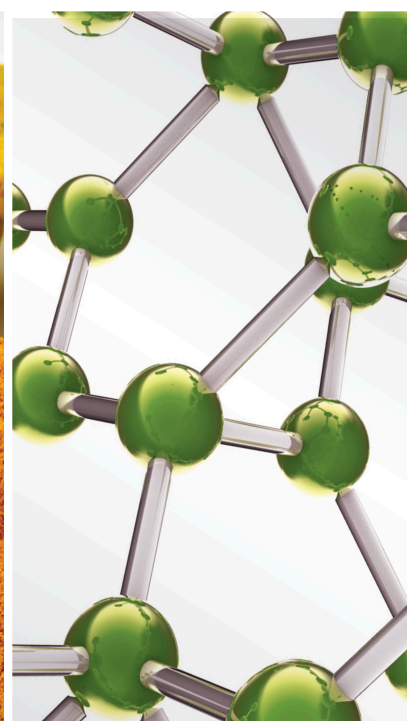


Herbal Medicine for Prevention and Therapy in Breast Cancer

Lead Guest Editor: Mohd Fadzelly Abu Bakar

Guest Editors: Azis Saifudin, Peng Cao, and Norhaizan Mohd Esa





Herbal Medicine for Prevention and Therapy in Breast Cancer

Evidence-Based Complementary and Alternative Medicine

Herbal Medicine for Prevention and Therapy in Breast Cancer

Lead Guest Editor: Mohd Fadzelly Abu Bakar
Guest Editors: Azis Saifudin, Peng Cao, and
Norhaizan Mohd Esa



Copyright © 2021 Hindawi Limited. All rights reserved.

This is a special issue published in "Evidence-Based Complementary and Alternative Medicine." All articles are open access articles distributed under the Creative Commons Attribution License, which permits unrestricted use, distribution, and reproduction in any medium, provided the original work is properly cited.

Editorial Board

Eman A. Mahmoud, Egypt
Smail Aazza, Morocco
Nahla S. Abdel-Azim, Egypt
Usama Ramadan Abdelmohsen, Germany
Essam A. Abdel-Sattar, Egypt
Mona Abdel-Tawab, Germany
Azian Azamimi Abdullah, Malaysia
Ana Lúcia Abreu-Silva, Brazil
Gustavo J. Acevedo-Hernández, Mexico
Jose C Adsuar, Spain
Duygu AĞAGÜNDÜZ, Turkey
Gabriel A. Agbor, Cameroon
Wan Mohd Aizat, Malaysia
Fahmida Alam, Malaysia
Ulysses Paulino Albuquerque, Brazil
Mohammed S. Ali-Shtayeh, Palestinian
Authority
Terje Alraek, Norway
Sergio R. Ambrosio, Brazil
Samson Amos, USA
Won G. An, Republic of Korea
Adolfo Andrade-Cetto, Mexico
Isabel Andújar, Spain
Letizia Angiolella, Italy
Makoto Arai, Japan
Daniel Dias Rufino Arcanjo, Brazil
Hyunsu Bae, Republic of Korea
Neda Baghban, Iran
Onesmo B. Balemba, USA
Winfried Banzer, Germany
Ahmed Bari, Saudi Arabia
Samra Bashir, Pakistan
Rusliza Basir, Malaysia
Jairo Kenupp Bastos, Brazil
Arpita Basu, USA
Daniela Beghelli, Italy
Mateus R. Beguelini, Brazil
Olfa Ben Braiek, Tunisia
Juana Benedí, Spain
Roberta Bernardini, Italy
Andresa A. Berretta, Brazil
Monica Borgatti, Italy

Francesca Borrelli, Italy
Samira Boulbaroud, Morocco
Mohammed Bourhia, Morocco
Célia Cabral, Portugal
Nunzio Antonio Cacciola, Italy
Giacchino Calapai, Italy
Giuseppe Caminiti, Italy
Raffaele Capasso, Italy
Francesco Cardini, Italy
María C. Carpinella, Argentina
Isabella Cavalcanti, Brazil
Shun-Wan Chan, Hong Kong
Harish Chandra, India
Wen-Dien Chang, Taiwan
Jianping Chen, China
Calvin Yu-Chian Chen, China
Kevin Chen, USA
Xiaojia Chen, Macau
Guang Chen, China
Mei-Chih Chen, Taiwan
Evan P. Cherniack, USA
Ching-Chi Chi, Taiwan
Giuseppina Chianese, Italy
Kok-Yong Chin, Malaysia
I. Chinou, Greece
Salvatore Chirumbolo, Italy
Jae Youl Cho, Republic of Korea
Hwi-Young Cho, Republic of Korea
Jun-Yong Choi, Republic of Korea
Seung Hoon Choi, Republic of Korea
Jeong June Choi, Republic of Korea
Kathrine Bisgaard Christensen, Denmark
Shuang-En Chuang, Taiwan
Ying-Chien Chung, Taiwan
Francisco José Cidral-Filho, Florianópolis
88040-900, SC, Brasil., Brazil
Ian Cock, Australia
Daniel Collado-Mateo, Spain
Marisa Colone, Italy
Lisa A. Conboy, USA
Kieran Cooley, Canada
Edwin L. Cooper, USA

José Otávio do Amaral Corrêa, Brazil
Maria T. Cruz, Portugal
Roberto K. N. Cuman, Brazil
Ademar A. Da Silva Filho, Brazil
Chongshan Dai, China
Giuseppe D'Antona, Italy
Vincenzo De Feo, Italy
Rocío De la Puerta, Spain
marinella de leo, Italy
Laura De Martino, Italy
Josué De Moraes, Brazil
Mozaniel de Oliveira, Brazil
Arthur De Sá Ferreira, Brazil
Nunziatina De Tommasi, Italy
Gourav Dey, India
Dinesh Dhamecha, USA
Claudia Di Giacomo, Italy
Antonella Di Sotto, Italy
Gabriel O. Dida, Japan
Vishal Diwan, Australia
Caigan Du, Canada
Shizheng Du, China
Jeng-Ren Duann, USA
Nativ Dudai, Israel
Rafael C. Dutra, Brazil
Thomas Efferth, Germany
Abir El-Alfy, USA
Mohamed Ahmed El-Esawi, Egypt
Mohd Ramli Elvy Suhana, Malaysia
Talha Bin Emran, Japan
Roger Engel, Australia
Karim Ennouri, Tunisia
Giuseppe Esposito, Italy
Tahereh Eteraf-Oskouei, Iran
Mohammad Faisal, Saudi Arabia
Sharida Fakurazi, Malaysia
Robson Xavier Faria, Brazil
Mohammad Fattahi, Iran
Keturah R. Faurot, USA
Piergiorgio Fedeli, Italy
Nianping Feng, China
Yibin Feng, Hong Kong
Glaura Fernandes, Brazil
Laura Ferraro, Italy
Antonella Fioravanti, Italy
Johannes Fleckenstein, Germany
Carmen Formisano, Italy

Harquin Simplicie Foyet, Cameroon
Filippo Fratini, Italy
Huiying Fu, China
Hua-Lin Fu, China
Liz G Müller, Brazil
Jian-Li Gao, China
Dolores García Giménez, Spain
Gabino Garrido, Chile
Safoora Gharibzadeh, Iran
Muhammad N. Ghayur, USA
Roxana Ghiulai, Romania
Angelica Oliveira Gomes, Brazil
Yuewen Gong, Canada
Elena González-Burgos, Spain
Susana Gorzalczany, Argentina
Sebastian Granica, Poland
Jiangyong Gu, China
Maruti Ram Gudavalli, USA
Shanshan Guo, China
Jianming GUO, China
Shuzhen Guo, China
Jian-You Guo, China
Hai-dong Guo, China
Zihu Guo, China
Narcís Gusi, Spain
Svein Haavik, Norway
Fernando Hallwass, Brazil
Gajin Han, Republic of Korea
Ihsan Ul Haq, Pakistan
Md. Areeful Haque, India
Hicham Harhar, Morocco
Kuzhuvélil B. Harikumar, India
Mohammad Hashem Hashempur, Iran
Muhammad Ali Hashmi, Pakistan
Waseem Hassan, Pakistan
Sandrina A. Heleno, Portugal
Soon S. Hong, Republic of Korea
Md. Akil Hossain, Republic of Korea
Muhammad Jahangir Hossen, Bangladesh
Shih-Min Hsia, Taiwan
Ching-Liang Hsieh, Taiwan
Weicheng Hu, China
Sen Hu, China
Tao Hu, China
Changmin Hu, China
Sheng-Teng Huang, Taiwan
Wei Huang, China

Ciara Hughes, Ireland
Attila Hunyadi, Hungary
Tarique Hussain, Pakistan
Maria-Carmen Iglesias-Osma, Spain
Elisha R. Injeti, USA
H. Stephen Injeyan, Canada
Amjad Iqbal, Pakistan
Chie Ishikawa, Japan
Angelo A. Izzo, Italy
Mohieddin Jafari, Finland
Rana Jamous, Palestinian Authority
G. K. Jayaprakasha, USA
Kamani Ayoma Perera Wijewardana
Jayatilaka, Sri Lanka
Kyu Shik Jeong, Republic of Korea
Qing Ji, China
Yanxia Jin, China
Hualiang Jin, China
Leopold Jirovetz, Austria
Won-Kyo Jung, Republic of Korea
Jeeyoun Jung, Republic of Korea
Takahide Kagawa, Japan
Nurkhalida Kamal, Saint Vincent and the
Grenadines
Atsushi Kameyama, Japan
Wenyi Kang, China
Kyungsu Kang, Republic of Korea
Shao-Hsuan Kao, Taiwan
Juntra Karbwang, Japan
Nasiara Karim, Pakistan
Morimasa Kato, Japan
Deborah A. Kennedy, Canada
Washim Khan, USA
Haroon Khan, Pakistan
Cheorl-Ho Kim, Republic of Korea
Jin-Kyung Kim, Republic of Korea
Kibong Kim, Republic of Korea
Bonglee Kim, Republic of Korea
Yun Jin Kim, Malaysia
Junghyun Kim, Republic of Korea
Kyungho Kim, Republic of Korea
Youn-Chul Kim, Republic of Korea
Dong Hyun Kim, Republic of Korea
Woojin Kim, Republic of Korea
Yoshiyuki Kimura, Japan
Nebojša Kladar, Serbia
Mi Mi Ko, Republic of Korea

Toshiaki Kogure, Japan
Jian Kong, USA
Malcolm Koo, Taiwan
Yu-Hsiang Kuan, Taiwan
Robert Kubina, Poland
Omer Kucuk, USA
Victor Kuete, Cameroon
Woon-Man Kung, Taiwan
Chan-Yen Kuo, Taiwan
Joey S. W. Kwong, China
Kuang C. Lai, Taiwan
Fanuel Lampiao, Malawi
Ilaria Lampronti, Italy
Chou-Chin Lan, Taiwan
Mario Ledda, Italy
Sang Yeoup Lee, Republic of Korea
Kyu Pil Lee, Republic of Korea
Dong-Sung Lee, Republic of Korea
Jeong-Sang Lee, Republic of Korea
Byung-Cheol Lee, Republic of Korea
Namhun Lee, Republic of Korea
Yun Jung Lee, Republic of Korea
Gihyun Lee, Republic of Korea
Harry Lee, China
Ju Ah Lee, Republic of Korea
Christian Lehmann, Canada
Marivane Lemos, Brazil
George B. Lenon, Australia
Marco Leonti, Italy
Xing Li, China
Min Li, China
XiuMin Li, Armenia
Hua Li, China
Xuqi Li, China
Yi-Rong Li, Taiwan
Chun-Guang Li, Australia
Yu-cui Li, China
Xi-Wen Liao, China
Shuibin Lin, China
Bi-Fong Lin, Taiwan
Shih-Chao Lin, Taiwan
Ho Lin, Taiwan
Kuo-Tong Liou, Taiwan
Chian-Jiun Liou, Taiwan
Christopher G. Lis, USA
Gerhard Litscher, Austria
I-Min Liu, Taiwan

Jingping Liu, China
Xiaosong Liu, Australia
Suhuan Liu, China, China
Yujun Liu, China
Emilio Lizarraga, Argentina
Monica Loizzo, Italy
Nguyen Phuoc Long, Republic of Korea
V́ctor Ĺpez, Spain
Zaira Ĺpez, Mexico
Chunhua Lu, China
Ángelo Luís, Portugal
Anderson Luiz-Ferreira, Brazil
Jian-Guang Luo, China
Ivan Luzardo Luzardo-Ocampo, Mexico
Zheng-tao Lv, China
Michel Mansur Machado, Brazil
Filippo Maggi, Italy
Jamal A. Mahajna, Israel
Juraj Majtan, Slovakia
Toshiaki Makino, Japan
Nicola Malafrente, Italy
Giuseppe Malfa, Italy
Francesca Mancianti, Italy
Subashani Maniam, Australia
Carmen Mannucci, Italy
Arroyo-Morales Manuel, Spain
Juan M. Manzaneeque, Spain
Fatima Martel, Portugal
Simona Martinotti, Italy
Carlos H. G. Martins, Brazil
Stefania Marzocco, Italy
Maulidiani Maulidiani, Malaysia
Andrea Maxia, Italy
Avijit Mazumder, India
Isac Medeiros, Brazil
Ahmed Mediani, Malaysia
Lewis Mehl-Madrona, USA
Ayikoé Guy Mensah-Nyagan, France
Oliver Micke, Germany
Maria G. Miguel, Portugal
Luigi Milella, Italy
Roberto Miniero, Italy
Letteria Minutoli, Italy
Prashant Modi, India
Daniel Kam-Wah Mok, Hong Kong
Changjong Moon, Republic of Korea
Albert Moraska, USA

Mark Moss, United Kingdom
Yoshiharu Motoo, Japan
Kamal D. Moudgil, USA
Yoshiki Mukudai, Japan
Sakthivel Muniyan, USA
Massimo Nabissi, Italy
Siddavaram Nagini, India
Hajime Nakae, Japan
Takao Namiki, Japan
Srinivas Nammi, Australia
Krishnadas Nandakumar, India
Vitaly Napadow, USA
Derek Tantoh Ndinteh, South Africa
Pratibha V. Nerurkar, USA
Benoit Banga N'guessan, Ghana
Marcello Nicoletti, Italy
Eliud Nyaga Mwaniki Njagi, Kenya
Cristina Nogueira, Brazil
Sakineh Kazemi Noureini, Iran
Rômulo Dias Novaes, Brazil
Martin Offenbaecher, Germany
Yoshiji Ohta, Japan
Oluwafemi Adeleke Ojo, Nigeria
Olumayokun A. Olajide, United Kingdom
Olufunmiso Olusola Olajuyigbe, Nigeria
Luís Flávio Oliveira, Brazil
Atolani Olubunmi, Nigeria
Abimbola Peter Oluyori, Nigeria
Vahidreza Ostadmohammadi, Iran
Chiagoziem Anariochi Otuechere, Nigeria
Mustafa Ozyurek, Turkey
Ester Pagano, Italy
Sokcheon Pak, Australia
Antônio Palumbo Jr, Brazil
Zongfu Pan, China
Yunbao Pan, China
Siyaram Pandey, Canada
Gunhyuk Park, Republic of Korea
Bong-Soo Park, Republic of Korea
Wansu Park, Republic of Korea
Rodolfo Parreira, Brazil
Matheus Pasquali, Brazil
Luiz Felipe Passero, Brazil
Visweswara Rao Pasupuleti, Malaysia
Bhushan Patwardhan, India
Claudia Helena Pellizzon, Brazil
Weijun Peng, China

Cheng Peng, Australia
Shagufta Perveen, Saudi Arabia
Raffaele Pezzani, Italy
Florian Pfab, Germany
Sonia Piacente, Italy
Andrea Pieroni, Italy
Richard Pietras, USA
Haifa Qiao, USA
Sheng Qin, China
Cláudia Quintino Rocha, Brazil
Khalid Rahman, United Kingdom
Nor Fadilah Rajab, Malaysia
Elia Ranzato, Italy
Manzoor A. Rather, India
Valentina Razmovski-Naumovski, Australia
Julita Regula, Poland
Kanwal Rehman, Pakistan
Gauhar Rehman, Pakistan
Ke Ren, USA
Man Hee Rhee, Republic of Korea
Daniela Rigano, Italy
José L. Rios, Spain
Francisca Rius Diaz, Spain
Eliana Rodrigues, Brazil
Maan Bahadur Rokaya, Czech Republic
Barbara Romano, Italy
Mariangela Rondanelli, Italy
Antonietta Rossi, Italy
DANIELA RUSSO, Italy
Mi Heon Ryu, Republic of Korea
Bashar Saad, Palestinian Authority
Abdul Sadiq, Pakistan
Sabiu Saheed, South Africa
Mohamed Z.M. Salem, Egypt
Avni Sali, Australia
Andreas Sandner-Kiesling, Austria
Manel Santafe, Spain
José Roberto Santin, Brazil
Antonietta Santoro, Italy
Tadaaki Satou, Japan
Roland Schoop, Switzerland
Sven Schröder, Germany
Sindy Seara-Paz, Spain
Veronique Seidel, United Kingdom
Terry Selfe, USA
Senthamil R. Selvan PhD, USA
Arham Shabbir, Pakistan

Suzana Shahar, Malaysia
Hongcai Shang, China
Wen-Bin Shang, China
Ronald Sherman, USA
Karen J. Sherman, USA
She-Po Shi, China
San-Jun Shi, China
Insop Shim, Republic of Korea
Im Hee Shin, Republic of Korea
Yukihiro Shoyama, Japan
Morry Silberstein, Australia
Samuel Martins Silvestre, Portugal
Moganavelli Singh, South Africa
Kuttulebbai N. S. Sirajudeen, Malaysia
Slim Smaoui, Tunisia
Eun Jung Sohn, Republic of Korea
Francisco Solano, Spain
Maxim A. Solovchuk, Taiwan
Young-Jin Son, Republic of Korea
Chang G. Son, Republic of Korea
Yanting Song, China
Chengwu Song, China
Klaokwan Srisook, Thailand
Vanessa Steenkamp, South Africa
Annarita Stringaro, Italy
Dan Su, China
Shan-Yu Su, Taiwan
Keiichiro Sugimoto, Japan
Valeria Sulsen, Argentina
Zewei Sun, China
Amir Syahir, Malaysia
Sharifah S. Syed Alwi, United Kingdom
Eryvaldo Sócrates Tabosa do Egito, Brazil
Orazio Tagliatela-Scafati, Italy
Shin Takayama, Japan
Takashi Takeda, Japan
Amin Tamadon, Iran
Gianluca Tamagno, Ireland
Ghee T. Tan, USA
Jing-Yu (Benjamin) Tan, Australia
qingfa Tang, China
Nader Tanideh, Iran
Jun-Yan Tao, China
Hamid Tebyanian, Iran
Lay Kek Teh, Malaysia
Norman Temple, Canada
Kamani H. Tennekoon, Sri Lanka

Mencherini Teresa, Italy
Mayank Thakur, Germany
Menaka Thounaojam, USA
Jinhui Tian, China
Michał Tomczyk, Poland
Loren Toussaint, USA
Md. Sahab Uddin, Bangladesh
Riaz Ullah, Saudi Arabia
Konrad Urech, Switzerland
Philip F. Uzor, Nigeria
Patricia Valentao, Portugal
Sandy van Vuuren, South Africa
Luca Vanella, Italy
Antonio Vassallo, Italy
Cristian Vergallo, Italy
Miguel Vilas-Boas, Portugal
Santos Villafaina, Spain
Aristo Vojdani, USA
Abraham Wall-Medrano, Mexico
Jin-Yi Wan, USA
Chunpeng(Craig) Wan, China
Almir Gonçalves Wanderley, Brazil
Youhua Wang, China
Huijun Wang, China
Ke-Lun Wang, Denmark
Chong-Zhi Wang, USA
Ting-Yu Wang, China
Jin''An Wang, China
Jia-bo Wang, China
Yong Wang, China
Xue-Rui Wang, China
Qi-Rui Wang, China
Shu-Ming Wang, USA
Xiao Wang, China
Ru-Feng Wang, China
Yun WANG, China
Kenji Watanabe, Japan
Jintanaporn Wattanathorn, Thailand
Silvia Wein, Germany
Meng-Shih Weng, Taiwan
Jenny M. Wilkinson, Australia
Katarzyna Winska, Poland
Christopher Worsnop, Australia
Xian Wu, USA
Jih-Huah Wu, Taiwan
Xu Wu, China
Sijin Wu, China



Zuoqi Xiao, China
Rafael M. Ximenes, Brazil
Guoqiang Xing, USA
JiaTuo Xu, China
Yong-Bo Xue, China
Mei Xue, China
Haruki Yamada, Japan
Nobuo Yamaguchi, Japan
Jing-Wen Yang, China
Longfei Yang, China
Wei-Hsiung Yang, USA
Qin Yang, China
Sheng-Li Yang, China
Junqing Yang, China
Mingxiao Yang, Hong Kong
Swee Keong Yeap, Malaysia
Albert S. Yeung, USA
Ebrahim M. Yimer, Ethiopia
Yoke Keong Yong, Malaysia
Fadia S. Youssef, Egypt
Zhilong Yu, Canada
Yanggang Yuan, China
Hilal Zaid, Israel
Paweł Zalewski, Poland
Armando Zarrelli, Italy
Y Zeng, China
Zhiqian Zhang, China
Jianliang Zhang, China
Mingbo Zhang, China
Jiu-Liang Zhang, China
Fangbo Zhang, China
Bimeng Zhang, China
Jing Zhao, China
RONGJIE ZHAO, China
Zhangfeng Zhong, Macau
Yan Zhu, USA
Guoqi Zhu, China
Suzanna M. Zick, USA
Stephane Zingue, Cameroon

Contents


Herbal Medicine for Prevention and Therapy in Breast Cancer

Mohd Fadzelly Abu Bakar , Azis Saifudin , Peng Cao , and Norhaizan Mohd Esa 
Editorial (4 pages), Article ID 9760586, Volume 2021 (2021)



Effects of Water Extract of *Cynanchum paniculatum* (Bge.) Kitag. on Different Breast Cancer Cell Lines

Shu-Yu Yang , Jen Ying Li , Guan-Jhong Huang , Badrinathan Sridharan , Jen-Shu Wang , Kai-Ming Chang , and Meng-Jen Lee 
Research Article (13 pages), Article ID 6665949, Volume 2021 (2021)


The Efficacy of Moxibustion for Breast Cancer Patients with Chemotherapy-Induced Myelosuppression during Adjuvant Chemotherapy: A Randomized Controlled Study

Yajie Ji, Siyu Li, Xinyue Zhang, Qiong Li, Qing Lu, Weili Chen, Yu Liu, Jiayu Sheng, Hongli Liang, Ke Jiang, Mengting Li, Shanyan Sha, Huangang Wu, Yan Huang, and Xiaohong Xue 
Research Article (10 pages), Article ID 1347342, Volume 2021 (2021)





Fuzheng Yiliu Formula Regulates Tumor Invasion and Metastasis through Inhibition of WAVE3 Expression

Wen-li Chen, Huan-huan Bai, Li-wei Liu, Hong-yu Chen, Qi Shi, Li-sheng Chang, Xiao-jun Gou , and Jun Qian 
Research Article (14 pages), Article ID 8898668, Volume 2021 (2021)







A Network Pharmacology Study on the Molecular Mechanisms of FDY003 for Breast Cancer Treatment

Ho-Sung Lee, In-Hee Lee, Kyungrae Kang, Sang-In Park, Seung-Joon Moon, Chol Hee Lee, and Dae-Yeon Lee 
Research Article (18 pages), Article ID 3919143, Volume 2021 (2021)

Unfermented Freeze-Dried Leaf Extract of Tongkat Ali (*Eurycoma longifolia* Jack.) Induced Cytotoxicity and Apoptosis in MDA-MB-231 and MCF-7 Breast Cancer Cell Lines

Lusia Barek Moses , Mohd Fadzelly Abu Bakar , Hasmadi Mamat , and Zaleha Abdul Aziz 
Research Article (16 pages), Article ID 8811236, Volume 2021 (2021)

Secondary Metabolites, Antioxidant, and Antiproliferative Activities of *Dioscorea bulbifera* Leaf Collected from Endau Rompin, Johor, Malaysia

Muhammad Murtala Mainasara , Mohd Fadzelly Abu Bakar , Abdah Md Akim , Alona C Linatoc , Fazleen Izzany Abu Bakar , and Yazan K. H. Ranneh 
Research Article (10 pages), Article ID 8826986, Volume 2021 (2021)

Aidi Injection as Adjuvant Drug Combined with Chemotherapy in Treatment of Breast Cancer: A Systematic Meta-Analysis

Chenhao Wu , Yongjun Qi , Juan Zhou , Chen Yao , Min Miao , and Chen Cheng 
Review Article (12 pages), Article ID 8832913, Volume 2021 (2021)

The Shuganhuazheng Formula in Triple-Negative Breast Cancer: A Study Based on Network Pharmacology and In Vivo Experiments

Bo Wang, Rui Fei, Yan Yang, Niancai Jing, Yi Lu, Hongyu Xiao, Jili Yang, and Yue Zhang 



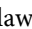

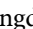
Research Article (10 pages), Article ID 8173147, Volume 2020 (2020)

Berberine Inhibits the Expression of SCT through miR-214-3p Stimulation in Breast Cancer Cells

Congyuan Zhu , Jianping Li , Yuming Hua , Jingli Wang, Ke Wang , and Jingqiu Sun 




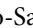
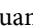
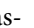


Research Article (13 pages), Article ID 2817147, Volume 2020 (2020)

In Vitro Cytotoxic Activity against Breast, Cervical, and Ovarian Cancer Cells and Flavonoid Content of Plant Ingredients Used in a Selected Thai Traditional Cancer Remedy: Correlation and Hierarchical Cluster Analysis

Thammarat Tuy-on , Arunporn Itharat , Ponlawat Maki , Pakakrong Thongdeeying , Weerachai Pipatrattanaseree , and Buncha Ooraikul


Research Article (10 pages), Article ID 8884529, Volume 2020 (2020)

Carvacrol: An In Silico Approach of a Candidate Drug on HER2, PI3K α , mTOR, hER- α , PR, and EGFR Receptors in the Breast Cancer

Oscar Herrera-Calderon , Andres F. Yepes-Pérez , Jorge Quintero-Saumeth , Juan Pedro Rojas-Armas , Miriam Palomino-Pacheco , José Manuel Ortiz-Sánchez , Edwin César Cieza-Macedo , Jorge Luis Arroyo-Acevedo , Linder Figueroa-Salvador , Gilmar Peña-Rojas , and Vidalina Andía-Ayme


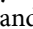
Research Article (12 pages), Article ID 8830665, Volume 2020 (2020)

Potential Molecular Mechanisms of Chaihu-Shugan-San in Treatment of Breast Cancer Based on Network Pharmacology

Kunmin Xiao, Kexin Li, Sidan Long, Chenfan Kong, and Shijie Zhu 


Research Article (9 pages), Article ID 3670309, Volume 2020 (2020)


Efficacy and Safety of Cinobufacin Combined with Chemotherapy for Advanced Breast Cancer: A Systematic Review and Meta-Analysis

Jing Xu, Dongyun Li , Kexin Du, and Jing Wang 

Research Article (13 pages), Article ID 4953539, Volume 2020 (2020)


Efficacy and Safety of Aidi Injection as an Adjuvant Therapy on Advanced Breast Cancer: A Systematic Review and Meta-Analysis of Randomized Controlled Trials

Yihui Chai, Yunzhi Chen, Wen Li , Zhong Qin, Jie Gao, Zhibin Jiang, Yuhong Ge, Liancheng Guan,

Mengzhi Zhang, Huaiquan Liu, Haiyang Yu, Qingxue Wang, and Changfu Yang 

Review Article (8 pages), Article ID 2871494, Volume 2020 (2020)

A Bioinformatics Research on Novel Mechanism of Compound Kushen Injection for Treating Breast Cancer by Network Pharmacology and Molecular Docking Verification

Shuyu Liu, Xiaohong Hu, Xiaotian Fan, Ruiqi Jin, Wenqian Yang, Yifei Geng, and Jiarui Wu 

Research Article (14 pages), Article ID 2758640, Volume 2020 (2020)

Editorial

Herbal Medicine for Prevention and Therapy in Breast Cancer

Mohd Fadzelly Abu Bakar ¹, Azis Saifudin ², Peng Cao ³, and Norhaizan Mohd Esa ⁴

¹Faculty of Applied Sciences and Technology, Universiti Tun Hussein Onn Malaysia (UTHM)–Pagoh Campus, Muar 84600, Johor, Malaysia

²Faculty of Pharmacy, Universitas Muhammadiyah Surakarta, Jalan A. Yani, Tromol Pos 1, Pabelan Kartasura, Surakarta, Central Java, Indonesia

³Department of Pharmacology, School of Pharmacy, Nanjing University of Chinese Medicine, Nanjing 210023, China

⁴Department of Nutrition, Faculty of Medicine and Health Sciences, Universiti Putra Malaysia, Serdang 43400, Selangor, Malaysia

Correspondence should be addressed to Mohd Fadzelly Abu Bakar; fadzelly@uthm.edu.my

Received 28 July 2021; Accepted 28 July 2021; Published 15 August 2021

Copyright © 2021 Mohd Fadzelly Abu Bakar et al. This is an open access article distributed under the Creative Commons Attribution License, which permits unrestricted use, distribution, and reproduction in any medium, provided the original work is properly cited.

Cancer is becoming more common globally. Breast cancer is one of the most prevalent forms of cancer and one of the main causes of cancer mortality. While modern medicine has been used as the primary cure for this disease, traditional herbal medicine has been commonly used as a complementary and alternative strategy in some developed and developing countries.

To provide scientific justification for the use of herbal medicine, it is necessary to record and publish preclinical and clinical evidence-based research. Concerns with herbal medicine including the consistency and standardisation of the herbal product (particularly the presence of bioactive compounds responsible for the effect), effectiveness, mode of action, safety, and herb-drug interaction if used as complementary and/or alternative medicine need to be further explored.

This special issue seeks to provide a forum for researchers to publish the most recent advances and clinical studies in the use of herbal medicines for breast cancer prevention and treatment, including ethnopharmacology, natural product chemistry, effectiveness, safety, dosage and toxicity, *in vitro* and *in vivo* preclinical trials, herb-drug relationship, clinical trials, and potential biochemical and molecular pathways. This special issue included fifteen articles which were carefully reviewed and accepted for publication and briefly described as follows.

Some of the papers of this special issue focus on plant extracts from different countries of the world, and their

potential to treat and prevent breast cancer using *in vitro* and/or *in vivo* methods. In some cases, a new generation of ICT technique (i.e., network pharmacology and molecular docking) was used to determine the potential plant phytochemicals and their possible mechanism of action to treat and/or prevent the incidence of breast cancer. In addition to that, *in vitro* and *in vivo* studies were also being conducted to confirm the anticancer activity from the network pharmacology results. In some cases, a partial phytochemical isolation and further characterization was performed. One clinical trial was conducted to determine the efficacy of herbal medicines to treat and/or prevent breast cancer in human patients. Of these, several works involve herbal preparations from single and/or polyherbal formulations from standardized herbal traditional Chinese medicine.

W. Chen et al. investigated the anticancer potential of herbal traditional Chinese medicine Fuzheng Yiliu formula (FZYLF) against MDA-MB-231/Adr cell line with high invasive ability and multidrug-resistant breast cancer cells. Using *in vitro* (established cancer cells) and *in vivo* (MDA-MB-231/Adr tumor xenografted in nude mice) approaches, they conclude that FZYLF can inhibit the invasion and metastasis as well as induce cytotoxicity in MDA-MB-231/Adr human breast cancer cells. They propose the regulation of WAVE3 expression as the possible molecular mechanism of action of FZYLF as anticancer agent.

L. B. Moses et al. investigated the anticancer capacity of *Eurycoma longifolia* (Jack.) or locally known as “Tongkat

Ali” leaf extracts and their probable anticancer mode of action *in vitro* against non-hormone-dependent MDA-MB-231 and hormone-dependent MCF-7 breast cancer cell lines. The leaves of *E. longifolia* were converted into both unfermented and fermented products, which were then screened with their action against both cancer cell lines. Flow cytometry was used to investigate apoptotic cell quantification, cell cycle distribution, and the expression of caspases and apoptotic proteins. MDA-MB-231 cells had substantial activities of cytochrome c, caspase-3, Bax, and Bcl-2 apoptotic proteins, while MCF-7 cells had significant activities of caspase-8, cytochrome c, Bax, p53, and Bcl-2 apoptotic protein. This extract has the highest levels of phenolics such as gallic acid, chlorogenic acid, ECG, and EGCG, which can contribute to its potent anticancer action.

The secondary metabolites, antioxidant, and anti-proliferative activity of *Dioscorea bulbifera* leaves collected from Endau Rompin, Johor, Malaysia, was explored by M. M. Mainasara et al. The results showed that the plant extracts displayed high antioxidant activity and induced cytotoxicity in both MCF-7 and MDA-MB-231 breast cancer cell lines. Apoptosis and cell cycle arrest have been shown to be part of the mechanism of action. These authors found that the plant contains at least of 39 metabolites that might synergistically contribute to the bioactivity.

C. Zhu et al. reported the anticancer potential of berberine (BBR), a kind of isoquinoline alkaloid that is extracted from *Coptidis Rhizoma* or Huanglian. BBR has been shown to display diverse health benefit properties such as antimicrobial, cardioprotective, and antidiabetic properties. They investigate the suppressive abilities of BBR on both MCF-7 and MDA-MB-231 breast cancer cells and confirm its underlying mechanisms with miR-214-3p. They found that BBR has the potential to suppress the proliferation of MCF-7 and MDA-MB-231 breast cancer cells by upregulating the expression of miR-214-3p and increasing its inhibition to stem cell transplant (SCT). As a conclusion, miR-214-3p/SCT axis is a potential therapeutic target in the mechanism of BBR to suppress breast cancer.

T. Tuy-on et al. investigated the anticancer potential of selected Thai traditional cancer remedies to induce cytotoxicity in breast, cervical, and ovarian cancer cells *in vitro*. The hierarchical cluster analysis (HCA) was used to classify the extracts by their cytotoxic characteristics. They design this method to predict the correlation between the plant's bioactive compounds and biological activities. The results showed that eleven plants normally used in Thai traditional medicine (TTM) were active against at least one of the cancer cell lines, while about 2/3 of all extracts were active against all tested cell lines. The remaining plant extracts might not be considered as active but may be needed as complementary medicine according to the TTM theory. They suggested further studies (i.e., *in vivo* work) to determine the exact efficacy of the herbal remedies.

Carvacrol is a phenol monoterpene and has been found as the dominant phytochemical in the essential oil of aromatic herb species in the family Lamiaceae such as oregano and thyme. This compound has been reported to display

protective effects in chemically induced breast cancer models *in vivo*. O. Herrera-Calderon et al. proposed and evaluated the possible mechanism of action of carvacrol by using an *in silico* study on selected receptors involved in breast cancer progression by docking analysis, molecular dynamics, and drug-likeness studies. Their findings suggest that mTOR signaling pathway could be a possible mechanism of action for its preventive properties on the breast cancer model.

Cynanchum paniculatum (Bge.) Kitag (CP) (also known as dog strangling vine, radix cynanchi paniculata, Shu Changching in Chinese) has been used in conjunction with other medicinal plants to treat cancer in TCM. S.-Y. Yang et al. investigated the anticancer potential of this plant extract against selected breast cancer cell lines with different mutation types (i.e., MDA-MB-231, MCF-7, and ZR-75-1 and SK-Br-3). They found out that negative estrogen receptor and progesterone receptor cells are more sensitive to CP treatment in terms of direct cytotoxicity, which is not regulated by caspase-3, but highly correlated to MMP-2 regulation. They conclude that CP displayed effective anticancer potential against selected breast cancer cells through diverse mechanisms of action specifically targeting the inhibition of proliferation of triple negative MDA-MB-231.

The systematic review and meta-analysis of the use of polyherbal traditional Chinese medicine using existing clinical data is also presented in three articles of the special issue.

Cinobufacin is a patent-protected traditional Chinese medicine that has been widely used for the treatment and prevention of breast cancer in China. The medicine is obtained from the skin of toad, *Bufo gargarizans* that contains diverse components such as toadotoxin, dehydroxytoluotoxin, serotonin, and arginine complex. J. Xu et al. reviewed the efficacy and safety of cinobufacin combined with chemotherapy for advanced breast cancer treatment. They found out that the ORR (overall response rate), CBR (clinical benefit rate), and pain relief rate of cinobufacin combined with the chemotherapy group were statistically better than in the chemotherapy group. Cinobufacin combined with the chemotherapy group can also reduce the tumour markers in cancer patients with low negative side effects.

Aidi injection (ADI) is a mixture of selected traditional Chinese herb injections that is composed of the extracts from *Panax ginseng* C. A. Mey, *Astragalus propinquus* Schischkin, *Acanthopanax senticosus* (Rupr. Maxim.) Harms, and *Mylabris phalerata* Pallas and has been used widely to treat breast cancer in China. Y. Chai et al. conducted the systematic review and meta-analysis of ADI to treat advanced breast cancer. They believe that, based on the few available clinical trials, therapy with ADI in advanced breast cancer patients dramatically alters the overall reaction rate and disease control rate, as well as improves quality of life with few side effects. More randomised control experiments with greater sample sizes, though, should be carried out, as should elucidation of the detailed mechanisms of action (biochemical and molecular level).

Meanwhile, C. Wu et al. investigated and compared the efficacy and safety of a combination of ADI and chemotherapy versus chemotherapy alone in the treatment of

breast cancer in a systematic review of clinical evidence. From the 20 studies available, they found out that the response rate (RR) and performance status (KPS) in the ADI + chemotherapy group were significantly higher than those of the chemotherapy alone group. They conclude that ADI could act synergistically to enhance the efficacy of chemotherapy drugs with reduced/no additional adverse side effects. They suggest the promotion of ADI as a potent adjunct anticancer drug especially in breast cancer treatment.

In this special issue, 4 bioinformatics research papers were published, particularly by using network pharmacology accompanied with molecular docking application. 1 paper further confirmed the bioinformatics results using a pre-clinical (*in vivo*) approach.

In China, compound Kushen injection (CKI) (made from *Sophora flavescens* and *Smilax glabra*) has been widely used to treat breast cancer. Its molecular mechanism, however, is unknown. As a result, S. Liu et al. used network pharmacology and molecular docking verification to explore alternative mechanisms of action. The findings revealed that 16 active CKI compounds were recognised, corresponding to 285 putative targets. They discovered that CKI is involved in numerous and complex mechanisms of action in the treatment of breast cancer, including several common cancer pathways, chemical carcinogenesis, oestrogen signalling pathway, TNF signalling pathway, and leukocyte transendothelial migration. Given that this study is primarily focused on data processing, additional biological studies are needed to validate the findings.

FDY003 is an herbal formulation that comprises three herbal preparations, namely, *Lonicera japonica* Thunberg, *Artemisia capillaris* Thunberg, and *Cordyceps militaris*, that have been shown to display potent antitumour effects in different types of cancer cells. As many herbal medicine preparations, the possible mechanism of action is still lacking. Using network pharmacology approaches, H.-S. Lee et al. investigated the mechanisms of FDY003 against breast cancer in the systemic level. They discovered that the herbal mixture modulated cellular processes such as cell proliferation, cell cycle mechanisms, and cell apoptosis, as well as many oncogenic pathways that play important roles in breast cancer pathology.

K. Xiao et al. reported the anticancer potential of Chaihu-Shugan-San, a traditional Chinese medicine that was formulated from seven different kinds of herbal preparations. According to the principles of traditional Chinese medicine, the clinical syndrome of breast cancer refers to the “Liver-Qi” stagnation and Chaihu-Shugan-San is one of the popular treatments for “Liver-Qi” stagnation. In this study, they investigated the possible pathway of Chaihu-Shugan-San in the treatment of breast cancer by network pharmacology. Preliminary results showed that 157 bioactive compounds and 8074 potential drug targets were obtained. Network pharmacology analysis showed that the pathway responsible for the potent anticancer agent includes (but not limited to) mRNA and RNA catabolic processes, telomere organization, apoptosis, cell cycle progression, transcriptional dysregulation, endocrine resistance, and viral

infection. They conclude that the treatment of Chaihu-Shugan-San on breast cancer involves multicomponent, multitarget, and multipathway interactions.

Shuganhuazheng formula (SGHZF) is an anticancer formulation that has been used widely in selected TCM and conventional hospitals in China for many years, especially to treat triple-negative breast cancer (TNBC). B. Wang et al. examined the medicinal effect and mechanism of SGHZF against TNBC using network pharmacology and further verified the efficacy in animal models. They found out that SGHZF has been shown to inhibit the proliferation of breast cancer growth in experimental animal models and the possible mechanism of action might involve the inhibition of Akt and HIF-1 α expression.

One randomised clinical trial was conducted using moxibustion, a type of TCM that involves the burning of moxa, a cone or stick made of ground mugwort leaves, on particular points on the body with the intention to protect health and prevent disease. Previous studies showed that moxibustion may reduce the incidence of cancer and the side effect of chemotherapy. As a result, Y. Ji et al. explored the therapeutic effectiveness of moxibustion for breast cancer patients undergoing adjuvant chemotherapy who have chemotherapy-induced myelosuppression (CIM). They conclude that moxibustion is useful for treating CIM in breast cancer patients undergoing adjuvant chemotherapy, especially in patients undergoing high-dose, long-term, and mixed chemotherapy regimens. Furthermore, moxibustion can reduce the occurrence of SAE (in myelosuppression) and AE (such as nausea, vertigo, bone, joint, and muscle pain, and incision pain) and improve the compliance and safety of chemotherapy.

A wide range of contributions from a diverse research scope that includes isolation and semipurification of bioactive compounds, preclinical (*in vitro* and *in vivo*) studies, possible mechanisms of action using molecular and bioinformatics (network pharmacology and molecular docking) approaches, systematic reviews and meta-analysis of published clinical data, and clinical trials of herbal medicine showed the promising potential of herbal medicine as prevention and therapy in breast cancer.

Data Availability

All data were obtained from the published studies.

Conflicts of Interest

The Guest Editors declare that they have no conflicts of interest regarding the publication of the special issue.

Acknowledgments

The Guest Editors of this special issue acknowledge all contributors to the success of this fantastic publication concerning the use of herbal products as prevention and treatment in breast cancer. In addition to that, the Guest Editors would like to thank all authors of the published articles of this special issue for their respected scientific

works, reviewers for their comments and suggestions and spending their valuable time to review the articles that made this special issue possible, and the editorial board and the person in charge of this journal for inviting them to host this special issue. The Lead Guest Editors acknowledge the support provided by the Ministry of Higher Education of Malaysia (MOHE) under Fundamental Research Grant Scheme (FRGS), Vot No. 1560 (FRGS/1/2015/WAB01/UTHM/02/1) that encourage scientific research related to complementary and alternative medicine in Malaysia, especially focusing on the use of natural products as prevention and treatment of cancer (breast cancer in this case).

*Mohd Fadzelly Abu Bakar
Azis Saifudin
Peng Cao
Norhaizan Mohd Esa*

Research Article

Effects of Water Extract of *Cynanchum paniculatum* (Bge.) Kitag. on Different Breast Cancer Cell Lines

Shu-Yu Yang ¹, Jen Ying Li ¹, Guan-Jhong Huang ², Badrinathan Sridharan ³,
Jen-Shu Wang ¹, Kai-Ming Chang ⁴, and Meng-Jen Lee ³

¹Department of Chinese Medicine, Taichung Tzu Chi Hospital, Buddhist Tzu Chi Medical Foundation, Taichung, Taiwan

²Department of Chinese Pharmaceutical Sciences and Chinese Medicine Resources, China Medical University, Taichung, Taiwan

³Department of Applied Chemistry, Chaoyang University of Technology, 168 Jifeng East Road, Taichung, Taiwan

⁴Department of Research, Koo Foundation Sun Yat-Sen Cancer Center, 125 LihDer Road, Pei-Tou District, Taipei, Taiwan

Correspondence should be addressed to Meng-Jen Lee; mjlee@cyut.edu.tw

Received 10 November 2020; Revised 13 February 2021; Accepted 10 March 2021; Published 26 May 2021

Academic Editor: Mohd Fadzelly Abu Bakar

Copyright © 2021 Shu-Yu Yang et al. This is an open access article distributed under the Creative Commons Attribution License, which permits unrestricted use, distribution, and reproduction in any medium, provided the original work is properly cited.

Cynanchum paniculatum (Bge.) Kitag. (CP) is an important medicinal herb used in Chinese herbal medicine, with a variety of biological activities including anticancer property. In this study, we explored the water extract of CP, for its anticancer effects against breast cancer cells with different mutation types. Cells were grouped as untreated (Control); CP direct treatment (dir-CP); Conditioned medium from CP treated (sup-CP), and untreated cells (sup-Control). Effects of dir-CP and sup-CP were compared to corresponding untreated cells on cytotoxicity, cell migration, and protein expression (cleaved caspase-3, caspase-9, and MMP-2 and 9). CP treatment showed time-dependent decrease in cell number of MDA-MB-231 and SK-Br-3 (both ER(-) PR(-)), while the decrease in cell number was not as significant in MCF-7 and ZR-75-1 cells (both ER(+) PR(+)). sup-CP treatment inhibited the cell migration of MDA-MB-231 and MCF-7 (Her2(-)) in a 24 h scratch assay. Our data suggested that ER(-) PR(-) cells are more sensitive to the CP in terms of direct cytotoxicity, which is not regulated by caspase-3. CP inhibited the migration of the two Her2(-) cells, and this correlated with MMP-2 regulation. The migration of ER(-) PR(-) cells was more sensitive to conditioned medium with CP treatment than to direct CP, and this is not regulated by MMP-2. Our data suggested that CP has anticancer potential on various breast cancer cells through different mechanisms and is specifically effective in inhibiting the migration of the triple negative MDA-MB-231. Our data provide insight into the mechanism of CP against breast cancer progression and would benefit the medical practitioners in better management with CP usage.

1. Introduction

Cynanchum paniculatum (Bge.) Kitag. (CP) (also known as dog strangling vine, radix cynanchi paniculata, Shu Changching in Chinese, SCC) belongs to the genus of *Cynanchum*, a genus of about 300 species including some swallow-worts, and the family Apocynaceae. They have slender and rigid stems which can grow about 1 meter and the roots are densely fibrous. The root and stem were traditionally used in Chinese medicine for symptoms including pain, arthritis, itching, swelling, and blood smoothing [1]. The 992 C.E. classical Chinese medicine book “Taiping Shenghui Fang” (the Taiping Holy Prescriptions for Universal Relief) described the usage of Shu Changching (i.e.,

Cynanchum paniculatum (Bge.) Kitag.) for curing heart ache and malicious ulcer, which indicated breast cancer. In modern Chinese medicine practice, it was used in conjunction with other medicinal plants for cancer [2, 3]. However, the mechanism of the action exerted in the treatment of cancer or other ailments by this plant extract is still under exploration [4, 5].

Breast cancer comprises the second largest population of cancer patients worldwide and is one of the important causes of death among women. The standard treatments for breast cancer have evolved from surgery, chemo/radiotherapy to antibody-based targeted therapy, due to the progress in cancer genomics. For example, among the early occurring population, patients with Her (+) overexpressing cells had

benefited from the target drug Herceptin [6]. Her2(+) breast cancer cells are highly metastatic in nature and Herceptin is a recombinant monoclonal antibody that is targeted towards growth factor receptors (HER) in Her2(+) metastatic breast cancer cells. On the other hand, patients with breast cancer that are triple negative (ER(-) PR(-) Her-2(-)) constitute about 15–20% of the breast cancer population lack Her2 gene and the specific disease metastasis with high recurrence rate challenges the medical experts in the management of the disease drug cannot be used for treatment [7]. These patients are generally younger and show a faster progression of the tumor which makes it very difficult to treat them [8]. For these patients, although other types of molecular target drug such as antiangiogenesis or immune therapy drug targeting the T cell checkpoint provide satisfactory results, the need for new chemical compounds that could act on this specific type of cancer still remains unattended [8, 9]. We intended to test whether CP extract could inhibit the proliferation of MDA-MB-231 cells (along with other breast cancer cells with different genetic variants) and also deduce the mechanism of cytotoxicity.

Several compounds were isolated from CP [2, 3, 10, 11] and two of them include paeonol [12, 13] and vanillic acid, which were among the components of the phenolic extract of food/medicine that tested positive for cancer cytotoxicity [14–16]. In this paper, we explore the action of water extract of CP on 4 different types of genomic compositions of breast cancer cells (for details, see Materials and Methods). The study intended mainly to explore and compare the mechanisms by which CP exhibit its antiproliferative and anti-metastatic potential on different breast cancer cells that vary by their genomic profile. Chemoresistance of cancer to molecular targeted therapy due to repeated administration is an important hurdle to overcome for oncologists and researchers by the exploration of new drugs. In this paper, we study the direct effect of CP and its conditioned medium on four different mutant types of breast cancer cells, wishing to pinpoint the molecular mechanism that could be affected.

2. Materials and Methods

2.1. Breast Cancer Cells and Their Genomic Composition. The human breast cancer cell lines MDA-MB-231, MCF-7, and ZR-75-1 were obtained from the BCRC (Bioresource Collection and Research Center, Hsinchu, Taiwan), whereas SK-Br-3 were obtained from the American Type Culture Collection (Manassas, VA). Their phenotypes for estrogen receptor (ER), progesterone receptor (PR), and human epidermal growth factor receptor 2 (Her2) are listed in Table 1.

2.2. Collection of CP Plant Material and Water Extraction. A voucher specimen of *Cynanchum paniculatum* was deposited in the Department of Applied Chemistry, Chaoyang University of Technology, and given a code “CY0001”, as advised by the Herbarium of National Research Institute of Chinese Medicine, Ministry of Health and Welfare (MOHW), Taiwan. Dry Xu Changqing (100 g) was extracted

TABLE 1: Breast cancer cell lines with different genomic variations used in this study.

Breast cancer cell lines	ER	PR	HER
MDA-MB-231	–	–	–
SK-Br-3	–	–	+
MCF-7	+	+	–
ZR-75-1	+	+	+

with 300 mL water, at 100°C for 1 hr, at 1 atm. They were extracted twice and pooled and then dried with a freeze dryer. The weight of the dry paste was 20% of the starting material.

2.3. Culture of Cells. The MDA-MB-231 cells were cultured in Leibovitz’s L-15 Medium (Gibco Life Technologies, NY, Grand Island), supplemented with 10% fetal bovine serum, in free gas exchange with atmospheric air. The MCF-7 cells were cultured in Eagle’s Minimum Essential Medium (Gibco Life Technologies, NY, Grand Island) supplemented with 0.1 mM nonessential amino acids, 1.0 mM sodium pyruvate, and 10% fetal bovine serum. The SK-Br-3 cells were cultured in McCoy’s 5a Medium Modified (Sigma-Aldrich, St Louis, MO), supplemented with 10% fetal bovine serum. The ZR-75-1 cells were cultured in RPMI-1640 Medium (Gibco Life Technologies, NY, Grand Island) supplemented with 4.5 g/L glucose, 10 mM HEPES, 1.0 mM sodium pyruvate, and 10% fetal bovine serum. The 184A1 cells were cultured in serum-free mammary epithelial basal medium (MEBM) supplemented with Bovine Pituitary Extract (BPE) 52 ug/ml, hEGF 10 ng/ml, Insulin 5 ug/ml, hydrocortisone 0.5 ug/ml, transferrin 10 ug/ml, using SingleQuot reagent packs from Lonza. Except for MDA-MB-231, the cells were cultured in a water-saturated atmosphere of 5% CO₂ and 95% atmospheric air at 37°C.

2.4. Crude Extract Treatment. The cells were plated at the density of 10⁴ cells in 96 wells for cytotoxicity or plated at the density of 7 × 10⁴ cells in 24 wells using culture inserts (Idibi, Martinsried, Germany) specially made for the scratch assay. The cells were plated in the respective medium with 10% serum until almost confluent. They were washed with PBS and changed to 5% exosome-free FBS in their respective medium for 24 hours. Then the cells were supplemented with medium without FBS and the various concentrations of CP extract for 24 hours before carrying out the cytotoxicity test using CCK8 kit or removing the culture insert. This treatment was referred to as direct-CP and different from those treated with conditioned medium (or sup-CP) which will be discussed in detail below.

2.5. Collection of Conditioned Medium and Treatment to the Naïve Cells. To test whether the certain effect was regulated by the secreted factors in the conditioned medium by an autocrine mechanism, some cells were treated with the CP extract as above described, and the 24-hour conditioned medium was collected, to treat naïve cells of the same cell

types. The naïve cells were plated and treated like those for the direct CP extract treatment, but the CP extract was replaced by the conditioned medium (see Figure 1). A conditioned medium without CP extract treatment was collected as a conditioned medium control (or sup-Control).

2.6. Proliferation/Cytotoxicity Assay. The cells were plated at the density of 10^4 cells in 96 wells until confluent and changed to CP extract containing serum-free medium for 24 hours before testing with a WST based proliferation/cytotoxicity assay using the CCK8 kit (cat no B34304, Bimake, Houston, USA). Four groups were tested, which include (1) the one treated directly with the CP extract (dir-CP), (2) cells treated with conditioned medium collected from the 24 hour CP extract treated cells (CP-sup), (3) cells treated with conditioned medium collected from the 24-hour incubation without CP extract (sup-Control), and (4) cells without any treatment (control).

2.7. Scratch Assay and Analyses of Cell Migration. The cells were plated at the density of 7×10^4 cells in 24 wells using culture inserts (Ibidi, Martinsried, Germany) until confluent in respective medium supplemented with 10% FBS and changed to CP extract added in 5% exosome-free FBS medium while the insert was removed. The gap left after removing the insert, which resembled the scratch, was photographed at 24 hours, 48 hours, 72 hours, and 5 days after the removal of insert treatment. The four treatment groups were the same as those for the cytotoxicity assay. The cell migration was calculated as follows.

A photograph was captured by the CCD camera and the border of the scratch was determined from the time zero photograph. Lines were drawn by connecting the location of the cells and the right or left border (whichever is nearer). The distance of migration was estimated by measuring the length of this line in the ImageJ software (NIH freeware). The average distance of all cells in the fields was calculated and compared among groups.

2.8. Western Blots. The cells were trypsinized and the cell pellet was collected. The cells were then lysed in RIPA buffer (cat no AI0011, Able-Bio) containing a protease inhibitor mix, and the supernatant was collected. The culture medium was collected and passed through 3 kDa flow-through column (cat no UFC900396, Millipore, Bedford, MA) to desalt and concentrate the protein. They were mixed with loading buffer to make final concentration of $2.5 \mu\text{g}/\mu\text{l} \sim 5 \mu\text{g}/\mu\text{l}$. Before immunoblotting, the cell lysate was boiled in a loading buffer with β -mercaptoethanol for 5 min. The cell lysates were separated on a 10%–12% SDS-PAGE and transferred to a polyvinyl difluoride (PVDF) membrane. The PVDF membranes were incubated in 0.1% milk in PBST (phosphate-buffered saline with 0.1% Tween-20) for 1 h to rid them of background staining, followed by overnight incubation in the primary antibodies at 4°C . Primary antibodies used were anti-MMP-9 (cat. nos. 3852; Cell Signaling Technology, Inc.), anti-MMP-2 (cat. no

13132; Cell Signaling Technology, Inc.), anticaspase-9 (cat. no 9502; Cell Signaling Technology, Inc.), anticlaved caspase-3 (cat. no 9661; Cell Signaling Technology, Inc.), and antiactin (cat. no. 4970; Cell Signaling Technology, Inc.). The secondary antibody used was anti-rabbit IgG conjugated with horseradish peroxidase (HRP) (Amersham) for all the proteins. After washing, blotted proteins were visualized using a Western blotting detection system (ECL Plus, Amersham, UK) and proteins bands were detected using Western Lightning™ Chemiluminescence Reagent Plus (Amersham Biosciences, Arlington Heights, IL, USA). Actin was stained and used as a normalization standard. After this normalization, each lane within the same blot was normalized against the control and the statistics were performed using this ratio.

2.9. Statistical Analyses. All the results obtained were analyzed with appropriate statistical tools. All the datasets were tested for normality using the Shapiro–Wilk test. One-way ANOVA was performed using Kruskal–Wallis test followed by post hoc pairwise comparison (Dunn’s test) for Figures 2–4. In case of Figure 5, one-way ANOVA using Welch F-test was used followed by post hoc pairwise comparison (Tukey’s method). Figure 6 was not analysed by statistical analysis and Figure 7 was also analysed by one-way ANOVA using Welch F-test which was used followed by post hoc pairwise comparison (Tukey’s method).

3. Results

3.1. LC_{50} of the Crude Extract to the 4 Cancer Cell Lines. We tested the LC_{50} for each cell line with a crude concentration range from 10 mg/ml to 0.01 mg/ml over 10 dilutions and plotted the survival rates over the concentrations. Linear regression was done using the 3–5 data points surrounding the 50 percent survival rates, and the LC_{50} was calculated by interpolation of the linear equation. The LC_{50} for the 4 cell lines is listed in Table 2.

LC_{50} values of CP on all the cell types fall between 2.5 and 5 mg/ml and survival rates of the cells treated with 2.5 mg/ml and 5 mg/ml of CP were compared and illustrated in Figure 2. When the cells were treated with 2.5 mg/ml, which is lower than all their LC_{50} , the cells demonstrated 40–80% survival rates depending on their susceptibility. When they were treated with 5 mg/ml, which is higher than the LC_{50} of all the cells, MCF-7 and ZR-75-1 cells (both ER(+) PR(+)), demonstrated about 40–50% survival, while MDA-MB-231 and SK-Br-3 (both ER(–) PR(–)), demonstrated only about 10% survival.

3.2. Time Course of Cell Survival after Treatment of CP. To test a longer cell survival, the effect of crude extract of CP on the cells was tested for a period of 3 days. The cells were treated with the LC_{50} concentration of the crude extract in a serum-free medium (see Materials and Methods) and were tested with WST based proliferation/cytotoxicity assay (CCK8) at 24, 48, and 72 hours after

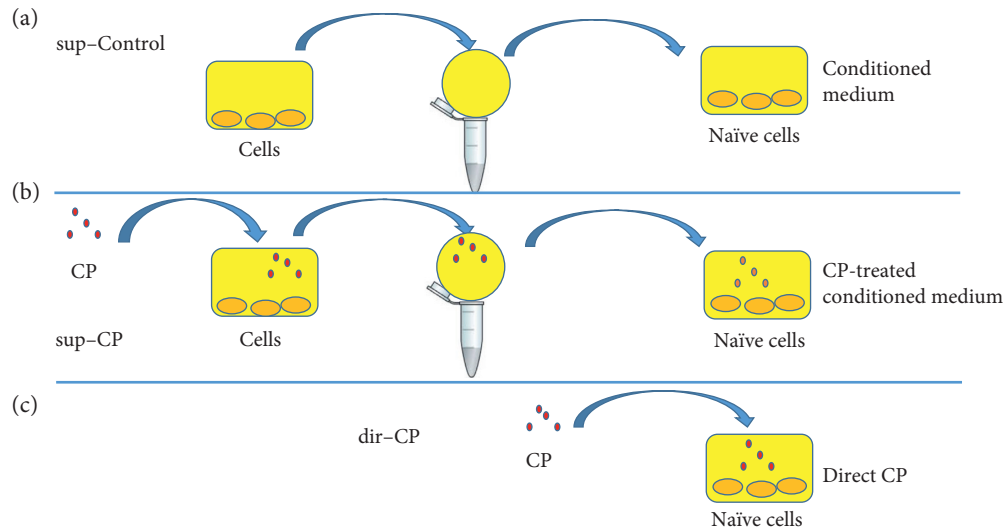


FIGURE 1: Schematic diagram for preparation of CP conditioned medium and treatment of CP extract and CP conditioned medium to the cells. (a) Conditioned medium without CP extract treatment was collected as a conditioned medium control (sup-Control); (b) Some cells were treated with the CP extract and the 24-hour conditioned medium was collected and the conditioned medium was used to treat naïve cells of the same cell types (sup-CP); (c) for the crude extract treatment (dir-CP), the naïve cells were treated directly with CP. The naïve cells were plated in the respective medium with 10% serum until almost confluent, washed with PBS, and changed to 5% exosome free FBS for 24 hours, and changed to medium without FBS and CP for 24 hours.

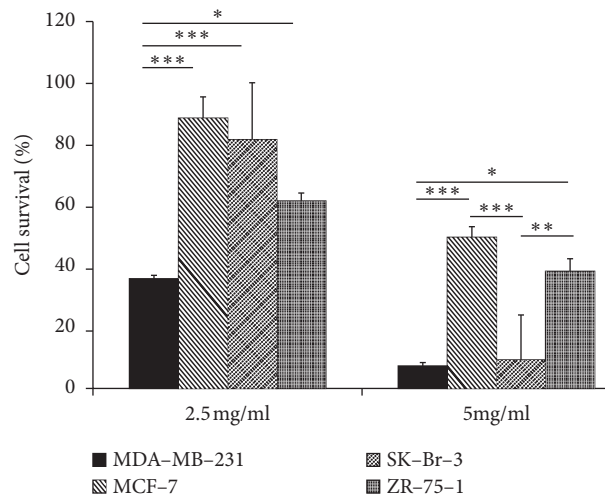


FIGURE 2: Cytotoxicity of CP extract on different cell types of breast cancer. The results were expressed as % survival of cells and were statistically analyzed by post hoc pairwise comparisons following the Kruskal-Wallis test: Dunn's method. The experiments were performed independently in replicated assays ($N=4$) and comparisons were made between the cells. ***- $p < 0.001$; *- $p < 0.05$.

initial treatment. The viable cell numbers were plotted against the cell number at time zero before drug treatment (Figure 3). The cell number of the treated cells showed time dependent decrease in MDA-MB-231 cells and SK-Br-3 cells (both ER PR negative), while in the case of MCF-7 cells, the decrease in cell number was observed up to 24 hours and then they replenished with increase in cell numbers by 48-72 hours.

3.3. Cytotoxicity: Comparison of CP-Treated Conditioned Medium to Direct CP Treatment.

The breast cancer cells were

known to alter the environment of their distant niche by extracellular secretions containing nucleic acid or protein to promote their survival or metastasis. To test whether treatment by CP to the cells would alter the biomolecular content of the medium to influence cytotoxicity, the CP treated conditioned medium (sup-CP) was collected and supplemented to the naïve cells. These were compared to the effect of direct treatment (dir-CP) on the naïve cells and the effect of 24-hour conditioned medium (sup-Control). We used a similar concentration of CP to be able to compare the cytotoxicity among cells. The MCF-7 cells, because of their higher LC_{50} , did not yield significant cytotoxicity when CP

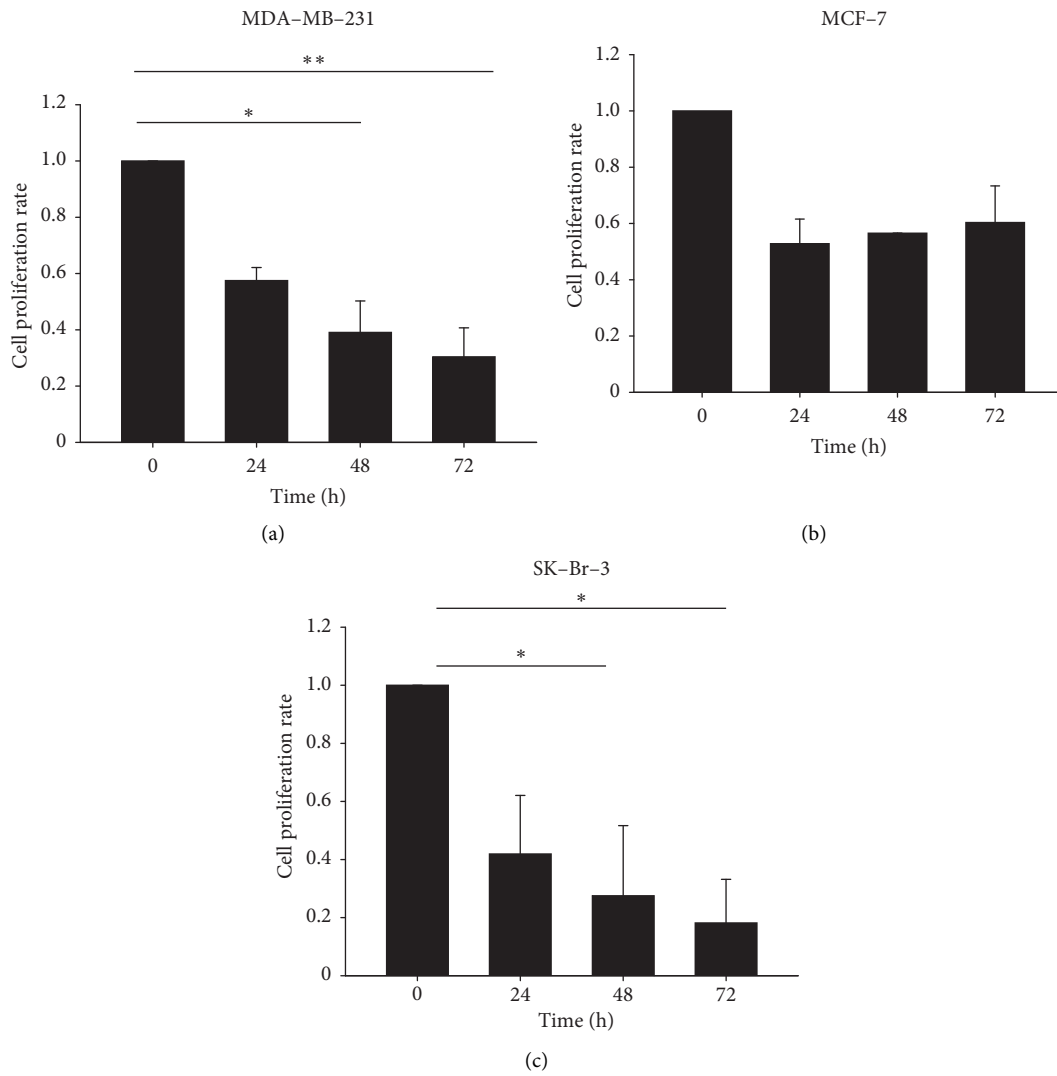


FIGURE 3: Time dependent cytotoxicity of CP extract on different cell types of breast cancer. The LC_{50} of CP extract on different cell types were determined and used for time dependent assay. The concentrations of CP treated are MDA-MB-231: 2.7 mg/ml, MCF-7: 3.1 mg/ml, and SK-Br-3: 3.05 mg/ml. Cytotoxicity was tested using the CCK8 kit after treatment of CP for 24, 48, and 72 hours. The results were statistically analyzed by nonparametric Kruskal-Wallis test for ANOVA and Dunn's post hoc pairwise comparison method. **- $p < 0.01$; *- $p < 0.05$.

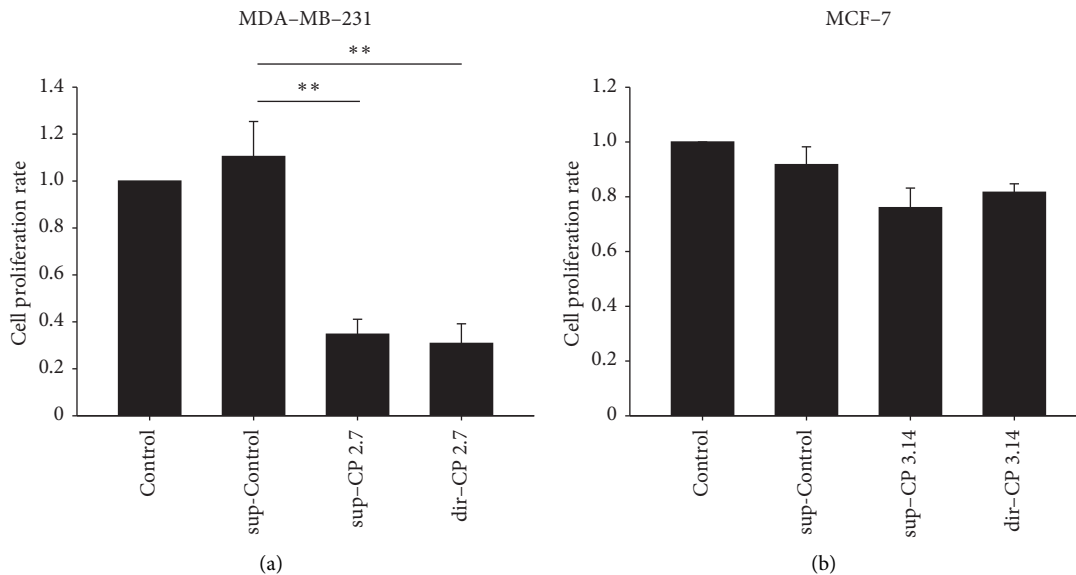


FIGURE 4: Continued.

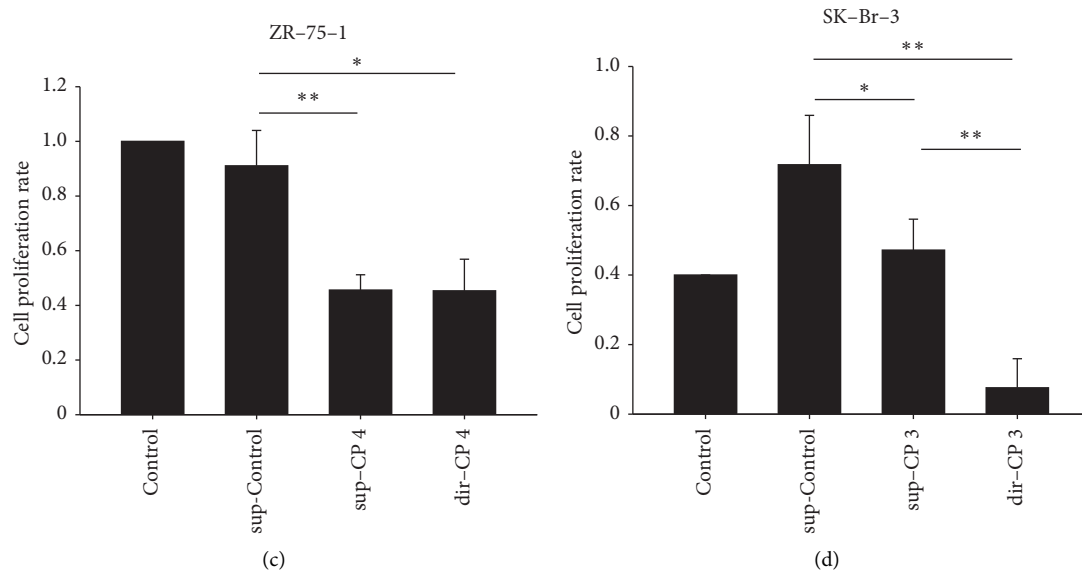


FIGURE 4: Cytotoxicity of sup-Control and sup-CP on naïve breast cancer cells. sup-Control and sup-CP preparation were prepared as explained in Figure 1. The results were statistically analyzed by post hoc pairwise comparisons following Kruskal-Wallis test. The experiments were performed independently in replicated assays ($N=4$). ***- $p < 0.001$, **- $p < 0.01$, and *- $p < 0.05$.

was added about 3 mg/ml. For MDA-MB-231 cells and ZR-75-1 cells, the sup-CP treatment does not result in significant cytotoxicity compared to direct CP treatment. For SK-Br-3, direct treatment yielded a much better effect than the CP treated conditioned medium (Figure 4).

3.4. The CP Crude Extract as Well as the CP-Treated Conditioned Medium Inhibited the Migration of MDA-MB-231 Cell and MCF-7 Cells in Scratch Assay. The effect of CP treatment on cell migration was tested using the scratch assay. The treatments were similar to the cytotoxicity study. The CP direct treatment (dir-CP), as well as the CP conditioned medium treatment (sup-CP), inhibited the cell migration of two Her2(-) cells lines, MDA-MB-231 and MCF-7, in a 24 hr scratch assay. When treated with 3 mg/ml crude extract, the MDA-MB-231 showed a significant reduction in the cells within the scratched area, demonstrating an inhibition to the cell migration (see Figure 5, dir-CP, and also Figure 6). In the case of MCF-7 cells, the direct CP treatment resulted in reduced cell migration even though it did not render significant cytotoxicity at 3 mg/ml. Therefore, the CP treatment in MCF-7 inhibits migration without enhancing significant cytotoxicity.

The CP extract and sup-CP both inhibited the migration of MCF-7 after 5 days of treatment, while the cells in untreated control or sup-Control had covered up the scratch area with significant migration. For MDA-MB-231, the inhibition was insignificant in the sup-CP treatment after 5 days (Figure 6).

3.5. CP-Treated Conditioned Medium (sup-CP) Inhibited the Migration Better than the Direct CP Crude Extract (dir-CP) in MDA-MB-231 cell and SK-Br-3 Cells in Scratch Assay.

According to Figures 6(a) and 6(b), in MDA-MB-231 cells, although some of the effects might be caused by the cytotoxicity of the crude extract, as 3 mg/ml was about the concentration of the LC_{50} for these cells, it is interesting that the CP treated conditioned medium (sup-CP) further inhibited the migration than direct treatment (dir-CP). In the case of SK-Br-3 cells, similar to MDA-MB-231 cells, the inhibitory effect of CP-treated conditioned medium on the migration of SK-Br-3 cells is significantly better than the direct CP treatment group (see Figure 6(b), SK-Br-3). A similar dose results in equal or even worse cytotoxicity in the direct CP treatment group. Therefore this discrepancy was not a result of cytotoxicity.

3.6. The MMPs and Caspase Expressions: Western Blots. To test the signaling pathways that were responsible for the cytotoxicity and cell migration, the proteins extracted from the naïve cells after treatment with direct CP, or CP-conditioned medium, were tested with Western blot using antibodies against caspase-9, cleaved caspase-3 (proteins involved in the apoptotic pathway), MMP-2, and MMP-9, (proteins responsible for cell migration).

For MDA-MB-231 cells, the expression level of MMP-9 protein was not regulated, while those of MMP-2 were regulated upon CP treatments. Both direct treatment (dir-CP) and CP conditioned medium (sup-CP) yield significantly reduced MMP-2 protein expression when compared to the sup-Control (see Figure 7, MDA-MB-231). However, there was no significant difference between the dir-CP and the sup-CP groups. The cleaved caspase-3, the active form, was also downregulated for the two groups when compared to the control group.

MCF-7 cells showed reduced MMP-2 expression in the sup-CP group. However, as both the dir-CP and sup-CP

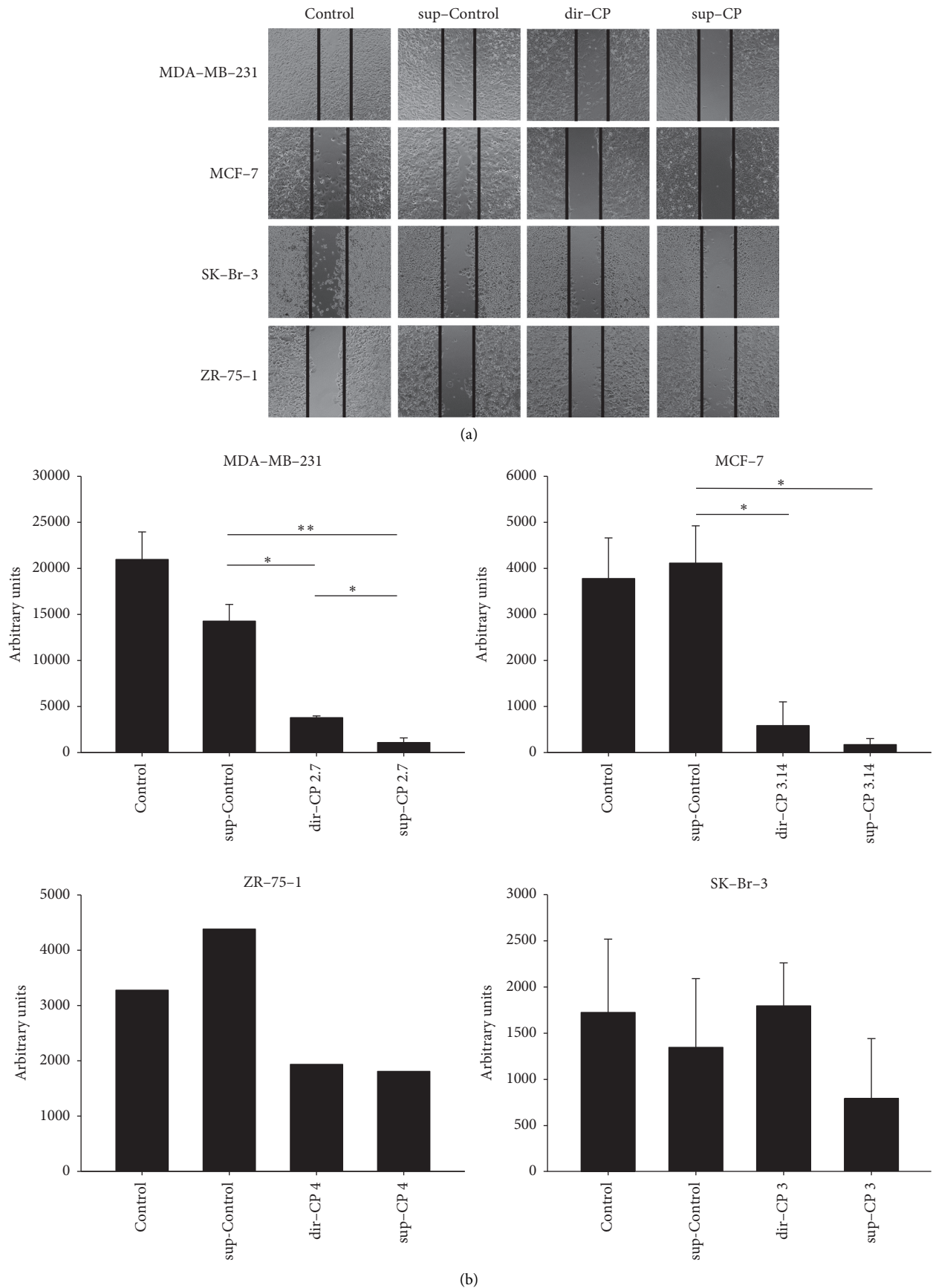


FIGURE 5: Scratch assay to study the migration of different types of cells treated with sup-Control; sup-CP & CP (dir-CP). The results were statistically analyzed by post hoc pairwise comparisons following Kruskal-Wallis test: Dunn's method and comparison was made as untreated vs. treated samples. The experiments were performed independently in replicated assays (N=4). **- $p < 0.01$; *- $p < 0.05$.

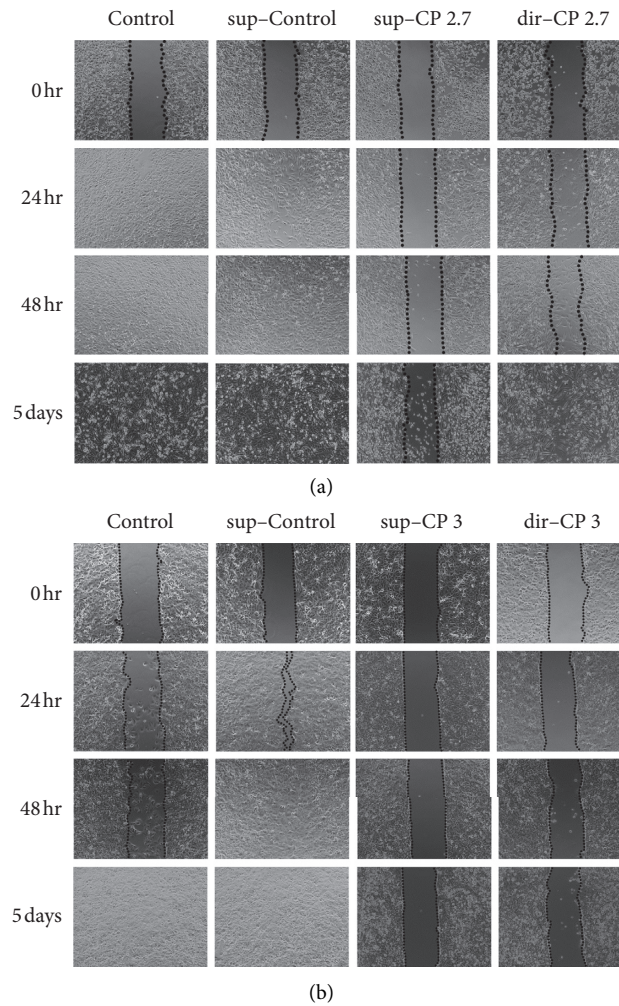


FIGURE 6: Scratch assay to study the time dependent migration of different types of cells treated with sup-Control; sup-CP, and CP (dir-CP). (a) is for MDA-MB-231 cells treated with 2.7 mg/ml of CP, and (b) is for MCF-7 cells treated with 3.14 mg/ml CP. The photos were taken at the beginning of various CP treatments (0, 24, and 48 hours and 5 days after treatment).

TABLE 2: LC_{50} values of the CP extract on different breast cancer cell lines.

Breast cancer cell lines	LC_{50} (mg/ml)
MDA-MB-231	2.68
MCF-7	5.6
SK-Br-3	3.05
ZR-75-1	3.99
184A1 (control)	6.94

inhibited the migration (see Figure 5, MCF-7), the anti-migration effect may not be solely contributed by the MMP-2 modulation. MMP-9 levels remained unregulated, so was the cleaved caspase-3 protein. Expression of cleaved caspase-3 was reduced when treated with dir-CP in comparison to its respective control (t -test, $p = 0.11$) but was not significant. In the case of SK-BR-3 cells, all the protein levels tested were not significantly altered (see Figure 5, SK-BR-3). Levels of cleaved caspase-3 showed a mild increase in the dir-CP treatment when compared to the treatment with CP conditioned medium (t -test, $p = 0.20$).

3.7. Sensitivity of ER(-) PR(-) Cells to CP Is Not Correlated to Caspase-3. When the CP treated cells were collected and examined, the levels of the caspase-9 and cleaved caspase-3 were not regulated except for the MDA-MB-231 cells (Figure 7). Usually, cells undergoing apoptosis show up-regulated expression of activated caspase-3 and in our study, MDA-MB-231 cells show a reduced expression of this protein. Hence, we could infer that CP mediated cellular damage was not caspase-3 dependent and further tests on other signaling pathways such as Sphingosine-1-phosphate [17] or Poly(ADP-ribose) polymerase (PARP) [12] might

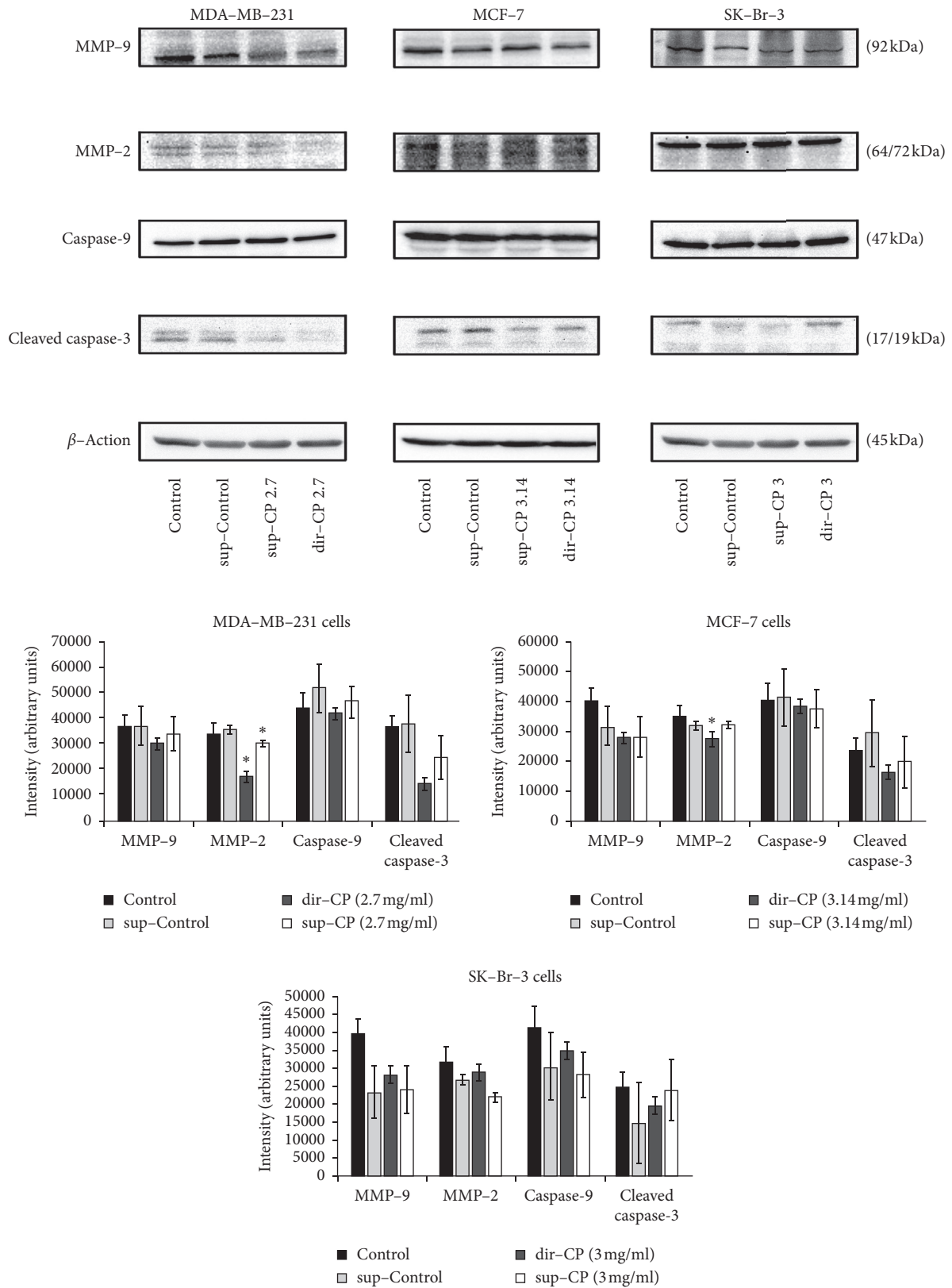


FIGURE 7: Immunoblotting studies of MMP-9, MMP-2, caspase-9, and cleaved caspase-3. Protein bands of different cell types of breast cancer treated with sup-Control, sup-CP, and dir-CP. The intensity of the bands was measured using ImageJ software. The results were statistically analyzed using post hoc pairwise comparisons for equal variance, i.e., Tukey's method, and the comparison was made as untreated vs. treated samples. The experiments were performed independently in replicated assays ($N = 4$). * $-p < 0.05$.

shed light on the molecules that regulate the cytotoxicity in these ER(-) PR(-) cells (MDA-MB-231 cells).

4. Discussion

Breast cancers can be subtyped according to their genotypic variations and metastasis characteristics. The ability of the drug against various types of breast cancer cells differs significantly due to alteration in the metabolic outcome of genotypic characteristics [18, 19]. In this paper, we used 4 different cell lines with varying genotypes to demonstrate a correlation among them with respect to sensitivity towards treatment with CP extract. The following experiments and observations were attempts to correlate the cytotoxicity, migration behavior, and signaling molecules to the genomic composition and responsible signaling molecules. After this, we further made an array of genotypes versus phenotypes to find out their correlation.

Cytotoxicity studies clearly showed that ER(-) PR(-) cells are more sensitive to the CP treatment in terms of direct cytotoxicity. The LC_{50} of these cells are in the increasing order MDA-MB-231 < SK-Br-3 < ZR-75-1 < MCF-7 < 184A1 (Table 2). If we use the criteria of whether this cell line could be killed significantly to about 20% of untreated cells, the two ER(-) PR(-) cells were sensitive while the double positive cells are resistant to CP treatment (summarized in Table 3). This is the same with other criteria, where cytotoxicity of CP extract after 24–72 hrs was tested (see Figure 3, summarized in Table 2). This demonstrated that the cytotoxicity of CP extract on the breast cancer cell lines is gene type dependent, and ER & PR phenotypes are correlated with the CP cytotoxicity.

Our comparative analysis on inhibition of migration revealed a correlation between Her2(-) phenotypes and partly regulated by MMP-2 level via autocrine fashion. CP crude extract, when administered directly or in a conditioned medium, inhibited the migration of MDA-MB-231 cells and MCF-7 cells (both Her(-)) (summarized in Table 4). SK-Br-3 supplemented with sup-CP did not show significant inhibition of migration compared to its corresponding control (Figure 5). But inhibition was significantly more when compared to dir-CP (Figure 5). Therefore, this inhibition of migration seemed to be correlated to the Her(-) phenotype. Further, the MMP-2 levels were downregulated in MDA-MB-231 cells and MCF-7 cells for the respective treatments. Though migration of Her(-) cells was inhibited by both dir-CP and sup-CP, the corresponding reduction in MMP-2 expression was not observed in dir CP, but MMP-2 expression was reduced in sup-CP treated cells. This clarifies that factors that regulate MMP-2 reduction was present only in CP treated conditioned medium which contains extracellular vesicles/exosomes (Comparison was illustrated in Table 4).

Cynanchum paniculatum is a significant part of traditional Chinese medicine where different parts of the plant were utilized to treat a number of ailments. Biological properties rendered by CP were through the bioactive polyphenolic compounds constituted in different plant parts of CP. According to Weon et al., Paeonol is the major constituent present in the 80% methanol extract of roots of

Cynanchum paniculatum Kitagawa (Asclepiadaceae), [10]. Paeonol is a major phenolic component of Moutan cortex Radicis, a traditional Chinese Medicine. It induces breast cancer cell apoptosis through the regulation of Bcl-2/Bax/caspase 3 signaling, or the CXCR3-B/CXCL4 signals [20, 21]. Paeonol synergizes with Epirubicin on the reduction of breast cancer cells growth via inhibiting PARP, Bax, caspase-3 and also by inhibition of p38/JNK/ERK MAPKs [22]. It was also reported that it could reverse paclitaxel resistance by upregulating the expressions of the adenosine-triphosphate binding cassette transporter proteins [23]. Therefore, it is reasonable to infer that the observed cytotoxicity effect of CP must be mediated through this compound. However, our data did not demonstrate downregulated caspase-3 expression, which suggests that multiple compounds might be responsible within the CP extract, and the compound in our extract responsible for the observed activities may not necessarily be Paeonol.

Until now, more than 440 compounds have been isolated and identified from plants that were classified under genus *Cynanchum*. These include C21 steroids, steroidal saponins, benzenes and derivatives, alkaloids, flavonoids, terpene, and so on [5]. The chemical composition of CP was previously extracted and single compounds were successfully isolated [2, 3, 11, 24, 25]. Among these compounds cynatratoside B exhibited potent inhibitory activities against HL-60, HT-29, PC-3, and MCF-7 cell lines and cynapanoside D-G displayed moderate cytotoxicity against the four cell lines [11].

Our results demonstrate the ER(-) PR(-) cells are highly sensitive towards CP extract, and comparatively less sensitivity was shown by MCF-7 & ZR-75-1 which expresses estrogen and progesterone receptors (ER & PR). These two receptors and their metabolic role towards cancer development are reported extensively that they play a key role in breast cancer development and their expression was high in the breast cancer cells than the normal human breast cells [26]. ER was well established for its oncogenic property through activation of MAPK pathway resulting in the upregulation of various growth factor receptors that can progress the cancer development. This information about the ER supports the LC_{50} value which is higher for the ER(+) PR(+) cells (MCF-7 & ZR-75-1). The estrogen receptors play a significant role in cancer survival and progression through PI3K/AKT/mTOR pathway [27]. This leads to the focus on the inhibition of these pathways to counter the growth of ER(+) breast cancer cells. Similar to ER, PR also plays a significant role in cancer progression through rapid activation c-Src and ERK2 in breast cancer cells leading to MAPK pathway mediated cancer cell growth. Hence, it was postulated that therapeutic strategies against ER(+) PR(+) breast cancer cells are targeted towards the downregulation of the MAPK/PI3K pathway [28]. The observations clearly depicted the cytotoxicity of CP on ER(-) PR(-) cells (MDA-MB-231) which shows that the molecular target for CP was apparently not similar to the mechanism in ER(+) PR(+) cells. Also, it can be assumed that whichever molecular mechanism the CP targets, the absence of estrogen and progesterone receptors and their downstream signaling is a prerequisite.

TABLE 3: Differential sensitivity to cytotoxicity is correlated to genomic characteristics.

Breast cancer cell lines	ER	PR	HER	5 mg/ml; 24 hr cytotoxicity less than 20%	3 mg/ml; 72 hr cytotoxicity less than 30%
MDA-MB-231	-	-	-	Y	Y
SK-Br-3	-	-	+	Y	Y
MCF-7	+	+	-	N	N
ZR-75-1	+	+	+	N	NA

The different genomic characteristics were listed in an array and compared to two traits (shown in the last two columns). The first result column demonstrated that when the cells were treated with 5mg/ml CP extract, MCF-7 and ZR-75-1 (both ER(+)-PR(+)) demonstrated about 40-50% survival, hence the N (no) for this phenotype, while MDA-MB-231 and SK-Br-3 (both ER(-)-PR(-)), demonstrated about 10% survival, hence the Y (yes). The second result column summarizes the results whether this cell line could be killed significantly to be less than 30% of control group with 3 mg/ml CP after 72 hours of incubation. The two ER(-)-PR(-) cells were sensitive (hence the Y result) while the two ER(+)-PR(+) cells are not. For details of the results, please see Figure 2 and respective text.

TABLE 4: Differential sensitivity to migration is correlated to genomic characteristics.

Breast cancer cell lines	ER	PR	HER	Direct CP inhibit migration	Direct CP reduced MMP-2 expression	Sup-CP inhibit migration	Sup-CP reduced MMP-2
MDA-MB-231	-	-	-	Y	Y	Y	Y
SK-Br-3	-	-	+	N	N	N	N
MCF-7	+	+	-	Y	N	Y	Y
ZR-75-1	+	+	+	N	N	N	N

The different genomic characteristics were listed in an array and compared to two traits (shown in the right four columns). The first result column demonstrated that when the cells were treated with similar CP extract, MDA-MB-231 and MCF-7 (both HER(-)), the migration of cells were inhibited, hence the Y (yes) for this phenotype, while SK-Br-3 and ZR-75-1 (both HER(+)) were not inhibited, hence the N (no). The second result column summarizes the results demonstrated that when the cells were treated with similar CP extract, only MDA-MB-231 cells demonstrated reduced MMP-2 level. There is no association to the genotypes. The third column demonstrated that when the cells were treated with similar CP extract, MDA-MB-231 and MCF-7 (both HER(-)), the migration of cells were inhibited by treatment of CP-treated conditioned medium, while SK-Br-3 and ZR-75-1 (both HER(+)) were not. The fourth column demonstrated that when the cells were treated with CP-treated conditioned medium, MDA-MB-231 and MCF-7 (both HER(-)), the MMP-2 levels were inhibited, while SK-Br-3 and ZR-75-1 (both HER(+)) were not. For details of the results, please see Figures 5-7 and respective text.

Though we found that MCF-7 cells were able to overcome the cytotoxic potential of CP extract, the cell migration property of this cell type was significantly reduced by sup-CP treatment and we could infer that the lack of growth factor receptor gene (Her2(-)) is one of the major reasons, because the ability of MDA-MB-231 cells (also Her2(-)) to migrate was reduced by sup-CP treatment. Her2 upregulation has shown to be linked to higher mortality, recurrence, and high metastatic potential of many cancer cells, including breast cancers. This was achieved by upregulation of an array of pathways which includes PI3K/Akt, Ras/MEK/ERK, and JAK/STAT pathways [29]. Surprisingly, the activity of sup-CP was significantly high compared dir-CP against migration of MDA-MB-231 cells. The fact that altered molecular profile of the conditioned medium, especially the exosome content, due to CP treatment might have shown the primal effect than polyphenols present in the CP extract. Corresponding results were obtained with western blotting analyses where the expression of MMP-2 in Her2(-) cells (MCF-7 & MDA-MB-231) was significantly reduced. The downregulation was observed in both dir-CP & sup-CP treatment in case of MDA-MB-231 cells and only sup-CP treatment had the effect on MCF-7 cells. This shows the role of extracellular vesicles, especially exosomes, on inhibition of cells migration through regulation of MMP-2 mediated mechanism on both the Her2(-) cells. Ramirez-Ricardo et al. has reported that circulating extracellular vesicles have significantly upregulated the cell migration through MMP-2 overexpression [30]. MMPs possess endopeptidase activity and degrade the extracellular matrix and in turn, the

basement membrane which during cancer progression is an important process that helps in cell migration, epithelial to mesenchymal transition (EMT), and metastasis [31]. In the case of breast cancer metastasis, MMP-2 & 9 play a pivotal role [32] and our study showed the polyphenolic compounds from CP extract were directly and through modulation of the extracellular profile has influenced the MMP-2 expression in MDA-MB-231 negatively. However, MMP-9 expression in MCF-7 & MDA-MB-231 cells was not downregulated significantly, and we could infer that bioactive compounds in CP extract possess a specific affinity towards MMP-2.

5. Conclusion

In summary, ER(-) PR(-) cells are more sensitive to the CP treatment in terms of direct cytotoxicity, which is not regulated by caspase-3. CP treatment inhibits the migration of Her2(-) cells, and this is correlated partly to MMP-2 regulation via autocrine fashion. This provided an interesting starting point for further study of the signaling pathways that regulate the genotype specific reaction to CP drug treatment. Further, given that the treatment of a triple negative breast cancer phenotype is complicated and challenging, the fact that CP targeted multiple phenotypes of this cell is a very interesting discovery. This illustrates that even the single formulation in Chinese medicine could act on multiple targets to hinder the disease progression.

The CP extract consists a group of single compounds and so it was not surprising that breast cancer cells with different genomic compositions would react very differently upon CP

treatment. They were differentially sensitive in terms of cytotoxicity or inhibition of migration. Therefore, it is possible to report that cells were responsive to different single compounds (individually or synergistically) within the extract rather than concluding that the same compound has altered different signaling pathways in different cells. Our study from the water extract of CP demonstrated its anticancer potential and also linked the activities to be specific to genotypes, which provide further evidence to explore the composition of CP and their specific targets to achieve precision in quality assurance and practice of Chinese medicine.

Data Availability

The Excel data used to support the findings of this study are available from the corresponding author upon request.

Conflicts of Interest

The authors declare that they have no conflicts of interest.

Acknowledgments

The authors are grateful to Dr. Ming-Tung Chen, Chinese Qi Healing Association, for assistance in herbal knowledge. This study was funded by the Ministry of Science and Technology, Taiwan, ROC (MOST) (108-2635-B-324-00), and Taichung Tzu Chi Hospital, Buddhist Tzu Chi Medical Foundation, Taichung, Taiwan ROC (TTCRD106-17).

Supplementary Materials

All details of statistical analysis are included in supplementary file 1. (*Supplementary Materials*)

References

- [1] P. Cheng, *Jhong Hua Dao Di Yao Tsai (The Classic Medicine of China) China Traditional Chinese Medicine*, Publishing House, Peiking, China, 2011.
- [2] C. S. Kim, J. Y. Oh, S. U. Choi, and K. R. Lee, "Chemical constituents from the roots of *Cynanchum paniculatum* and their cytotoxic activity," *Carbohydrate Research*, vol. 381, pp. 1–5, 2013.
- [3] H. L. Yu, Q. Long, W. F. Yi et al., "Two new C21 steroidal glycosides from the roots of *Cynanchum paniculatum*," *Natural Products and Bioprospecting*, vol. 9, no. 3, pp. 209–214, 2019.
- [4] J.-x. Chen, C.-s. Cheng, J. Chen et al., "*Cynanchum paniculatum* and its major active constituents for inflammatory-related diseases: a review of traditional use, multiple pathway modulations, and clinical applications," *Evidence-Based Complementary and Alternative Medicine*, vol. 2020, Article ID 7259686, 16 pages, 2020.
- [5] L. Han, X. Zhou, M. Yang et al., "Ethnobotany, phytochemistry and pharmacological effects of plants in genus *Cynanchum* Linn.(Asclepiadaceae)," *Molecules*, vol. 23, no. 5, p. 1194, 2018.
- [6] R. Nahta and F. J. Esteva, "Herceptin: mechanisms of action and resistance," *Cancer Letter*, vol. 232, no. 2, pp. 123–138, 2006.
- [7] R. Dent, M. Trudeau, K. I. Pritchard et al., "Triple-negative breast cancer: clinical features and patterns of recurrence," *Clinical Cancer Research*, vol. 13, no. 15 Pt 1, pp. 4429–4434, 2007.
- [8] F. S. Cyprian, S. Akhtar, Z. Gatalica, and S. Vranic, "Targeted immunotherapy with a checkpoint inhibitor in combination with chemotherapy: a new clinical paradigm in the treatment of triple-negative breast cancer," *Bosnian Journal of Basic Medical Sciences*, vol. 19, no. 3, p. 227, 2019.
- [9] C. A. Hudis and L. Gianni, "Triple-negative breast cancer: an unmet medical need," *Oncologist*, vol. 16, no. Suppl 1, pp. 1–11, 2011.
- [10] J. B. Weon, C. Y. Kim, H. J. Yang, and C. J. Ma, "Neuroprotective compounds isolated from *Cynanchum paniculatum*," *Archives of Pharmacal Research*, vol. 35, no. 4, pp. 617–621, 2012.
- [11] D. Zhao, B. Feng, S. Chen et al., "C21 steroidal glycosides from the roots of *Cynanchum paniculatum*," *Fitoterapia*, vol. 113, pp. 51–57, 2016.
- [12] Y. Shi, F. Zhou, F. Jiang, H. Lu, J. Wang, and C. Cheng, "PARP inhibitor reduces proliferation and increases apoptosis in breast cancer cells," *Chinese Journal of Cancer Research*, vol. 26, no. 2, p. 142, 2014.
- [13] W. Zhang, J. Cai, S. Chen et al., "Paclitaxel resistance in MCF-7/PTX cells is reversed by paeonol through suppression of the SET/phosphatidylinositol 3-kinase/Akt pathway," *Molecular Medicine Reports*, vol. 12, no. 1, pp. 1506–1514, 2015.
- [14] J. Hilbig, P. de Britto Policarpi, V. M. A. de Souza Grinevicius et al., "Aqueous extract from pecan nut [*Carya illinoensis* (Wangenh) C. Koch] shell show activity against breast cancer cell line MCF-7 and Ehrlich ascites tumor in Balb-C mice," *Journal of Ethnopharmacology*, vol. 211, pp. 256–266, 2018.
- [15] C. Khamphukdee, O. Monthakantirat, Y. Chulikhit et al., "Chemical constituents and antidepressant-like effects in ovarietomized mice of the ethanol extract of *Alternanthera philoxeroides*," *Molecules*, vol. 23, no. 9, p. 2202, 2018.
- [16] E. Spilioti, M. Jaakkola, T. Tolonen et al., "Phenolic acid composition, antiatherogenic and anticancer potential of honeys derived from various regions in Greece," *PLoS One*, vol. 9, no. 4, Article ID e94860, 2014.
- [17] J. Tsuchida, M. Nagahashi, K. Takabe, and T. Wakai, "Clinical impact of sphingosine-1-phosphate in breast cancer," *Mediators of Inflammation*, Article ID 2076239, 2017.
- [18] X. Dai, H. Cheng, Z. Bai, and J. Li, "Breast cancer cell line classification and its relevance with breast tumor subtyping," *Journal of Cancer*, vol. 8, no. 16, p. 3131, 2017.
- [19] B. Mansoori, A. Mohammadi, S. Davudian, S. Shirjang, and B. Baradaran, "The different mechanisms of cancer drug resistance: a brief review," *Advanced Pharmaceutical Bulletin*, vol. 7, no. 3, p. 339, 2017.
- [20] Y. Ou, Q. Li, J. Wang, K. Li, and S. Zhou, "Antitumor and apoptosis induction effects of paeonol on mice bearing EMT6 breast carcinoma," *Biomol Ther (Seoul)*, vol. 22, no. 4, pp. 341–346, 2014.
- [21] R. O. Saahene, J. Wang, M. L. Wang, E. Agbo, and D. Pang, "The antitumor mechanism of paeonol on CXCL4/CXCR3-B signals in breast cancer through induction of tumor cell apoptosis," *Cancer Biother Radiopharm*, vol. 33, no. 6, pp. 233–240, 2018.
- [22] J. Wu, X. Xue, B. Zhang et al., "Enhanced antitumor activity and attenuated cardiotoxicity of Epirubicin combined with Paeonol against breast cancer," *Tumour Biology*, vol. 37, no. 9, pp. 12301–12313, 2016.
- [23] J. Cai, S. Chen, W. Zhang et al., "Paeonol reverses paclitaxel resistance in human breast cancer cells by regulating the

- expression of transgelin 2," *Phytomedicine*, vol. 21, no. 7, pp. 984–991, 2014.
- [24] J. Q. Yu, A. J. Deng, and H. L. Qin, "Nine new steroidal glycosides from the roots of *Cynanchum stauntonii*," *Steroids*, vol. 78, no. 1, pp. 79–90, 2013.
- [25] D. Zhao, H. F. Wang, G. Chen, Y. P. Li, H. M. Hua, and Y. H. Pei, "Two new 13,14:14,15-disecopregnane-type compounds from the roots of *Cynanchum paniculatum*," *Journal of Asian Natural Products Research*, vol. 18, no. 4, pp. 339–343, 2016.
- [26] V. Walter, C. Fischer, T. M. Deutsch et al., "Estrogen, progesterone, and human epidermal growth factor receptor 2 discordance between primary and metastatic breast cancer," *Breast Cancer Research and Treatment*, vol. 183, no. 1, pp. 137–144, 2020.
- [27] A. B. McMartin, M. Palese, and T. R. Tephly, "Formate assay in body fluids: application in methanol poisoning," *Biochemical Medicine*, vol. 13, pp. 117–126, 1975.
- [28] P. Bhateja, M. Cherian, S. Majumder, and B. Ramaswamy, "The Hedgehog signaling pathway: a viable target in breast cancer?" *Cancers*, vol. 11, no. 8, p. 1126, 2019.
- [29] P. Zeng, S. Sun, R. Li, Z.-X. Xiao, and H. Chen, "HER2 upregulates ATF4 to promote cell migration via activation of ZEB1 and downregulation of E-cadherin," *International Journal of Molecular Sciences*, vol. 20, no. 9, p. 2223, 2019.
- [30] J. Ramírez-Ricardo, E. Leal-Orta, E. Martínez-Baeza et al., "Circulating extracellular vesicles from patients with breast cancer enhance migration and invasion via a Src-dependent pathway in MDA-MB-231 breast cancer cells," *Molecular Medicine Reports*, vol. 22, no. 3, pp. 1932–1948, 2020.
- [31] M. K. Jena and J. Janjanam, "Role of extracellular matrix in breast cancer development: a brief update," *F1000Research*, vol. 7, 2018.
- [32] H. Li, Z. Qiu, F. Li, and C. Wang, "The relationship between MMP-2 and MMP-9 expression levels with breast cancer incidence and prognosis," *Oncology Letters*, vol. 14, no. 5, pp. 5865–5870, 2017.

Research Article

The Efficacy of Moxibustion for Breast Cancer Patients with Chemotherapy-Induced Myelosuppression during Adjuvant Chemotherapy: A Randomized Controlled Study

Yajie Ji,^{1,2} Siyu Li,¹ Xinyue Zhang,¹ Qiong Li,¹ Qing Lu,¹ Weili Chen,¹ Yu Liu,¹ Jiayu Sheng,¹ Hongli Liang,¹ Ke Jiang,¹ Mengting Li,¹ Shanyan Sha,¹ Huangan Wu,^{2,3} Yan Huang,^{2,3} and Xiaohong Xue¹ 

¹Department of Breast Surgery, Yueyang Hospital of Integrated Chinese and Western Medicine, Shanghai University of Traditional Chinese Medicine, Shanghai 200437, China

²Shanghai Research Institute of Acupuncture and Meridian, Shanghai University of Traditional Chinese Medicine, Shanghai 200030, China

³Key Laboratory of Acupuncture and Immunological Effects, Shanghai University of Traditional Chinese Medicine, Shanghai 200030, China

Correspondence should be addressed to Xiaohong Xue; 195641459@qq.com

Received 2 August 2020; Revised 5 April 2021; Accepted 15 April 2021; Published 26 April 2021

Academic Editor: Mohd Fadzelly Abu Bakar

Copyright © 2021 Yajie Ji et al. This is an open access article distributed under the Creative Commons Attribution License, which permits unrestricted use, distribution, and reproduction in any medium, provided the original work is properly cited.

Objective. The randomized controlled clinical trial aims to investigate the clinical efficacy of moxibustion for breast cancer patients with chemotherapy-induced myelosuppression (CIM) during adjuvant chemotherapy. **Methods.** Surgically resected breast cancer patients were randomly divided into the moxibustion group (MOX; $n = 48$) and control group (CON; $n = 44$). Routine adjuvant chemotherapy (every 21 days, 4–8 cycles) and supportive recombinant human granulocyte colony-stimulating factor were given to both groups, while MOX received an additional moxibustion treatment (once daily after each cycle of chemotherapy). Primary endpoints included the grade of myelosuppression in terms of white blood cell (WBC) and absolute neutrophil count (ANC) and the incidence of myelosuppression-related serious adverse events (SAEs). Other measures included treatment compliance, adverse events (AEs), and survival. **Results.** WBC counts were generally higher in MOX and were dramatically higher than those in CON at the 7th course of chemotherapy ($P = 0.008$), while grade 1 ANC reduction was dramatically lower than that in CON at the 7th course of chemotherapy ($P = 0.006$). These effects were particularly significant in patients receiving anthracycline-taxane combination regimens. Moreover, MOX had fewer febrile neutropenia than CON ($P = 0.051$). MOX demonstrated a lower incidence of grade 3–4 myelosuppression ($P < 0.05$). AEs including grade 2–3 severe nausea, various kinds of pains, and vertigo occurred less frequently in MOX ($P < 0.05$). No difference in survival was observed between the two groups ($P > 0.05$). **Conclusion.** Moxibustion is effective for treating CIM in breast cancer patients during adjuvant chemotherapy, especially for patients receiving high-dose, long-term, and combined chemotherapy regimens. Moxibustion can reduce the incidence of myelosuppression-related SAE and improve the compliance and safety of chemotherapy in breast cancer.

1. Introduction

Breast cancer is a chemotherapy-sensitive malignant disease [1]. Dose-dense anthracycline-taxane combination chemotherapy is usually recommended in early-stage patients [2] and is beneficial to overall survival in selected endocrine-

sensitive patients [3]. However, this combination regimen causes high cytotoxicity to noncancerous normal tissue and leads to obvious chemotherapy-induced myelosuppression (CIM). Of which, febrile neutropenia (FN) is the major dose-limiting toxicity, which is associated with an increase in the risk of infection and can even be life-threatening [4, 5].

Hence, the prevention of CIM-related toxicities, as well as improving patients' quality of life (QoL), is the key to breast cancer management.

Myeloid growth factor (MGF) such as recombinant human granulocyte colony-stimulating factor (rhG-CSF) is currently used to treat and prevent CIM [6]. The use of MGF can improve disease-free survival (DFS) and overall survival (OS) in breast cancer [7]. The WBC-increasing effect is fast but rather short-lived. Moreover, 20–30% of the patients receiving MGF reported adverse events (AEs) and even serious adverse events (SAEs) including myelodysplastic syndrome [8] and acute myeloid leukemia [9]. These greatly hampered the patients' prognosis and QoL.

Traditional Chinese Medicine (TCM) that adjusts the body's Yin-Yang balance and emphasizes holistic concepts and pattern identification may be a potential alternative for MGF. Moxibustion is one of the TCM therapies that stimulate specific acupoints of the patient's body with dried moxa, intending to protect the health and prevent diseases [10]. Chen found that moxibustion can effectively prevent leukopenia and reduce gastrointestinal side effects after chemotherapy in breast cancer patients [11]. A recent study also revealed that moxibustion can improve the general conditions of patients with malignant tumors [12]. Given its convenience and low cost, moxibustion may be applied as a complementary treatment for breast cancer.

Currently, there is a lack of high-level clinical evidence (i.e., RCTs) in applying moxibustion to relieve CIM in breast cancer [13]. The consensus on choices of acupoints, methods, and course of moxibustion treatment is urgently warranted. Therefore, we aimed to systematically evaluate the effect of moxibustion for breast cancer patients receiving adjuvant chemotherapy in a randomized controlled setting.

2. Materials and Methods

2.1. Study Design. This is a randomized controlled trial (RCT) conducted at Shanghai Yueyang Integrated Traditional Chinese Medicine and Western Medicine Hospital. Postoperative breast cancer patients who were expected to receive adjuvant chemotherapy were recruited during 2015 and 2016. Inclusion criteria included the following: (1) diagnosed with breast cancer according to both Chinese and Western standards, (2) female, (3) aged between 18 and 80 years old, (4) pathologically confirmed primary breast cancer, (5) patients expected to receive adjuvant chemotherapy according to the "CACA Guidelines for Breast Cancer Diagnosis and Treatment (2015 edition)", (6) agreed to complete a full course of chemotherapy, (7) good compliance, and (8) written informed consent obtained. Exclusion criteria included the following: (1) history of receiving systemic chemotherapy or radiotherapy, (2) abnormal liver and kidney functions, serum alanine aminotransferase (ALT)/aspartate aminotransferase (AST) ≥ 2.5 times higher than the normal upper limit, and serum creatine (sCr) $\geq 150 \mu\text{mol/L}$, (3) major organ dysfunction such as severe heart disease, (4) coexistence of other primary malignancies, (5) pregnant or lactating women (according to blood β -HCG test), (6) language or geographic issues that

affect the follow-up of patients, and (7) other conditions that may cause risks to the patients or confuse the results as determined by the investigators. Eligible patients were randomly assigned into the moxibustion group (MOX) which received an additional moxibustion treatment and the control group (CON) which received the routine adjuvant chemotherapy without moxibustion. Primary endpoints included the grade of myelosuppression in terms of white blood cell (WBC) and absolute neutrophil count (ANC) and the incidence of myelosuppression-related SAE. Other measures included treatment compliance, AE, DFS, and OS.

This study was approved by the Ethics Committee of the Shanghai Yueyang Integrated Traditional Chinese Medicine and Western Medicine Hospital (Approval number: 2015-050) and was conducted in accordance with the Declaration of Helsinki. Written informed consent was obtained from each participant before study enrollment.

2.2. Diagnostic Standards. For the Western diagnostic standards, clinical diagnosis was based on the Tumor of the Breast (2nd Edition) edited by Shao Zhimin; the pathological diagnosis was based on the WHO Classification of Tumors of the Breast (4th Edition); the staging was based on the American Joint Committee on Cancer Staging Form (8th Edition). For the Chinese diagnostic standards, the diagnosis was based on the Practical Surgery of Traditional Chinese Medicine (2nd Edition).

2.3. Sample Size Estimation. According to our preliminary study, the occurrence rates of grade 2 or above myelosuppression in MOX and CON were 39% and 81%, respectively. Patients were randomly assigned to the two groups at a 1:1 ratio. The Z-pooled normal approximation was used to estimate the required sample size. Assuming that the two-sided significance level (α) is 0.05 and the power ($1-\beta$) is 0.2, the calculated sample size was 44 cases in MOX and 44 cases in CON.

3. Method for Randomization

A stratified randomization method was applied in this study using the online clinical trial random grouping management system which automatically assigned participants into groups after data entry. Patients were stratified according to the received chemotherapy regimens (in particular, anthracycline-only, taxane-only, and anthracycline-taxane combination chemotherapy). The administrative staff was responsible for generating the random allocation sequence and providing the treatment allocation to the physicians in sealed envelopes. The physicians were then responsible for assigning participants to corresponding interventions.

3.1. Moxibustion Treatment. Shenque (CV8), bilateral Zusanli (ST36), and bilateral Sanyinjiao (SP6) were selected as the acupoints for moxibustion based on the Science of Meridian and Acupuncture [14]. Shenque is located in the umbilicus. Zusanli is located in the outer side of the legs, 3

inches below Dubi (ST35), and between Dubi (ST35) and Jiexi (ST41). Sanyinjiao is located in the inner side of the legs, 3 inches above the tip of the medial malleolus, and at the posterior margin of medial tibia.

Mild moxibustion was applied to fully expose the above-selected acupoints. Hanyi® Pure Moxa Sticks for Mild Moxibustion was purchased from Nanyang Ltc. The moxa sticks were cut into 1.5 cm long to ensure constant size and density. When performing moxibustion, the lighted moxa stick was held accurately at the acupoint (about 2–3 cm away from the skin) so that the subject can feel warm but not burning. The skin areas applied with moxibustion should appear red. The subject first took a lying position for moxibustion at the Shenque and then took a sitting position for moxibustion at the bilateral Zusanli, followed by the bilateral Sanyinjiao. Moxibustion at each acupoint lasted for 15 minutes, followed by a gentle massage of the acupoints.

Moxibustion was performed once daily in MOX, started on the second day after each cycle of chemotherapy, and continued until the day before the next chemotherapy cycle. No moxibustion was planned on the days receiving chemotherapy. Moxibustion was applied until 3 weeks after the last cycle of chemotherapy. The exact treatment course depended on the chemotherapy cycles which were 4–8 cycles in this study.

3.2. Chemotherapy Regimen. Both MOX and CON received adjuvant chemotherapy treatment for breast cancer (every 21 days). Anthracycline-only, taxane-only, or anthracycline-taxane combination regimen was administered as decided by the investigators according to the CACA Guidelines for Breast Cancer Diagnosis and Treatment (2015 edition) [15]. rhG-CSF was applied to patients according to NCCN Clinical Practice Guidelines in Oncology: Myeloid Growth Factors (Version 1.2015) [16]. In brief, patients were closely followed up when grade 1 myelosuppression occurred. For patients with grade 2 or above myelosuppression, rhG-CSF was applied until their WBC counts and ANC returned to normal.

General supportive care for preventing and curing other chemotherapy-related AEs and certain medications that must be taken for patients with comorbidities were allowed as concurrent treatments in this study. However, Chinese herbal medicinal extracts and other TCM treatments for treating myelosuppression were prohibited.

3.3. Laboratory Tests and Technical Examination. Routine blood tests were performed at the first (day 1–7), second (day 8–14), and third (day 15–20) weeks after each cycle of chemotherapy (every 21 days). Parameters including WBC counts, ANC, hemoglobin (HGB), and platelet (PLT) were recorded. The reductions in WBC counts and ANC were compared between MOX and CON. Besides, liver functions including alanine transaminase (ALT), aspartate transaminase (AST), and γ -glutamyltranspeptidase (GGT); kidney functions including serum creatinine (sCr); blood lipids including triglyceride (TG) and total cholesterol (TC); heart

responses including creatine kinase (CK), and left ventricular ejection fraction (LVEF) were also recorded.

3.4. Adverse Effects. The incidences of common adverse effects such as general systemic conditions, gastrointestinal reactions, and pain were recorded. Particularly, the incidence rates of CIM-related SAEs including the proportion of patients with FN, grade 3–4 WBC counts and/or ANC reduction, and grade 3–4 abnormal laboratory indicators of the two groups were compared. Moxibustion-related AEs including skin reactions, burns, and heat symptoms were also recorded. The grading was determined according to the CTCAE 4.0.2.

3.5. Chemotherapy Compliance. Poor compliance was defined as a shortened course of chemotherapy and/or a reduction in chemotherapy dose. The proportion of patients who complete the standard course of treatment with standard dosing was compared between the two groups.

3.6. Survival Analysis. Follow-up was performed by the investigator through face-to-face interviews, telephone calls, and a WeChat management platform (ID: yanyueesf). The WeChat management platform was provided by Shanghai Ruochu Information and Technology Co. Ltd. The company has signed a nondisclosure agreement to protect the participants' confidentiality. DFS was defined as the time from the day of randomization to the day of disease progression or death, while OS was defined as the time from the day of randomization to the day of death. Kaplan–Meier method was used to generate the survival curves and calculate the survival rates. A Rank-sum test was used to compare the survival rates between the two groups.

3.7. Statistical Analysis. Two datasets were generated for subsequent analysis: a full analysis set (FAS) including all selected intent-to-treat (ITT) populations and a per-protocol set (PPS) including the per-protocol (PP) populations among the selected ones who completed the trial. Baseline and survival analyses were performed using the FAS, while the other data analyses were performed using the PPS.

Data analysis was performed using SPSS 22.0 software. All analysis was two-tailed and a P value of less than 0.05 was regarded statistically significant. Continuous variables that follow normal distribution were compared by using independent t -tests or ANOVA; otherwise, the Kruskal–Wallis H test and Nemenyi test were used. For categorical variables, the Chi-square test or Fisher's exact test was used for comparison.

4. Results

4.1. Demographic Information. From July 1, 2015, to July 31, 2016, a total of 132 postoperative breast cancer patients were recruited. 98 of them (49 in MOX and 49 in CON) were included as the FAS population and 92 of them (48 in MOX and 44 in CON) were included as the PPS population

(Supplementary Figure 1). The ITT population showed no significant statistical difference (Supplementary Table 1) in basic information, and the PPS population was also comparable at baseline (Supplementary Table 2).

4.2. Effects of Moxibustion on Myelosuppression. Generally, during the whole course of chemotherapy, no significant difference ($P > 0.05$) was found in the incidence of grade 0–4 WBC count reduction, ANC reduction, HGB reduction, and PLT reduction between the two groups (Supplementary Table 3).

Next, we compared the WBC counts of the two groups at specific time points (Table 1). There was no significant difference in WBC counts in the first, second, and third weeks after cycle 1–5 chemotherapy treatment between MOX and CON. But as the course of chemotherapy progressed, the difference in WBC counts began to occur. The WBC count of MOX in the first week after cycle 6 chemotherapy was slightly higher than that of the CON ($P = 0.084$). In the 7th cycle, the WBC count in the first week after chemotherapy was significantly higher in MOX (5.38 ± 1.41 vs $3.78 \pm 1.46 \times 10^9/L$, $P < 0.01$). However, the difference returned nonsignificant in the 8th cycle of treatment. We also found no difference in the incidence of grade 0–4 WBC count reduction between the two groups (Supplementary Table 4).

Throughout the courses of chemotherapy, there was no significant difference in ANC between MOX and CON (Supplementary Table 5). However, a trend of a higher percentage of grade 0 ANC patients was observed in cycle 5 (79.4% vs 60.6%, $P = 0.057$) and cycle 7 (75.0% vs 45.5%, $P = 0.051$) in the MOX group. In addition, grade 1 ANC reduction in MOX was significantly lower than that in CON (0% vs 31.8%, $P < 0.01$; Table 2) in cycle 7.

4.3. Stratified Analysis according to the Applied Chemotherapy Regimens. The majority of the patients (65/92, 70.7%) received an anthracycline-taxane combination regimen in this study, including 32 patients in the MOX group and 33 patients in the CON group. According to Figures 1(a) and 1(b), the lowest WBC counts and ANC in the MOX group were higher compared to the CON group since the 4th cycle of chemotherapy.

Further analysis stratifying the patients who received an anthracycline-taxane combination regimen according to the total course of treatment was performed. For the 44 patients who received 8-course of chemotherapy (21 in MOX and 23 in CON), the lowest WBC counts in the MOX group were higher than those of the CON group in cycles 4, 5, and 7 (Figure 2(a)). The MOX group also showed a higher value of the lowest ANC compared to the CON group since cycle 5 of chemotherapy (Figure 2(b)). For the 21 patients who received 6-course of chemotherapy (11 in MOX and 10 in CON), the lowest WBC counts and the lowest ANC in the MOX group were higher than those of the CON group at any time point (Figures 2(c) and 2(d)).

Other than the anthracycline-taxane combination regimen, 5 patients (5.4%; 2 in MOX and 3 in CON) received an anthracycline-only regimen and 22 patients (23.9%; 14 in

MOX and 8 in CON) received a taxane-only regimen in this study, respectively. No statistically significant differences in the lowest WBC count and the lowest ANC were found between the anthracycline-only group and the taxane-only group.

4.4. Effects of Moxibustion on AEs. There were no significant differences observed in liver and kidney functions (ALT elevation, AST elevation, GGT elevation, and sCr elevation), blood lipids (TG elevation and TC elevation), and cardiac response (CK elevation and LVEF reduction) between the two groups (Supplementary Table 6).

No significant differences in fatigue, malaise, and weight loss were observed between the two groups. Trends of fewer cases of grade 2 fatigue (12.5% vs 20.5%) and grade 2 malaise (8.3% vs 15.9%) were observed in the MOX group compared to the CON group (Supplementary Table 7).

For gastrointestinal reactions, grade 2–3 severe nausea in the MOX group was significantly less frequent compared to the CON group (27.1% vs 47.7%, $P < 0.05$). A trend of fewer cases of vomiting, diarrhea, and constipation was also observed in the MOX group (Supplementary Table 8).

The incidence of pain was slightly lower in the MOX group (89.6% vs 97.7%). Subdividing this into different sites of pain, we observed that bone, joint, muscle, and incision pain were less frequent in the MOX group ($P < 0.05$; Supplementary Table 9).

The cases of hot flashes were higher in the MOX group (25.0% vs 11.4%, $P = 0.092$), but the proportion of vertigo was significantly less than that in the CON group (4.2% vs 27.3%, $P < 0.01$; Supplementary Table 10).

No moxibustion-related toxic side effects including skin reactions, burns, and heat syndrome were observed in the MOX group.

4.5. Chemotherapy Compliance. For myelosuppression-related SAE, the number of FN cases in the MOX group was fewer than that in the CON group (1 vs 6, $P = 0.051$); the number of grade 3–4 severe myelosuppression cases (WBC count and/or ANC reduction) in the MOX group was significantly fewer than that in the CON group (30 vs 36, $P < 0.05$); no significant difference in the incident of grade 3 ALT and/or AST elevation was found between the two groups.

The above-mentioned SAEs may cause the early termination of chemotherapy; however, the number of cases that terminated chemotherapy earlier than expected showed no difference between the two groups (Supplementary Table 11). In contrast, the MOX group had a slightly lower chance of dose reduction compared to the CON group (2.1% vs 11.4%, $P = 0.100$).

4.6. Survival Analysis. All the 98 patients in the FAS population were successfully followed up with a median follow-up duration of 45.1 months (38.0–51.6 months). Distant recurrence was observed in 6 cases (6.1%) with a median time to distant recurrence of 22.9 months (13.0–25.2

TABLE 1: Comparison of the WBC counts at specific time points between the two groups.

Chemotherapy course	Group	n	WBC count		
			1 st week after chemotherapy (1–7 d)	2 nd week after chemotherapy (8–14 d)	3 rd week after chemotherapy (15–20d)
1 st course	MOX	48	5.03 ± 1.93 (36)	3.25 ± 1.76 (45)	6.67 ± 2.12 (47)
	CON	44	4.61 ± 1.68 (36)	3.11 ± 1.31 (39)	6.33 ± 2.35 (44)
2 nd course	MOX	48	5.08 ± 1.70 (38)	3.41 ± 1.42 (44)	5.86 ± 1.67 (46)
	CON	44	5.33 ± 2.07 (33)	3.21 ± 1.12 (38)	5.47 ± 1.85 (44)
3 rd course	MOX	48	4.92 ± 1.68 (35)	3.50 ± 1.25 (44)	5.50 ± 1.85 (45)
	CON	44	4.74 ± 1.98 (34)	3.22 ± 1.44 (40)	5.19 ± 1.15 (44)
4 th course	MOX	48	4.86 ± 1.94 (23)	3.51 ± 1.61 (33)	5.71 ± 1.63 (38)
	CON	44	5.04 ± 1.82 (25)	3.66 ± 2.17 (33)	5.22 ± 2.74 (36)
5 th course	MOX	33	5.22 ± 2.74 (19)	4.72 ± 1.63 (29)	5.79 ± 1.66 (33)
	CON	34	5.05 ± 2.11 (23)	5.20 ± 1.84 (25)	6.15 ± 1.79 (34)
6 th course	MOX	33	6.40 ± 2.00 (20) [#]	4.33 ± 2.09 (21)	5.40 ± 1.75 (24)
	CON	34	4.33 ± 2.09 (14) [#]	4.71 ± 1.27 (22)	5.42 ± 1.42 (14)
7 th course	MOX	20	5.38 ± 1.41 (12) ^{**}	4.87 ± 1.82 (18)	5.08 ± 1.42 (20)
	CON	23	3.78 ± 1.46 (15) ^{**}	4.67 ± 1.79 (20)	5.21 ± 1.01 (21)
8 th course	MOX	20	5.19 ± 2.43 (9)	5.35 ± 2.44 (8)	5.03 ± 1.66 (7)
	CON	23	3.95 ± 1.27 (6)	4.19 ± 1.04 (8)	5.86 ± 1.07 (7)

WBC counts are expressed as mean ± standard deviation $\times 10^9/L$ (number of cases). [#] $P = 0.084$, ^{**} $P < 0.01$.

TABLE 2: Comparison of the ANC count reduction grading between the two groups.

Chemotherapy course	Group	n	ANC reduction grading				
			Grade 0	Grade 1	Grade 2	Grade 3	Grade 4
1 st course	MOX	48	15 (31.3)	3 (6.3)	8 (16.7)	15 (31.3)	7 (14.6)
	CON	44	10 (22.7)	5 (11.4)	6 (13.6)	13 (29.5)	10 (22.7)
2 nd course	MOX	48	15 (31.3)	4 (8.3)	16 (33.3)	11 (22.9)	2 (4.2)
	CON	44	14 (31.8)	7 (15.9)	7 (15.9)	15 (34.1)	1 (2.3)
3 rd course	MOX	48	16 (33.3)	3 (6.3)	14 (29.2)	12 (25.0)	3 (6.3)
	CON	43	14 (32.6)	2 (4.7)	13 (30.2)	11 (25.6)	3 (7.0)
4 th course	MOX	42	22 (52.4)	2 (4.8)	8 (19.0)	6 (14.3)	4 (9.5)
	CON	37	13 (35.1)	5 (13.5)	7 (18.9)	10 (27.0)	2 (5.4)
5 th course	MOX	34	27 (79.4) [#]	3 (8.8)	1 (2.9)	2 (5.9)	1 (2.9)
	CON	33	20 (60.6) [#]	1 (3.0)	4 (12.1)	5 (15.2)	3 (9.1)
6 th course	MOX	27	18 (66.7)	5 (18.5)	2 (7.4)	1 (3.7)	1 (3.7)
	CON	25	16 (64.0)	1 (4.0)	3 (12.0)	3 (12.0)	2 (8.0)
7 th course	MOX	20	15 (75.0) [*]	0 (0.0) ^{**}	2 (10.0)	1 (5.0)	2 (10.0)
	CON	22	10 (45.5) [*]	7 (31.8) ^{**}	2 (9.1)	2 (9.1)	1 (4.5)
8 th course	MOX	12	10 (83.3)	1 (8.3)	1 (8.3)	0 (0.0)	0 (0.0)
	CON	13	7 (53.8)	3 (23.1)	2 (15.4)	0 (0.0)	1 (7.7)

Variables are expressed as the number of cases (percentage). [#] $P = 0.057$, ^{*} $P = 0.051$, ^{**} $P < 0.01$.

months). Death was observed in 2 cases (2.0%), with a survival time of 31.1 and 33.2 months, respectively.

According to the Kaplan-Meier analysis shown in Figure 3(a), the median DFS in MOX and CON was 49.0 months (95% CI: 46.8–51.2 months) and 50.0 months (95% CI: 48.6–51.8 months), respectively. The median OS in MOX and CON was 50.6 months (95% CI: 49.8–51.4 months) and 51.3 months (95% CI: 50.8–51.8 months), respectively (Figure 3(b)). The DFS and OS were comparable between the two groups ($P > 0.05$).

The analysis of the sites of distant recurrence revealed 5 cases of lung metastasis and 1 case of liver metastasis, with 1

case of death in each group. However, there were 2 cases in MOX that standard treatments were not given due to economic factors (Supplementary Table 12).

5. Discussion

Postoperative CIM in breast cancer often causes fatigue, dizziness, and unwillingness to speak, palpitations, insomnia and dreaminess, spontaneous sweating and tachypnea, pale and enlarged tongue, weak pulses, etc. Jiang has proven that the effect of moxibustion comes from the warm and hot stimulus produced by the burning of moxa [17] so that the

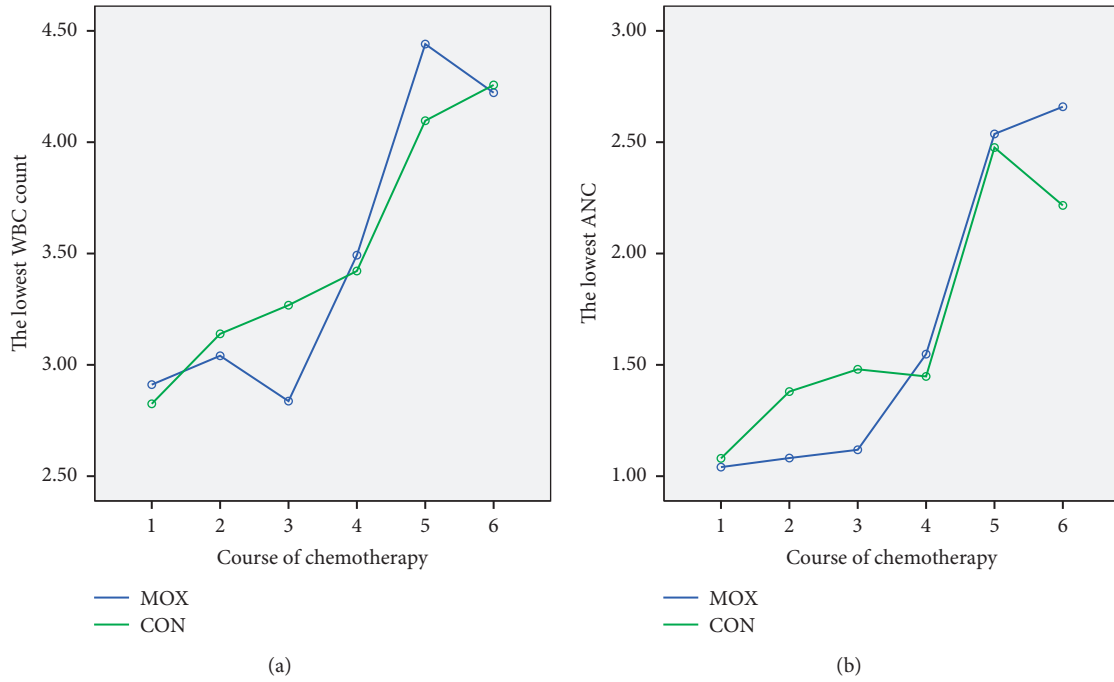


FIGURE 1: Comparisons of the lowest WBC counts and ANC between the two groups. Line charts showing (a) the lowest WBC counts and (b) the lowest ANC of the MOX and CON groups during the course of chemotherapy.

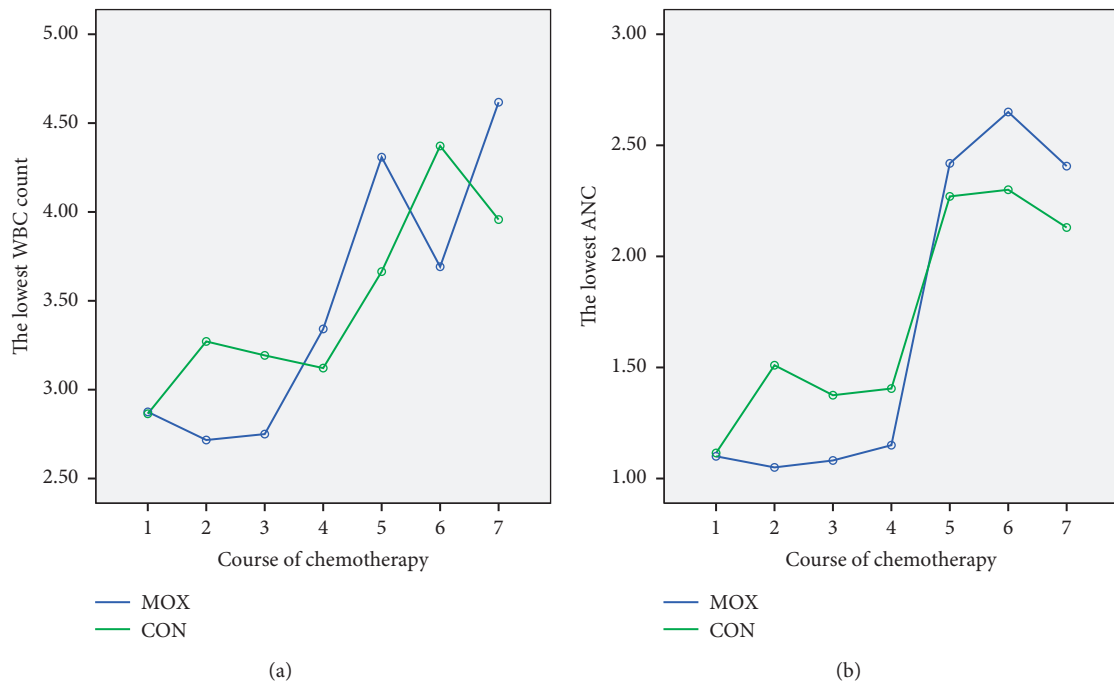


FIGURE 2: Continued.

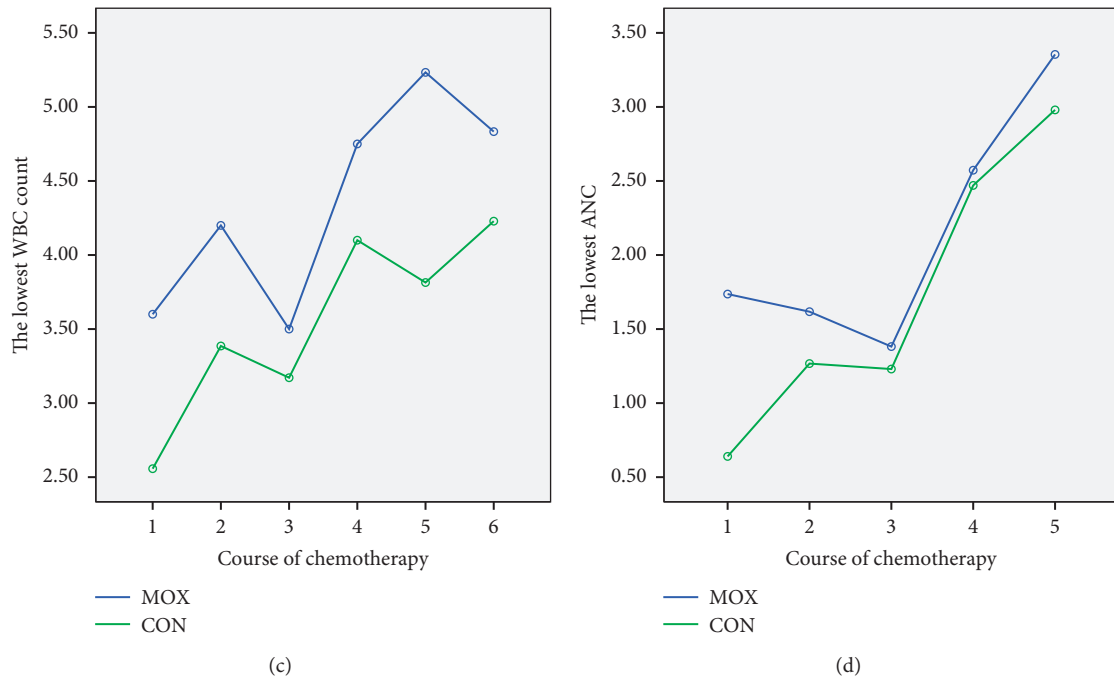


FIGURE 2: Comparisons of the lowest WBC counts and ANC in the subgroup of patients who received 8-course chemotherapy. Line charts showing (a) the lowest WBC counts and (b) the lowest ANC of the MOX and CON groups during the course of chemotherapy. Comparisons of the lowest WBC counts and ANC in the subgroup of patients who received 6-course chemotherapy. Line charts showing (c) the lowest WBC counts and (d) the lowest ANC of the MOX and CON groups during the course of chemotherapy.

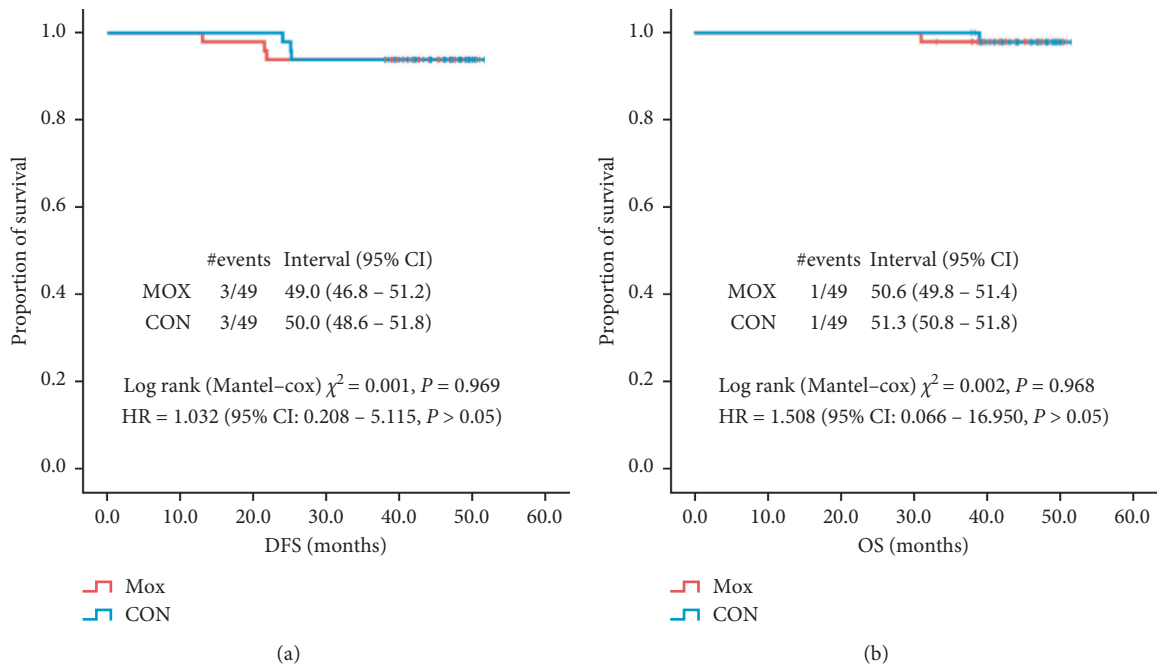


FIGURE 3: Comparisons of the DFS and OS between the two groups. Kaplan-Meier curves showing (a) the DFS and (b) the OS of the MOX and CON groups.

neuroendocrine-immune network can be gradually regulated.

Previous clinical studies showed that moxibustion can increase the WBC count for 55.9–84.0% and improve the patients' QoL [18–22]. However, the physicians have not yet come to a consensus on the acupoints, methods, courses, and volume of moxibustion. The evidence supporting moxibustion on CIM is of low quality. Further research is needed to provide a well-evaluated moxibustion protocol for supportive treatment in breast cancer patients.

The primary outcome measures of this study were WBC count and ANC. Different chemotherapy regimens and courses of treatment may also influence the blood test results [23]. Therefore, we compared the WBC counts and ANC at different time points during chemotherapy and carried out stratified analysis according to chemotherapy regimens. Consistent with Chen's and Jiang's conclusion [11, 24], our results revealed that the WBC counts and ANC reduction grade gradually showed a slight difference between the two groups as the course of chemotherapy progressed, indicating that moxibustion can stabilize the WBC count and ANC in the latter course of the chemotherapy. Although moxibustion did not show significant advantages for patients receiving anthracycline-only and taxane-only regimens, beneficial effects were observed in patients receiving combination regimens, especially for those receiving high-dose and multiple courses of chemotherapy. Interestingly, it is found that WBC count and ANC reduction grade are more sensitive in evaluating moxibustion on CIM.

In this study, there were no significant differences in the occurrence of gastrointestinal-related AEs between the two groups. However, the incidence of grade 2–3 severe nausea in MOX was significantly less than that in CON, indicating that moxibustion has an effect on preventing nausea and vomiting. Consistent with our findings, Zhao had also reported that moxibustion at Shenque and Zusanli acupoints can prevent gastrointestinal reactions caused by chemotherapy [25].

With the help of the WeChat management platform, the follow-up rate of the FAS population was 100% (98/98). The median follow-up duration is 45.1 (38.0–51.6) months. The occurrence rates of events were lower than those previously reported [26]. Six cases of patients who had survival events showed a median time to distant recurrence of 22.9 months, which seems logical regarding that the peak period of distant recurrence is 2–3 years after surgical treatment in breast cancer [27]. Survival data showed that moxibustion is not detrimental to the patients' DFS and OS.

6. Conclusions

This RCT study suggested that moxibustion could prevent CIM in breast cancer patients, especially in the 7th course of chemotherapy. For patients receiving high-dose and multiple courses of anthracycline-taxane combined chemotherapy, the efficacy of moxibustion was particularly obvious. Additionally, moxibustion may lower the incidence of SAE (in myelosuppression), reduce AE (such as nausea, vertigo, bone, joint, and muscle pain, and incision pain), and

increase compliance and safety of chemotherapy. In this RCT, our results provided systematic evidence for the use of a simple, convenient, and inexpensive (relatively, compared to rhG-CSF) moxibustion protocol to relieve CIM in breast cancer patients receiving adjuvant chemotherapy. A study of the combination therapy of moxibustion and Traditional Chinese Medicine is ongoing [28].

Abbreviation

E:	Epirubicin
C:	Cyclophosphamide
T:	Taxol
F:	Fluorouracil
H:	Herceptin
AI:	Aromatase inhibitor
OFS:	Ovarian function suppression
TAM:	Tamoxifen.

Data Availability

All the study data are available upon reasonable request.

Conflicts of Interest

The authors declare that they have no conflicts of interest.

Authors' Contributions

Yajie Ji and Siyu Li contributed equally to this work.

Acknowledgments

This work was supported by grants from the Three-Year Program of Shanghai Hospital Development Center (No. 16CR2026B) and the National Natural Science Foundation of China (No. 82004446), as a preliminary study.

Supplementary Materials

Supplementary Figure 1: flow chart of patient enrollment. Supplementary Table 1: baseline characteristics of the FAS population. Variables are expressed as either mean \pm standard deviation or number of cases (percentage). Supplementary Table 2: baseline characteristics of the PPS population. Variables are expressed as either mean \pm standard deviation or number of cases (percentage). Supplementary Table 3: comparison of myelosuppression occurred during chemotherapy between the two groups. Supplementary Table 4: comparison of the WBC count reduction grading between the two groups. Variables are expressed as number of cases (percentage). Supplementary Table 5: comparison of the ANCs at specific time points between the two groups. ANCs are expressed as mean \pm standard deviation $\times 10^9/L$ (number of cases). Supplementary Table 6: comparison of adverse effects between the two groups. Variables are expressed as number of cases (percentage). Supplementary Table 7: comparison of systemic general adverse effects between the two groups. Variables are expressed as number of cases (percentage).

Supplementary Table 8: comparison of gastrointestinal adverse effects between the two groups. Variables are expressed as number of cases (percentage). * $P < 0.05$. Supplementary Table 9: comparison of the pain adverse effects between the two groups. Variables are expressed as number of cases (percentage). Musculoskeletal and connective tissue disorders include bone pain, arthralgia, and muscle pain. * $P < 0.05$. Supplementary Table 10: comparison of the other adverse effects between the two groups. Variables are expressed as number of cases (percentage). # $P = 0.092$, ** $P < 0.01$. 1: infection includes oral mucositis, rhinitis, pneumonia, cholecystitis, gastroenteritis, pelvic inflammatory disease, incision infection, and urinary tract infection. 2: paresthesia includes dysesthesia, dysgeusia, scalp numbness, and general numbness. 3: edema includes facial edema, pedal edema, and periocular edema. 4: hemorrhage includes bleeding gums, nosebleed, and subconjunctival hemorrhage. 5: surgical and medical procedures include 1 case of venous thrombosis and 2 cases of breast surgery. Supplementary Table 11: comparison of the chemotherapy compliance between the two groups. Variables are expressed as number of cases (percentage). Supplementary Table 12: clinical characteristics of the 6 cases with survival events observed. *Death interval is defined as the time between distant recurrence and death. (*Supplementary Materials*)

References

- [1] R. Horii, F. Akiyama, Y. Ito et al., "Histological features of breast cancer, highly sensitive to chemotherapy," *Breast Cancer*, vol. 14, no. 4, pp. 393–400, 2008.
- [2] E. P. Mamounas and G. W. Sledge Jr., "Combined anthracycline-taxane regimens in the adjuvant setting," *Seminars in Oncology*, vol. 28, no. 4J, pp. 24–31, 2001.
- [3] M. Joerger and B. Thürlimann, "Chemotherapy regimens in early breast cancer: major controversies and future outlook," *Expert Review of Anticancer Therapy*, vol. 13, no. 2, pp. 165–178, 2013.
- [4] L. R. Baden, S. Swaminathan, M. Angarone et al., "Prevention and treatment of cancer-related infections, version 2.2016, NCCN clinical practice guidelines in oncology," *Journal of the National Comprehensive Cancer Network*, vol. 14, no. 7, pp. 882–913, 2016.
- [5] T. J. Smith, K. Bohlke, G. H. Lyman et al., "Recommendations for the use of WBC growth factors: American Society of Clinical Oncology clinical practice guideline update," *Journal of Clinical Oncology*, vol. 33, no. 28, pp. 3199–3212, 2015.
- [6] K. S. Antman, J. D. Griffin, A. Elias et al., "Effect of recombinant human granulocyte-macrophage colony-stimulating factor on chemotherapy-induced myelosuppression," *New England Journal of Medicine*, vol. 319, no. 10, pp. 593–598, 1988.
- [7] S. Cortés De Miguel, M. Á. Calleja-Hernández, S. Menjón-Beltrán, and I. Vallejo-Rodríguez, "Granulocyte colony-stimulating factors as prophylaxis against febrile neutropenia," *Supportive Care in Cancer*, vol. 23, no. 2, pp. 547–559, 2015.
- [8] D. Hershman, A. I. Neugut, J. S. Jacobson et al., "Acute myeloid leukemia or myelodysplastic syndrome following use of granulocyte colony-stimulating factors during breast cancer adjuvant chemotherapy," *JNCI: Journal of the National Cancer Institute*, vol. 99, no. 3, pp. 196–205, 2007.
- [9] G. H. Lyman, D. C. Dale, D. A. Wolff et al., "Acute myeloid leukemia or myelodysplastic syndrome in randomized controlled clinical trials of cancer chemotherapy with granulocyte colony-stimulating factor: a systematic review," *Journal of Clinical Oncology*, vol. 28, no. 17, pp. 2914–2924, 2010.
- [10] h Wu, *Modern Research on Chinese Moxibustion Treatment*, Shanghai Scientific & Technological Publishers, Shanghai, China, 2013.
- [11] L. Chen, C. Guan, W. Zhang et al., "Clinical study on leukopenia with moxibustion on Dazhui Zusanli acupoint, prevention and treatment of breast cancer after chemotherapy," *Nei Mongol Journal of Traditional Chinese Medicine*, vol. 5, pp. 72–73, 2017.
- [12] X. Hou and G. Ni, "Advances in the study of moxibustion treatment on malignant tumors," *World Journal of Integrated Traditional and Western Medicine*, vol. 9, pp. 101–104, 2014.
- [13] Y. Ji and X. Xue, "Research status of moxibustion in preventing chemotherapy-induced myelosuppression in malignant tumors," *Guangming Journal of Chinese Medicine*, vol. 34, no. 14, pp. 2266–2271, 2019.
- [14] X. Shen, *Science of Meridians and Acupoints*, China Press of Traditional Chinese Medicine, Beijing, China, 2016.
- [15] Chinese Association for Clinical Oncologists, "The Chinese Anti-Cancer Association, the Society of Chemotherapy and Editorial Committee National Medical Journal of China. Chinese expert consensus on clinical application of recombinant human granulocyte-colony stimulating factor during cancer therapy (2015 edition)," *National Medical Journal of China*, vol. 95, pp. 3001–3003, 2015.
- [16] NCCN, *NCCN Clinical Practice Guidelines in Oncology: Myeloid Growth Factors*, vol. 6, NCCN, Plymouth, UK, 2015. <https://www.nccn.org/>.
- [17] J. Jiang, L. Wang, B. Xu et al., "Anti-inflammatory effect mechanism of warming-dredging in moxibustion," *Chinese Acupuncture & Moxibustion*, vol. 9, pp. 860–864, 2013.
- [18] L. Zhong and C. Li, "Observation on the therapeutic effects of moxibustion on 40 cases of leukopenia caused by chemotherapy," *Journal of Qiqihar University of Medicine*, vol. 24, p. 3451, 2012.
- [19] H. Tian, H. Lin, L. Zhang et al., "Effective research on treating leukopenia following chemotherapy by moxibustion," *Clinical Journal of Chinese Medicine*, vol. 10, pp. 35–38, 2015.
- [20] L. Zhang and H. Yang, "Application of selective acupoint moxibustion on leukocytopenia induced to antitumor," *Clinical Journal of Chinese Medicine*, vol. 10, no. 15, pp. 117–119, 2018.
- [21] H. Wu, X. Su, Q. Su et al., "50 cases of leukopenia after breast cancer chemotherapy treated by flumigating the navel with Chinese herbs beneath the moxa cone," *Guangming Journal of Chinese Medicine*, vol. 11, pp. 2107–2108, 2013.
- [22] S. Yue, Z. Fan, H. Lin et al., "Observation on the therapeutic effects of ginger interposed moxibustion combined with superficial acupuncture on leukopenia after breast cancer radiotherapy and chemotherapy," *Shenzhen Journal of Integrated Traditional Chinese and Western Medicine*, vol. 8, pp. 29–31, 2015.
- [23] N. An, Q. Huang, H. Zhou et al., "Retrospective analysis of influencing factors of grade IV myelosuppression," *China Journal of Chinese Materia Medica*, 2016.
- [24] S. Jiang, D. Xie, and L. Jiang, "Clinical study on treating chemotherapy-associated leukopenia with traditional Chinese medicine and moxibustion in breast cancer," *Journal of*

- Guangdong Pharmaceutical University*, vol. 35, pp. 451–455, 2019.
- [25] B. Zhao and W. Zhang, “Observation of the therapeutic effects of moxibustion on at Shenque and Zusanli in 47 cases on prevention and treatment of gastrointestinal reactions caused by chemotherapy,” *Asia-Pacific Traditional Medicine*, vol. 11, pp. 75–76, 2013.
- [26] W. Cao, Y. He, J. Li et al., “Impact of adjuvant chemotherapy on the survival of patients with estrogen receptor $\geq 50\%$, human epidermal growth factor receptor-2 negative, lymph node negative breast cancer,” *Chinese Journal of General Surgery*, vol. 33, no. 3, pp. 223–227, 2018.
- [27] W. Yin, L. Zhou, J. Lu et al., “Time distribution of the recurrence hazard for breast cancer patients undergoing surgery,” *Journal of Practical Oncology*, vol. 6, pp. 527–531, 2007.
- [28] Y. Ji, S. Li, X. Zhang et al., “The prophylactic and therapeutic effects of moxibustion combined with traditional Chinese medicine decoction for treating chemotherapy-induced myelosuppression in early-stage breast cancer: study protocol for a randomized controlled trial,” *Trials*, vol. 21, p. 844, 2020.

Research Article

Fuzheng Yiliu Formula Regulates Tumor Invasion and Metastasis through Inhibition of WAVE3 Expression

Wen-li Chen,¹ Huan-huan Bai,² Li-wei Liu,¹ Hong-yu Chen,¹ Qi Shi,¹ Li-sheng Chang,¹ Xiao-jun Gou ,¹ and Jun Qian ³

¹Baoshan District Hospital of Integrated Traditional Chinese and Western Medicine of Shanghai, Shanghai 201999, China

²School of Pharmacy, Shaanxi University of Traditional Chinese Medicine, Xianyang, Shaanxi 712046, China

³Department of Diagnostics of Chinese Medicine, School of Chinese Medicine,

School of Integrated Chinese and Western Medicine, Nanjing University of Chinese Medicine, Nanjing, Jiangsu 210023, China

Correspondence should be addressed to Xiao-jun Gou; gouxiaojun1975@163.com and Jun Qian; junqian_njucm@163.com

Received 7 August 2020; Revised 22 February 2021; Accepted 26 February 2021; Published 28 March 2021

Academic Editor: Mohd Fadzelly Abu Bakar

Copyright © 2021 Wen-li Chen et al. This is an open access article distributed under the Creative Commons Attribution License, which permits unrestricted use, distribution, and reproduction in any medium, provided the original work is properly cited.

Objective. To explore the mechanism of action of Fuzheng Yiliu formula (FZYLF) in regulation of the invasion and metastasis of MDA-MB-231/Adr human breast cancer cells through WAVE3. **Methods.** The MDA-MB-231/Adr cells with high invasive ability were screened by Transwell, and the plasmid with high WAVE3 expression was made for transfection. Plasmid transfection efficiency and protein expression level were verified by polymerase chain reaction (PCR) and western blotting (WB). The effect of FZYLF on cell proliferation and invasion was investigated before and after WAVE3 silencing by flow cytometry. A nude mouse model of tumor metastasis was established to study the antitumor activity of FZYLF. **Results.** The expression levels of mRNA and proteins of intracellular WAVE3 increased significantly after plasmid transfection, mRNA from 1.37 ± 0.41 to 9.88 ± 1.31 and protein from 1 ± 0.08 to 5.09 ± 0.03 ($P < 0.01$). Intervention with FZYLF could significantly affect the activity of MDA-MB-231/Adr cells and inhibit invasion and metastasis, IC_{50} from 71.04 to 46.41 mg/mL and from 162 ± 14.82 to 81.4 ± 12.05 ($P < 0.05$ or $P < 0.01$), and significantly reduce the expression levels of WAVE3 (from 1 ± 0.02 to 0.63 ± 0.04), MMP-9 (from 1 ± 0.05 to 0.63 ± 0.03), NF- κ B (p65) (from 1 ± 0.02 to 0.62 ± 0.02), and p-I κ B α (from 1 ± 0.03 to 0.68 ± 0.02) ($P < 0.05$ or $P < 0.01$). The T/C (%) of FZYLF (13 g crude drug/kg) was 62.06% for MDA-MB-231/Adr tumor xenografted in nude mice, with a tumor inhibition rate of 39.64%. **Conclusion.** FZYLF can inhibit the invasion and proliferation of the MDA-MB-231/Adr human breast cancer cells, and the mechanism of action may be related to the regulation of WAVE3 expression.

1. Introduction

Breast cancer is one of the most common malignant tumors in women all over the world and has gradually evolved into the first female malignant tumor in recent years [1]. This disease tends to recur and metastasize and its biological behavior is dangerous, especially in triple negative breast cancer (TNBC), which has the characteristics of poor histological grade, advanced clinical stage, poor prognosis and high mortality, and a tendency to occur at a younger age. The 3- and 5-year disease-free survival (DFS) and overall survival (OS) are lower in TNBC than in non-TNBC [2]. The prognosis of TNBC gets worse with the increase in N staging,

and the probability of recurrence and metastasis increases significantly at stage N2 or above, but there is no significant correlation with T staging and histological grade [3]. It is estimated that up to 30% of patients with lymph node negative breast cancer and most patients with lymph node positive breast cancer will have metastasis even with standardized treatment. With the continuous application of chemotherapy drugs, chemotherapy-induced multidrug resistance (MDR) of breast cancer not only limits the clinical efficacy of drugs but also promotes the occurrence of invasion and metastasis. The mechanism of MDR development is complex in breast cancer and is often believed to be the combined result of multiple mechanisms, including high

expression of membrane transporters, disorders in drug transport and activation, changes in the nature and number of drug targets, changes in the enzyme system, enhancement of DNA repair, and inhibition of cell apoptosis [4].

WAVE3 plays an important role in migration and invasion of breast cancer cells. Breast cancer cells degrade the extracellular matrix and basement membrane at the primary site, migrate into blood vessels, and reach the distal organs through blood flow to form metastatic foci [5]. WAVE3 (also known as WASF3) is a member of the WASP (Wiskott-Aldrich syndrome) protein family, which is a newly discovered group of proteins in recent years that mediates actin polymerization by activating actin-related protein 2/3 (Arp2/3) complex and participates in the formation of filamentous pseudopodia and lamellar pseudopodia during cell migration, membrane transport, and cell adhesion. WAVE3 plays a critical role in tumor proliferation, differentiation, and invasion, especially in invasion and metastasis. In breast cancer, the expression of WAVE3 is positively correlated with the grade, drug resistance, invasion, and progression of tumor. In TNBC, the high expression of WAVE3 is closely related to the metastasis of breast cancer [6]. WAVE3 is also an important link in TGF β -induced epithelial matrix transformation in breast cancer [7]. Silencing the expression of WAVE3 in invasive breast cancer cells by siRNA can effectively reduce the number of lamellar pseudopodia on the edge of tumor cell membrane and weaken the ability of tumor cells to invade and migrate. After the breast cancer cells with further knockout of WAVE3 are inoculated into nude mice, it is found out that compared to the negative control group, the growth of tumor *in situ* is significantly slower and the distant metastasis rate of tumor decreases significantly [8]. In addition, WAVE3 knockout also increases the sensitivity of TNBC to chemotherapy by inhibiting STAT-HIF-1 α -mediated angiogenesis [9]. In our recent study, it has been confirmed that the expression of WAVE3 is also higher in tissues of invasive breast cancer than in tissues of breast cancer *in situ* [10]. These results suggest that WAVE3 plays an important role in the invasion and metastasis of breast cancer, especially in chemotherapy-resistant breast cancer.

Matrix metalloproteinase-9 (MMP-9) is a secreted multidomain enzyme that regulates the composition of cell matrix. It belongs to the gelatinase subfamily of MMPs. Therefore, its main substrate is gelatin (collagen), which is the main component of basement membrane. MMP-9 destroys the basement membrane and promotes tumor invasion and metastasis by enzymolysis. Christine et al. have found that MMP-9 secreted by human breast cancer cells promotes the invasion of tumor cells in cell culture and lung metastasis *in situ* mouse model of basal-like TNBC [11]. Zhao et al. have revealed that in TNBC, prognosis is worse in patients with high expression of MMP-9 than in patients with low expression of MMP-9 [12].

I κ B α is the most classic member of I κ B protein family. The NF- κ B family is composed of five members, namely, P50, P52, P65, c-Rel, and RelB. In the classic NF- κ B signaling pathway, I κ B α binds with the most common NF- κ B dimer P65 : P50 to prevent it from entering the nucleus and binding

with DNA, thus inhibiting the activation of NF- κ B signaling pathway. When I κ B α is phosphorylated by activated IKK to p-I κ B α , the classic NF- κ B signaling pathway is activated. NF- κ B plays an important role in the occurrence and development of breast cancer. Hossain et al. have found out that Notch signal regulates mitochondrial metabolism and NF- κ B activity in TNBC cells through IKK α -dependent nonclassical pathway, thus promoting the invasion and metastasis of breast cancer [13]. El-Hafeez et al. have revealed that norwogonin can further inhibit the activation of NF- κ B and STAT3 signaling pathways by inhibiting the expression of TAK1, thus playing an anticancer role [14].

Traditional Chinese medicine (TCM) has unique advantages in preventing tumor recurrence and metastasis [15, 16]. A study by Zheng et al. [4] has suggested several reversal strategies of MDR in breast cancer, including reversal by chemical drugs, cytokines, immunotherapy, gene technology, and Chinese medicines, and treatment with TCM compound formulas has the advantages of multitarget, safety, effectiveness, and low cost. Fuzheng Yiliu formula (FZYLF, formula that reinforces healthy qi and inhibits tumor) is a commonly used prescription in our department that has been used over 10 years in patients after operation for breast cancer. It is composed of Dangshen (Radix Codonopsis, DS), Maidong (Radix Ophiopogonis, MD), Maorenshen (*Actinidia valvata* Dunn, MRS), Shijianchuan (*Salviae Chinensis* Herba, SJC), stir-fried Biejia (*Carapax Trionycis*, BJ), crude Yiyren (*Semen Coicis*, YJR) (DS 15 g, MD 10 g, MRS 15 g, SJC 15 g, BJ 15 g, and YJR 15 g), and so on. In this prescription, DS tonifies qi and engenders fluid; MD nourishes yin and moistens the lung; stir-fried BJ softens the lumps and dissipates the nodules; MRS clears heat and removes toxin; SJC clears heat and removes toxin, activates blood, and suppresses pain; crude YJR invigorates the spleen and drains dampness, eliminates impediment and checks diarrhea, clears heat, and expels pus. These drugs used in combination strengthen healthy qi and inhibit tumor. Previous clinical studies have confirmed that this prescription can significantly improve the patients' quality of life [17, 18]. From the perspective of basic research, the present study discusses the effect and mechanism of FZYLF on the invasion and metastasis of multidrug-resistant breast cancer cells.

2. Materials and Methods

2.1. Experimental Materials

2.1.1. Cell Lines. The MCF-7 and MDA-MB-231 human breast cancer cells and the drug-resistant cell lines MCF-7/Taxol, MCF-7/Adr, MDA-MB-231/Taxol, and MDA-MB-231/Adr were cultured in DMEM medium containing 10% fetal bovine serum (FBS) at 37°C with 5% CO₂.

2.1.2. Animals. 25 female SPF BALB/c nude mice were provided by Changzhou Cavens Laboratory Animal Co., Ltd. (Changzhou, China) (laboratory animal production license: SCXK (SU) 2016-0010; laboratory animal use license: SYXK (SU) 2017-0007).

2.1.3. Reagents and Consumables. DMEM (high sugar) medium was purchased from Gibco (NY, USA); FBS was obtained from ScienCell Research Laboratories (CA, USA). CCK8 cell viability test kit was purchased from Enjing Biotech Co., Ltd. (Nanjing, China) (E1CK-000208-10). Transwell chamber with pore size of 8.0 μm was manufactured by Corning Incorporated (REF 3422, LOT: 14416045). BD Matrigel matrix (basement membrane) was purchased from BD Biosciences (356234). WAVE3 antibody was from EnoGene, rabbit antihuman/mouse (E20-74899); I κ B- α antibody from EnoGene, rabbit antihuman/mouse (E2344534); P-I κ B- α antibody from EnoGene, rabbit antihuman/mouse (E2340776); NF- κ B antibody from EnoGene, rabbit antihuman (E10-20406); MMP-9 antibody from EnoGene, rabbit antihuman (E11-0275C); GAPDH antibody from EnoGene, rabbit antihuman/mouse (E90062). Hydrophobic PVDF membrane was obtained from Millipore; ECL chemiluminescence reagent was obtained from Beyotime (P0018A). RIPA Lysis solution, BSA, prestain protein marker, HRP labeled goat anti-rabbit secondary antibody, developer, fixer, and BCA protein assay kit were all purchased from Enjing Biotech Co., Ltd. (Nanjing, China). WAVE3 plasmid was purchased from Nanjing GenScript Biotechnology Co., Ltd. (Nanjing, China).

MRS (Lot no. 160108) in FZYLF was grown in Zhejiang Province, produced on January 08, 2016, and processed by Hongqiao Chinese Medicine Crude Slices Co., Ltd. (Shanghai, China). Other medicinal materials (Lot no. 1512068) were grown in Zhejiang Province and processed by Shanghai Lei Yunshang Chinese Medicine Crude Slices Factory (Shanghai, China). Amount of the drugs used in the prescription was as follows: DS 15 g, MD 10 g, MRS 15 g, SJC 15 g, stir-fried BJ 15 g (decocted first), and YYR 15 g.

2.1.4. Instruments. The instruments used in this study are shown in Table 1.

2.1.5. Preparation of FZYLF. 3 bags of the abovementioned herbs were taken in an appropriate amount. Powder of the herbs was mixed, added with 10 times water, and soaked overnight. Reflux extraction was carried out for 2 h. The extract was recovered and filtered, then evaporated and concentrated in an evaporating dish on a water bath, and the water extract of FZYLF was obtained. The extract was concentrated to 200 mL at a concentration of 1.5 g crude drugs/mL and stored at 4°C. Quality control of Fuzheng Yiliu formula can be seen in Supplementary Materials.

2.2. Methods

2.2.1. Effect of FZYL on Proliferation of MDA-MB-231 Human Breast Cancer Cells In Vitro. Tumor cells were cultured separately. Cells in logarithmic growth phase were inoculated into a 96-well plate at 1×10^5 cells/mL, 100 μL /well, and cultured for 24 h at 37°C, 5% CO₂. Water and alcohol extracts at corresponding concentrations were added, and a negative control group was set up. After incubation with

cells for 24 h, the growth of cells in each group was observed under a microscope. 10 μL CCK-8 was added to each well and let stand at room temperature for 4 h. Absorbance was detected at 450 nm and IC₅₀ was calculated.

2.2.2. Detection of WAVE3 Expression Level. The expression of WAVE3 gene in human breast cancer cell lines MCF-7 and MDA-MB-231 and drug-resistant cell lines MCF-7/Taxol, MCF-7/Adr, MDA-MB-231/Taxol, and MDA-MB-231/Adr was detected by real-time PCR. In the previous experiment on asiatic acid, the results showed that asiatic acid could significantly inhibit proliferation in the MDA-MB-231 and MCF-7 cell lines, with the strongest inhibitory activity on MDA-MB-231. Therefore, MDA-MB-231 cells were selected for follow-up study [10].

Real-time PCR: cells were lysed in TriPure Regent at 1 mL per well in a 6-well plate. The lysate was extracted with chloroform, precipitated with isopropanol, and washed with 75% ethanol to precipitate total RNA. Total RNA was reverse-transcribed into cDNA following instructions of the reverse transcription kit, and the expression of each target gene was detected by real-time quantitative PCR with β -actin as internal reference. SYBR green real-time PCR was used for amplification, and the threshold value and Ct value were obtained automatically by software. The specific operation is shown in the literature [10]. The sequences of primers were used as follows: β -actin (5'-AGTCCTGTGGCATCCAC-GAAAC-3' and 5'-CACACGGAGTACTTGCCTCAG-3') and WAVE3 (5'-CACCAATCAGTGATGCTCGAAG-3' and 5'-AGTCGGACCAGTCGTTCTCG-3').

2.2.3. Expression of WAVE3 at Gene and Protein Levels after Transfection. MDA-MB-231/Adr cells were transfected with shRNA-WAVE3, and pcDNA3.1-WAVE3 was transfected into MDA-MB-231 cells. The MDA-MB-231/Adr and MDA-MB-231 cells in logarithmic growth phase were inoculated into a 6-well plate and cultured in an incubator until a cell density of 60~80% at the bottom of the well. The cells were ready for transfection. Before transfection, the culture medium in the wells was replaced by 1 mL antibiotics-free DMEM medium. Following Lipo2000 operation instructions, 200 μL each of opti-MEM was used to dilute shRNA-WAVE3 (50 nmol) or pcDNA3.1-WAVE3 and Lipo2000 (5 μL), and a negative control group was set up. Cells in the control group were transfected as mentioned above with blank vector plasmid containing no WAVE3 gene. The diluted Lipo2000 was incubated for 5 min at room temperature and then gently mixed with the diluted shRNA and let it stand for 20 min at room temperature to form the shRNA-RNAiMAX complex, which was added into the cell culture plate and mixed by shaking gently. The plate was put into an incubator for incubation at 37°C, 5% CO₂. The DMEM complete medium was replaced 6 h later.

Gene and protein expression levels of WAVE3 in the human breast cancer cell line MDA-MB-231 and the drug-resistant cell line MDA-MB-231/Adr after transfection were detected by real-time PCR and western blotting. Protein

TABLE 1: List of instruments.

Instrument	Purchased from	Model
Biological safety cabinet	Suzhou Purification Equipment Co., Ltd.	BHC-1300A/B2
Carbon dioxide incubator	SANYO Japan	MCO-15AC
Fluorescence inverted biomicroscope	Nanjing Jiangnan Novel Optics Co., Ltd.	XD-202
Tabletop high-speed centrifuge	SCILOGEX	D2012
Low-temperature high-speed centrifuge	SCILOGEX	D3024R
Microplate reader	Thermo Scientific	MUTISKAN MK3
Precision electronic balance	Satorius	BSA224S
Microvertical electrophoresis tank	Shanghai Tanon Technology Co., Ltd.	VE 180
Transfer electrophoresis cell	Shanghai Tanon Technology Co., Ltd.	VE 186
Electrophoresis apparatus	Shanghai Tanon Technology Co., Ltd.	EPS 300
Decolorizing shaker	Jiangsu Jintan Ronghua Instrument Manufacturing Co., Ltd.	TY-80B
Mute mixer	Jiangsu Haimen Qilin Beier Instrument Manufacturing Co., Ltd.	WH-986

expression levels of WAVE3, $\text{I}\kappa\text{B}\alpha$, NF- KB , and MMP-9 in the human breast cancer cell line MDA-MB-231/Adr shRNA after transfection were investigated by western blotting. The real-time PCR is the same as mentioned in Section 2.2.2, and the specific operation of western blot is shown in the literature [10]. In the previous experiment on asiatic acid in FZYLf, the expression of WAVE3 increased significantly in ductal carcinoma in situ tissue, and it was even higher in the metastasis group. WAVE3 might be involved in drug resistance, invasion, and metastasis of tumor cells. Therefore, MDA-MB-231/Adr cells were selected for follow-up study [10].

2.2.4. Detection of Cell Proliferation, Metastasis, and Invasion after Transfection. The transfected cells were inoculated into a 96-well plate and treated with FZYLf at different concentrations (100 mg crude drugs/mL, 50 mg crude drugs/mL, 25 mg crude drugs/mL, 12.5 mg crude drugs/mL, 6.25 mg crude drugs/mL, 3.125 mg crude drugs/mL, 1.56 mg crude drugs/mL, and 0.78 mg crude drugs/mL) on the next day. CCK-8 was added 72 h later to determine OD450 and calculate the inhibition rate and IC_{50} . Effect of FZYLf on in vitro cell proliferation activity, metastasis, and invasion of the human breast cancer cell line MDA-MB-231 and the drug-resistant cell line MDA-MB-231/Adr after transfection was investigated with CCK-8 kit and by Transwell assay.

Transwell method: the Transwell chamber coated with matrix gel was put into a culture plate; 300 μL prewarmed serum-free medium was added into the upper chamber and kept for 15~30 min at room temperature to rehydrate the matrix gel. The residual culture medium was removed. The cells were starved for 12 h and resuspended in serum-free medium containing BSA to make cell suspension. The cell density was adjusted to 1×10^5 cells/mL. 100 μL cell suspension was inoculated into the Transwell chamber and 500 μL of a medium containing FBS was added into the lower chamber for routine culture for 12~48 h. The matrix gel and cells in the upper chamber were wiped off with cotton swabs. The cells were stained with 0.1% crystal violet, and the number of cells passing through the membrane was counted under a microscope. The cells were decolorized with 33% acetic acid for complete elution of crystal violet. The

eluent was collected and OD value was determined at 570 nm to indirectly reflect the number of cells.

2.2.5. Model Establishment and Administration. The cell lines MDA-MB-231/Adr-siC in logarithmic growth phase and MDA-MB-231/Adr-si WAVE3 with low expression of WAVE3 were used for the experiment. Cell suspension was inoculated subcutaneously under the right armpit of nude mice at 5×10^6 cells/mice under sterile conditions. Diameter of the xenografted tumor was measured with a Vernier caliper. When the tumor grew to about 100 mm^3 , the tumor-bearing nude mice that grew well and showed uniformity in tumor size were selected and divided into four groups.

Group assignment: MDA-MB-231/Adr-siC xenografted tumor group, MDA-MB-231/Adr-siC xenografted tumor + FZYLf (13 g crude drugs/kg) group, MDA-MB-231/Adr-siWAVE3 xenografted tumor group, and MDA-MB-231/Adr-siWAVE3 xenografted tumor + FZYLf (13 g crude drugs/kg) group.

FZYLf was administered by gavage to mice in each group, once daily at a dosing volume of 0.1 mL/10 g body weight. The antitumor effect of the test article was observed dynamically by measuring the tumor diameter every other day. Body weight of the mice was measured while measuring tumor diameter. The mice were sacrificed at day 15. The tumor mass was surgically removed, weighted, and preserved in formalin.

Tumor volume (TV) was calculated as follows:

$$\text{TV} = \frac{1}{2} \times a \times b^2, \quad (1)$$

where a and b represent the length and width, respectively.

Relative tumor volume (RTV) was calculated based on the measurement results using the following formula: $\text{RTV} = V_t/V_0$, where V_0 is the tumor volume measured at dosing at cage assignment (d_0) and V_t is the tumor volume at each measurement. Antitumor activity was evaluated by relative tumor proliferation rate T/C (%) which was calculated as follows:

$$\frac{T}{C} (\%) = \frac{T_{\text{RTV}}}{C_{\text{RTV}}} \times 100, \quad (2)$$

where T_{RTV} is RTV in the treatment groups; C_{RTV} is RTV in the negative control groups.

2.2.6. Statistical Analysis. Data were expressed as mean \pm SD. The GraphPad Prism 5.0 software was used for statistical analysis. T-test was performed for comparison between two groups. $P < 0.05$ indicated statistical significance.

3. Results

3.1. Effect of FZYLF on Proliferation of the Human Breast Cancer Cell Line MDA-MB-231. Results (Figure 1) showed that FZYLF significantly inhibited proliferation of the human breast cancer cell line MDA-MB-231 ($P < 0.01$, or $P < 0.001$).

3.2. Gene Expression Level of WAVE3 in the Tumor Cells MCF-7, MCF-7/Taxol, MCF-7/Adr, MDA-MB-231, MDA-MB-231/Adr, and MDA-MB-231/Taxol. Results (Figure 2) showed that the expression level of WAVE3 was higher in the drug-resistant MDA-MB-231/Adr and MDA-MB-231/Taxol cells than in the nondrug-resistant MDA-MB-231 cells, and it was higher in the drug-resistant MCF-7/Adr and MCF-7/Taxol cells than in the nondrug-resistant MCF-7 cells. The expression level of WAVE3 was the highest in the MDA-MB-231/Adr cells.

3.3. mRNA and Protein Expression Levels of WAVE3 in the MDA-MB-231 and MDA-MB-231/Adr Cells after Transfection. Results (Figure 3) showed that the mRNA and protein expression levels of WAVE3 increased significantly in the MDA-MB-231 cells transfected with pcDNA3.1-WAVE3 plasmid ($P < 0.01$), and Figure 4 shows that the levels decreased significantly in the MDA-MB-231/Adr cells with WAVE3 knocked out ($P < 0.05$ or $P < 0.01$).

3.4. Changes in Proliferation Activity of the MDA-MB-231 and MDA-MB-231/Adr Cells before and after Transfection with Plasmid with High WAVE3 Expression or shRNA. Results (Figure 5) showed that proliferation activity of the MDA-MB-231 cells increased significantly after transfection with pcDNA3.1-WAVE3 plasmid ($P < 0.05$), and it decreased significantly in the MDA-MB-231/Adr cells with WAVE3 knocked out ($P < 0.05$).

3.5. Changes in Invasion Ability of the MDA-MB-231 and MDA-MB-231/Adr Cells before and after Transfection with Plasmid with High WAVE3 Expression or shRNA. Results (Figure 6) showed that invasion ability of the MDA-MB-231 cells increased significantly after transfection with pcDNA3.1-WAVE3 plasmid, and it decreased significantly in the MDA-MB-231/Adr cells with WAVE3 knocked out.

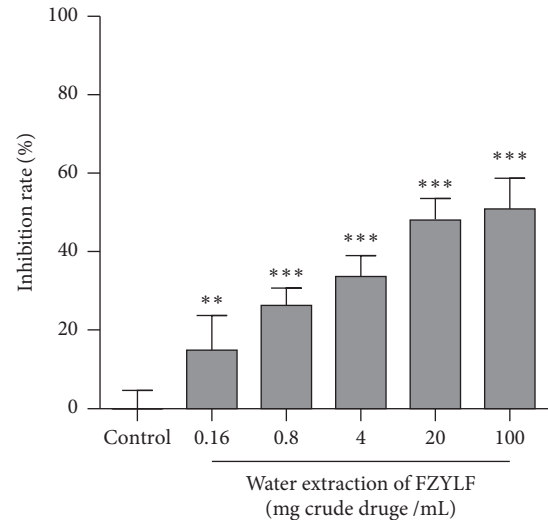


FIGURE 1: Effect of FZYLF on in vitro proliferation activity of the MDA-MB-231 human breast cancer cells. Compared with the control group, * $P < 0.05$, ** $P < 0.01$, and *** $P < 0.001$ (mean \pm SD, $n = 5$).

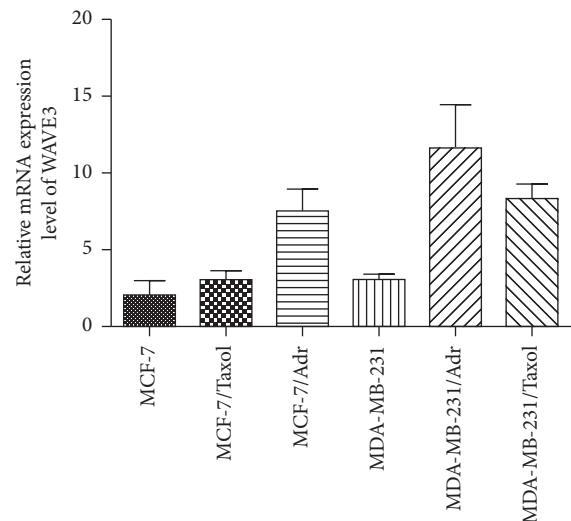


FIGURE 2: Relative expression level of WAVE3 gene in the tumor cells.

3.6. Effect of FZYLF on In Vitro Proliferation Activity of Human Breast Cancer Cells before and after WAVE3 Gene Silencing in Human Breast Cancer Cell Lines. Results (Figure 7) showed that the MDA-MB-231 cells transfected with pcDNA3.1-WAVE3 plasmid had an increased resistance to FZYLF, with increase of IC_{50} from 30.74 mg/mL to 61.05 mg/mL, and the MDA-MB-231/Adr cells with WAVE3 knocked out had significantly increased sensitivity to FZYLF, with decrease in IC_{50} from 71.04 mg/mL to 46.41 mg/mL ($P < 0.05$ or $P < 0.01$). FZYLF could reduce the invasion ability of the MDA-MB-231 and MDA-MB-231/Adr cells, and its intervention with the expression level of WAVE3 also had an

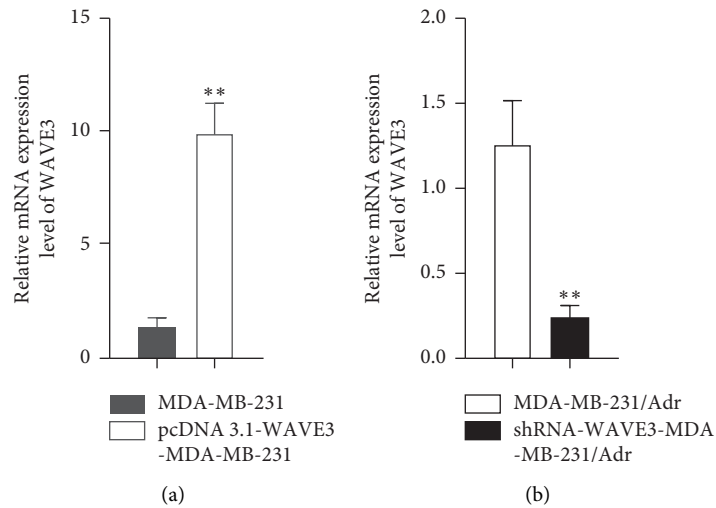


FIGURE 3: mRNA expression level of WAVE3 in the MDA-MB-231 and MDA-MB-231/Adr cells after transfection. Compared with the control group, ** $P < 0.01$.

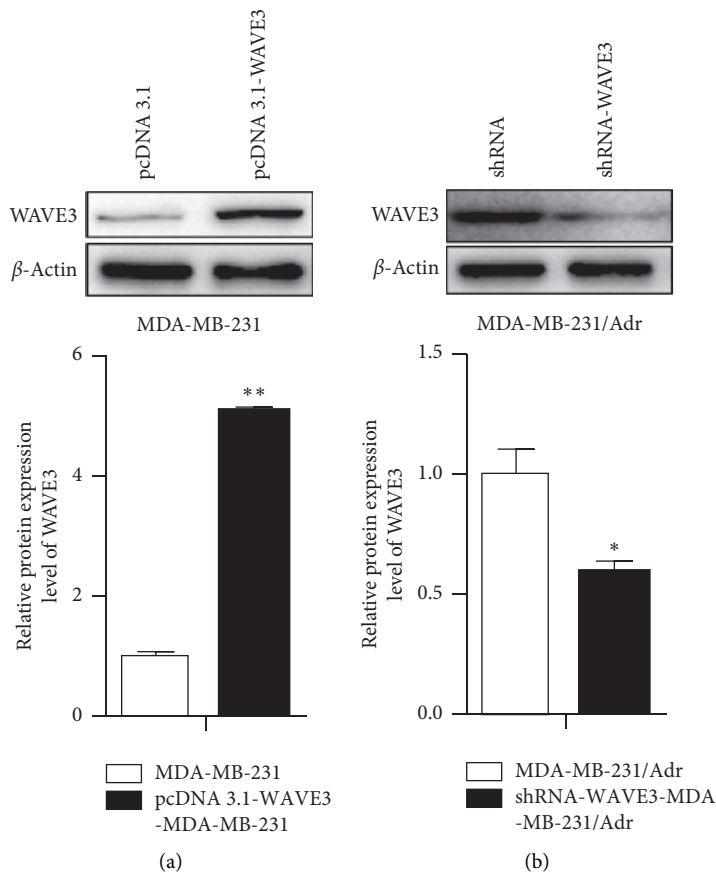


FIGURE 4: Protein expression level of WAVE3 in the MDA-MB-231 and MDA-MB-231/Adr cells after transfection. Compared with the control group, * $P < 0.05$ and ** $P < 0.01$.

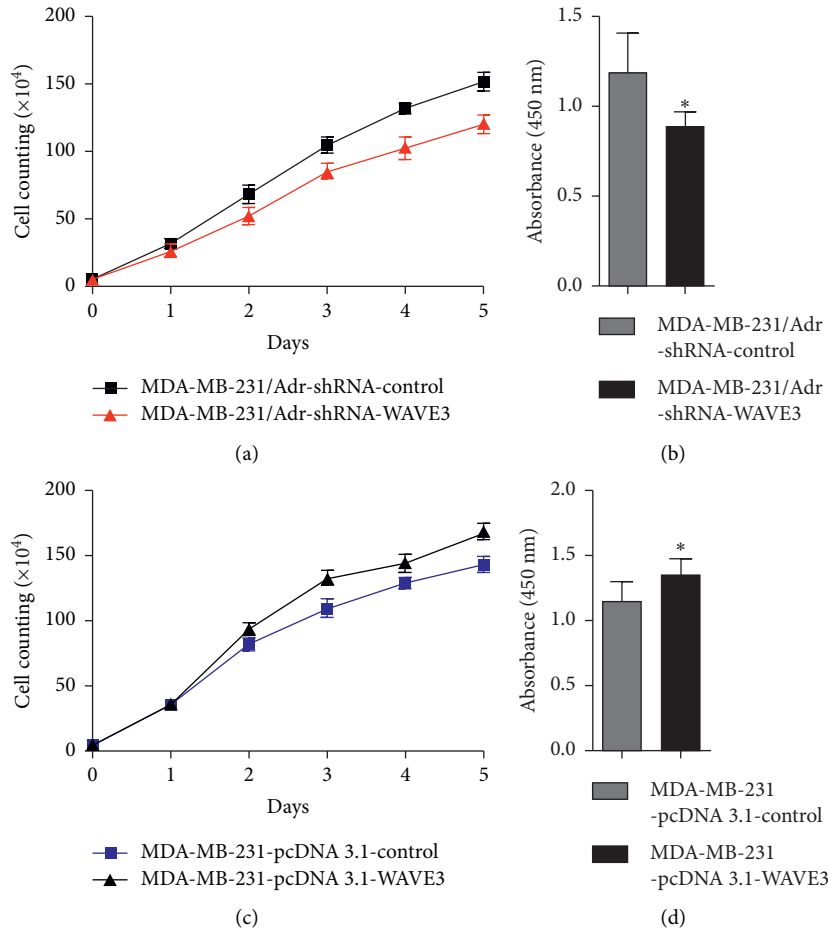


FIGURE 5: Changes of the number of the MDA-MB-231 and MDA-MB-231/Adr cells over time after transfection. Compared with the control group, * $P < 0.05$.

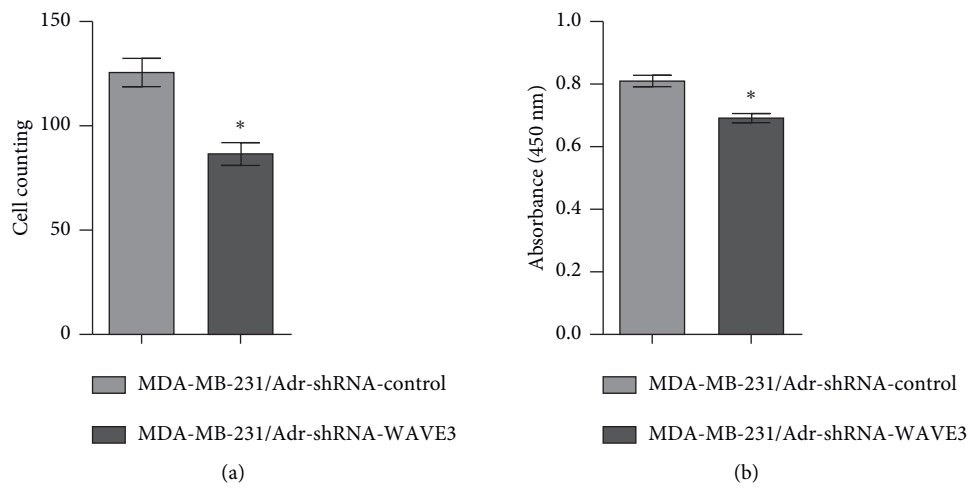


FIGURE 6: Continued.

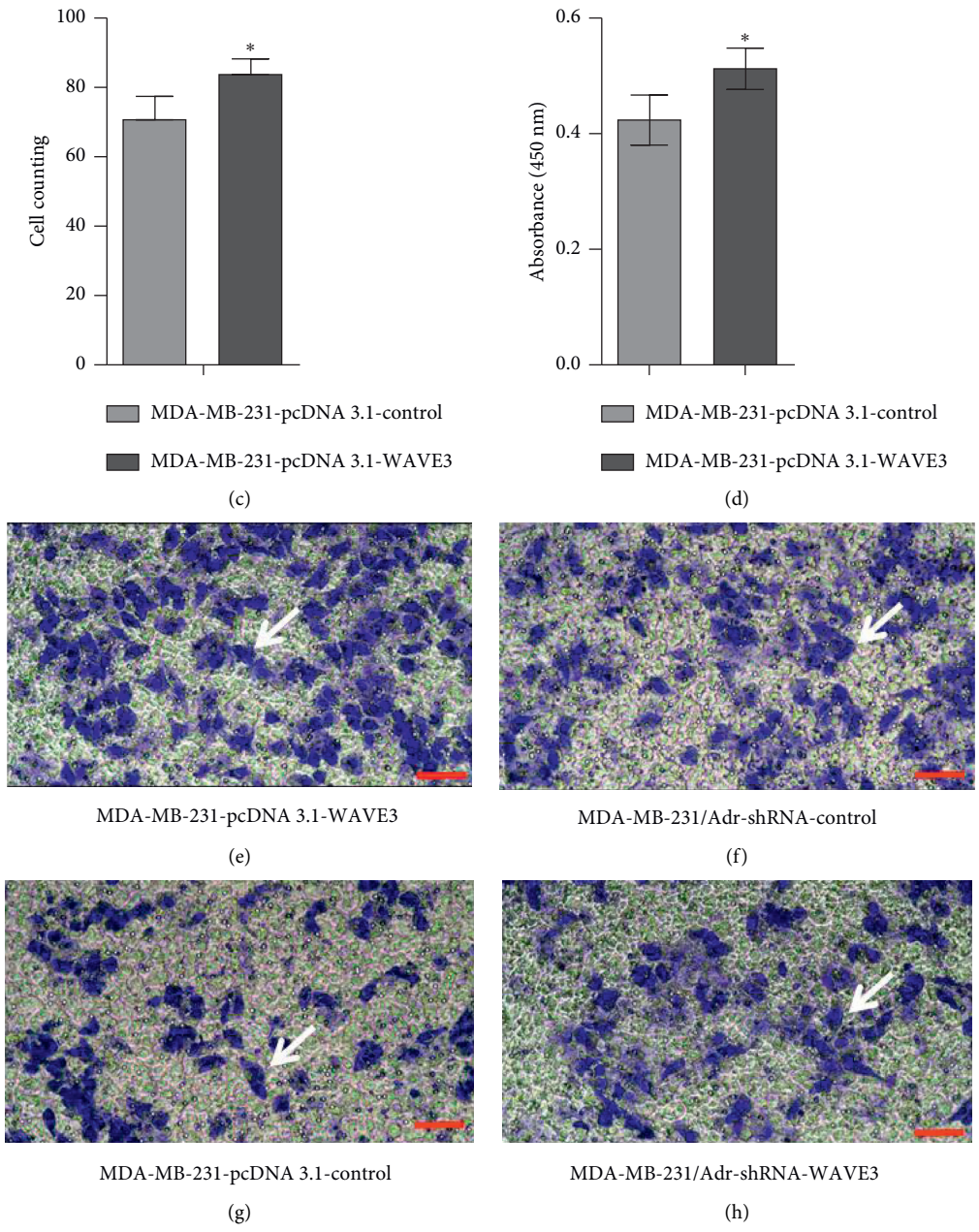


FIGURE 6: Changes in invasion ability of the MDA-MB-231 and MDA-MB-231/Adr cells after transfection. Compared with the control group, * $P < 0.05$ and ** $P < 0.01$. The magnification of the photomicrograph is 300 times.

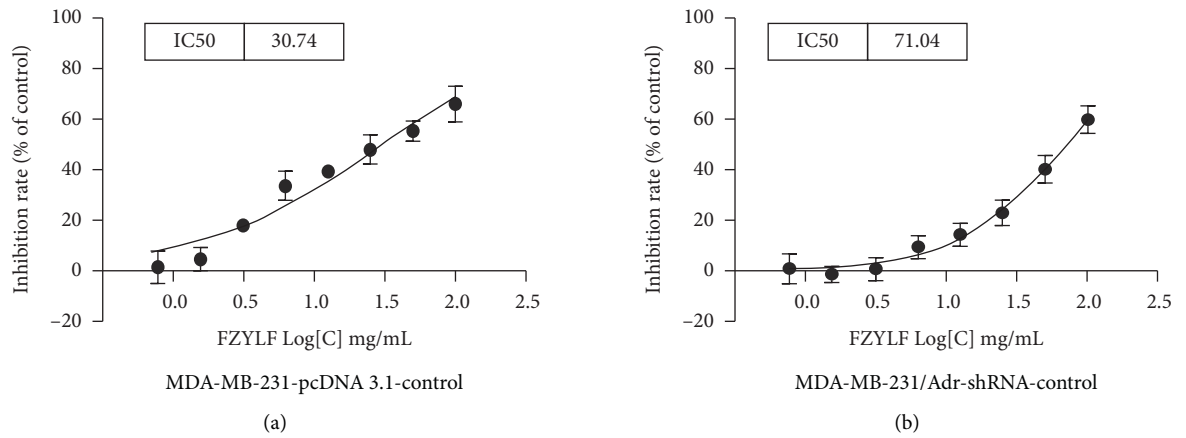


FIGURE 7: Continued.

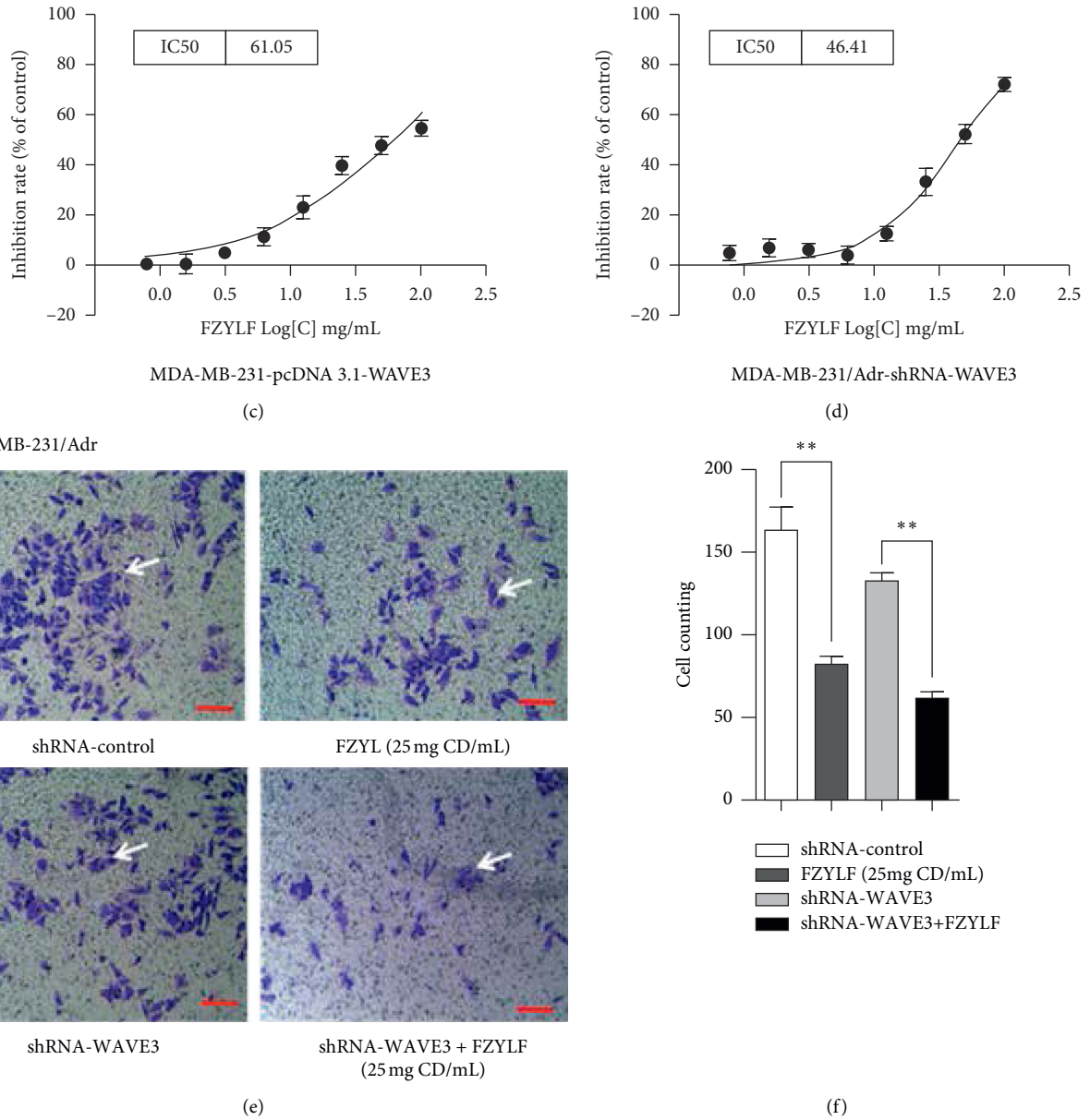


FIGURE 7: Effect of FZYLf on in vitro invasion ability of the drug-resistant human breast cancer cells before and after WAVE3 gene silencing. Compared with the control group, * $P < 0.05$ and ** $P < 0.01$. The magnification of the photomicrograph is 300 times.

effect on the invasion ability of the cells ($P < 0.05$ or $P < 0.01$).

3.7. Effect of FZYLf on Protein Expression of WAVE3, IκBα, NF-κB, and MMP-9 in Human Breast Cancer Cells before and after WAVE3 Gene Silencing in Drug-Resistant Human Breast Cancer Cell Lines. Results (Figure 8) showed that the MDA-MB-231/Adr cells with WAVE3 knocked out were more sensitive to regulation by FZYLf, which could significantly inhibit the protein expression levels of WAVE3, MMP-9, p-IκBα, and NF-κB (p65) ($P < 0.05$ or $P < 0.01$), but FZYLf had no significant effect on the protein expression level of

t-IκBα. GAPDH was the internal reference for cytoplasmic proteins and H3 for nuclear proteins.

3.8. Effect of FZYLf on MDA-MB-231/Adr and MDA-MB-231/Adr-siRNA WAVE3 Xenografted Tumor. The cell lines MDA-MB-231/Adr-siC and MDA-MB-231/Adr-siWAVE3 with low WAVE3 expression were inoculated into nude mice under the armpit, and the test article FZYLf (13 g crude drugs) was administered by gavage for 15 days consecutively. Results (Figures 9–13) showed that at day 9 of administration, FZYLf significantly reduced the tumor volume compared to the volume of the MDA-MB-231/Adr-siC

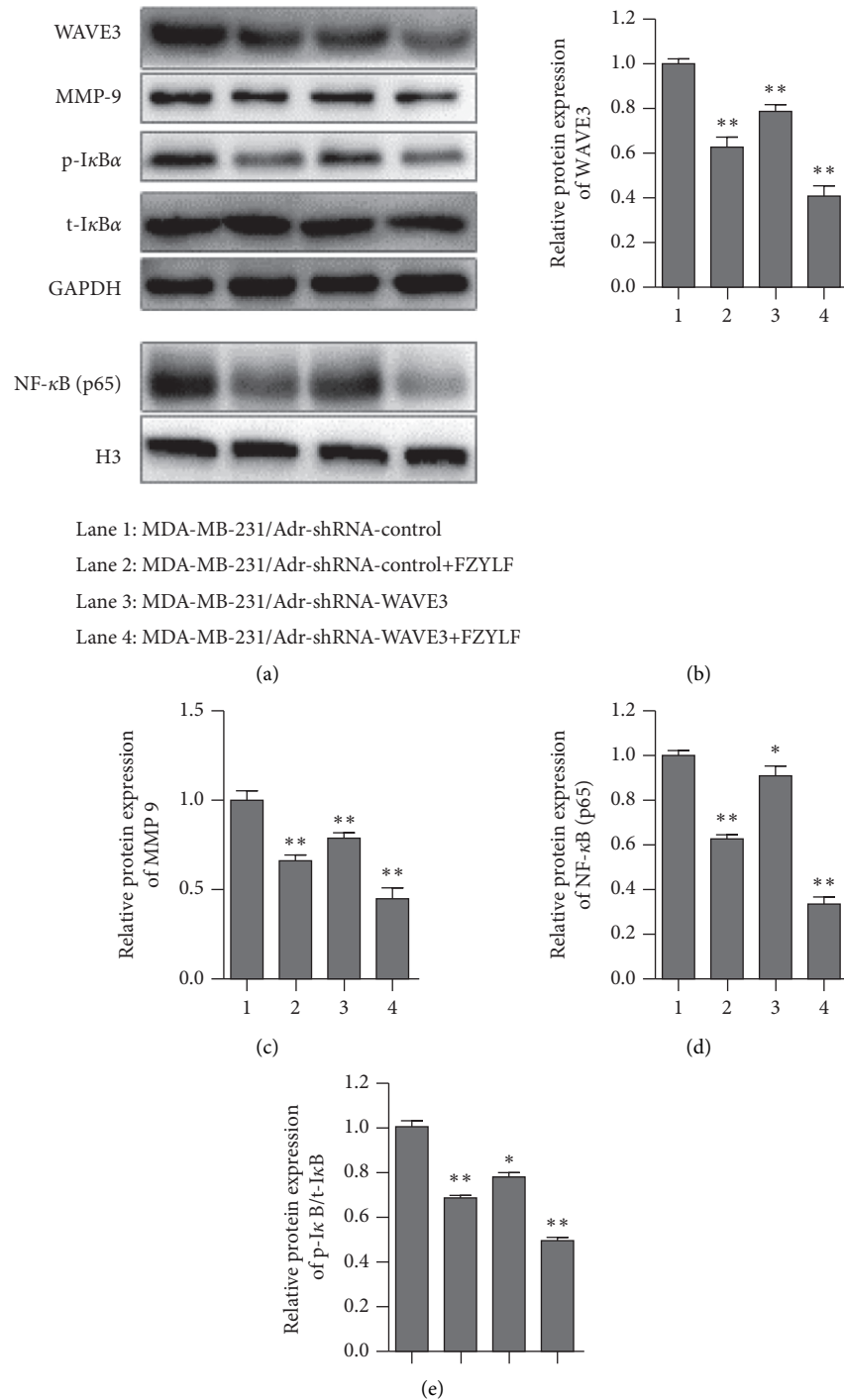


FIGURE 8: Effect of FZYLF on protein expression of WAVE3, IκBα, NF-κB, and MMP-9 in human breast cancer cells before and after WAVE3 gene silencing (FZYLF 20 mg crude drugs/mL). Compared with the control group, * $P < 0.05$ and ** $P < 0.01$.

xenografted tumor ($P < 0.05$). At day 15, compared to the MDA-MB-231/Adr-siC xenografted tumor group, T/C (%) was 52.29%, 71.74%, and 33.40% in the MDA-MB-231/Adr-siC + FZYLF, MDA-MB-231/Adr-siWAVE3, and MDA-

MB-231/Adr-siWAVE3+FZYLF groups, respectively, and the tumor inhibition rate was 41.92%, 23.81%, and 64.87% in the MDA-MB-231/Adr + FZYLF, MDA-MB-231/Adr-siWAVE3, and MDA-MB-231/Adr-siWAVE3+FZYLF groups,

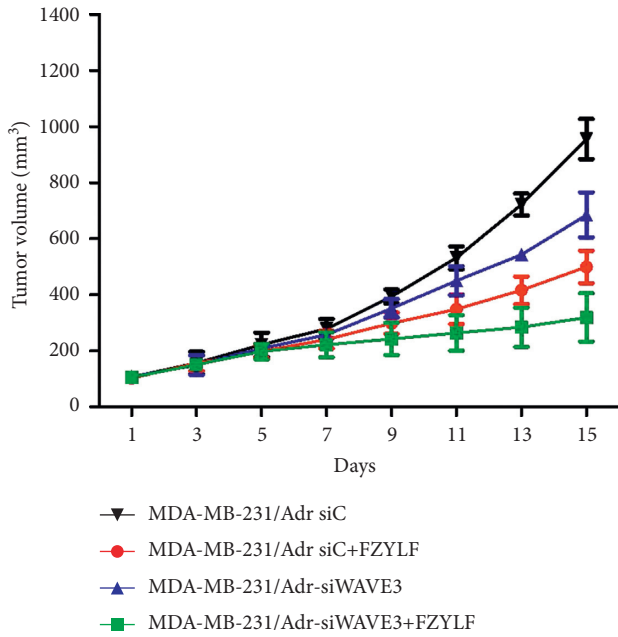


FIGURE 9: Effect of FZYLF on growth volume of xenografted tumor of the adriamycin-resistant human breast cancer cell line MDA-MB-231/Adr in nude mice.

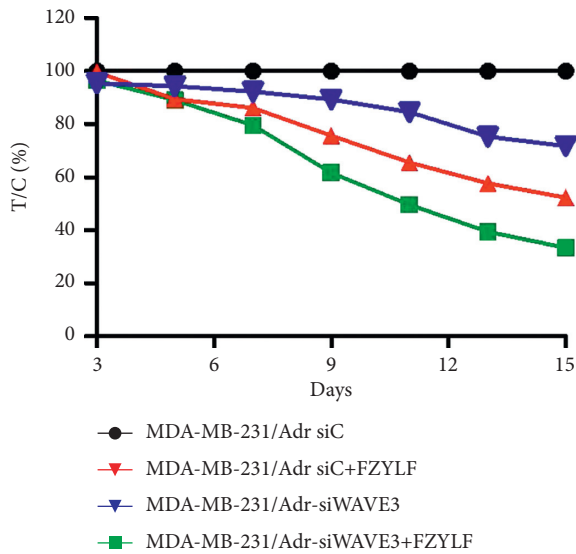


FIGURE 10: Effect of FZYLF on relative proliferation rate of xenografted tumor of adriamycin-resistant human breast cancer cell lines in nude mice.

respectively. FZYLF (13 g crude drugs/kg) had a T/C (%) of 62.06% and a tumor inhibition rate of 39.64% for MDA-MB-231/Adr xenografted tumor in nude mice.

4. Discussion

As a highly heterogeneous tumor, breast cancer is a heterogeneous disease composed of different solid tissues with different gene expression patterns and its heterogeneity may be caused by different types of gene mutation of normal

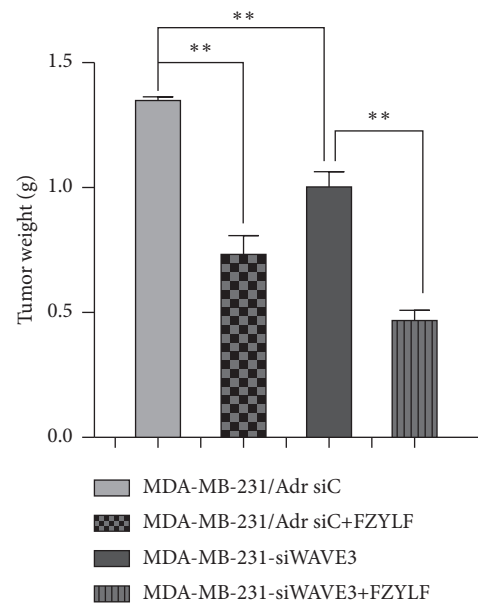


FIGURE 11: Effect of FZYLF on tumor weight of xenografted tumor of adriamycin-resistant human breast cancer cell lines in nude mice. Compared with the MDA-MB-231/Adr-siC group, * $P < 0.05$ and ** $P < 0.01$.

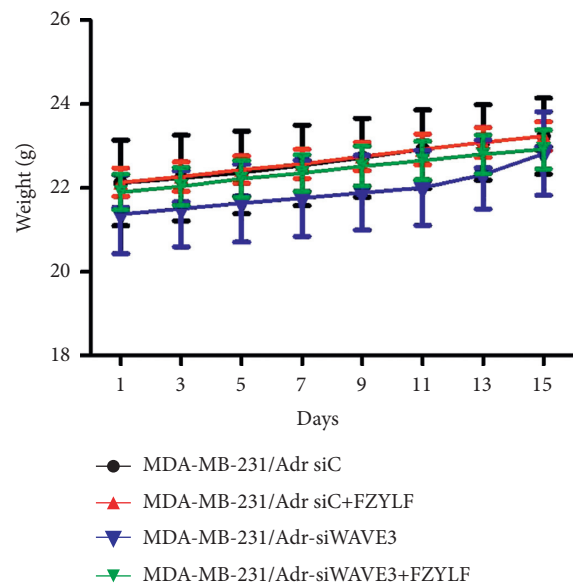


FIGURE 12: Effect of FZYLF on body weight of the nude mice bearing xenografted tumor of adriamycin-resistant human breast cancer cell lines.

epithelial cells of the breast that result in different groups of tumor cells. Through analysis of the molecular markers by immunohistochemistry, breast cancer is classified into four types based on different expressions of estrogen receptor (ER), progesterone receptor (PR), human epidermal growth factor receptor-2 (HER-2), and Ki67 index [19–21]. In TNBC, there is the absence of expression of the three receptors ER, PR, and HER-2, so TNBC is not sensitive to

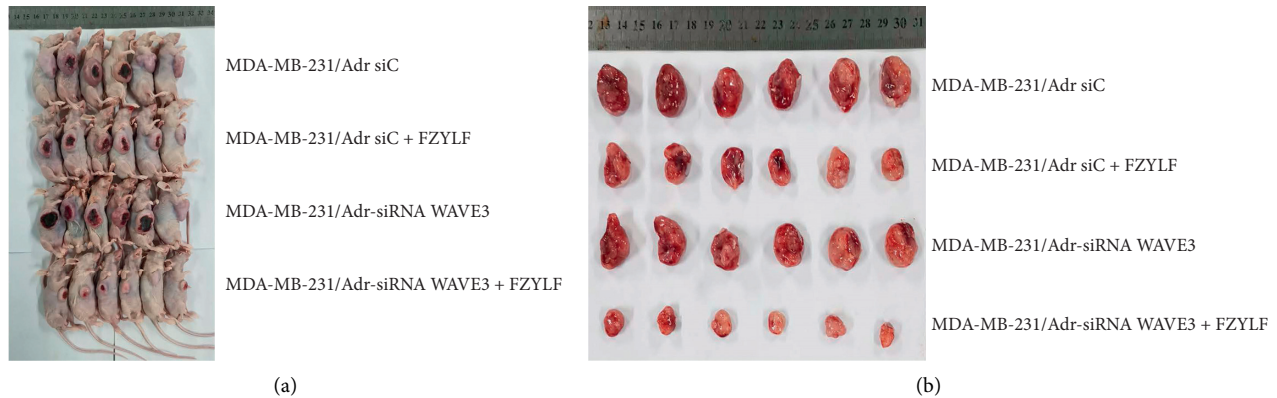


FIGURE 13: Tumor-bearing nude mice in each group and size of tumor.

standard targeted therapies against breast cancer. Breast cancer of different types has different histopathological, molecular, and clinical features and requires different treatment methods. In Western countries, patients with TNBC account for 12~17% of those with breast cancer, and the incidence rate of TNBC in Asian women is quite similar to that in white women. TNBC has the clinical features of high invasiveness, common local recurrence, and distant metastasis, and it has an obviously poor prognosis compared to the other types of breast cancer [22–24]. Currently, radiotherapy and chemotherapy are still the main treatments for breast cancer. High risk of relapse and metastasis and high mortality of TNBC require more research to improve the prognosis of this special type of breast cancer. Multidrug resistance of tumor is the main cause of chemotherapy failure, and the main mechanism of MDR involves reduced cellular uptake of drugs, increased cellular efflux of drugs, changes in apoptosis-related pathways, changes in drug-targeting molecules, enhanced DNA repair mechanism, increased activity of drug-metabolizing enzymes, etc. [25]. Therefore, it is important to further understand the processes of invasion and metastasis and find out the mechanism of action in invasion and metastasis of multidrug-resistant human breast cancer cells.

WAVE3 is a new actin-regulatory protein and its absence causes cellular abnormality in structure, migration, and invasion [26]. The NF- κ B pathway is an important mechanism in WAVE3-mediated cell migration, and Teng et al. [27] have found out that WAVE3 gene knockout in breast cancer cells can lead to decrease in MMP-9 and inhibit the activation and nuclear transport of NF- κ B. The expression of WAVE3 is positively correlated with the extent of tumor invasion and progression and negatively correlated with clinic pathological parameters of tumor [6].

Breast cancer metastasis causes high economic burden to patients. Metastasis is an intrinsic feature of biological behavior of malignant tumor and also one of the root causes of treatment failure. TCM has unique advantages in the prevention of tumor recurrence and metastasis and the development of clinically effective Chinese compound formulas provides support for solving this clinical problem. According to TCM, “deficiency of healthy qi” is the ultimate

cause of occurrence and development of tumor and it is present through the course of disease. Insufficiency of healthy qi is the pathological basis of tumor occurrence and deficiency is the root cause of disease. Reinforcing healthy qi is an essential approach in tumor treatment. Many studies have demonstrated that this treatment approach can not only improve the quality of life of patients with malignant tumor and reduce the adverse reactions of radiotherapy and chemotherapy but also optimize the therapeutic effect of chemotherapy through combined use with chemotherapy, and this approach can also prolong the progression-free survival and overall survival of patients [28–30]. FZYLf is a prescription used commonly in our department to treat deficiency of both qi and yin after breast cancer surgery and radiotherapy and chemotherapy. Breast cancer is a disease of root (actual) deficiency and branch (seeming) excess, or specifically, deficiency resulted from deficiency and concurrent deficiency and excess. Root deficiency occurs mainly in the liver, spleen, and kidney, and branch excess is mainly qi stagnation, blood stasis, phlegm turbidity, and heat toxin. Internal deficiency of healthy qi and yin-yang disharmony in Zang-Fu organs are the basis and the seven emotions and internal damage are the important factors in occurrence of breast cancer. FZYLf improves the quality of life of breast cancer patients and reduces the adverse reactions of surgery, chemotherapy, and radiotherapy.

WAVE3 had different expression levels in different drug-resistant breast cancer cells: the expression of WAVE3 was higher in the drug-resistant MDA-MB-231/Adr and MDA-MB-231/Taxol cells than in the nondrug-resistant MDA-MB-231 cells, and it was higher in the drug-resistant MCF-7/Adr and MCF-7/Taxol cells than in the nondrug-resistant MCF-7 cells. The expression of WAVE3 was the highest in the MDA-MB-231/Adr cells. It was indicated in the cell transfection experiment in the present study that the mRNA and protein expression levels of WAVE3 increased significantly in the MDA-MB-231 cells transfected with pcDNA3.1-WAVE3 plasmid, and the levels decreased significantly in the MDA-MB-231/Adr cells with WAVE3 knocked out. Experiments funded by the National Natural Science Foundation of China (NSFC) and conducted in our hospital have demonstrated that the expression level of

WAVE3 increases significantly in the tissues of breast carcinoma *in situ* and the expression level of WAVE3 is also higher in the tissues of invasive breast carcinoma than in those of breast carcinoma *in situ*. These results suggest that WAVE3 is correlated to the proliferation and invasion of breast cancer. This correlation is confirmed clinically and cellularly.

In the *in vitro* experiment, intervention with FZYL F reduced the invasion ability of the MDA-MB-231 cells transfected with pcDNA3.1-WAVE3 plasmid and the MDA-MB-231/Adr cells with WAVE3 knocked out. In the *in vivo* experiment, FZYL F (13 g crude drugs/kg) showed a T/C (%) of 62.06% and a tumor inhibition rate of 39.64% for the MDA-MB-231/Adr xenografted tumor in nude mice and could significantly inhibit the growth of the xenografted tumor. It can be seen from the changes in tumor weight and growth volume of the drug-resistant human breast cancer cell line MDA-MB-231/Adr xenografted tumor in nude mice that FZYL F inhibits the proliferation and metastasis of the MDA-MB-231/Adr cells.

It was demonstrated in the mechanism study that FZYL F could significantly inhibit the protein expression levels of WAVE3, MMP-9, p-I κ B α , and NF- κ B (p65), but it had no significant effect on the protein expression level of t-IkBa. So, it is deduced that FZYL F may inhibit the MDA-MB-231/Adr cells through regulation of WAVE3, by influencing the protein expression of MMP-9, p-I κ B α , and NF- κ B (p65). MMP-9, p-I κ B α , and NF- κ B (p65) have a certain relationship with the invasion and metastasis of breast cancer, and further study is needed to find out the pathway(s) through which they work.

5. Conclusion

This study explores the mechanism of action of FZYL F in regulation of the invasion and metastasis of the MDA-MB-231/Adr human breast cancer cells through WAVE3. The effect of FZYL F on proliferation and invasion of the cells before and after WAVE3 knockout is investigated by Transwell assay, PCR, WB, and flow cytometry. The antitumor activity of FZYL F is studied by establishing a xenografted tumor in nude mice. It is revealed that FZYL F significantly inhibits the invasion and metastasis of the multidrug-resistant breast cancer cells MDA-MB-231/Adr and the mechanism of action may be related to its inhibition of the abnormal protein expression of WAVE3 gene, MMP-9, p-I κ B α , and NF- κ B (p65). That FZYL F regulating the invasion and metastasis of human breast cancer cells through WAVE3 is a complex process which involves many proteins and pathways, the specific links in mediation of cell metastasis mechanism by FZYL F are still unclear, and further experiment is needed in the future to verify the effect of FZYL F and the related mechanism.

Data Availability

All data used during the study are available from the corresponding author.

Conflicts of Interest

The authors declare that they have no conflicts of interest.

Authors' Contributions

Wen-li Chen and Huan-huan Bai contributed equally to this work and should be considered co-first authors. Xiao-jun Gou and Jun Qian contributed equally to this work and should be considered co-corresponding authors.

Acknowledgments

This study was financially supported by Shanghai Baoshan District Science and Technology Commission Science and Technology Innovation Special Fund Project (no. 16-E-15) and Natural Resources Fund Breeding Project of Baoshan District Hospital of Integrated Traditional Chinese and Western Medicine of Shanghai (no. GZRPYJ-201704).

Supplementary Materials

Quality control of Fuzheng Yiliu formula . Figure S1: HPLC chromatogram of asiatic acid reference substance. Figure S2: HPLC chromatogram of Fuzheng Yiliu formula. Figure S3: HPLC chromatogram of Maorenshen (*Actinidia valvata* Dunn, MRS) negative sample. (*Supplementary Materials*)

References

- [1] J. Ferlay, M. Colombet, I. Soerjomataram et al., "Estimating the global cancer incidence and mortality in 2018: GLOBOCAN sources and methods," *International Journal of Cancer*, vol. 144, no. 8, pp. 1941–1953, 2019.
- [2] G. J. Morris, S. Naidu, A. K. Topham et al., "Differences in breast carcinoma characteristics in newly diagnosed African-American and Caucasian patients," *Cancer*, vol. 110, no. 4, pp. 876–884, 2007.
- [3] R. Ao, Z. X. Qiang, and L. Hao, "Relationship between pathological staging and prognosis of triple negative breast cancer," *Cancer Clinical and Rehabilitation in China*, vol. 24, no. 11, pp. 1301–1303, 2017.
- [4] X. W. Zheng, S. Y. Chen, W. P. Zhng, and Y. L. Dong, "Research Progress on mechanism and reversal strategy of multidrug resistance in breast cancer," *Chinese Pharmacy*, vol. 26, no. 20, pp. 2864–2867, 2015.
- [5] J. B. Maxhimer, R. M. Quiros, R. Stewart et al., "Heparanase-1 expression is associated with the metastatic potential of breast cancer," *Surgery*, vol. 132, no. 2, pp. 326–333, 2002.
- [6] K. Swati, A. Katarzyna, R. Louis et al., "Increased expression levels of WAVE3 are associated with the progression and metastasis of triple negative breast cancer," *PLoS One*, vol. 7, no. 8, Article ID e42895, 2012.
- [7] M. A. Taylor, G. Davuluri, J. G. Parvani et al., "Upregulated WAVE3 expression is essential for TGF- β -mediated EMT and metastasis of triple-negative breast cancer cells," *Breast Cancer Research and Treatment*, vol. 142, no. 2, pp. 341–353, 2013.
- [8] S.-A. Khalid, S. Alfiya, and L. Xiurong, "Down-regulation of WAVE3, a metastasis promoter gene, inhibits invasion and

- metastasis of breast cancer cells,” *The American Journal of Pathology*, vol. 170, no. 6, pp. 2112–2121, 2007.
- [9] D. Gangarao, W. P. Schiemann, E. F. Plow, and S.-A. Khalid, “Loss of WAVE3 sensitizes triple-negative breast cancers to chemotherapeutics by inhibiting the STAT-HIF-1 α -mediated angiogenesis,” *JAK-STAT*, vol. 3, no. 4, Article ID e1009276, 2015.
- [10] X.-j. Gou, H.-h. Bai, L.-w. Liu et al., “Asiatic acid interferes with invasion and proliferation of breast cancer cells by inhibiting WAVE3 activation through PI3K/AKT signaling pathway,” *BioMed Research International*, vol. 2020, Article ID 41874387, 12 pages, 2020.
- [11] M. Christine, H. Alexandra, M. Erin, and R. Sophia, “Tumor cell-produced matrix metalloproteinase 9 (MMP-9) drives malignant progression and metastasis of basal-like triple negative breast cancer,” *Oncotarget*, vol. 5, no. 9, pp. 2736–2749, 2014.
- [12] S. Zhao, W. Ma, M. Zhang et al., “High expression of CD147 and MMP-9 is correlated with poor prognosis of triple-negative breast cancer (TNBC) patients,” *Medical Oncology*, vol. 30, no. 1, p. 335, 2013.
- [13] F. Hossain, C. Sorrentino, D. A. Ucar et al., “Notch signaling regulates mitochondrial metabolism and NF- κ B activity in triple-negative breast cancer cells via ikk α -dependent non-canonical pathways,” *Frontiers in Oncology*, vol. 8, p. 575, 2018.
- [14] A. A. A. El-Hafeez, H. O. Khalifa, E. A. M. Mahdy et al., “Anticancer effect of nor-wogonin (5, 7, 8-trihydroxyflavone) on human triple-negative breast cancer cells via down-regulation of TAK1, NF- κ B, and STAT3,” *Pharmacological Reports*, vol. 71, no. 2, pp. 289–298, 2019.
- [15] R. F. Zhou and P. X. Liu, “Research Progress on reversal of multidrug resistance of breast cancer by traditional Chinese Medicine,” *Chinese Journal of Traditional Chinese Medicine*, no. 22, pp. 77–80, 2005.
- [16] B. Guo, S. Liu, Y. Y. Ye, and X. H. Han, “Effects of osthole, psoralen, aconitine on breast cancer MDA-MB-231BO cell line inhibition in vitro,” *Journal of Chinese Integrative Medicine*, vol. 9, no. 10, pp. 1110–1117, 2011.
- [17] W. L. Chen, L. M. Zhang, Q. Shi, X. F. Zhou, and H. Y. Chen, “Clinical observation of Fuzheng Yiliu decoction combined with psychological intervention on emotion of breast cancer patients,” *World Traditional Chinese Medicine*, vol. 11, no. 6, pp. 986–992, 2016.
- [18] W. L. Chen and L. M. Zhang, “Fuzheng Yiliu decoction combined with psychological intervention to improve the quality of life of patients with advanced breast cancer,” *Jilin Traditional Chinese Medicine*, vol. 36, no. 8, pp. 802–807, 2016.
- [19] J.-J. Hao, T. Gong, Y. Zhang et al., “Characterization of gene rearrangements resulted from genomic structural aberrations in human esophageal squamous cell carcinoma KYSE150 cells,” *Gene*, vol. 513, no. 1, pp. 196–201, 2013.
- [20] L. V. Rhodes, C. R. Tate, V. T. Hoang et al., “Regulation of triple-negative breast cancer cell metastasis by the tumor-suppressor liver kinase B1,” *Oncogenesis*, vol. 4, no. 10, p. e168, 2015.
- [21] C. M. Perou, T. Sorlie, M. B. Eisen et al., “Molecular portraits of human breast tumours,” *Nature*, vol. 406, no. 6797, pp. 747–752, 2000.
- [22] R. L. Siegel, K. D. Miller, and A. Jemal, “Cancer statistics, 2017,” *CA: A Cancer Journal for Clinicians*, vol. 67, no. 1, pp. 7–30, 2017.
- [23] L. Fan, K. Strasser-Weippl, J.-J. Li et al., “Breast cancer in China,” *The Lancet Oncology*, vol. 15, no. 7, pp. e279–e289, 2014.
- [24] A. Giordano, M. Giuliano, M. De Laurentiis et al., “Circulating tumor cells in immunohistochemical subtypes of metastatic breast cancer: lack of prediction in HER2-positive disease treated with targeted therapy,” *Annals of Oncology*, vol. 23, no. 5, pp. 1144–1150, 2012.
- [25] Q. L. Yu and R. G. Sa, “Current situation of anti-tumor metastasis treatment with traditional Chinese Medicine,” *Jilin Traditional Chinese Medicine*, vol. 30, no. 5, pp. 456–458, 2010.
- [26] M. Binks, G. E. Jones, P. M. Brickell, C. Kinnon, D. R. Katz, and A. J. Thrasher, “Intrinsic dendritic cell abnormalities in Wiskott-Aldrich syndrome,” *European Journal of Immunology*, vol. 28, no. 10, pp. 3259–3267, 1998.
- [27] Y. Teng, M. Liu, and J. K. Cowell, “Functional interrelationship between the WASF3 and KISS1 metastasis-associated genes in breast cancer cells,” *International Journal of Cancer*, vol. 129, no. 12, pp. 2825–2835, 2011.
- [28] H. L. Li and G. Z. Sun, “Sun Guizhi’s theory on the etiology and pathogenesis of malignant tumor,” *Chinese Journal of Traditional Chinese Medicine Information*, vol. 17, no. 1, pp. 88–89, 2010.
- [29] X. J. Lin, G. R. Dan, H. L. Situ, and Y. Lin, “Immunotherapy mechanism of traditional Chinese medicine reinforcing the body method in preventing malignant tumor metastasis,” *Clinical Research of Traditional Chinese Medicine*, vol. 7, no. 24, pp. 22–24, 2015.
- [30] S. L. Wu and Z. H. Xu, “Progress in principles and methods of traditional Chinese medicine for malignant tumor in recent ten years,” *Journal of Traditional Chinese Medicine Literature*, vol. 36, no. 3, pp. 69–72, 2018.

Research Article

A Network Pharmacology Study on the Molecular Mechanisms of FDY003 for Breast Cancer Treatment

Ho-Sung Lee,^{1,2} In-Hee Lee,¹ Kyungrae Kang,² Sang-In Park,³ Seung-Joon Moon,² Chol Hee Lee,² and Dae-Yeon Lee ^{1,2}

¹The Fore, 87 Ogeum-ro, Songpa-gu, Seoul 05542, Republic of Korea

²Forest Hospital, 129 Ogeum-ro, Songpa-gu, Seoul 05549, Republic of Korea

³Forestheal Hospital, 173 Ogeum-ro, Songpa-gu, Seoul 05641, Republic of Korea

Correspondence should be addressed to Dae-Yeon Lee; foresthrnd@gmail.com

Received 29 May 2020; Revised 25 January 2021; Accepted 29 January 2021; Published 6 February 2021

Academic Editor: Azis Saifudin

Copyright © 2021 Ho-Sung Lee et al. This is an open access article distributed under the Creative Commons Attribution License, which permits unrestricted use, distribution, and reproduction in any medium, provided the original work is properly cited.

Herbal medicines have drawn considerable attention with regard to their potential applications in breast cancer (BC) treatment, a frequently diagnosed malignant disease, considering their anticancer efficacy with relatively less adverse effects. However, their mechanisms of systemic action have not been understood comprehensively. Based on network pharmacology approaches, we attempted to unveil the mechanisms of FDY003, an herbal drug comprised of *Lonicera japonica* Thunberg, *Artemisia capillaris* Thunberg, and *Cordyceps militaris*, against BC at a systemic level. We found that FDY003 exhibited pharmacological effects on human BC cells. Subsequently, detailed data regarding the biochemical components contained in FDY003 were obtained from comprehensive herbal medicine-related databases, including TCMSP and CancerHSP. By evaluating their pharmacokinetic properties, 18 chemical compounds in FDY003 were shown to be potentially active constituents interacting with 140 BC-associated therapeutic targets to produce the pharmacological activity. Gene ontology enrichment analysis using g:Profiler indicated that the FDY003 targets were involved in the modulation of cellular processes, involving the cell proliferation, cell cycle process, and cell apoptosis. Based on a KEGG pathway enrichment analysis, we further revealed that a variety of oncogenic pathways that play key roles in the pathology of BC were significantly enriched with the therapeutic targets of FDY003; these included PI3K-Akt, MAPK, focal adhesion, FoxO, TNF, and estrogen signaling pathways. Here, we present a network-perspective of the molecular mechanisms via which herbal drugs treat BC.

1. Introduction

Breast cancer (BC) is a common female malignancy and a cause of mortality globally [1]. The genetic and epigenetic dysregulations in multiple cancer-associated genes and their key oncogenic signalings are implicated in the pathology of BC; these include the phosphoinositide 3-kinase- (PI3K-) Akt, tumor necrosis factor (TNF), forkhead box O (FoxO), erythroblastic leukemia viral oncogene homolog (ErbB), vascular endothelial growth factor (VEGF), hypoxia-inducible factor- (HIF-) 1, estrogen, p53, focal adhesion, and mitogen-activated protein kinase (MAPK) pathways [2–4]. Currently, chemotherapy, molecular-targeted therapy, and endocrine therapy are the major pharmacological

approaches for BC treatment [5–10]. However, the long-term and frequent use of the aforementioned therapeutic drugs may induce toxic events that deteriorate quality of life of cancer patients, including gastrointestinal dysfunction, fatigue, peripheral neuropathy, immunosuppression and myelosuppression, cardiotoxicity, and osteoporosis [11–18]. In addition, the pharmacological efficacy of most molecular-targeted agents often falls short of expectations because of their limited capacity to therapeutically modulate the cancerous activities of various oncogenic cellular components [19]. These issues emphasize the need for anticancer agents that can pharmacologically regulate multiple oncogenes and pathways with safety. Herbal drugs are multicomponent therapeutics that elicit their pharmacological effects via

multiple chemical compounds that target diverse disease-related genes, proteins, and pathways [20, 21]. Herbal medicines have attracted much attention due to their promising anticancer effects, reduced toxicities, and lower side effects [20, 21]. Previous clinical research studies have further shown that the use of herbal drugs can improve the tumor response, survival, health status, and quality of life of patients undergoing cancer therapy [22, 23].

FDY003 is an herbal formula composed of three herbal medicines [24, 25], namely, *Lonicera japonica* Thunberg (LjT), *Artemisia capillaris* Thunberg (AcT), and *Cordyceps militaris* (Cm), that have been reported to exert prominent anticancer effects in various cancer types [26–35]. It has been shown that FDY003 is a potent inhibitor of proliferation while promoting the apoptotic death of cancer cells and tumors [24, 25]. These activities involve regulation of key modulators of cell cycle and apoptosis, such as p53, p21, caspase-3, and Bcl-2-associated X protein (Bax) [24]. However, the molecular mechanisms of FDY003 against BC at the systemic level remain unclear.

Network pharmacology is a multidisciplinary research approach that uncovers complex disease mechanisms and can be used to formulate promising treatment strategies based on a systems perspective [36–39]. The interdisciplinary methodology integrates diverse scientific fields, such as medicine, pharmacology, network biology, systems biology, and computer science [36–39]. Network pharmacology has been demonstrated to be an efficient tool for the acquisition of comprehensive and systematic insights into the “multicomponent, multitarget, multipathway” polypharmacological properties of herbal medicines, and it is extensively used to explore the active chemical compounds of herbal drugs and their therapeutic targets responsible for their pharmacological activities [36–39]. Network pharmacology investigates how associated systematic mechanisms are regulated through interactions among various key components and targets [36–39]. Here, we attempted to unravel the molecular mechanisms of anti-BC effects of FDY003 based on network pharmacology approaches.

2. Materials and Methods

2.1. Cell Culture. The MCF-7, MDA-MB-453, and MDA-MB-231 human BC cell lines were purchased from the Korean Cell Line Bank (Seoul, Korea). The cells were cultured in Dulbecco's Modified Eagle's Medium (DMEM, WELGENE Inc., Daegu, Korea) supplemented with 10% fetal bovine serum, 100 U/mL penicillin, and 100 μ g/mL streptomycin (Thermo Fisher Scientific Inc., Waltham, MA, USA). The cultured cells were maintained in a humidified atmosphere with 5% CO₂ at 37°C.

2.2. Preparation of FDY003 Herbal Formula. The preparation of FDY003 was conducted as previously described [25]. In brief, the raw herbal constituents of FDY003 were obtained from Green Myeong-Poom Pharm. Co., Ltd. (Namyangju, Korea). The dried plant materials of LjT (4.16 g), AcT (6.25 g), and Cm (6.25 g) were ground, added to 70% ethanol

(500 mL), and subjected to reflux extraction at 80°C for 3 h. Then, the herbal extract was filtered through a 1 μ m pore filter (Hyundai Micro, Seoul, Korea) and successively purified with 80% and 90% ethanol. The resulting solution was lyophilized at –80°C. The samples were stored at –20°C and then dissolved in distilled water before the experiments.

2.3. Cell Viability Assay. The cell viability assay was performed following the previous procedures [25]. 3-(4,5-Dimethylthiazol-2-yl)-2,5-diphenyltetrazolium bromide (MTT) was obtained from Sigma-Aldrich Inc. (St. Louis, MO, USA). Cell viability was measured using the MTT assay. The cells were seeded in 96-well plates (5.0×10^4 cells per well) and then treated with the indicated drugs for 72 h in a 5% CO₂ incubator at 37°C. Subsequently, MTT solution (200 μ L) was added to each well, and the cells were further incubated for 2 h. Thereafter, the resulting formazan crystals were dissolved in dimethyl sulfoxide, and the absorbance was read with an Epoch 2 Microplate Spectrophotometer at 550 nm (BioTek, Winooski, VT, USA).

2.4. Exploration of Active Chemical Compounds. Comprehensive information on the phytochemical components of FDY003 was integrated from traditional Chinese medicine systems pharmacology (TCMSP) and anticancer herbs database of systems pharmacology (CancerHSP) databases [40, 41]. To determine the bioactive compounds of FDY003, we assessed the key absorption, distribution, metabolism, and excretion (ADME) pharmacokinetic parameters (i.e., oral bioavailability (OB), drug-likeness (DL), and Caco-2 permeability) of chemical constituents obtained from the TCMSP database [40]. OB, a pivotal consideration in drug development, is a measurement of the rate, fraction, and extent of an orally administered drug that reaches the expected site of drug action [40, 42]. Caco-2 permeability is a parameter widely used for the evaluation of the intestinal absorption rate and extent of a given substance using Caco-2 human intestinal epithelial cells [40, 43–45]. In general, drug molecules with a Caco-2 permeability less than –0.4 are considered not permeable across the epithelium of intestines [40, 46, 47]. DL is an indicator that is used to assess whether a compound has the potential to be developed into a drug with respect to its physical and chemical properties; it is calculated based on the Tanimoto coefficient and relevant molecular descriptors [40, 48]. A chemical compound is considered active if it meets the following criteria: OB \geq 30%, Caco-2 permeability \geq –0.4, and DL \geq 0.18 [37, 40, 49, 50].

2.5. Target Identification for the Active Compounds. Molecular targets of the bioactive compounds of FDY003 were determined using comprehensive information regarding chemical-protein interactions obtained from various relevant databases, including Search Tool for Interactions of Chemicals (STITCH) 5 [51], SwissTargetPrediction [52, 53], PharmMapper [54], and Similarity Ensemble Approach (SEA) [55]. We also used *in silico* models, such as systematic drug targeting tool (SysDT) [56]

and weighted ensemble similarity (WES) algorithm [57], for target identification according to previously described procedures [58–63]. Human genes/proteins related to the pathology of BC were obtained from the following databases: Therapeutic Target Database (TTD) [64], GeneCards [65], Comparative Toxicogenomics Database (CTD) [66], DisGeNET [67], Human Genome Epidemiology (HuGE) Navigator [68], Online Mendelian Inheritance in Man (OMIM) [69], Pharmacogenomics Knowledgebase (PharmGKB) [70], and DrugBank [71].

2.6. Network Construction. The herbal medicine-bioactive compound (H-C) and bioactive compound-target (C-T) networks were generated by connecting the three herbal constituents of FDY003 with the bioactive compounds and the bioactive compounds with the targets. The target-pathway (T-P) network was generated by connecting the targets with relevant biological pathways. The protein-protein interaction (PPI) network was generated based on the interactions between the targets (confidence score ≥ 0.9) using the STRING database [72]. Network visualization and analysis were performed with Cytoscape [73]. In the presented data, nodes indicate the herbal constituents, active chemical constituents, targets, or pathways, and edges (or links) indicate their interactions [74]. The degree indicates the number of edges of a node in a network [74].

2.7. Contribution Index Analysis. The contribution of chemical compounds to the pharmacological activity of FDY003 was analyzed using a contribution index (CI) [50] that can be calculated using the following formula:

$$\begin{aligned} \text{NE}(j) &= \sum_{i=1}^n d_i, \\ \text{CI}(j) &= \frac{c_j \times \text{NE}(j)}{\sum_{i=1}^m c_i \times \text{NE}(i)} \times 100\%, \end{aligned} \quad (1)$$

where NE indicates the network-based efficacy, n indicates the number of targets of chemical component j , d_i indicates the number of links of target i of chemical component j , m indicates the number of chemical components, and c_i (or c_j) indicates the number of previous literatures containing the terms “breast cancer” and the common name of chemical component i (or j) in their title or abstract that were retrieved from the PubMed (<https://pubmed.ncbi.nlm.nih.gov/>). If the sum of the highest CIs is greater than 85%, the compounds with those CIs are considered the major contributors, as previously suggested [50].

2.8. Functional Enrichment Analysis. Gene ontology (GO) enrichment analysis was performed using g:Profiler [75], and pathway enrichment analysis was carried out with Kyoto Encyclopedia of Genes and Genomes (KEGG) databases [76].

3. Results

3.1. Anticancer Properties of FDY003 against Breast Cancer. To investigate whether FDY003 exerts therapeutic effects on BC cells, we treated MCF-7 (an estrogen receptor-positive human BC cell line), MDA-MB-453 (a human epidermal growth factor receptor 2- (HER2-) positive human BC cell line), and MDA-MB-231 (a triple-negative human BC cell line) cells with FDY003 for 72 h and observed their responses. We found that FDY003 repressed the viability of MCF-7 ($\text{IC}_{50} = 242.90 \mu\text{g}/\text{mL}$), MDA-MB-453 ($\text{IC}_{50} = 156.01 \mu\text{g}/\text{mL}$), and MDA-MB-231 ($\text{IC}_{50} = 197.56 \mu\text{g}/\text{mL}$) cells (Supplementary Figure S1), suggesting that the herbal medicine possesses anti-BC properties.

3.2. Chemical Components of FDY003. The chemical compounds that are present in FDY003 were obtained from the comprehensive databases associated with herbal medicine such as TCMSP and CancerHSP [40, 41]. Accordingly, 323 compounds were retrieved for FDY003 after removing duplicates (Supplementary Table S1).

3.3. Active Chemical Compounds in FDY003. Compounds whose pharmacokinetic parameters met the following criteria were considered active as described in Section 2.4: $\text{OB} \geq 30\%$, Caco-2 permeability ≥ -0.4 , and $\text{DL} \geq 0.18$ [49, 50]. A number of compounds not satisfying the aforementioned criteria were also considered bioactive because they were present in large amounts in herbal medicines and were known to have potent pharmacological efficacy. As a result, we obtained 20 active compounds for FDY003 (Supplementary Table S2).

3.4. Targets of Active Chemical Compounds in FDY003. We used comprehensive chemical-protein interaction data obtained from various relevant databases, including STITCH [51], SEA [55], SwissTargetPrediction [52, 53], and PharmMapper [54] to explore the molecular targets for the bioactive chemical components in FDY003. In addition, in silico models, such as SysDT [56] and WES algorithms [57], were used for the target exploration based on previously described procedures [58–63]. Consequently, we obtained 196 targets for the 18 active compounds (i.e., 4'-methylcapillarisin, arcapillin, artemillin A, capillarisin, chrysoeriol, cirsimaritin, cordycepin, corymbosin, eriodictiol (flavone), eupalitin, eupatolitin, genkwanin, isoarcapillin, isorhamnetin, kaempferol, luteolin, quercetin, and β -sitosterol) in FDY003 (Figure 1 and Supplementary Table S3). No interacting targets were retrieved for the compounds “loniceracetalides B_qt” and “demethoxycapillarisin.”

3.5. Network Pharmacology Study on the Molecular Mechanisms of FDY003. To conduct network pharmacology analysis of the molecular mechanisms of FDY003 against BC, we first generated an herbal medicine-bioactive compound-target (H-C-T) network of the herbal formula by linking the herbal medicines with their bioactive chemical components and the components with the targets (Figure 2).

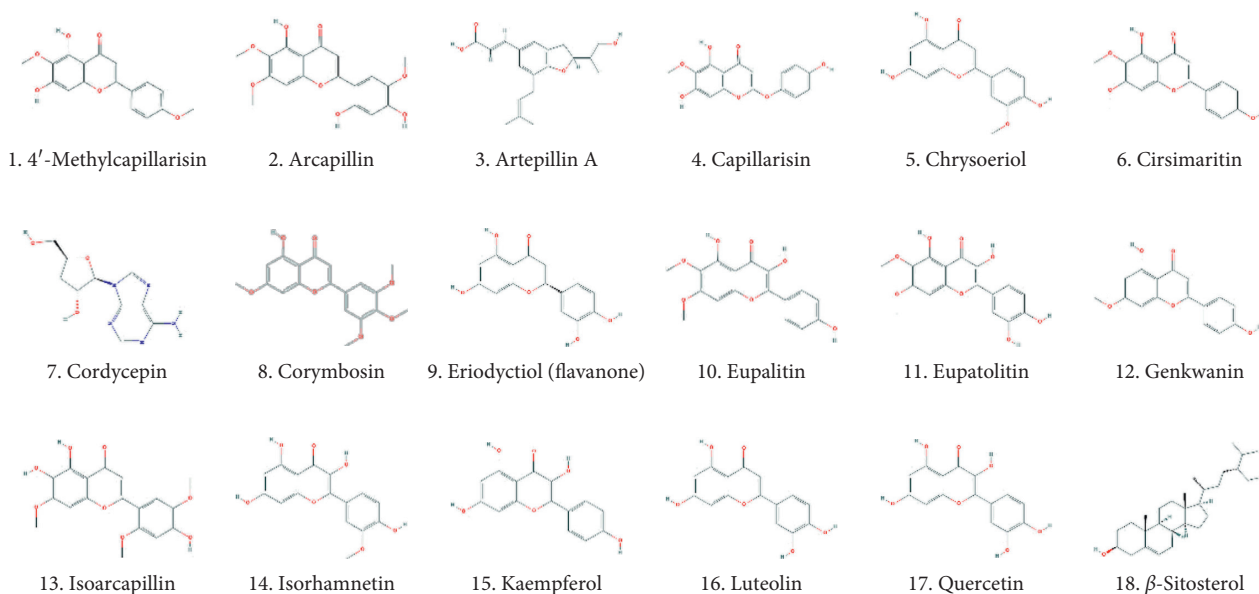


FIGURE 1: The active chemical compounds of FDY003.

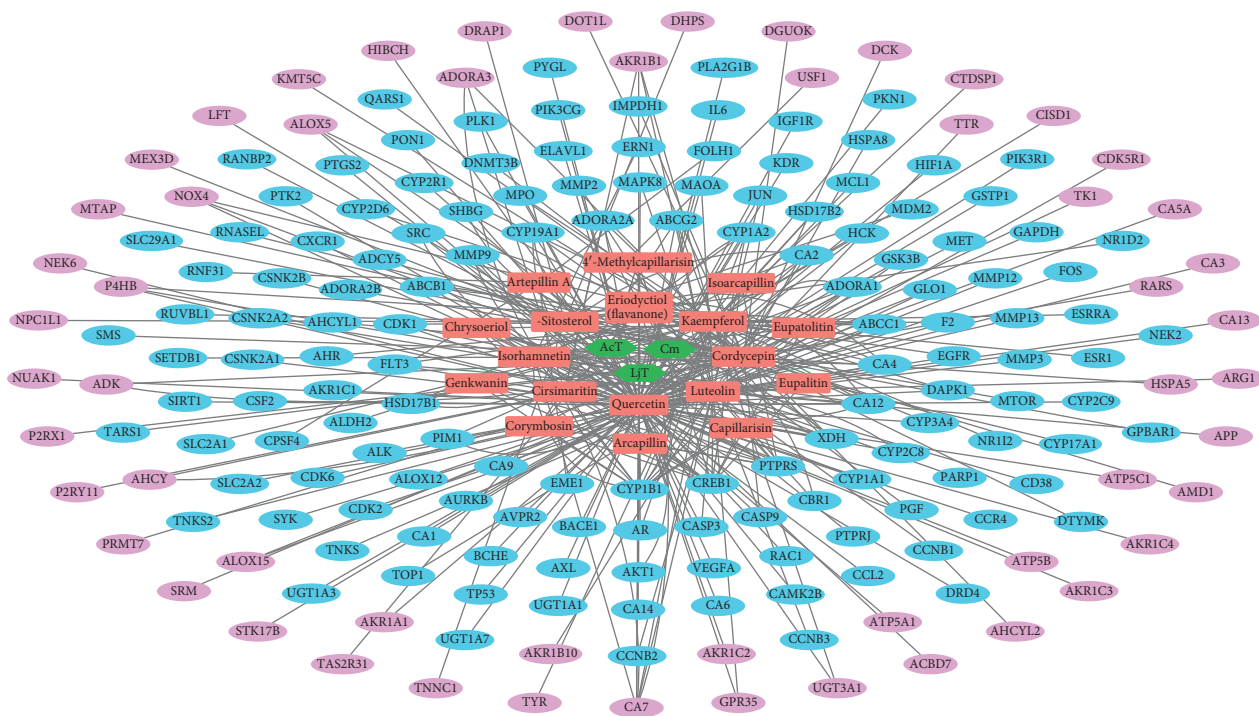


FIGURE 2: Herbal medicine-active chemical compound-target network of FDY003. Green hexagons, herbal medicines; red rectangles, active chemical compounds; blue ellipses, BC-associated targets; purple ellipses, non-BC-associated targets.

The resulting H-C-T network contained 217 nodes (3 herbal medicines, 18 active chemical components, and 196 targets) and 354 edges (Figure 2). In addition, to obtain insight into the BC-associated pharmacological features of FDY003, we constructed a C-T network (158 nodes with 254 edges) by connecting the bioactive chemical components with the BC-associated targets (Figure 3 and Supplementary Table S3). The quercetin, luteolin,

kaempferol, cordycepin, eriodyctiol (flavanone), isorhamnetin, and β -sitosterol exhibited the highest degrees (Figure 3 and Supplementary Table S3), implying that they are essential for the mediation of the anticancer effects of FDY003 against BC. Furthermore, 42 BC-associated targets interacted with two or more compounds (Figure 3 and Supplementary Table S3), supporting the poly-pharmacological characteristics of FDY003.

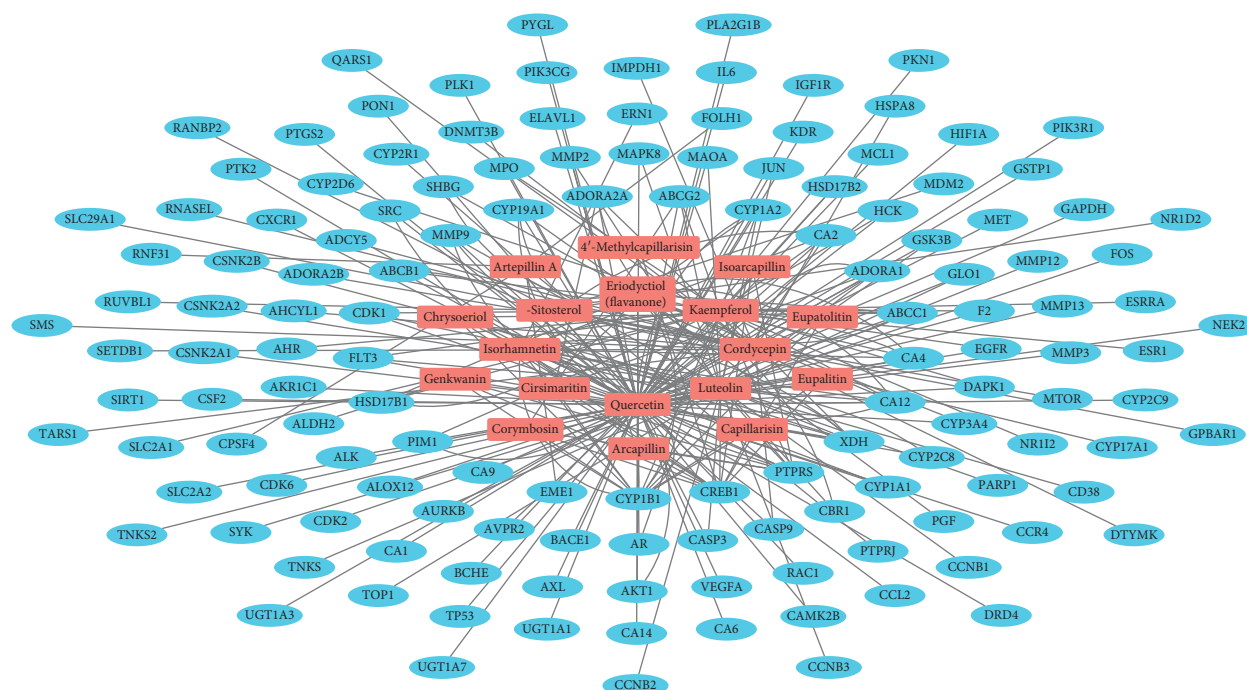


FIGURE 3: Active chemical component-target network of FDY003. Red rectangles, bioactive chemical components; blue ellipses, breast cancer-associated targets.

To investigate the interactive associations among the targets, we built a PPI network (106 nodes and 315 edges) consisting of the BC-associated therapeutic targets of FDY003 (Figure 4). Subsequently, we explored the existence of hubs (i.e., nodes with relatively high degrees that tend to play prominent roles in the cellular processes in a network) [77, 78]. In the analysis, we defined hubs as nodes with degrees equal to or greater than twice the mean node degree [79, 80]. Among the BC-associated targets of FDY003, TP53, SRC, PIK3R1, VEGFA, AKT1, EGFR, CYP1A1, CYP3A4, JUN, CDK1, and ESR1 were hub nodes (Figure 4), suggesting that the nodes act as important targets mediating the therapeutic effects of FDY003 against BC cells. Loss of function of p53 (encoded by *TP53*) due to genetic alterations has been shown to drive the tumorigenesis, progression, and metastasis of BC; p53 expression has been reported to be a potential prognostic indicator for BC patients [81–89]. The dysregulation and elevated activity of the kinase Src (encoded by *SRC*) is frequently observed in multiple human malignancies, including BC, and it promotes the invasion, metastasis, migration, and proliferation of BC cells [90–94]. The expression and activity of *SRC* or *PIK3R1* are highly upregulated in malignant breast tumor tissues and have been correlated with decreased survival of BC patients [95–97]. VEGF-A (encoded by *VEGFA*) is a crucial regulator in the proliferation, angiogenesis, and metastatic behavior of BC cells, and it confers resistance against chemotherapy [98–101]. The overexpression or hyperactivation of AKT (encoded by *AKT1*), epidermal growth factor receptor (EGFR; encoded by *EGFR*), or c-Jun (encoded by *JUN*) promotes various cancerous processes, including proliferation, growth, survival, invasion, and migration of BC cells

and is further related to the poorer clinical outcomes of BC patients [102–127]. Such targets have been implicated in reduced drug sensitivity of cancer cells to chemotherapeutics; therefore, targeting them could improve the therapeutic efficacy of chemotherapy and radiotherapy in BC [104–106, 109, 111–113, 117, 119, 123, 125, 126, 128–131]. Cytochrome P450 1A1 (encoded by *CYP1A1*) and cytochrome P450 3A4 (encoded by *CYP3A4*) are modulators of estrogen metabolism, and their activities are involved in the cancerous processes of BC cells [132–139]. Genetic polymorphism and expression of *CYP3A1* or *CYP3A4* in breast tumor tissues have been reported to be potentially useful factors for the prediction of treatment responses to chemotherapy [140, 141]. *CDK1* (encoded by *CDK1*) functions as a crucial regulator in cell cycle progression, and its dysregulation leads to aberrant proliferation of BC cells [142]. Previous studies have indicated that *CDK1* activity may act as a prognostic indicator in BC, and *CDK1* targeting can increase chemotherapeutic efficacy [143–147]. Abnormal activity of estrogen receptor α (encoded by *ESR1*) is considered primarily responsible for tumorigenesis and progression of BC, and the receptor is the most promising therapeutic target [134–139].

To assess the contribution of the chemical components to the pharmacological effects of FDY003, we calculated CIs for the individual active compounds (Section 2.7) [50, 148]. As a result, quercetin and luteolin had the highest CIs with a sum of 91.83% (Supplementary Figure S2), which suggests that the two active components are key factors contributing to the FDY003 anticancer properties in BC treatment.

Overall, the results of the analyses above facilitate the identification of the polypharmacological mechanisms of FDY003 activity against BC.

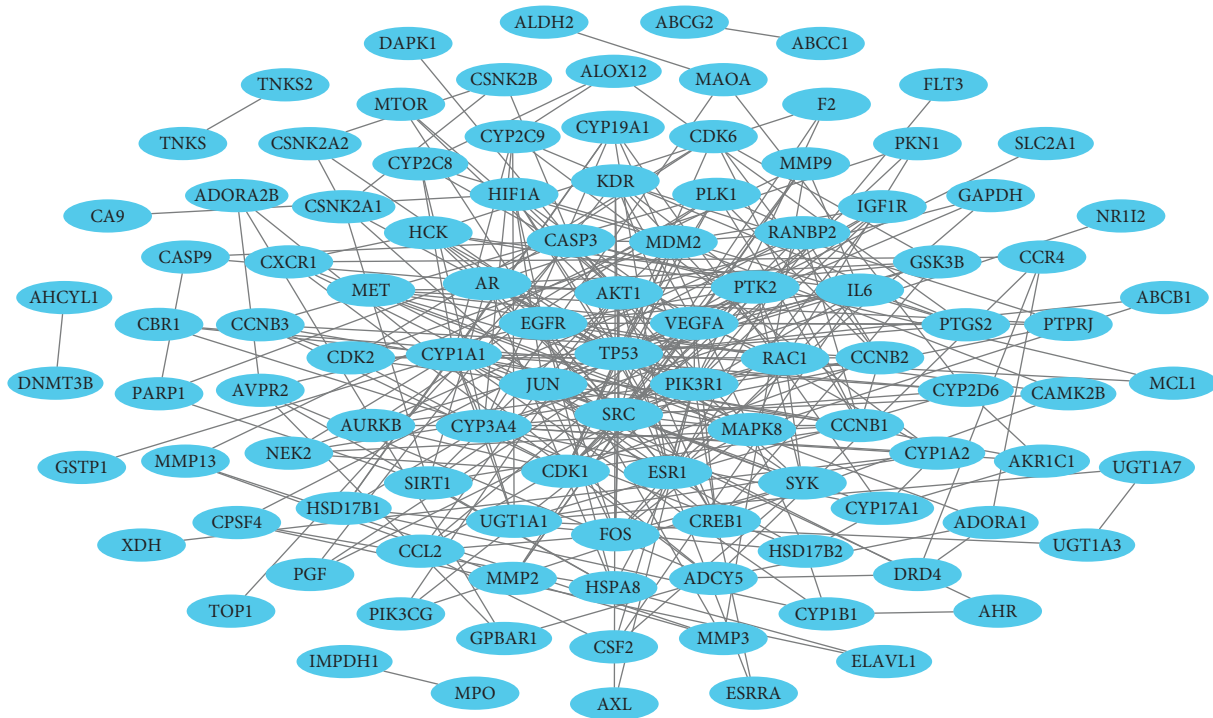


FIGURE 4: Protein-protein interaction network for breast cancer-associated targets of FDY003. Nodes refer to the breast cancer-related targets of FDY003.

3.6. Functional Enrichment Analysis for the FDY003 Network.

To investigate the biological roles of the BC-related targets of FDY003, we carried out GO enrichment analysis for the targets. These targets were enriched in GO terms for the modulation of biological processes, involving cell proliferation, cell cycle progression, and cell apoptosis (Supplementary Figure S3), highlighting the molecular properties of FDY003 activity.

The aberrant activities of oncogenic cellular signalings are known to be responsible for cancer development and progression [149]. To this end, we next carried out pathway enrichment analysis for its BC-related targets (Figure 5 and Supplementary Figure S3). We found that the following diverse pathways, which importantly function in the tumorigenesis and progression of BC, were significantly enriched with the FDY003 targets: “Pathways in cancer,” “PI3K-Akt signaling pathway,” “Endocrine resistance,” “MAPK signaling pathway,” “Focal adhesion,” “Cellular senescence,” “FoxO signaling pathway,” “TNF signaling pathway,” “EGFR tyrosine kinase inhibitor resistance,” “Estrogen signaling pathway,” “Ras signaling pathway,” “Steroid hormone biosynthesis,” “Apoptosis,” “Breast cancer,” “HIF-1 signaling pathway,” “PD-L1 expression and PD-1 checkpoint pathway in cancer,” “Cell cycle,” “ErbB signaling pathway,” “Wnt signaling pathway,” “p53 signaling pathway,” “VEGF signaling pathway,” and “Platinum drug resistance” (Figure 5 and Supplementary Figure S3). The dysregulation of PI3K-Akt, MAPK, focal adhesion, and Ras signaling pathways promotes diverse cancerous cell processes, including the uncontrolled cell proliferation, invasion, migration, survival, metastasis, and angiogenesis of

BC cells [3, 126, 150–154]. Abnormalities of crucial cellular function, such as senescence, apoptosis, and cell cycle, are the important pathological processes of BC [155–160]. The TNF signaling pathway is a mediator of the inflammatory process, and its activity is closely linked with the progression, metastasis, and poor prognosis of BC [161, 162]. The estrogen signaling pathway functions as the most critical regulator of tumor initiation and malignant progression in BC, and therapeutic modulation of its activity serves as a primary treatment strategy [163–167]. Previous studies have suggested that expression of programmed death-ligand 1 (PD-L1) serves as a prognostic factor for the survival of patients with BC and that inhibition of the programmed cell death protein 1 (PD-1)/PD-L1 pathway can enhance anti-tumor responses [168–172]. The HIF-1 and Wnt signaling regulate various cellular behaviors, involving cell proliferation, metastasis, and stem cell-like characteristics in BC cells [173–180]. The p53 signaling pathway exerts tumor-suppressive activity associated with cell cycle arrest, apoptosis, and cellular senescence, and loss of function of its key pathway components has been implicated in the carcinogenesis of BC and is a negative prognostic factor for patient survival [85, 181]. The VEGF signaling pathway plays a protumoral role by increasing angiogenesis, thus promoting the survival, migration, and invasion of BC cells [101, 182]. In addition, resistance to platinum-based drugs, endocrine therapy, and EGFR signaling inhibitors are major obstacles in BC treatment [183–189].

We further analyzed the functional associations among FDY003 targets using GeneMANIA [190], an algorithm useful for the analysis of biological functions of cellular

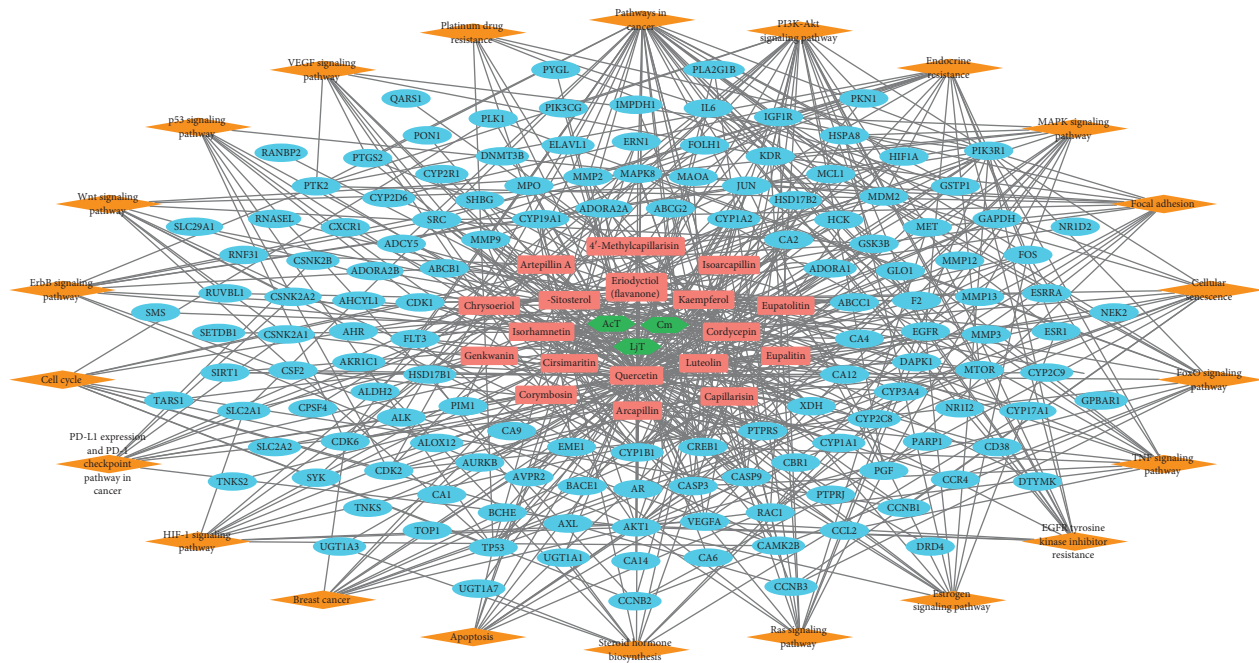


FIGURE 5: Herbal medicine-compound-target-pathway network of FDY003. Green hexagons, herbal medicines; red rectangles, bioactive chemical components; blue ellipses, breast cancer-related targets; orange diamonds, signaling pathways.

components based on extensive network integration. Among the BC-associated targets of FDY003, 38.32% and 33.65% of them tended to be coexpressed and physically interacting, respectively (Supplementary Figure S4), suggesting that they have similar biological roles and functions.

Together, the results above suggest that FDY003 exerts the pharmacological activity by targeting diverse BC-associated oncogenic signaling pathways and the modulation of relevant biological functions.

4. Discussion

BC is a common cancer type and ranks as the leading cause of death among women globally [1]. Herbal medicines are attracting considerable attention for potential applications in cancer treatment owing to their high anticancer activities, reduced toxicity, and minimal adverse effects [21]. Based on a network pharmacology analysis, we explored the molecular mechanisms of the therapeutic effects of FDY003 for BC. (i) FDY003 exhibited anticancer effects on human BC cells (Supplementary Figure 1). (ii) Eighteen potentially active compounds (i.e., 4'-methylcapillarisin, arcapillin, artemillin A, capillarisin, chrysoeriol, cirsimaritin, cordycepin, corymbosin, eriodyctiol (flavanone), eupalitin, eupatolitin, genkwanin, isorcapillin, isorhamnetin, kaempferol, luteolin, quercetin, and β -sitosterol) present in FDY003 may interact with 140 BC-associated therapeutic targets and induce the pharmacological activity of the herbal drug (Figures 1–4). (iii) GO terms for the modulation of cellular processes were significantly enriched for the FDY003 targets, including cell proliferation, cell cycle process, and cell apoptosis (Supplementary Figure 3). In addition, (iv) diverse pathways that play key roles in BC pathology were enriched

for the targets that included PI3K-Akt, MAPK, focal adhesion, FoxO, TNF, and estrogen signaling pathways (Figure 5 and Supplementary Figure 3).

The FDY003 constituents have been reported to exert inhibitory effects against BC. Act inhibited the proliferation but induced the death of BC cells [191]. Cm has been previously demonstrated to reduce the migratory and proliferative capacities of BC cells and to stimulate apoptosis by promoting caspase activation and Akt inactivation [29, 35, 192, 193]. Cm also has immunomodulatory properties that can inhibit the growth of breast tumors [194]. Capillarisin exhibits its anticancer effects by attenuating the invasive and proliferative properties of BC cells [195]. Chrysoeriol treatment has been reported to promote apoptosis and cell cycle arrest and further repress the invasion, proliferation, and migration of BC cells [196, 197]. Cirsimaritin inhibits proliferation and angiogenesis via the downregulation of VEGF, Akt, and extracellular signal-regulated kinase (ERK) [198]. Cordycepin is a potent inhibitor of the invasion and proliferation of BC cells while inducing their apoptosis through the regulation of MAPK and caspase-dependent pathways [199–203]. Cordycepin has also been shown to function as a radiosensitizer that can enhance the efficacy of radiotherapy toward BC cells [204]. Genkwanin modulates the activities of CYP1 enzymes and PI3K/Akt/mammalian target of rapamycin (mTOR) pathways, thereby suppressing proliferation and inducing apoptosis of BC cells [205–207]. Isorhamnetin exerts the anticancer activity against BC cells by inhibiting their proliferative and invasive abilities [208–210]. β -Sitosterol activates key apoptotic pathways, including Fas and caspase signaling pathways, and reduces the viability of BC cells [211–214]. Furthermore, β -sitosterol has been demonstrated

to elevate the pharmacological effectiveness of tamoxifen, a selective estrogen receptor modulator that is extensively applied in clinical practice [215]. Kaempferol, luteolin, and quercetin stimulate apoptotic cell death but inhibit cell processes, including proliferation, cell cycle progression, angiogenesis, migration, invasion, metastasis, and cancer stemness; such effects occur via the regulation of important BC-associated pathways such as the Akt, caspase, EGFR, estrogen, HER2, MAPK, insulin-like growth factor (IGF)-1, Notch, and Wnt signaling pathways [216–266]. The three chemical compounds have also been shown to sensitize BC cells to various anticancer drugs, including cisplatin, docetaxel, doxorubicin, lapatinib, paclitaxel, rapamycin, sorafenib, tamoxifen, topotecan, and vincristine [267–286]. For instance, luteolin can synergistically enhance the growth-suppression and apoptosis-inducing activities of the anticancer agent celecoxib against BC cells by blocking the activation of oncogenic Akt and ERK signaling [271, 272]. The combined treatment of quercetin with kaempferol or luteolin has synergistic antiproliferative effects that are greater than those of either treatment exclusively [287, 288]. The risk of BC incidence showed a tendency to be lower in women with higher quercetin intakes [289].

Pharmacologic effects of FDY003 in cancer cells have been previously reported [24, 25]. FDY003 has been reported to exert its anticancer effects through the regulation of the activities of key mediators of apoptosis and cell cycle progression; these involved Bax, caspase-3, p21, and p53 that induce apoptosis while suppressing the proliferative and survival capacities of cancer cells [24, 25]. Treatment with the herbal formula further inhibited tumor growth in xenograft mice bearing human cancer cells [24], suggesting in vivo therapeutic effects against cancer. Contrary to the treatment with irinotecan, a clinically used cytotoxic chemotherapeutic agent [290], body weight loss (a parameter used to evaluate the potential toxicity of drug treatments in animal experiments) did not occur in FDY003-administered xenograft mice [24], suggesting tolerability of the herbal drug as well as its antitumor activity. Future experimental studies should (i) investigate the pharmacological effects of FDY003 in diverse types of cancer, (ii) explore the mechanisms underlying the anticancer activity of the herbal formula such as its immunomodulatory effects, and (iii) evaluate the anticancer effectiveness and safety of FDY003 combined with other widely used therapeutic approaches (i.e., chemotherapy, endocrine therapy, and targeted molecular therapy). Such studies would facilitate the development of safer and more effective herbal medicine-based strategies for BC treatment.

5. Conclusions

We explored the systematic mechanisms of FDY003 activity against BC based on a network pharmacology analysis. FDY003 elicited anticancer effects on human BC cells. Eighteen chemical compounds in FDY003 were identified as potentially bioactive compounds that could target 140 BC-associated genes/proteins and exhibit therapeutic effects. The FDY003 targets were enriched in GO terms associated

with the modulation of cellular processes, involving cell proliferation, cell cycle progression, and cell apoptosis. Pathway enrichment analysis of the targets further demonstrated that diverse pathways crucial for the BC pathology were significantly enriched with the FDY003 targets, involving the PI3K-Akt, MAPK, focal adhesion, FoxO, TNF, and estrogen signaling pathways. Based on a network perspective, our findings offer in-depth insights into the therapeutic properties of herbal medicines in BC treatment. Future studies should explore the potential efficacy of the herbal formula in other cancer types as well as its potential efficacy and safety profiles in combination with other therapies.

Abbreviations

AcT:	<i>Artemisia capillaris</i> Thunberg
ADME:	Absorption, distribution, metabolism, and excretion
Bax:	Bcl-2-associated X protein
C-T:	Compound-target
CI:	Contribution index
Cm:	<i>Cordyceps militaris</i>
CTD:	The Comparative Toxicogenomics Database
CYP:	Cytochrome P450
DL:	Drug-likeness
EGFR:	Epidermal growth factor receptor
ErbB:	Erythroblastic leukemia viral oncogene homolog
FoxO:	Forkhead box protein O
GO:	Gene ontology
H-C:	Herb-compound
H-C-T:	Herb-target-pathway
HIF-1:	Hypoxia-inducible factor 1
HuGE Navigator:	Human Genome Epidemiology Navigator
KEGG:	Kyoto Encyclopedia of Genes and Genomes
LjT:	<i>Lonicera japonica</i> Thunberg
MAPK:	Mitogen-activated protein kinase
MTT:	3-(4,5-Dimethylthiazol-2-yl)-2,5-diphenyltetrazolium bromide
NE:	Network-based efficacy
OB:	Oral bioavailability
OMIM:	Online Mendelian Inheritance in Man
PD-1:	Programmed cell death protein 1
PD-L1:	Programmed death-ligand 1
PharmGKB:	Pharmacogenomics Knowledgebase
PI3K:	Phosphoinositide 3-kinase
PPI:	Protein-protein interaction
QOL:	Quality of life
SEA:	Similarity ensemble approach
STITCH:	Search Tool for Interactions of Chemicals
SysDT:	Systematic drug targeting tool
TCMSP:	Traditional Chinese medicine systems pharmacology
TTD:	Therapeutic Target Database
TNF:	Tumor necrosis factor
T-P:	Target-pathway
VEGF:	Vascular endothelial growth factor

WES Weighted ensemble similarity algorithm.
algorithm:

Data Availability

The data used to support the findings of this study are included within the article.

Conflicts of Interest

The authors declare that there are no conflicts of interest.

Acknowledgments

This study was funded by the Fore and Forest Hospital.

Supplementary Materials

Supplementary Figure S1. Effects of FDY003 on the viability of breast cancer cells. Supplementary Figure S2. Contribution index of active compounds in FDY003. Supplementary Figure S3. Functional enrichment analysis for the breast cancer-associated targets of FDY003. Supplementary Figure S4. Functional interaction analysis for the breast cancer-associated targets of FDY003. Supplementary Table S1. List of the chemical compounds in FDY003. Supplementary Table S2. List of the active chemical compounds in FDY003. Supplementary Table S3. List of the targets of active chemical compounds in FDY003. (*Supplementary Materials*)

References

- [1] C. E. DeSantis, J. Ma, M. M. Gaudet et al., "Breast cancer statistics, 2019," *CA: A Cancer Journal for Clinicians*, vol. 69, no. 6, pp. 438–451, 2019.
- [2] R. Garcia-Becerra, N. Santos, L. Diaz, and J. Camacho, "Mechanisms of resistance to endocrine therapy in breast cancer: focus on signaling pathways, miRNAs and genetically based resistance," *International Journal of Molecular Sciences*, vol. 14, no. 1, pp. 108–145, 2020.
- [3] P. F. McAuliffe, F. Meric-Bernstam, G. B. Mills, and A. M. Gonzalez-Angulo, "Deciphering the role of PI3K/Akt/mTOR pathway in breast cancer biology and pathogenesis," *Clinical Breast Cancer*, vol. 10, no. 3, pp. S59–S65, 2010.
- [4] D. Zardavas, J. Baselga, and M. Piccart, "Emerging targeted agents in metastatic breast cancer," *Nature Reviews Clinical Oncology*, vol. 10, no. 4, pp. 191–210, 2013.
- [5] P. den Hollander, M. I. Savage, and P. H. Brown, "Targeted therapy for breast cancer prevention," *Frontiers in Oncology*, vol. 3, p. 250, 2013.
- [6] X. Li, M. T. Lewis, J. Huang et al., "Intrinsic resistance of tumorigenic breast cancer cells to chemotherapy," *Journal of the National Cancer Institute*, vol. 100, no. 9, pp. 672–679, 2008.
- [7] R. Nahta, D. Yu, M. C. Hung, G. N. Hortobagyi, and F. J. Esteva, "Mechanisms of disease: understanding resistance to HER2-targeted therapy in human breast cancer," *Nature Clinical Practice Oncology*, vol. 3, no. 5, pp. 269–280, 2006.
- [8] M. J. Piccart-Gebhart, M. Procter, B. Leyland-Jones et al., "Trastuzumab after adjuvant chemotherapy in HER2-positive breast cancer," *The New England Journal of Medicine*, vol. 353, no. 16, pp. 1659–1672, 2005.
- [9] E. H. Romond, E. A. Perez, J. Bryant et al., "Trastuzumab plus adjuvant chemotherapy for operable HER2-positive breast cancer," *The New England Journal of Medicine*, vol. 353, no. 16, pp. 1673–1684, 2005.
- [10] R. Rouzier, C. M. Perou, W. F. Symmans et al., "Breast cancer molecular subtypes respond differently to preoperative chemotherapy," *Clinical Cancer Research*, vol. 11, no. 16, pp. 5678–5685, 2005.
- [11] M. Abotaleb, P. Kubatka, M. Caprnda et al., "Chemotherapeutic agents for the treatment of metastatic breast cancer: an update," *Biomedicine & Pharmacotherapy*, vol. 101, pp. 458–477, 2018.
- [12] S. Ali, M. Rasool, H. Chaudhry et al., "Molecular mechanisms and mode of tamoxifen resistance in breast cancer," *Bioinformatics*, vol. 12, no. 3, pp. 135–139, 2016.
- [13] E. A. Ariazi, J. L. Ariazi, F. Cordera, and V. C. Jordan, "Estrogen receptors as therapeutic targets in breast cancer," *Current Topics in Medicinal Chemistry*, vol. 6, no. 3, pp. 181–202, 2006.
- [14] A. Farolfi, E. Melegari, M. Aquilina et al., "Trastuzumab-induced cardiotoxicity in early breast cancer patients: a retrospective study of possible risk and protective factors," *Heart*, vol. 99, no. 9, pp. 634–639, 2013.
- [15] M. Fiuza, "Cardiotoxicity associated with trastuzumab treatment of HER2+ breast cancer," *Advances in Therapy*, vol. 26, no. 1, pp. S9–S17, 2009.
- [16] E. L. Mayer and H. J. Burstein, "Chemotherapy for metastatic breast cancer," *Hematology/Oncology Clinics of North America*, vol. 21, no. 2, pp. 257–272, 2007.
- [17] A. H. Partridge, H. J. Burstein, and E. P. Winer, "Side effects of chemotherapy and combined chemohormonal therapy in women with early-stage breast cancer," *JNCI: Journal of the National Cancer Institute*, vol. 30, pp. 135–142, 2001.
- [18] B. Ramaswamy and C. L. Shapiro, "Osteopenia and osteoporosis in women with breast cancer," *Seminars in Oncology*, vol. 30, no. 6, pp. 763–775, 2003.
- [19] G. R. Zimmermann, J. Lehar, and C. T. Keith, "Multi-target therapeutics: when the whole is greater than the sum of the parts," *Drug Discovery Today*, vol. 12, no. 1-2, pp. 34–42, 2007.
- [20] S. Ohnishi and H. Takeda, "Herbal medicines for the treatment of cancer chemotherapy-induced side effects," *Frontiers in Pharmacology*, vol. 6, p. 14, 2015.
- [21] P. Poornima, J. D. Kumar, Q. Zhao, M. Blunder, and T. Efferth, "Network pharmacology of cancer: from understanding of complex interactomes to the design of multi-target specific therapeutics from nature," *Pharmacological Research*, vol. 111, pp. 290–302, 2016.
- [22] S. Y. Yin, W. C. Wei, F. Y. Jian, and N. S. Yang, "Therapeutic applications of herbal medicines for cancer patients," *Evidence-Based Complementary and Alternative Medicine*, vol. 2013, Article ID 302426, 15 pages, 2013.
- [23] L. Zhu, L. Li, Y. Li, J. Wang, and Q. Wang, "Chinese herbal medicine as an adjunctive therapy for breast cancer: a systematic review and meta-analysis," *Evidence-Based Complementary and Alternative Medicine*, vol. 2016, Article ID 9469276, 17 pages, 2016.
- [24] I.-H. Lee and D.-Y. Lee, "FDY003 inhibits colon cancer in a Colo205 xenograft mouse model by decreasing oxidative stress," *Pharmacognosy Magazine*, vol. 15, no. 65, p. 675, 2019.
- [25] H.-S. Lee, I.-H. Lee, K. Kang et al., "Systems pharmacology study of the anticervical cancer mechanisms of FDY003," *Natural Product Communications*, vol. 15, no. 12, 2020.

- [26] G. Feng, X. Wang, C. You et al., "Antiproliferative potential of *Artemisia capillaris* polysaccharide against human nasopharyngeal carcinoma cells," *Carbohydrate Polymers*, vol. 92, no. 2, pp. 1040–1045, 2013.
- [27] M. Hokin-Neaverson and J. W. Jefferson, "Deficient erythrocyte NaK-ATPase activity in different affective states in bipolar affective disorder and normalization by lithium therapy," *Neuropsychobiology*, vol. 22, no. 1, pp. 18–25, 1989.
- [28] E. Jang, S. Y. Kim, N. R. Lee et al., "Evaluation of antitumor activity of *Artemisia capillaris* extract against hepatocellular carcinoma through the inhibition of IL-6/STAT3 signaling axis," *Oncology Reports*, vol. 37, no. 1, pp. 526–532, 2017.
- [29] C. Y. Jin, G. Y. Kim, and Y. H. Choi, "Induction of apoptosis by aqueous extract of *Cordyceps militaris* through activation of caspases and inactivation of Akt in human breast cancer MDA-MB-231 Cells," *Journal of Microbiology and Biotechnology*, vol. 18, no. 12, pp. 1997–2003, 2008.
- [30] J. Kim, K. H. Jung, H. H. Yan et al., "Artemisia Capillaris leaves inhibit cell proliferation and induce apoptosis in hepatocellular carcinoma," *BMC Complementary Medicine and Therapies*, vol. 18, no. 1, p. 147.
- [31] K. I. Park, H. Park, A. Nagappan et al., "Polyphenolic compounds from Korean *Lonicera japonica* Thunb. induces apoptosis via AKT and caspase cascade activation in A549 cells," *Oncology Letters*, vol. 13, no. 4, pp. 2521–2530, 2017.
- [32] Y. K. Rao, S. H. Fang, W. S. Wu, and Y. M. Tzeng, "Constituents isolated from *Cordyceps militaris* suppress enhanced inflammatory mediator's production and human cancer cell proliferation," *Journal of Ethnopharmacology*, vol. 131, no. 2, pp. 363–367, 2010.
- [33] H. S. Yoo, J. W. Shin, J. H. Cho et al., "Effects of *Cordyceps militaris* extract on angiogenesis and tumor growth," *Acta Pharmacologica Sinica*, vol. 25, no. 5, pp. 657–665, 2004.
- [34] Q. Zhou, Z. Zhang, L. Song et al., "Cordyceps militaris fraction inhibits the invasion and metastasis of lung cancer cells through the protein kinase B/glycogen synthase kinase 3beta/beta-catenin signaling pathway," *Oncology Letters*, vol. 16, no. 6, pp. 6930–6939, 2018.
- [35] C. Chen, M.-L. Wang, C. Jin et al., "Cordyceps militaris polysaccharide triggers apoptosis and G0/G1 cell arrest in cancer cells," *Journal of Asia-Pacific Entomology*, vol. 18, no. 3, pp. 433–438, 2015.
- [36] C. Hao da and P. G. Xiao, "Network pharmacology: a Rosetta Stone for traditional Chinese medicine," *Drug Discovery Today*, vol. 75, no. 5, pp. 299–312, 2014.
- [37] H. S. Lee, I. H. Lee, S. I. Park, and D. Y. Lee, "Network pharmacology-based investigation of the system-level molecular mechanisms of the hematopoietic activity of samul-tang, a traditional Korean herbal formula," *Evidence-Based Complementary and Alternative Medicine*, vol. 2020, Article ID 9048089, 2020.
- [38] W. Y. Lee, C. Y. Lee, Y. S. Kim, and C. E. Kim, "The methodological trends of traditional herbal medicine employing network pharmacology," *Biomolecules*, vol. 9, p. 8, 2019.
- [39] G. B. Zhang, Q. Y. Li, Q. L. Chen, and S. B. Su, "Network pharmacology: a new approach for Chinese herbal medicine research," *Evidence-Based Complementary and Alternative Medicine*, vol. 2013, Article ID 621423, 9 pages, 2013.
- [40] J. Ru, P. Li, J. Wang et al., "TCMSP: a database of systems pharmacology for drug discovery from herbal medicines," *Journal of Cheminformatics*, vol. 6, p. 13, 2014.
- [41] W. Tao, B. Li, S. Gao et al., "CancerHSP: anticancer herbs database of systems pharmacology," *Scientific Reports*, vol. 5, p. 11481, 2015.
- [42] C. K. Wang and D. J. Craik, "Cyclic peptide oral bioavailability: lessons from the past," *Biopolymers*, vol. 106, no. 6, pp. 901–909, 2016.
- [43] M. N. Garcia, C. Flowers, and J. D. Cook, "The Caco-2 cell culture system can be used as a model to study food iron availability," *Journal of Nutrition*, vol. 126, no. 1, pp. 251–258, 1996.
- [44] Y. Kono, A. Iwasaki, K. Matsuoka, and T. Fujita, "Effect of mechanical agitation on cationic liposome transport across an unstirred water layer in caco-2 cells," *Biological and Pharmaceutical Bulletin*, vol. 39, no. 8, pp. 1293–1299, 2016.
- [45] D. A. Volpe, "Variability in Caco-2 and MDCK cell-based intestinal permeability assays," *Journal of Pharmaceutical Sciences*, vol. 97, no. 2, pp. 712–725, 2008.
- [46] Y. Li, J. Zhang, L. Zhang et al., "Systems pharmacology to decipher the combinational anti-migraine effects of Tianshu formula," *Journal of Ethnopharmacology*, vol. 174, pp. 45–56, 2015.
- [47] J. Zhang, Y. Li, X. Chen, Y. Pan, S. Zhang, and Y. Wang, "Systems pharmacology dissection of multi-scale mechanisms of action for herbal medicines in stroke treatment and prevention," *PLoS One*, vol. 9, no. 8, Article ID e102506, 2014.
- [48] A. Y. Lee, W. Park, T. W. Kang, M. H. Cha, and J. M. Chun, "Network pharmacology-based prediction of active compounds and molecular targets in Yijin-Tang acting on hyperlipidaemia and atherosclerosis," *Journal of Ethnopharmacology*, vol. 221, pp. 151–159, 2018.
- [49] J. Huang, F. Cheung, H. Y. Tan et al., "Identification of the active compounds and significant pathways of yinchenhao decoction based on network pharmacology," *Molecular Medicine Reports*, vol. 16, no. 4, pp. 4583–4592, 2017.
- [50] S. J. Yue, L. T. Xin, Y. C. Fan et al., "Herb pair Danggui-Honghua: mechanisms underlying blood stasis syndrome by system pharmacology approach," *Scientific Reports*, vol. 7, p. 40318, 2017.
- [51] D. Szklarczyk, A. Santos, C. von Mering, L. J. Jensen, P. Bork, and M. Kuhn, "STITCH 5: augmenting protein-chemical interaction networks with tissue and affinity data," *Nucleic Acids Research*, vol. 44, no. D1, pp. D380–D384, 2015.
- [52] A. Daina, O. Michielin, and V. Zoete, "SwissTargetPrediction: updated data and new features for efficient prediction of protein targets of small molecules," *Nucleic Acids Research*, vol. 47, no. W1, pp. W357–W364, 2019.
- [53] D. Gfeller, A. Grosdidier, M. Wirth, A. Daina, O. Michielin, and V. Zoete, "SwissTargetPrediction: a web server for target prediction of bioactive small molecules," *Nucleic Acids Research*, vol. 42, pp. W32–W38, 2014.
- [54] X. Wang, Y. Shen, S. Wang et al., "PharmMapper 2017 update: a web server for potential drug target identification with a comprehensive target pharmacophore database," *Nucleic Acids Research*, vol. 45, no. W1, pp. W356–W360, 2017.
- [55] M. J. Keiser, B. L. Roth, B. N. Armbruster, P. Ernsberger, J. J. Irwin, and B. K. Shoichet, "Relating protein pharmacology by ligand chemistry," *Nat Biotechnol*, vol. 25, no. 2, pp. 197–206, 2007.
- [56] H. Yu, J. Chen, X. Xu et al., "A systematic prediction of multiple drug-target interactions from chemical, genomic,

- and pharmacological data,” *PLoS One*, vol. 7, no. 5, Article ID e37608, 2012.
- [57] C. Zheng, Z. Guo, C. Huang et al., “Large-scale direct targeting for drug repositioning and discovery,” *Scientific Reports*, vol. 5, p. 11970, 2015.
- [58] J. Liu, M. Jiang, Z. Li et al., “A novel systems pharmacology method to investigate molecular mechanisms of scutellaria barbata D. Don for non-small cell lung cancer,” *Frontiers in Pharmacology*, vol. 9, p. 1473, 2018.
- [59] X. Su, Y. Li, M. Jiang et al., “Systems pharmacology uncover the mechanism of anti-non-small cell lung cancer for *Hedyotis diffusa* Willd.,” *Biomedicine & Pharmacotherapy*, vol. 109, pp. 969–984, 2019.
- [60] J. Wang, L. Zhang, B. Liu et al., “Systematic investigation of the *Erigeron breviscapus* mechanism for treating cerebrovascular disease,” *Journal of Ethnopharmacology*, vol. 224, pp. 429–440, 2018.
- [61] J. Liu, J. Liu, F. Shen et al., “Systems pharmacology analysis of synergy of TCM: an example using saffron formula,” *Scientific Reports*, vol. 8, no. 1, p. 380, 2018.
- [62] J. Liu, J. Zhu, J. Xue et al., “In silico-based screen synergistic drug combinations from herb medicines: a case using *Cistanche tubulosa*,” *Scientific Reports*, vol. 7, no. 1, p. 16364, 2017.
- [63] J. Liu, T. Pei, J. Mu et al., “Systems pharmacology uncovers the multiple mechanisms of xijiao dihuang decoction for the treatment of viral hemorrhagic fever,” *Evidence-Based Complementary and Alternative Medicine*, vol. 2016, Article ID 9025036, 17 pages, 2016.
- [64] F. Zhu, B. Han, P. Kumar et al., “Update of TTD: therapeutic target database,” *Nucleic Acids Research*, vol. 38, pp. D787–D791, 2009.
- [65] M. Safran, I. Dalah, J. Alexander et al., “GeneCards Version 3: the human gene integrator,” *Database*, vol. 2010, p. baq020, 2010.
- [66] A. P. Davis, C. J. Grondin, R. J. Johnson et al., “The comparative Toxicogenomics database: update 2019,” *Nucleic Acids Research*, vol. 47, no. D1, pp. D948–D954, 2019.
- [67] J. Pinero, A. Bravo, N. Queralt-Rosinach et al., “DisGeNET: a comprehensive platform integrating information on human disease-associated genes and variants,” *Nucleic Acids Research*, vol. 45, no. D1, pp. D833–D839, 2017.
- [68] W. Yu, M. Gwinn, M. Clyne, A. Yesupriya, and M. J. Khoury, “A navigator for human genome epidemiology,” *Nature Genetics*, vol. 40, no. 2, pp. 124–125, 2008.
- [69] J. S. Amberger, C. A. Bocchini, F. Schiettecatte, A. F. Scott, and A. Hamosh, “OMIM.org: Online Mendelian Inheritance in Man (OMIM(R)), an online catalog of human genes and genetic disorders,” *Nucleic Acids Research*, vol. 43, pp. D789–D798, 2015.
- [70] M. Whirl-Carrillo, E. M. McDonagh, J. M. Hebert et al., “Pharmacogenomics knowledge for personalized medicine,” *Clin Pharmacol Ther*, vol. 92, no. 4, pp. 414–417, 2012.
- [71] D. S. Wishart, Y. D. Feunang, A. C. Guo et al., “DrugBank 5.0: a major update to the DrugBank database for 2018,” *Nucleic Acids Research*, vol. 46, no. D1, pp. D1074–D1082, 2017.
- [72] D. Szklarczyk, A. L. Gable, D. Lyon et al., “STRING v11: protein-protein association networks with increased coverage, supporting functional discovery in genome-wide experimental datasets,” *Nucleic Acids Research*, vol. 47, no. D1, pp. D607–D613, 2019.
- [73] P. Shannon, A. Markiel, O. Ozier et al., “Cytoscape: a software environment for integrated models of biomolecular interaction networks,” *Genome Research*, vol. 13, no. 11, pp. 2498–2504, 2003.
- [74] A. L. Barabasi and Z. N. Oltvai, “Network biology: understanding the cell’s functional organization,” *Nature Reviews Genetics*, vol. 5, no. 2, pp. 101–113, 2004.
- [75] U. Raudvere, L. Kolberg, I. Kuzmin et al., “g:Profiler: a web server for functional enrichment analysis and conversions of gene lists (2019 update),” *Nucleic Acids Research*, vol. 47pp. W191–W198, W1, 2019.
- [76] M. Kanehisa and S. Goto, “KEGG: kyoto encyclopedia of genes and genomes,” *Nucleic Acids Research*, vol. 28, no. 1, pp. 27–30, 2000.
- [77] D. Y. Cho, Y. A. Kim, and T. M. Przytycka, “Chapter 5: network biology approach to complex diseases,” *PLoS Computational Biology*, vol. 8, no. 12, Article ID e1002820, 2012.
- [78] H. Jeong, S. P. Mason, A. L. Barabasi, and Z. N. Oltvai, “Lethality and centrality in protein networks,” *Nature*, vol. 411, no. 6833, pp. 41–42, 2001.
- [79] J. Zhu, X. Yi, Y. Zhang, Z. Pan, L. Zhong, and P. Huang, “Systems pharmacology-based approach to comparatively study the independent and synergistic mechanisms of danhong injection and naoxintong capsule in ischemic stroke treatment,” *Evidence-Based Complementary and Alternative Medicine*, vol. 2019, Article ID 1056708, 17 pages, 2010.
- [80] J. Zhong, Z. Liu, X. Zhou, and J. Xu, “Synergic anti-pruritus mechanisms of action for the radix sophorae flavescens and fructus cnidii herbal pair,” *Molecules*, vol. 229 pages, 2017.
- [81] L. D. Miller, J. Smeds, J. George et al., “An expression signature for p53 status in human breast cancer predicts mutation status, transcriptional effects, and patient survival,” *Proceedings of the National Academy of Sciences of the United States of America*, vol. 102, no. 38, pp. 13550–13555, 2005.
- [82] P. Yang, C. W. Du, M. Kwan, S. X. Liang, and G. J. Zhang, “The impact of p53 in predicting clinical outcome of breast cancer patients with visceral metastasis,” *Scientific Reports*, vol. 3, p. 2246, 2020.
- [83] M. D. Wellenstein, S. B. Coffelt, D. E. M. Duits et al., “Loss of p53 triggers WNT-dependent systemic inflammation to drive breast cancer metastasis,” *Nature*, vol. 572, no. 7770, pp. 538–542, 2019.
- [84] L. Y. Lim, N. Vidnovic, L. W. Ellisen, and C. O. Leong, “Mutant p53 mediates survival of breast cancer cells,” *British Journal of Cancer*, vol. 101, no. 9, pp. 1606–1612, 2009.
- [85] M. Lacroix, R. A. Toillon, and G. Leclercq, “p53 and breast cancer, an update,” *Endocrine-Related Cancer*, vol. 13, no. 2, pp. 293–325, 2006.
- [86] H. Yamashita, T. Toyama, M. Nishio et al., “p53 protein accumulation predicts resistance to endocrine therapy and decreased post-relapse survival in metastatic breast cancer,” *Breast Cancer Research*, vol. 8, no. 4, p. R48, 2006.
- [87] D. Walerych, M. Napoli, L. Collavin, and G. Del Sal, “The rebel angel: mutant p53 as the driving oncogene in breast cancer,” *Carcinogenesis*, vol. 33, no. 11, pp. 2007–2017, 2012.
- [88] N. Turner, E. Moretti, O. Siclari et al., “Targeting triple negative breast cancer: is p53 the answer?” *Cancer Treatment Reviews*, vol. 39, no. 5, pp. 541–550, 2013.
- [89] B. Na, X. Yu, T. Withers et al., “Therapeutic targeting of BRCA1 and TP53 mutant breast cancer through mutant p53 reactivation,” *NPJ Breast Cancer*, vol. 5, p. 14, 2019.
- [90] E. L. Mayer and I. E. Krop, “Advances in targeting SRC in the treatment of breast cancer and other solid malignancies,”

- Clinical Cancer Research*, vol. 16, no. 14, pp. 3526–3532, 2010.
- [91] S. Hiscox, L. Morgan, T. P. Green, D. Barrow, J. Gee, and R. I. Nicholson, “Elevated Src activity promotes cellular invasion and motility in tamoxifen resistant breast cancer cells,” *Breast Cancer Research and Treatment*, vol. 97, no. 3, pp. 263–274, 2006.
- [92] X. H. Zhang, Q. Wang, W. Gerald et al., “Latent bone metastasis in breast cancer tied to Src-dependent survival signals,” *Cancer Cell*, vol. 16, no. 1, pp. 67–78, 2009.
- [93] F. Saad and A. Lipton, “SRC kinase inhibition: targeting bone metastases and tumor growth in prostate and breast cancer,” *Cancer Treatment Reviews*, vol. 36, no. 2, pp. 177–184, 2010.
- [94] H. Jallal, M. L. Valentino, G. Chen, F. Boschelli, S. Ali, and S. A. Rabbani, “A Src/Abl kinase inhibitor, SKI-606, blocks breast cancer invasion, growth, and metastasis in vitro and in vivo,” *Cancer Research*, vol. 67, no. 4, pp. 1580–1588, 2007.
- [95] B. Elsberger, R. Fullerton, S. Zino et al., “Breast cancer patients’ clinical outcome measures are associated with Src kinase family member expression,” *British Journal of Cancer*, vol. 103, no. 6, pp. 899–909, 2010.
- [96] B. S. Verbeek, T. M. Vroom, S. S. Adriaansen-Slot et al., “c-Src protein expression is increased in human breast cancer. An immunohistochemical and biochemical analysis,” *The Journal of Pathology*, vol. 180, no. 4, pp. 383–388, 1996.
- [97] Y. Yang, M. Li, and Y. Li, “High expression of PIK3R1 (p85 α) correlates with poor survival in patients with metastatic breast cancer,” *Int Journal of Clinical and Experimental Pathology*, vol. 9, no. 12, pp. 12797–12806.
- [98] H. J. Burstein, Y. H. Chen, L. M. Parker et al., “VEGF as a marker for outcome among advanced breast cancer patients receiving anti-VEGF therapy with bevacizumab and vinorelbine chemotherapy,” *Clinical Cancer Research*, vol. 14, no. 23, pp. 7871–7877, 2008.
- [99] Y. Liang, R. A. Brekken, and S. M. Hyder, “Vascular endothelial growth factor induces proliferation of breast cancer cells and inhibits the anti-proliferative activity of anti-hormones,” *Endocrine-Related Cancer*, vol. 13, no. 3, pp. 905–919, 2006.
- [100] M. Luo, L. Hou, J. Li et al., “VEGF/NRP-1 axis promotes progression of breast cancer via enhancement of epithelial-mesenchymal transition and activation of NF-kappaB and beta-catenin,” *Cancer Letters*, vol. 373, no. 1, pp. 1–11, 2016.
- [101] M. Perrot-Appianat and M. Di Benedetto, “Autocrine functions of VEGF in breast tumor cells: adhesion, survival, migration and invasion,” *Cell Adhesion & Migration*, vol. 6, no. 6, pp. 547–553, 2012.
- [102] S. B. Vestey, C. Sen, C. J. Calder, C. M. Perks, M. Pignatelli, and Z. E. Winters, “Activated Akt expression in breast cancer: correlation with p53, Hdm2 and patient outcome,” *European Journal of Cancer*, vol. 41, no. 7, pp. 1017–1025, 2005.
- [103] G. Perez-Tenorio, O. Stal, and G. Southeast Sweden Breast Cancer, “Activation of AKT/PKB in breast cancer predicts a worse outcome among endocrine treated patients,” *British Journal of Cancer*, vol. 86, no. 4, pp. 540–545, 2002.
- [104] T. Kirkegaard, C. J. Witton, L. M. McGlynn et al., “AKT activation predicts outcome in breast cancer patients treated with tamoxifen,” *The Journal of Pathology*, vol. 207, no. 2, pp. 139–146, 2005.
- [105] P. Grell, P. Fabian, M. Khoylou et al., “Akt expression and compartmentalization in prediction of clinical outcome in HER2-positive metastatic breast cancer patients treated with trastuzumab,” *International Journal of Oncology*, vol. 41, no. 4, pp. 1204–1212, 2012.
- [106] E. Tokunaga, A. Kataoka, Y. Kimura et al., “The association between Akt activation and resistance to hormone therapy in metastatic breast cancer,” *European Journal of Cancer*, vol. 42, no. 5, pp. 629–635, 2006.
- [107] M. M. Vleugel, A. E. Greijer, R. Bos, E. van der Wall, and P. J. van Diest, “c-Jun activation is associated with proliferation and angiogenesis in invasive breast cancer,” *Human Pathology*, vol. 37, no. 6, pp. 668–674, 2006.
- [108] X. Jiao, S. Katiyar, N. E. Willmarth et al., “c-Jun induces mammary epithelial cellular invasion and breast cancer stem cell expansion,” *Journal of Biological Chemistry*, vol. 285, no. 11, pp. 8218–8226, 2010.
- [109] Y. Zhang, X. Pu, M. Shi et al., “c-Jun, a crucial molecule in metastasis of breast cancer and potential target for biotherapy,” *Oncology Reports*, vol. 18, no. 5, pp. 1207–1212, 2007.
- [110] Y. Zhang, X. Pu, M. Shi et al., “Critical role of c-Jun overexpression in liver metastasis of human breast cancer xenograft model,” *BMC Cancer*, vol. 7, p. 145, 2007.
- [111] A. E. Teschendorff, L. Li, and Z. Yang, “Denosing perturbation signatures reveal an actionable AKT-signaling gene module underlying a poor clinical outcome in endocrine-treated ER+ breast cancer,” *Genome Biology*, vol. 16, p. 61, 2015.
- [112] N. M. Davis, M. Sokolosky, K. Stadelman et al., “Deregulation of the EGFR/PI3K/PTEN/Akt/mTORC1 pathway in breast cancer: possibilities for therapeutic intervention,” *Oncotarget*, vol. 5, no. 13, pp. 4603–4650, 2014.
- [113] H. Nogi, T. Kobayashi, M. Suzuki et al., “EGFR as paradoxical predictor of chemosensitivity and outcome among triple-negative breast cancer,” *Oncology Reports*, vol. 21, no. 2, pp. 413–417, 2009.
- [114] D. Liu, J. He, Z. Yuan et al., “EGFR expression correlates with decreased disease-free survival in triple-negative breast cancer: a retrospective analysis based on a tissue microarray,” *Medical Oncology*, vol. 29, no. 2, pp. 401–405, 2012.
- [115] S. O. Lim, C. W. Li, W. Xia et al., “EGFR signaling enhances aerobic glycolysis in triple-negative breast cancer cells to promote tumor growth and immune escape,” *Cancer Research*, vol. 76, no. 5, pp. 1284–1296, 2016.
- [116] K. L. Mueller, K. Powell, J. M. Madden, S. T. Eblen, and J. L. Boerner, “EGFR tyrosine 845 phosphorylation-dependent proliferation and transformation of breast cancer cells require activation of p38 MAPK,” *Translational Oncology*, vol. 5, no. 5, pp. 327–334, 2012.
- [117] L. Dihge, P. O. Bendahl, D. Grabau et al., “Epidermal growth factor receptor (EGFR) and the estrogen receptor modulator amplified in breast cancer (AIB1) for predicting clinical outcome after adjuvant tamoxifen in breast cancer,” *Breast Cancer Research and Treatment*, vol. 109, no. 2, pp. 255–262, 2008.
- [118] H. S. Park, M. H. Jang, E. J. Kim et al., “High EGFR gene copy number predicts poor outcome in triple-negative breast cancer,” *Modern Pathology*, vol. 27, no. 9, pp. 1212–1222.
- [119] S. E. Ghayad and P. A. Cohen, “Inhibitors of the PI3K/Akt/mTOR pathway: new hope for breast cancer patients,” *Recent Patents on Anti-Cancer Drug Discovery*, vol. 5, no. 1, pp. 29–57.
- [120] S. Langer, C. F. Singer, G. Hudelist et al., “Jun and Fos family protein expression in human breast cancer: correlation of protein expression and clinicopathological parameters,” *European Journal of Gynaecological Oncology*, vol. 27, no. 4, pp. 345–352, 2014.

- [121] X. L. Yan, C. J. Fu, L. Chen et al., "Mesenchymal stem cells from primary breast cancer tissue promote cancer proliferation and enhance mammosphere formation partially via EGF/EGFR/Akt pathway," *Breast Cancer Research and Treatment*, vol. 132, no. 1, pp. 153–164, 2012.
- [122] B. S. Verbeek, S. S. Adriaansen-Slot, T. M. Vroom, T. Beckers, and G. Rijksen, "Overexpression of EGFR and c-erbB2 causes enhanced cell migration in human breast cancer cells and NIH3T3 fibroblasts," *FEBS Letters*, vol. 425, no. 1, pp. 145–150, 1998.
- [123] C. A. Castaneda, H. Cortes-Funes, H. L. Gomez, and E. M. Ciruelos, "The phosphatidylinositol 3-kinase/AKT signaling pathway in breast cancer," *Cancer and Metastasis Reviews*, vol. 29, no. 4, pp. 751–759, 2010.
- [124] G. Kallergi, S. Agelaki, A. Kalykaki, C. Stournaras, D. Mavroudis, and V. Georgoulas, "Phosphorylated EGFR and PI3K/Akt signaling kinases are expressed in circulating tumor cells of breast cancer patients," *Breast Cancer Research*, vol. 10, no. 5, p. R80.
- [125] E. Paplomata and R. O'Regan, "The PI3K/AKT/mTOR pathway in breast cancer: targets, trials and biomarkers," *Therapeutic Advances in Medical Oncology*, vol. 6, no. 4, pp. 154–166, 2008.
- [126] K. S. Saini, S. Loi, E. de Azambuja et al., "Targeting the PI3K/AKT/mTOR and Raf/MEK/ERK pathways in the treatment of breast cancer," *Cancer Treatment Reviews*, vol. 39, no. 8, pp. 935–946, 2013.
- [127] J. Briggs, S. Chamboredon, M. Castellazzi, J. A. Kerry, and T. J. Bos, "Transcriptional upregulation of SPARC, in response to c-Jun overexpression, contributes to increased motility and invasion of MCF7 breast cancer cells," *Oncogene*, vol. 21, no. 46, pp. 7077–7091, 2002.
- [128] N. J. Jordan, J. M. Gee, D. Barrow, A. E. Wakeling, and R. I. Nicholson, "Increased constitutive activity of PKB/Akt in tamoxifen resistant breast cancer MCF-7 cells," *Breast Cancer Research and Treatment*, vol. 87, no. 2, pp. 167–180, 2004.
- [129] J. M. Albert, K. W. Kim, C. Cao, and B. Lu, "Targeting the Akt/mammalian target of rapamycin pathway for radiosensitization of breast cancer," *Molecular Cancer Therapeutics*, vol. 5, no. 5, pp. 1183–1189, 2006.
- [130] K. Liang, W. Jin, C. Knuefermann et al., "Targeting the phosphatidylinositol 3-kinase/Akt pathway for enhancing breast cancer cells to radiotherapy," *Molecular Cancer Therapeutics*, vol. 2, no. 4, pp. 353–360, 2003.
- [131] J. J. Lee, K. Loh, and Y. S. Yap, "PI3K/Akt/mTOR inhibitors in breast cancer," *Cancer Biology & Medicine*, vol. 12, no. 4, pp. 342–354, 2015.
- [132] M. Rodriguez and D. A. Potter, "CYP1A1 regulates breast cancer proliferation and survival," *Molecular Cancer Research*, vol. 11, no. 7, pp. 780–792, 2013.
- [133] Y. Huang, A. Trentham-Dietz, M. Garcia-Closas et al., "Association of CYP1B1 haplotypes and breast cancer risk in Caucasian women," *Cancer Epidemiology, Biomarkers & Prevention*, vol. 18, no. 4, pp. 1321–1323, 2009.
- [134] C. S. Huang, H. D. Chern, K. J. Chang, C. W. Cheng, S. M. Hsu, and C. Y. Shen, "Breast cancer risk associated with genotype polymorphism of the estrogen-metabolizing genes CYP17, CYP1A1, and COMT: a multigenic study on cancer susceptibility," *Cancer Research*, vol. 59, no. 19, pp. 4870–4875, 1999.
- [135] R. Mitra, Z. Guo, M. Milani et al., "CYP3A4 mediates growth of estrogen receptor-positive breast cancer cells in part by inducing nuclear translocation of phospho-Stat3 through biosynthesis of (+/-)-14,15-epoxyeicosatrienoic acid (EET)," *Journal of Biological Chemistry*, vol. 286, no. 20, pp. 17543–17559, 2011.
- [136] N. Napoli, D. T. Villareal, S. Mumm et al., "Effect of CYP1A1 gene polymorphisms on estrogen metabolism and bone density," *Journal of Bone and Mineral Research*, vol. 20, no. 2, pp. 232–239, 2005.
- [137] A. M. Yu, K. Fukamachi, K. W. Krausz, C. Cheung, and F. J. Gonzalez, "Potential role for human cytochrome P450 3A4 in estradiol homeostasis," *Endocrinology*, vol. 146, no. 7, pp. 2911–2919, 2005.
- [138] Z. N. Cheng, Y. Shu, Z. Q. Liu, L. S. Wang, D. S. Ou-Yang, and H. H. Zhou, "Role of cytochrome P450 in estradiol metabolism in vitro," *Acta Pharmacologica Sinica*, vol. 22, no. 2, pp. 148–154, 2001.
- [139] E. Taioli, H. L. Bradlow, S. V. Garbers et al., "Role of estradiol metabolism and CYP1A1 polymorphisms in breast cancer risk," *Cancer Detection and Prevention*, vol. 23, no. 3, pp. 232–237, 1999.
- [140] X. Zhou, G. Qiao, X. Wang et al., "CYP1A1 genetic polymorphism is a promising predictor to improve chemotherapy effects in patients with metastatic breast cancer treated with docetaxel plus thiotepa vs. docetaxel plus capecitabine," *Cancer Chemotherapy and Pharmacology*, vol. 81, no. 2, pp. 365–372, 2018.
- [141] K. Sakurai, K. Enomoto, S. Matsuo, S. Amano, and M. Shiono, "CYP3A4 expression to predict treatment response to docetaxel for metastasis and recurrence of primary breast cancer," *Surgery Today*, vol. 41, no. 5, pp. 674–679, 2011.
- [142] S. Izadi, A. Nikkhoo, M. Hojjat-Farsangi et al., "CDK1 in breast cancer: implications for theranostic potential," *Anti-Cancer Agents in Medicinal Chemistry*, vol. 20, no. 7, pp. 758–767, 2020.
- [143] Q. Xia, Y. Cai, R. Peng, G. Wu, Y. Shi, and W. Jiang, "The CDK1 inhibitor RO3306 improves the response of BRCA-pro deficient breast cancer cells to PARP inhibition," *International Journal of Oncology*, vol. 44, no. 3, pp. 735–744, 2014.
- [144] S. J. Kim, N. Masuda, F. Tsukamoto et al., "The cell cycle profiling-risk score based on CDK1 and 2 predicts early recurrence in node-negative, hormone receptor-positive breast cancer treated with endocrine therapy," *Cancer Letters*, vol. 355, no. 2, pp. 217–223, 2014.
- [145] S. J. Kim, S. Nakayama, Y. Miyoshi et al., "Determination of the specific activity of CDK1 and CDK2 as a novel prognostic indicator for early breast cancer," *Annals of Oncology*, vol. 19, no. 1, pp. 68–72, 2008.
- [146] S. Nakayama, Y. Torikoshi, T. Takahashi et al., "Prediction of paclitaxel sensitivity by CDK1 and CDK2 activity in human breast cancer cells," *Breast Cancer Research*, vol. 11, no. 1, p. R12, 2009.
- [147] J. Kang, C. M. Sergio, R. L. Sutherland, and E. A. Musgrove, "Targeting cyclin-dependent kinase 1 (CDK1) but not CDK4/6 or CDK2 is selectively lethal to MYC-dependent human breast cancer cells," *BMC Cancer*, vol. 14, p. 32, 2014.
- [148] S. J. Yue, J. Liu, W. W. Feng et al., "System pharmacology-based dissection of the synergistic mechanism of Huangqi and Huanglian for diabetes mellitus," *Frontiers in Pharmacology*, vol. 8, p. 694, 2017.
- [149] W. Kolch, M. Halasz, M. Granovskaya, and B. N. Kholodenko, "The dynamic control of signal transduction networks in cancer cells," *Nature Reviews Cancer*, vol. 15, no. 9, pp. 515–527, 2015.

- [150] K. M. Hardy, B. W. Booth, M. J. Hendrix, D. S. Salomon, and L. Strizzi, "ErbB/EGF signaling and EMT in mammary development and breast cancer," *Journal of Mammary Gland Biology and Neoplasia*, vol. 15, no. 2, pp. 191–199, 2010.
- [151] M. Luo and J. L. Guan, "Focal adhesion kinase: a prominent determinant in breast cancer initiation, progression and metastasis," *Cancer Letters*, vol. 289, no. 2, pp. 127–139, 2010.
- [152] M. Bullock, "FOXO factors and breast cancer: outfoxing endocrine resistance," *Endocrine-Related Cancer*, vol. 23, no. 2, pp. R113–R130, 2016.
- [153] M. Farhan, H. Wang, U. Gaur, P. J. Little, J. Xu, and W. Zheng, "FOXO signaling pathways as therapeutic targets in cancer," *International Journal of Biological Sciences*, vol. 13, no. 7, pp. 815–827, 2017.
- [154] T. Li and J. A. Sparano, "Inhibiting Ras signaling in the therapy of breast cancer," *Clinical Breast Cancer*, vol. 3, no. 6, pp. 405–416, 2003.
- [155] P. D. Angelini, M. F. Zacarias Fluck, K. Pedersen et al., "Constitutive HER2 signaling promotes breast cancer metastasis through cellular senescence," *Cancer Res*, vol. 73, no. 1, pp. 450–458, 2013.
- [156] P. Lipponen, "Apoptosis in breast cancer: relationship with other pathological parameters," *Endocrine-Related Cancer*, vol. 6, no. 1, pp. 13–16, 1999.
- [157] R. Pare, T. Yang, J. S. Shin, and C. S. Lee, "The significance of the senescence pathway in breast cancer progression," *Journal of Clinical Pathology*, vol. 66, no. 6, pp. 491–495, 2013.
- [158] M. Parton, M. Dowsett, and I. Smith, "Studies of apoptosis in breast cancer," *BMJ*, vol. 322, no. 7301, pp. 1528–1532, 2001.
- [159] P. G. Roy and A. M. Thompson, "Cyclin D1 and breast cancer," *Breast*, vol. 15, no. 6, pp. 718–727, 1998.
- [160] R. L. Sutherland and E. A. Musgrove, "Cyclins and breast cancer," *Journal of Mammary Gland Biology and Neoplasia*, vol. 9, no. 1, pp. 95–104, 2004.
- [161] J. E. Goldberg and K. L. Schwertfeger, "Proinflammatory cytokines in breast cancer: mechanisms of action and potential targets for therapeutics," *Current Cancer Drug Targets*, vol. 11, no. 9, pp. 1133–1146, 2010.
- [162] M. F. Mercogliano, S. Bruni, P. V. Elizalde, and R. Schillaci, "Tumor necrosis factor alpha blockade: an opportunity to tackle breast cancer," *Frontiers in Oncology*, vol. 10, p. 584, 2020.
- [163] S. Hayashi, T. Niwa, and Y. Yamaguchi, "Estrogen signaling pathway and its imaging in human breast cancer," *Cancer Sciences*, vol. 100, no. 10, pp. 1773–1778, 2009.
- [164] R. Nahta and R. M. O'Regan, "Therapeutic implications of estrogen receptor signaling in HER2-positive breast cancers," *Breast Cancer Research and Treatment*, vol. 135, no. 1, pp. 39–48, 2012.
- [165] J. M. Renoir, V. Marsaud, and G. Lazennec, "Estrogen receptor signaling as a target for novel breast cancer therapeutics," *Biochemical Pharmacology*, vol. 85, no. 4, pp. 449–465, 2013.
- [166] S. Saha Roy and R. K. Vadlamudi, "Role of estrogen receptor signaling in breast cancer metastasis," *International Journal of Breast Cancer*, vol. 2012, Article ID 654698, 2012.
- [167] T. Saha, S. Makar, R. Swetha, G. Gutti, and S. K. Singh, "Estrogen signaling: an emanating therapeutic target for breast cancer treatment," *European Journal of Medicinal Chemistry*, vol. 177, pp. 116–143, 2019.
- [168] G. P. Andrieu, J. S. Shafran, C. L. Smith et al., "BET protein targeting suppresses the PD-1/PD-L1 pathway in triple-negative breast cancer and elicits anti-tumor immune response," *Cancer Letters*, vol. 465, pp. 45–58, 2019.
- [169] S. Chretien, I. Zerdes, J. Bergh, A. Matikas, and T. Foukakis, "Beyond PD-1/PD-L1 inhibition: what the future holds for breast cancer immunotherapy," *Cancers (Basel)*, vol. 115 pages, 2019.
- [170] Y. Guo, P. Yu, Z. Liu et al., "Prognostic and clinicopathological value of programmed death ligand-1 in breast cancer: a meta-analysis," *PLoS One*, vol. 11, no. 5, Article ID e0156323, 2016.
- [171] X. Jing, S. Shao, Y. Zhang et al., "BRD4 inhibition suppresses PD-L1 expression in triple-negative breast cancer," *Experimental Cell Research*, vol. 392, no. 2, Article ID 112034, 2010.
- [172] S. Muenst, A. R. Schaerli, F. Gao et al., "Expression of programmed death ligand 1 (PD-L1) is associated with poor prognosis in human breast cancer," *Breast Cancer Research and Treatment*, vol. 146, no. 1, pp. 15–24, 2014.
- [173] G. B. Jang, J. Y. Kim, S. D. Cho et al., "Blockade of Wnt/beta-catenin signaling suppresses breast cancer metastasis by inhibiting CSC-like phenotype," *Scientific Reports*, vol. 5, p. 12465, 2015.
- [174] L. P. Schwab, D. L. Peacock, D. Majumdar et al., "Hypoxia-inducible factor 1alpha promotes primary tumor growth and tumor-initiating cell activity in breast cancer," *Breast Cancer Research*, vol. 14, no. 1, p. R6, 2012.
- [175] G. L. Semenza, "Hypoxia-inducible factors: coupling glucose metabolism and redox regulation with induction of the breast cancer stem cell phenotype," *The EMBO Journal*, vol. 36, no. 3, pp. 252–259, 2017.
- [176] D. M. Gilkes and G. L. Semenza, "Role of hypoxia-inducible factors in breast cancer metastasis," *Future Oncology*, vol. 9, no. 11, pp. 1623–1636, 2013.
- [177] R. Lamb, M. P. Ablett, K. Spence, G. Landberg, A. H. Sims, and R. B. Clarke, "Wnt pathway activity in breast cancer subtypes and stem-like cells," *PLoS One*, vol. 8, no. 7, Article ID e67811, 2013.
- [178] N. Dey, B. G. Barwick, C. S. Moreno et al., "Wnt signaling in triple negative breast cancer is associated with metastasis," *BMC Cancer*, vol. 13, p. 537, 2013.
- [179] S. G. Pohl, N. Brook, M. Agostino, F. Arfuso, A. P. Kumar, and A. Dharmarajan, "Wnt signaling in triple-negative breast cancer," *Oncogenesis*, vol. 6, no. 4, p. e310, 2017.
- [180] J. R. Prospero and K. H. Goss, "A Wnt-ow of opportunity: targeting the Wnt/beta-catenin pathway in breast cancer," *Current Cancer Drug Targets*, vol. 11, no. 9, pp. 1074–1088, 2010.
- [181] M. Gasco, S. Shami, and T. Crook, "The p53 pathway in breast cancer," *Breast Cancer Research*, vol. 4, no. 2, pp. 70–76, 2002.
- [182] A. M. Mercurio, E. A. Lipscomb, and R. E. Bachelder, "Non-angiogenic functions of VEGF in breast cancer," *Journal of Mammary Gland Biology and Neoplasia*, vol. 10, no. 4, pp. 283–290, 2005.
- [183] E. A. Musgrove and R. L. Sutherland, "Biological determinants of endocrine resistance in breast cancer," *Nature Reviews Cancer*, vol. 9, no. 9, pp. 631–643, 2009.
- [184] A. S. Clark, K. West, S. Streicher, and P. A. Dennis, "Constitutive and inducible Akt activity promotes resistance to chemotherapy, trastuzumab, or tamoxifen in breast cancer cells," *Molecular Cancer Therapeutics*, vol. 1, no. 9, pp. 707–717, 2002.
- [185] R. Clarke, J. J. Tyson, and J. M. Dixon, "Endocrine resistance in breast cancer--An overview and update," *Molecular and Cellular Endocrinology*, vol. 418, no. 3, pp. 220–234, 2015.

- [186] N. Eckstein, "Platinum resistance in breast and ovarian cancer cell lines," *Journal of Experimental & Clinical Cancer Research*, vol. 30, p. 91, 2011.
- [187] M. P. Decatris, S. Sundar, and K. J. O'Byrne, "Platinum-based chemotherapy in metastatic breast cancer: current status," *Cancer Treatment Reviews*, vol. 30, no. 1, pp. 53–81, 2004.
- [188] P. R. Pohlmann, I. A. Mayer, and R. Mernaugh, "Resistance to trastuzumab in breast cancer," *Clinical Cancer Research*, vol. 15, no. 24, pp. 7479–7491, 2009.
- [189] C. K. Osborne and R. Schiff, "Mechanisms of endocrine resistance in breast cancer," *Annual Review of Medicine*, vol. 62, pp. 233–247, 2011.
- [190] J. Montojo, K. Zuberi, H. Rodriguez, G. D. Bader, and Q. Morris, "GeneMANIA: fast gene network construction and function prediction for Cytoscape," *F1000Research*, vol. 3, p. 153, 2014.
- [191] J.-H. Kim, D.-H. Kim, J.-H. You et al., "Comparison of cytotoxin and immune activities between natural and tissue cultured plant in *Artemisia capillaris* thunb," *Korean Journal of Medicinal Crop Science*, vol. 13, no. 4, pp. 154–160, 2005.
- [192] J. Song, Y. Wang, M. Teng et al., "Cordyceps militaris induces tumor cell death via the caspasedependent mitochondrial pathway in HepG2 and MCF7 cells," *Molecular Medicine Reports*, vol. 13, no. 6, pp. 5132–5140, 2016.
- [193] H. C. Wu, S. T. Chen, J. C. Chang et al., "Radical scavenging and antiproliferative effects of cordycepin-rich ethanol extract from Brown rice-cultivated *Cordyceps militaris* (ascomycetes) mycelium on breast cancer cell lines," *International Journal of Medicinal Mushrooms*, vol. 21, no. 7, pp. 657–669, 2019.
- [194] M. H. Jeong, C. M. Lee, S. W. Lee et al., "Cordycepin-enriched *Cordyceps militaris* induces immunomodulation and tumor growth delay in mouse-derived breast cancer," *Oncology Reports*, vol. 30, no. 4, pp. 1996–2002, 2013.
- [195] S. O. Lee, Y. J. Jeong, M. Kim, C. H. Kim, and I. S. Lee, "Suppression of PMA-induced tumor cell invasion by capillarisin via the inhibition of NF-kappaB-dependent MMP-9 expression," *Biochemical and Biophysical Research Communications*, vol. 366, no. 4, pp. 1019–1024, 2008.
- [196] K. Amrutha, P. Nanjan, S. K. Shaji et al., "Discovery of lesser known flavones as inhibitors of NF-kappaB signaling in MDA-MB-231 breast cancer cells—a SAR study," *Bioorganic & Medicinal Chemistry Letters*, vol. 24, no. 19, pp. 4735–4742, 2014.
- [197] H. Takemura, H. Uchiyama, T. Ohura et al., "A methoxy-flavonoid, chrysoeriol, selectively inhibits the formation of a carcinogenic estrogen metabolite in MCF-7 breast cancer cells," *The Journal of Steroid Biochemistry and Molecular Biology*, vol. 118, no. 1-2, pp. 70–76, 2009.
- [198] J. Yeon Park, H. Young Kim, T. Shibamoto et al., "Beneficial effects of a medicinal herb, *Cirsium japonicum* var. *maackii*, extract and its major component, cirsimaritin on breast cancer metastasis in MDA-MB-231 breast cancer cells," *Bioorganic & Medicinal Chemistry Letters*, vol. 27, no. 17, pp. 3968–3973, 2017.
- [199] E. M. Noh, H. J. Youn, S. H. Jung et al., "Cordycepin inhibits TPA-induced matrix metalloproteinase-9 expression by suppressing the MAPK/AP-1 pathway in MCF-7 human breast cancer cells," *International Journal of Molecular Medicine*, vol. 25, no. 2, pp. 255–260, 2010.
- [200] D. Wang, Y. Zhang, J. Lu et al., "Cordycepin, a natural antineoplastic agent, induces apoptosis of breast cancer cells via caspase-dependent pathways," *Natural Product Communications*, vol. 11, no. 1, pp. 63–68, 2016.
- [201] S. Choi, M. H. Lim, K. M. Kim, B. H. Jeon, W. O. Song, and T. W. Kim, "Cordycepin-induced apoptosis and autophagy in breast cancer cells are independent of the estrogen receptor," *Toxicology and Applied Pharmacology*, vol. 257, no. 2, pp. 165–173, 2011.
- [202] D. Lee, W. Y. Lee, K. Jung et al., "The inhibitory effect of cordycepin on the proliferation of MCF-7 breast cancer cells, and its mechanism: an investigation using network pharmacology-based analysis," *Biomolecules*, vol. 9, no. 9, 2019.
- [203] H. J. Lee, P. Burger, M. Vogel, K. Friese, and A. Bruning, "The nucleoside antagonist cordycepin causes DNA double strand breaks in breast cancer cells," *Invest New Drugs*, vol. 30, no. 5, pp. 1917–1925, 2012.
- [204] J. Dong, Y. Li, H. Xiao et al., "Cordycepin sensitizes breast cancer cells toward irradiation through elevating ROS production involving Nrf2," *Toxicology and Applied Pharmacology*, vol. 364, pp. 12–21, 2019.
- [205] V. P. Androutsopoulos, K. Ruparelia, R. R. Arroo, A. M. Tsatsakis, and D. A. Spandidos, "CYP1-mediated antiproliferative activity of dietary flavonoids in MDA-MB-468 breast cancer cells," *Toxicology*, vol. 264, no. 3, pp. 162–170, 2009.
- [206] H. W. Zhang, J. J. Hu, R. Q. Fu et al., "Flavonoids inhibit cell proliferation and induce apoptosis and autophagy through downregulation of PI3Kgamma mediated PI3K/AKT/mTOR/p70S6K/ULK signaling pathway in human breast cancer cells," *Scientific Reports*, vol. 8, no. 1, p. 11255, 2018.
- [207] Y. Li, J. Hong, H. Li et al., "Genkwanin nanosuspensions: a novel and potential antitumor drug in breast carcinoma therapy," *Drug Delivery*, vol. 24, no. 1, pp. 1491–1500, 2017.
- [208] Q. Wu, P. A. Kroon, H. Shao, P. W. Needs, and X. Yang, "Differential effects of quercetin and two of its derivatives, isorhamnetin and isorhamnetin-3-glucuronide, in inhibiting the proliferation of human breast-cancer MCF-7 cells," *Journal of Agricultural and Food Chemistry*, vol. 66, no. 27, pp. 7181–7189, 2018.
- [209] C. Li, D. Yang, Y. Zhao et al., "Inhibitory effects of isorhamnetin on the invasion of human breast carcinoma cells by downregulating the expression and activity of matrix metalloproteinase-2/9," *Nutrition and Cancer*, vol. 67, no. 7, pp. 1191–1200, 2015.
- [210] J. Hu, Y. Zhang, X. Jiang et al., "ROS-mediated activation and mitochondrial translocation of CaMKII contributes to Drp1-dependent mitochondrial fission and apoptosis in triple-negative breast cancer cells by isorhamnetin and chloroquine," *Journal of Experimental & Clinical Cancer Research*, vol. 38, no. 1, p. 225, 2019.
- [211] A. Alvarez-Sala, A. Attanzio, L. Tesoriere, G. Garcia-Llatas, R. Barbera, and A. Cilla, "Apoptotic effect of a phytosterol-ingredient and its main phytosterol (beta-sitosterol) in human cancer cell lines," *International Journal of Food Sciences and Nutrition*, vol. 70, no. 3, pp. 323–334, 2019.
- [212] C. Park, D. O. Moon, C. H. Ryu et al., "Beta-sitosterol sensitizes MDA-MB-231 cells to TRAIL-induced apoptosis," *Acta Pharmacologica Sinica*, vol. 29, no. 3, pp. 341–348, 2008.
- [213] A. B. Awad, R. Roy, and C. S. Fink, "Beta-sitosterol, a plant sterol, induces apoptosis and activates key caspases in MDA-MB-231 human breast cancer cells," *Oncology Reports*, vol. 10, no. 2, pp. 497–500, 2003.
- [214] A. B. Awad, A. C. Downie, and C. S. Fink, "Inhibition of growth and stimulation of apoptosis by beta-sitosterol treatment of MDA-MB-231 human breast cancer cells in

- culture," *International Journal of Molecular Medicine*, vol. 5, no. 5, pp. 541–545, 2000.
- [215] A. B. Awad, S. L. Barta, C. S. Fink, and P. G. Bradford, "beta-Sitosterol enhances tamoxifen effectiveness on breast cancer cells by affecting ceramide metabolism," *Molecular Nutrition & Food Research*, vol. 52, no. 4, pp. 419–426, 2008.
- [216] C. Azevedo, A. Correia-Branco, J. R. Araujo, J. T. Guimaraes, E. Keating, and F. Martel, "The chemopreventive effect of the dietary compound kaempferol on the MCF-7 human breast cancer cell line is dependent on inhibition of glucose cellular uptake," *Nutrition and Cancer*, vol. 67, no. 3, pp. 504–513, 2015.
- [217] S. Y. Chien, Y. C. Wu, J. G. Chung et al., "Quercetin-induced apoptosis acts through mitochondrial- and caspase-3-dependent pathways in human breast cancer MDA-MB-231 cells," *Human & Experimental Toxicology*, vol. 28, no. 8, pp. 493–503, 2009.
- [218] E. J. Choi and W. S. Ahn, "Kaempferol induced the apoptosis via cell cycle arrest in human breast cancer MDA-MB-453 cells," *Nutrition Research and Practice*, vol. 2, no. 4, pp. 322–325, 2008.
- [219] C. C. Chou, J. S. Yang, H. F. Lu et al., "Quercetin-mediated cell cycle arrest and apoptosis involving activation of a caspase cascade through the mitochondrial pathway in human breast cancer MCF-7 cells," *Archives of Pharmacological Research*, vol. 33, no. 8, pp. 1181–1191, 2010.
- [220] M. T. Cook, Y. Liang, C. Besch-Williford, S. Goyette, B. Mafuvadze, and S. M. Hyder, "Luteolin inhibits progesterin-dependent angiogenesis, stem cell-like characteristics, and growth of human breast cancer xenografts," *Springerplus*, vol. 4, p. 444, 2015.
- [221] M. T. Cook, Y. Liang, C. Besch-Williford, and S. M. Hyder, "Luteolin inhibits lung metastasis, cell migration, and viability of triple-negative breast cancer cells," *Breast Cancer (Dove Med Press)*, vol. 9, pp. 9–19, 2017.
- [222] X. H. Deng, H. Y. Song, Y. F. Zhou, G. Y. Yuan, and F. J. Zheng, "Effects of quercetin on the proliferation of breast cancer cells and expression of survivin in vitro," *Experimental and Therapeutic Medicine*, vol. 6, no. 5, pp. 1155–1158, 2013.
- [223] J. Duo, G. G. Ying, G. W. Wang, and L. Zhang, "Quercetin inhibits human breast cancer cell proliferation and induces apoptosis via Bcl-2 and Bax regulation," *Molecular Medicine Reports*, vol. 5, no. 6, pp. 1453–1456, 2012.
- [224] G. Gao, R. Ge, Y. Li, and S. Liu, "Luteolin exhibits anti-breast cancer property through up-regulating miR-203," *Artificial Cells, Nanomedicine, and Biotechnology*, vol. 47, no. 1, pp. 3265–3271, 2019.
- [225] L. Huang, K. Jin, and H. Lan, "Luteolin inhibits cell cycle progression and induces apoptosis of breast cancer cells through downregulation of human telomerase reverse transcriptase," *Oncology Letters*, vol. 17, no. 4, pp. 3842–3850, 2019.
- [226] H. Hung, "Inhibition of estrogen receptor alpha expression and function in MCF-7 cells by kaempferol," *Journal of Cellular Physiology*, vol. 198, no. 2, pp. 197–208, 2004.
- [227] L. Jia, S. Huang, X. Yin, Y. Zan, Y. Guo, and L. Han, "Quercetin suppresses the mobility of breast cancer by suppressing glycolysis through Akt-mTOR pathway mediated autophagy induction," *Life Sciences*, vol. 208, pp. 123–130, 2018.
- [228] Y. Jiang, K. P. Xie, H. N. Huo, L. M. Wang, W. Zou, and M. J. Xie, "[Inhibitory effect of luteolin on the angiogenesis of chick chorioallantoic membrane and invasion of breast cancer cells via downregulation of AEG-1 and MMP-2]," *Sheng Li Xue Bao*, vol. 65, no. 5, pp. 513–518, 2013.
- [229] G. Y. Kang, E. R. Lee, J. H. Kim et al., "Downregulation of PLK-1 expression in kaempferol-induced apoptosis of MCF-7 cells," *European Journal of Pharmacology*, vol. 611, no. 1–3, pp. 17–21, 2009.
- [230] B. W. Kim, E. R. Lee, H. M. Min et al., "Sustained ERK activation is involved in the kaempferol-induced apoptosis of breast cancer cells and is more evident under 3-D culture condition," *Cancer Biology & Therapy*, vol. 7, no. 7, pp. 1080–1089, 2008.
- [231] M. J. Kim, J. S. Woo, C. H. Kwon, J. H. Kim, Y. K. Kim, and K. H. Kim, "Luteolin induces apoptotic cell death through AIF nuclear translocation mediated by activation of ERK and p38 in human breast cancer cell lines," *Cell Biology International*, vol. 36, no. 4, pp. 339–344, 2012.
- [232] S. H. Kim, K. A. Hwang, and K. C. Choi, "Treatment with kaempferol suppresses breast cancer cell growth caused by estrogen and triclosan in cellular and xenograft breast cancer models," *Journal of Nutritional Biochemistry*, vol. 28, pp. 70–82, 2016.
- [233] E. J. Lee, S. Y. Oh, and M. K. Sung, "Luteolin exerts anti-tumor activity through the suppression of epidermal growth factor receptor-mediated pathway in MDA-MB-231 ER-negative breast cancer cells," *Food and Chemical Toxicology*, vol. 50, no. 11, pp. 4136–4143, 2012.
- [234] G. A. Lee, K. C. Choi, and K. A. Hwang, "Kaempferol, a phytoestrogen, suppressed triclosan-induced epithelial-mesenchymal transition and metastatic-related behaviors of MCF-7 breast cancer cells," *Environmental Toxicology and Pharmacology*, vol. 49, pp. 48–57, 2017.
- [235] Y. K. Lee, S. Y. Park, Y. M. Kim, W. S. Lee, and O. J. Park, "AMP kinase/cyclooxygenase-2 pathway regulates proliferation and apoptosis of cancer cells treated with quercetin," *Experimental & Molecular Medicine*, vol. 41, no. 3, pp. 201–207, 2009.
- [236] C. Li, Y. Zhao, D. Yang et al., "Inhibitory effects of kaempferol on the invasion of human breast carcinoma cells by downregulating the expression and activity of matrix metalloproteinase-9," *Biochemistry and Cell Biology*, vol. 93, no. 1, pp. 16–27, 2015.
- [237] S. Li, Q. Zhao, B. Wang, S. Yuan, X. Wang, and K. Li, "Quercetin reversed MDR in breast cancer cells through down-regulating P-gp expression and eliminating cancer stem cells mediated by YB-1 nuclear translocation," *Phytotherapy Research*, vol. 32, no. 8, pp. 1530–1536, 2018.
- [238] X. Li, N. Zhou, J. Wang et al., "Quercetin suppresses breast cancer stem cells (CD44(+)/CD24(-)) by inhibiting the PI3K/Akt/mTOR-signaling pathway," *Life Sciences*, vol. 196, pp. 56–62, 2018.
- [239] C. H. Lin, C. Y. Chang, K. R. Lee, H. J. Lin, T. H. Chen, and L. Wan, "Flavones inhibit breast cancer proliferation through the Akt/FOXO3a signaling pathway," *BMC Cancer*, vol. 15, p. 958, 2015.
- [240] C. W. Lin, W. C. Hou, S. C. Shen et al., "Quercetin inhibition of tumor invasion via suppressing PKC delta/ERK/AP-1-dependent matrix metalloproteinase-9 activation in breast carcinoma cells," *Carcinogenesis*, vol. 29, no. 9, pp. 1807–1815, 2008.
- [241] D. Lin, G. Kuang, J. Wan et al., "Luteolin suppresses the metastasis of triple-negative breast cancer by reversing epithelial-to-mesenchymal transition via downregulation of beta-catenin expression," *Oncology Reports*, vol. 37, no. 2, pp. 895–902, 2017.

- [242] B. M. Markaverich, K. Shoulars, and M. A. Rodriguez, "Luteolin regulation of estrogen signaling and cell cycle pathway genes in MCF-7 human breast cancer cells," *International Journal of Biomedical Science*, vol. 7, no. 2, pp. 101–111, 2011.
- [243] L. T. Nguyen, Y. H. Lee, A. R. Sharma et al., "Quercetin induces apoptosis and cell cycle arrest in triple-negative breast cancer cells through modulation of Foxo3a activity," *The Korean Journal of Physiology & Pharmacology*, vol. 21, no. 2, pp. 205–213, 2017.
- [244] S. M. Oh, Y. P. Kim, and K. H. Chung, "Biphasic effects of kaempferol on the estrogenicity in human breast cancer cells," *Archives of Pharmacal Research*, vol. 29, no. 5, pp. 354–362, 2006.
- [245] S. H. Park, S. Ham, T. H. Kwon et al., "Luteolin induces cell cycle arrest and apoptosis through extrinsic and intrinsic signaling pathways in MCF-7 breast cancer cells," *Journal of Environmental Pathology, Toxicology, and Oncology*, vol. 33, no. 3, pp. 219–231, 2014.
- [246] K. Phromnoi, S. Yodkeeree, S. Anuchapreeda, and P. Limtrakul, "Inhibition of MMP-3 activity and invasion of the MDA-MB-231 human invasive breast carcinoma cell line by bioflavonoids," *Acta Pharmacologica Sinica*, vol. 30, no. 8, pp. 1169–1176, 2009.
- [247] S. Ranganathan, D. Halagowder, and N. D. Sivasithambaram, "Quercetin suppresses twist to induce apoptosis in MCF-7 breast cancer cells," *PLoS One*, vol. 10, no. 10, Article ID e0141370, 2015.
- [248] P. S. Rao, A. Satelli, M. Moridani, M. Jenkins, and U. S. Rao, "Luteolin induces apoptosis in multidrug resistant cancer cells without affecting the drug transporter function: involvement of cell line-specific apoptotic mechanisms," *International Journal of Cancer*, vol. 130, no. 11, pp. 2703–2714, 2012.
- [249] K. M. Reipas, J. H. Law, N. Couto et al., "Luteolin is a novel p90 ribosomal S6 kinase (RSK) inhibitor that suppresses Notch4 signaling by blocking the activation of Y-box binding protein-1 (YB-1)," *Oncotarget*, vol. 4, no. 2, pp. 329–345, 2013.
- [250] A. Rivera Rivera, L. Castillo-Pichardo, Y. Gerena, and S. Dharmawardhane, "Anti-breast cancer potential of quercetin via the Akt/AMPK/mammalian target of rapamycin (mTOR) signaling cascade," *PLoS One*, vol. 11, no. 6, Article ID e0157251, 2016.
- [251] G. Scambia, F. O. Ranelletti, P. Benedetti Panici et al., "Quercetin inhibits the growth of a multidrug-resistant estrogen-receptor-negative MCF-7 human breast-cancer cell line expressing type II estrogen-binding sites," *Cancer Chemotherapy and Pharmacology*, vol. 28, no. 4, pp. 255–258, 1991.
- [252] H. S. Seo, J. M. Ku, H. S. Choi et al., "Quercetin induces caspase-dependent extrinsic apoptosis through inhibition of signal transducer and activator of transcription 3 signaling in HER2-overexpressing BT-474 breast cancer cells," *Oncology Reports*, vol. 36, no. 1, pp. 31–42, 2016.
- [253] A. Srinivasan, C. Thangavel, Y. Liu et al., "Quercetin regulates beta-catenin signaling and reduces the migration of triple negative breast cancer," *Including results for Mol Carcinogenesis*, vol. 55, no. 5, pp. 743–756, 2015.
- [254] J. Q. Sui, K. P. Xie, and M. J. Xie, "Inhibitory effect of luteolin on the proliferation of human breast cancer cell lines induced by epidermal growth factor," *Sheng Li Xue Bao*, vol. 68, no. 1, pp. 27–34, 2016.
- [255] D. W. Sun, H. D. Zhang, L. Mao et al., "Luteolin inhibits breast cancer development and progression in vitro and in vivo by suppressing Notch signaling and regulating miRNAs," *Cellular Physiology and Biochemistry*, vol. 37, no. 5, pp. 1693–1711, 2015.
- [256] S. F. Tao, H. F. He, and Q. Chen, "Quercetin inhibits proliferation and invasion acts by up-regulating miR-146a in human breast cancer cells," *Molecular and Cellular Biochemistry*, vol. 402, no. 1–2, pp. 93–100, 2015.
- [257] L. M. Wang, K. P. Xie, H. N. Huo, F. Shang, W. Zou, and M. J. Xie, "Luteolin inhibits proliferation induced by IGF-1 pathway dependent ERalpha in human breast cancer MCF-7 cells," *Asian Pacific Journal of Cancer Prevention*, vol. 13, no. 4, pp. 1431–1437, 2012.
- [258] R. Wang, L. Yang, S. Li et al., "Quercetin inhibits breast cancer stem cells via downregulation of aldehyde dehydrogenase 1A1 (ALDH1A1), chemokine receptor type 4 (CXCR4), mucin 1 (MUC1), and epithelial cell adhesion molecule (EPCAM)," *Medical Science Monitor*, vol. 24, pp. 412–420, 2018.
- [259] T. D. Way, M. C. Kao, and J. K. Lin, "Degradation of HER2/neu by apigenin induces apoptosis through cytochrome c release and caspase-3 activation in HER2/neu-overexpressing breast cancer cells," *FEBS Letters*, vol. 579, no. 1, pp. 145–152, 2005.
- [260] X. Yi, J. Zuo, C. Tan et al., "Kaempferol, a flavonoid compound from gynura medica induced apoptosis and growth inhibition in mcf-7 breast cancer cell," *African Journal of Traditional, Complementary and Alternative Medicines*, vol. 13, no. 4, pp. 210–215, 2016.
- [261] X. Zhao, Q. Wang, S. Yang et al., "Quercetin inhibits angiogenesis by targeting calcineurin in the xenograft model of human breast cancer," *European Journal of Pharmacology*, vol. 781, pp. 60–68, 2016.
- [262] L. Zhu and L. Xue, "Kaempferol suppresses proliferation and induces cell cycle arrest, apoptosis, and DNA damage in breast cancer cells," *Oncology Research*, vol. 27, no. 6, pp. 629–634, 2019.
- [263] Y.-K. Lee, S. Y. Park, W.-S. L. Young-Min Kim, and O. Park, "Regulation of MCF-7 cell apoptosis by phytochemical quercetin through AMPK-mTOR signaling pathway," *Cancer Prevention Research*, vol. 15, no. 4, pp. 320–325.
- [264] Y. Pandey, S. H. Mehdi, M. A. Khan, P. Bhatt, and C. Pant, "TRAIL (Tumor Necrosis Factor-Related Apoptosis-Inducing Ligand) mediated Apoptosis of human breast cancer cells sensitized by dietary flavonoid Kaempferol," *International Journal of Biological Sciences*, vol. 5, p. 6, 2019.
- [265] J. Stapel, C. Oppermann, D. Richter, W. Ruth, and V. J. Briese, "Polyphenol compounds with anti-carcinogenic qualities: effects of quercetin (flavonol), chrysin (flavon), kaempferol (flavanol), naringenin (flavanon) and hesperidin (flavanoid) on in vitro breast cancer," *J Journal of Medicinal Plants Research*, vol. 7, no. 29, pp. 2187–2196, 2013.
- [266] A. S. Sultan, M. I. Khalil, B. M. Sami, A. F. Alkhouriji, and O. J. Sadek, "Quercetin induces apoptosis in triple-negative breast cancer cells via inhibiting fatty acid synthase and β -catenin," *International Journal of Clinical and Experimental Pathology*, vol. 10, no. 1, pp. 156–172, 2017.
- [267] S. H. Akbas, M. Timur, and T. Ozben, "The effect of quercetin on topotecan cytotoxicity in MCF-7 and MDA-MB 231 human breast cancer cells," *Journal of Surgical Research*, vol. 125, no. 1, pp. 49–55, 2005.
- [268] C. T. Chiang, T. D. Way, and J. K. Lin, "Sensitizing HER2-overexpressing cancer cells to luteolin-induced apoptosis

- through suppressing p21(WAF1/CIP1) expression with rapamycin," *Molecular Cancer Therapeutics*, vol. 6, no. 7, pp. 2127–2138, 2007.
- [269] G. Du, H. Lin, M. Wang et al., "Quercetin greatly improved therapeutic index of doxorubicin against 4T1 breast cancer by its opposing effects on HIF-1 α in tumor and normal cells," *Cancer Chemotherapy and Pharmacology*, vol. 65, no. 2, pp. 277–287, 2010.
- [270] G. J. Du, Z. H. Song, H. H. Lin, X. F. Han, S. Zhang, and Y. M. Yang, "Luteolin as a glycolysis inhibitor offers superior efficacy and lesser toxicity of doxorubicin in breast cancer cells," *Biochemical and Biophysical Research Communications*, vol. 372, no. 3, pp. 497–502, 2008.
- [271] Y. W. Jeon, Y. E. Ahn, W. S. Chung, H. J. Choi, and Y. J. Suh, "Synergistic effect between celecoxib and luteolin is dependent on estrogen receptor in human breast cancer cells," *Tumor Biology*, vol. 36, no. 8, pp. 6349–6359, 2015.
- [272] Y. W. Jeon and Y. J. Suh, "Synergistic apoptotic effect of celecoxib and luteolin on breast cancer cells," *Oncology Reports*, vol. 29, no. 2, pp. 819–825, 2013.
- [273] M. R. Kim, H. S. Choi, J. W. Yang, B. C. Park, J. A. Kim, and K. W. Kang, "Enhancement of vascular endothelial growth factor-mediated angiogenesis in tamoxifen-resistant breast cancer cells: role of Pin1 overexpression," *Molecular Cancer Therapeutics*, vol. 8, no. 8, pp. 2163–2171, 2009.
- [274] S. Li, S. Yuan, Q. Zhao, B. Wang, X. Wang, and K. Li, "Quercetin enhances chemotherapeutic effect of doxorubicin against human breast cancer cells while reducing toxic side effects of it," *Biomedicine & Pharmacotherapy*, vol. 100, pp. 441–447, 2018.
- [275] S. Z. Li, S. F. Qiao, J. H. Zhang, and K. Li, "Quercetin increase the chemosensitivity of breast cancer cells to doxorubicin via PTEN/Akt pathway," *Anti-Cancer Agents in Medicinal Chemistry*, vol. 15, no. 9, pp. 1185–1189, 2015.
- [276] H. Liu, J. I. Lee, and T. G. Ahn, "Effect of quercetin on the anti-tumor activity of cisplatin in EMT6 breast tumor-bearing mice," *Obstetrics & Gynecology Science*, vol. 62, no. 4, pp. 242–248, 2019.
- [277] N. Orsolich and N. Car, "Quercetin and hyperthermia modulate cisplatin-induced DNA damage in tumor and normal tissues in vivo," *Tumor Biology*, vol. 35, no. 7, pp. 6445–6454, 2014.
- [278] R. Sharma, L. Gatchie, I. S. Williams et al., "Glycyrrhiza glabra extract and quercetin reverses cisplatin resistance in triple-negative MDA-MB-468 breast cancer cells via inhibition of cytochrome P450 1B1 enzyme," *Bioorganic & Medicinal Chemistry Letters*, vol. 27, no. 24, pp. 5400–5403, 2017.
- [279] S. H. Tu, C. T. Ho, M. F. Liu et al., "Luteolin sensitises drug-resistant human breast cancer cells to tamoxifen via the inhibition of cyclin E2 expression," *Food Chemistry*, vol. 141, no. 2, pp. 1553–1561, 2013.
- [280] H. Wang, L. Tao, K. Qi et al., "Quercetin reverses tamoxifen resistance in breast cancer cells," *Journal of B.U.ON.: Official Journal of the Balkan Union of Oncology*, vol. 20, no. 3, pp. 707–713, 2015.
- [281] M. Y. Wong and G. N. Chiu, "Simultaneous liposomal delivery of quercetin and vincristine for enhanced estrogen-receptor-negative breast cancer treatment," *Anticancer Drugs*, vol. 21, no. 4, pp. 401–410, 2010.
- [282] M. Y. Wong and G. N. Chiu, "Liposome formulation of co-encapsulated vincristine and quercetin enhanced antitumor activity in a trastuzumab-insensitive breast tumor xenograft model," *Nanomedicine*, vol. 7, no. 6, pp. 834–840, 2011.
- [283] M. Y. Yang, C. J. Wang, N. F. Chen, W. H. Ho, F. J. Lu, and T. H. Tseng, "Luteolin enhances paclitaxel-induced apoptosis in human breast cancer MDA-MB-231 cells by blocking STAT3," *Chemico-Biological Interactions*, vol. 213, pp. 60–68, 2014.
- [284] L. Zhang, F. Yang, L. Huang, A. Liu, and J. Zhang, "Luteolin enhances the antitumor activity of lapatinib in human breast cancer cells," *Biomed Res*, vol. 28, no. 11, pp. 4902–4907, 2017.
- [285] S. Soltanian, H. Riahirad, A. Pabarja, M. R. Karimzadeh, and K. J. B. Saeidi, "Kaempferol and docetaxel diminish side population and down-regulate some cancer stem cell markers in breast cancer cell line MCF-7," *Biocell*, vol. 41, no. 2&3, p. 33, 2018.
- [286] M. Louisa and B. Wardhani, "Quercetin improves the efficacy of sorafenib in triple negative breast cancer cells through the modulation of drug efflux transporters expressions," *International Journal of Applied Pharmaceutics*, vol. 11, pp. 129–134, 2019.
- [287] M. L. Ackland, S. van de Waarsenburg, and R. Jones, "Synergistic antiproliferative action of the flavonols quercetin and kaempferol in cultured human cancer cell lines," *In Vivo*, vol. 19, no. 1, pp. 69–76, 2005.
- [288] Y. L. Shih, H. C. Liu, C. S. Chen et al., "Combination treatment with luteolin and quercetin enhances anti-proliferative effects in nicotine-treated MDA-MB-231 cells by down-regulating nicotinic acetylcholine receptors," *Journal of Agricultural and Food Chemistry*, vol. 58, no. 1, pp. 235–241, 2009.
- [289] P. Knekt, J. Kumpulainen, R. Jarvinen et al., "Flavonoid intake and risk of chronic diseases," *The American Journal of Clinical Nutrition*, vol. 76, no. 3, pp. 560–568, 2002.
- [290] U. Vanhoefer, A. Harstrick, W. Achterrath, S. Cao, S. Seeber, and Y. M. Rustum, "Irinotecan in the treatment of colorectal cancer: clinical overview," *Journal of Clinical Oncology*, vol. 19, no. 5, pp. 1501–1518, 2001.

Research Article

Unfermented Freeze-Dried Leaf Extract of *Tongkat Ali* (*Eurycoma longifolia* Jack.) Induced Cytotoxicity and Apoptosis in MDA-MB-231 and MCF-7 Breast Cancer Cell Lines

Lusia Barek Moses ^{1,2}, Mohd Fadzelly Abu Bakar ¹, Hasmadi Mamat ³,
and Zaleha Abdul Aziz ⁴

¹Faculty of Applied Sciences and Technology, Universiti Tun Hussein Onn Malaysia (UTHM), Pagoh Campus, Hub Pendidikan Tinggi Pagoh, KM1, Jalan Panchor, 84600, Muar, Johor, Malaysia

²Institute for Tropical Biology and Conservation, Universiti Malaysia Sabah, Jalan UMS, Kota Kinabalu, Sabah 88400, Malaysia

³Faculty of Food Science and Nutrition, Universiti Malaysia Sabah, Jalan UMS, Kota Kinabalu, Sabah 88400, Malaysia

⁴Faculty of Science and Natural Resources, Universiti Malaysia Sabah, Jalan UMS, Kota Kinabalu, Sabah 88400, Malaysia

Correspondence should be addressed to Mohd Fadzelly Abu Bakar; fadzelly@uthm.edu.my and Zaleha Abdul Aziz; zalehaaz@ums.edu.my

Received 12 August 2020; Revised 29 November 2020; Accepted 12 January 2021; Published 31 January 2021

Academic Editor: Hamid Tebyanian

Copyright © 2021 Lusia Barek Moses et al. This is an open access article distributed under the Creative Commons Attribution License, which permits unrestricted use, distribution, and reproduction in any medium, provided the original work is properly cited.

The present study was conducted to determine the cytotoxicity effect of *Eurycoma longifolia* (Jack.) leaf extracts and also its possible anticancer mechanism of action against breast cancer cell lines: non-hormone-dependent MDA-MB-231 and hormone-dependent MCF-7. The leaves of *E. longifolia* were processed into unfermented and fermented batches before drying using freeze and microwave-oven drying techniques. Obtained extracts were tested for cytotoxicity effect using MTT assay and phenolic determination using HPLC-DAD technique. The most toxic sample was analyzed for its apoptotic cell quantification, cell cycle distribution, and the expression of caspases and apoptotic protein using flow cytometry technique. Fragmentation of DNA was tested using an agarose gel electrophoresis system. The results determined that the unfermented freeze-dried leaf extract was the most toxic towards MDA-MB-231 and MCF-7 cells, in a dose-dependent manner. This extract contains the highest phenolics of gallic acid, chlorogenic acid, ECG, and EGCG. The DNA fragmentation was observed in both cell lines, where cell cycle was arrested at the G₂/M phase in MCF-7 cells and S phase in MDA-MB-231 cells. The number of apoptotic cells for MDA-MB-231 was increased when the treatment was prolonged from 24 h to 48 h but slightly decreased at 72 h, whereas apoptosis in MCF-7 cells occurred in a time-dependent manner. There were significant activities of cytochrome c, caspase-3, Bax, and Bcl-2 apoptotic protein in MDA-MB-231 cells, whereas MCF-7 cells showed significant activities for caspase-8, cytochrome c, Bax, p53, and Bcl-2 apoptotic protein. These results indicate the ability of unfermented freeze-dried leaf extract of *E. longifolia* to induce apoptosis cell death on MDA-MB-231 and MCF-7, as well as real evidence on sample preparation effect towards its cytotoxicity level.

1. Introduction

Globally, 1 in 6 deaths is due to cancer, which ranked it as the second leading cause of death [1]. According to GLOBOCAN produced by the International Agency for Research on Cancer, out of 185 countries, approximately 18.1 million new cancer incidence and 9.6 million deaths were reported in 2018 [2]. The most commonly diagnosed is lung cancer, with 2.09 million

cases and closely followed by female breast cancer, also with 2.09 million cases. Breast cancer is ranked fifth for mortality with 627 000 deaths after lung cancer (1.76 million deaths), colorectal cancer (862 000 deaths), stomach cancer (783 000 deaths), and liver cancer (782 000 deaths) [1]. By 2040, the cancer incidence expected to grow to 27.5 million new cases and 16.3 million deaths due to the growth and ageing of the population [3]. As the second leading of diagnosed cancer,

breast cancer has increased concern worldwide, especially among females. However, the frequency of its diagnosed and mortality cases significantly varied across countries and within each country, depending on the degree of economic development as well as the social and lifestyle factors. The reported incidences have been occurring in both developed and less developed countries, where almost 70% of deaths occur in less developed countries [1]. The GLOBACAN of the International Agency for Research on Cancer has estimated the age-standardized rate (ASR) of breast cancer in Malaysia as 38.7 per 100,000 with 5,410 new cases in 2012 [4].

Traditional and complementary medicine has also been suggested as an alternative treatment besides surgery, chemotherapy, and pharmacogenomics therapy to reduce the breast cancer occurrence [5]. Up to 64% of traditional and complementary medicines, uptakes were reported by women with breast cancer. However, up to date, only a few traditional or complementary therapies have been tested scientifically [4]. In the early stage of developing an anticancer drug, a study on the biochemical reaction of a sample and its mechanism of action is crucial, especially on the determination of its cell death mode [6]. Apoptosis is a natural programmed cell death mode triggered by anticancer drugs as well as other physical and chemical factors [7]. Once apoptosis showed a defective regulation, it would lead to an uncontrollable proliferation of cancer cell [8, 9]. Therefore, regulated apoptosis becomes a major target and principal mechanism in the development of an effective anticancer chemotherapeutic agent [6].

Eurycoma longifolia Jack. (Simaroubaceae family) is prevalent among traditional medicinal practitioners. This medicinal plant is commonly known as Tongkat Ali (Malaysia), Pasak Bumi (Indonesia), Tung Saw (Thailand), Cay Ba Binh (Vietnam), Tho Nan (Laos), and Babi Kurus (Java) [10]. The decoction of this plant is mainly used to increase energy and vitality for man and as a tonic for a woman after childbirth. Some of its uses are to treat fatigue, malaria, diarrhoea, dysentery, glandular swelling, bleeding, dropsy, cough, fever, ulcer, and high blood pressure [11, 12]. Scientifically, there have been numerous studies and a wide range of pharmaceutical properties discovered from its roots [13]. It has shown anticancer activities on various types of cancer, including lung, breast, and cervical cancers. Salahi et al. [14] have reported the antitumour activity of *E. longifolia* root extracts against leukemic cell line of K-562. Meanwhile, its branch extract-mediated silver nanoparticles exhibited significant anticancer activity against human glioma cells (DBTRG and U87) and human breast cancer cells (MCF-7 and MDA-MB-231) [15]. Yet, the utilization of its leaf remains minimal as it usually discarded after harvesting its root. Hence, utilizing its leaf by preparing it as herbal tea in this present study was to highlight its significance as one of the potential alternative medicines for breast cancer, as well as to maximize the utilization of this plant.

In the meantime, sample preparation also plays a crucial factor to maximize its potential. The fermentation process can cause alteration or reduction of phytochemical content which may affect the anticancer potential. Apart from fermentation, drying technique also plays an essential factor in the quality preservation of the end-product. Efficient drying techniques will enhance the quality of dried product such as

aroma and appearance by hindering any biochemical changes or microbial growth [16]. Through this study, the most effective procedure of processing and preparation of *E. longifolia* leaves to obtain the optimum cytotoxicity effect against cancer cells were outlined.

2. Materials and Methods

2.1. Preparation of Unfermented and Fermented Leaves. About 1.0 kg of fresh intermediate leaves (from 2nd axis to 4th axis) of *Eurycoma longifolia* leaves was collected from the hilly area of Universiti Malaysia Sabah (UMS), and a voucher specimen was deposited into BORNEENSIS Herbarium (BORH), Institute for Tropical Biology and Conservation in UMS. The leaves were washed with distilled water and blotted with a paper towel to remove excess water. Then, the cleaned leaves were divided into two batches (approximately about 0.5 kg/batch) of unfermented and fermented leaves. The unfermented and fermented leaves were prepared as described by Lusya Barek et al. [17]. For unfermented one, the leaves were firstly steam blanched at $98 \pm 2^\circ\text{C}$ for 30 sec to inactivate degradative enzymes and immediately soaked in an ice-cold water bath for 30 sec before blended for 5 sec using a blender (Panasonic Mx-337, Malaysia) and dried. Meanwhile, those fermented leaves were firstly left in the open air for 18 hours before ground using a blender for 5 sec. The ground leaves were then sprayed with distilled water in a ratio of 1 : 1 (w/v) and left in dark condition at room temperature ($25 \pm 1^\circ\text{C}$) for 5 h to undergo oxidation-fermentation process.

For drying, each unfermented and fermented leaves of *E. longifolia* were further divided into two batches and dried using microwave-oven and freeze-drying techniques. For microwave-oven dried, ground leaves were dried using a microwave-oven (Samsung MW71 E, South Korea) at 600 W for 5 min; meanwhile, freeze-dried leaves were firstly frozen at -80°C for 48 h before subjecting into the freeze dryer (Labconco FreeZone, United State) for 48 h.

The leaf extract was prepared by infusing 2.0 g of dried leaves in 200 ml boiling distilled water ($100 \pm 2^\circ\text{C}$), stirred using a magnetic stirrer (Stuart SD162, United Kingdom) at 300 rpm for 2 min and left to cool for 10 min before filtering through Whatman No.4 filter paper. Resultant infusions were lyophilized by freezing those at -80°C for 48 h before subjecting into the freeze dryer for 48 h. Two commercial tea *Camellia sinensis* products, namely, "BOH green tea" (unfermented) and "SABAH black tea" (fermented), were used as a comparison to *E. longifolia* herbal teas. These teas were prepared as the same as the *E. longifolia* herbal extracts. Each 1.0 g of extracts was dissolved in 1.0 ml dimethyl sulfoxide and stored in -20°C for further used.

2.2. Cell Culture. Human breast cancer cells (MCF-7 and MDA-MB-231) and normal mouse embryonic fibroblast, 3T3-NIH, were obtained from the American Type Culture Collection (ATCC) (Manassas, United States). The MCF-7 and MDA-MB-231 cancer cells were maintained in an RPMI 1640 medium supplemented with heat-inactivated fetal bovine serum (FBS) and penicillin-streptomycin in a ratio of

100:10:1 (v/v/v); meanwhile, the 3T3-NIH normal cell was maintained in DMEM and supplemented as the same as the cancer cells. These cells were kept until they grew exponentially in a humidified cell incubator (Sanyo, Japan) with an atmosphere of 5% CO₂ at 37°C.

2.3. MTT Cytotoxicity Assay. MCF-7, MDA-MB-231, and 3T3-NIH cells were seeded at a concentration of 1×10^3 cells/ml in a 96-well plate and incubated for 24 h in an incubator at 37°C with 5% CO₂. After incubation, the old medium was replaced with the extract diluted with the respective complete growth medium (200, 100, 50, 25, 12.5, 6.5, and 0.0 µg/ml) and followed by incubation for 72 h. After the incubation, each well was added with 20 µl of 5 mg/ml MTT solution and incubated in dark condition for another 3 h [18]. Then, the medium with the MTT solution was removed, and 100 µl of absolute dimethyl sulfoxide (DMSO) was added to each well to dissolve formazan crystal that has been formed by viable cells. Each well was measured at 540 nm using an ELISA plate reader (FLUOstar Omega, BMG LABTECH, Germany). The percentage of cell viability was calculated as follows:

$$\text{percentage of cell viability (\%)} = \frac{\text{OD sample}}{\text{OD control}} \times 100\%, \quad (1)$$

where OD = optical density, control = without treatment of extract, and sample = with treatment of extract. The IC₅₀ values were determined as the concentration of the extracts that caused 50% inhibition or cell death.

2.4. HPLC-DAD Analysis for Phenolic Determination. HPLC analysis was performed to determine phenolic content using an HPLC 1200 series equipped with column Agilent ZORBAX Eclipse (XDB-C18), 5 µm, (250 × 4.6 mm internal diameter), G1322 vacuum degasser, G1311 quaternary pump, G1329 autosampler, G1316 thermostatted column compartment, and G1315 diode array detector (DAD) with ChemStation Software. Twelve (12) phenolic standards of *p*-coumaric acid, chlorogenic acid, vanillic acid, ferulic acid, gallic acid, caffeic acid, (-)-epicatechin (EC), (-)-epigallocatechin (EGC), (-)-epicatechin gallate (ECG), (-)-epigallocatechin gallate (EGCG), hesperidin, and naringin were prepared in a series of concentrations ranged from 20 to 100 µg/ml for calibration of individual phenolic quantification. Each *E. longifolia* infusion was filtered through a 0.5 µm nylon membrane filter before injection into the HPLC apparatus. The sample flow rate was set up for 1 ml/min with 20 µl of injection volume. The phenolic content was measured at 280 nm. The mobile phases were composed of (A) 10% acetic acid in acetonitrile and (B) water, filtered under vacuum through a 4.5 µm membrane filter before used. Gradient elution was performed as 10% solvent A constantly for 9 min before increased to 20% for 2 min. At 12 min, the elution increased to 35% for 4 min before drastically decreased to 10% at 18 min and remained constant for 2 min.

2.5. DNA Fragmentation Analysis. Cancer cells at the density of 5×10^5 cells/well were seeded in a 6-well plate and grown for 24 h in an incubator at 37°C with 5% CO₂. The cells were treated with selected *E. longifolia* leaf extract at IC₅₀ value and incubated again for 72 h. The treated cells were harvested and transferred into a Falcon tube before centrifuged at 2000 rpm for 5 min to obtain a cell pellet. The pellet was washed twice with 1x PBS. Positive control of drug doxorubicin was treated similarly as the extract. DNA laddering analysis was performed according to the procedure described in Cayman DNA Laddering Assay Kit (Ann Arbor, Michigan) to obtain a dry cell pellet. Before electrophoresis, the dry pellet was resuspended in 25 µl of TE buffer. Each 10 µl of cell extract was mixed with 2 µl of loading buffer. DNA fragments were separated in 0.8% agarose gel stained with 5.0 mg/ml ethidium bromide at 75 V for 60 min using an agarose gel electrophoresis system. A 1 kb plus of DNA ladder (Invitrogen, USA) was used as a marker to determine the DNA fragment size. DNA fragmentation was visualized using under UV light using FluorChem 5500 Chemiluminescent (Alpha Innotech, United State).

2.6. Cell Cycle Determination. The cell cycle distributions of treated cells were determined according to Abu Bakar et al. [19]. The cells at the density of 5×10^5 cells/well were seeded in the 6-well plates and incubated at 37°C with 5% CO₂ for 24 h before treated with selected leaf extract at its IC₅₀ values and incubated again for 24 h, 48 h, and 72 h. The treated cells were then harvested after reaching the respective treatment period, washed twice with 1x cold PBS, and centrifuged. Obtained cell pellets were added with 500 µl 1x cold PBS and 4.5 ml of ice-cold 70% ethanol before incubated for overnight at -20°C. The cell pellets were rewashed twice with 1x cold PBS before resuspended in 500 µl propidium iodide staining solution (containing 100 µg/ml propidium iodide and 40 µg/ml RNase). Finally, the cells were incubated for 30 min at 37°C in dark condition before analyzing using Summit 4.3 software of flow cytometer (Alpha Innotech, California, USA).

2.7. FITC Annexin V Apoptosis Analysis. The FITC Annexin V apoptosis staining was conducted using FITC Annexin V Apoptosis detection kit (BD Pharmingen, Bioscience, Austria). The cells (5×10^5 cells/well) were seeded in the 6-well plates and grown for 24 h at 37°C with 5% CO₂ in an incubator. After incubation, the cells were treated with selected leaf extract at IC₅₀ values for 24 h, 48 h, and 72 h. All adhering and floating cells were collected into centrifuged tubes before washing twice with 1x cold PBS. The cell pellets were resuspended in 1 ml 1x binding buffer (containing 0.1 M HEPES/NaOH (pH 7.4), 1.4 M NaCl, and 25 mM CaCl₂). Then, 500 µl was transferred into Cryovial tubes and added with 5 µl of FITC Annexin V and 10 µl of propidium iodide. The tubes were incubated in dark condition at room temperature (25 ± 2°C) for 15 min before analyzing using Summit 4.3 software of flow cytometer.

2.8. Caspase-3 and -8 and Cytochrome c Determination Assay. Cells at the density of 5×10^5 cells/well were seeded in the 6-well plates, grown, and treated with selected leaf extract at its IC_{50} values before harvested. The activity of caspase-3 of the tested herbal extract was determined using the caspase-3 assay kit, colourimetric (SIGMA, Germany). Briefly, the harvested cells were then lysed using 1x lysis buffer (containing 250 mM HEPES, pH 7.4, 25 mM CHAPS, and 25 mM DTT) before added with 85 μ l of 1x cell buffer (containing 200 mM HEPES, pH 7.4, 1% CHAPS, 50 mM DTT, and 20 mM EDTA) and 5 μ l of caspase-3 substrate (Acetyl-Asp-Glu-Val-Asp p-nitroanilide (Ac-DEVD-pNA)). The absorbance values of light yellow colour formed solutions were measured at 405 nm using the ELISA reader.

For caspase-8 and cytochrome c activities, Human Caspase-8/FLICE Platinum ELISA assay kit (eBioscience, Austria) and Human Cytochrome c Platinum ELISA assay kit (eBioscience, Austria) were used, respectively. Briefly, the harvested cells were lysed using 200 μ l of 1x lysis buffer. In the caspase-8 analysis, a total of 50 μ l cell lysate was added in a 96-microwell plate coated with a monoclonal antibody to human caspase-8, before added with 50 μ l of detection antibody, 100 μ l of diluted anti-rabbit-IgG-HRP, and 100 μ l of TMB substrate solution. Meanwhile, for cytochrome c activity, 50 μ l of lysed cells were added in a 96-microwell plate coated with a monoclonal antibody to human cytochrome c, before added with 50 μ l of biotin-conjugated, 100 μ l of diluted streptavidin-HRP, and TMB substrate solution. The stop solution (100 μ l) was added into each well before measured at 450 nm using the ELISA reader. All the final results of treated cells were compared with untreated cells (control) and were expressed as fold of increase in caspases or cytochrome c activity.

2.9. p53, Bax, and Bcl-2 Expression. Protein expression of p53, Bax, and Bcl-2 was analyzed based on the flow cytometry protocol for staining intracellular molecules as described by the Research and Development (R&D) system (NY) [20] with slight modification. Each cancer cell line at a density of 5×10^5 cells/well was seeded in a 6-well plate and grown for 24 h at 37°C in an incubator with 5% CO₂. After the incubation, the cell was treated with selected leaf extract at IC_{50} values and incubated again for 24 h, 48 h, and 72 h. The untreated cell was used as a control. Adhering and floating cells were collected and centrifuged at 2000 rpm in 4°C for 5 min. Briefly, the cell pellet was fixed by adding 100 μ l of 1% (w/v) freshly prepared paraformaldehyde and incubated at room temperature (25°C \pm 2) for 10 min. The cell pellet was then permeabilized in 100 μ l of 1% Triton X-100 for 10 min before proceeding to staining with antibodies. For direct staining of p53 antibody, the permeabilized cell was added with 10 μ l of 2.5 μ g/ml p53 antibody, followed by incubation in dark condition at room temperature (25°C \pm 2) for 30 min. The stained cell was then centrifuged (2000 rpm in 4°C for 5 min) and washed again with cold 1x PBS before added with 400 μ l of cold 1x PBS before flow cytometer analysis. For indirect staining of Bax and Bcl-2 antibodies, the permeabilized cell was added with

10 μ l of 2.5 μ g/ml Bax or Bcl-2 antibodies and incubated in dark condition at room temperature (25°C \pm 2) for 30 min. Then, 500 μ l of cold 1x PBS was added and centrifuged at 2000 rpm in 4°C for 5 min. Each cell pellet was added with 10 μ l of IgG polyclonal anti-mouse secondary antibody and incubated in dark condition at room temperature (25°C \pm 2) for another 30 min. The stained cell was washed twice with cold 1x PBS, and the centrifugation step was repeated. Finally, the cell pellet was resuspended in 400 μ l of cold 1x PBS before flow cytometer analysis.

2.10. Data Analysis. All data were analyzed using GraphPad Prism version 5.01 and expressed as means \pm standard deviation (S.D.) of five replicate analyses in five independent experiments. One-way analysis of variance (ANOVA) followed by Tukey's multiple range test was carried out to determine the significance between means. The statistically significant level was set at $P < 0.05$.

3. Result

3.1. Cytotoxicity Effect of Commercial Teas and *E. longifolia* Leaf Extracts. In the present study, the percentage of cell viability of MDA-MB-231 (Figure 1(a)), MCF-7 (Figure 1(b)), and NIH-3T3 (Figure 1(c)) displayed a clear decreasing pattern in a dose-dependent manner for all extracts of *C. sinensis* and *E. longifolia* leaves. Doxorubicin at a concentration of 0–20 μ g/ml (Figure 2) also displayed a similar pattern with IC_{50} values less than 3 μ g/ml for both cancer cell lines.

The most prominent result was shown by the inhibition in the unfermented freeze-dried leaf extract of *E. longifolia* on the cell viability of breast cancer cell line, especially against MCF-7 cells with an IC_{50} value of 45.0 ± 3.5 μ g/ml (Table 1). The amount of this extract was lower compared to SABAH black tea (50.5 ± 0.5 μ g/ml). Besides, this extract also showed a potent cytotoxicity effect against MDA-MB-231 cells with an IC_{50} value of 69.3 ± 17.2 μ g/ml and significantly lower compared to SABAH black tea (92.3 ± 3.2 μ g/ml). Both cancer cell lines displayed a similar pattern, where the freeze-dried leaf extract showed lower IC_{50} values compared to those microwave-oven dried regardless it was fermented or not. Still, fermented leaves always possess higher values than those were unfermented.

3.2. Phenolic Determination of Commercial Teas and *E. longifolia* Leaf Extracts. In the phenolic determination, complete baseline separation of an individual compound by HPLC-DAD was obtained by a combination of gradient and isocratic elution. The retention time of different compounds were 3.565 min for gallic acid, 4.203 for chlorogenic acid, 5.726 for (-)-epicatechin (EC), 6.066 for (-)-epigallocatechin gallate (EGCG), 6.878 for caffeic acid, 7.190 for vanillic acid, 7.595 for (-)-epigallocatechin (EGC), 10.339 for (-)-epicatechin gallate (ECG), 10.696 for *p*-coumaric acid, 12.041 for ferulic acid, 13.401 for naringin, and 13.818 for hesperidin. Based on Table 2, phenolics in the unfermented freeze-dried leaf extract such as gallic acid (9.81 ± 0.02 mg/

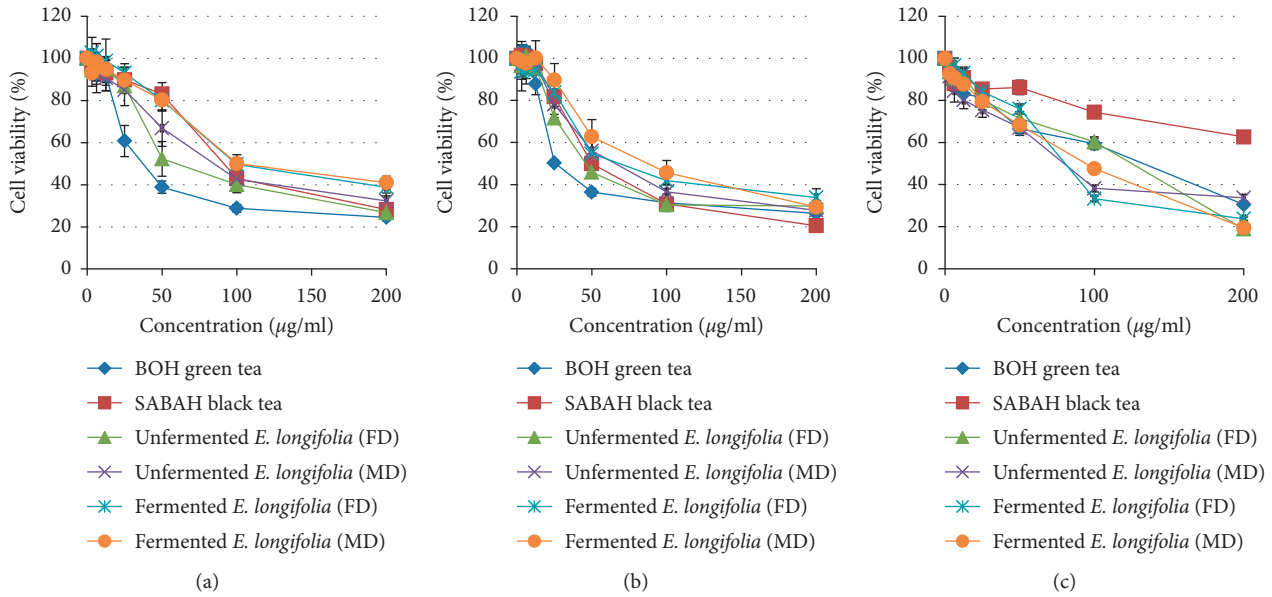


FIGURE 1: Cell viability after treated with commercial teas and *E. longifolia* leaf extracts against (a) non-hormone-dependent breast cancer cell MDA-MB-231, (b) hormone-dependent breast cancer cell MCF-7, and (c) normal mouse embryonic fibroblast cell NIH-3T3. FD: freeze-dried. MD: microwave-oven dried.

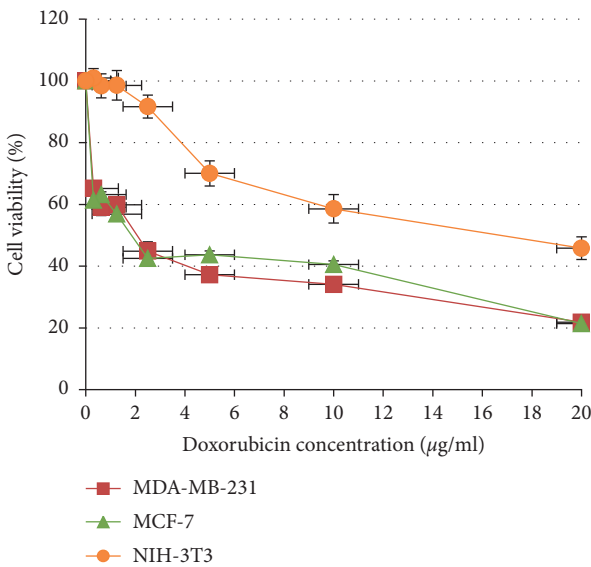


FIGURE 2: Cell viability after treated with positive control of drug doxorubicin against breast cancer cell lines, MCF-7 and MDA-MB-231, and normal mouse embryonic fibroblast cell NIH-3T3.

L), chlorogenic acid (7.70 ± 0.08 mg/L), and catechin derivatives of ECG (3.07 ± 0.02 mg/L) and EGCG (2.28 ± 0.01 mg/L) were recorded highest compare to other types of *E. longifolia*.

3.3. *Effect of Unfermented Freeze-Dried Leaf Extract of E. longifolia at IC₅₀ Values on DNA Fragmentation.* In DNA laddering analysis, all treated MDA-MB-231 and MCF-7 cell lines showed DNA fragmentation after 72 h of treatment with the extract. Treated MDA-MB-231 cells developed

TABLE 1: IC₅₀ (µg/ml) of commercial teas and *E. longifolia* leaf extracts against breast cancer cell lines, MCF-7 and MDA-MB-231, and normal mouse embryonic fibroblast cell NIH-3T3.

Sample	MDA-MB-231	MCF-7	NIH-3T3
Doxorubicin	2.1 ± 0.07^f	1.8 ± 0.01^e	15.4 ± 1.45^e
Commercial tea (<i>C. sinensis</i>)			
BOH green tea	35.0 ± 5.3^e	26.2 ± 2.0^d	133.3 ± 5.6^a
SABAH black tea	92.3 ± 3.2^{bc}	50.5 ± 0.5^{bc}	>200
<i>E. longifolia</i>			
Unfermented (FD)	69.3 ± 17.2^d	45.0 ± 3.5^c	125.5 ± 6.2^b
Unfermented (MD)	84.7 ± 8.4^c	65.7 ± 20.3^b	79.7 ± 7.2^d
Fermented (FD)	98.3 ± 11.5^{ab}	66.7 ± 20.5^b	81.8 ± 16.2^{cd}
Fermented (MD)	99.7 ± 6.8^a	97.3 ± 13.6^a	96.4 ± 3.6^c

Values are expressed as mean \pm standard deviation ($n=5$); means with different superscript lowercase letters within the same column were significantly different at the level of $P < 0.05$. FD: freeze-dried. MD: microwave-oven dried.

multiple DNA bands ranging from 2000 bp to >12,000 bp with RNA smear (Figure 3(a)). Similarly, treated MCF-7 cells also developed multiple DNA bands ranging from 1000 bp to >12,000 bp with RNA smear (Figure 3(b)).

3.4. *Effect of Unfermented Freeze-Dried Leaf Extract of E. longifolia at IC₅₀ Value on Cell Cycle Distribution and Apoptosis.* For MDA-MB-231 cells (Figures 4 and 5), a significant cell cycle arrest at S phase was observed as early as 24 h (12.6%) and slightly increased at 48 h (14.2%) before decrease at 72 h of treatment (10.2%). At the meantime, the number of cells in G₀/G₁ and G₂/M phases was reduced significantly at 48 h compared to 24 h treatment and showed a moderate increment at 72 h. As early as 24 h treatment, the apoptosis (sub-G₁ phase) increases from 21.6% to 27.0% at

TABLE 2: Phenolic content (mg/L) in commercial teas and *E. longifolia* leaf infusions.

Sample	Commercial tea (<i>Camellia sinensis</i>)			<i>Eurycoma longifolia</i>		
	BOH green tea	SABAH black tea	Unfermented (FD)	Unfermented (MD)	Fermented (FD)	Fermented (MD)
Gallic acid	18.50 ± 0.07 ^b	19.23 ± 0.05 ^a	9.81 ± 0.02 ^c	8.53 ± 0.06 ^d	9.78 ± 0.02 ^c	7.52 ± 0.02 ^c
Chlorogenic acid	ND	ND	7.70 ± 0.08 ^b	4.36 ± 0.03 ^d	8.00 ± 0.09 ^a	4.98 ± 0.09 ^c
<i>p</i> -Coumaric acid	9.43 ± 0.01 ^a	5.71 ± 0.01 ^b	ND	ND	ND	ND
Vanillic acid	ND	ND	5.44 ± 0.01 ^a	5.51 ± 0.01 ^a	5.23 ± 0.01 ^b	5.29 ± 0.01 ^b
Caffeic acid	ND	ND	ND	ND	ND	ND
Ferulic acid	ND	ND	ND	ND	ND	ND
EC	88.95 ± 0.15 ^a	83.13 ± 0.11 ^b	ND	ND	ND	ND
ECG	23.60 ± 0.16 ^a	12.51 ± 0.14 ^b	3.07 ± 0.02 ^c	2.66 ± 0.03 ^d	ND	ND
EGC	173.36 ± 1.13 ^b	240.01 ± 0.77 ^a	ND	ND	ND	ND
EGCG	314.89 ± 0.88 ^a	160.74 ± 0.57 ^b	2.28 ± 0.01 ^c	1.55 ± 0.01 ^d	ND	ND
Hesperidin	ND	ND	ND	ND	ND	ND
Naringin	ND	ND	ND	ND	ND	ND

EC: (-)-epicatechin; EGC: (-)-epigallocatechin; ECG: (-)-epicatechin gallate; EGCG: (-)-epigallocatechin gallate; FD: freeze-dried; MD: microwave-oven dried; ND: not detected; values are expressed as mean ± standard deviation ($n=5$); means with different superscript lowercase letters within the same row were significantly different at the level of $P < 0.05$.

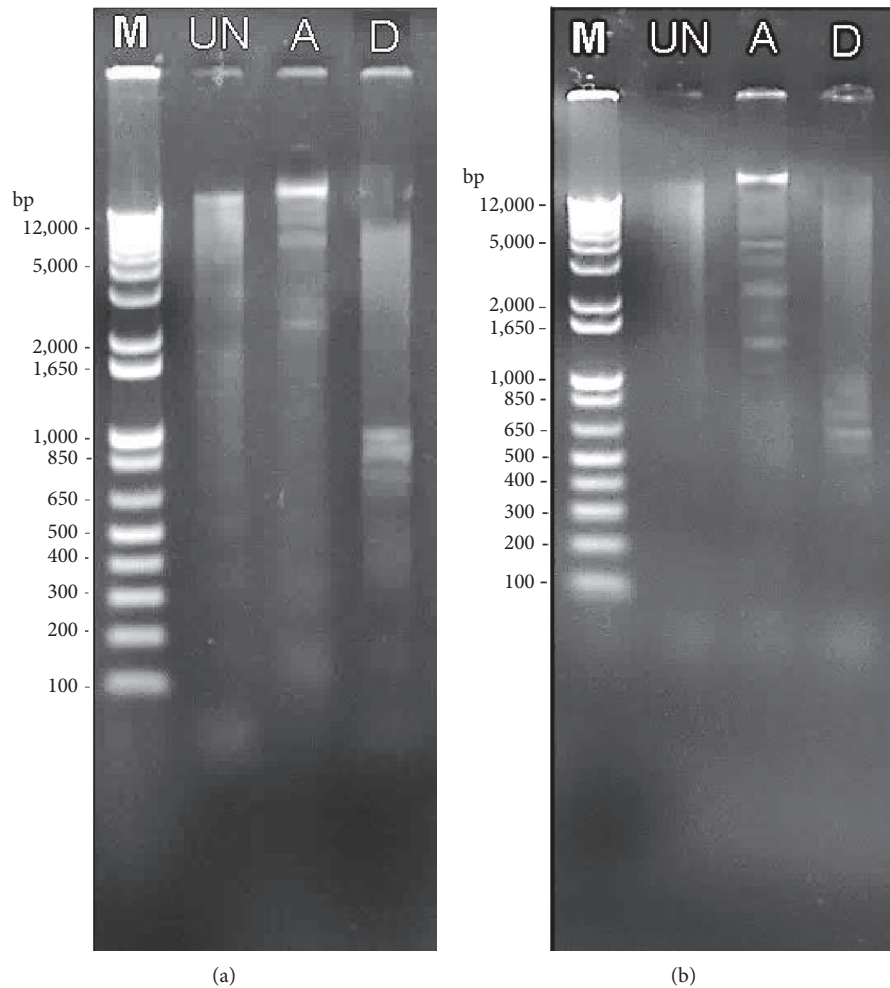


FIGURE 3: DNA fragmentation of (a) MDA-MB-231 and (b) MCF-7 cell lines after treated with unfermented freeze-dried leaf extract of *E. longifolia* at IC_{50} value for 72 h. M: DNA marker; UN: untreated; A: unfermented freeze-dried leaf extract of *E. longifolia*; D: positive control drug doxorubicin.

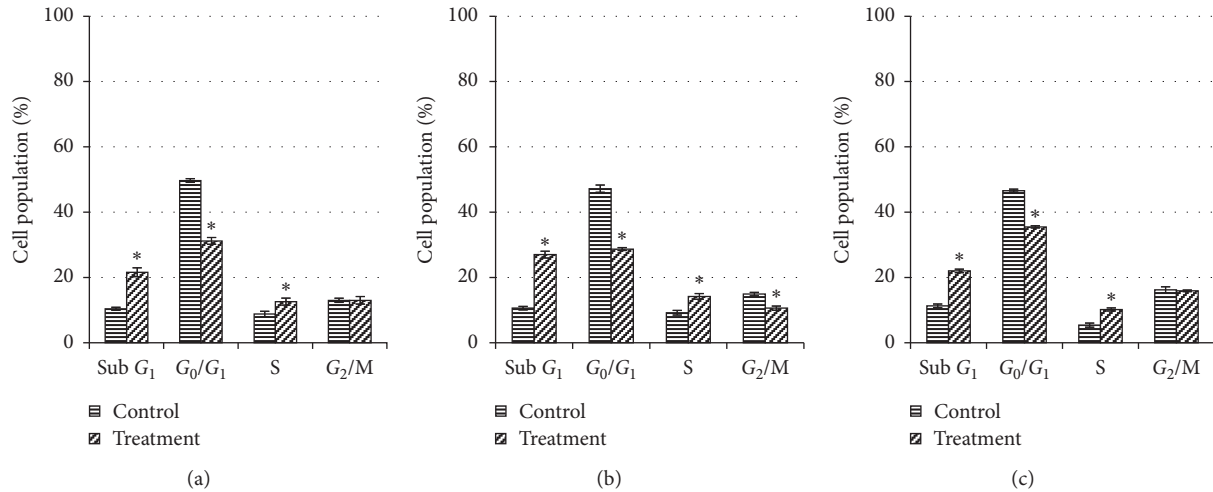


FIGURE 4: Cell cycle distribution of untreated MDA-MB-231 cells and those treated with unfermented freeze-dried leaf extract of *E. longifolia* at IC₅₀ value for (a) 24 h, (b) 48 h, and (c) 72 h. The data are presented as mean ± standard deviation for three replicates and indicated by an asterisk showed a significant difference ($P < 0.05$) relative to respective control.

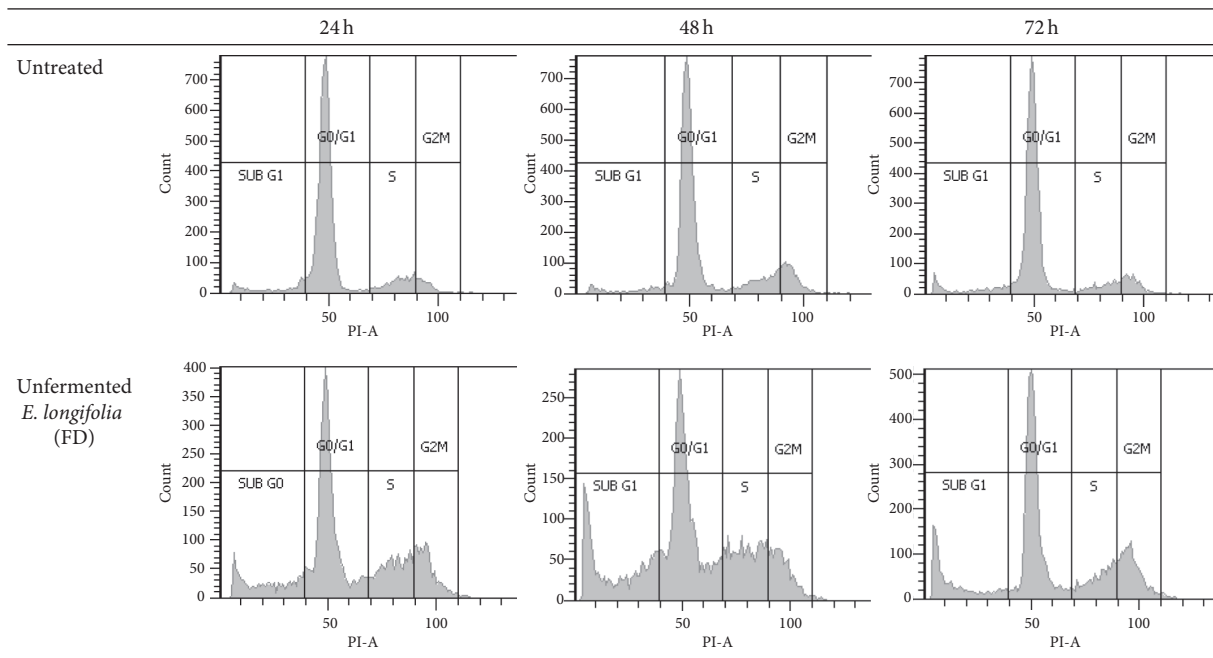


FIGURE 5: Representative flow cytometric scan of untreated MDA-MB-231 cells and those treated with unfermented freeze-dried leaf extract of *E. longifolia* at IC₅₀ value for 24 h, 48 h, and 72 h. FD: freeze-dried.

48 h but decreases to 22.0% at 72 h; however, all were significantly higher ($P < 0.05$) compared to their respective controls (10.4%, 10.6%, and 11.3%). This indicates that the selected extract at IC₅₀ value was more effective to induce apoptosis at 48 h of treatment compared to 24 h or 72 h.

In contrast, MCF-7 cells (Figures 6 and 7) showed a significant arrest at G₂/M phase at 24 h of treatment (22.8%) ($P < 0.05$) compared to control before suddenly decrease and shifting to apoptosis (sub G₁) with the drastic increase at 48 h (16.9%) and 72 h (12.8%) of treatment. Meanwhile, the numbers of cell in G₀/G₁ and S phases were reduced

significantly ($P < 0.05$). Apoptosis also occurred during G₂/M arrest for the first 24 h of the treatment (14.4%) and significantly increased up to 38.0% at 48 h and 48.8% at 72 h compared to their respective controls (5.3%, 10.1%, and 12.0%) ($P < 0.05$). Also, the proportion of cells in G₀/G₁ and G₂/M phases was decreased significantly ($P < 0.05$) compared to their control after 24 h, 48 h, and 72 h of treatment.

3.5. Effect of Unfermented Freeze-Dried Leaves of *E. longifolia* at IC₅₀ Value on Early and Late Apoptosis. The exposure of

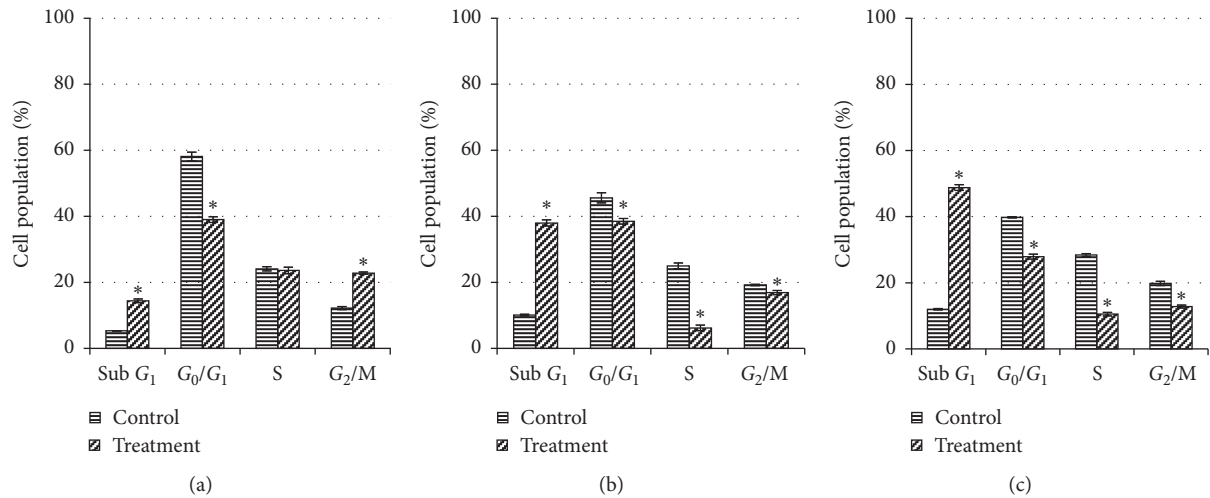


FIGURE 6: Cell cycle distribution of untreated MCF-7 cells and those treated with unfermented freeze-dried leaf extract of *E. longifolia* at IC₅₀ value for (a) 24 h, (b) 48 h, and (c) 72 h. The data are presented as mean ± standard deviation for three replicates and indicated by an asterisk showed a significant difference ($P < 0.05$) relative to respective control.

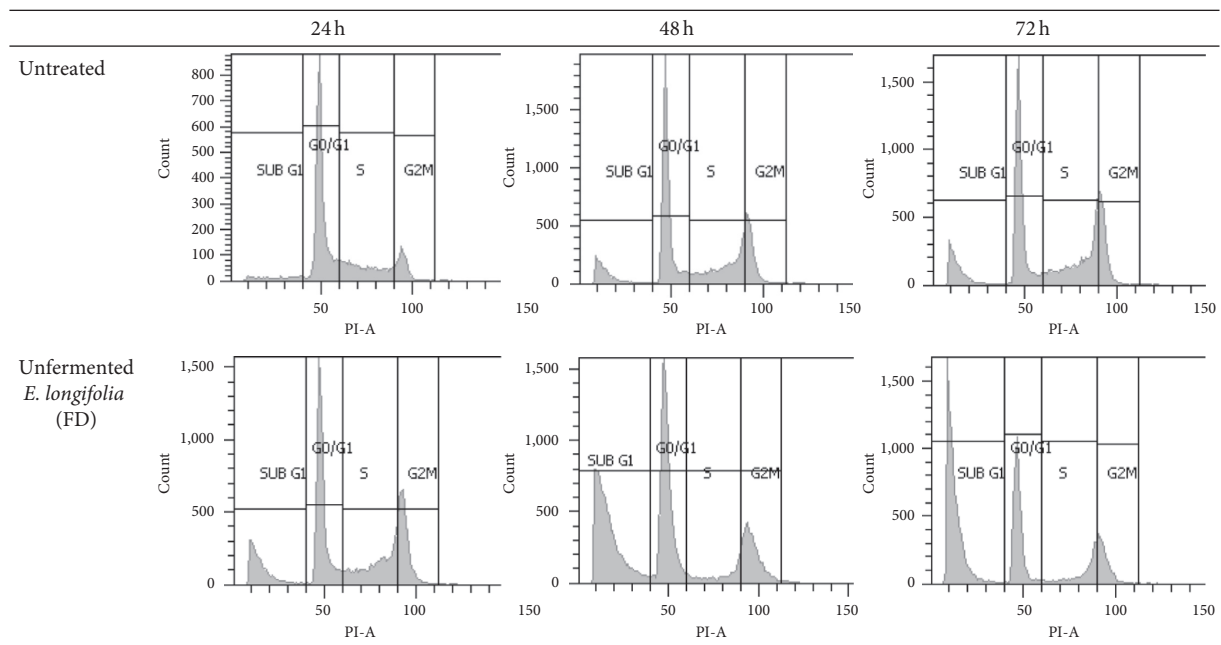


FIGURE 7: Representative flow cytometric scan of untreated MCF-7 cells and those treated with unfermented freeze-dried leaf extract of *E. longifolia* at IC₅₀ value for 24 h, 48 h, and 72 h. FD: freeze-dried.

unfermented freeze-dried leaf extract of *E. longifolia* on MDA-MB-231 cells (Figures 8 and 9) for 24 h showed significant ($P < 0.05$) small percentage of early apoptosis (8.0%) event occurred when compared to the control (2.5%). Following 48 h of treatment, it has resulted in a substantial shift from live cells to early and late apoptotic cell populations with the value of 39.8% and 17.6%, respectively ($P < 0.05$). However, total apoptosis decreased to a level of 39.8% (early apoptosis: 29.4%; late apoptosis: 10.4%) for 72 h of treatment.

For MCF-7 cells (Figures 10 and 11), after 24 h exposure of this extract, there was a significant ($P < 0.05$) late

apoptosis event (4.8%) occurred when compared to the control (0.6%). Following 48 h of treatment, treated cells showed a strong shift from live cells to early and late apoptotic cell populations with the value of 29.7% and 8.2%, respectively ($P < 0.05$). After 72 h of treatment, the total apoptosis increased up to 48.2% (early apoptosis: 19.3%; late apoptosis: 28.9%). This suggested the apoptosis in MCF-7 cells occurred in a time-dependent manner.

3.6. Possible Anticancer Mechanism of Unfermented Freeze-Dried Leaf Extract of *E. longifolia* at IC₅₀ Value on the Activity of Caspase-3, Caspase-8, and Cytochrome c and Also Protein

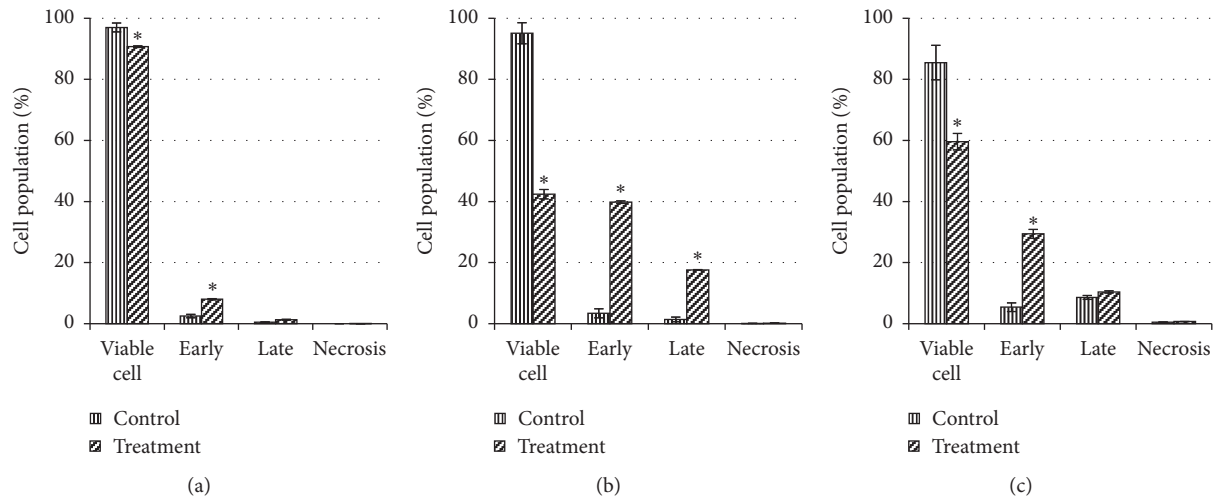


FIGURE 8: The cell population of untreated MDA-MB-231 cells and those treated with unfermented freeze-dried leaf extract of *E. longifolia* at IC_{50} value for (a) 24 h, (b) 48 h, and (c) 72 h. The values are presented as mean \pm standard deviation for three replicates and indicated by an asterisk showed a significant difference ($P < 0.05$) relative to respective control.

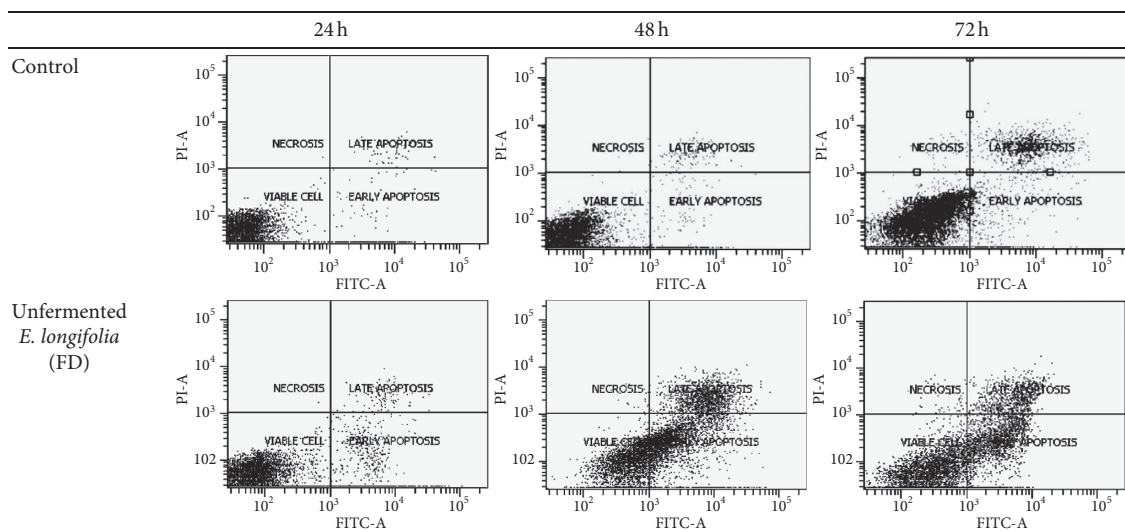


FIGURE 9: Representative flow cytometric scan of untreated MDA-MB-231 cells and those treated with unfermented freeze-dried leaf extract of *E. longifolia* at IC_{50} value for 24 h, 48 h, and 72 h.

Expression of Bcl-2, Bax, and p53. Treated MDA-MB-231 cells showed the activation ($P < 0.05$) of caspase-3 at 24 h and increase at 48 h with 2-fold than the control but decrease after 72 h of treatment. In contrast, the cytochrome c activity was higher ($P < 0.05$) at 24 h but decreased at 48 h and 72 h of treatment. Only caspase-8 showed no activity in MDA-MB-231 cells throughout the treatment periods (Figure 12). Differently, treated MCF-7 cells showed activities in caspase-8 and cytochrome c but no activation of caspase-3 throughout the treatment periods. The cytochrome c activity was increased with time and led to more than 2-fold ($P < 0.05$) activity at 72 h of treatment. In contrast, caspase-

8 activity was decreased with time compared to their respective controls (Figure 13).

The extract caused the increase of Bax and p53 expression in MDA-MB-231 cells from 24 h (34.0% and 61.3%, respectively) to 48 h (62.5% and 77.4%, respectively) but reduced moderately after 72 h (38.7% and 69.2%, respectively) (Figures 14 and 15(a)). Meanwhile, the expression of Bcl-2 was gradually decreased through the treatment periods of 24 h, 48 h, and 72 h (31.8%, 17.7%, and 0.9%, respectively) ($P > 0.05$).

Treated MCF-7 showed the expression of Bcl-2 in an antagonistic manner with the p53 and Bax, with decreases of Bcl-2 and increases of p53 and Bax activities throughout the

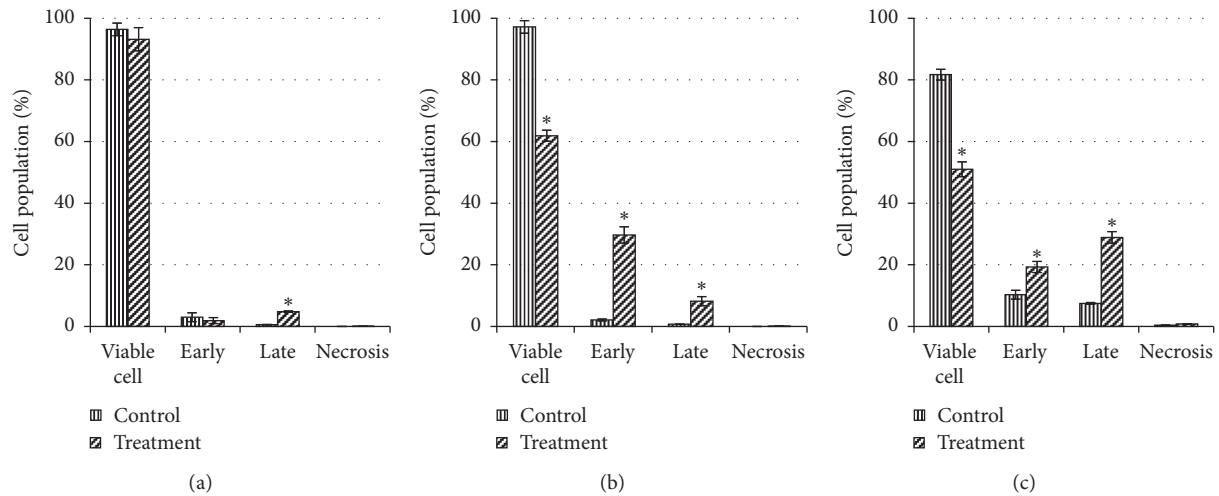


FIGURE 10: The cell population of untreated MCF-7 cells and those treated with unfermented freeze-dried leaf extract of *E. longifolia* at IC_{50} value for (a) 24 h, (b) 48 h, and (c) 72 h. The values are presented as mean \pm standard deviation for three replicates and indicated by an asterisk showed a significant difference ($P < 0.05$) relative to respective control.

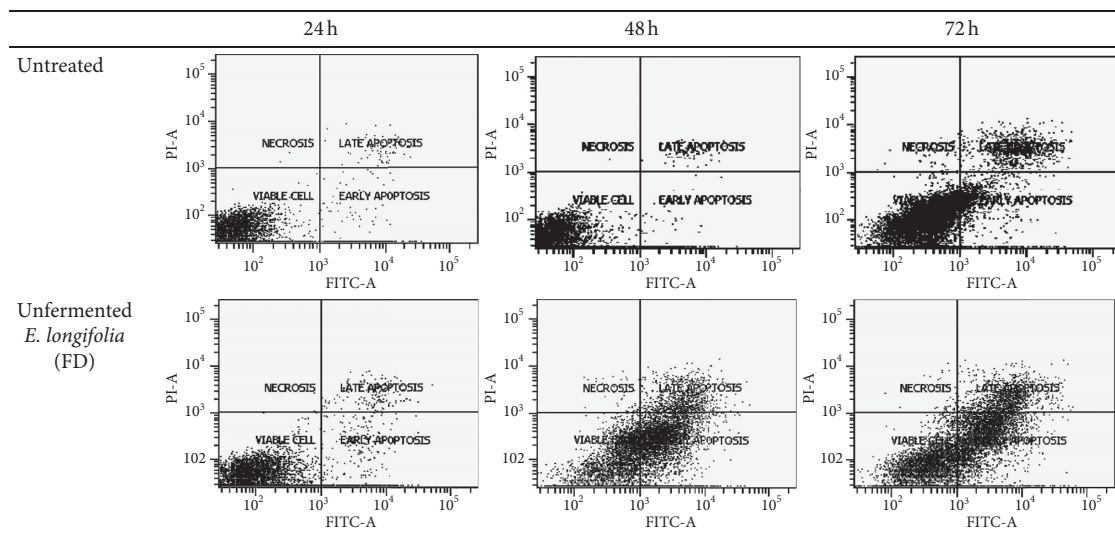


FIGURE 11: Representative flow cytometric scan of untreated MCF-7 cells and those treated with unfermented freeze-dried leaf extract of *E. longifolia* at IC_{50} value for 24 h, 48 h, and 72 h. FD: freeze-dried.

treatment periods of 24 h, 48 h, and 72 h, which significantly different to respective controls ($P < 0.05$) (Figures 16 and 15(b)). In contrast with treated MDA-MB-231 cells, the caspase-3 was not activated in the treated MCF-7 cells. There was the only activation of caspase-8 and cytochrome c.

4. Discussion

As the result of cytotoxicity effect evaluation, the leaf extract of *E. longifolia*, which was unfermented and freeze-dried had been further studied for its possible anticancer mechanism of action. The selection was made as it is fulfilling three crucial criteria: (1) possessed the lowest IC_{50} value than the other extracts which indicate the most substantial cytotoxic effect, (2) IC_{50} value was lower than $100 \mu\text{g/ml}$ of sample

concentration (50% less than total concentration tested of $200 \mu\text{g/ml}$), and (3) IC_{50} value was lower than IC_{50} value of NIH-3T3 cell ($125.5 \pm 6.2 \mu\text{g/ml}$) indicated that this extract at IC_{50} value was not toxic to normal cell line. The phenolics such as gallic acid, chlorogenic acid, vanillic acid, and catechin derivatives (i.e., ECG and EGCG) that were determined in this extract might contribute to the cytotoxicity effect against MCF-7 and MDA-MB-231 cancer cell lines. Previously, many of these compounds were proven scientifically to inhibit the growth of breast cancer cells [21, 22]. A study by Rezaei-Seresht et al. [23] had shown the cytotoxicity effect of caffeic acid and gallic acid against MCF-7 cells by the activation of intrinsic apoptotic signalling pathways along with the expression of p53, Mcl-1, and p21 genes. Similarly, a study by Schröder et al. [24] also had reported

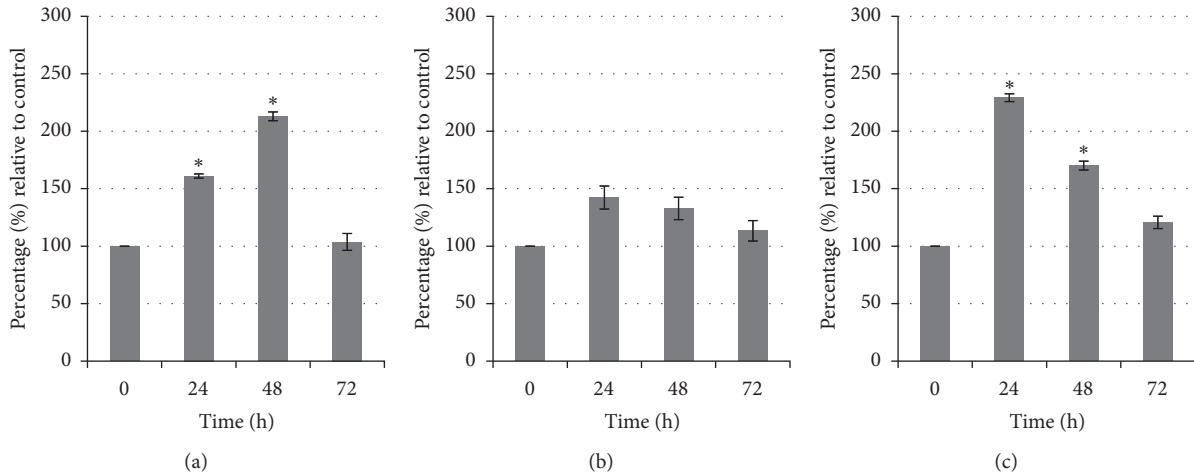


FIGURE 12: (a) Caspase-3, (b) caspase-8, and (c) cytochrome c activities of MDA-MB-231 cells treated with unfermented freeze-dried leaf extract of *E. longifolia* at IC_{50} value. The values are presented as mean \pm standard deviation for three replicates and indicated by an asterisk showed a significant difference ($P < 0.05$) relative to respective control.

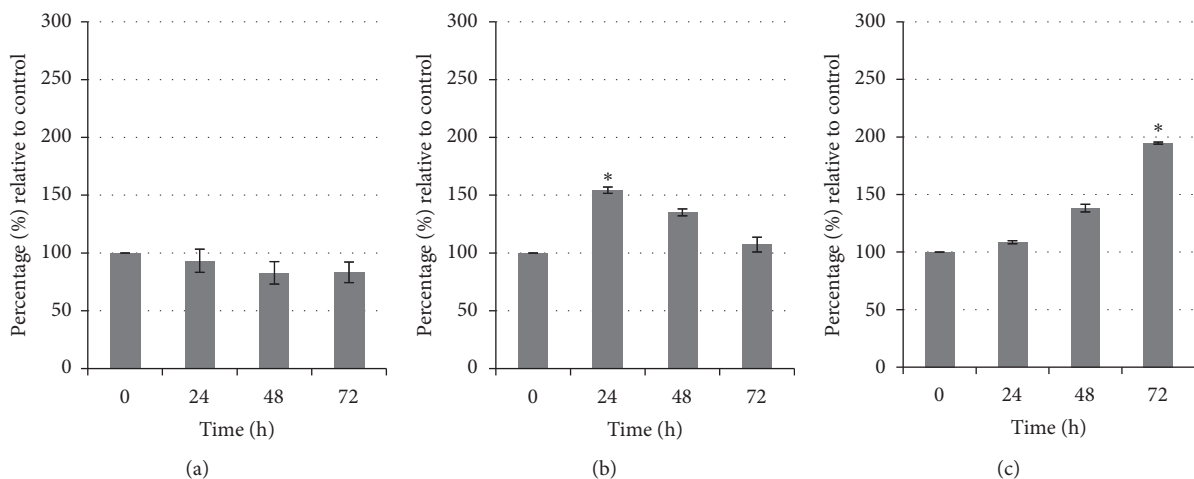


FIGURE 13: (a) Caspase-3, (b) caspase-8, and (c) cytochrome c activities of MCF-7 cells treated with unfermented freeze-dried leaf extract of *E. longifolia* at IC_{50} value. The values are presented as mean \pm standard deviation for three replicates and indicated by an asterisk showed a significant difference ($P < 0.05$) relative to respective control.

the cytotoxicity effect of ECGC derived from green tea on both MCF-7 and MDA-MB-231 cancer cells, which might be caused by the activation of estrogen receptor-independent pathways.

Apart from phenolics determined in the present study, a recent study by Supartini et al. [25] had revealed the presence of flavonoids, tannins, triterpenoid, carotenoid, kumarin, carbohydrate, and saponin in both ethanolic and water extracts of *E. longifolia* leaves. Moreover, 3 major chemical compounds in its ethanol extract were identified, i.e., 4H-pyran-4-one, 2,3-dihydro-3,5-dihydroxy-6-methyl- (6.78%), 2-cyclohexene-1-one, 4-hydroxy-3,5,6-trimethyl-4-(3-oxo-1-butenyl)- (6.46%), and acetic acid, 2-(2,2,6-trimethyl-7-oxabicyclo[4.1.0]hept-1-yl)-propenyl ester (5.61%). They stated that these compounds had been numerous reported to have biological activities such as antimicrobial, anti-inflammatory,

strong antioxidant capacity, anticancer, antimutagenic, antipeptic, antiseptic, antispasmodic, antiandrogenic, and hypocholesterolemic activities. In a different study by Jiwa-jinda et al. [26], the ethanolic extract of *E. longifolia* leaves consisted of 7 quassinoid compounds of lonilactone, 6-dehydro lonilactone, 11-dehydroklaineaneone, 12-epi dehydroklaineaneone, 15 β -hydroxyklaineaneone, 14,15 β -dihydroxyklaineaneone, and 15- β -O-acetyl-14-hydroxyklaineaneone. Quassinoids are a well-known compound to exhibit a wide range of inhibitory effects, including anti-inflammatory, antiviral, antimalarial, and anti-proliferative effects on various cancer cell types including breast cancer [27]. Meanwhile, Zakaria et al. [28] have detected the presence of eurycomanone and 14,15 β -dihydroxyklaineaneone in leaf extracts of *E. longifolia*. These compounds have also been found significantly in its roots,

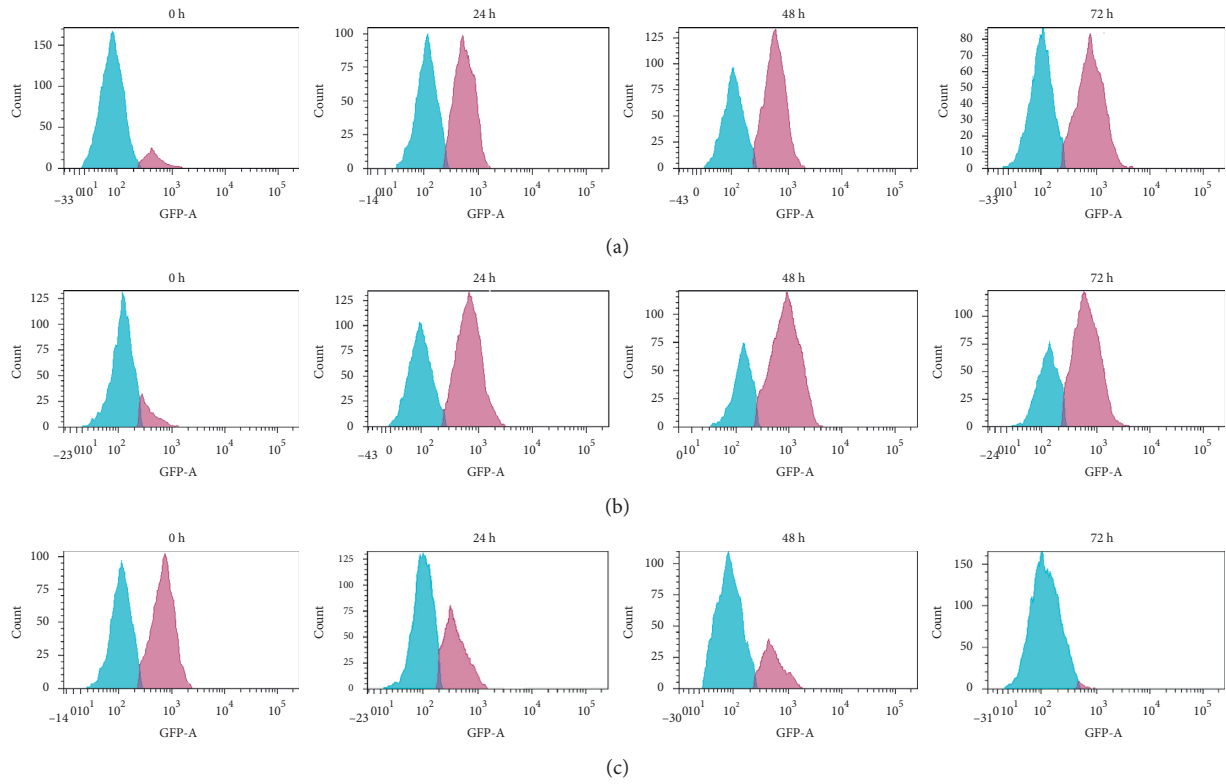


FIGURE 14: Representative flow cytometric scan of untreated MDA-MB-231 cells and those treated with unfermented freeze-dried leaf extract of *E. longifolia* at IC₅₀ value for 24 h, 48 h, and 72 h. (a) p53, (b) Bax, and (c) Bcl-2 expressions. Blue peak = unstained cells. The purple peak at 0 h = untreated cells. Purple peaks at 24, 48, and 72 h = treated cells with extract at the respective treatment period.

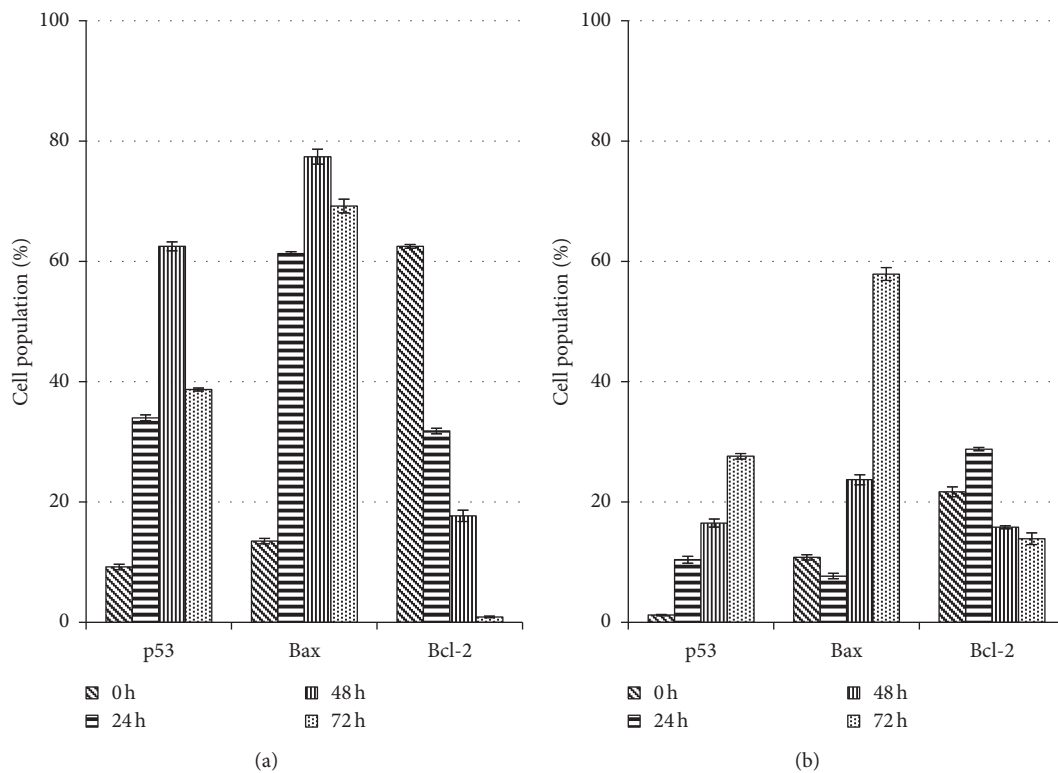


FIGURE 15: p53, Bax and Bcl-2 proteins expression of A. MDA-MB-231 and B. MCF-7 cancer cell lines treated with unfermented freeze-dried leaf extract of *E. longifolia* at IC₅₀ value. -e values are presented as mean \pm standard deviation for three replicates and indicated by an asterisk were showed a significant difference ($P < 0.05$) relative to respective control (values at 0 h).

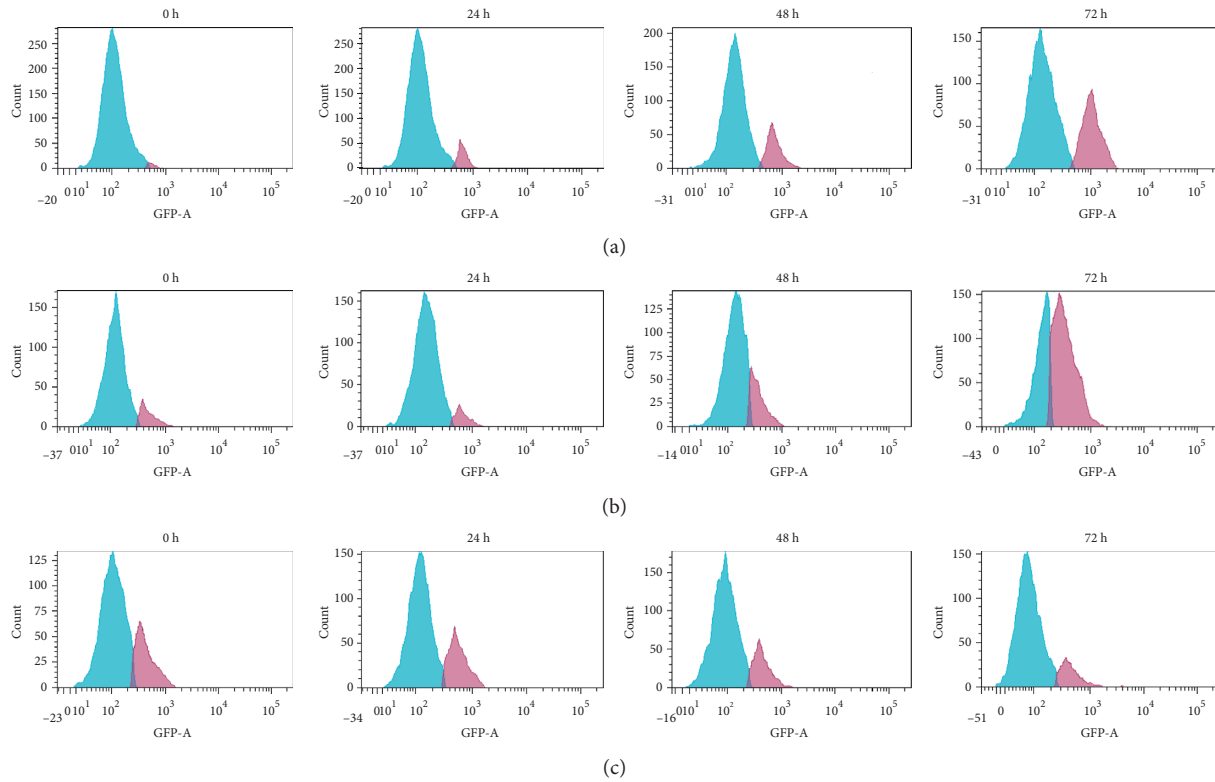


FIGURE 16: Representative flow cytometric scan of untreated MCF-7 cells and those treated with unfermented freeze-dried leaf extract of *E. longifolia* at IC_{50} value for 24 h, 48 h and 72 h. (a) p53, (b) Bax and (c) Bcl-2 expressions. Blue peak = unstained cells. The purple peak at 0 h = Untreated cells. The purple peak at 24, 48 and 72 h = Treated cells with extract at the respective treatment period.

where eurycomanone, in particular, had been proven to exert antiproliferation or cytotoxicity effect against breast carcinoma cell of MCF-7 [29].

However, those phenolics appear to be affected by processing factors since the present result of the cytotoxicity effect between different types of *E. longifolia* extracts was obvious. The steam blanching process acts as the pretreatment to deactivate the degradative enzymes called polyphenol oxidase (PPO) to prevent the oxidation of polyphenol compounds and retaining more phenolic content in the unfermented leaves. Differently, the absence of this crucial step in the fermented leaf preparation caused the deterioration of phenolic compounds. The withering and fermentation processes also might cause the oxidation or degradation of phenolic compounds in fermented leaves [30]. In terms of drying techniques, the nonthermal of freeze-drying gave the end-product with higher phenolic content compared to the microwave-oven drying due to its low temperature, vacuum conditions and very low deterioration reaction rates [31]. The primary structure of dried leaves was preserved during drying due to the developed frozen water molecules or ice crystal within the leaf tissue matrix has lower movement compared to its liquid form [31]. This present finding was in agreement with a recent study by Roslan et al. [32], as the freeze-dried leaves of *Camellia sinensis* or authentic tea showed the highest phenolics, flavonoids, and antioxidant activity compared to superheated steam and oven drying techniques.

At the cellular level, chemotherapeutic agents act primarily by inducing cancer cell death through the mechanism of apoptosis [33]. In the present study, there was an evident selected *E. longifolia* extract was able to induce apoptosis in both breast cancer cells: MCF-7 and MDA-MB-231. DNA fragmentation or the cleavage of DNA into oligonucleosomal size fragments suggesting this extract had caused the cells to undergo apoptosis cell death mode. The dying cells during apoptosis would leave a minimum impact to neighbouring tissues *in vivo* compared to those of necrosis, another form of cell death, which accompanied by membrane rupture and leakage of cellular contents causing tissue inflammation [34], thus making it a promising agent for chemotherapy, which merits further study.

A flow cytometry result showed the number of apoptotic cells by calculation based on the appearance of cells in G_1 . The number of apoptotic MDA-MB-231 cells was increased as the treatment period was prolonged from 24 h to 48 h but decreased at 72 h, which also displayed in the similar manner of S phase cells in population, indicated that the S phase was arrested as the synthesis of DNA was inhibited and the cells were prevented from entering G_2/M phase [35, 36]. The activity of Bax increased from 24 h to 48 h but decreased of Bcl-2 at the same time suggesting that this extract induced the upregulation of Bax and downregulation of Bcl-2. The Bax gene is a transcriptional target of p53 and could be upregulated in response to p53-dependent apoptosis triggers. Meanwhile, the downregulation of Bcl-2 has caused the

release of cytochrome c from mitochondria into the cytosol. In turn, the release of cytochrome c binds with Apaf-1 which activates caspase-9 before activates downstream effector caspases such as caspase-3, -6, and -7 [37]. In this current study, the activated caspase-3 might then lead to apoptotic cell death. A similar finding in Birjandian et al.'s research [38] had shown the crude methanolic extract of *Echinophora platyloba* promotes MDA-MB-231 cell death at IC_{50} $534.6 \pm 7.2 \mu\text{g/mL}$ by inducing cell arrest at S phase after 24 h of incubation and significantly upregulates the expression of Bax and p27 gene, as well as the downregulation of Bcl-2 gene expression.

Differently, the percent of MCF-7 apoptotic cells rose as the time of treatment was prolonged from 24 h, 48 h, and then 72 h, similarly with the distribution of G_2/M phase cells in its population, being evident that the G_2/M phase became the dominant phase during apoptosis in treated cells in a time-dependent manner. These findings indicate that the cytotoxicity effect of this extract on MCF-7 cells could be attributed primarily to the induction of G_2/M arrest. MCF-7 cells got accumulated at G_2/M phase as the DNA was damaged or unreplicated and prevented cells from undergoing mitosis process [18, 39]. In contrast with the treated MDA-MB-231 cells, the caspase-3 was not activated in treated MCF-7 cells. There was the only activation of caspase-8 and cytochrome c. There is a possibility that this extract might induce two apoptosis pathways, i.e., caspase-8-initiated pathway and mitochondrial-initiated caspase-9-mediated pathway [40, 41]. Moreover, since the caspase-3 was not activated, another downstream effector caspase-6 and -7 might be triggering the apoptosis initiation [37]. Ali et al. [42] have also reported that a curcumin derivative of (Z)-3-hydroxy-1-(2-hydroxyphenyl)-3-phenylprop-2-en-1-one (DK1) activates the upregulation of p53 and p21 and downregulation of PLK-1 which promote phosphorylation of CDC2 which caused the arrest of G_2/M phase. Besides, results of increase reactive oxygen species and decrement of antioxidant glutathione level were associated with apoptosis along with elevation of cytochrome c and then activation of caspase-9.

5. Conclusion

The unfermented freeze-dried leaf extract of *E. longifolia* was determined as the most effective anticancer source against MDA-MB-231 and MCF-7 cell lines compared to other *E. longifolia* extracts. The extract was proven to induce apoptosis cell death which leads to DNA fragmentation. A significant cell cycle arrest at S phase was observed as early as 24 h for MDA-MB-231 which was caused by the failure of DNA synthesis. In contrast, the cell cycle arrest on G_2/M of MCF-7 indicates that DNA was damaged and unable to be duplicated. The upregulation of Bax and downregulation of Bcl-2 expression in MDA-MB-231 cells might be responsible for cytochrome c and caspase-3 activities which lead to apoptosis cell death. The actions of caspase-8 and cytochrome c in MCF-7 with upregulation of Bax and p53 and also downregulation of Bcl-2 expression showed the possibility of this extract might induce two apoptosis pathways, i.e., caspase-8-initiated pathway and mitochondrial-initiated

caspase-9-mediated pathway, triggering downstream effector caspase-6 and -7 and initiating the apoptosis mechanism. These results indicate the ability of unfermented freeze-dried leaf extract of *E. longifolia* to induce apoptosis cell death on MDA-MB-231 and MCF-7, as well as providing fundamental evidence on the sample preparation effect towards its cytotoxicity level. In future, these data can act as initial guidance towards developing chemotherapeutic agent for cancer treatment. Additional *in vivo* studies on the toxicology, bioavailability, and anticancer activity are however needed to clarify the efficacy and safety of this extract in breast cancer treatment.

Data Availability

The datasets generated and analyzed during the current study are available from the first author on reasonable request.

Conflicts of Interest

The authors declare that they have no conflicts of interest.

Acknowledgments

The authors would like to acknowledge the Ministry of Higher Education of Malaysia (MOHE) for financial assistance under the Fundamental Research Grant Scheme (FRGS) Vot no. 1560 (FRGS/1/2015/WAB01/UTHM/02/1). The authors acknowledge the opportunity to use facilities for cell culture and anticancer research purposes in Nutrition Laboratory at the Department of Nutrition and Dietetics, Faculty of Medicine and Health Sciences, Universiti Putra Malaysia. The authors also would like to acknowledge the Seaweed Research Unit, Faculty of Food Science and Nutrition, Faculty of Science and Natural Resources and Institute for Tropical Biology and Conservation, Universiti Malaysia Sabah, Malaysia, for the use of the laboratory facilities and technical assistance. Special thanks to the loving memory of late Prof. Dr. Asmah Rahmat for her contribution in this research.

References

- [1] World Health Organization (WHO), *Cancer*, World Health Organization, Geneva, Switzerland, 2018, <https://www.who.int/news-room/fact-sheets/detail/cancer>.
- [2] F. Bray, J. Ferlay, I. Soerjomataram, R. L. Siegel, L. A. Torre, and A. Jemal, "Global cancer statistics 2018: GLOBOCAN estimates of incidence and mortality worldwide for 36 cancers in 185 countries," *CA: A Cancer Journal for Clinicians*, vol. 68, no. 6, pp. 394–424, 2018.
- [3] American Cancer Society, *Global Cancer Facts & Figures*, American Cancer Society, Atlanta, Georgia, 4th edition, 2018.
- [4] C. H. Yip, N. Bhoo Pathy, and S. H. Teo, "A review of breast cancer research in Malaysia," *Medical Journal Malaysia*, vol. 69, pp. 8–22, 2014.
- [5] S. Y. Yin, W. C. Wei, F. Y. Jian, and N. S. Yang, "Therapeutic applications of herbal medicines for cancer patients," *Evidence-based Complementary and Alternative Medicine*, vol. 2013,

- 15 pages, 2013, <https://doi.org/10.1155/2013/302426>, Article ID 302426.
- [6] G. Pistritto, D. Trisciuglio, C. Ceci, A. Garufi, and G. D’Orazi, “Apoptosis as anticancer mechanism: function and dysfunction of its modulators and targeted therapeutic strategies,” *Aging*, vol. 8, no. 4, pp. 603–619, 2016.
- [7] R. Jan and G.-e.-S. Chaudhry, “Understanding apoptosis and apoptotic pathways targeted cancer therapeutics,” *Advanced Pharmaceutical Bulletin*, vol. 9, no. 2, pp. 205–218, 2019.
- [8] P. Erb, J. Ji, M. Wernli, E. Kump, A. Glaser, and S. A. Büchner, “Role of apoptosis in basal cell and squamous cell carcinoma formation,” *Immunology Letters*, vol. 100, no. 1, pp. 68–72, 2005.
- [9] H. Huang, A. Y. Chen, X. Ye et al., “Myricetin inhibits proliferation of cisplatin-resistant cancer cells through a p53-dependent apoptotic pathway,” *International Journal of Oncology*, vol. 47, no. 4, pp. 1494–1502, 2015.
- [10] N. M. Chen, N. Mohamed, N. Muhammad, I. N. Mohamad, and A. N. Shuid, “*Eurycoma longifolia*: medicinal plant in the prevention and treatment of male osteoporosis due to androgen deficiency,” *Evidence-Based Complementary and Alternative Medicine*, vol. 2012, 9 pages, 2012, <https://doi.org/10.1155/2012/125761>, Article ID 125761.
- [11] R. Bhat and A. A. Karim, “Tongkat Ali (*Eurycoma longifolia* Jack): a review on its ethnobotany and pharmacological importance,” *Fitoterapia*, vol. 81, no. 7, pp. 669–679, 2010.
- [12] A. N. Mohamed, J. Vejayam, and M. M. Yusoff, “Review on *Eurycoma longifolia* pharmacological and phytochemical properties,” *Journal of Applied Sciences*, vol. 15, no. 6, pp. 831–844, 2015.
- [13] S. U. Rehman, K. Choe, and H. H. Yoo, “Review on a traditional herbal medicine, *Eurycoma longifolia* Jack (Tongkat ali): its traditional uses, chemistry, evidence-based pharmacology and toxicology,” *Molecules*, vol. 27, no. 331, pp. 1–31, 2016.
- [14] O. S. Al-Salahi, D. Ji, A. M. Majid et al., “Anti-tumor activity of *Eurycoma longifolia* root extracts against K-562 cell line: in vitro and in vivo study,” *PLoS One*, vol. 9, no. 1, Article ID e83818, 2014.
- [15] D. Nallappan, P. N. V. K. V. Tollamadugu, A. N. Fauzi, N. S. Yaacob, and V. R. Pasupuleti, “Biomimetic synthesis and anticancer activity of *Eurycoma longifolia* branch extract-mediated silver nanoparticles,” *IET Nanobiotechnology*, vol. 11, no. 7, pp. 889–897, 2017.
- [16] M. S. Rabeta and S. Y. Lai, “Effects of drying, fermented and unfermented tea of *Ocimum tenuiflorum* Linn. on the antioxidant capacity,” *International Food Research Journal*, vol. 20, no. 4, pp. 1601–1608, 2013.
- [17] M. Lusía Barek, M. Hasnadi, A. A. Zaleha, and A. B. Mohd Fadzelly, “Effect of different drying methods on phytochemicals and antioxidant properties of unfermented and fermented teas from Sabah Snake Grass (*Clinacanthus nutans* Lind.) leaves,” *International Food Research Journal*, vol. 22, no. 2, pp. 661–670, 2015.
- [18] M. F. Abu Bakar, *Chemopreventive and Chemotherapeutic Properties of Selected Fruits Endemic to Borneo: Investigation on Mangifera Pajang and Artocarpus Odoratissimus*, University of Nottingham, Nottingham, UK, 2010.
- [19] M. F. Abu Bakar, M. Mohamad, A. Rahmat, S. A. Burr, and J. R. Fry, “Cytotoxicity, cell cycle arrest, and apoptosis in breast cancer cell lines exposed to an extract of the seed kernel of *Mangifera pajang* (bambangan),” *Food and Chemical Toxicology*, vol. 48, no. 6, pp. 1688–1697, 2010.
- [20] Research and Development (R&D) Systems (NY), *Flow Cytometry Protocol for Staining Intracellular Molecules Using Detergents to Permeabilize the Cell Membrane*, Research and Development (R&D) Systems (NY), New York, NY, USA, 2015, <https://www.rndsystems.com/resources/protocols/flow-cytometry-protocol-staining-intracellular-molecules-using-detergents>.
- [21] F. Li, S. Li, H.-B. Li, G.-F. Deng, W.-H. Ling, and X.-R. Xu, “Antiproliferative activities of tea and herbal infusions,” *Food & Function*, vol. 4, no. 4, pp. 530–538, 2013.
- [22] D. O. Levitsky and V. M. Dembitsky, “Anti-breast cancer agents derived from plants,” *Natural Products and Bioprospecting*, vol. 5, no. 1, pp. 1–16, 2015.
- [23] H. Rezaei-Seresht, H. Cheshomi, F. Falanji, F. Movahedi-Motlagh, M. Hashemian, and E. Mireskandari, “Cytotoxic activity of caffeic acid and gallic acid against MCF-7 human breast cancer cells: an *in silico* and *in vitro* study,” *Avicenna Journal of Phytomedicine*, vol. 9, no. 6, pp. 574–586, 2019.
- [24] L. Schröder, P. Marahrens, J. G. Koch et al., “Effects of green tea, matcha tea and their components epigallocatechin gallate and quercetin on MCF-7 and MDA-MB-231 breast carcinoma cells,” *Oncology Reports*, vol. 41, no. 1, pp. 387–396, 2019.
- [25] Supartini, R. Maharani, A. Fernandes, and T. K. Waluyo, “Herbal tea of yellow bitter charm (*Eurycoma longifolia* Jack.) leaves and its potential analysis for commercial herbs drink,” *IOP Conference Series: Earth and Environmental Science*, vol. 415, 2019.
- [26] S. Jiwajinda, V. Santisopasri, A. Murakami, N. Hirai, and H. Ohigashi, “Quassinoids from *Eurycoma longifolia* as plant growth inhibitors,” *Phytochemistry*, vol. 58, no. 6, pp. 959–962, 2001.
- [27] G. Fiaschetti, M. Grotzer, T. Shalaby, D. Castelletti, and A. Arcaro, “Quassinoids: from traditional drugs to new cancer therapeutics,” *Current Medicinal Chemistry*, vol. 18, no. 3, p. 316, 2011.
- [28] N. Zakaria, K. Mohd, M. S. R. Hamil, A. H. Memon, M. Asmawi, and Z. Ismail, “Characterization of primary and secondary metabolites of leaf and stem extracts of *Eurycoma longifolia* Jack,” *Journal of Fundamental and Applied Sciences*, vol. 9, pp. 661–679, 2017.
- [29] H. Yusuf, D. Satria, and Zulkarnain, “The activity of eurycomanone derivatives on cancer cell lines,” *International Journal of Pharmaceutical Sciences and Research*, vol. 10, no. 6, pp. 2947–2950, 2019.
- [30] M. F. Abu Bakar, A. H. Teh, F. Othman, N. Hashim, and S. Fakurazi, “Anti-proliferative properties and antioxidant activity of various type of *Strobilanthes crispus* tea,” *International Journal of Cancer Research*, vol. 2, no. 2, pp. 152–158, 2006.
- [31] C. Bonazzi and E. Dumoulin, “Quality changes in food materials as influenced by drying processes,” *Modern Drying Technology*, vol. 1, pp. 1–20, 2011.
- [32] A. S. Roslan, A. Ismail, Y. Ando, and A. Azlan, “Effect of drying methods and parameters on the antioxidant properties of tea (*Camellia sinensis*) leaves,” *Food Production Process and Nutrient*, vol. 2, p. 8, 2020.
- [33] C. M. Pfeffer and A. Singh, “Apoptosis: a target for anticancer therapy,” *International Journal of Molecular Sciences*, vol. 19, no. 2, p. 448, 2018.
- [34] J. H. Zhang and M. Xu, “DNA fragmentation in apoptosis,” *Cell Research*, vol. 10, no. 3, pp. 205–211, 2000.
- [35] W. M. Becker, L. J. Kleinsmith, and J. Hardin, *The World of the Cell*, Pearson Benjamin Cummings, San Francisco, CA, USA, 6th edition, 2006.

- [36] K. J. Barnum and M. J. O'Connell, "Cell cycle regulation by checkpoints," *Methods in Molecular Biology*, vol. 1170, pp. 29–40, 2014.
- [37] G. Bjelakovic, A. Nagora, M. Bjelakovic, I. Stamenkovic, R. Arsic, and V. Katic, "Apoptosis: programmed cell death and its clinical implications," *Medicine and Biology*, vol. 12, no. 1, pp. 6–11, 2005.
- [38] E. Birjandian, N. Motamed, and N. Yassa, "Crude methanol extract of *Echinophora platyloba* induces apoptosis and cell cycle arrest at S-phase in human breast cancer cells," *Iranian Journal of Pharmaceutical Research*, vol. 17, no. 1, pp. 307–316, 2018.
- [39] S.-M. Jangi, J. L. Díaz-Pérez, B. Ochoa-Lizarralde et al., "H1 histamine receptor antagonists induce genotoxic and caspase-2-dependent apoptosis in human melanoma cells," *Carcinogenesis*, vol. 27, no. 9, pp. 1787–1796, 2006.
- [40] Z. Hongmei, "Chapter 1 Extrinsic and apoptosis signal pathway review- Apoptosis and Medicine," in *Apoptosis and Medicine*, pp. 3–22, InTechOpen, London, UK, 2012.
- [41] J. Zhang, L. Ma, Z.-F. Wu et al., "Cytotoxic and apoptosis-inducing activity of C 21 steroids from the roots of *Cynanchum atratum*," *Steroids*, vol. 122, pp. 1–8, 2017.
- [42] N. M. Ali, S. K. Yeap, N. Abu et al., "Synthetic curcumin derivative DK1 possessed G2/M arrest and induced apoptosis through accumulation of intracellular ROS in MCF-7 breast cancer cells," *Cancer Cell International*, vol. 17, p. 30, 2017.

Research Article

Secondary Metabolites, Antioxidant, and Antiproliferative Activities of *Dioscorea bulbifera* Leaf Collected from Endau Rompin, Johor, Malaysia

Muhammad Murtala Mainasara ^{1,2}, Mohd Fadzelly Abu Bakar ¹, Abdah Md Akim ³,
Alona C Linatoc ¹, Fazleen Izzany Abu Bakar ¹, and Yazan K. H. Ranneh ¹

¹Faculty of Applied Sciences & Technology, Universiti Tun Hussein Onn Malaysia (UTHM), Hab Pendidikan Tinggi Pagoh, KM1, Jalan Panchor, Muar 84600, Johor, Malaysia

²Faculty of Science, Department of Biological Sciences, Usmanu Danfodiyo University Sokoto, PMB 1046, Sokoto, Nigeria

³Department of Biomedical Sciences, Faculty of Medicine and Health Sciences, Universiti Putra Malaysia, Seri Kembangan 43400, Selangor, Malaysia

Correspondence should be addressed to Mohd Fadzelly Abu Bakar; fadzelly@uthm.edu.my

Received 11 August 2020; Revised 26 October 2020; Accepted 14 December 2020; Published 11 January 2021

Academic Editor: Amin Tamadon

Copyright © 2021 Muhammad Murtala Mainasara et al. This is an open access article distributed under the Creative Commons Attribution License, which permits unrestricted use, distribution, and reproduction in any medium, provided the original work is properly cited.

Breast cancer is among the most commonly diagnosed cancer and the leading cause of cancer-related death among women globally. Malaysia is a country that is rich in medicinal plant species. Hence, this research aims to explore the secondary metabolites, antioxidant, and antiproliferative activities of *Dioscorea bulbifera* leaf collected from Endau Rompin, Johor, Malaysia. Antioxidant activity was assessed using 2,2-diphenyl-1-picrylhydrazyl (DPPH), ferric reducing antioxidant power (FRAP), and 2,2'-azino-bis-3-ethylbenzthiazoline-6-sulphonic acid (ABTS) assays, while the cytotoxicity of *D. bulbifera* on MDA-MB-231 and MCF-7 breast cancer cell lines was tested using 3-(4,5-dimethylthiazol-2-yl)-2,5-diphenyl tetrazolium bromide (MTT) assay. Cell cycle analysis and apoptosis were assessed using flow cytometry analysis. Phytochemical profiling was conducted using gas chromatography-mass spectrometry (GC-MS). Results showed that methanol extract had the highest antioxidant activity in DPPH, FRAP, and ABTS assays, followed by ethyl acetate and hexane extracts. *D. bulbifera* tested against MDA-MB-231 and MCF-7 cell lines showed a pronounced cytotoxic effect with IC₅₀ values of 8.96 µg/mL, 6.88 µg/mL, and 3.27 µg/mL in MCF-7 and 14.29 µg/mL, 11.86 µg/mL, and 7.23 µg/mL in MDA-MB-231, respectively. Cell cycle analysis also indicated that *D. bulbifera* prompted apoptosis at various stages, and a significant decrease in viable cells was detected within 24 h and substantially improved after 48 h and 72 h of treatment. Phytochemical profiling of methanol extract revealed the presence of 39 metabolites such as acetic acid, n-hexadecanoic acid, acetin, hexadecanoate, 7-tetradecenal, phytol, octadecanoic acid, cholesterol, palmitic acid, and linolenate. Hence, these findings concluded that *D. bulbifera* extract has promising anticancer and natural antioxidant agents. However, further study is needed to isolate the bioactive compounds and validate the effectiveness of this extract in the *In vivo* model.

1. Introduction

Millions of mortalities were reported globally as a result of cancer, and the numbers of new cases are expected to increase in the future [1]. Breast tumour is the second highest cancer recorded worldwide and the most common cause of cancer death among women. It has been ascertained that

about 25% of all new identified cancer case is breast cancer, which accounts for 15% of deaths in women each year [2, 3].

Breast cancer is a commonly diagnosed cancer in Malaysia, having a standardized age rate of 47.4 per 100,000 [4, 5]. The National Cancer Registry of Malaysia (NCR) records that 21,773 Malaysians who are perceived with cancer and approximations show that unregistered cases

have reached about 10,000 cases every year. It is likely that by 75 years old, ¼ of Malaysians will be diagnosed with cancer [6]. Therefore, discovering new drugs with minimal toxicity is a broad scientific challenge, and there is an immediate need to search for a new agent to mitigate the menace by using alternative evidence-based herbal medicines.

Dioscorea bulbifera (Figure 1) is a member of the family Dioscoreaceae, categorised in the order Dioscoreales and genus *Dioscorea*. It is usually referred to as air potato, air yam, or bulbil-bearing yam. It is a prolific climbing plant indigenous to Southern Asia and West Africa, mostly found along forest edges. The direction of circular twinning had been reported in *D. bulbifera* and can grow to a height of 12 m. It has shiny green leaves that are alternate with a long leafstalk. Resembling true yam leaves, *D. bulbifera* has an annual vegetative cycle. Hence, this study was directed toward discovering secondary metabolites, antioxidant, and antiproliferative effects of *D. bulbifera* leaf extract from Kampung Peta, Endau Rompin, Mersing, Johor, Malaysia.

2. Materials and Methods

2.1. Sample Collection and Preparation. *D. bulbifera* fresh leaves were collected at Kampung Peta, Johor, Malaysia, on 5th May 2017 with the permission of Perbadanan Taman Negara Johor (PTJN) and with full observation of rules and regulations on collection practices of medicinal plants as laid down by the World Health Organisation (WHO) collection of plant materials [7]. Identification was made, and the voucher specimen was deposited in the Herbarium of Centre

of Research for Sustainable Uses of Natural Resources (CoR-SUNR), Faculty of Applied Sciences and Technology, Universiti Tun Hussein Onn Malaysia. Fresh sample was cleaned using tap water to eliminate impurities or soil debris. The sample was crushed to a fine powder with an electric blender after shade drying at room temperature and kept in a zip lock bag in a freezer (−20°C) for further analysis [8, 9].

2.2. Sample Extraction. Methanol, ethyl acetate, and hexane solvents were used for the extraction of plant samples by successive maceration methods as described by Bhunu et al. [10] with some modifications. The mixture was filtered using a vacuum filter and then evaporated using a rotary evaporator where the yield of extracts was found; hexane (6.22%), ethyl acetate (8.63%), and methanol (20.6%) were used. The extract was later used to identify its phytochemicals, antioxidant, and antiproliferative effects.

2.3. Determination of Antioxidant Activities

2.3.1. 2,2-Diphenyl-1-picrylhydrazyl (DPPH) Assay. DPPH scavenging activity of the sample was determined according to Bakar et al. [11] and Hassan and Bakar [12]. Briefly, a methanol solution of DPPH (0.3 mM) was added into the samples (2.5 mL). The extract was kept in a light protected place at room temperature for 30 min after mixing vigorously. The absorbance was read at 518 nm. The following equation was used for calculating the scavenging or antioxidant activity (AA):

$$AA (\%) = \frac{\text{Absorbance (sample)} - \text{absorbance (empty sample)}}{\text{absorbance (control)}} \times 100. \quad (1)$$

2.3.2. Ferric Reducing Antioxidant Power (FRAP) Assay. FRAP assay was conducted according to Dusuki et al. [13] with some modifications. The FRAP mixture was formed by mixing 300 mM acetate buffer with 3.6 pH, 2.5 mL of 10 mM TPTZ solution in 40 mM HCl, and 0.25 mL of 20 mM FeCl₃, and the substances were tested in 0.1 mL methanol, ethyl acetate, and hexane or methanol. Plain reading was recorded at 593 nm using a test tube with extra 3 mL of FRAP reagent. Plant extract (100 µL) and distilled water (300 µL) were supplemented to the test tube. Using a spectrometer, after 30 min of incubation, absorbance was read at 593 nm. Ferric reducing capacity in 1 g of dried sample (mM/g) was measured as mM for the final result. All tests were run in triplicate.

2.3.3. 2,2'-Azino-bis-3-ethylbenzthiazoline-6-sulphonic Acid (ABTS) Assay. ABTS assay was carried in line with Re et al. [14] with some modifications. Reacting of ABTS solution (7 mM) with 2.45 mM of potassium persulfate produced the

performed radical monocation of ABTS. The solution was kept in the dark and left to stand for 15 h at room temperature. To obtain the units of absorbance at 734 nm, the solution was diluted with either methanol, ethyl acetate, or hexane; aliquot for every sample (200 µL) was added to 2000 µL of ABTS. Using a spectrometer, the absorbance was monitored for 5 min at 734 nm. Blank solvents were run appropriately in every assay. The proportion of inhibition was calculated against control and matched to a vitamin C standard curve (10–100 µM), and the percentage was used to express the radical scavenging activities.

2.4. Anticancer Activities

2.4.1. Cell Culture Condition. MCF-7 and MDA-MB-231 breast cancer cell lines were purchased from American Type Culture Collection (ATCC). The cells were maintained in Roswell Park Memorial Institute (RPMI) 1640 media supplemented with L-glutamine, 1% penicillin-streptomycin,



FIGURE 1: *D. bulbifera* plant (leaves).

and 10% fetal bovine serum in a humidified atmosphere of 5% carbon dioxide (CO₂) at 37°C.

2.4.2. Extracts Preparation. To solubilise the plant extract, dimethyl sulphoxide (DMSO) at a concentration of 10 mM which was kept at 4°C under light protection was used. DMSO concentration that does not exceed 1% was used for the whole experiment. Fresh complete culture media were diluted with 20 mg/10 mL of standard drug (doxorubicin), and the extract was serially diluted to the cell plates at varying concentrations from 100 µg/mL to 1.5625 µg/mL.

2.4.3. 3-(4,5-Dimethylthiazol-2-yl)-2,5-diphenyl Tetrazolium Bromide (MTT) Assay. Following a procedure described by Rahmat et al. [15], 6.9×10^5 of MDA-MB-231 and MCF-7 cells were plated in 96-well plate and grown in 200 µL complete growth media (CGM) and treated for 24 h, 48 h, and 72 h, respectively. IC₅₀ of the extract was added in 96-well plates in serial dilution (100 µg/mL–5.625 µg/mL), and then, 20 µL of MTT was added into each well and nurtured for 4 h. Afterward, to liquefy and solubilize the colored crystals, 100 µL of DMSO was added into each well, and absorbance was read at 570 nm using an ELISA reader (AWARENESS-State Fax, USA). The following formula was used to determine the cytotoxicity of the extract:

$$\text{Cytotoxicity \%} = \frac{\text{optical density of sample}}{\text{optical density control}} \times 100. \quad (2)$$

For the suppression concentration (IC₅₀), the quality of sample that readily inhibits cell division by half was determined explicitly for every cell multiplying curve.

2.4.4. Cell Cycle Analysis by Propidium Iodide (PI) Staining. Cell cycle analysis was carried out with some modifications as described by Queiroz et al. [16]. Cells (1×10^6) were nurtured for 24 h and subsequently treated for 24 h, 48 h, and 72 h using crude extracts at the IC₅₀ values. Altogether, the detached and adhering cells were reaped and reassigned in a disinfected centrifuge tube. The cells were then centrifuged (1,200 rpm) for 15 min at 4°C. Cold phosphate buffered saline (PBS) was used to wash the cells where the cells were resuspended with 0.5 mL of cold PBS, and ice-cold ethanol (70%) was then added to the cell suspension and

incubated at –20°C for 2 h. Then, the ethanol was expelled from the sample after centrifugation. The cells that have been rinsed twice using cool PBS previously were stained with propidium iodide (500 µL of 10 µg/mL) and RNase (100 µg/mL) at room temperature for about 30 min. Dispersion of the cell cycle was analysed using flow cytometry.

2.4.5. Annexin V/PI Apoptosis Assay. This method was performed according to Tor et al. [17]. Briefly, cells were plated in 6-well plates and treated with IC₅₀ values for 24 h, 48 h, and 72 h. The viability of the cells was measured using an annexin V-FITC/PI kit, following the manufacturer's procedure. Both treated and control cells were centrifuged and washed twice using PBS. At room temperature, cell staining was carried out using FITC annexin V (5 µL) and 10 µL PI for 15 min, and cell death was also analysed using flow cytometry.

2.5. Gas Chromatography-Mass Spectrometry (GC-MS) Analysis. The selected crude extract was analysed using gas chromatography (GC-MS-2010 Plus-Shimadzu) in order to determine the secondary metabolites present. The segment (30.0 m length, 0.25 mm ID, and 0.25 µm thickness) was set at 50°C for 4 min which was then expanded to 300°C at the rate of 3°C/min, and after that supported for 10 min. The temperature at the injector was set at 250°C, and the volume was set at 0.1 L. The present helium rate of the bearer gas was set at 1 mL/min with an aggregate run span of an hour. Electron ionization and mass spectra were performed at 70 eV and between the range of 40–700 m/z [18].

2.6. Statistical Analysis. All the data were presented as mean ± standard error of mean (S.E.M). The data were statistically analysed by one-way ANOVA, followed by Dunnett's posthoc using Prism version 15.0. The level of statistical significance was set at $p < 0.05$.

3. Results

3.1. Antioxidant Activity of the Plant Extracts. Since one antioxidant assay is not sufficient to provide an adequate picture of the scavenging activities, *D. bulbifera* leaf extracts were subjected to several antioxidant assays. Antioxidant

TABLE 1: Antioxidants activities of *D. bulbifera* leaves extract.

Sample name	DPPH (%)	FRAP (mM/g)	ABTS (mg AEAC/g)
Ascorbic acid	97.0 ± 0.21	76.5 ± 0.5	47.1 ± 0.81
Methanol extract	79.0 ± 0.31	65.6 ± 0.35	31.34 ± 2.06
Ethyl acetate extract	23.2 ± 0.05	59.5 ± 0.10	10.98 ± 0.64
Hexane extract	11.5 ± 0.31	14.9 ± 0.05	9.50 ± 0.48

potential of *D. bulbifera* leaf extracts was evaluated using DPPH, FRAP, and ABTS assays (Table 1). For the DPPH assay, the methanol extract of *D. bulbifera* had the highest scavenging activity with the value of 79.0 ± 0.31 %, followed by the ethyl acetate extract with 23.2 ± 0.05 % and hexane extract with 11.5 ± 0.31 %, respectively. The same observation was also found in the FRAP assay where the methanol extract demonstrated highest reducing capacity with a value of 65.6 ± 0.35 mM Fe²⁺/g, followed by ethyl acetate with 59.5 ± 0.10 mM Fe²⁺/g and hexane extract with 14.9 ± 0.05 mM Fe²⁺/g, respectively. Whereas for the ABTS assay, the methanol extract also had the highest scavenging activity with a value of 31.34 ± 2.06 mg AEAC/g, followed by the ethyl acetate extract with 10.98 ± 0.64 mg AEAC/g and hexane extract with a value of 9.50 ± 0.48 mg AEAC/g. Plant phenolics are a significant group of compounds that serve as major antioxidants or free radical scavengers. Hence, in this analysis, the observed high free radical scavenging behavior of the methanol extract may have accounted for its polarity for the radical scavenging ability of the plant extracts. The radical scavenging activities may be due to the presence of some flavonoids with a free hydroxyl group, capable of donating hydrogen and electron [12].

The findings showed that the plant extracts had substantial disparities in their ability to compare ascorbic acid, which may also be ascribed to various characteristics, reaction, and mechanisms. Organic media can be used in solubilising DPPH radical chromogens. A strong positive correlation ($R^2 = 0.9399$, $p < 0.05$) was observed between the activities. There was also a similar relationship in FRAP, where a strong positive linear correlation ($R^2 = 0.8143$, $p < 0.05$) was found. FRAP also correlates with ABTS•+ ($R^2 = 0.87$), whereas ABTS•+ showed a stiff positive association to VCEAC ($R^2 = 0.6784$). The practical difference in these comparisons was DPPH•, which also correlates poorly with ABTS ($R^2 = 0.53$).

3.2. Anticancer Activities of *D. bulbifera*

3.2.1. 3-(4,5-Dimethylthiazol-2-yl)-2,5-diphenyl Tetrazolium Bromide (MTT) Assay. Cytotoxic activity of the plant extracts against the breast cancer cells lines was assessed using MTT assay. The IC₅₀ values of extracts on the viability of cancer cells after 24 h, 48 h, and 72 h of incubation were evaluated. IC₅₀ values were determined which lower IC₅₀ values signifying a higher antiproliferative activity. All the three extracts tested have demonstrated significant and effective antiproliferative activities in both dosage and time-dependent manner.

The IC₅₀ values of the extract on the viability of cells in MCF-7 after 24 h, 48 h, and 72 h of incubation were 41.17 µg/mL, 15.71 µg/mL, and 11.53 µg/mL, respectively, while the standard drug, doxorubicin, has shown the potent antiproliferative effect on the tested cell line with the IC₅₀ values of 5.87 µg/mL, 3.23 µg/mL, and 1.98 µg/mL for 24 h, 48 h, and 72 h, respectively. For the MDA-MB-231 cell line, the methanol extract of *D. bulbifera* had IC₅₀ values of 4.29 µg/mL, 1.86 µg/mL, and 1.23 µg/mL, respectively, at 24 h, 48 h, and 72 h. On the other hand, doxorubicin displayed potent cytotoxicity against the tested cell line with IC₅₀ values of 11.21 µg/mL, 8.1 µg/mL, and 3.07 µg/mL for 24 h, 48 h, and 72 h, respectively.

3.2.2. Cell Cycle Arrest. Using the IC₅₀ concentration from MTT assay for 24 h, 48 h, and 72 h, cell cycle analysis was evaluated after exposure of *D. bulbifera* methanol extract (Figure 2). In MCF-7, there was a momentous arrest at sub-G₁, at 24 h–72 h, and the number of cells at S and G₂/M phases and the number of cells at G₀/G₁ were reduced substantially. In MDA-MB-231, there was a significant arrest at sub-G₁ and G₂/M for 24 h, 48 h, and 72 h, and the number of cells in G₀/G₁ and the number of cells in G₂/M were markedly reduced. At 48 h, there was also considerable arrest at sub-G₁ and G₀/G₁, and the number of cells in S and the number of cells in G₂/M phases were markedly reduced, and eventually at 72 h, there was a substantial arrest at sub-G₁ and S, and the number of cells in G₀/G₁ and G₂/M phases decreased significantly.

3.2.3. Apoptosis. Cell lines were treated, and the IC₅₀ values for 24 h, 48 h and 72 h were obtained. The cells were stained with both FITC-conjugated annexin V and PI. FACS was utilised to acquire the stained cell populace. Histograms from FACS investigation at each concentrate fixation are shown in Figure 2. Graphical presentation (Figure 3) shows the proportion of annexin-V-FITC and PI-stained cells at the different time of treatment, at an early stage of apoptosis, apoptotic, and late apoptotic cells. Plant extracts for the treatment were examined for 24 h, 48 h, and 72 h in cell lines.

Figure 3 shows the percentages of cell viability after treatment of *D. bulbifera* methanol extract in MCF-7. At the end of treatment (after 72 h), the percentage of feasible cells decreased ominously by 7.78%, while the percentage of cells increased by 3.99% at early apoptosis. The cell proportion also rises by 1.06% in the late apoptotic period. Nevertheless, the percentage of cells in early apoptosis decreased by 3.8% for the control culture at 72 h; the late apoptotic stage also decreased by 0.02%, while the number of viable cells

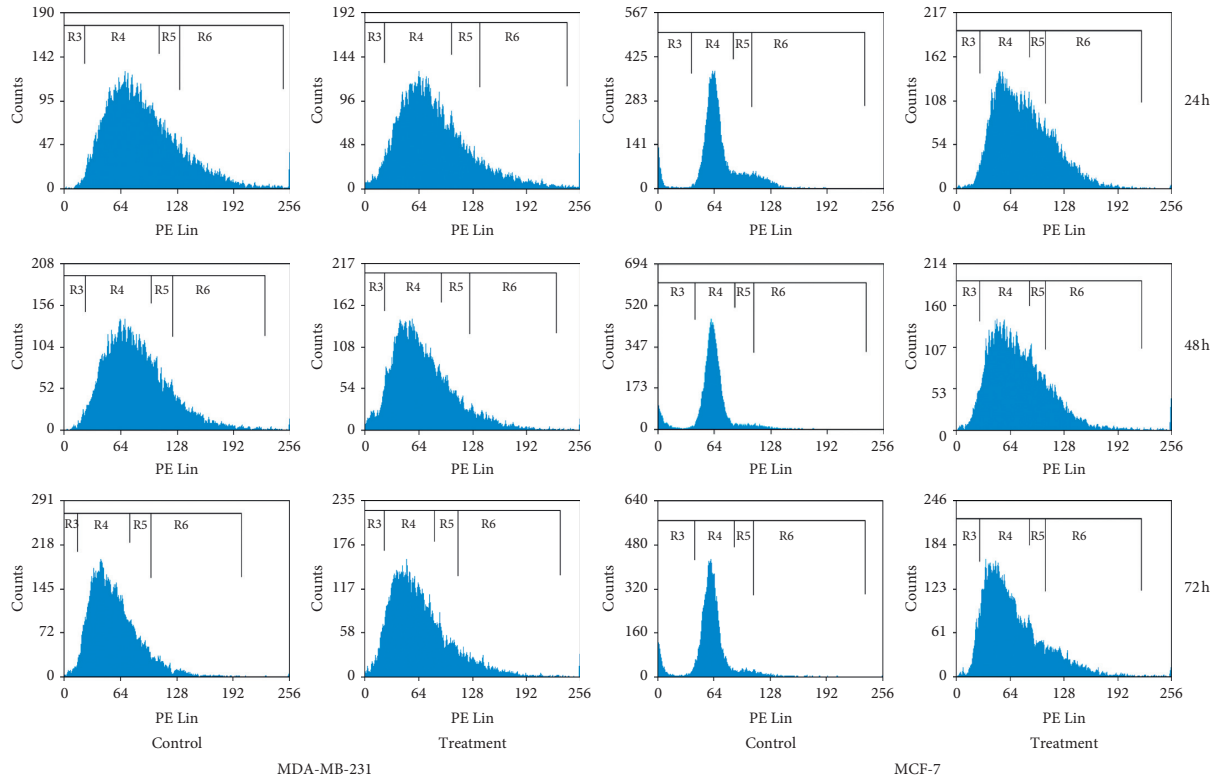


FIGURE 2: Flow cytometric scans of treated and untreated (control) cells.

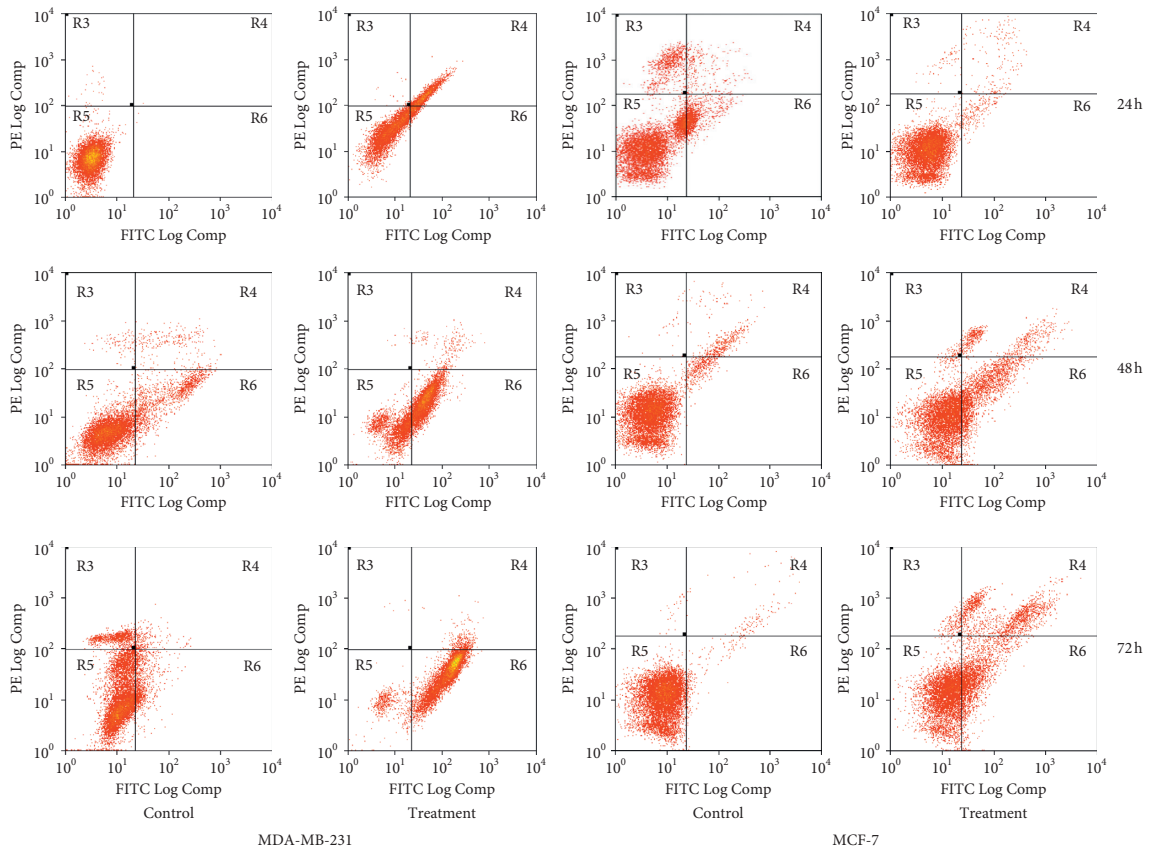


FIGURE 3: Annexin V FITC of treated and untreated (control) cells.

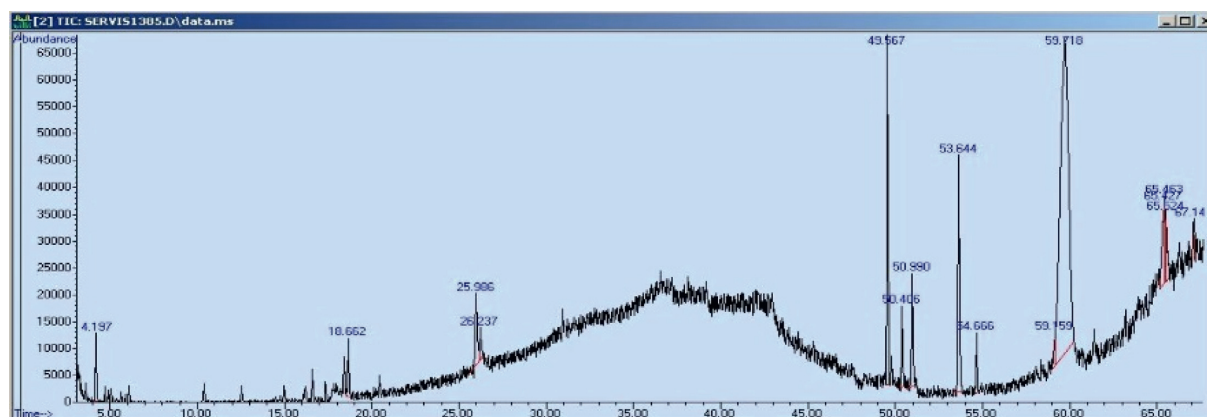


FIGURE 4: GC chromatograms of *D. bulbifera* methanol crude extract.

increased by 8.02%. Although the proportion of cells in the group of live cells decreased significantly by 28.43% in MDA-MB-231 after 72 h of treatment, the percentage of cells in early apoptosis increased by 29.37%. Similarly, at the necrotic level, the proportion of cells increased by 41.46% but decreased by 0.74% in the late apoptotic period. However, for the control culture at 72 h, the proportion of cells with early apoptosis decreased by 4.14%, the late apoptotic stage also decreased by 14.62%, while the apoptotic period increased by 1.08%, and a number of viable cells also decreased by 11.92%.

3.3. Gas Chromatography-Mass Spectroscopy (GC-MS) Analysis. GC/MS investigation was conducted on *D. bulbifera* methanol extract. The peaks in the chromatogram were integrated and matched with the database spectra of recognised compounds stored in the GC-MS libraries of Pfleger–Maurer–Weber–drug, National Institute of Standard and Technology (NIST), WILEY229.LIB, Flavour, Fragrance, Natural and Synthetic Compounds (FFNSC1.3.lib), and Pesticides Library for toxicology (PMW_tox2).

The result of *D. bulbifera* methanol extract revealed 50 peaks, with 45 compounds identified, representing 98.49% of the entire extract (Figure 4). The major among them were acetic acid (34.68%), n-hexadecanoic acid (14.89%), 1,2,3-propanetriol, 1-acetate (acetin) (7.28%), hexadecanoate <methyl-> (4.01%), 7-tetradecenal (Z)- (2.92%), glycerol alpha-monoacetate (2.80%), phytol (2.46%), octadecanoic acid (2.26%), cholesterol (2.10%), palmitic acid (1.35%), linolenate <methyl-> (1.32%), megastigmatrienone and 8-oxabicyclo-oct-5-en-2-ol, 1,4,4-trimethyl (1.28%) each, 1,2,3-propanetriol (1.23%), and 4,4,5,8-tetramethylchroman-2-ol (1.22%).

4. Discussion

Medicinal plants have been of great interest as a source of natural antioxidants used for health promotion such as anticancer properties. In this present study, the radical scavenging activities of *D. bulbifera* leaf extracts were quantified using DPPH, FRAP, and ABTS assays. All the

extracts demonstrated scavenging of stable DPPH and ABTS as well as reducing activity in FRAP assay. The secondary metabolites, namely, phenolics and flavonoids, present in this species make it potential for antioxidant activities by functioning as reducing agents [15, 19–22]. Numerous antioxidants that are described to have therapeutic potential such as vanillic acid, isovanillic acid, epicatechin, and myricetin are essential bioactive compounds in *D. bulbifera*. Tubers of *D. bulbifera* have displayed higher scavenging activity, reducing power, and ferrous ion chelating due to its high content of polyphenols such as oxalic acid, citric acid, malic acid, and succinic acid. Thus, the secondary metabolites might be the key role players behind its biological activities [23]. The methanolic extract of *D. bulbifera* has been reported to demonstrate DPPH radical-scavenging activity [24]. Studies of antioxidants from different platinum–palladium bimetallic nanoparticles (PtNPs) made from *D. bulbifera* indicates that PtNPs could inhibit radical DPPH by up to 30.16%, while palladium (PdNPs) showed up to 28.97% of the activity. Despite this, Ptfor–PdNPs reveal 38.49% scavenging when compared separately with PtNPs and PdNPs. In addition, for Pt–PdNPs (56.71%), a synergistic enhancement activity against radical superoxide was also observed as contrasted and only PtNPs (31.87%) or PdNPs (27.1%).

Another study which was conducted by Li et al. [25] revealed that *D. bulbifera* and other *Dioscorea* species possessed high antioxidant activity as in the following order *D. bulbifera*, followed by *D. collettii*, *D. nipponica*, and *D. opposita*. This indicates that members of the genus *Dioscorea* have therapeutic potential due to high antioxidants contents. Comparable study was carried out by Ghosh et al. [26]; copper nanoparticles (CuNPs) synthesised by *D. bulbifera* showed high radical scavenging activities that are slightly lesser when compared with ascorbic acid. Vitamin C also showed 14.11% of superoxide scavenging activity while CuNPs showed 48.39% of the activity.

The results of the present study indicated that the methanolic extract of *D. bulbifera* was found to be the most cytotoxic extract in both cell lines due to the presence of plentiful active compounds, namely, diosgenin in yam, the

edible tubers of *Dioscorea* spp. These results are compatible with the studies conducted by Li et al. [27] and Lee et al. [28]. Diosgenin has been shown to enhance metabolism of lipids, improve antioxidant activities, reduce glucose levels, and suppress inflammation [29]. Previous research presented that foods rich in diosgenin such as yam species (known as air potatoes) found to have a protective effect on myocardial I/R wound in rats due to apoptosis and necrosis and showed a cytotoxic effect on cancer cell lines [29–34].

It was reported by Nur and Nugroho [32] that *D. bulbifera* extracts demonstrated a cytotoxic effect on T47D cell lines. This research result indicated that the chloroform extract of the *D. bulbifera* leaves was stronger in inhibiting the growth of the cells than the methanol extract. Similarly, Ghosh and his colleagues [26] revealed that different nanoparticles Pt₀-PdNPs, PdNPs, and PtNPs made from *D. bulbifera* tuber extract exhibited the anti-proliferative effect where Pt-PdNPs had been the most cytotoxic nanoparticles at concentration 10 µg/mL. *In vivo* studies conducted on cytotoxic activities of the water extract, nonethyl acetate extract, ethyl acetate extract, ethanol extract, and diosbulbin B isolated from *D. bulbifera* showed that ethanol and ethyl acetate extracts reduced the lump weight in S180 and H22 tumour cells bearing mice while no such effect was observed in water and nonethyl acetate extracts [35].

In this study, cell cycle analysis was conducted in MCF-7 and MDA-MB-231 cell lines after treated with *D. bulbifera* methanol extract at IC₅₀ concentration for 24 h, 48 h, and 72 h. At 24 h, the extract induced S and G₂/M phases arrest in MCF-7 and G₀/G₁ and G₂/M phases arrest in MDA-MB-231. At 48 h, growth in a number of the treated cells was observed in the sub-G₁ phase in MCF-7 and sub-G₁ and G₀/G₁ in MDA-MB-231, while significant decreases in the number of cells were observed in G₀/G₁, S, and G₂/M in MCF-7 and S and G₂/M in MDA-MB-231. At 72 h, *D. bulbifera* methanol extracts arrested MCF-7 at the sub-G₁ phase and MDA-MB-231 at sub-G₁ and S phases.

The result of the present study was similar with Srivivasan et al. [36] where diosgenin led to cell growth in the G₁ phase, consisting of 72% of cells in G₁ at 24 h and 82% and 76% at 48 h and 72 h posttreatment, respectively, compared to untreated cells. Similar observation was found in diosgenin-treated MDA-MB-231 cells where there was aggregation of cells in the G₁ process occurred (82% at 24 h, 81% at 48 h, and 71% at 72 h). In addition, Moalic et al. [37] found that cells treated with diosgenin suppressed 1547 cell proliferation rate after 12 h along with a significant accumulation of cells in the G₁ phase which was increased at 24 h. Consequently, the fraction of S phase cells decreased at 12 h. A sub-G₁ population, typically associated with apoptotic cells, appeared at 48 h when compared to controls. According to a similar study conducted by Wang and Weller [38], HepG2 cells treated with different concentrations of protodioscin (bioactive component in *D. collettii*) for up to 24 h, accumulated mainly in the G₂/M phase in a dose-dependent and time-dependent manner with consequent increase in the sub-G₁ phase of cell cycle. Moreover, diosgenin isolated from *D. bulbifera* was reported to induce

S-phase arrest at a concentration of 13 µM in DU-145 prostate cancer cells. At 24 h of incubation phase, S arrest was relatively substantial, but at 48 h of incubation, there was no such effect, and arrest was not found to be important in MCF-7 compared to DU-145 [39].

In 2005, Liu et al. [40] reported that NB4 cells treated with diosgenin resulted in the enlargement of cell size, and arrest was made at G₂/M. Diosgenin increased the p53 levels in NB4 cells, indicating its importance in controlling cell cycle arrest. Flow cytometric sub-G₁ analysis showed that a dramatic hypodiploid number of K562 cells appeared after treatment with diosgenin for 48 h along with DNA fragmentation. Another research carried out by Hsu et al. [41] presented that treatment of squamous cell carcinoma-25 (SCC-25) with red mold *Dioscorea* cell cycle for 24 h caused arrest at the G₂/M phase. This effect was also connected to the repression of CDK1 and cyclin B1 mRNA levels, ensuring cell proliferation inhibition.

On comparative research by Liu and his colleagues [40], it was found that dioscin fundamentally hinders multiplication of C6 glioma cells at the S stage because of an expansion in a few cells in the stage following expanding dosages of dioscin increment in sub-G₁ arrest. Demonstrating that dioscin caused cell cycle capture at the S stage, G₀/G₁ stage decline in a few cells was observed. It has been recently detailed that dioscin restrained ROS creation, brought about DNA harm, and made cell cycle captured at the S stage, when contrasted and untreated, gathering the extent of the G₀/G₁ stage decreased from 61.38% to 35.43%, and S stage increased from 30.62% to 59.77% by 5.0 mg/ml of dioscin while the extents of G₂/M stage had small changes. These findings showed that dioscin was able to block human HEp-2 and TU212 cells at the S stage [42].

A study performed by Li et al. [27] showed that diosgenin treatment in focus subordinate caused increment of G₂/M stage cell population in Bel-7721, SMMC7721, and HepG2 HCC cells, suggesting that diosgenin could arrest the cell cycle in the G₂/M stage because of the way that extent of G₂/M stage cells with expanded in centralization of diosgenin. Lee and his colleagues [28] presented the anti-proliferative impacts of diosgenin from yam (*D. pseudojaponica*) on malignant growth (MCF-7, A 549, and Hep G2) and typical (HS68 and clone 9) cells. The outcome demonstrated that diosgenin from *D. pseudojaponica* hindered MCF-7 cells multiplication through G₀/G₁ arrest.

The importance of the apoptosis idea for oncology lies in its being a directed marvel subject to incitement and hindrance. Even though little was thought about how settled helpful operators for disease influence its introduction, it appears to be sensible to propose that more prominent comprehension of the procedures included may prompt the advancement of enhanced treatment regimens [43]. Apoptosis is a physiological process of cell death that is in charge of the destruction of cells in normal tissues; it likewise occurs in different pathologic settings. Morphologically, it involves quick build up and sprouting of the cells with the arrangement of membrane-enclosed apoptotic bodies containing well-preserved organelles which are phagocytosed

and digested by nearby resident cells [44]. Generally, apoptosis involved two central pathways; the first one is the stimulation of death receptors (DRs) in the tumour necrosis factor (TNF) superfamily, and the second one is the mitochondrial pathway initiated by Bcl-2 family proteins [45].

Several drugs that are used for cancer treatment have been appeared to cause apoptosis in quickly dividing normal cell numbers and tumours. Consequently, enhanced apoptosis is liable for a significant number of the antagonistic impacts of chemotherapy and tumour regression. Clear understanding of the procedures involved might lead to the improved treatment regimen. Hence, the realization of anticancer drugs that mediated the therapeutic impact by activating apoptosis is an additional necessary outcome [44].

Annexin-V-FITC/PI-flow cytometry analysis ascertained the induction of apoptosis by plant crude in both MCF-7 cells and MDA-MB-231. Distinctive biochemical features characterise apoptosis in the removal of damaged cells or tumour cells without causing irritation. The commencement of enzymatic and catabolic procedures in apoptosis in this manner empower cell morphological changes, for example, externalization of the plasma layer, phosphatidylserine (PS), shrinking of the cells, blebbing in cell membrane, condensation of chromatin, nuclear fragmentation, and apoptotic bodies formation [46–49].

5. Conclusion

In conclusion, the effort presented herein has proved that *D. bulbifera* methanol extract had resilient antiproliferative activity when compared with a standard drug. The antioxidant activities shown by methanol, ethyl acetate, and hexane extracts of the plant were significant compared with ascorbic acid, indicating the potential of the leaves of this species as natural antioxidants. Hence, antiproliferative activities demonstrated by leaf extracts authenticate the old style uses of this plant against various diseases of breast cancer inclusive.

Data Availability

The datasets generated and/or analysed during the current study are available from the first author upon request.

Conflicts of Interest

The authors declare that they have no conflicts of interest.

Acknowledgments

This research was financially supported by the Ministry of Higher Education of Malaysia (MOHE) under Fundamental Research Grant Scheme, FRGS, Vot No. 1560 (FRGS/1/2015/WAB01/UTHM/02/1) and also GPPS grant by UTHM (Vot No. U608). The authors would also like to thank Universiti Putra Malaysia (UPM) and Universiti Tun Hussein Onn Malaysia (UTHM) for providing infrastructural facilities to carry out this study.

References

- [1] M. F. Abu Bakar, M. Mohamad, A. Rahmat, S. A. Burr, and J. R. Fry, "Cytotoxicity, cell cycle arrest, and apoptosis in breast cancer cell lines exposed to an extract of the seed kernel of *Mangifera pajang* (bambangan)," *Food and Chemical Toxicology*, vol. 48, no. 6, pp. 1688–1697, 2010.
- [2] C. E. DeSantis, S. A. Fedewa, A. Goding Sauer, J. L. Kramer, R. A. Smith, and A. Jemal, "Breast cancer statistics, 2015: convergence of incidence rates between black and white women," *CA: A Cancer Journal for Clinicians*, vol. 66, no. 1, pp. 31–42, 2016.
- [3] R. A. Smith and C. E. DeSantis, "Breast Cancer Epidemiology," *Breast Imaging*, United State of America in Oxford University Press, New York, NY, USA, 2018.
- [4] N. A. Taib, M. Akmal, I. Mohamed, and C. H. Yip, "Improvement in survival of breast cancer patients—trends in survival over two time periods in a single institution in an Asia Pacific Country, Malaysia," *Asian Pacific Journal of Cancer Prevention*, vol. 12, pp. 345–349, 2011.
- [5] C. H. Yip, N. A. Taib, and I. Mohamed, "Epidemiology of breast cancer in Malaysia," *Asian Pacific Journal of Cancer Prevention*, vol. 7, no. 3, pp. 369–374, 2006.
- [6] C. E. DeSantis, J. Ma, A. Goding Sauer, L. A. Newman, and A. Jemal, "Breast cancer statistics, 2017, racial disparity in mortality by state," *CA: A Cancer Journal for Clinicians*, vol. 67, no. 6, pp. 439–448, 2017.
- [7] World Health Organization and Ś. O. Zdrovia, *WHO Guidelines on Good Agricultural and Collection Practices [GACP] for Medicinal Plants*, World Health Organization, Geneva, Switzerland, 2003.
- [8] H. Jaberian, K. Piri, and J. Nazari, "Phytochemical composition and in vitro antimicrobial and antioxidant activities of some medicinal plants," *Food Chemistry*, vol. 136, no. 1, pp. 237–244, 2013.
- [9] B. Saad, S. Dakwar, O. Said et al., "Evaluation of medicinal plant hepatotoxicity in co-cultures of hepatocytes and monocytes," *Evidence-Based Complementary and Alternative Medicine*, vol. 3, no. 1, pp. 93–98, 2006.
- [10] B. Bhunu, R. Mautsa, and S. Mukanganyama, "Inhibition of biofilm formation in *Mycobacterium smegmatis* by *Parinari curatellifolia* leaf extracts," *BMC Complementary and Alternative Medicine*, vol. 17, no. 1, p. 285, 2017.
- [11] M. F. A. Bakar, F. A. Karim, M. Suleiman, A. Isha, and A. Rahmat, "Phytochemical constituents, antioxidant and antiproliferative properties of a liverwort, *Lepidozia borneensis* Stephani from Mount Kinabalu, Sabah, Malaysia," *Evidence-based Complementary and Alternative Medicine*, vol. 2015, Article ID 936215, 9 pages, 2015.
- [12] S. H. A. Hassan and M. F. A. Bakar, "Antioxidative and anticholinesterase activity of *Cyphomandra betacea* fruit," *The Scientific World Journal*, vol. 2013, Article ID 278071, 7 pages, 2013.
- [13] N. J. S. Dusuki, M. F. Abu Bakar, F. I. Abu Bakar, N. A. Ismail, and M. I. Azman, "Proximate composition and antioxidant potential of selected tubers peel," *Food Research*, vol. 4, no. 1, pp. 121–126, 2019.
- [14] R. Re, N. Pellegrini, A. Proteggente, A. Pannala, M. Yang, and C. Rice-Evans, "Antioxidant activity applying an improved ABTS radical cation decolorization assay," *Free Radical Biology and Medicine*, vol. 26, no. 9–10, pp. 1231–1237, 1999.
- [15] A. Rahmat, S. Edrini, A. M. Akim, P. Ismail, T. Y. Y. Hin, and M. F. Abu Bakar, "Anticarcinogenic properties of *Strobilanthes crispus* extracts and its compounds in vitro,"

- International Journal of Cancer Research*, vol. 2, no. 1, pp. 47–49, 2006.
- [16] E. A. Queiroz, S. Puukila, R. Eichler et al., “Metformin induces apoptosis and cell cycle arrest mediated by oxidative stress, AMPK and FOXO3a in MCF-7 breast cancer cells,” *PLoS One*, vol. 9, no. 5, Article ID e98207, 2014.
- [17] Y. S. Tor, L. S. Yazan, J. B. Foo et al., “Induction of apoptosis through oxidative stress-related pathways in MCF-7, human breast cancer cells, by ethyl acetate extract of *Dillenia suffruticosa*,” *BMC Complementary and Alternative Medicine*, vol. 14, no. 1, p. 55, 2014.
- [18] M. Sermakkani and V. Thangapandian, “GC-MS analysis of *Cassia italica* leaf methanol extract,” *Asian Journal of Pharmaceutical and Clinical Research*, vol. 5, no. 2, pp. 90–94, 2012.
- [19] W. I. Wan-Ibrahim, K. Sidik, and U. R. Kuppusamy, “A high antioxidant level in edible plants is associated with genotoxic properties,” *Food Chemistry*, vol. 122, no. 4, pp. 1139–1144, 2010.
- [20] M. F. A. Bakar, F. A. Karim, and E. Perisamy, “Comparison of phytochemicals and antioxidant properties of different fruit parts of selected artocarpus species from Sabah, Malaysia,” *Sains Malaysiana*, vol. 44, no. 3, pp. 355–363, 2015.
- [21] B. Adaramola and A. Onigbinde, “Influence of extraction technique on the mineral content and antioxidant capacity of edible oil extracted from ginger rhizome,” *Chemistry International*, vol. 3, no. 1, pp. 1–7, 2017.
- [22] Z. Zhang, D. Lin, W. Li, H. Gao, Y. Peng, and J. Zheng, “Sensitive bromine-based screening of potential toxic furanoids in *Dioscorea bulbifera* L,” *Journal of Chromatography B*, vol. 1057, pp. 1–14, 2017.
- [23] M. E. Sharlina, W. Yaacob, A. M. Lazim et al., “Physico-chemical properties of starch from *Dioscorea pyriformis* tubers,” *Food Chemistry*, vol. 220, pp. 225–232, 2017.
- [24] S. Ghosh, P. More, A. Derle et al., “Diosgenin functionalized iron oxide nanoparticles as novel nanomaterial against breast cancer,” *Journal of Nanoscience and Nanotechnology*, vol. 15, no. 12, pp. 9464–9472, 2015a.
- [25] S. Li, S.-K. Li, R.-Y. Gan, F.-L. Song, L. Kuang, and H.-B. Li, “Antioxidant capacities and total phenolic contents of infusions from 223 medicinal plants,” *Industrial Crops and Products*, vol. 51, pp. 289–298, 2013.
- [26] S. Ghosh, P. More, R. Nitnavare et al., “Antidiabetic and antioxidant properties of copper nanoparticles synthesized by medicinal plant *Dioscorea bulbifera*,” *Journal of Nanomedicine & Nanotechnology*, vol. S6, 2015.
- [27] Y. Li, X. Wang, S. Cheng et al., “Diosgenin induces G2/M cell cycle arrest and apoptosis in human hepatocellular carcinoma cells,” *Oncology Reports*, vol. 33, no. 2, pp. 693–698, 2015.
- [28] Y.-C. Lee, J.-T. Lin, C.-K. Wang, C.-H. Chen, and D.-J. Yang, “Antiproliferative effects of fractions of furostanol and spirostanol glycosides from yam (*Dioscorea pseudojaponica* yamamoto) and diosgenin on cancer and normal cells and their apoptotic effects for mcf-7 cells,” *Journal of Food Biochemistry*, vol. 36, no. 1, pp. 75–85, 2012.
- [29] C.-T. Chen, Z.-H. Wang, C.-C. Hsu, H.-H. Lin, and J.-H. Chen, “In vivo protective effects of diosgenin against doxorubicin-induced cardiotoxicity,” *Nutrients*, vol. 7, no. 6, pp. 4938–4954, 2015.
- [30] S. Ghosh, R. Nitnavare, A. Dewle et al., “Novel platinum–palladium bimetallic nanoparticles synthesized by *Dioscorea bulbifera*: anticancer and antioxidant activities,” *International Journal of Nanomedicine*, vol. 10, pp. 7477–7490, 2015c.
- [31] J. Jagadeesan, N. Nandakumar, T. Rengarajan, and M. P. Balasubramanian, “Diosgenin, a steroidal saponin, exhibits anticancer activity by attenuating lipid peroxidation via enhancing antioxidant defense system during NMU-induced breast carcinoma,” *Journal of Environmental Pathology, Toxicology and Oncology*, vol. 31, no. 2, pp. 121–129, 2012.
- [32] R. M. Nur and L. H. Nugroho, “Cytotoxic activities of fractions from *Dioscorea bulbifera* L. chloroform and methanol extracts on T47D breast cancer cells,” *Pharmacognosy Journal*, vol. 10, no. 1, pp. 33–38, 2018.
- [33] S. Selim and S. Al Jaouni, “Anticancer and apoptotic effects on cell proliferation of diosgenin isolated from *Costus speciosus* (Koen.) Sm,” *BMC Complementary and Alternative Medicine*, vol. 15, no. 1, p. 301, 2015.
- [34] S.-L. Wang, B. Cai, C.-B. Cui, H.-W. Liu, C.-F. Wu, and X.-S. Yao, “Diosgenin-3-O- α -l-Rhamnopyranosyl-(1 \rightarrow 4)- β -d-glucopyranoside obtained as a new anticancer agent from *Dioscorea futschauensis* induces apoptosis on human colon carcinoma HCT-15 cells via mitochondria-controlled apoptotic pathway,” *Journal of Asian Natural Products Research*, vol. 6, no. 2, pp. 115–125, 2004.
- [35] J.-M. Wang, L.-L. Ji, C. J. Branford-White et al., “Antitumor activity of *Dioscorea bulbifera* L. rhizome in vivo,” *Fitoterapia*, vol. 83, no. 2, pp. 388–394, 2012.
- [36] S. Srinivasan, S. Koduru, R. Kumar, G. Venguswamy, N. Kyprianou, and C. Damodaran, “Diosgenin targets Akt-mediated prosurvival signaling in human breast cancer cells,” *International Journal of Cancer*, vol. 125, no. 4, pp. 961–967, 2009.
- [37] S. Moalic, B. Liagre, C. Corbière et al., “A plant steroid, diosgenin, induces apoptosis, cell cycle arrest and COX activity in osteosarcoma cells,” *FEBS Letters*, vol. 506, no. 3, pp. 225–230, 2001.
- [38] L. Wang and C. L. Weller, “Recent advances in extraction of nutraceuticals from plants,” *Trends in Food Science & Technology*, vol. 17, no. 6, pp. 300–312, 2006.
- [39] A. A. Hamid, T. Kaushal, R. Ashraf et al., “(2 β , 25R)-3 β -Hydroxy-spiro-5-en-7-iminoxy-heptanoic acid exhibits anti-prostate cancer activity through caspase pathway,” *Steroids*, vol. 119, pp. 43–52, 2017.
- [40] M.-J. Liu, Z. Wang, Y. Ju, R. N.-S. Wong, and Q.-Y. Wu, “Diosgenin induces cell cycle arrest and apoptosis in human leukemia K562 cells with the disruption of Ca²⁺ homeostasis,” *Cancer Chemotherapy and Pharmacology*, vol. 55, no. 1, pp. 79–90, 2005.
- [41] W.-H. Hsu, B.-H. Lee, and T.-M. Pan, “Red mold dioscorea-induced G2/M arrest and apoptosis in human oral cancer cells,” *Journal of the Science of Food and Agriculture*, vol. 90, no. 15, pp. 2709–2715, 2010.
- [42] L. Si, L. Zheng, L. Xu et al., “Dioscin suppresses human laryngeal cancer cells growth via induction of cell-cycle arrest and MAPK-mediated mitochondrial-derived apoptosis and inhibition of tumor invasion,” *European Journal of Pharmacology*, vol. 774, pp. 105–117, 2016.
- [43] I. M. Ghobrial, T. E. Witzig, and A. A. Adjei, “Targeting apoptosis pathways in cancer therapy,” *CA: A Cancer Journal for Clinicians*, vol. 55, no. 3, pp. 178–194, 2005.
- [44] J. F. R. Kerr, C. M. Winterford, and B. V. Harmon, “Apoptosis. Its significance in cancer and cancer therapy,” *Cancer*, vol. 73, no. 8, pp. 2013–2026, 1994.
- [45] E. H. Zhang, R. F. Wang, S. Z. Guo, and B. Liu, “An update on antitumor activity of naturally occurring chalcones,” *Evidence-based Complementary and Alternative Medicine*, vol. 2013, Article ID 815621, 22 pages, 2013.

- [46] U. Ziegler and P. Groscurth, "Morphological features of cell death," *Physiology*, vol. 19, no. 3, pp. 124–128, 2004.
- [47] F. Doonan and T. G. Cotter, "Morphological assessment of apoptosis," *Methods*, vol. 44, no. 3, pp. 200–204, 2008.
- [48] J. B. Foo, L. Saiful Yazan, Y. S. Tor et al., "Induction of cell cycle arrest and apoptosis by betulinic acid-rich fraction from *Dillenia suffruticosa* root in MCF-7 cells involved p53/p21 and mitochondrial signalling pathway," *Journal of Ethnopharmacology*, vol. 166, pp. 270–278, 2015.
- [49] G. Banfalvi, "Methods to detect apoptotic cell death," *Apoptosis*, vol. 22, no. 2, pp. 306–323, 2017.

Review Article

Aidi Injection as Adjuvant Drug Combined with Chemotherapy in Treatment of Breast Cancer: A Systematic Meta-Analysis

Chenhao Wu ¹, Yongjun Qi ², Juan Zhou ², Chen Yao ², Min Miao ²,
and Chen Cheng ²

¹Breast Surgery Department, Hainan Women and Children's Medical Center, No. 75 Longkun Nan Road, Hai Kou, Hainan Province, China

²Obstetrics and Gynecology Department, Jiangdu People's Hospital of Yangzhou, No. 9 Dongfang Hong Road, Jiangdu District, Yangzhou, Jiangsu Province, China

Correspondence should be addressed to Chen Cheng; chengsis996@163.com

Received 2 September 2020; Revised 2 November 2020; Accepted 11 December 2020; Published 8 January 2021

Academic Editor: Azis Saifudin

Copyright © 2021 Chenhao Wu et al. This is an open access article distributed under the Creative Commons Attribution License, which permits unrestricted use, distribution, and reproduction in any medium, provided the original work is properly cited.

Objective. To compare the efficacy and safety of combination of Aidi injection and chemotherapy and chemotherapy alone in treatment of breast cancer. **Methods.** The related control and randomized studies till August 1st, 2020, were retrieved in the database including PubMed, Embase, Cochrane Library, CNKI, CBM, Wang-Fang, and VIP. Primary outcomes were response rate (RR) and performance status (KPS) improvement rate; secondary outcomes were rate of adverse drug reactions (ADR) including myelosuppression, digestive tract reaction, liver dysfunction, and cardiac toxicity. Review Manager 5.3 was used in the present analysis. **Results.** In total, 20 studies (18 articles) were included in the present analysis. RR (OR 1.76 (1.32, 2.35); $p = 0.0001$) and KPS improvement rate (OR: 2.68 (1.34, 6.46); $p = 0.007$) in Aidi injection plus chemotherapy group were significantly higher than those of chemotherapy alone group. Addition of Aidi injection significantly reduced the rate of myelosuppression, digestive tract reaction, leukocyte decrease, II-IV cardiac function abnormality, atrial dysrhythmia, ventricular arrhythmia, ST segment T wave inversion, and abnormal ECG (all $p < 0.05$). **Conclusion.** Aidi injection could increase the efficacy of chemotherapy, could reduce myelosuppression, digestive tract reaction, and cardiac toxicity induced by chemotherapy, and did not lead to additional toxicity and side effect. Therefore, it is an anticancer drug with good efficacy and low toxicity, worth further popularization.

1. Introduction

Breast cancer is a common cancer type and is the fifth most common cause of cancer death [1]. In 2012, there were 1.67 million newly diagnosed breast cancer cases, comprising 25% of all sorts of cancers among females [2]. In China, the number of breast cancer cases increased dramatically. The number of newly diagnosed breast cancer cases in 2000 was 121,2693, and this number reached 168,013 in 2005 [3], and 278900 in 2014 [4]. The main options in breast cancer treatment included surgery, chemotherapy, and radiation. Among them, chemotherapy has been a widely accepted and applied treatment method. However, chemotherapy usually temporarily relieves symptoms, lengthens survival, but

occasionally cures the disease, so its treatment efficacy is still to be improved [5]. On the other hand, the related toxicity greatly affected quality of life of patients. Therefore, much work has been made to find alternative treatment methods. In recent years, Traditional Chinese Medicine (TCM) received much attention in the field of cancer treatment due to its capability of efficacy improvement and toxicity reduction [6].

Aidi injection was one of the Chinese Patent Medicines with anticancer activity included in Catalogue of Drugs for Basic National Medical Insurance and Countermeasures of China [7]. It is extracted from Chinese herbal medicines of catharides, ginseng, astragalus, and acanthopanax senticosus. In opinion of TCM, Aidi

injection has the ability of clearing away heat and toxin, removing stasis, and dispersing accumulation. Cantharidin is the major component for toxicity of cantharides and also is an effective anticancer component. It can inhibit cancer cells without decreasing the pericirculation leucocytes level and has obvious immune-suppression effect, which is quite outstanding for current anticancer drugs [8]. Ginseng, astragalus, and acanthopanax senticosus have showed anticancer capability of inducing apoptosis of cancer cells, inhibiting proliferation of cancer cells, inhibiting cancerous angiogenesis, and so on, and they usually also have features of low toxicity, low drug resistance, and obvious immune-improvement capability. In China, Aidi injection was extensively used in the treatment of primary liver cancer [9], lung cancer [10], gastric cancer [11], colon cancer [12], lymphadenoma [13], gynecology cancer [14], and so on. In clinical practice, Aidi injection is usually used as adjuvant drug in chemotherapy in cancer treatment to decrease toxicity of chemotherapy and improve quality of life [15]. There have been a number of clinical studies investigating combination of Aidi injection with chemotherapy in cancer treatment. In the studies among breast cancer patients, addition of Aidi injection had showed certain benefits. Therefore, we performed this meta-analysis to systematically review and evaluate the efficacy and safety of Aidi injection as adjuvant drug in chemotherapy in the treatment of breast cancer.

2. Materials and Methods

2.1. Inclusion and Exclusion Criteria. The inclusion criteria were as follows: (1) types of studies: randomized controlled trials; retrospective or observational studies were not eligible; (2) types of participants: pathologically or cytologically diagnosed with breast cancer; Karnofsky performance status score ≥ 60 ; (3) intervention: patients in control group received pure chemotherapy and the patients in the experimental group received chemotherapy plus Aidi injection; (4) outcome measurements: at least one of the three measurements was evaluated: short-term response rate for solid tumor, performance status improvement rate, and adverse events rate.

Exclusion criteria were as follows: (1) other Traditional Chinese Medicines were used during study period; (2) other cancer treatments such as radiation therapy or immunological or target treatment were used during study period.

2.2. Retrieval Strategy. We searched the related studies till August 1st, 2020, using the database including PubMed, Cochrane library, Embase, and Chinese medical databases: CNKI, CBM, Wang-Fang, and VIP. The retrieval terms were "Aidi injection" or "Aidi", AND "breast cancer", OR "breast tumor" OR "breast carcinoma" in retrieval using PubMed, Cochrane library, and Embase. These terms in English and Chinese both were used for CNKI, CBM, Wang-Fang, and VIP. The references of important articles were also searched.

2.3. Literature Screening, Data Extraction, and Quality Assessment. Two independent reviewers (WCH and QY) made the literature screening and data extraction, respectively. For each literature screening, duplication, title, abstract, and main text were examined. The screening results by the two reviewers were compared and decided through discussion. When agreement could not be made with discussion, a third independent reviewer (YC) was invited to make final decision. The extracted information included author name, publication year, sample size, TNM stage, intervention methods, treatment cycles, and outcome measurements.

Quality assessments were made with Cochrane risk of bias tool as suggested by Cochrane handbook for systematic reviews of interventions. The assessed measurements include random sequence generation, allocation concealment, blinding of participants and personnel, blinding of outcome assessment, incomplete outcome data, and selective reporting. Each measurement was rated with low, unclear, and high bias risk.

2.4. Outcome Measurements. Short-term treatment efficacy was determined according to the modified Response Evaluation Criteria in Solid Tumours 1.1 (RECIST 1.1) [16]. Response rate = number of patients with complete response + number of patients with partial response rate / total patient number. Performance status was assessed with Karnofsky Performance Status (KPS) score. After treatment, increase of KPS score from baseline ≥ 10 was considered as KPS improvement; decrease of KPS score from baseline ≥ 10 was considered as KPS reduction; KPS score above or below < 10 was considered as stable KPS. KPS improvement rate = number of patients with KPS improvement / total patient number. The toxicity and adverse events were assessed as I°, II°, III°, and IV°, according to the common toxicity criteria of chemotherapy drugs drafted by WHO (1991); cardiac function abnormality was also assessed according to the WHO anticancer drug toxicity criteria. Grade 0 indicates that heart rate, rhythm, and function are normal; I° indicates no symptoms of cardiac insufficiency and may present abnormal cardiac signs; grade II° indicates transient cardiac insufficiency, no treatment needed; grade III° indicates presenting symptoms of cardiac function insufficiency which are manageable; IV° indicates presenting symptoms of cardiac function insufficiency which are unmanageable.

2.5. Statistical Analysis. Review Manager 5.3 was used for meta-analysis. Odds ratios (OR) for categorial or continuous variables of experimental group (Aidi injection plus chemotherapy) and control group (chemotherapy alone) were calculated and compared. $P < 0.05$ was considered to be statistically significant. The heterogeneity between the included studies was tested with the standard Chi-squared (I^2Q) test. If $p < 0.1$, $I^2 < 50\%$, fixed effect model was used for analysis; if $p < 0.1$, $I^2 > 50\%$, random effect model was used. Subgroup analyses according to number of cycles (≤ 3 vs > 3) were made to identify the heterogeneity source. Funnel plot

was used for estimation of publication bias. If the number of included studies was less than 10, publication bias was not assessed.

3. Results

3.1. Literature Screening Results and Characteristics of the Included Studies. Following the search strategy described above, 96 articles were retrieved. Among them, 23 were retrieved from CNKI, 26 were retrieved from CBM, 22 were retrieved from VIP, 24 were retrieved from Wan-Fang, 1 was retrieved from PubMed, 0 were retrieved from EMBASE, and 0 were retrieved from Cochrane library. After duplicate checking, 26 articles were obtained. After title and abstract examination, 3 articles were excluded. After main-text examination, 5 articles were excluded: 1 study did not evaluate the measurements of response rate or performance status improvement rate; 1 study did not provide TNM stage of included patients; 1 study was single arm study rather than randomized controlled study; 1 study was performed among patients with cancer other than breast cancer; 1 study used TCMs other than Aidi injection. Finally, 18 articles (20 studies) were included in the present meta-analysis. The flowchart of article selection process is shown as Figure 1.

The characteristics of the 20 included studies are shown in Table 1 [17–34]. All the 20 studies were published in Chinese journals. The study performed by Gao et al. compared Aidi plus chemotherapy and chemotherapy alone, respectively, among treatment naïve patients and patients with drug resistance for anthracycline and paclitaxel, so the two comparisons were both included and regarded as two studies: Gao QH 2013a and Gao QH 2013b [21]. The study performed by Wang GD et al. compared low-dose Aidi plus chemotherapy and high-dose Aidi plus chemotherapy and chemotherapy alone, so two comparisons (low dose vs control; high dose vs control) were included and regarded as two studies: Wang GD 2012a and Wang GD 2012b [30]. The patients in four studies performed by Chen WM et al. [17], Han et al. [22], Wang GD et al. [30], and Jin et al. [23] received chemotherapy after surgery. The other studies out of the four studies did not administrate surgery. The chemotherapies were regular regimen but varied among the studies. The dosage of Aidi injection ranged from 50 ml to 100 ml.

3.2. Quality Assessment Result. All the included studies were randomized controlled studies. The baseline characteristics of patients were well balanced between the experimental group and control group. Five studies reported the randomized sequence generation methods [19, 20, 25, 29, 32]; 5 studies had evaluated long-term efficacy so they reported follow-up [20, 27, 29, 31, 34] and the rest studies did not as they only evaluated short-term efficacy; 6 studies evaluated adverse events rate and reported multiple adverse events but did not provide overall data of all adverse events that

occurred [20, 21, 24, 26, 31] and the rest of studies had made complete reports of all or certain adverse events; 1 study reported drop-out rate [22]. However, in all the studies, the blindness of allocation and assessment was not described, so they were rated as unclear; the blindness of participants and personals was not described either and was rated as high risk based on the general practice in hospital of China (Figures 2 and 3).

3.3. Outcomes

3.3.1. Response Rate. 15 studies were included in the analysis of response rate, which included 970 patients, 508 in Aidi plus chemotherapy group and 462 in chemotherapy alone group (Figure 4). The heterogeneity between the included studies was not significant ($p = 0.92$; $I^2 = 0\%$), so fixed-effect model was used. The analysis results indicated that the pooled response rate in Aidi plus chemotherapy group was significantly higher than that of the chemotherapy alone group (OR 1.76 (1.32, 2.35); $p = 0.0001$). Funnel plot was adopted to estimate the publication bias and the result suggested no obvious publication bias (Figure 5).

3.3.2. Performance Status Improvement Rate. Eight studies were included in the analysis of performance status improvement rate, which included 700 patients, 345 in Aidi plus chemotherapy group and 355 in chemotherapy alone group (Figure 6). Heterogeneity between the included studies was significant ($p = 0.03$, $I^2 = 54\%$), so random-effects model was used. The analysis result showed that performance status improvement rate in the patients receiving Aidi plus chemotherapy was significantly higher than that in the patients receiving chemotherapy alone (OR: 2.68 (1.34, 6.46); $p = 0.007$).

However, in subgroup analysis in respect to cycle numbers, the difference of performance status improvement rate was significant in the subgroup in which chemotherapy cycles were >3 (OR: 12.42 (4.56, 33.85); $p < 0.00001$), and heterogeneity was not significant ($p = 0.95$, $I^2 = 0\%$) (Figure 7); the performance status improvement rate was not significantly different in the subgroup in which chemotherapy cycles were ≤ 3 (OR: 1.66 (0.95, 2.89); $p = 0.07$), and the heterogeneity was not significant between the studies ($p = 0.51$, $I^2 = 0\%$) (Figure 7). Furthermore, the heterogeneity between the two subgroups was significant ($p = 0.0006$; $I^2 = 91.6\%$) (Figure 7), indicating that chemotherapy cycles >3 or ≤ 3 were a source of heterogeneity in the total analysis.

Again, subgroup analysis regarding Aidi injection of high (100 mL) or low (50 mL) dose was also performed (Figure 8) to determine the source of heterogeneity. In the subgroup of low-dose Aidi, heterogeneity was not significant ($p = 0.38$, $I^2 = 1\%$). The pooled performance improvement rate was significantly higher in low-dose Aidi plus

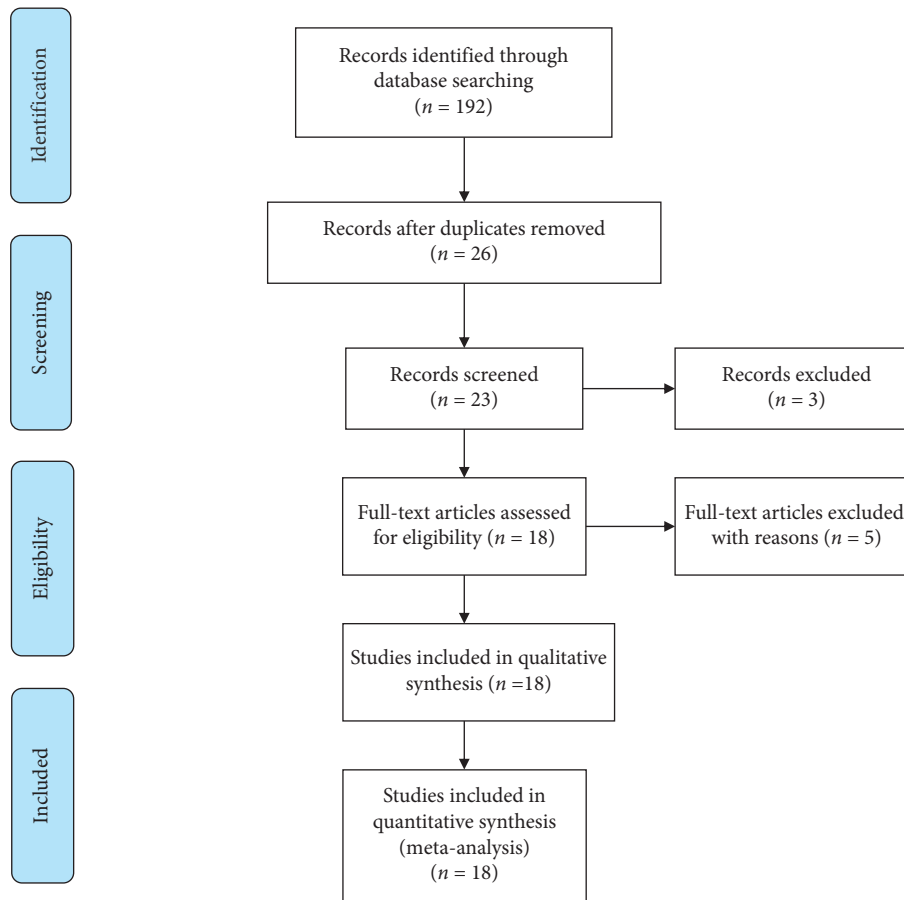


FIGURE 1: Flowchart of the studies selection process.

chemotherapy group [OR: 2.11 (1.12, 3.99); $p = 0.02$]. In the subgroup of high-dose Aidi, the heterogeneity between studies was significant ($p = 0.01$, $I^2 = 73\%$); the pooled performance improvement rate was not significantly different in this subgroup analysis [OR: 3.48 (0.70, 17.36); $p = 0.13$] (Figure 8). However, the difference between the subgroups was not significant ($p = 0.57$, $I^2 = 0\%$).

3.4. Adverse Drug Events Rate

Myelosuppression Rate. Seven studies were included in the analysis for myelosuppression rate, which included 486 patients, 246 in Aidi injection plus chemotherapy group and 240 in chemotherapy group (Figure 9). The heterogeneity between the included studies was not significant ($p = 0.8$, $I^2 = 0\%$). The analysis result indicated that the pooled myelosuppression rate of Aidi plus chemotherapy group was significantly lower than that of the chemotherapy alone group (OR: 0.34 (0.20, 0.55); $p < 0.0001$).

Furthermore, 4 studies were included in the analysis for III-IV grade myelosuppression rate. Heterogeneity was not significant ($p = 0.25\%$, $I^2 = 28\%$) (Table 2). The pooled III-IV grade myelosuppression rate was significantly lower in Aidi plus chemotherapy group (OR: 0.43 (0.25, 0.76); $p = 0.03$) (Table 2).

Digestive Tract Reaction Rate. Eight studies were included in the analysis for digestive tract reaction rate, which included 623 patients (Figure 10). The heterogeneity between studies was not significant ($p = 0.72$, $I^2 = 0\%$). The analysis result indicated that the pooled digestive tract reaction rate was significantly lower in Aidi plus chemotherapy group, when compared with chemotherapy alone group (OR: 0.50 (0.17, 1.47); $p = 0.001$).

The analysis for III-IV grade digestive tract reaction rate included 4 studies (Table 2). The heterogeneity was shown between studies ($p = 0.06$; $I^2 = 59\%$). The III-IV grade digestive tract reaction rate was significantly lower in Aidi plus chemotherapy group (OR: 0.42 (0.22, 0.80); $p = 0.008$).

Other ADRs. The other adverse drug reaction rates were also compared, as shown in Table 2. The pooled total and II-IV grade leukocyte decrease rate were shown to be significantly lower in Aidi plus chemotherapy group (both $p < 0.05$). The adverse events rates related to cardiac toxicity, including II-IV cardiac function abnormality, atrial dysrhythmia, ventricular arrhythmia, ST segment T wave inversion, and abnormal ECG, were significantly lower in Aidi plus chemotherapy group (all $p < 0.05$). The total and III-IV grade liver dysfunction rate, total and III-IV hair loss rate, phlebitis rate, and atrioventricular block rate were not significantly different between the two groups (all $p < 0.05$).

TABLE 1: Characteristics of included studies.

First author	Year	No. E/C	Age	Stage	Surgery	Intervention		Experimental group
						Control group	Experimental group	
Eisenhauer [16]	2016	40/39	46.73 ± 14.29/ 45.98 ± 15.78	III-IVa	Yes	CEF (6 cycles): CTX 600 mg/m ² , d1, 8; EPI 100 mg/m ² , d1; 5-FU 500 mg/m ² , d1, 8; 21d	CT + Aidi 100 ml, qd, d1-8	
Chen [17]	2012	30/26	42.5/42.5	II-III	No	AC-T (3 courses): ADM 60 mg/m ² , d1 + CTX 600 mg/m ² , d1; 14d, for 4 cycles; followed by TAX 175 mg/m ² , d1, 14d, 4 cycles	CT + Aidi 100 ml, qd, 4d	
Chen [18]	2010	28/20	36.2/37.5	I-IIIa	No	CTF (3 cycles): CTX 400–600 mg/m ² , 5-Fu 400–600 mg/m ² , d1, 8; THP 40–50 mg/m ² , d1; 21d	CT + Aidi 100 ml, qd, 10d	
Fu [19]	2007	44/44	42/48	IV	No	NP (above 2 cycles): NVB 25 mg/m ² , d1, 8; DDP 30 mg/m ² , d2-4; 28d	CT + Aidi 50 ml, qd, d1-15	
Dang [20]	2014	64/64	46.7 ± 20.3	Not clear	Yes	CEF (6 cycles): CTX 600 mg/m ² , d1, 8; EPI 100 mg/m ² , d1; 5-FU 500 mg/m ² , d1, 8; 21d	CT + Aidi 100 ml, qd, d1-8	
Gao [21]	2013a	32/32	33–69	III-IV	No	TAC (at least 2 cycles): TXT 75 mg/m ² , d1; EPI 90 mg/m ² , d1; CTX 500 mg/m ² , d1; 21d	CT + Aidi 80 ml, qd, d1-15	
Gao [21]	2013b	16/16	33–69	III-IV	No	GEM + CAPE (at least 2 cycles): GEM 1 g/m ² , d1, d8; CAPE 1 g/m ² , bid, d1-14; 21d	CT + Aidi 80 ml, qd, d1-15	
Han [22]	2016	60/60	53.9 ± 11.5/ 54.2 ± 12.1	Not clear	Yes	CAF/CEF/TAC (6 cycles)	CT + Aidi 100 ml, qd	
Jin [23]	2005	50/50	45	II-III	No	CEF (2 cycles): CTX 600 mg/m ² , d1, 8; EPI 75 mg/m ² , d1; 5-FUDR 750 mg, d1, 8; 21d	CT + Aidi 100 ml, qd, d1-15	
Liu [24]	2006	32/20	46.2 ± 2.6/44.5 ± 3.2	I-IIIa	No	CEF (3 cycles): CTX 400–600 mg/m ² , 5-FU 400–600 mg/m ² , d1, 8; EPI 75–90 mg/m ² , d1; 21d	CT + Aidi 100 ml, qd, 10d	
Li [25]	2012	24/28	57.2 ± 3.5/55.7 ± 3.4	IIb-III	No	TAC (2 cycles): TXT 75 mg/m ² , d1; EPI 100 mg/m ² , d1; CTX 600 mg/m ² , d1; 21d	CT + Aidi 80 ml, qd, d1-15	
Lu [26]	2005	60/40	39.5 (20–68)	II-III	No	CMF (3 cycles): CTX 600 mg/m ² , d1, 8; MTX 30 mg/m ² , d1; 5Fu 500 mg/m ² , d1, 8; 21d	CT + Aidi 80 ml, qd, d1-15	
Ren [27]	2013	26/22	42.3/42.2	II-III	No	TC-P (3 courses): THP 60 mg/m ² , d1, CTX 600 mg/m ² d1, 14 d/cycle, for 4 cycles; followed by TAX 175 mg/m ² , d1, 14d, 4 cycles	CT + Aidi 100 ml qd, 4d	
Shen [28]	2006	48/48	51/50	IV	No	CAF or TA (2 cycles): CAF: CTX 600 mg/m ² , d1, THP 40 mg/m ² , d1; 5-FU 750 mg, d1, d8; 21d. TA: Taxol 135 mg/m ² , d1; THP 40 mg/m ² , d1; 21d	CT + Aidi 50 ml d1-15	
Song [29]	2012a	38/41	53.28 ± 11.32/ 53.02 ± 11.37	Not clear	Yes	CAF/CEF/AC/AT/TAC (6 cycles)	CT + Aidi 50 ml, qd	
Song [29]	2012b	32/41	52.67 ± 11.85/ 53.02 ± 11.37	Not clear	Yes	CAF/CEF/AC/AT/TAC (6 cycles)	CT + Aidi 100 ml, qd	
Wang [30]	2016	21/21	46.5 (33–67)	IV	No	NP (at least 2 cycles): NVB 25 mg/m ² , d1, d8; DDP 30 mg/m ² , d2, 4; 28d	CT + Aidi 50 ml, qd, d1-15	
Wang [31]	2004	31/28	53.5 (31–70)/54.2 (32–69)	IV	No	NT (at least 2 cycles): NVB 25 mg/m ² , d1, 8; THP 40–50 mg/m ² , d1; 21	CT + Aidi 50 mg, qd, d1-15; 21d	
Yang [32]	2005	30/30	48.4 (31–67)/47.6 (30–65)	III-IV	No	CAF (2 cycles): CTX 600 mg/m ² , d1, 8; ADM 50 mg/m ² , d1; 5-FU 500 mg/m ² , d1, 8; 21d	CT + Aidi 100 ml, qd, d1-10	
Yang [33]	2016	36/37	53 (41–67)/54 (38–69)	III-IV	No	TXT + CAPE (6 cycles): TXT 75 mg/m ² , d1; CAPE 900 mg/m ² , bid, d1-14; 21d	CT + Aidi 100 ml, d1-14	

CT = chemotherapy; E/C = experimental group/control group; 5-FU = 5-fluorouracil; TAX = paclitaxel; NVB = vinorelbine; DDP = cisplatin; ADM = adriamycin; CTX = cyclophosphamide; EPI = epirubicin; ADM = adriamycin; THP = pirarubicin; TXT = docetaxel; 5-FUDR = floxuridin; GEM = gemcitabine; CAPE = capecitabine. * Gao Qinghua 2013a were among the treatment-native patients; Gao Qinghua 2013b were among the patients failed in treatment with anthracycline and paclitaxel.

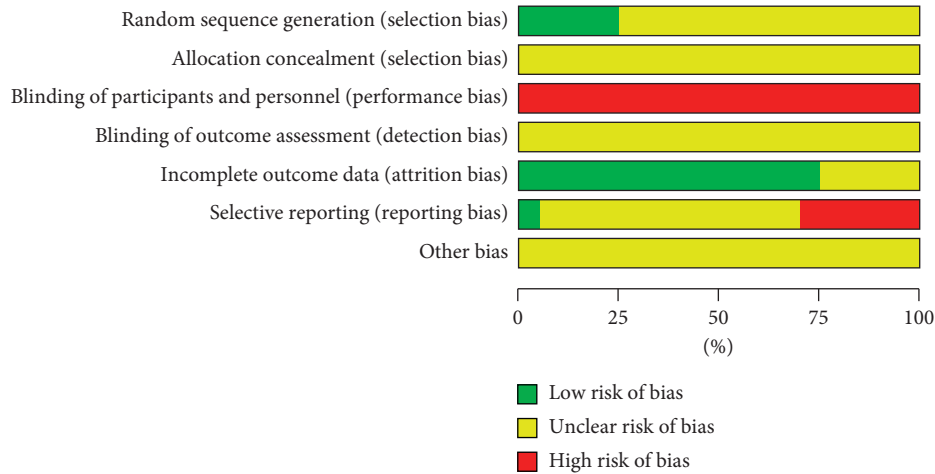


FIGURE 2: Risk of bias graph of included studies.

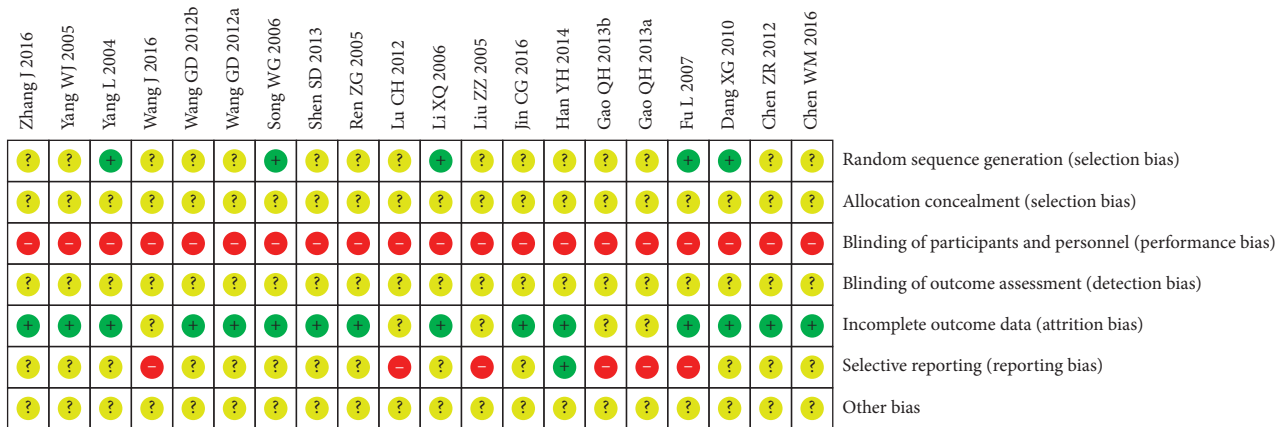


FIGURE 3: Summary of risk bias of included studies.

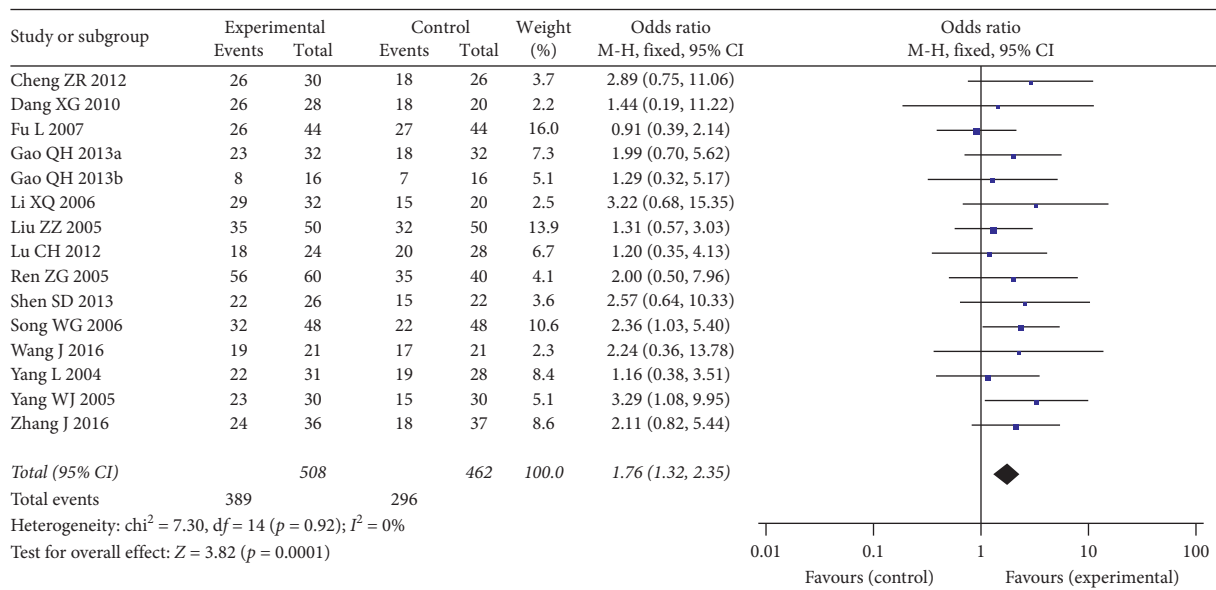


FIGURE 4: Forest plot of response rate in breast cancer patients receiving chemotherapy alone and chemotherapy plus Aidi injection.

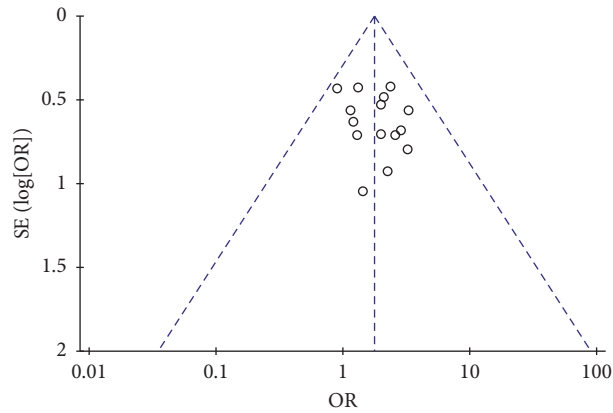


FIGURE 5: Funnel plot of response rate for the publication bias.

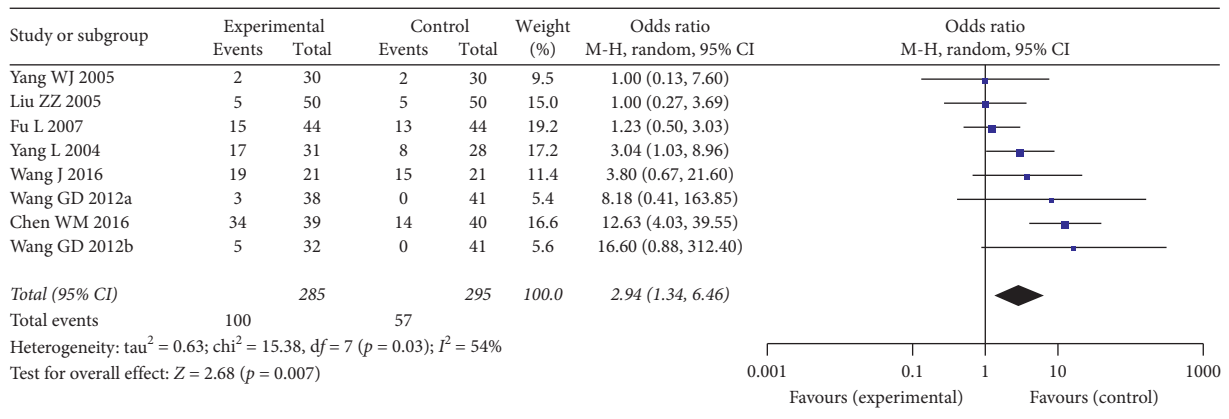


FIGURE 6: Forest plot of performance status improvement rate in patients receiving chemotherapy alone and chemotherapy plus Aidi injection.

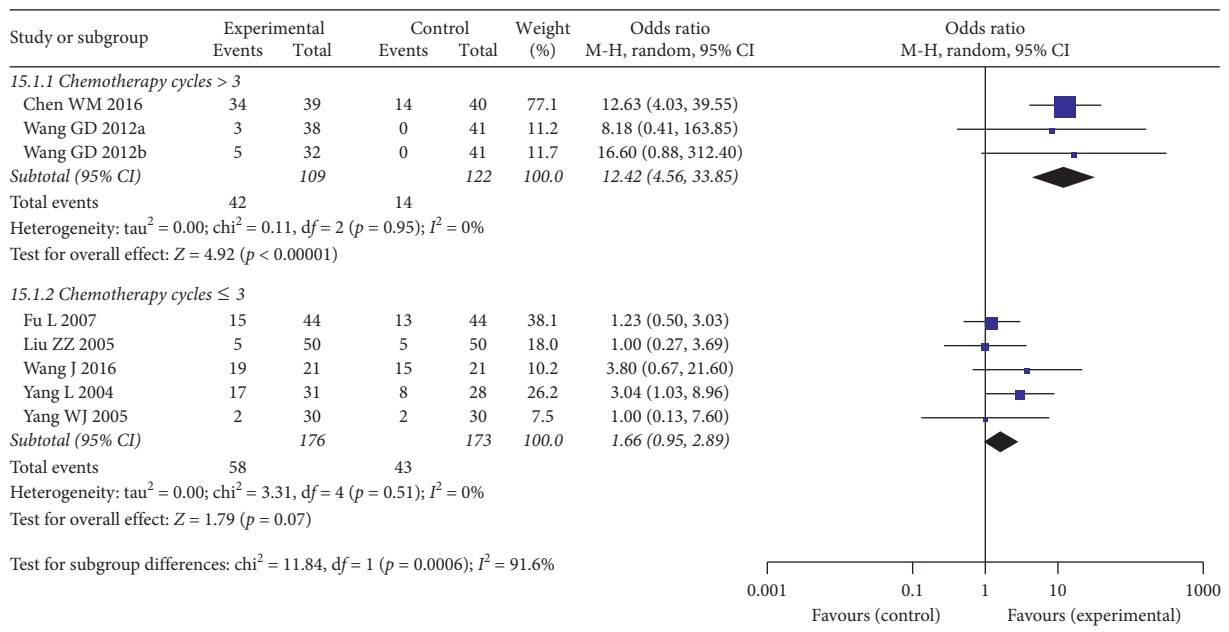


FIGURE 7: Forest plot of performance status in subgroup analysis regarding chemotherapy cycles.

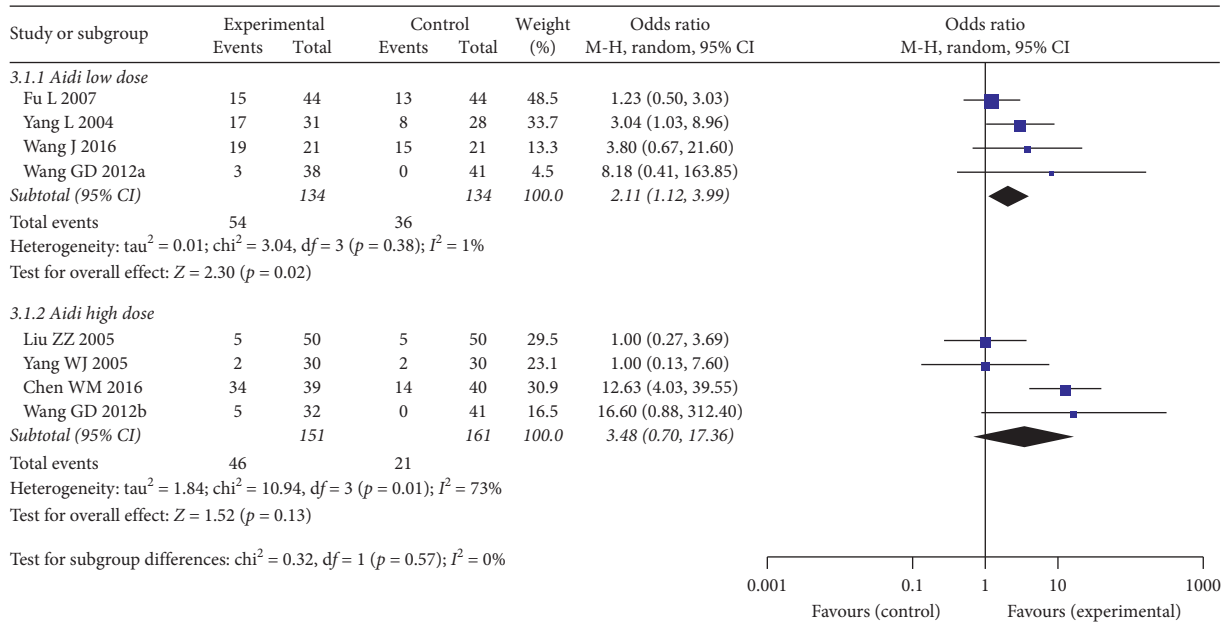


FIGURE 8: Forest plot of performance status in subgroup analysis regarding Aidi injection high or low dose.

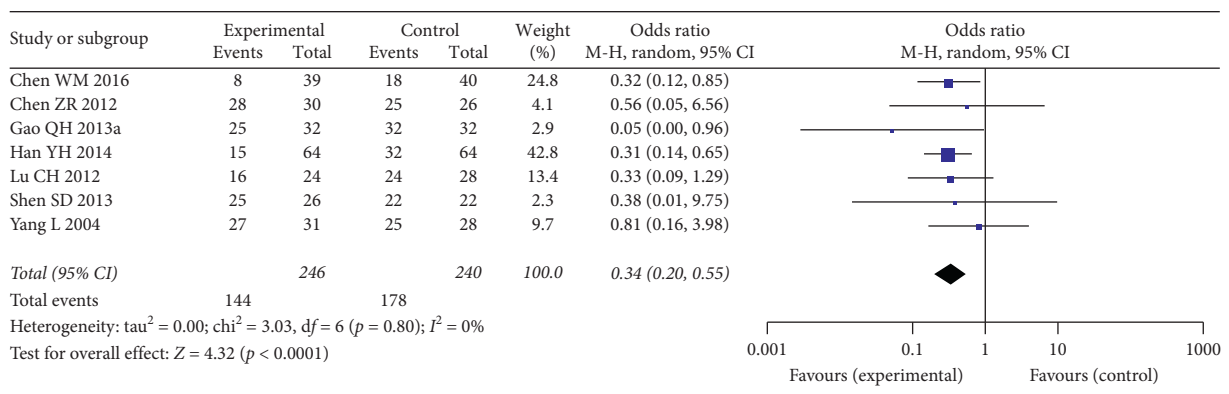


FIGURE 9: Forest plot of myelosuppression rate among patients receiving chemotherapy alone and chemotherapy plus Aidi injection.

TABLE 2: Summary of comparisons of ADRs among the patients receiving chemotherapy alone and chemotherapy plus Aidi injection.

ADRs	Number of studies	Number of patients	Heterogeneity (p/I ²)	Model	OR	p
Myelosuppression	7	486	0.80/0%	Fixed	0.34 [0.200, 55]	<0.0001
III-IV myelosuppression	4	259	0.25/28%	Fixed	0.43 [0.25, 0.76]	0.003
Digestive tract reaction	8	623	0.72/0%	Fixed	0.50 [0.33, 0.76]	0.001
III-IV digestive tract reaction	4	269	0.06/59%	Random	0.42 [0.22, 0.80]	0.008
Liver dysfunction	5	432	0.80/0%	Fixed	0.90 [0.48, 1.68]	0.74
III-IV liver dysfunction	1	96	NA	NA	0.48 [0.08, 2.74]	0.41
Leukocyte decrease	3	152	0.41/0%	Fixed	0.43 [0.19, 0.97]	0.04
III-IV leukocyte decrease	4	313	0.03/67%	Random	0.40 [0.24, 0.66]	0.0003
Hair loss	1	88	NA	NA	0.78 [0.30, 2.07]	0.62
III-IV hair loss	1	96	NA	NA	0.71 [0.23, 2.24]	0.56
Phlebitis	2	132	0.61/0%	Fixed	0.89 [0.40, 1.96]	0.77
II-IV cardiac function abnormality	4	320	0.78/0%	Fixed	0.16 [0.13, 0.38]	<0.00001
Atrial dysrhythmia	3	272	0.56/0%	Fixed	0.24 [0.13, 0.45]	<0.00001
Ventricular arrhythmia	3	272	0.96/0%	Fixed	0.08 [0.01, 0.42]	0.003
Atrioventricular block	3	272	0.94/0%	Fixed	0.29 [0.05, 1.80]	0.18
ST segment T wave inversion	3	272	0.91/0%	Fixed	0.25 [0.15, 0.42]	<0.00001
Abnormal ECG	3	272	0.80/0%	Fixed	0.17 [0.06, 0.47]	<0.00001

NA = not applicable; ADRs = adverse drug reactions; OR = odds ratio; ECG = electrocardiogram.

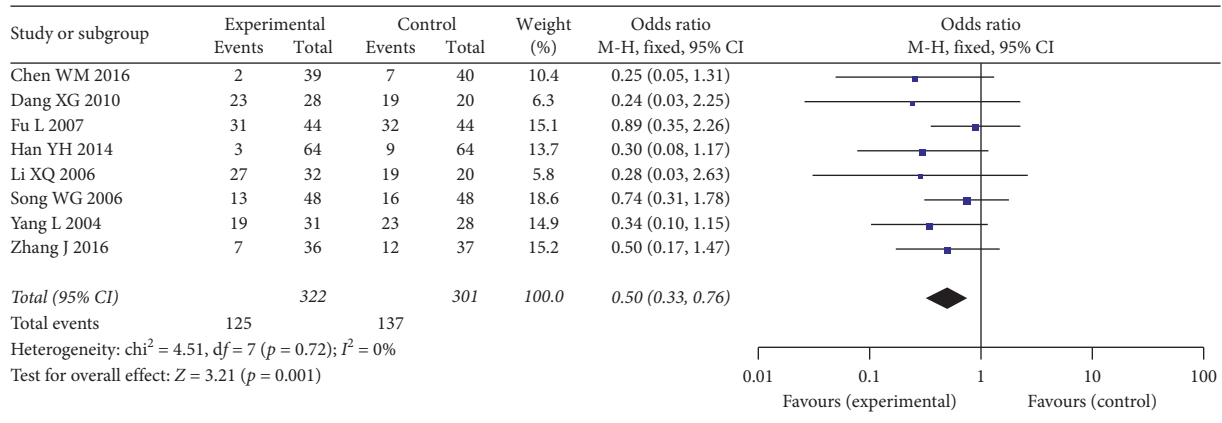


FIGURE 10: Forest plot of digestive tract reaction rate among patients.

4. Discussion

Side effects in the treatment of breast cancer seriously affect the quality of life of patients and make development of alternative treatment necessary. In hospital of China, Chinese Patent Medicine Aidi injection was widely used as adjuvant drug in chemotherapy for breast cancer. We performed this meta-analysis to compare the efficacy and safety of Aidi injection plus chemotherapy and chemotherapy alone in treatment of breast cancer.

Our analysis demonstrated that addition of Aidi to chemotherapy significantly improved response rate and performance status improvement rate; Aidi plus chemotherapy group significantly decreased the rate of all grade and III-IV grade myelosuppression, the rate of all grade and III-IV grade digestive tract reaction, the rate of all grade and II-IV grade leukocyte decrease, and the rate of most of cardiac toxicity related adverse events. In regards of the other adverse drug reactions, the ADR rate was slightly reduced in Aidi plus chemotherapy group but showed no significance.

The heterogeneity in the analysis for response rate, myelosuppression rate, and digestive tract reaction rate was not significant but was significant in the analysis for performance status improvement rate. In order to identify source of heterogeneity, we made subgroup analysis according to chemotherapy cycle number and Aidi of high or low dosage, respectively. The subgroup analysis demonstrated that the chemotherapy cycle number, namely, the treatment duration of Aidi, was a source of heterogeneity, since the difference between two subgroup analyses was significant. We speculate that TCM usually takes a longer action time; on the other hand, longer Aidi usage may increase its effect compared with shorter usage. The two aspects together might explain the increased KPS improvement rate in subgroup with chemotherapy cycle number ≥ 3 .

The high dose Aidi might increase the KPS improvement rate since OR in high-dose subgroup analysis was higher than OR in low-dose subgroup analysis, but the difference between the high-dose and low-dose subgroup was not significant. Therefore, the dosage of Aidi might not be the

source of heterogeneity in the total analysis for KPS improvement rate. We speculate that the high-dose and low-dose Aidi might not be very different regarding their effect on KPS, but it is also possible that the sample size is not large enough to identify their difference.

Chemotherapy is important treatment option for breast cancer for its clinical benefit, but it can also lead to side effects such as myelosuppression, digestive tract reactions, and cardiac toxicity. Its toxicity apparently affects patients that sometimes patients could not complete the whole chemotherapy cycle number. Our study demonstrated that addition of Aidi injection could significantly reduce the chemotherapy related toxicities, and Aidi injection itself did not show any obvious toxicity. The safe profile of Aidi injection had been validated by previous studies; for example, in the study by Hu et al., among the cancer patients who received Aidi injection in 2013–2015 in their department, the adverse drug reaction rate was about 1% [35]. Thus, we may conclude that Aidi injection has obvious toxicity-protection effect during chemotherapy treatment, which might partially explain the improved quality of life of patients, and the increased response rate since it may help patients to better complete chemotherapy courses.

Many studies explored the mechanism for activity of Aidi injection in cancer treatment. Aidi injection is prepared from Cantharidin, Ginsen, Astragaloside, and Acanthopanax santicosus. These Chinese herbal medicines have the ability to inhibit cancers and improve immunity as evidenced by a series of laboratory studies [36–39]. Cantharidin, as the central component in the whole preparation, is featured with anticancer activity and no concurrent myelosuppression [40, 41]. Experimental studies reported that cantharidin sodium injection is effective in the management of breast cancer [42], through inhibiting proliferation of breast cancer cells [43], suppressing autophagy, and inducing apoptosis [44]. Aidi injection as the whole preparation has shown anticancer activity and ability of immunological function improvement [45]. For laboratory studies, it was reported that addition of Aidi injection to chemotherapy could significantly increase tumor inhibition rate and reduce Her-2/neu expression level in the nude mice breast carcinoma implanted of Her-2/neu over expression

[46]; it could significantly inhibit cancer cell proliferation, induce cell apoptosis, and reduce cell diameter in the ErbB2 positive breast cancer cell BT-474, SK-BR-3, and HCC-1954 [47]; it significantly inhibited proliferation of MCF-9 cells in dose-dependent manner, accompanying altered expression profiles of microRNAs in MCF-9 cells [48]. For human studies, it was reported that Aidi injection treatment could reverse the suppression or promotion effect of chemotherapy on the peripheral blood level of CD3+, CD4+, CD8+, CD4+/CD8+, and NK cells [17, 22, 24, 26, 32, 33, 49]; Aidi injection plus chemotherapy decreased level of tumor markers CEA, CA153 more than chemotherapy alone [17]; addition of Aidi injection to chemotherapy could reduce serum VEGF level of breast cancer patients, that its anti-cancer action may be achieved through inhibition of tumor angiogenesis to inhibit proliferation, invasion, and metastasis of tumor cells [50].

Limitations. (1) Long-term efficacy is important measurement in breast cancer treatment, but the present study only evaluated short-term efficacy. The long-term efficacy measurements such as overall survival and 5-year survival rate were reported in a few included studies, but the measurements were different so pooled effect size could not be calculated. (2) Some included studies also evaluated the effect of addition of Aidi injection on the level of cardiac enzymes, liver function measurements, immune cells, and tumor markers, but those measurements could not be pooled in meta-analysis due to the presentation way of the results. (3) All studies were performed in China and published in Chinese journals, which may lead to certain bias. (4) The overall quality of the included studies was not high, and the blindness was not described by all the studies, so the results still shall be interpreted cautiously. (5) The adverse events were selectively reported in some included studies: for example, in some studies, multiple adverse events were recorded, but not each event was reported in standard with severity grades that the less common adverse events were roughly described with text, which may lead to reporting bias.

Finally, this is the second meta-analysis evaluated efficacy and safety of Aidi injection plus chemotherapy versus chemotherapy alone among breast cancer patients. Compared with the first published one, our analysis has included larger number of studies, thoroughly discussing adverse events of Aidi injections, and made subgroup analysis to identify the effect of treatment duration and dosage on KPS. According to our analysis, Aidi injection could increase the efficacy of chemotherapy and reduce myelosuppression, digestive tract reaction, and cardiac toxicity induced by chemotherapy and did not lead to additional toxicity and side effects. Therefore, it is an anticancer drug which might have good efficacy and low toxicity and worth further investigation.

Data Availability

The data used to support the findings of this study are included within the article.

Conflicts of Interest

The authors declare that they have no conflicts of interest in this paper.

Authors' Contributions

C. Chen contributed to conceptualization. Q. Yongjun and Y. Chen contributed to data curation. H. Jinzhi and Z. Jun contributed to formal analysis. W. Chenhao and Q. Yongjun contributed to investigation. C. Chen contributed to supervision. H. Jinzhi and Y. Chen contributed to validation. H. Jinzhi, Z. Juan, and M. Min contributed to visualization. W. Chenhao wrote the original draft. W. Chenhao and M. Min contributed to review and editing.

References

- [1] M. Akram, M. Iqbal, M. Daniyal, and A. U. Khan, "Awareness and current knowledge of breast cancer," *Biological Research*, vol. 50, no. 1, p. 33, 2017.
- [2] S.-J. Han, Q.-Q. Guo, T. Wang et al., "Prognostic significance of interactions between ER alpha and ER beta and lymph node status in breast cancer cases," *Asian Pacific Journal of Cancer Prevention*, vol. 14, no. 10, pp. 6081–6084, 2013.
- [3] L. Yang, D. M. Parkin, J. Ferlay, L. Li, and Y. Chen, "Estimates of cancer incidence in China for 2000 and projections for 2005," *Cancer Epidemiology, Biomarkers & Prevention*, vol. 14, no. 1, pp. 243–250, 2005.
- [4] H. Li, R. S. Zheng, S. W. Zhang et al., "Incidence and mortality of female breast cancer in China, 2014," *Zhonghua Zhong Liu Za Zhi*, vol. 40, no. 3, pp. 166–171, 2018.
- [5] J. Raphael and S. Verma, "Overall survival (OS) endpoint: an incomplete evaluation of metastatic breast cancer (MBC) treatment outcome," *Breast Cancer Research and Treatment*, vol. 150, no. 3, pp. 473–478, 2015.
- [6] Y. Sun, "Experience and prospective of integrated medicine in treatment and prevention of cancer," *China Cancer*, vol. 2, pp. 436–438, 2003.
- [7] Chinese Pharmacopoeia Commission, *Pharmacopoeia of the People's Republic of China: Part I*, China Medical Science and Technology Press, Beijing, China, 2010.
- [8] Z. Y. An, Z. Wang, and Y. Zhao, "Anti-cancer research progress of cantharidin and its derivatives," *Asia-Pacific Traditional Medicine*, vol. 5, no. 1, pp. 128–130, 2009.
- [9] L. Liu, J. Liang, and X. Deng, "Effects of Aidi injection (艾迪注射液) with western medical therapies on quality of life for patients with primary liver cancer: a systematic review and meta-analysis," *Chinese Journal of Integrative Medicine*, vol. 25, no. 10, pp. 785–790, 2019.
- [10] Z. Xiao, C. Wang, M. Zhou et al., "Clinical efficacy and safety of Aidi injection plus paclitaxel-based chemotherapy for advanced non-small cell lung cancer: a meta-analysis of 31 randomized controlled trials following the PRISMA guidelines," *Journal of Ethnopharmacology*, vol. 228, pp. 110–122, 2019.
- [11] W. Jiancheng, G. Long, Y. Zhao et al., "Effect of Aidi injection plus chemotherapy on gastric carcinoma: a meta-analysis of randomized controlled trials," *Journal of Traditional Chinese Medicine*, vol. 35, no. 4, pp. 361–374, 2015.
- [12] G. Li, P. J. Ye, X. J. Ying et al., "Clinical effect of Aidi injection combined with folfiri program in treatment of advanced

- colorectal cancer," *Chinese Journal of General Practice*, vol. 13, pp. 1414–1416, 2015.
- [13] Y. S. Zhang, Q. Li, F. L. Sun, and L. Zhao, "Meta-analysis of Aidi injection treatment combining chop chemotherapy in treatment of malignant lymphoma," *Chinese Journal of New Drugs and Clinical Remedies*, vol. 33, pp. 807–812, 2014.
- [14] R. Z. Zhong, W. H. Xiao, J. Lin, and L. He, "Analysis of the clinical effects of Aidi injection combined with TC regimen on advanced epithelial ovarian cancer," *Anti-tumor Pharmacy*, vol. 5, pp. 366–369, 2014.
- [15] G. Xie, Z. H. Cui, K. Peng, X. H. Zhou, Q. Xia, and D. Xu, "Aidi injection, a traditional Chinese medicine injection, could be used as an adjuvant drug to improve quality of life of cancer patients receiving chemotherapy: a propensity score matching analysis," *Integrative Cancer Therapies*, vol. 18, Article ID 1534735418810799, 2019.
- [16] E. A. Eisenhauer, P. Therasse, J. Bogaerts et al., "New response evaluation criteria in solid tumours: revised recist guideline (version 1.1)," *European Journal of Cancer*, vol. 45, no. 2, pp. 228–247, 2009.
- [17] W. M. Chen, "Clinical observation of Aidi injection combined with CEF regimen for post-surgery patients with breast cancer," *Chinese Journal of Modern Drug Application*, vol. 10, pp. 185–186, 2016.
- [18] Z. R. Chen, S. D. Shen, and Z. Huang, "Effect of dose-dense AC→T regimen plus Aidi injection on triple-negative breast cancer," *Chinese Journal of Surgical*, vol. 4, no. 2, pp. 85–87, 2012.
- [19] X. G. Dang and L. Wang, "Evaluation of efficacy on breast cancer treated by Aidi injection plus CTF program of neo-adjuvant chemotherapy and the impacts on serum sFas," *World Journal of Integrated Traditional and Western Medicine*, vol. 5, no. 1, pp. 54–56, 2010.
- [20] L. Fu and X. G. Kou, "Aidi injection combined with chemotherapy in treatment of 44 patients with advanced breast cancer," *Traditional Chinese Medicine*, vol. 23, no. 8, p. 517, 2007.
- [21] Q. H. Gao, "Clinical observation of Aidi combined with chemotherapy in treatment of metastatic breast cancer," *Chinese Journal of Modern Drug*, vol. 7, pp. 121–122, 2013.
- [22] Y. H. Han, X. Q. Jiang, H. Yang, Z. Y. Wu, and M. Jiang, "Clinical observation of Aidi injection combined with CEF regimen chemotherapy in treatment of postoperative breast cancer," *Hubei Journal of TCM*, vol. 36, pp. 7–8, 2014.
- [23] C. G. Jin, "Study of protective effect of supportive anti-cancer therapy for heart injury induced by post-surgery anthracycline chemotherapy for breast cancer," *Heilongjiang Medicine Journal*, vol. 29, pp. 270–272, 2016.
- [24] Z. Z. Liu, H. Liu, L. F. Li, and S. D. Cui, "Clinical observation of Aidi injection combined with chemotherapy in treatment of local advanced breast cancer," *Shandong Medical Journal*, vol. 45, no. 19, p. 62, 2005.
- [25] X. Q. Li and S. B. Gong, "Analysis of efficacy of Aidi injection combined with CEF regimen for breast cancer," *Pharmacology and Clinics of Chinese Materia Medica*, vol. 22, no. 3–4, pp. 176–177, 2006.
- [26] C. H. Lu, M. Hong, J. You et al., "Clinical Observation of Aidi injection combined with TAC regimen as post-surgery adjuvant chemotherapy for breast cancer," *Traditional Chinese Medicine Journal*, vol. 113, pp. 50–52, 2012.
- [27] Z. G. Ren and F. Zhang, "Efficacy observation on high dose of Aidi injection combined with chemotherapy in treatment of 60 patients with breast cancer," *Journal of Linyi Medical College*, vol. 27, no. 5, pp. 341–343, 2005.
- [28] S. D. Shen, Z. R. Chen, and G. F. Xiao, "Clinical observation of dose-dense TC→P regimen plus Aidi injection on triple-negative breast cancer," *Guide of China Medicine*, vol. 11, no. 8, pp. 84–85, 2013.
- [29] W. G. Song, Y. F. Wang, L. X. Yang et al., "Clinical observation of Aidi combined with chemotherapy in treatment of recurrent or metastatic breast cancer," *Chinese Journal of Cancer Prevention and Treatment*, vol. 13, no. 16, pp. 1275–1280, 2006.
- [30] G. D. Wang, M. D. Lei, J. Y. Li et al., "Protective effect of compound cantharis injection on anthracycline chemotherapy induced cardiac injury in breast cancer patients," *China Pharmacy*, vol. 12, pp. 1100–1103, 2012.
- [31] J. Wang, "Efficacy of Aidi injection combined with chemotherapy in treatment of advanced breast cancer," *Yiyao Qianyan*, vol. 6, pp. 61–62, 2016.
- [32] L. Yang, "Clinical observation of Aidi injection combined with chemotherapy in treatment of advanced breast cancer," *Chinese Journal of Integrated Traditional and Western Medicine*, vol. 24, no. 8, pp. 755–756, 2004.
- [33] W. J. Yang, "Aidi injection combined with CAF regimen in treatment of 30 cases of advanced breast cancer," *Jiangxi Journal of Traditional Chinese Medicine*, vol. 36, no. 7, pp. 46–47, 2005.
- [34] J. Zhang, K. Xu, and S. L. Wang, "Randomized controlled trial of the supportive function of the Aidi injection in the process of chemotherapy in treating anthracycline-resistant metastatic breast cancer patients," *Guiding Journal of Traditional Chinese Medicine and Pharmacology*, vol. 22, pp. 27–30, 2016.
- [35] M. M. Hu, X. Q. Zhu, and M. Y. Zhu, "Analysis on application of traditional Chinese medicine injections in inpatients with tumor in Wenzhou People's Hospital during 2013–2015," *Evaluation and Analysis of Drug-Use in Hospitals of China*, vol. 16, pp. 1088–1090, 2016.
- [36] S. Ren, H. Zhang, Y. Mu, M. Sun, and P. Liu, "Pharmacological effects of Astragaloside IV: a literature review," *Journal of Traditional Chinese Medicine*, vol. 33, no. 3, pp. 413–416, 2013.
- [37] A. Ahuja, J. H. Kim, J.-H. Kim, Y.-S. Yi, and J. Y. Cho, "Functional role of ginseng-derived compounds in cancer," *Journal of Ginseng Research*, vol. 42, no. 3, pp. 248–254, 2018.
- [38] J. X. Du, Y. H. Gu, B. Zhang, and X. H. Zhu, "Research and evaluation on the antitumor effect of the active components from acanthopanax," *Evaluation and Analysis of Drug-Use in Hospitals of China*, vol. 10, pp. 199–200, 2010.
- [39] R. Rauh, S. Kahl, H. Boechzeh, R. Bauer, B. Kaina, and T. Efferth, "Molecular biology of cantharidin in cancer cells," *Chinese Medicine*, vol. 2, pp. 8–16, 2007.
- [40] J. M. Chang and Y. Q. Zhang, "Analysis of the factors affecting efficacy and toxicity of cantharidin," *Clinical Journal of Chinese Medicine*, vol. 4, no. 4, pp. 67–68, 2012.
- [41] K. Bonness, I. V. Aragon, R. Beth, N. M. Dean, and R. E. Honkanen, "Cantharidin-induced mitotic arrest is associated with the formation of aberrant mitotic spindles and lagging chromosomes resulting, in part, from the suppression of PP2A α ," *Molecular Cancer Therapeutics*, vol. 5, no. 11, pp. 2727–2736, 2006.
- [42] S. Huang and K. Cao, "Anti-invasive and anti-metastasis effect of norcantharidin on high-metastatic human breast cancer cell lines," *Journal of Tropical Medicine*, vol. 9, pp. 1034–1045, 2010.
- [43] J. Y. Wang, J. L. Liang, and G. J. Liu, "Effect of Norcantharidin on expression of VEGF mRNA in human breast cancer cell

- lines,” *Chinese Archives of Traditional Chinese Medicine*, vol. 27, no. 11, pp. 2369–2371, 2009.
- [44] H.-C. Li, Z.-H. Xia, Y.-F. Chen et al., “Cantharidin inhibits the growth of triple-negative breast cancer cells by suppressing autophagy and inducing apoptosis in vitro and in vivo,” *Cellular Physiology and Biochemistry*, vol. 43, no. 5, pp. 1829–1840, 2017.
- [45] J. Xu, W. Z. Ju, and H. S. Tan, “Summary of studies investigating action mechanisms and clinical application of Aidi injection,” *Pharmaceutical and Clinical Research*, vol. 20, no. 1, pp. 48–51, 2012.
- [46] X. M. Zhang, X. Liu, and Q. Pan, “Effects of chemotherapy and Aidi injection on nude mice breast carcinoma implanted of Her-2/neu over-expression,” *Journal of Emergency of Traditional Chinese Medicine*, vol. 18, pp. 1654–1657, 2009.
- [47] J. Tang and G. J. Wang, “Antitumor effect of Aidi injection on ErbB2-positive breast cancer cells and mechanisms of action,” *Journal of Chinese Pharmaceutical Sciences*, vol. 34, pp. 333–340, 2018.
- [48] H. Zhang, Q.-M. Zhou, Y.-Y. Lu, J. Du, and S.-B. Su, “Aidi injection () alters the expression profiles of MicroRNAs in human breast cancer cells,” *Journal of Traditional Chinese Medicine*, vol. 31, no. 1, pp. 10–16, 2011.
- [49] L. W. Chu, Z. Y. Wen, L. G. Zhang, Y. Z. Pei, and W. L. Gong, “Analysis of effect of Aidi injection on cellular immunology of breast cancer patients,” *China Medical Engineering*, vol. 21, pp. 36–37, 2013.
- [50] M. Wang and L. Wu, “Effect of Aidi injection on serum VEGF in patients with breast cancer,” *Chinese Journal of Clinical Research*, vol. 26, pp. 1151–1158, 2013.

Research Article

The Shuganhuazheng Formula in Triple-Negative Breast Cancer: A Study Based on Network Pharmacology and In Vivo Experiments

Bo Wang,¹ Rui Fei,² Yan Yang,³ Niancai Jing,³ Yi Lu,³ Hongyu Xiao,³ Jili Yang,³ and Yue Zhang³ 

¹Changchun University of Chinese Medicine, Changchun, Jilin 130117, China

²Cell Biology Department, School of Basic Medicine, Jilin University, Changchun, Jilin 130021, China

³Department of Integrated Chinese and Western Medicine, Jilin Cancer Hospital, Changchun, Jilin 130000, China

Correspondence should be addressed to Yue Zhang; zhangyuejlc@163.com

Received 22 July 2020; Revised 18 November 2020; Accepted 26 November 2020; Published 14 December 2020

Academic Editor: Azis Saifudin

Copyright © 2020 Bo Wang et al. This is an open access article distributed under the Creative Commons Attribution License, which permits unrestricted use, distribution, and reproduction in any medium, provided the original work is properly cited.

Breast cancer is the most common cancer in women. Among breast cancer subtypes, triple-negative breast cancer (TNBC) has the highest degree of malignancy and the worst prognosis. The Shuganhuazheng formula (SGHZF) is a traditional Chinese herbal formula for the treatment of TNBC, but the mechanism of SGHZF in the treatment of TNBC remains unclear. In this study, the therapeutic effect and mechanism of SGHZF against TNBC were preliminarily determined based on in vivo experimental verification and network pharmacology. In terms of therapeutic effects, the antitumour effect was verified by measuring and calculating tumour volume, and the expression of proto-oncogene c-Myc was verified by PCR. In terms of the mechanism, potential therapeutic targets were identified by overlapping the SGHZF-related and TNBC-related targets. After comprehensively analysing the results of the protein-protein interaction (PPI), gene ontology (GO) function, and Kyoto Encyclopedia of Genes and Genomes (KEGG) pathway enrichment analyses, Akt and HIF-1 α were selected for verification by using immunohistochemical and Western blot analyses. The results of the study indicated that SGHZF can inhibit breast tumour growth in mice and that the mechanism may be related to the inhibition of Akt and HIF-1 α expression.

1. Introduction

Malignant tumour disease has become a major threat to human life and health. According to the Global Cancer Statistics of the World Health Organization (WHO) in 2018, 1/10 women will suffer from cancer in her lifetime; breast cancer is the most common cancer in women, accounting for 24.2% of female cancer cases. Breast cancer is also the leading cause of cancer-related death in women, accounting for 15% of female cancer-related deaths [1]. Triple-negative breast cancer (TNBC) accounts for 10–20% of all breast cancers [2]. TNBC is highly invasive, has a poor prognosis, and is prone to local recurrence and distant metastasis [3, 4]. At present, chemotherapy is still the main treatment for TNBC, but several unavoidable side effects are associated with this strategy [5, 6]. Therefore, people have searched for effective complementary and alternative medical methods

for a long time [7]. As an important type of complementary and alternative medicine, traditional Chinese medicine (TCM), has been widely used in the treatment of TNBC in China and many other countries and regions of the world with significant curative effects and few side effects [8, 9].

The Shuganhuazheng formula (SGHZF) is an empirical formula for the treatment of TNBC that was created by Professor Zhang Yue, a famous expert in TCM in Jilin Province. It consists of Chai Hu, Bie Jia, Dang Gui, Bai Zhu, Bai Shao, Zhe Bei, Fu Ling, and Gan Cao. It has been widely used in the Department of Integrated Traditional Chinese and Western Medicine of Jilin Cancer Hospital for many years. However, the mechanism by which SGHZF helps to treat TNBC remains unclear, and this lack of understanding affects its potential clinical application to some degree. In this study, the therapeutic effect and mechanism of SGHZF against TNBC was preliminarily determined based on

network pharmacology and in vivo experimental verification. The purpose of this study is to provide an important experimental basis for the clinical application of SGHZF in the treatment of TNBC. The specific research process is as follows.

2. Materials and Methods

2.1. Drugs, Cells, Animals, and Reagents. SGHZF patent medicine was provided by the Jilin Institute of TCM (1 g is equivalent to 5.3125 g of crude drugs), and it was prepared at different concentrations as needed for the experiments. The 4T1 cells were purchased from the Shanghai Cell Bank of the Chinese Academy of Sciences. Female BALB/c mice were purchased from Changchun Yisi Experimental Animal Technology company with limited liability (SCXK (Ji)-2016-0003). c-Myc, Akt, and HIF-1 α antibodies were purchased from Abcam. Relevant primers were purchased from Yugong Bioengineering (Shanghai) Co., Ltd. Other reagents were purchased from (Changchun) Fengsheng Biological Co., Ltd.

2.2. Establishment of Tumour-Bearing Mice with TNBC and Determination of the Antitumour Effect of SGHZF. All animal experiments were conducted under the guidelines of the Animal Care and Use Committee of Changchun University of Chinese Medicine. After 1 week of adaptive feeding, the mice were fasted in a barrier environment at room temperature for 12 hours. Forty female BALB/c mice weighing 18 g–22 g and aged 8 weeks were selected. After anaesthesia by intraperitoneal injection of 2% pentobarbital at doses of 3–4 μ l/g, 4T1 cells (3×10^5 cells/ml) were inoculated into the anterior breast of their axillary sternum, and each mouse was injected with 0.1 mL. On the 3rd day, tumour nodules with diameters of 3 mm–4 mm were observed at the inoculation site, which was considered successful modelling [10]. On the second day after successful modelling, 40 mice (8 per group) were randomly divided into a model control group and SGHZF experimental groups receiving 0.01 g/kg, 0.1 g/kg, 1 g/kg, and 10 g/kg doses. Each experimental group was administered 0.2 ml of the corresponding concentration of SGHZF by intragastric administration, while the model control group was administered the same amount of distilled water by intragastric administration once a day for 21 days. The longest and shortest diameters of the tumours were measured on days 3, 7, 14, and 21 to calculate the tumour volume and tumour inhibition rate. The formula for calculating the tumour volume was as follows: tumour volume = (longest tumour diameter \times shortest tumour diameter²)/2. The formula for calculating the tumour inhibition rate was as follows: tumour inhibition rate = (average volume of tumours in the model control group – average volume of tumours in each experimental group)/average volume of tumours in the model control group * 100%.

2.3. Immunohistochemical Analysis. The mice were treated via the method described in section 2.2. On the 21st day, the

mice were killed by asphyxiation, and the tumour tissues were dissected. Then, tumour tissues were fixed in 10% neutral formalin solution according to routine tissue treatment protocols. After paraffin embedding, serial sections were made (2 μ m thick). Finally, the tissue morphology was observed by haematoxylin and eosin staining (H&E) under an electron microscope. Immunohistochemical analysis was performed by staining the sections using different antibodies (according to the antibody instructions). Motic Images Advanced 3.2 was used as the image analysis software.

2.4. PCR. The mice were treated via the method described in section 2.2. On the 21st day, the mice were killed by air asphyxia to dissect the tumour tissues. After the tumours were harvested from the mice, they were fully ground in liquid nitrogen, total RNA was extracted strictly following the kit instructions, and PCR amplification was followed by 1.5% agarose gel electrophoresis. Finally, the greyscale values of the bands were analysed by ImageJ software.

2.5. Western Blot Detection. The mice were treated with the method described in section 2.2. On the 21st day, the mice were killed by air asphyxia to dissect the tumour tissues. Then, protein extraction and quantitative analysis were performed on tumour tissues. After routine detection of protein concentration and denaturation of proteins, SDS-PAGE electrophoresis and membrane transfer were carried out. Finally, the grey values were analysed by ImageJ software.

2.6. Data Preparation of Network Pharmacology Research. TCMSP [11] (<http://lsp.nwu.edu.cn/tcmsp.php>) and TCMID [12] (<http://119.3.41.228:8000/tcmid>) databases were used to search for the active components of SGHZF. The search terms were “Chai Hu”, “Bai Shao”, “Bai Zhu”, “Chuan Bei”, “Dang Gui”, “Fu Ling”, and “Gan Cao”. Then, the TCMSP database was used to screen the active components and retrieve their relevant targets. The screening conditions were oral bioavailability (OB) \geq 30%, drug-likeness (DL) \geq 0.18, and Caco-2 permeability $>$ –0.4. Finally, the retrieval results were combined and duplicates were removed to obtain the targets of the active components of SGHZF. Because turtle shells are not suitable for network pharmacology research, we decided to exclude them.

The GENECARDS [13] (<https://www.genecards.org/>) and OMIM [14] (<https://www.omim.org/>) disease databases were used to search disease targets of TNBC. The search term was “triple-negative breast cancer.” Finally, the retrieval results were combined and duplicates were removed to obtain the targets of TNBC.

2.7. Construction of Network Graph and Potential Therapeutic Targets Analysis. R language software was used to analyse the interaction between drugs and disease targets to obtain potential therapeutic targets, and the results are presented in the form of a Venn diagram and a table. Cytoscape 3.6.1

software was used to construct the interaction relationship between drugs and potential therapeutic targets, and the results are presented in the form of a network diagram. Then, the STRING (string-db.org/) platform was used to construct the protein-protein interaction (PPI) network of potential therapeutic targets, and the minimum interaction threshold was set as the highest confidence (>0.9) to show the interactions between potential therapeutic targets. Finally, the cytoHubba plugin of Cytoscape 3.6.1 was used to calculate the correlation frequency of potential therapeutic targets, and the results are presented in the form of a network diagram. Then, gene ontology (GO) function and Kyoto Encyclopedia of Genes and Genomes (KEGG) pathway enrichment analyses were performed on the potential therapeutic targets to obtain the gene functions and molecular pathways of the potential therapeutic targets, and the results are presented in the form of bar and dot charts.

2.8. Statistical Analysis. SPSS 19.0 software was used to calculate the mean and standard deviation ($\bar{x} \pm s$) of each group of data, and the differences between each index were compared by ANOVA, with $P < 0.05$ and $P < 0.01$ as the statistical standards. The greyscale values of the protein and nucleic acid images were analysed by ImageJ software, and semiquantitative analysis was carried out. Differences of more than 2-fold were considered significant.

3. Results

3.1. Inhibitory Effect of SGHZF on Mice with Breast Cancer

3.1.1. Antitumour Effect of SGHZF on Tumour-Bearing Mice. To verify the inhibitory effect of SGHZF on TNBC, we first conducted tumour inhibition experiments on a mouse model of breast cancer and observed and measured breast cancer tumour growth in each group of mice. The results showed that tumour growth of mice in the model control group was rapid on day 3, while the tumour growth of mice in each experimental group was slow, with no significant difference. The tumour growth of mice in all experimental groups was slow on day 7, while the tumours of mice in the model control group and the 10 g/kg experimental group did not grow significantly. The tumour growth of mice in the model control group was rapid on days 14 and 21, while the tumour growth of mice in each experimental group was significantly inhibited, with a certain concentration dependence observed. Among these observations, the inhibition effect was the most obvious on day 21 in the 1 g/kg and 10 g/kg groups (see Figure 1). The above results indicated that SGHZF inhibits tumour growth in tumour-bearing mice.

3.1.2. Effect of SGHZF on the Expression of *c-Myc* in Tumour-Bearing Mice. To further verify the inhibitory effect of SGHZF on TNBC, we used PCR technology to detect the expression of the oncogene *c-Myc* in the tumour tissues of mice in each group. The results showed that the expression of *c-Myc* in the 0.1 g/kg, 1 g/kg, and 10 g/kg experimental

groups was significantly lower than that in the model control group ($P < 0.05$ or $P < 0.01$). However, there was no significant difference between the 1 g/kg and 10 g/kg experimental groups. The 0.01 g/kg experimental group showed no significant decrease compared with the model control group (see Figure 2). The above results indicated that SGHZF inhibits the expression of the oncogene *c-Myc* in tumour-bearing mice.

3.2. Active Components and Targets of Drugs in SGHZF.

To obtain the active components and targets of SGHZF, we searched according to the search terms and screening conditions in 2.6 and combined and deduplicated the search results. The results showed that the active components and quantity of the drugs in SGHZF were as follows: 15 species of Chai Hu, 18 species of Bai Shao, 4 species of Bai Zhu, 11 species of Chuan Bei, 6 species of Dang Gui, 7 species of Fu Ling, and 133 species of Gan Cao. After combination and deduplication, 174 active components were obtained. The targets of these 174 active components were further searched, and a total of 214 targets were obtained after combination and deduplication (see Figure 3).

3.3. Analysis of the Interaction between SGHZF and TNBC Targets.

To clarify the interaction relationship between SGHZF and targets of TNBC, we first searched according to the search terms of section 2.6, and then we combined the search results and removed the duplicates. In total, 3606 disease targets were retrieved from the GENECARDS database, and 462 disease targets were retrieved from the OMIM database. After the results of the two databases were combined and duplicates were removed, a total of 3971 TNBC targets were obtained. Then, potential therapeutic targets were obtained by overlapping the SGHZF-related and TNBC-related targets. Ultimately, 172 potential therapeutic targets were obtained through interaction analysis, accounting for more than 80% of TNBC-related targets (Figure 4(a)). Further PPI analysis of potential therapeutic targets revealed that 164 of them were correlated with each other (Figure 4(b)). Among them, highly correlated potential therapeutic targets such as EGFR, ESRI, AKT1, STAT3, and IL6 also showed high disease-related scores in the GENECARDS database (Table 1), which indicated that these potential therapeutic targets may have greater therapeutic effects.

3.4. GO Function and KEGG Pathway Enrichment Analysis of Potential Therapeutic Targets.

To further investigate the molecular mechanism of potential therapeutic targets, we applied the GO function and KEGG enrichment analysis of potential therapeutic targets. The results of GO functional enrichment showed that the molecular functions of potential therapeutic targets mainly include DNA-binding transcription activator activity, RNA polymerase II-specific activity, and cytokine receptor activity (Figures 5(a) and 5(b)). The results of KEGG enrichment analysis showed that the signalling pathways related to potential therapeutic

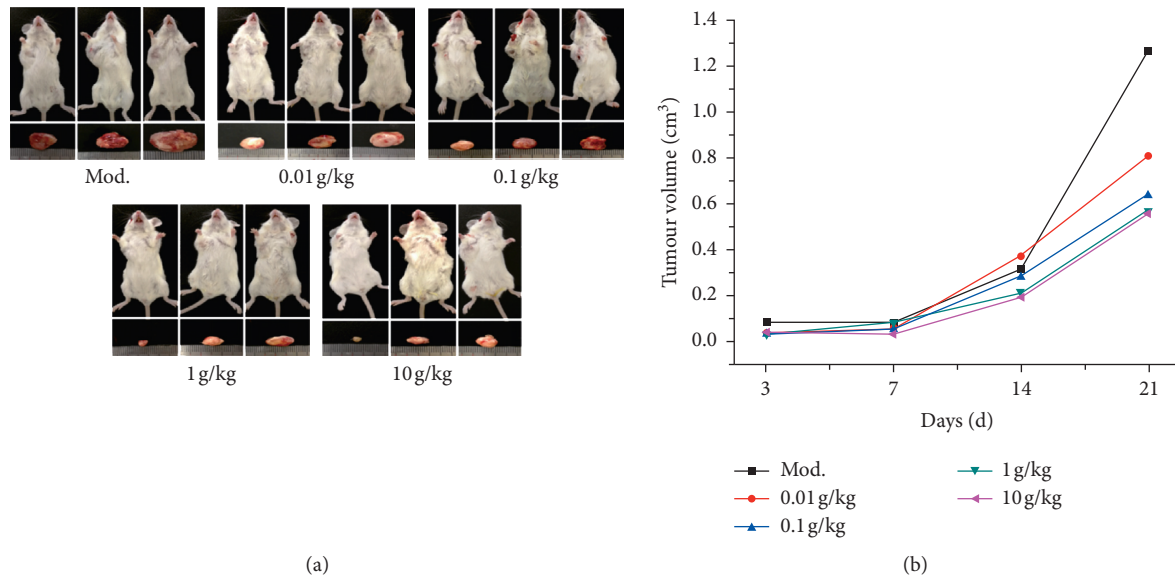


FIGURE 1: Antitumour effect of SGHZF on tumour-bearing mice. The tumour volume of each mouse was measured and calculated on days 3, 7, 14, and 21, and the inhibition rate was calculated ($n = 8$). On day 21, mice in each group were sacrificed, tumour tissues were harvested, and photographs were taken. (a) Comparison of tumour size among groups on the 21st day. Three typical pictures in each group are shown. (b) Changes in tumour volume.

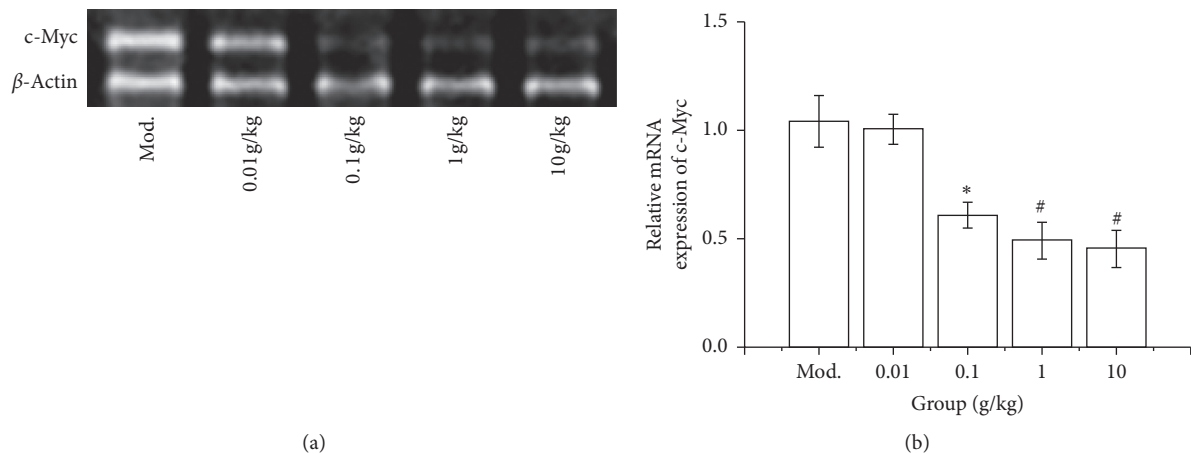


FIGURE 2: Effect of SGHZF on c-Myc expression in mice with breast cancer. (a) PCR gel map of tumour tissues of mice in each group. (b) Histogram of c-Myc expression in tumour tissues of mice in each group. * Compared with Mod, $P < 0.05$; # compared with Mod, $P < 0.01$.

targets (excluding other disease pathways) mainly included the IL-17 signalling pathway, TNF signalling pathway, and HIF-1 signalling pathway (Figures 5(c) and 5(d)). The above results indicate that the treatment of TNBC with SGHZF is closely related to multiple targets and multiple signalling pathways.

3.5. Gene Expression Analysis of Related Targets

3.5.1. Effect of SGHZF on Akt Expression in Mice with Breast Cancer. To prove the therapeutic mechanism of SGHZF in mice with breast cancer, we investigated the expression of Akt in the tumour tissue of mice by immunohistochemistry

and Western blot analyses. The immunohistochemistry results showed that the tumour tissue of the model control group was dark colour, the cytoplasm was brown-yellow, and the nucleus was light blue, which indicated that the expression of protein molecules was high. In each experimental group, the tumour tissue staining gradually reduced, the brown colour of the cytoplasm gradually weakened, and the blue colour of the nucleus gradually deepened, which indicated that the expression of protein molecules was gradually reduced. The optical density values of immune tissues in each group were Mod > 0.01 g/kg > 0.1 g/kg > 1 g/kg > 10 g/kg. Compared with the values of the model control group, the values of each experimental group were

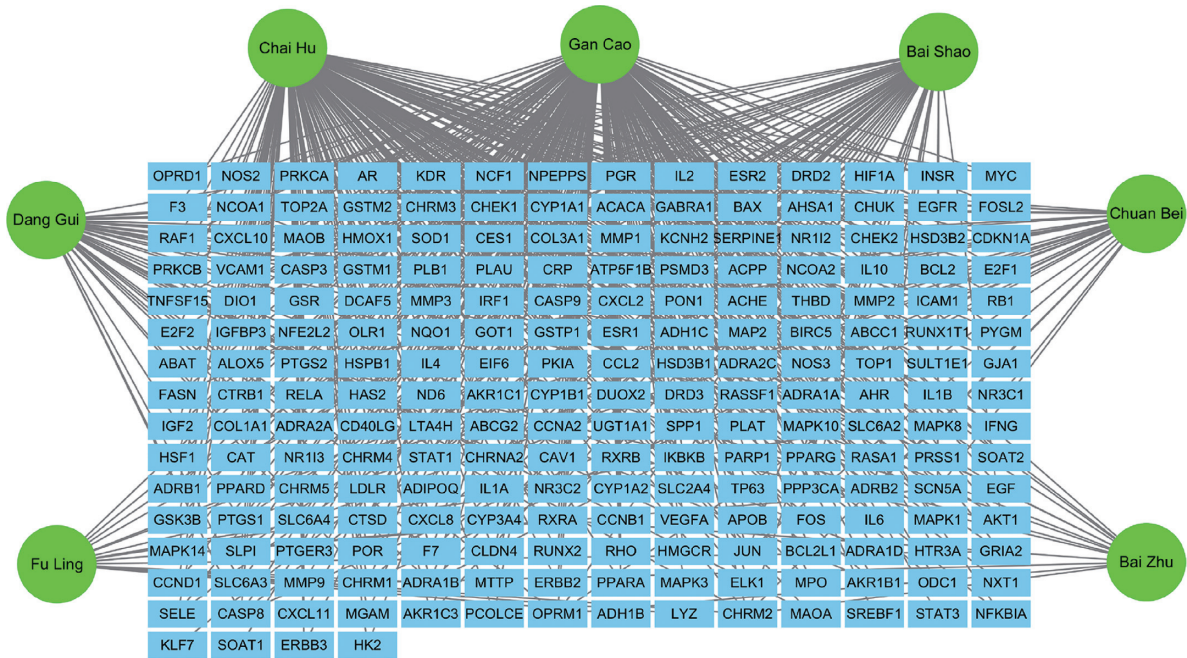


FIGURE 3: The Chinese herbal medicine-target network. The blue squares represent targets, and the green circles represent the names of the medicines in SGHZF. The line represents the relationship between the active components and the targets.

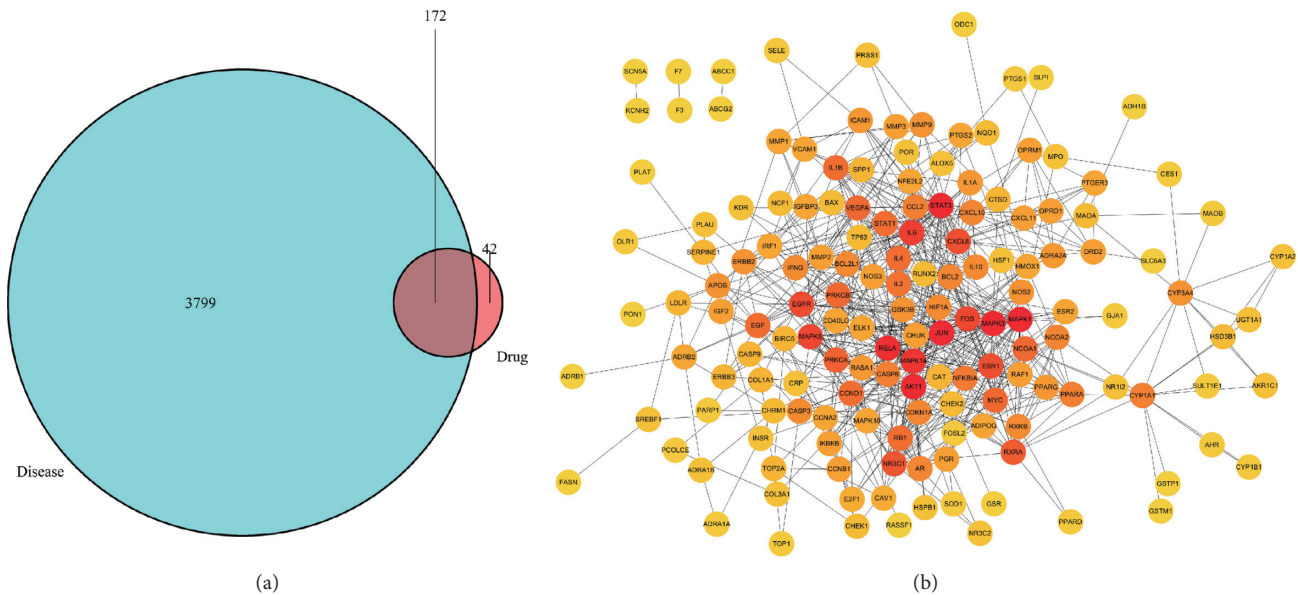


FIGURE 4: Acquisition and analysis of potential therapeutic targets. (a) Venn diagram of the interaction between the target of drugs in SGHZF and the target of TNBC disease. The blue circle represents the number of targets. The red circle represents the number of drug targets, and the intersection represents the number of potential therapeutic targets. (b) PPI network map with associated potential therapeutic targets. The circle represents the abbreviation of the target, while the line indicates the association between the targets, and the darker the colour, the higher the correlation.

significantly different ($P < 0.05$ or $P < 0.01$), and the differences were most obvious in the 1 g/kg and 10 g/kg groups (see Figure 6(a)). The Western blotting results showed that the expression of AKT in each group showed a downward trend with a significant concentration dependence ($P < 0.05$ or $P < 0.01$), which was consistent with the immunohistochemical

results (see Figures 6(b) and 6(c)). The above results indicate that SGHZF inhibits the expression of Akt in mice with breast cancer.

3.5.2. Effect of SGHZF on HIF-1 α Expression in Mice with Breast Cancer. To prove the therapeutic mechanism of

TABLE 1: Potential therapeutic targets with high PPI correlation and high disease correlation scores in the GENECARDS database.

Target	Interactions in the PPI network	Disease-related scores in the GENECARDS database
EGFR	22	104.07
ESR1	21	102.25
AKT1	36	82.32
STAT3	38	70.64
IL6	26	67.01

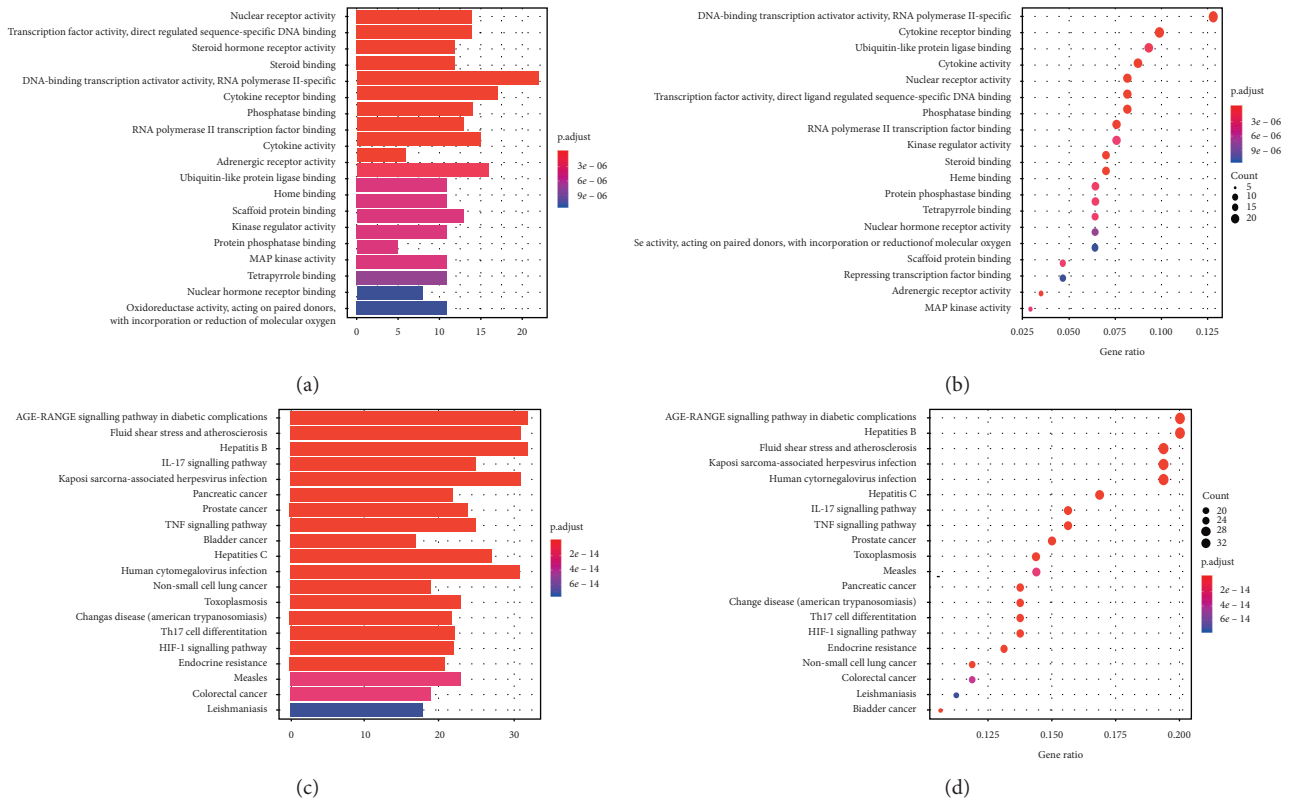


FIGURE 5: Enrichment analysis of potential therapeutic targets. (a) Bar chart of GO enrichment analysis results; (b) dot chart of GO enrichment analysis results; (c) bar chart of KEGG enrichment analysis results; and (d) dot chart of KEGG enrichment analysis results. In the bar chart, the abscissa represents the number of targets, and the ordinate represents the name of the enrichment result. The redder the colour, the smaller the adjusted P value. The bluer the colour, the larger the adjusted P value. In the dot chart, the abscissa represents the ratio of targets, and the ordinate represents the name of the enrichment result. The larger the circle, the greater the enrichment and vice versa. The redder the circle, the smaller the adjusted P value. The bluer the circle, the larger the adjusted P value.

SGHZF in mice with breast cancer, we further investigated the expression of HIF-1 α in the tumour tissue of mice by immunohistochemistry and Western blot analyses. The immunohistochemistry results showed that the tumour tissue of each group was brown yellow, while the colour of the model control group was darker, and the distribution was uniform. In each experimental group, the tumour tissue was light coloured; the brown-yellow staining of the cytoplasm was gradually reduced, but the light blue staining of the nuclei gradually deepened, making the whole tissue appear as light blue-white. The optical density values of the immune tissues in each group were ranked Mod >0.01 g/kg >0.1 g/kg >1 g/kg >10 g/kg, which showed an obvious concentration dependence. The difference between the values of the model control group and the 0.1 g/kg

experimental group was significant ($P < 0.05$); the difference between the values of the 1 g/kg and 10 g/kg experimental groups was extremely significant ($P < 0.01$) (see Figure 7(a)). The Western blotting results showed that the expression of HIF-1 α in each group showed a downward trend with a significant concentration dependence ($P < 0.05$ or $P < 0.01$), which was consistent with the immunohistochemical results (see Figures 7(b) and 7(c)). The above results indicate that SGHZF has an inhibitory effect on the expression of HIF-1 α in mice with breast cancer.

4. Discussion

TNBC is a kind of heterogeneous tumour. Compared with other molecular types of breast cancer, it has a higher

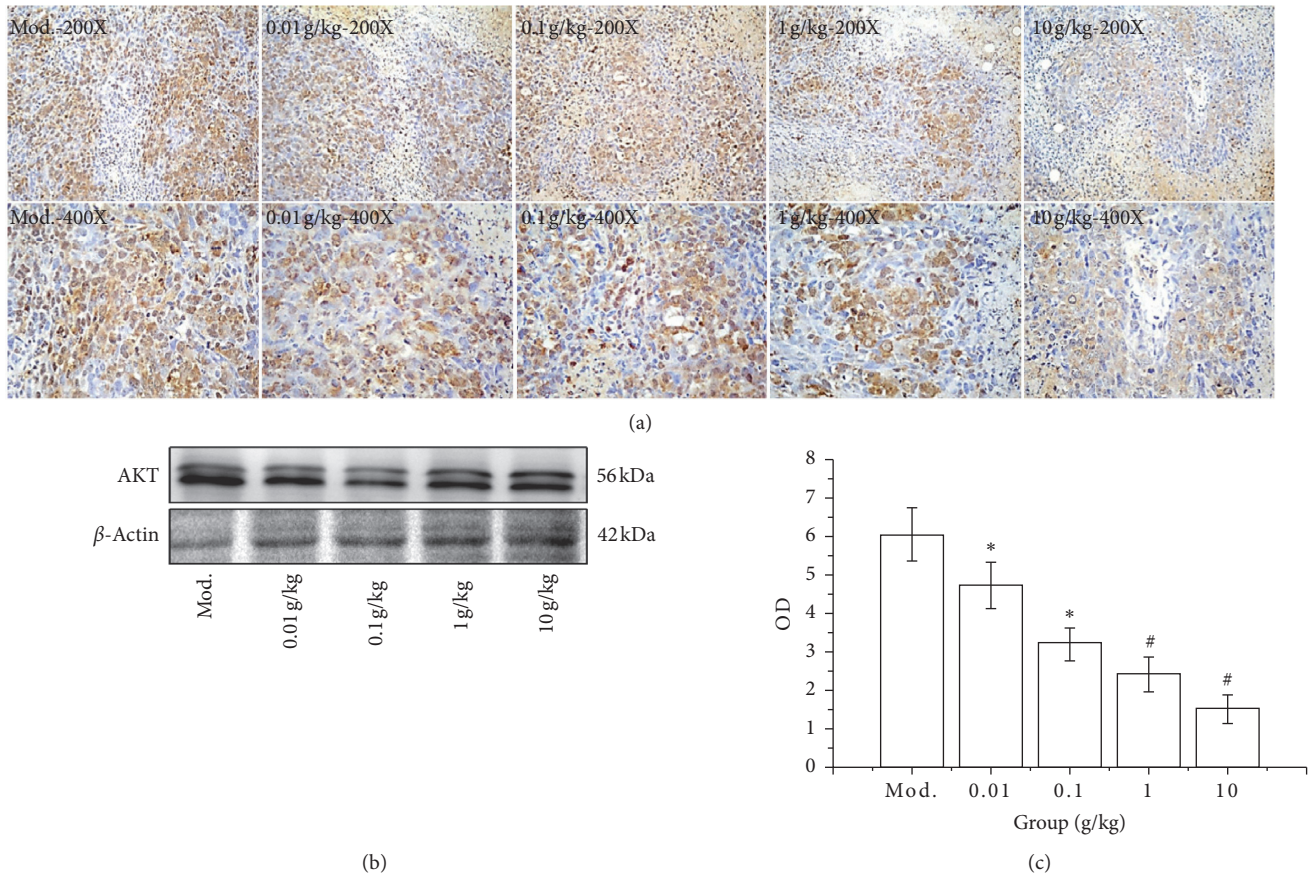


FIGURE 6: Effect of SGHZF on the expression of AKT in mice with breast cancer. (a) Immunohistochemistry images at 200x and 400x. (b) Gel map of the Western blotting results of each group. (c) OD value of the Western blot in each group. *Compared with Mod, $P < 0.05$; #compared with Mod, $P < 0.01$.

recurrence rate and a poorer prognosis [15, 16]. At present, chemotherapy is still the main treatment for TNBC. Despite aggressive systemic chemotherapy, the survival of patients with TNBC is unacceptable [17, 18], and this is exemplified in older patients [19]; chemotherapy also leads to inevitable drug resistance and side effects [20]. Although scholars have continued their search for druggable molecular targets in TNBC, to date, no specific drug has been found to be effective [21]. A large number of studies have shown that the treatment of cancer with traditional Chinese herbal formulas involves the interaction of multiple targets and multiple signalling pathways [22–24]. Therefore, TCM may have great potential for the treatment of TNBC.

Considering that the growth of tumours can be observed directly in animal experiments *in vivo* and that tumour tissues can be assessed more conveniently, we used the mouse 4T1 breast cancer animal model to study the inhibitory effect of SGHZF on TNBC. This model is a recognized animal model of TNBC in mice, and its tumour growth rate and metastasis status are very similar to those of humans, which makes it an ideal animal model for the study of TNBC [25, 26]. In this study, we calculated the tumour volume of mice in this model and found that the tumour volume and tumour inhibition rate of different experimental groups did not change over time. However, on day 21, there

were statistically significant differences in the tumour volumes and tumour inhibition rates between groups, which may be related to the metabolism and blood drug concentration of the traditional Chinese herbal formula in mice. Our experiment confirmed that SGHZF inhibits tumour growth in tumour-bearing mice.

As an important member of the Myc family, c-Myc is an oncogene in breast cancer [27]. It plays an important role in promoting the occurrence and development of tumours [28] and in promoting and maintaining tumour cell proliferation [29], differentiation, and apoptosis [30]. In recent years, a large number of studies have shown that c-Myc plays an important role in regulating the metabolism, proliferation, and apoptosis of TNBC cells [30–32]. Therefore, we measured the expression of c-Myc in tumour tissue. The results showed that the expression of c-Myc in the high-dose SGHZF experimental group was significantly reduced compared to that in the control group, which indicates that SGHZF had an inhibitory effect on c-Myc in mouse breast cancer.

After confirming that SGHZF has an inhibitory effect on breast cancer in tumour-bearing mice, we investigated the active components and targets of drugs in SGHZF. SGHZF contains a large number of traditional Chinese herbs, and its active components and molecular functions are complex and

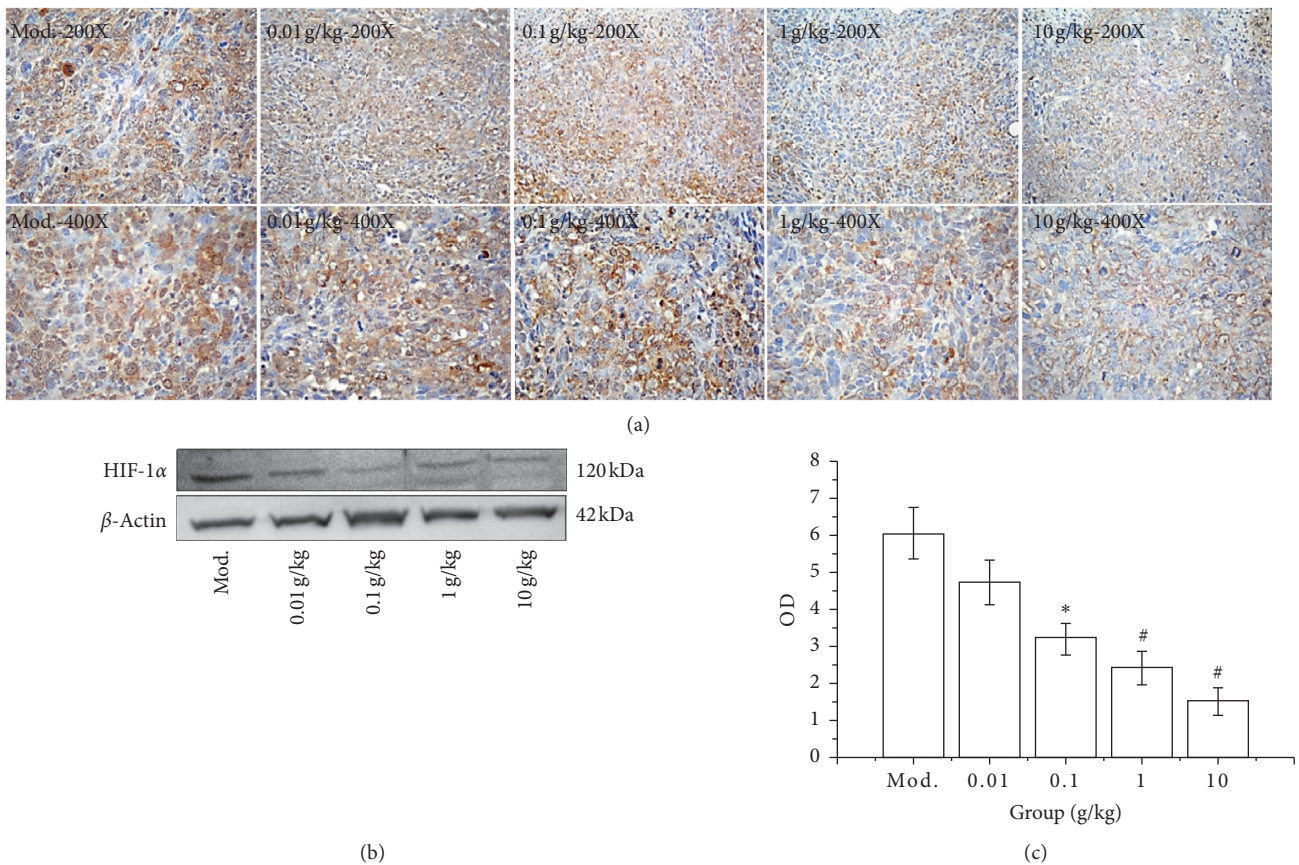


FIGURE 7: Effect of SGHZF on the expression of HIF-1 α in mice with breast cancer. (a) Immunohistochemistry images at 200x and 400x. (b) Gel map of the Western blotting results of each group. (c) OD value of the Western blot in each group. *Compared with Mod, $P < 0.05$; # compared with Mod, $P < 0.01$.

diverse, so it is difficult for traditional research methods to comprehensively study the molecular mechanism of its treatment. Therefore, we applied the network pharmacology research method to explore the potential therapeutic targets of SGHZF. Through network pharmacology research, we obtained 174 active components and 214 targets in SGHZF. The active components and targets of Chai Hu and Gan Cao are relatively high, indicating that these two drugs may be the main drugs in SGHZF. According to the literature, glycyrrhizin and glycyrrhetic acid combined with etoposide could inhibit proliferation and promote apoptosis of TNBC cells [33]. Saikosaponin *D* from Chai Hu suppresses TNBC cell growth by targeting β -catenin signalling [34].

Through further study, we found that there were 172 potential therapeutic targets of SGHZF, accounting for more than 80% of the targets of SGHZF, among which 164 potential therapeutic targets were correlated with each other. By comparing the correlation scores of disease targets, we found that the potential therapeutic targets with high PPI correlations, such as EGFR, ESR1, AKT1, STAT3, and IL6, also showed high disease correlation scores in the GENECARDS database, indicating that these targets are closely related to TNBC and suggesting that their potential therapeutic effects may be greater. The results of GO functional enrichment analysis showed that the molecular functions of

potential therapeutic targets mainly included DNA-binding transcription activator activity, RNA polymerase II-specific activity, and cytokine receptor activity. These molecular functions and characteristics are closely related to tumour cells. The results of the KEGG pathway enrichment analysis showed that the pathways related to potential therapeutic targets (excluding other disease pathways) mainly included the IL-17 signalling pathway, the TNF signalling pathway, and the HIF-1 signalling pathway, which have been associated with tumours [35–37].

Among the enriched KEGG pathways, the HIF-1 signalling pathway is most closely related to TNBC [38]. An increase in HIF-1 expression is one of the main molecular characteristics of TNBC [39]. HIF-1 α is the main target of the HIF-1 signalling pathway [40], and the overactivation of Akt upstream can activate the expression of HIF-1 α downstream [41]. A large number of studies have shown that hypoxia can enhance the invasive ability of cancer [42], which is closely related to chemotherapeutic resistance [43]. Considering that TNBC is highly invasive and is mainly treated with chemotherapy, we believe that the HIF-1 signalling pathway is very important to TNBC. Moreover, the PPI analysis revealed that HIF-1 α and AKT1 of the Akt family were highly correlated with potential therapeutic targets. Therefore, we chose Akt and HIF-1 α for further

experimental verification. The results indicated that SGHZF can inhibit the expression of AKT and HIF-1 α , which is consistent with the network pharmacology prediction. Through this study, we found that SGHZF has an inhibitory effect on mouse TNBC and that its mechanism may be related to the inhibition of Akt and HIF-1 α expression. Thus far, we have preliminarily explored the molecular mechanism of SGHZF in the treatment of TNBC.

In summary, as a complex Chinese herbal compound, SGHZF has a multifaceted molecular mechanism in the treatment of TNBC. In this study, we preliminarily identified and verified this mechanism, which lays a foundation for the follow-up study of SGHZF in the treatment of TNBC.

5. Conclusions

SGHZF inhibits breast cancer tumour growth in mice, and the underlying mechanism may be related to the inhibition of Akt and HIF-1 α expression.

Data Availability

The data used to support the findings of this study are available from the corresponding author upon request.

Conflicts of Interest

The authors declare that there are no conflicts of interest regarding the publication of this paper.

Acknowledgments

The project was supported by the Department of Science and Technology of Jilin Province (201603046YY).

References

- [1] F. Bray, J. Ferlay, I. Soerjomataram, R. L. Siegel, L. A. Torre, and A. Jemal, "Global cancer statistics 2018: GLOBOCAN estimates of incidence and mortality worldwide for 36 cancers in 185 countries," *CA: A Cancer Journal for Clinicians*, vol. 68, no. 6, pp. 394–424, 2018.
- [2] P. Kumar and R. Aggarwal, "An overview of triple-negative breast cancer," *Archives of Gynecology and Obstetrics*, vol. 293, no. 2, pp. 247–269, 2016.
- [3] A. C. Garrido-Castro, N. U. Lin, and K. Polyak, "Insights into molecular classifications of triple-negative breast cancer: improving patient selection for treatment," *Cancer Discovery*, vol. 9, no. 2, pp. 176–198, 2019.
- [4] J. M. Lebert, R. Lebert, E. Powell, M. Seal, and J. McCarthy, "Advances in the systemic treatment of triple-negative breast cancer," *Current Oncology*, vol. 25, pp. S142–S150, 2018.
- [5] S. Peter, A. Sylvia, H. S. Rugo et al., "Atezolizumab and nab-paclitaxel in advanced triple-negative breast cancer," *The New England Journal of Medicine*, vol. 379, no. 22, pp. 2108–2121, 2018.
- [6] E. L. Mayer and H. J. Burstein, "Chemotherapy for triple-negative breast cancer: is more better?" *Journal of Clinical Oncology*, vol. 34, no. 28, pp. 3369–3371, 2016.
- [7] P. Khosravi-Shahi, L. Cabezón-Gutiérrez, and A. M. I. Salcedo, "State of art of advanced triple negative breast cancer," *The Breast Journal*, vol. 25, no. 5, pp. 967–970, 2019.
- [8] J. Chen, Y. Qin, C. Sun et al., "Clinical study on postoperative triple-negative breast cancer with Chinese medicine: study protocol for an observational cohort trial," *Medicine*, vol. 97, no. 25, Article ID e11061, 2018.
- [9] H. Meng, N. Peng, M. Yu et al., "Treatment of triple-negative breast cancer with Chinese herbal medicine: a prospective cohort study protocol," *Medicine*, vol. 96, no. 44, Article ID e8408, 2017.
- [10] Z. D. Y. Screening, *Mechanisms of Anti-triple Negative Breast Cancer Activity of Natural Product from Ginkgo Biloba Sarcotestas*, Shenyang Agricultural University, Shenyang, China, 2018.
- [11] J. Ru, P. Li, J. Wei et al., "TCMSP: a database of systems pharmacology for drug discovery from herbal medicines," *Journal of Cheminformatics*, vol. 6, p. 13, 2014.
- [12] L. Huang, D. Xie, Y. Yu et al., "TCMID 2.0: a comprehensive resource for TCM," *Nucleic Acids Research*, vol. 46, pp. D1117–D1120, 2018.
- [13] S. Fishilevich, S. Zimmerman, A. Kohn et al., "Genic insights from integrated human proteomics in GeneCards," *Database: The Journal of Biological Databases and Curation*, vol. 2016, p. baw030, 2016.
- [14] J. S. Amberger, C. A. Bocchini, F. Schiettecatte, A. F. Scott, and A. Hamosh, "OMIM org: online Mendelian Inheritance in Man (OMIM®), an online catalog of human genes and genetic disorders," *Nucleic Acids Research*, vol. 43, pp. D789–D798, 2015.
- [15] D. Y. Wang, Z. Jiang, B.-D. Yaacov, J. R. Woodgett, and E. Zacksenhaus, "Molecular stratification within triple-negative breast cancer subtypes," *Scientific Reports*, vol. 9, no. 1, Article ID 19107, 2019.
- [16] X. Li, J. Yang, L. Peng et al., "Triple-negative breast cancer has worse overall survival and cause-specific survival than non-triple-negative breast cancer," *Breast Cancer Research and Treatment*, vol. 161, no. 2, pp. 279–287, 2017.
- [17] Y. Cheng, Y. Guan, J. Wang et al., "Platinum-based chemotherapy in advanced triple-negative breast cancer: a multicenter real-world study in China," *International Journal of Cancer*, vol. 147, 2020.
- [18] L. Y. Xia, Q. L. Hu, J. Zhang, W. Y. Xu, and X. S. Li, "Survival outcomes of neoadjuvant versus adjuvant chemotherapy in triple-negative breast cancer: a meta-analysis of 36,480 cases," *World Journal of Surgical Oncology*, vol. 18, no. 1, p. 129, 2020.
- [19] A. K. Tzikas, S. Nemes, and Linderholm, "A comparison between young and old patients with triple-negative breast cancer: biology, survival and metastatic patterns," *Breast Cancer Research And Treatment*, vol. 182, no. 3, pp. 643–654, 2020.
- [20] R. Oun, Y. E. Moussa, and N. J. Wheate, "The side effects of platinum-based chemotherapy drugs: a review for chemists," *Dalton Transactions*, vol. 47, no. 19, pp. 6645–6653, 2018.
- [21] S. Y. Park, J. H. Choi, and J. S. Nam, "Targeting cancer stem cells in triple-negative breast cancer," *Cancers*, vol. 11, no. 7, 2019.
- [22] B. Duan, L. Han, S. Ming et al., "FUling-guizhi herb pair in coronary heart disease: integrating network pharmacology and in vivo pharmacological evaluation," *Evidence-based Complementary and Alternative Medicine*, vol. 2020, Article ID 1489036, 10 pages, 2020.
- [23] C. Fan, F. R. Wu, J. F. Zhang, and H. Jiang, "A network pharmacology approach to explore the mechanisms of shugan jianpi formula in liver fibrosis," *Evidence-Based Complementary and Alternative Medicine*, vol. 2020, Article ID 4780383, 13 pages, 2020.

- [24] Z. Zhuang, Q. Chen, C. Huang, J. Wen, H. Huan, and Z. Liu, "A comprehensive network pharmacology-based strategy to investigate multiple mechanisms of HeChan tablet on lung cancer," *Evidence-based Complementary and Alternative Medicine*, vol. 2020, Article ID 7658342, 17 pages, 2020.
- [25] L. Yang, L. Yong, X. Zhu et al., "Disease progression model of 4T1 metastatic breast cancer," *Journal Of Pharmacokinetics and Pharmacodynamics*, vol. 47, no. 1, pp. 105–116, 2020.
- [26] J. Steenbrugge, V. N. Elast, K. Demeyere et al., "Comparative profiling of metastatic 4T1-vs. Non-metastatic py230-based mammary tumors in an intraductal model for triple-negative breast cancer," *Frontiers in Immunology*, vol. 10, p. 2928, 2019.
- [27] D. J. Liao and R. B. Dickson, "c-Myc in breast cancer," *Endocrine-Related Cancer*, vol. 7, no. 3, pp. 143–164, 2000.
- [28] A. Dalal, E. Kavanagh, S. O'Grady et al., "The novel low molecular weight MYC antagonist MYCMI-6 inhibits proliferation and induces apoptosis in breast cancer cells," *Investigational New Drugs*, vol. 102, 2020.
- [29] Y. Liu, H. Song, S. Yu et al., "Protein Kinase D3 promotes the cell proliferation by activating the ERK1/c-MYC axis in breast cancer," *Journal Of Cellular And Molecular Medicine*, vol. 24, no. 3, pp. 2135–2144, 2020.
- [30] O. Wang, F. Yang, Y. Liu et al., "C-MYC-induced upregulation of lncRNA SNHG12 regulates cell proliferation, apoptosis and migration in triple-negative breast cancer," *American Journal of Translational Research*, vol. 9, no. 2, pp. 533–545, 2017.
- [31] J. Du, J. J. Fan, C. Dong, H. T. Li, and B. L. Ma, "Inhibition effect of exosomes-mediated Let-7a on the development and metastasis of triple negative breast cancer by down-regulating the expression of c-Myc," *European Review for Medical and Pharmacological Sciences*, vol. 23, no. 12, pp. 5301–5314, 2019.
- [32] J. Wang, M. Li, D. Chen et al., "Expression of C-myc and β -catenin and their correlation in triple negative breast cancer," *Minerva Medica*, vol. 108, no. 6, pp. 513–517, 2017.
- [33] Y. Cai, B. Zhao, Q. Liang, Y. Zhang, J. Cai, and G. Li, "The selective effect of glycyrrhizin and glycyrrhetic acid on topoisomerase II α and apoptosis in combination with etoposide on triple negative breast cancer MDA-MB-231 cells," *European Journal Of Pharmacology*, vol. 809, pp. 87–97, 2017.
- [34] J. Wang, H. Qi, X. Zhang et al., "Saikosaponin D from Radix Bupleuri suppresses triple-negative breast cancer cell growth by targeting β -catenin signaling," *Biomedicine & Pharmacotherapy = Biomedecine & Pharmacotherapie*, vol. 108, pp. 724–733, 2018.
- [35] S. B. Coffelt, K. Kersten, C. W. Doornebal et al., "IL-17-producing $\gamma\delta$ T cells and neutrophils conspire to promote breast cancer metastasis," *Nature*, vol. 522, no. 7556, pp. 345–348, 2015.
- [36] R. Courtney, D. C. Ngo, N. Malik, K. Ververis, S. M. Tortorella, and T. C. Karagiannis, "Cancer metabolism and the Warburg effect: the role of HIF-1 and PI3K," *Molecular Biology Reports*, vol. 42, no. 4, pp. 841–851, 2015.
- [37] L. Schlicher, M. Wissler, F. Preiss et al., "SPATA2 promotes CYLD activity and regulates TNF-induced NF- κ B signaling and cell death," *EMBO Reports*, vol. 17, no. 10, pp. 1485–1497, 2016.
- [38] N. Kachamakova-Trojanowska, P. Podkalicka, T. Barwacz et al., "HIF-1 stabilization exerts anticancer effects in breast cancer cells in vitro and in vivo," *Biochemical Pharmacology*, vol. 175, Article ID 113922, 2020.
- [39] C. Y. Kuo, C. T. Cheng, P. Hou et al., "HIF-1-alpha links mitochondrial perturbation to the dynamic acquisition of breast cancer tumorigenicity," *Oncotarget*, vol. 7, no. 23, pp. 34052–34069, 2016.
- [40] G. L. Semenza, "Targeting HIF-1 for cancer therapy," *Nature Reviews Cancer*, vol. 3, no. 10, pp. 721–732, 2003.
- [41] F. Agani and B. H. Jiang, "Oxygen-independent regulation of HIF-1: novel involvement of PI3K/AKT/mTOR pathway in cancer," *Current Cancer Drug Targets*, vol. 13, no. 3, pp. 245–251, 2013.
- [42] B. Muz, P. de la Puente, F. Azab, and A. K. Azab, "The role of hypoxia in cancer progression, angiogenesis, metastasis, and resistance to therapy," *Hypoxia*, vol. 3, pp. 83–92, 2015.
- [43] A. M. Shannon, D. J. Bouchier-Hayes, C. M. Condrin, and D. Toomey, "Tumour hypoxia, chemotherapeutic resistance and hypoxia-related therapies," *Cancer Treatment Reviews*, vol. 29, no. 4, pp. 297–307, 2003.

Research Article

Berberine Inhibits the Expression of SCT through miR-214-3p Stimulation in Breast Cancer Cells

Congyuan Zhu , Jianping Li , Yuming Hua , Jingli Wang, Ke Wang ,
and Jingqiu Sun 

Department of General Surgery, The Affiliated Hospital of Jiangnan University, Wuxi Third People's Hospital, Wuxi, Jiangsu 214002, China

Correspondence should be addressed to Congyuan Zhu; brlx12001@sohu.com

Received 9 July 2020; Revised 21 September 2020; Accepted 24 October 2020; Published 29 November 2020

Academic Editor: Azis Saifudin

Copyright © 2020 Congyuan Zhu et al. This is an open access article distributed under the Creative Commons Attribution License, which permits unrestricted use, distribution, and reproduction in any medium, provided the original work is properly cited.

In this study, we aimed to evaluate the suppressive abilities of berberine (BBR) on MCF-7 and MDA-MB-231 cells and confirm its underlying mechanisms on miR-214-3p. We first built a panel of 18 miRNAs and 9 lncRNAs that were reported to participate in the mechanism of breast cancer. The RT-qPCR results suggested that BBR illustrated a dosage-dependent pattern in the stimulation to miR-214-3p in both MCF-7 and MDA-MB-231 cells. Then, we performed gain-and-lose function tests to validate the role of miR-214-3p contributing to the anticancer effects of BBR. Both BBR and miR-214-3p mimic reduced the cell viability, repressed migration and invasion capacities, increased rates of total apoptotic cells and ratio of Bax/Bcl-2, and increased the percentage of G2/M cells of MCF-7 and MDA-MB-231 cells by colony formation and CKK8 assay, scratch wound healing and gelatin-based 3D conformation assay, transwell invasion assay, and cell cycle analysis, respectively. However, miR-214-3p inhibitor counteracted all these effects of BBR. Based on the bioinformatics analysis and dual-luciferase reporter test, we identified binding sites between SCT and miR-214-3p. We further confirmed that BBR massively and dose-dependently reduced the mRNA expression and protein levels of SCT in both MCF-7 and MDA-231 cells. We testified that both miR-214-3p mimic and BBR could decrease the mRNA expression and protein levels of SCT, while miR-214-3p inhibitor weakened these reductions. In conclusion, BBR suppressed MCF-7 and MDA-MB-231 breast cancer cells by upregulating miR-214-3p and increasing its inhibition to SCT.

1. Introduction

Based on the results of epidemiological investigation, it has been reported that breast cancer is becoming one of the major types of cancer and contributes to the highest mortality rate in gynecologic malignancies [1]. Currently, the mainstream treatments of breast cancer are regional avenues, including radiation and surgery and general tools like chemotherapy and biologic therapies [2]. In order to improve the management of breast cancer, it is necessary to exploit novel therapeutic target.

Noncoding RNA, including microRNA (miRNA) and long noncoding RNA (lncRNA), participate in various biological processes [3]. Both miRNAs and lncRNAs related to human cancers are referred to as “oncomirs” [4], which are identified as two types: (i) miRNAs or lncRNAs called

oncogenes are upregulated or amplified in cancer; (ii) miRNAs or lncRNAs called suppressors are downregulated or deleted in cancer [5]. A handful of miRNAs and lncRNAs, such as miR-101 [6], miR-21 [7], miR-155 [8], lncRNA-H19 [9], lncRNA-SNHG6 [10], and lncRNA-TALNEC2 [11], are considered to participate in the mechanism of proliferation, invasion, apoptosis, and molecular signaling in breast cancer. Therefore, these small regulatory miRNAs work as novel targets for anticancer therapeutic strategies.

The chemical name of berberine (BBR) is 2,3-methylenedioxy-9,10-dimethoxyprotoberberine chloride. BBR is a kind of isoquinoline alkaloid that is extracted from *Coptidis Rhizoma* or *Huanglian*. BBR has been proved to possess numerous protective properties, like antimicrobial, cardioprotective, and antidiabetic activities [12, 13]. Among these properties, anticancer activity of BBR has been widely

accepted. BBR shows anticancer activity in plenty of cancers, including breast cancers [14]. It is believed that BBR moderates mitochondria and pathway of caspase to induce the apoptosis of breast cancer cells [15]. However, how miRNA regulation plays a role in the inhibition of breast cancer cells by BBR to is still under ambiguous.

In this study, we first made a panel of 18 miRNAs [6–8, 16–30] and 9 lncRNAs [9, 10, 15, 29–34] that were previously reported to be related with breast cancer. Then, based on a series of tests, we identified miR-214-3p as the crucial miRNA mediating in the antitumor effects of BBR in MCF-7 and MDA-MB-231 breast cancer cells. Furthermore, according to target scan software and a series of tests, we ensured that BBR promoted miR-214-3p expression and suppressed the protein expression of its targets secretin (SCT).

2. Materials and Methods

2.1. Cell Culture. Two human breast cancer cell lines (MCF-7 and MDA-MB-231) were purchased from Chinese Academy of Sciences cell bank (Shanghai, China). The cells were cultured in RPMI-1640 medium (Gibco, Thermo) supplemented with 10% fetal bovine serum (Gibco, Thermo) and incubated in an atmosphere of 37°C humidified and 5% CO₂.

2.2. Introduction of Plasmids and siRNA into Cells. Lipofectamine® 3000 (Thermo Fisher Scientific, Inc.) was used to transfect the plasmids into cells in accordance with the protocols. Reagent of miR-214-3p mimic or miR-214-3p inhibitor (Guangzhou RiboBio Co., Ltd.) was employed to up- or downregulate the levels of miR-214-3p in 6-well plates with a density of 2×10^5 cells in each well. The negative control (NC) was manipulated by a scrambled miRNA.

2.3. Cell Proliferation Assay. We used the Cell Counting Kit 8 (CCK8, Beyotime, China) assay and colony formation assay to estimate the effect of BBR on cell proliferation. Briefly, 7×10^3 cells/well were seeded in 96-well plates and treated with BBR (HPLC $\geq 99\%$, purchased from Meilun Biologics, Dalian China). After 72 h of incubation, a microplate reader was used at a 450 nm optical density to test the viability of each group cells. In colony formation assay, cells were placed into 6-well plates and maintained in media for two weeks and fixed by methanol and stained by 0.1% crystal violet (Sigma, USA) for 20 min.

2.4. Cell Migration and Invasion Assay. The activity of cell migration was evaluated by scratch wound healing assay and gelatin-based 3D conformation assay. In scratch wound healing assay, a sterile tip was used to scratch each well to form a thin “wound.” Before adding the serum-free medium, PBS was manipulated to wash the floating cells. At 0 and 12 h after cell recovery, Image-Pro Plus software was manipulated for measuring cell migration distance, and the data were averaged. In gelatin-based 3D conformation assay,

fully-formed 3D structures were transferred to 0.1% gelatin-coated plates and treated with BBR or miR-214-3p mimic or miR-214-3p inhibitor. The migration levels were evaluated after 24 and 48 h. The medium containing 2% FBS was employed to reduce influence of cell proliferation in this test. 3D structures were imaged by microscope Nikon Eclipse TS 110 and quantified by ImageJ software. The migration index was calculated by the area of cells migrating outwards the 3D structure.

Invasion activities of MCF-7 and MDA-MB-231 cells were analyzed by using transwell invasion assay. On the upper surface of the membrane, the chambers were coated with Matrigel (1 : 5; 80 μ l/well, BD Biosciences). DMEM with 10% FBS was added to the lower chamber. After 24 h incubation, 4% paraformaldehyde was used to fix the upper chambers for 10 min. Then, it was stained by crystal violet. The microscope (Olympus) was used to count the numbers of passed cells.

2.5. Apoptosis Assay and Cell Cycle Analysis. The levels of apoptosis were measured by annexin-V and propidium iodide (PI) staining as previously described [35]. Cells were seeded to 6-well plate and treated with DMSO, BBR, miR-214-3p mimic, or BBR with miR-214-3p inhibitor. After 24 h, cells were harvested and stained with annexin-V and propidium iodide for 20 min and then run on a BD FACSCanto II cell analyser (BD Biosciences, USA). At least 10000 single cell events were acquired per sample and analyzed by FlowJo software v10.5.0 (FlowJo, USA).

The methods of cell cycle analysis were performed according to previous report [36]. Cells were seeded to 6-well plate and treated with DMSO, BBR, miR-214-3p mimic, or BBR with miR-214-3p inhibitor. After 24 h, cells were resuspended in ice-cold Dulbecco’s phosphate buffered saline (DPBS) with 70% ethanol. Cells were centrifuged at 300 $\times g$ for 5 min and resuspended in DPBS. After 2 h staining of propidium iodide and bovine pancreas ribonuclease, cells were run in BD FACSCanto II cell analyser (BD Biosciences, USA). 50000 single cell events were captured per sample and analysed by FlowJo software v10.5.0 (FlowJo, USA).

2.6. Detection of miRNAs and lncRNAs. We used TRIzol reagent (Invitrogen, CA) to extract total RNA of MCF-7 and MDA-MB-231 cells in each group. SYBR Green PCR kit (Thermo) was used for PCR amplification. Each sample was provided with three repeated holes. Internal reference of GAPDH was manipulated to adjusting and the data of mRNA expression were calculated by the $2^{-\Delta\Delta Ct}$ method. Primer sequences were shown in Table 1.

2.7. Protein Detection of Levels of SCT. The total protein of MCF-7 and MDA-MB-231 cells was extracted with RIPA lysis method. The protein concentration of each well was detected with a BCA method. Protein content was adjusted to 4 μ g/ μ l, 12% SDS-PAGE electrophoresis separation was carried out, and the membrane was transferred to PVDF membranes after ionization. Staining was carried out with Ponceau working solution. The antibodies of GAPDH

TABLE 1: Primer sequences.

	Forward	Reverse
miR-101	5'-UACAGUACUGUGUAUACUGAA-3'	5'-CAGUUAUCACAGUACUGUAUU-3'
miR-21	5'-CGCGCTAGCTTATCAGACTGA-3'	5'-GTGCAGGGTCCGAGGT-3'
miR-155-3p	5'-CCACAGGTGATGGGCAGAAT-3'	5'-TTCCTGTGGGGGATCGGTAT-3'
miR-381	5'-CCAGAUUGUAAGUGGUACCGUU-3'	5'-CUCUACACCGAACUAUAUCAGU-3'
miR-216b-5p	5'-CCTGGCGTCGTGATTAGTG-3'	5'-TCAGTCCTGTCCATAATTAGCC-3'
miR-205-3p	5-GAGGATCCCCGGGTACCGGTAGGCCTTT-3'	5'-CACACATTCCACAGGCTGCTACGGTGGTGGCGT-3'
miR-200c	5'-GGGAACACACCTGGTTAAC-3'	5'-CAGTGCCTGTCGTGGAGT-3'
miR-188-5p	5'-GCC CAT CCC TTG CAT GGT-3'	5'-AGT GCA GGGTCCGAG GTATT-3'
miR-214-3p	5'-GCACAGCAGGCACAGACA-3'	5'-CAGAGCAGGGTCAGCGGTA-3'
miR-616	5'-ACACTC CAGCTGGGAGTCATTGGAGGGTTT-3'	5'-TGGTGTCTGGAGTCCG -3'
miR-129-5p	5'-AATCTAGAA CCCTGCCTGTGGTCTCTGA-3'	5'-AACTCTAGA AGAGAGTCCCTAGT-3'
miR-26a-5p	5'-AGAAGATGGCA GCAAGAGCG-3'	5'-TCAAGTCAGGCTGAGATGCTAGT-3'
miR-203a	5'-TTGGATCACAGCGATACAAACTT-3'	5'-AGCGCACGCCAATAAAGACAT-3'
miR-7	5'-AAAAGAACACGTGGAAGGATG-3'	5'-CGCCTAACGTACCGCGAATTT-3'
miR-211-5p	5'-CCCTTTGTCATCCTTCGCCT-3'	5'-GCGAGCACAGAATTAATACGACTC-3'
miR-138-5p	5'-TGCAAT GGGTTTGGCGTAGAAC-3'	5'-CCAGTGCCG CAGGGTAGGT-3'
miR-186-5p	5'-CCCGA TAAAGCTAGATAACC-3'	5'-CAGTGCCT GTCGTGGAGT-3'
LINC02582	5'-ATCAACAGCCAACAAATACC-3'	5'-TTCTTATCACCGTCACCCT-3'
SNHG3	5'-TTCCGGGCGTTACTTAAGG-3'	5'-GGTCAAGAACAAGCACACCAA-3'
AC073284.4	5'-TCATGGCTCACTGCAGCCTC-3'	5'-TGGGAGGCCAAGGTGACAGA-3'
H19	5'-ATCGGTGCCTCAGCGTTCGG-3'	5'-CTGTCTCGCCGTCAACCCG-3'
Lnc101069	5'-GCTTAGAAATTTCTTCCACCTG-3'	5'-CTGCCCTAGCGATTGTGAA-3'
DRHC	5'-CAGTGGGAACCTCTGACT CG-3'	5'-GTGCCTGGTGTCT CTCTTACC-3'
RUNXOR	5'-ATGTTTAGTATTTTAAATGATGGGATT-3'	5'-ACCTACCCTCCCCAAAATATAC-3'
LINC01287	5'-CCGCATCCAAACCTACATACTAACCC-3'	5'-CGACCGAAAAAATTCATTCCCTCAA-3'
SNHG6	5'-TTGGGATGTTGATAGTTTTAGATGGAGGT-3'	5'-AATAAATCCATCCCTCATAACRA-3'
GAPDH	5'-GGGAGCCAAAAGGGTCAT-3'	5'-GAGTCCTTCCACGATACCAA-3'

(Sigma no. 2275-PC-020) and SCT (Sigma no. AF6387-SP) were diluted to 1 : 5000 and 1 : 1000, respectively. The diluents were added to be sealed overnight at 4°C. Quantity One software was employed to analyze the gray value of scanned protein bands. The relative expression was equal to the ratio of target protein gray value and GAPDH gray value.

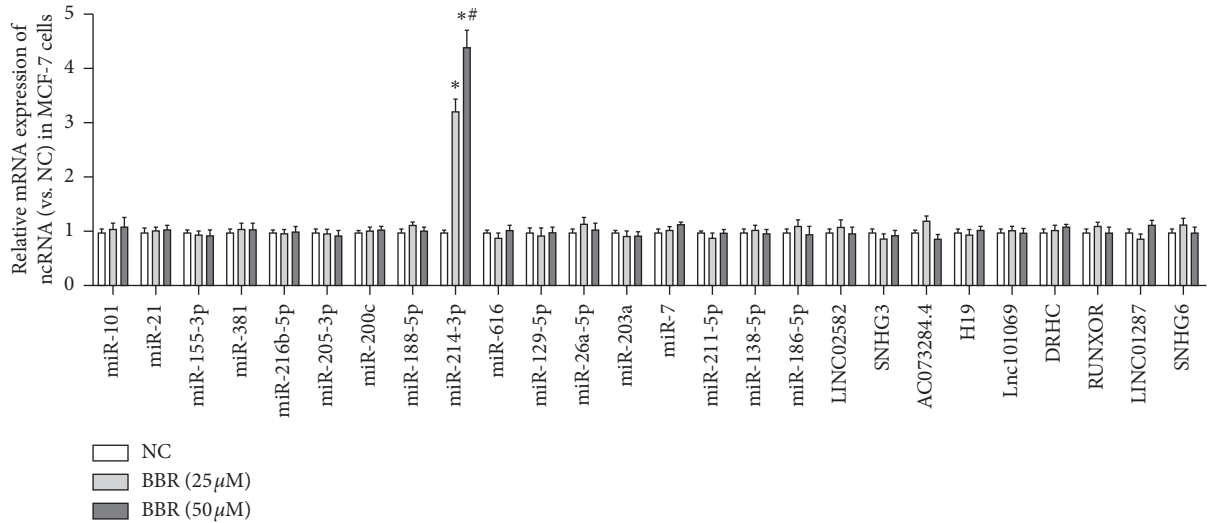
2.8. Prediction of Target Genes. Targetscan7.2 and miRwalk were used to predict downstream target gene of miR-214-3p. Reporter gene plasmids containing wild-type and mutant SCT 3'UTR, psiCHECK-2 plasmids (Promega, C8021, USA), miR-214-3p mimic, and their controls were transfected into MCF-7 and MDA-MB-231 cells for 48 hours and then used. Dual-luciferase reporter gene detection kits were used for operation. Finally, collected cells were detected by chemiluminescence. Three repetitions were designed for each group of experiments, and each experiment was repeated for three times.

2.9. Statistical Analysis. The data were analyzed by SPSS 20.0 software and the results were drawn by Graph Prism 8.0. All the data were expressed as mean \pm standard deviation (SD \pm means). The comparisons of each group were calculated by Student's *t*-test or one-way ANOVA methods. When $p < 0.05$, there were statistical differences.

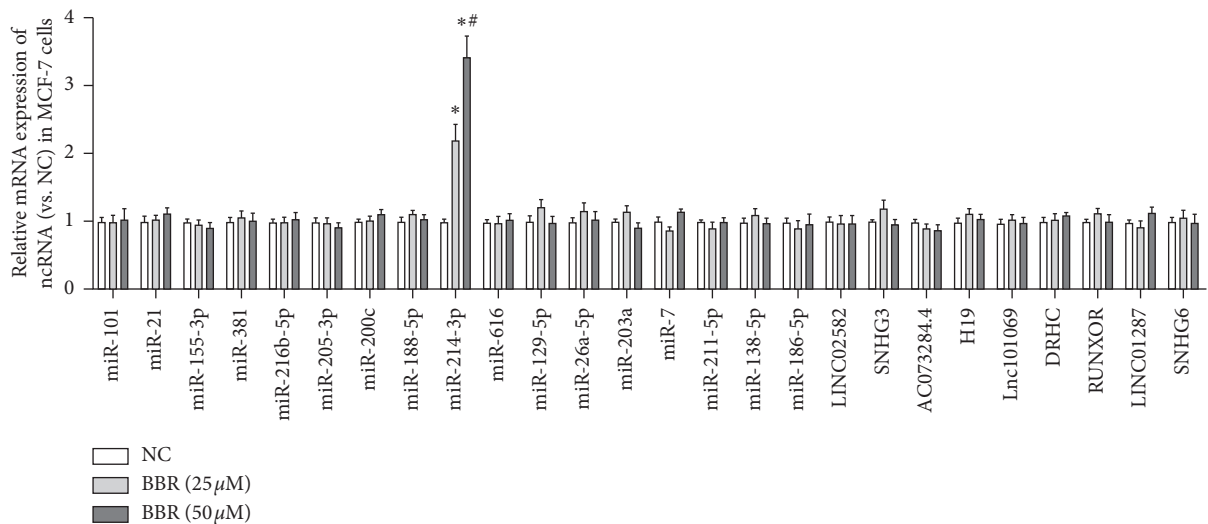
3. Results

3.1. BBR Can Obviously Increase the Expression of miR-214-3p in Both MCF-7 and MDA-MB-231 Cells. We first built a panel of 18 miRNAs and 9 lncRNAs that were reported to participate in the mechanism of breast cancer. The RT-qPCR results suggested that BBR illustrated a dosage-dependent pattern in the stimulation to miR-214-3p in both MCF-7 and MDA-MB-231 cells (Figure 1).

3.2. BBR Upregulates miR-214-3p Expression to Repress Cell Growth, Invasion, and Migration. Then, we performed gain-and-lose function tests to validate the role of miR-214-3p contributing to the anticancer effects of BBR on MCF-7 and MDA-MB-231 cells. The transfection efficiency was confirmed by RT-qPCR (Figure 2(a)). The results of colony formation assay demonstrated that both BBR treatment and miR-214-3p mimic could reduce the colony numbers of MCF-7 cells by 56.62% and 60.33% and MDA-MB-231 cells by 50.42% and 56.21%, respectively (Figure 2(b)). CKK8 assay showed that both BBR treatment and miR-214-3p mimic could reduce the cell viability of MCF-7 cells by 35.4% and 27.4% and MDA-MB-231 cells by 27.4% and 11.5%, respectively (Figure 2(c)). These results indicated that both BBR treatment and miR-214-3p mimic could inhibit the proliferation of MCF-7 and MDA-MB-231 cells. Scratch wound healing assay (Figure 3) and gelatin-based 3D



(a)



(b)

FIGURE 1: BBR increases the levels of miR-214-3p in both MCF-7 and MDA-MB-231 cells. RT-qPCR results suggested that BBR illustrated a dosage-dependent pattern in the stimulation of miR-214-3p in both MCF-7 and MDA-MB-231 cells in a panel of 18 miRNAs and 9 lncRNAs that were reported to participate in the mechanism of breast cancer. * $p < 0.05$ vs. NC group. # $p < 0.05$ vs. BBR (25μm) group.

conformation assay (Figure 4) suggested that both BBR treatment and miR-214-3p mimic could repress the migration capacities of MCF-7 and MDA-MB-231 cells. It was observed that both BBR and miR-214-3p mimic prevented the invasion capacities of MCF-7 and MDA-MB-231 cells by transwell invasion assay (Figure 5). However, miR-214-3p inhibitor counteracted all these suppressions of BBR treatment (Figures 2–5).

3.3. BBR Upregulates miR-214-3p Expression to Induce Cell Apoptosis and G2/M Arrest. After BBR and miR-214-3p mimic administration, there were significant increases of 8.3-fold and 6.9-fold in the rates of total apoptotic cells in MCF-7 cells and 6.3-fold and 4.8-fold in MDA-MB-231 cells, respectively (Figure 6(a)). BBR and miR-214-3p mimic treatment increased the ratio of Bax/Bcl-2 by 4.8-fold and

3.1-fold in MCF-7 cells and by 3.9-fold and 3.2-fold in MDA-MB-231 cells, respectively (Figure 6(b)). All these indicated that both BBR and miR-214-3p mimic induce apoptosis of breast cancer cells. Cell cycle analysis was employed to compare the levels of cell combination dose induced by cell loss. The results indicated that BBR and miR-214-3p mimic administration could increase the percentage of G2/M cells by 20% and 17% in MCF-7 cells and by 13% and 9% in MDA-MB-231 cells, respectively (Figure 7). However, miR-214-3p inhibitor counteracted all these stimulations of BBR treatment (Figures 6 and 7).

3.4. BBR Promotes miR-214-3p Expression and Represses Protein Expression of Its Targets SCT. Based on the TargetsCan7.2 and miRwalk bioinformatics analysis, it was identified that SCT and miR-214-3p had targeted binding

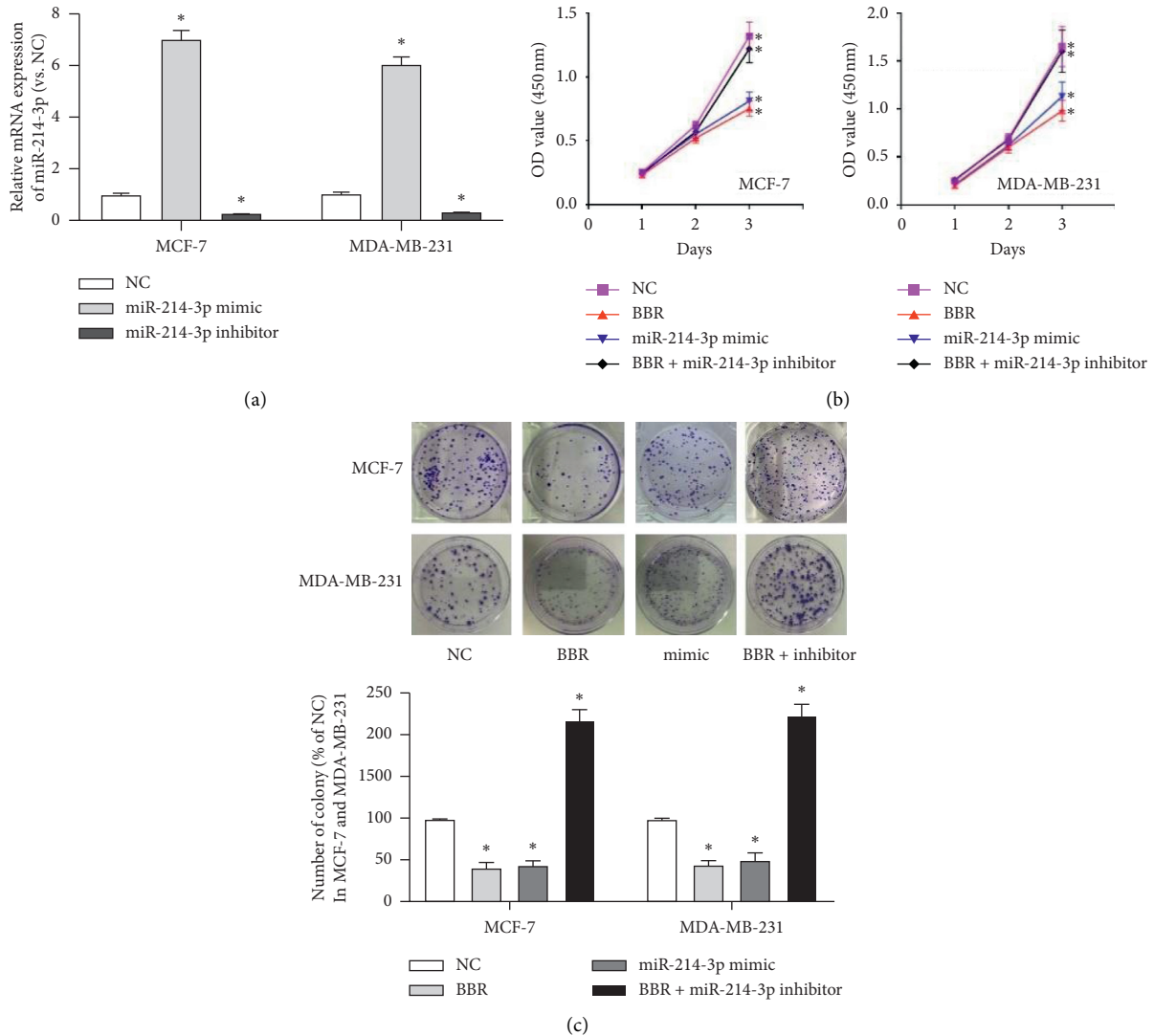


FIGURE 2: Transfection efficiency and proliferation evaluation. (a) The transfection efficiency was confirmed by RT-qPCR. (b) Colony formation assay demonstrated that both BBR treatment and miR-214-3p mimic could reduce the colony numbers of MCF-7 cells by 56.62% and 60.33% and MDA-MB-231 cells by 50.42% and 56.21%, respectively. (c) CCK8 assay showed that both BBR treatment and miR-214-3p mimic could reduce the cell viability of MCF-7 cells by 35.4% and 27.4%, and MDA-MB-231 cells by 27.4% and 11.5%, respectively. * $p < 0.05$ vs. NC group. # $p < 0.05$ vs. BBR group.

sites (Figures 8(a) and 8(b)). So, we first verified it by dual-luciferase reporter. Activity of luciferase in miR-214-3p mimic group in psiCHECK-2-SCT-WT was obviously lower than that of independent sequence group ($p < 0.05$), while activity of luciferase in miR-214-3p mimic group in psiCHECK-2-SCT-MUT group was not significantly different from that of independent sequence group ($p > 0.05$) (Figure 8(c)). Then, to ensure the assumption that BBR could promote miR-214-3p expression and suppress the protein expression of its targets SCT, we further confirmed that BBR could massively and dose-dependently reduce the mRNA expression and protein levels of SCT in both MCF-7 and MDA-231 cells ($p < 0.05$) (Figures 8(d) and 8(e)). Next, we testified that both miR-214-3p mimic and BBR could decrease the mRNA expression and protein levels of SCT, while miR-214-3p inhibitor weakened these reductions

(Figures 8(f) and 8(g)). These results indicated that BBR promoted miR-214-3p expression and repressed the protein expression of its targets SCT.

4. Discussion

BBR is a natural alkaloid mainly found in the famous Chinese herb *Coptidis Rhizoma*. In the beginning, BBR was used in treating diarrhea and gastroenteritis [37]. In subsequent studies, BBR was proved to possess other properties, for instance, antibiosis, cardioprotection, glucose regulation, and antineoplastic activity [12, 13, 35, 38]. In this study, it was found that BBR obviously suppressed the abilities of growth and invasiveness in both MCF-7 and MDA-MB-231 cells. These results were consistent with previous studies [39, 40]. Kim et al. found that berberine could efficiently

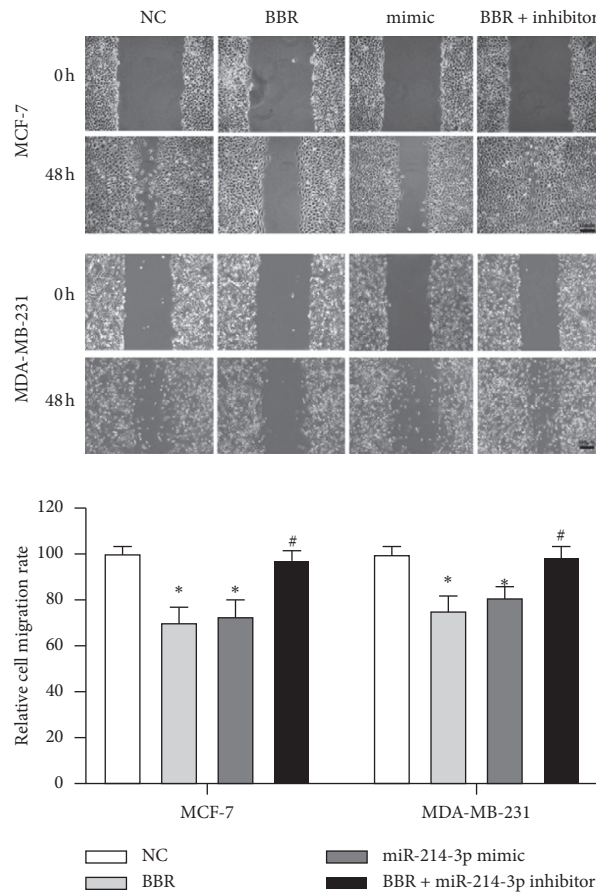


FIGURE 3: Scratch wound healing assays. MCF-7 and MDA-MB-231 cells were cultured in DMEM 0.1% FBS and treated with 50 μ M of BBR, miR-214-3p mimic, or miR-214-3p inhibitor for 48 h. Wound closure was monitored and calculated using the software ImageJ. * $p < 0.05$ vs. NC group. # $p < 0.05$ vs. BBR group.

inhibit growth by inducing cell cycle arrest in anoikis-resistant MCF-7 and MDA-MB-231 cells [39]. It was also indicated that the growth inhibitory effects of berberine treatment on MCF-7 cells might be partly due to the effects on side population cells and ABCG2 expression [40]. Further analysis of these phenotypes is essential for understanding the effect of berberine on anoikis-resistant breast cancer cells. Nonetheless, the antitumor mechanism of BBR in breast cancer cells still remains ambiguous.

In our investigation, the focus was to seek the key ncRNA and its target pathway in the antibreast cancer mechanism of BBR. We first listed a panel of 18 miRNAs [6–8, 16–30] and 9 lncRNAs [9, 10, 15, 29–34] that were previously reported to be related with breast cancer, and we found that BBR illustrated a dosage-dependent pattern in the stimulation to miR-214-3p in both MCF-7 and MDA-MB-231 cells. miRNA is one of the important regulators that act as a posttranscriptional suppression officer. Abnormal levels of miRNA could result in a diversity of regulation in diverse cellular pathways. There is a strong proof that some crucial miRNAs are involved in the progress of breast cancer [41]. To validate the role of miR-214-3p in the suppression of BBR to breast cancer cells, we performed a rescue test and observed that both BBR and miR-214-3p mimic could repress the abilities of growth, invasiveness, and migration in MCF-

7 and MDA-MB-231 cells, while miR-214-3p inhibitor counteracted these suppression. We also found that BBR upregulated miR-214-3p expression to induce cell apoptosis and G2/M arrest. These results indicated that BBR presented anticancer effects through miR-214-3p. Another study showed that lncRNATSLNC8 inhibited miR-214-3p/FOXP2 axis to suppress the proliferation and G1/S phase transition of breast cancer cells [42]. It has been reported that the expression of miR-214-3p is correlated with the proliferation and apoptosis of breast cancer cells [21] and acts as a breast tumor suppressor through the regulation of EMT [43]. In the fields of breast cancer, these studies have established that miR-214-3p had a vital role in the progress of breast cancer. Our results indicated that miR-214-3p was also the target of BBR to present anticancer effects.

Then, after using bioinformatics analysis and searching previous studies, we identified that SCT might be the downstream target of miR-214-3p. To confirm the assumption that BBR could promote miR-214-3p transcription and raise the suppression of its downstream target SCT, we first confirmed that BBR could dose-dependently reduce SCT in both levels of mRNA and protein. After that, we found that both miR-214-3p mimic and BBR repressed SCT mRNA and protein, while miR-214-3p inhibitor weakened these reductions. In physiological conditions, SCT binds to

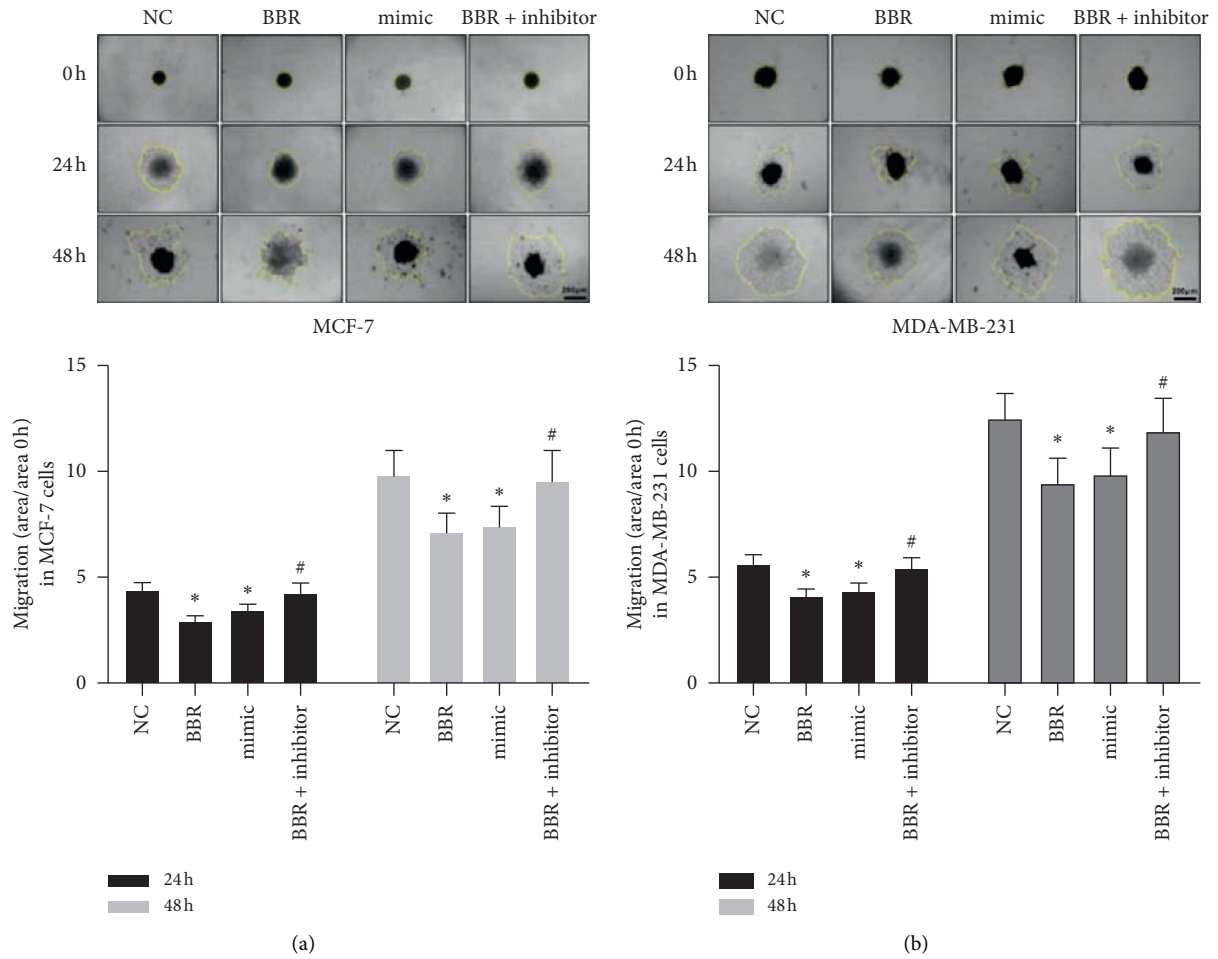


FIGURE 4: Gelatin-based 3D conformation assays. BBR treatment and miR-214-3p mimic could repress MCF-7 (a) and MDA-MB-231 (b) moving outwards from the 3D structures and being confined to the center region, where they were initially seeded. * $p < 0.05$ vs. NC group. # $p < 0.05$ vs. BBR group.

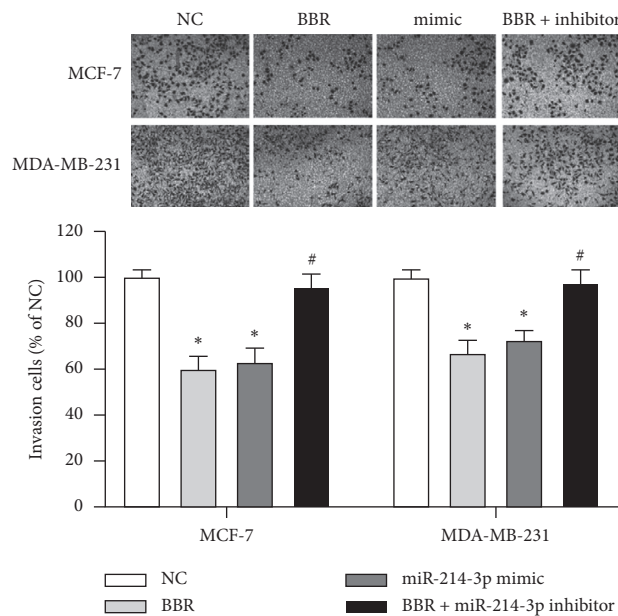


FIGURE 5: Transwell invasion assays. BBR and miR-214-3p mimic prevented the invasion capacities of MCF-7 and MDA-MB-231 cells. * $p < 0.05$ vs. NC group. # $p < 0.05$ vs. BBR group.

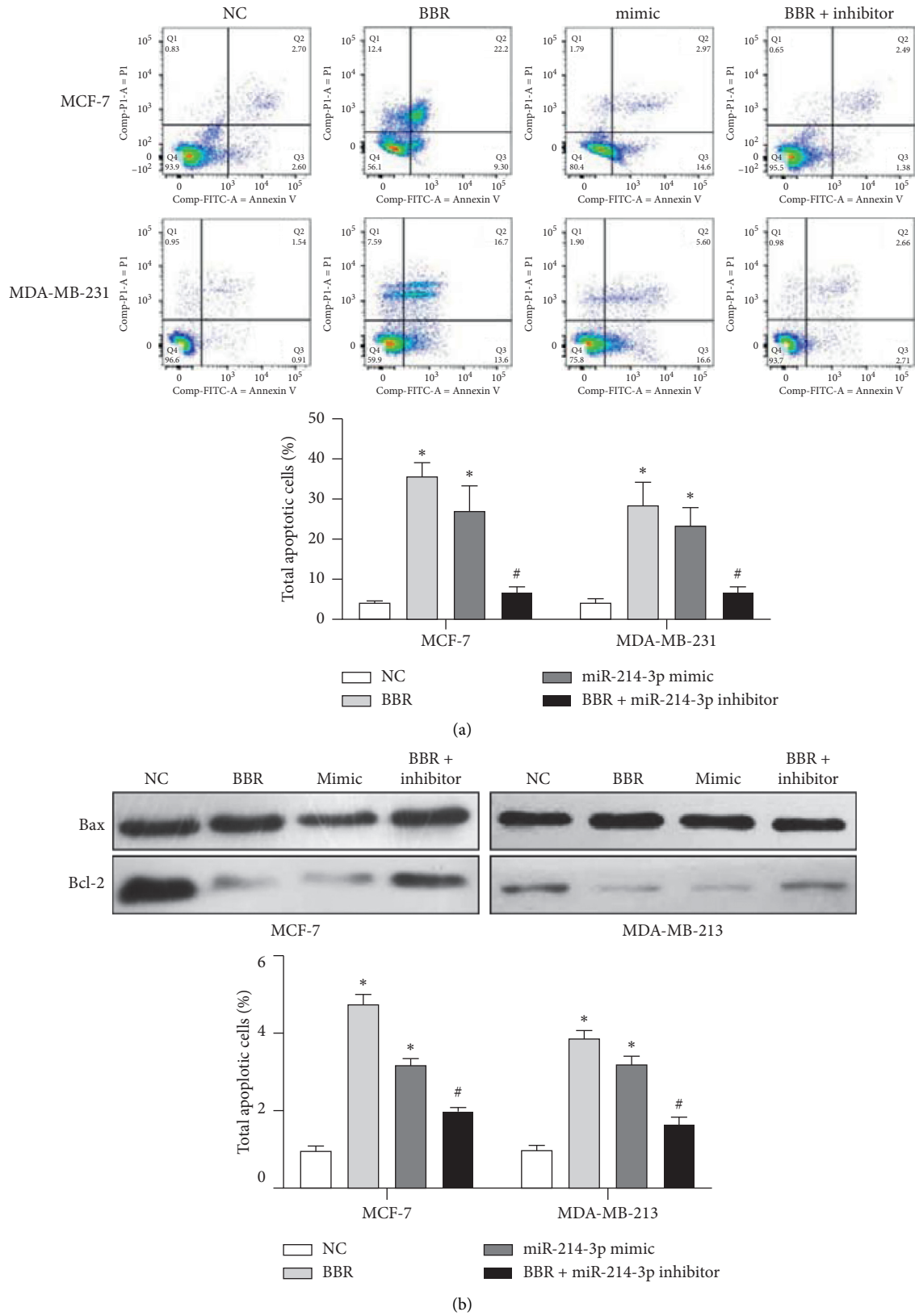


FIGURE 6: Cell apoptosis assays. (a) The total apoptotic cells and representative scatter plots. After BBR and miR-214-3p mimic administration, there were significant increases of 8.3-fold and 6.9-fold in the rates of total apoptotic cells in MCF-7 cells and 6.3-fold and 4.8-fold in MDA-MB-231 cells. (b) Western blot showed BBR and miR-214-3p mimic treatment increased the ratio of Bax/Bcl-2 by 4.8-fold and 3.1-fold in MCF-7 cells and by 3.9-fold and 3.2-fold in MDA-MB-231 cells. * $p < 0.05$ vs. NC group. # $p < 0.05$ vs. BBR group.

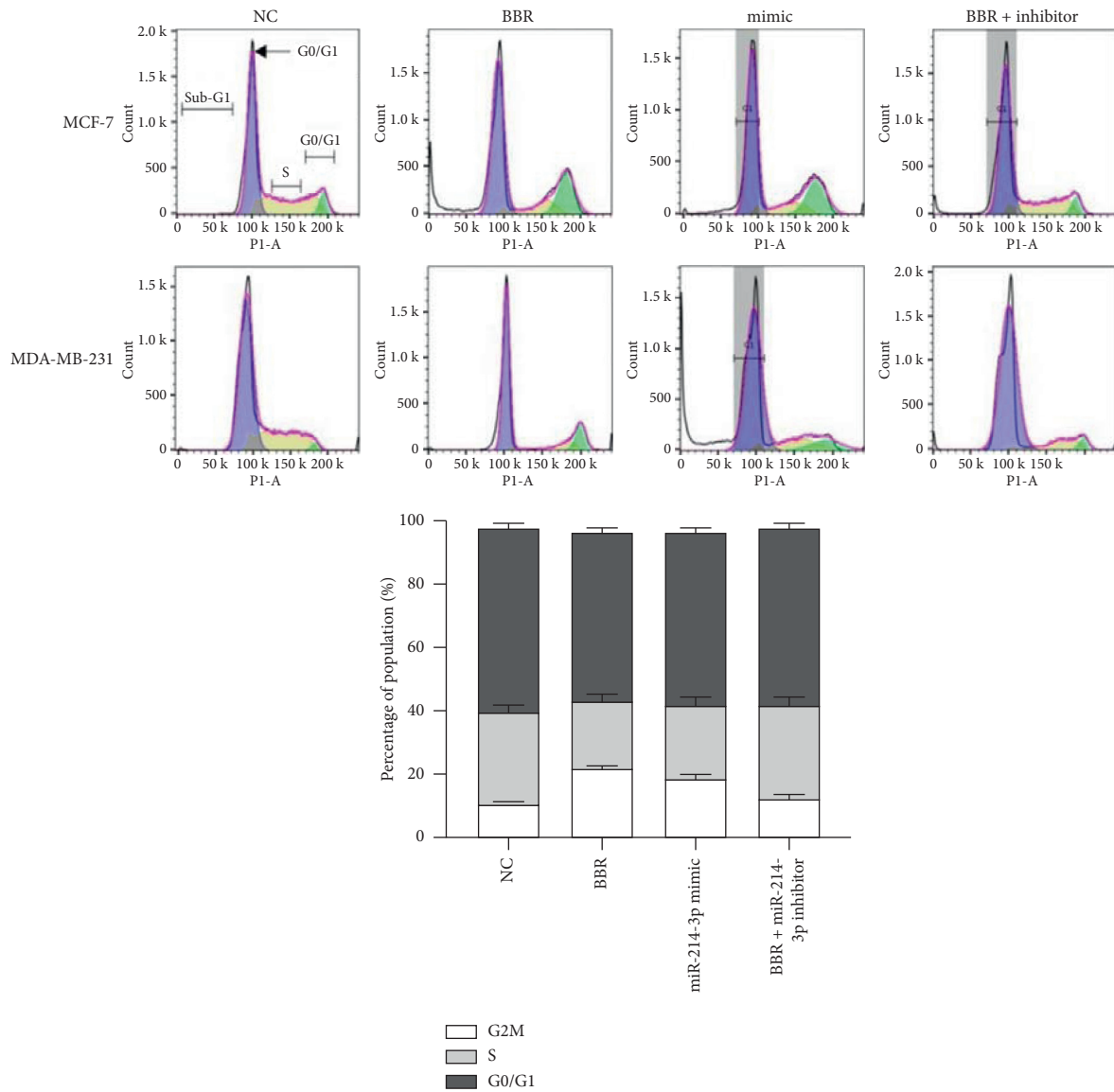
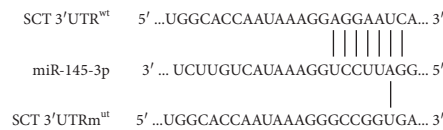


FIGURE 7: Cell cycle analyses. BBR and miR-214-3p mimic administration could increase the percentage of G2/M cells by 20% and 17% in MCF-7 cells and by 13% and 9% in MDA-MB-231 cells, respectively. * $p < 0.05$ vs. NC group. # $p < 0.05$ vs. BBR group.

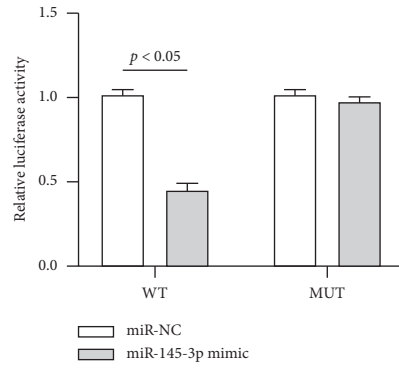
	Predicted consequential pairing of target region (top) and miRNA (bottom)	Side type	Context** score	Context** score percentile	Weighted context** score	Conserved branch length	PCT
Position 107-114 of SCT 3' UTR hsa-miR-145-3p	5' ...UGGCACCAUAAAGGAGGAAUCA... 3' ...UCUUGUCAUAAAGGUCCUAGG	8mer	-0.67	99	-0.67	0	N/A

(a)

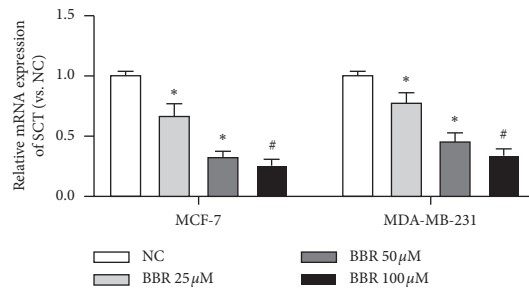


(b)

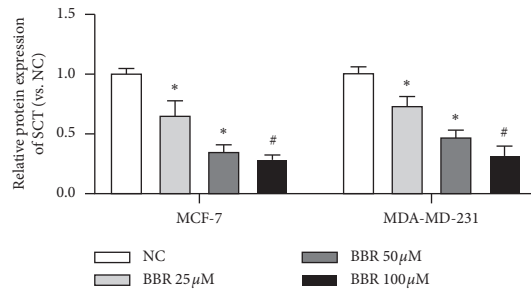
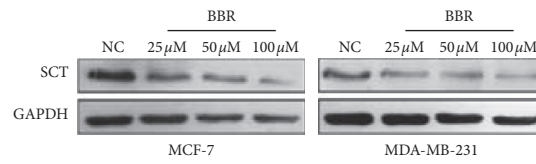
FIGURE 8: Continued.



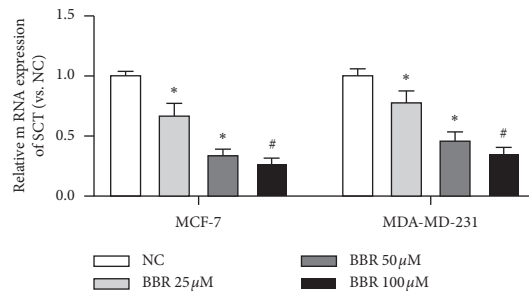
(c)



(d)



(e)



(f)

FIGURE 8: Continued.

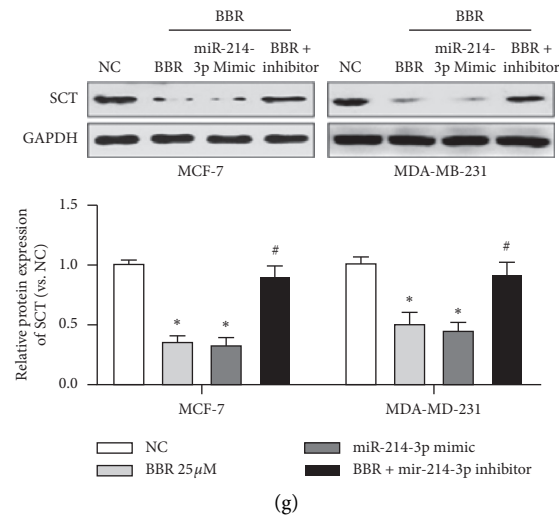


FIGURE 8: (a and b) Targetscan7.2 and miRwalk bioinformatics analysis identified that SCT and miR-214-3p had targeted binding sites. (c) Activity detection of dual-luciferase reporter gene. (d and e) BBR massively and dose-dependently reduced the mRNA expression and protein levels of SCT in both MCF-7 and MDA-231 cells. (f and g) Both miR-214-3p mimic and BBR decreased the mRNA expression and protein levels of SCT, while miR-214-3p inhibitor weakened these reductions. * $p < 0.05$ vs. NC group. # $p < 0.05$ vs. BBR group.

its receptor to mediate the effect of the gastrointestinal hormone on digestion and water homeostasis. The over-expression of SCT in MCF-7 cells led to an increase of the cell proliferation index and cellular migration [44]. The data of this study revealed the fact that miR-214-3p inversely acted on SCT in both MCF-7 and MDA-MB-231 cells. However, whether SCT is an oncogene or a tumor suppressor is still controversial. A number of studies hold the idea that it is an oncogene, as high expression was observed in breast cancer [44], whereas other studies indicated the downregulation of the gene in colorectal cancer [45] and prostate cancer [46]. SCT acts as a gene with double-edge sword activities, which possesses both oncogenic and tumor-suppressive effects. It plays a tumor-suppressive role in normal cells and a proliferation and migration stimulating role in cancer cells. It has been reported that SCT suppresses the proliferation of normal breast cells, while the gene stimulates the proliferation and migration of cancer cells [44].

In conclusion, BBR is indicative of the suppression to MCF-7 and MDA-MB-231 breast cancer cells by upregulating the expression of miR-214-3p and increasing its inhibition to SCT. The miR-214-3p/SCT axis is the therapeutic target in the mechanism of BBR to suppress breast cancer.

Data Availability

The datasets used and/or analyzed in the present study are available from the corresponding author upon reasonable request.

Conflicts of Interest

The authors declare that they have no competing interests.

Authors' Contributions

Congyuan Zhu, the principal investigator, designed the study, performed the statistical evaluations, assisted in writing the paper and edited it in all its revisions. Jianping Li and Hua Yunming participated in the paper's design and coordination. Congyuan Zhu, Jingli Wang, and Ke Wang performed the experiments. Jingqiu Sun revised drafts of the article critically for intellectual content.

Acknowledgments

The authors would like to thank everyone who had taken part in this study. This study was supported by the Science Research Foundation of Wuxi Sanitary Bureau (XM1010).

References

- [1] M. Ghoncheh, Z. Pournamdar, and H. Salehiniya, "Incidence and mortality and epidemiology of breast cancer in the world," *Asian Pacific Journal of Cancer Prevention*, vol. 17, no. 3, pp. 43–46, 2016.
- [2] M. S. Hizir, M. Balcioglu, M. Rana, N. M. Robertson, and M. V. Yigit, "Simultaneous detection of circulating oncomiRs from body fluids for prostate cancer staging using nanographene oxide," *ACS Applied Materials & Interfaces*, vol. 6, no. 17, pp. 14772–14778, 2014.
- [3] Y. Zhong, Y.-H. Pei, J. Wang, J. Chen, S.-S. Jiang, and J.-B. Gong, "MicroRNA expression profile in myocardial bridging patients," *Scandinavian Journal of Clinical and Laboratory Investigation*, vol. 74, no. 7, pp. 582–587, 2014.
- [4] E. D'Asti, A. Huang, M. Kool et al., "Tissue factor regulation by miR-520g in primitive neuronal brain tumor cells," *The American Journal of Pathology*, vol. 186, no. 2, pp. 446–459, 2016.
- [5] S. Dhar, A. Kumar, A. M. Rimando, X. Zhang, and A. S. Levenson, "Resveratrol and pterostilbene epigenetically

- restore PTEN expression by targeting oncomiRs of the miR-17 family in prostate cancer," *Oncotarget*, vol. 6, no. 29, pp. 27214–27226, 2015.
- [6] S. Manvati, K. C. Mangalhar, P. Kalaiarasan, N. Srivastava, B. Kumar, and R. N. K. Bamezai, "MiR-101 induces senescence and prevents apoptosis in the background of DNA damage in MCF7 cells," *PLoS One*, vol. 9, no. 10, p. e111177, 2014.
- [7] M. D. Chanyshev, Y. V. Razumova, V. Y. Ovchinnikov, and L. F. Gulyaeva, "MiR-21 regulates the ACAT1 gene in MCF-7 cells," *Life Sciences*, vol. 209, pp. 173–178, 2018.
- [8] D. M. Tiago, N. Conceição, H. Caiado, V. Laizé, and M. L. Cancela, "Matrix Gla protein repression by miR-155 promotes oncogenic signals in breast cancer MCF-7 cells," *FEBS Letters*, vol. 590, no. 8, pp. 1234–1241, 2016.
- [9] H. Si, P. Chen, H. Li, and X. Wang, "Long non-coding RNA H19 regulates cell growth and metastasis via miR-138 in breast cancer," *American Journal of Translational Research*, vol. 11, no. 5, pp. 3213–3225, 2019.
- [10] Y. Nie, L. Zhou, H. Wang et al., "Profiling the epigenetic interplay of lncRNA RUNXOR and oncogenic RUNX1 in breast cancer cells by gene in situ cis-activation," *American Journal of Cancer Research*, vol. 9, no. 8, pp. 1635–1649, 2019.
- [11] E. Qiao, D. Chen, Q. Li et al., "Long noncoding RNA TALNEC2 plays an oncogenic role in breast cancer by binding to EZH2 to target p57 KIP2 and involving in p-p38 MAPK and NF- κ B pathways," *Journal of Cellular Biochemistry*, vol. 120, no. 3, pp. 3978–3988, 2019.
- [12] N. N. Yuan, C. Z. Cai, M. Y. Wu, H. X. Su, M. Li, and J. H. Lu, "Neuroprotective effects of berberine in animal models of Alzheimer's disease: a systematic review of pre-clinical studies," *BMC Complementary and Alternative Medicine*, vol. 19, no. 1, p. 109, 2019.
- [13] L.-S. Zhang, J.-H. Zhang, R. Feng et al., "Efficacy and safety of berberine alone or combined with statins for the treatment of hyperlipidemia: a systematic review and meta-analysis of randomized controlled clinical trials," *The American Journal of Chinese Medicine*, vol. 47, no. 4, pp. 751–767, 2019.
- [14] J. Tak, A. Sabarwal, R. K. Shyanti, and R. P. Singh, "Berberine enhances posttranslational protein stability of p21/cip1 in breast cancer cells via down-regulation of Akt," *Molecular and Cellular Biochemistry*, vol. 458, no. 1-2, pp. 49–59, 2019.
- [15] N. Yao, Y. Fu, L. Chen et al., "Long non-coding RNA NONHSAT101069 promotes epirubicin resistance, migration, and invasion of breast cancer cells through NON-HSAT101069/miR-129-5p/Twist1 axis," *Oncogene*, vol. 38, no. 47, pp. 7216–7233, 2019.
- [16] Z. Bolandghamat Pour, M. Nourbakhsh, K. Mousavizadeh et al., "Up-regulation of miR-381 inhibits NAD⁺ salvage pathway and promotes apoptosis in breast cancer cells," *EXCLI Journal*, vol. 18, pp. 683–696, 2019.
- [17] M.-N. Menbari, K. Rahimi, A. Ahmadi et al., "MiR-216b-5p inhibits cell proliferation in human breast cancer by down-regulating HDAC8 expression," *Life Sciences*, vol. 237, Article ID 116945, 2019.
- [18] C. Qiu, F. Huang, Q. Zhang, W. Chen, and H. Zhang, "miR-205-3p promotes proliferation and reduces apoptosis of breast cancer MCF-7 cells and is associated with poor prognosis of breast cancer patients," *Journal of Clinical Laboratory Analysis*, vol. 33, no. 8, Article ID e22966, 2019.
- [19] H. Tang, C. Song, F. Ye et al., "miR-200c suppresses stemness and increases cellular sensitivity to trastuzumab in HER2+ breast cancer," *Journal of Cellular and Molecular Medicine*, vol. 23, no. 12, pp. 8114–8127, 2019.
- [20] X. Zhu, J. Qiu, T. Zhang et al., "MicroRNA-188-5p promotes apoptosis and inhibits cell proliferation of breast cancer cells via the MAPK signaling pathway by targeting Rap2c," *Journal of Cellular Physiology*, vol. 235, no. 5, 2019.
- [21] L. C. Han, H. Wang, F. L. Niu, J. Y. Yan, and H. F. Cai, "Effect miR-214-3p on proliferation and apoptosis of breast cancer cells by targeting survivin protein," *European Review for Medical and Pharmacological Sciences*, vol. 23, no. 17, pp. 7469–7474, 2019.
- [22] C. Yuan, "miR-616 promotes breast cancer migration and invasion by targeting TIMP2 and regulating MMP signaling," *Oncology Letters*, vol. 18, no. 3, pp. 2348–2355, 2019.
- [23] R. Meng, J. Fang, Y. Yu et al., "miR-129-5p suppresses breast cancer proliferation by targeting CBX4," *Neoplasma*, vol. 65, no. 4, pp. 572–578, 2018.
- [24] Z. M. Huang, H. F. Ge, C. C. Yang et al., "MicroRNA-26a-5p inhibits breast cancer cell growth by suppressing RNF6 expression," *The Kaohsiung Journal of Medical Sciences*, vol. 35, no. 8, pp. 467–473, 2019.
- [25] J. Liu, L. Yang, X. Guo et al., "Sevoflurane suppresses proliferation by upregulating microRNA-203 in breast cancer cells," *Molecular Medicine Reports*, vol. 18, no. 1, pp. 455–460, 2018.
- [26] Q. Huang, Y. Y. Wu, S. J. Xing, and Z. W. Yu, "Effect of miR-7 on resistance of breast cancer cells to adriamycin via regulating EGFR/PI3K signaling pathway," *European Review for Medical and Pharmacological Sciences*, vol. 23, no. 12, pp. 5285–5292, 2019.
- [27] S. Yarahmadi, Z. Abdolvahabi, Z. Hesari et al., "Inhibition of sirtuin 1 deacetylase by miR-211-5p provides a mechanism for the induction of cell death in breast cancer cells," *Gene*, vol. 711, p. 143939, 2019.
- [28] C. Zhao, X. Ling, X. Li, X. Hou, and D. Zhao, "MicroRNA-138-5p inhibits cell migration, invasion and EMT in breast cancer by directly targeting RHBDD1," *Breast cancer*, vol. 26, pp. 817–825, 2019.
- [29] B. Wang, J. Zheng, R. Li et al., "Long noncoding RNA LINC02582 acts downstream of miR-200c to promote radioresistance through CHK1 in breast cancer cells," *Cell Death & Disease*, vol. 10, no. 10, p. 764, 2019.
- [30] Q. Ma, X. Qi, X. Lin, L. Li, L. Chen, and W. Hu, "LncRNA SNHG3 promotes cell proliferation and invasion through the miR-384/hepatoma-derived growth factor axis in breast cancer," *Human Cell*, vol. 33, no. 1, pp. 232–242, 2019.
- [31] Y. Y. Wang, L. Yan, S. Yang et al., "Long noncoding RNA AC073284.4 suppresses epithelial-mesenchymal transition by sponging miR-18b-5p in paclitaxel-resistant breast cancer cells," *Journal of Cellular Physiology*, vol. 234, no. 12, pp. 23202–23215, 2019.
- [32] F. Yu, L. Wang, and B. Zhang, "Long non-coding RNA DRHC inhibits the proliferation of cancer cells in triple negative breast cancer by downregulating long non-coding RNA HOTAIR," *Oncology Letters*, vol. 18, no. 4, pp. 3817–3822, 2019.
- [33] C. Song, P. Sun, Q. He, L. L. Liu, J. Cui, and L. M. Sun, "Long non-coding RNA LINC01287 promotes breast cancer cells proliferation and metastasis by activating Wnt/ss-catenin signaling," *European Review for Medical and Pharmacological Sciences*, vol. 23, no. 10, pp. 4234–4242, 2019.
- [34] K. Li, Y.-b. Ma, Y.-h. Tian et al., "Silencing lncRNA SNHG6 suppresses proliferation and invasion of breast cancer cells through miR-26a/VASP axis," *Pathology-Research and Practice*, vol. 215, no. 10, Article ID 152575, 2019.

- [35] Y. S. Lin, Y. C. Chiu, Y. H. Tsai et al., "Different mechanisms involved in the berberine-induced antiproliferation effects in triple-negative breast cancer cell lines," *Journal of Cellular Biochemistry*, vol. 120, no. 8, pp. 13531–13544, 2019.
- [36] H. M. Palethorpe, E. Smith, Y Tomita et al., "Bacopasides I and II act in synergy to inhibit the growth, migration and invasion of breast cancer cell lines," *Molecules*, vol. 24, no. 19, 2019.
- [37] G. H. Rabbani, T. Butler, J. Knight, S. C. Sanyal, and K. Alam, "Randomized controlled trial of berberine sulfate therapy for diarrhea due to enterotoxigenic *Escherichia coli* and *Vibrio cholerae*," *Journal of Infectious Diseases*, vol. 155, no. 5, pp. 979–984, 1987.
- [38] J. Wang, Y. Jiang, B. Wang, and N. Zhang, "A review on analytical methods for natural berberine alkaloids," *Journal of Separation Science*, vol. 42, no. 9, pp. 1794–1815, 2019.
- [39] J. B. Kim, J.-H. Yu, E. Ko et al., "The alkaloid Berberine inhibits the growth of Anoikis-resistant MCF-7 and MDA-MB-231 breast cancer cell lines by inducing cell cycle arrest," *Phytomedicine*, vol. 17, no. 6, pp. 436–440, 2010.
- [40] J. Kim, E. Ko, W. Han, I. Shin, S. Park, and D.-Y. Noh, "Berberine diminishes the side population and ABCG2 transporter expression in MCF-7 breast cancer cells," *Planta Medica*, vol. 74, no. 14, pp. 1693–1700, 2008.
- [41] Q. Du, X. Zhang, X. Zhang, M. Wei, H. Xu, and S. Wang, "Propofol inhibits proliferation and epithelial-mesenchymal transition of MCF-7 cells by suppressing miR-21 expression," *Artificial Cells, Nanomedicine, and Biotechnology*, vol. 47, no. 1, pp. 1265–1271, 2019.
- [42] C. X. Qin, X. Q. Yang, G. C. Jin, and Z. Y. Zhan, "LncRNA TSLNC8 inhibits proliferation of breast cancer cell through the miR-214-3p/FOXP2 axis," *European Review for Medical and Pharmacological Sciences*, vol. 23, no. 19, pp. 8440–8448, 2019.
- [43] L. Min, C. Liu, J. Kuang, X. Wu, and L. Zhu, "miR-214 inhibits epithelial-mesenchymal transition of breast cancer cells via downregulation of RNF8," *Acta Biochimica et Biophysica Sinica*, vol. 51, no. 8, pp. 791–798, 2019.
- [44] S. Kang, B. Kim, H.-S. Kang et al., "SCTR regulates cell cycle-related genes toward anti-proliferation in normal breast cells while having pro-proliferation activity in breast cancer cells," *International Journal of Oncology*, vol. 47, no. 5, pp. 1923–1931, 2015.
- [45] J. Fang, S.-L. Wang, S.-B. Zhao et al., "Impact of intraduodenal acetic acid infusion on pancreatic duct cannulation during endoscopic retrograde cholangiopancreatography: a double-blind, randomized controlled trial," *Journal of Gastroenterology and Hepatology*, vol. 33, no. 10, pp. 1804–1810, 2018.
- [46] J. Devaney, C. Stirzaker, W. Qu et al., "Epigenetic deregulation across chromosome 2q14.2 differentiates normal from prostate cancer and provides a regional panel of novel DNA methylation cancer biomarkers," *Cancer Epidemiology Biomarkers & Prevention*, vol. 20, no. 1, pp. 148–159, 2011.

Research Article

***In Vitro* Cytotoxic Activity against Breast, Cervical, and Ovarian Cancer Cells and Flavonoid Content of Plant Ingredients Used in a Selected Thai Traditional Cancer Remedy: Correlation and Hierarchical Cluster Analysis**

Thammarat Tuy-on ¹, **Arunporn Itharat** ^{2,3}, **Ponlawat Maki** ¹,
Pakakrong Thongdeeying ^{2,3}, **Weerachai Pipatrattanaseree** ⁴, and **Buncha Ooraikul**⁵

¹Graduate School, Faculty of Medicine, Thammasat University, Bangkok, Pathumthani 12120, Thailand

²Department of Applied Thai Traditional Medicine, Faculty of Medicine, Thammasat University, Bangkok, Klongluang, Pathumthani 12120, Thailand

³Center of Excellence in Applied Thai Traditional Medicine, Faculty of Medicine, Thammasat University, Klongluang, Bangkok, Pathumthani 12120, Thailand

⁴Regional Medical Science Center 12 Songkhla, Department of Medical Sciences, Ministry of Public Health, Muang, Songkhla 90100, Thailand

⁵Department of Agricultural Food and Nutritional Science, Faculty of Agricultural Life and Environmental Sciences, University of Alberta, Edmonton, AB, Canada

Correspondence should be addressed to Arunporn Itharat; iarunporn@yahoo.com

Received 22 August 2020; Revised 25 October 2020; Accepted 7 November 2020; Published 17 November 2020

Academic Editor: Mohd Fadzelly Abu Bakar

Copyright © 2020 Thammarat Tuy-on et al. This is an open access article distributed under the Creative Commons Attribution License, which permits unrestricted use, distribution, and reproduction in any medium, provided the original work is properly cited.

This study aimed to investigate *in vitro* cytotoxic activity of selected plant ingredients from a traditional Thai remedy for the treatment of cancer patients against cancer cells occurring in women such as MCF-7 (breast cancer), SKOV3 (ovarian cancer), and HeLa (cervical cancer) cell lines. The plants and the remedy were macerated with 95% ethanol and boiled in water. Cytotoxic activity of the extracts was analyzed by SRB assay. Total flavonoid contents of the extracts were determined and their correlation with cytotoxic activity was evaluated. The hierarchical cluster analysis (HCA) was used to classify the extracts by their cytotoxic characteristics. A total of 66.7% of the plants was active against the tested cancer cell lines. Among the 44 plants in the remedy used for cancer treatment, nine plants that are also used in Thai cuisine exerted significant cytotoxicity against tested cancer cell lines. Eleven plants in the remedy were active against at least one of the tested cancer cell lines. All extracts were grouped into three groups and illustrated as heat map and hierarchical dendrogram. Total flavonoid content showed weak or no correlation with cytotoxic activity. *A. dahurica*, *F. albopurpurea*, and *T. indica* selectively exerted potent cytotoxic activity against MCF-7 with SI value more than 6. *A. galanga*, *P. amarus*, *L. striatum*, *H. indicum*, and *F. vulgare* exerted moderate cytotoxicity to all tested cell with low toxicity to normal cells. The correlation and HCA performed in this study provided an alternative way to investigate biological activities of plant ingredients in polyherbal traditional remedies.

1. Introduction

Cancers of breast, cervical, and ovarian are common cancers occurring in the female population. Breast cancer is the most common and the most leading cause of cancer death among

women worldwide. Cervical and ovary cancers are the fourth and seventh most common, respectively [1]. Although each cancer has its own established treatment guidelines, the conventional treatments are surgery, radiation, and chemotherapy. The current treatments, particularly anticancer

drugs, may be inadequate for patients due to some severe side effects arising from toxicity on normal cells or tissues. These side effects of chemotherapy often affect patient's quality of life [2]. Therefore, novel substances or plant extracts need to be developed for the treatment and prevention of cancers.

Herbal medicines for cancer treatment are known to cancer patients. These medicinal plants have become increasingly recognized either as alternative medicines for cancer treatment or dietary supplements for cancer prevention. In Thai traditional medicine (TTM) prescribed by traditional doctors, several medicinal plants are combined as remedies [3, 4]. TTM is a cultural heritage and indigenous wisdom that has been used by Thai people for over a thousand years. It utilizes several herbs rather than a single herb to design a remedy for cancer treatment. The selected TTM remedy in this study was a cancer remedy prescribed at the Jitmeatta Mercy Foundation for Cancer Patients of Thailand (JFCT), Phetchaburi province, Thailand. This remedy is composed of 44 plants mixed by equal weight. This traditional cancer remedy was prepared by the decoction method and it was used to treat cancer patients more than 30 years ago. Previous research showed that almost all cancer patients treated at JFCT were women, so this research pointed to prove that this cancer remedy can cure cancers in women [5].

Phytochemical compounds in herbal medicines play an important role in the expression of biological and pharmacological activities. Flavonoids, a group of phenolic compounds, provide potential benefits in health promotion and prevention of several chronic diseases including cancer. Due to the variation of substitutions on the skeletal structure of flavonoids, an extremely diverse range of flavonoid derivatives in herbal medicines have been discovered [6]. Many flavonoids showed cytotoxic activity and antitumor, such as epigallocatechin gallate and quercetin [7].

Thus, the aim of this study was to investigate *in vitro* cytotoxic activity of the extracts of this TTM remedy and its 44 plant ingredients in this remedy against commonly occurring cancers in women, i.e., MCF-7 (breast cancer), SKOV3 (ovarian cancer), and HeLa (cervical cancer). The total flavonoid content of the extracts was also studied, and its correlation with cytotoxic activity was also evaluated. The statistical cluster analysis was used to visualize the cytotoxic pattern of plants and remedies. This study also evaluated an alternative method for screening the cytotoxic activity of plant ingredients in polyherbal remedies used in traditional medicines. The correlation of cytotoxic activity with total flavonoid content may be used in the search for cytotoxic compounds from flavonoids against cancers occurring in women in the future.

2. Materials and Methods

2.1. Plant Materials. All plants were collected from Phetchaburi Province, Thailand, in 2018. The herbarium specimens were prepared and deposited at the herbarium of Southern Center of Thai Medicinal Plants at the Faculty of Pharmaceutical Science, Prince of Songkla University, Songkhla, Thailand, and the relevant voucher numbers are shown in Table 1.

2.2. Preparation of Plant and TTM Extracts. Each plant was washed, thinly sliced, dried in an oven at 45°C, and powdered. Dried plants (1000 g) were macerated with 3.0 L of 95% ethanol for 3 days, filtered, and evaporated to dryness. The selected traditional Thai cancer remedy was prepared according to the proportion used at the JFCT foundation by combining an equal weight of each dried plant, mixed together, and powdered. The resulting remedy was extracted by two methods, maceration (as described above), and decoction. The decoction method was carried out by boiling the remedy (1000 g) with an equal amount of water for 15 minutes and the aqueous extract filtered and evaporated to dryness with a freeze drier. The ethanolic extract of TTM was named TTE and the aqueous extract obtained from decoction was named TTW. The %yield was calculated (Table 1) and all extracts were kept at -20°C until use.

2.3. Cell Lines and Culture. Breast cancer cell lines (MCF-7 ATCC NO HTB-22), ovarian cancer (SKOV-3 ATCC NO HTB-77), and cervical cancer (HeLa ATCC NO CCL-2) were purchased from the American Type Culture Collection (Manassas, VA, USA). Normal human keratinocyte immortal cell line (HaCat) was purchased from the CLS cell line service (No. 300493-SF).

MCF-7 and HeLa cell lines were cultured in minimum essential medium (MEM). SKOV-3 was cultured in Roswell Park Memorial Institute medium 1640 (RPMI-1640) and HaCat was cultured in Dulbecco's Modified Eagle's Medium (DMEM). All cultured media were supplemented with 10% fetal bovine serum and 1% penicillin-streptomycin. The cells were incubated in 5% CO₂ at 37°C and 95% humidity.

2.4. In Vitro Assay for Cytotoxic Activity. Cytotoxicity of the extracts was investigated by using sulphorhodamine B (SRB) assay according to the method previously described [8, 9]. Briefly, cells were seeded in a 96-well microtiter plate and incubated for 24 hours. Each extract was diluted by DMSO to produce stock solution at a concentration of 10 mg/ml except TTW, which was diluted by water. The stock solution was diluted serially by culture medium to produce a working solution (2, 20, 100, and 200 µg/ml). The seeded cells were treated with various concentrations of working solution of plant and remedy extracts and incubated for 72 hours. The final concentrations of extract in the seeded cell were 1, 10, 50, and 100 µg/ml and the maximum final concentration of DMSO in the seeded cell was 1%v/v. The medium was replaced with cell culture media and the plates were continuously incubated at 37°C for three days in order to observe cytotoxicity after a recovery period. The cells were fixed with 40% trichloroacetic acid and the plates left at 4°C for 45 min. The media were removed and the cells were stained with 0.4% SRB in acetic acid. The %survival was determined by colorimetric measurement at 492 nm and calculated by the following equation. The half inhibitory concentrations (IC₅₀) of the extracts were calculated by using GraphPad Prism software (CA, USA)

TABLE 1: Plant ingredients in the selected Thai traditional remedy and their extraction yield (% w/w of dried crude plant powder).

Botanical name	Family	Common name	Part used	% yield	Voucher number
<i>Acanthus ebracteatus</i> vahl.	Acanthaceae	Sea holly	Leaf	3.14	SKP 001 01 05 01
<i>Andrographis paniculata</i> (Burm.f.) Wall ex Nees.	Acanthaceae	Kariyat, Creat	Leaf	10.23	SKP 001 01 16 01
<i>Rhinacanthus nasutus</i> (L.) Kurz.	Acanthaceae	White crane flower	Leaf	17.90	SKP 001 18 14 01
<i>Ananas comosus</i> (L.) Merr.	Bromeliaceae	Pineapple	Fruit	3.65	SKP 029 01 03 01
<i>Commiphora myrrha</i> (NEES) Engler.	Burseraceae	Bullet Wood	Resin	15.01	SKP 031 03 13 01
<i>Carica papaya</i> L.	Caricaceae	Papaya	Root	9.64	SKP 040 03 16 01
<i>Artemisia vulgaris</i> Linn.	Compositae	Mugwort	Rhizome	3.29	SKP 051 01 22 01
<i>Mammea siamensis</i> Kosterm.	Calophyllaceae	Negkassar	Flower	5.62	SKP 216 13 19 01
<i>Mesua ferrea</i> Linn.	Calophyllaceae	Iron wood	Flower	4.71	SKP216 13 06 01
<i>Dioscorea opposita</i> thumb.	Dioscoreaceae	Nagaimo	Rhizome	3.14	SKP 062 04 15 01
<i>Equisetum arvense</i> L.	Equisetaceae	Horsetails	Leaf	1.45	SKP 224 05 01 01
<i>Croton stellatopilosus</i> Ohba.	Euphorbiaceae	Plow-noi (Thai)	Leaf	14.29	SKP 071 03 19 01
<i>Phyllanthus amarus</i> Schmach&Thonn.	Euphorbiaceae	Egg Woman.	Leaf	34.5	SKP 071 16 01 01
<i>Astragalus membranaceus</i> Bge. Var. mongolicu.	Fabaceae	Milkvetch Root	Root	9.12	SKP 072 01 13 01
<i>Heliotropium indicum</i> L.	Fabaceae	Alacransillo	Stem	2.98	SKP 072 08 09 01
<i>Enhalus acoroides</i> (L.f.) Royle.	Hydrocharitaceae	Sea Acorus	Root	2.18	SKP 088 05 01 01
<i>Ocimum tenuiflorum</i> L.	Lamiaceae	Holy Basil	Leaf	16.26	SKP 099 15 20 01
<i>Pogostemon cablin</i> (Blanco) Benth.	Lamiaceae	Patchoull	Stem	27.16	SKP 099 16 03 01
<i>Cinnamomum verum</i> J. Presl.	Lauraceae	Camphor	Bark	12.42	SKP 096 03 22 01
<i>Tamarindus indica</i> Linn.	Leguminosae	Tamarind	Leaf	12.5	SKP 098 20 09 01
<i>Ligusticum striatum</i> Dc.	Menispermaceae	Szechuan lovage	Rhizome	10.3	SKP 114 12 19 01
<i>Maclura cochinchinensis</i> Corner.	Moraceae	Cockspur thorn	Fruit	6.28	SKP 117 13 03 01
<i>Myristica fragrans</i> Houtt.	Myrisicaceae	Nutmeg tree.	Flower	12.57	SKP 121 13 06 01
<i>Nelumbo nucifera</i> Gaerth.	Nelumbonaceae	Sacred lotus	Root	1.89	SKP 125 14 14 01
<i>Jasminum sambac</i> Ait.	Oleaceae	Jasmine	Flower	20.1	SKP 129 10 19 01
<i>Flickingeria albopurpurea</i> Seidenf.	Orchidaceae	Fading Flickingeria	Flower	2.34	SKP 132 06 01 01
<i>Cardiospermum halicacalum</i> L.	Sapindaceae	Balloon vine	Vine	8.38	SKP 170 03 08 01
<i>Mimusops elengi</i> Linn.	Sapotaceae	Spash Cherry	Flower	6.92	SKP 171 13 05 01
<i>Schisandra chinensis</i> .	Schisandraceae	Schizandra Berry	Fruit	14.16	SKP 223 19 03 01
<i>Rehmannia glutinosa</i> (Gaertn.) libosch.	Scrophulariac	Chinese foxglove	Root	15.0	SKP 177 18 07 02
<i>Lycium barbarum</i> .	Solannaceae	Goji berry, Wolfberry	Leaf	9.81	SKP 180 12 02 01
<i>Solanum indicum</i> L.	Solannaceae	Black nightshade	Fruit	4.24	SKP 180 19 09 01
<i>Angelica sinensis</i> (Oliv.) Diels.	Umbelliferae	Dong quai	Bulb	2.5	SKP 199 01 19 01
<i>Foeniculum vulgare</i> mill subsp. piperatum (Ucr.) Beguinot.	Umbelliferae	Fennel	Fruit	3.07	SKP 199 06 22 01
<i>Linacia triadra</i> Miers.	Umbelliferae	Bai-ya-nang (Thai)	Rhizome	7.31	SKP 199 12 20 01
<i>Angelica dahurica</i> Benth.	Umbelliferae	African Tulip Tree	Bulb	6.23	SKP 206 01 04 01
<i>Vitis vinifera</i> L.	Vitaceae	Grape	Fruit	3.43	SKP 204 22 22 01
<i>Alpinia galangal</i> (L.) Willd.	Zingiberaceae	Galanga.	Rhizome	1.78	SKP 206 01 07 01
<i>Amomum villosum</i> Lour var. Xanthiodes.	Zingiberaceae	Bastard cardamom,	Fruit	19.7	SKP 206 01 22 01
<i>Boesenbergia rotunda</i> (L.) Mansf.	Zingiberaceae	Fingerroot	Rhizome	9.62	SKP 206 02 18 01
<i>Curcuma aromatic</i> Salisb.	Zingiberaceae	Wild Turmeric	Rhizome	28.58	SKP 206 03 01 01
<i>Curcuma comosa</i> Roxb.	Zingiberaceae	Wanchakmodlook (Thai)	Bulb	12.96	SKP 206 03 03 01
<i>Kaempferia galanga</i> L.	Zingiberaceae	Aromatic ginger	Rhizome	1.14	SKP 206 11 07 01

$$\text{Inhibition (\%)} = \left(\frac{\text{OD}_{\text{control}} - \text{OD}_{\text{sample}}}{\text{OD}_{\text{control}}} \right) \times 100. \quad (1)$$

2.5. Total Flavonoid Content. Total flavonoid content was measured by the aluminum chloride colorimetric assay [10]. Briefly, an aliquot (1 mL) of the extracts or standard solution of quercetin (20, 40, 60, 80, 100, 120, and 240 mg/L) was added to a volumetric flask. To the flask were added 75 μL of 5% NaNO_2 and 150 μL of 10% AlCl_3 . After 5 min, 500 μL of 1 M NaOH was added, and the volume was adjusted by H_2O . The solution was mixed well, and the absorbance was

measured against the prepared reagent blank at 510 nm. The concentration of total flavonoid content in the test samples was calculated from the calibration plot ($Y = 0.0162x + 0.0044$, $r^2 > 0.999$) and expressed as mg quercetin equivalent/g of dried plant. All the determinations were carried out in triplicate.

2.6. Statistical Analysis. All experiments were carried out by three independent experiments, and the data were reported as the mean and standard error of means. The correlation of total flavonoid content and cytotoxic activity was plotted and the correlation coefficient (r) calculated by using

Microsoft® excel. The similarity of cytotoxic activity to the three cancer cells of the tested plants was classified using the hierarchical cluster analysis (HCA) and visualized as a heat map using Heatmap Illustrator (HemI) version 1.0 software [11].

3. Results

3.1. Cytotoxic Activity. The cytotoxic activity of the plant and remedy extracts is shown in Tables 2 and 3. The extracts obtained from the selected cancer remedy, TTW and TTE, were not active ($IC_{50} > 100 \mu\text{g/ml}$). However, TTE exerted moderate activity against MCF-7 with IC_{50} of $52.33 \pm 2.05 \mu\text{g/ml}$. Of the 46 extracts tested, 30 (65.2%) exerted cytotoxic activity against the cancer cells with various degrees of potency. Four plant extracts exerted potent cytotoxic activity against MCF-7 with IC_{50} values less than $20 \mu\text{g/ml}$, including *A. dahurica*, *M. siamensis*, *F. albopurpurea*, and *T. indica*. The other 26 extracts exerted low to moderate cytotoxic activity. With regard to normal cells (HaCat), 15 extracts showed no cytotoxic activity with IC_{50} values more than $100 \mu\text{g/ml}$. The selective index (SI) of the extracts was calculated. SI is the ratio between IC_{50} values of HaCaT (normal cell) and cancer cell lines. The greater the SI value, the more selective it is. SI value more than 2 indicates that the herbal extract is toxic against cancer cells but less toxic to normal cells. SI value less than 2 indicates the general toxicity of the extract [12]. Based on this criterion, the extracts of *A. dahurica*, *F. albopurpurea*, *M. siamensis*, *C. halicacalum*, *C. papaya*, *K. galanga*, *P. cablin*, and *T. indica* were remarkably selective to breast cancer (MCF-7) cells. Plant extracts which exerted activities against all tested cancer cells were from *A. galaga*, *L. striatum*, *P. amarus*, and *H. indicum*.

3.2. Total Flavonoid Content and Correlation with Cytotoxic Activity. The total flavonoid content of the extracts is shown in Table 3. *C. aromatica* showed the highest content ($259.7 \pm 3.21 \text{ mg quercetin eq./g}$) followed by *A. sinensis* ($259.70 \pm 2.59 \text{ mg quercetin eq./g}$) and *A. dahurica* ($227.95 \pm 5.69 \text{ mg quercetin eq./g}$). The ethanolic extract of the Thai traditional remedy showed total flavonoid content of $105.67 \pm 4.33 \text{ mg quercetin eq./g}$. The correlation between flavonoid content and cytotoxic activity of the extracts was investigated. Total flavonoid contents of the extracts were plotted against their cytotoxic activities, and the correlation coefficients (r) were evaluated. The results showed that there was no correlation between the total flavonoid content of the extracts and their cytotoxic activity against all tested cell lines ($r < 0.35$) (Figure 1). However, in MCF-7, when some outlier data were excluded, there was a strong correlation between flavonoid content and cytotoxicity with r value -0.81 (Figure 2).

3.3. Hierarchical Cluster Analysis. HCA is a multivariate statistical method to evaluate the pattern of data, which is classified into clusters according to their similar characteristics. The similarity or dissimilarity of the extracts is

illustrated, as shown in the dendrogram (Figure 3). In this study, 44 plant extracts and two Thai traditional remedy extracts were classified by HemI software based on their cytotoxic activity against all tested cancer cells. The euclidean metric was selected to evaluate the similarity of the cytotoxic pattern. The heat map was generated to visualize the intensity of cytotoxic activity, and the linkages of similar extracts were shown in the horizontal dimension. As shown in Figure 3, HCA classified 46 extracts into three main groups. The extracts expressing low cytotoxicity against cancer cells were clustered into group I. Group II was composed of the extracts that selectively exhibited cytotoxicity against MCF-7. The extracts showing cytotoxicity against two or more cancer cells were clustered in group III.

4. Discussion

There has been an increasing interest in herbal medicine as an alternative treatment and prevention of cancer. Traditional Thai medicine is an alternative healthcare approach utilizing medicinal plants as a component in the holistic treatment of cancer patients [3]. In this study, we investigated the cytotoxic activity of selected Thai medicinal plants and remedy against cancer cells commonly occurred in women: breast (MCF-7), ovarian (SKOV3), and cervical cancer (HeLa). In the cytotoxic screening of 44 plants and two TTM extracts, the results were analyzed by HCA and visualized them into a heat map (Figure 3). Three major groups of the extracts were categorized by their cytotoxicity characteristics. Group I is composed of plant extracts which exerted less or no cytotoxic activity. Group II was the extracts that selectively exerted cytotoxicity against MCF-7. The extracts with moderate to high activity against all cancer cells were clustered into group III. With regard to the extracts obtained from the selected cancer remedy, TTW was not active against all tested cells, while TTE exerted moderate cytotoxicity against MCF-7. These results indicated that the cytotoxic compounds were extracted from the remedy in a small amount. However, the results of cancer treatment by TTM may occur by the accumulation of the cytotoxic compounds in the body when it was taken for long-term multiple doses. In TTM, many plants in remedy are used as many functions or biological activities related to cancer such as antiinflammation, increase immunology, antimicrobial, antioxidant activities. Another reason, TTM extract may help with another mechanism on cancer treatment such as increased immunology or angiogenesis, when this remedy was absorbed in the patient's body. Thus, this suggestion should be clarify further studied including *in vivo* and clinical trials investigation.

According to the heat map and HCA shown in Figure 3 along with IC_{50} and SI values presented in Tables 1 and 3, *A. dahurica*, *F. albopurpurea*, and *T. indica* exerted potent activity against MCF-7 with IC_{50} less than $20 \mu\text{g/ml}$ and SI more than 6. *M. siamensis* exerted potent cytotoxicity against MCF-7 with SI more than 2. The results indicated that these extracts might have particularly beneficial effects for use in breast cancer treatment and prevention. *A. galanga*, *P. amarus*, and *L. striatum* exerted moderate

TABLE 2: Cytotoxic activity (IC₅₀; µg/ml) of plant extracts against breast cancer (MCF-7), ovarian cancer (SKOV3), cervical cancer (HeLa), and human keratinocyte (HaCat) cell lines (mean ± SEM; n = 3).

Plant	Cytotoxicity (IC ₅₀ (µg/ml) ± SEM)			
	MCF -7	SKOV3	Hela	HaCat
<i>A. ebracteatus</i>	>100	21.52 ± 1.28	25.31 ± 2.25	80.95 ± 0.94
<i>A. galanga</i>	34.79 ± 4.24	33.75 ± 1.21	34.88 ± 1.13	93.18 ± 2.20
<i>A. villosum</i>	30.66 ± 1.29	80.79 ± 3.82	59.42 ± 2.02	52.25 ± 0.58
<i>A. comosus</i>	>100	>100	>100	>100
<i>A. paniculata</i>	87.02 ± 3.21	>100	>100	38.29 ± 3.20
<i>A. sinensis</i>	34.15 ± 1.33	89.78 ± 1.25	72.25 ± 2.05	71.47 ± 2.55
<i>A. dahurica</i>	9.87 ± 2.13	>100	>100	>100
<i>A. valgaris</i>	49.16 ± 3.65	35.44 ± 1.07	46.54 ± 2.92	27.30 ± 3.71
<i>A. membranaceus</i>	>100	>100	>100	>100
<i>B. rotunda</i>	29.96 ± 1.09	35.05 ± 0.75	60.22 ± 2.15	34.25 ± 0.62
<i>C. halicacalum</i>	45.65 ± 2.32	>100	>100	>100
<i>C. papaya</i>	42.2 ± 2.11	>100	>100	>100
<i>C. verum</i>	20.88 ± 1.82	46.25 ± 1.25	24.12 ± 0.88	46.16 ± 1.43
<i>C. myrrha</i>	>100	>100	68.77 ± 4.10	>100
<i>C. sativus</i>	>100	>100	>100	>100
<i>C. stellatopilosus</i>	87.65 ± 3.21	>100	>100	34.21 ± 0.10
<i>C. aromatica</i>	90.43 ± 3.12	>100	>100	8.78 ± 0.21
<i>C. comosa</i>	68.56 ± 2.32	61.21 ± 1.26	73.21 ± 2.01	39.34 ± 0.96
<i>D. opposite</i>	>100	>100	>100	>100
<i>E. acoroides</i>	>100	>100	>100	>100
<i>F. albopurpurea</i>	14.63 ± 4.54	>100	>100	>100
<i>F. vulgare</i>	20.34 ± 2.64	45.27 ± 2.12	68.25 ± 1.85	>100
<i>H. indicum</i>	29.55 ± 3.21	35.13 ± 3.01	47.85 ± 2.02	>100
<i>E. arvense</i>	>100	>100	>100	>100
<i>J. sambac</i>	>100	>100	>100	>100
<i>K. galanga</i>	49.33 ± 1.45	>100	>100	>100
<i>L. triadra</i>	>100	46.25 ± 3.01	>100	81.53 ± 4.17
<i>L. striatum</i>	30.22 ± 2.32	28.32 ± 1.52	36.24 ± 2.20	>100
<i>L. barbarum</i>	>100	>100	>100	>100
<i>M. cochinchinensis</i>	53.47 ± 1.07	>100	>100	37.68 ± 0.85
<i>M. siamensis</i>	11.23 ± 2.82	>100	>100	33.39 ± 0.40
<i>M. ferrea</i>	86.42 ± 3.21	>100	>100	6.84 ± 0.39
<i>M. elengi</i>	>100	>100	>100	>100
<i>M. fragrans</i>	64.57 ± 2.22	>100	>100	32.58 ± 0.61
<i>N. nucifera</i>	>100	>100	>100	>100
<i>O. tenuiflorum</i>	50.56 ± 1.97	>100	>100	95.08 ± 0.59
<i>P. amarus</i>	23.23 ± 1.13	28.84 ± 2.15	35.21 ± 1.08	75.28 ± 1.40
<i>P. cablin</i>	24.65 ± 2.13	>100	>100	>100
<i>R. glutinosa</i>	>100	>100	>100	>100
<i>R. nasutus</i>	65.81 ± 3.28	48.28 ± 3.13	>100	>100
<i>S. chinensis.</i>	>100	>100	>100	>100
<i>S. indicum</i>	>100	>100	>100	>100
<i>T. indica</i>	14.76 ± 2.73	>100	>100	92.57 ± 0.94
<i>V. vinifera</i>	>100	>100	>100	>100
TTW	>100	>100	>100	47.12 ± 3.14
TTE	52.33 ± 2.05	>100	>100	>100

TTE = ethanolic extract of the Thai traditional cancer remedy; TTW = aqueous extract of the Thai traditional cancer remedy.

cytotoxicity (IC₅₀ > 20 µg/ml) against all tested cancer cells with low toxicity to normal cells (SI > 2). *H. indicum* and *F. vulgare* also selectively exerted mild to moderate cytotoxicity against the cancer cells.

Flavonoids, a group of phenolic compounds found in several medicinal plants, have a diverse range of derivatives depending on the substituted groups on their skeletal structure. This variety of flavonoids make the medicinal plants more valuable for their role in health promotion and

prevention of several chronic diseases including cancer. In this study, we investigated the total flavonoid contents of the plants and analyzed their correlation with cytotoxicity against cancer cells. As shown in Figure 1, the total flavonoid content of the extracts exhibited weak or no correlation to cytotoxicity against all tested cancer cells with coefficient (*r*) less than 0.35. However, in MCF-7, when the outlier data were excluded and the correlation recalculated, some extracts showed a strong correlation between total flavonoid

TABLE 3: Selectivity index (SI) of cytotoxic activity and total flavonoid content of the plant and remedy extracts.

Plant extracts	Selectivity index (SI)			Total flavonoid (mean \pm SEM; mg quercetin eq./g)
	HaCat/MCF7 ratio	HaCat/SKOV3 ratio	HaCat/Hela ratio	
<i>A. ebracteatus</i>	0.81	3.76	3.20	151.32 \pm 3.59
<i>A. galanga</i>	2.68	2.76	2.67	140.84 \pm 4.47
<i>A. villosum</i>	1.70	0.65	0.88	79.72 \pm 7.94
<i>A. comosus</i>	1.00	1.00	1.00	75.07 \pm 4.14
<i>A. paniculata</i>	0.44	0.38	0.38	96.1 \pm 5.87
<i>A. sinensis</i>	2.09	0.80	0.99	246.56 \pm 2.58
<i>A. dahurica</i>	10.13	1.00	1.00	227.95 \pm 5.69
<i>A. valgaris</i>	0.56	0.77	0.59	64.83 \pm 3.47
<i>A. membranaceus</i>	1.00	1.00	1.00	185.91 \pm 6.78
<i>B. rotunda</i>	1.14	0.98	0.57	175.38 \pm 5.19
<i>C. halicacalum</i>	2.19	1.00	1.00	138.29 \pm 3.98
<i>C. papaya</i>	2.37	1.00	1.00	134.27 \pm 2.61
<i>C. verum</i>	2.21	1.00	1.91	220.97 \pm 4.12
<i>C. myrrha</i>	1.00	1.00	1.45	143.77 \pm 4.37
<i>C. stellatopilosus</i>	0.39	0.34	0.34	46.38 \pm 5.02
<i>C. aromatic</i>	0.10	0.09	0.09	259.7 \pm 3.21
<i>C. Comosa</i>	0.57	0.64	0.54	139.28 \pm 3.04
<i>D. opposite</i>	1.00	1.00	1.00	113.73 \pm 5.71
<i>E. acoroides</i>	1.00	1.00	1.00	31.96 \pm 2.29
<i>F. albopurpurea</i>	6.83	1.00	1.00	25.47 \pm 2.13
<i>F. vulgare</i>	4.92	2.21	1.47	81.57 \pm 2.97
<i>H. indicum</i>	3.39	2.85	2.09	33.64 \pm 2.61
<i>E. arvense</i>	1.00	1.00	1.00	33.25 \pm 2.42
<i>J. sambac</i>	1.00	1.00	1.00	30.06 \pm 2.73
<i>K. galanga</i>	2.03	1.00	1.00	88.23 \pm 2.71
<i>L. triadra</i>	0.82	1.76	0.82	136.84 \pm 2.68
<i>L. striatum</i>	3.31	3.53	2.76	34.39 \pm 3.07
<i>L. barbarum.</i>	1.00	1.00	1.00	85.6 \pm 2.98
<i>M. cochinchinensis</i>	0.71	0.38	0.38	93.77 \pm 3.4
<i>M. siamensis</i>	2.97	0.33	0.33	204.94 \pm 2.72
<i>M. ferrea</i>	0.08	0.07	0.07	216.49 \pm 7.31
<i>M. elengi</i>	1.00	1.00	1.00	190.5 \pm 3.54
<i>M. fragrans</i>	0.51	0.33	0.33	72.23 \pm 3.59
<i>N. nucifera</i>	1.00	1.00	1.00	82.43 \pm 2.53
<i>O. tenuiflorum</i>	1.88	0.95	0.95	124.35 \pm 2.74
<i>P. amarus</i>	3.24	2.61	2.14	164.6 \pm 6.21
<i>P. cablin</i>	4.06	1.00	1.00	73.58 \pm 4.98
<i>R. glutinosa</i>	1.00	1.00	1.00	101.58 \pm 2.06
<i>R. nasutus</i>	1.52	2.07	1.00	183.57 \pm 5.46
<i>S. chinensis.</i>	1.00	1.00	1.00	94.79 \pm 5.57
<i>S. indicum</i>	1.00	1.00	1.00	163.17 \pm 3.44
<i>T. indica</i>	6.27	0.93	0.93	158 \pm 5.50
<i>V. vinifera</i>	1.00	1.00	1.00	14.8 \pm 2.73
TTW	0.47	0.47	0.47	41.92 \pm 4.04
TTE	1.91	1.00	1.00	105.67 \pm 4.33

content and cytotoxicity with the coefficient of -0.81 (Figure 2). This indicated that flavonoids found in plants such as *T. indica*, *B. rotunda*, and *A. dahurica* might be related to their cytotoxicity against MCF-7.

Several flavonoids from *T. indica* have been reported, including vitexin, isovitrexin, orientin, and iso-orientin [13]. A previous report showed that vitexin and orientin exhibited mild to moderate cytotoxic activity against MCF-7 cell line with IC_{50} more than $50 \mu\text{g/ml}$ [14]. Another report showed that the rhizome of *B. rotunda* contained flavonoids and chalcone compounds such as alpinetin, pinocembrin, cardamonin, pinostrobin, and panduratin A [15]. A

cyclohexenyl chalcone, panduratin A, in *B. rotunda* showed potent cytotoxic activity against MCF-7 with IC_{50} of $3.75 \mu\text{g/ml}$ [16]. *A. dahurica* showed high flavonoid content and exerted potent cytotoxic activity against MCF-7. The major constituents of *A. dahurica* were furocoumarins, imperatorin, phelloptorin, and isoimperatorin [17]. Imperatorin and isoimperatorin exhibited low to moderate cytotoxic activity against L1210, HL-60, K562, and B16F10 cell lines [18]. Components found in *M. siamensis* are coumarins such as mammae A, mammae B, mammae E, and other derivatives. Mammae A/AA exerted potent cytotoxic activity against breast cancer (MDA-MB-231) [19]. In *P. amarus*, the

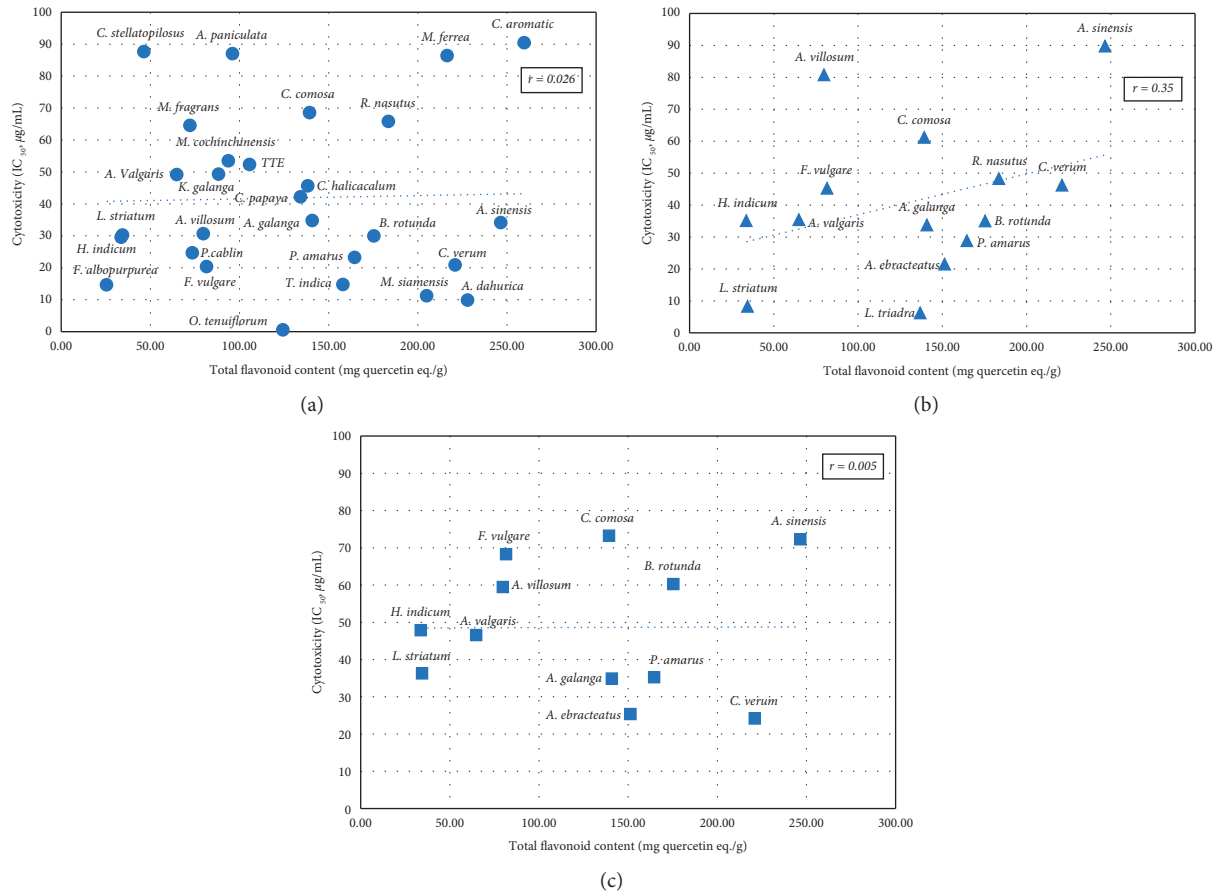


FIGURE 1: Scatter plots of flavonoid content and cytotoxicity of the plant extracts ($IC_{50} < 100 \mu\text{g/ml}$) against cancer cell lines. r = correlation coefficient, (a) = MCF-7, (b) = SKOV, (c) = HeLa.

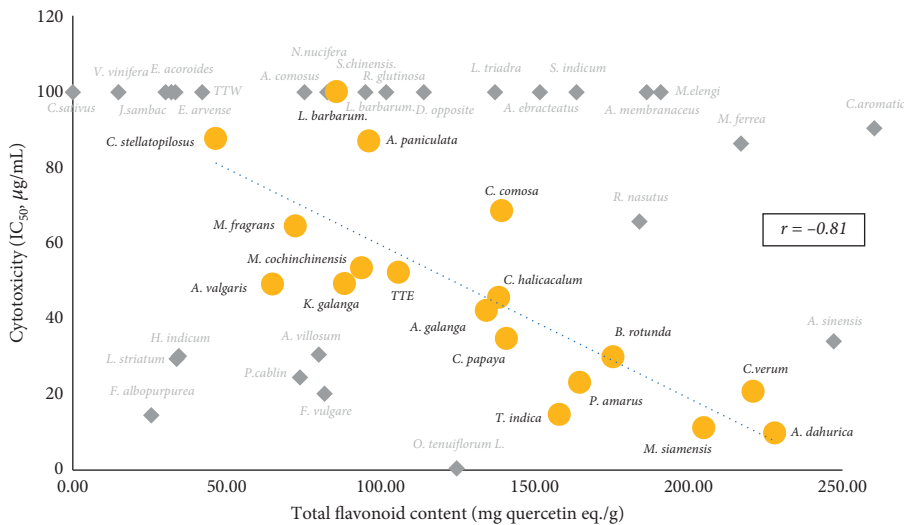


FIGURE 2: Scatter plot of cytotoxicity to MCF-7 and total flavonoid content of some selected plant extracts. r = correlation coefficient. (●) = the selected plant extracts that showed the correlation between total flavonoid content and cytotoxicity with correlation coefficient (r) value -0.81 ; (◆) = the plant extracts that showed lesser correlation.

major chemical components are lignans. Crude methanolic extract of *P. amarus* exerted cytotoxic activity against MCF-7 and could reduce invasion, migration, and adhesion [20].

C. aromatica showed the highest content of flavonoids; however, it exerted mild cytotoxicity to all tested cancer cells indicating that the flavonoids in *C. aromatica* were not

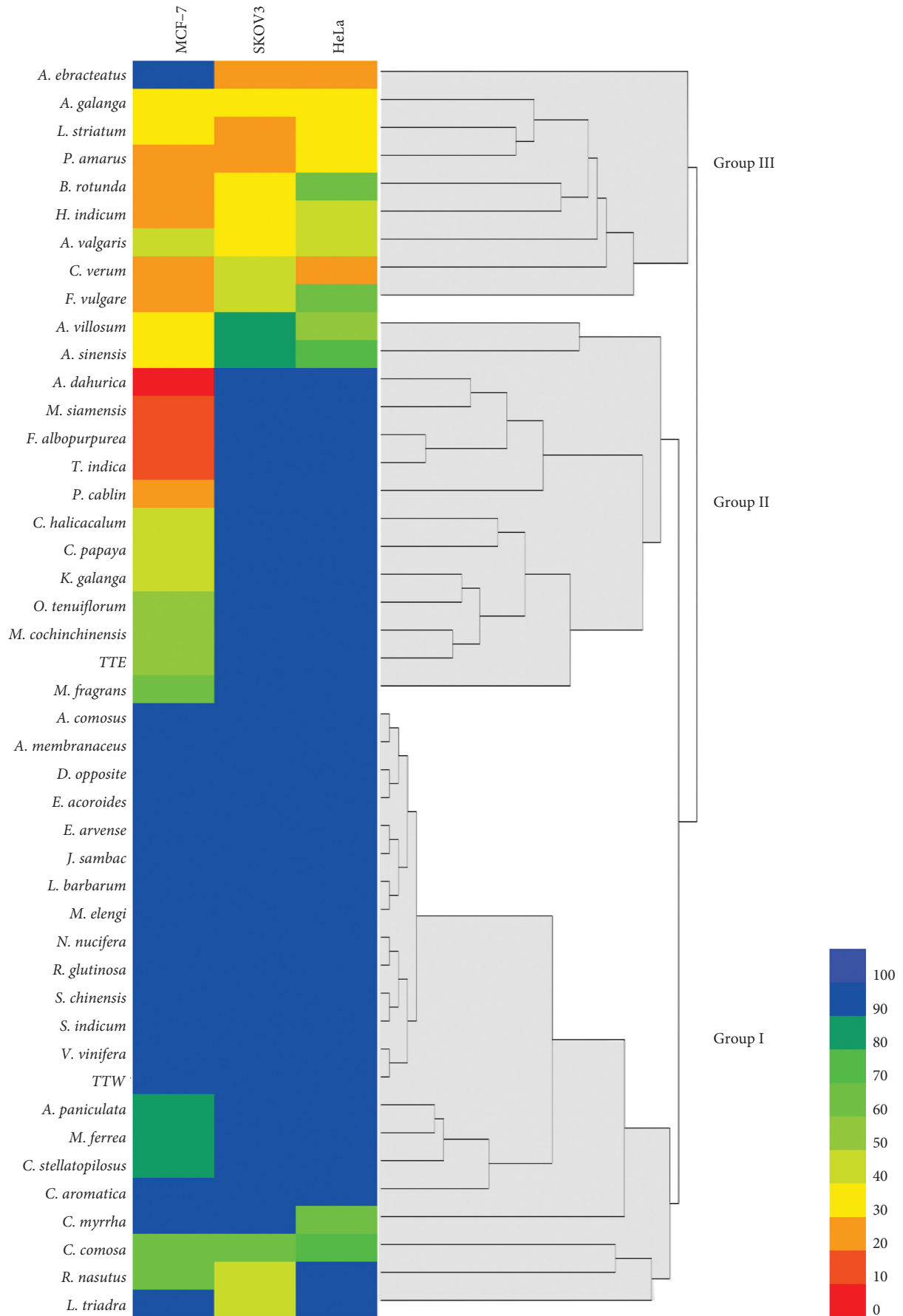


FIGURE 3: Heat map and hierarchical cluster analysis of plant and remedy extracts. Color scale bar showed a range of IC₅₀, red color bar represents more potent cytotoxic activity (0–10 µg/ml) incrementing to a blue color bar which represents weak cytotoxic activity (90–100 µg/ml).

related to cytotoxicity against the cancer cells. Major chemical constituents found in *C. aromatica* were volatile terpenes, sesquiterpenes, and curcuminoids. These compounds may react with the chemicals used in the total flavonoid assay leading to the overestimation of the values [21]. *C. verum* also showed high content of flavonoids, the major components being cinnamaldehyde and methyl eugenol [22].

Among the plants that showed high total flavonoid content, *C. aromatica* extract which possessed the highest flavonoid content exerted mild cytotoxic activity while *A. dahurica* exerted potent cytotoxicity. This indicated that the flavonoids in *C. aromatica* differed from those in *A. dahurica*, leading to the differences in their cytotoxic activity. In phytochemical reviews, the major constituent in *C. aromatica* is terpenes, while in *A. dahurica* are furocoumarins. These indicated that these compounds might cause overestimation of total flavonoid content, which underscores the limitation of this study. Hence, the determination of the total flavonoid content of the plants alone may be insufficient to describe the correlation with their biological activities. Therefore, more in-depth phytochemical studies should be pursued by more powerful analytical methods and instruments.

5. Conclusion

Among the 44 plants in a selected cancer remedy used for cancer treatments, 17 plants are food ingredients in Thai cuisine and nine of them exerted significant cytotoxicity against the tested cancer cell lines. Eleven plants normally used in TTM were active against at least one of the cancer cell lines, while 66.7% of all extracts were active against all the tested cell lines. The remaining plant extracts may not have any cytotoxic activity but may be necessary adjuvants according to the TTM theory which considers the correction of the imbalance of body functions as an important aspect in designing a medicine. The correlation and HCA studies provided an alternative way to investigate the biological activities of plant ingredients in polyherbal traditional remedies. This method was designed to predict the correlation between their active components and biological activities. However, the results may not show a strong correlation between the active components in traditional remedies or mixed herbs and their cytotoxicity against cancer cells. This is because only some herbs in the remedy possess cytotoxic effects while the others are included to balance other physiological functions in the body to improve patient's well-being. Therefore, *in vivo* studies are necessary to elucidate the true efficacy of herbal medicines. Hierarchical cluster analysis can help interpret the results of *in vitro* studies of herbals extracts by classifying them into groups that show different degrees of cytotoxicity in relation to the content of their bioactive components.

Data Availability

The data supporting the conclusions of the study are available from the corresponding author upon request.

Conflicts of Interest

The authors declare that they have no conflicts of interest.

Acknowledgments

This work was supported by the Centre of Excellence in Applied Thai Traditional Medicine Research, Bualuang ASEAN Chair Professorship, and Faculty of Medicine, Thammasat University, Thailand.












References

- [1] B. W. Stewart and C. P. Wild, *World Cancer Report 2014*, World Health Organization, Lyon, France, 2014.
- [2] S. Akin, G. Can, A. Aydiner, K. Ozdilli, and Z. Durna, "Quality of life, symptom experience and distress of lung cancer patients undergoing chemotherapy," *European Journal of Oncology Nursing*, vol. 14, no. 5, pp. 400–409, 2010.
- [3] B. Poonthananiwatkul, R. H. M. Lim, R. L. Howard, P. Pibanpaknatee, and E. M. Williamson, "Traditional medicine use by cancer patients in Thailand," *Journal of Ethnopharmacology*, vol. 168, pp. 100–107, 2015.
- [4] N. Ali and M. Hussain-Gambles, "Complementary and alternative medicine (CAM) use among South Asian patients with cancer in Britain," *Diversity Health Social Care*, vol. 2, no. 1, pp. 41–45, 2005.
- [5] T. Tuy-on, P. Maki, and A. Itharat, "Factors affecting treatment decision with traditional Thai approach; treatment results and quality of life of cancer patients treated at the Jitmeatta Mercy Foundation for Cancer Patients of Thailand (JFCT), Phetchaburi province, Thailand," *The Journal of the Thai Khadi Research Institute*, vol. 18, no. 1, 2021, In press.
- [6] T. Y. Wang, Q. Li, and K. S. Bi, "Bioactive flavonoids in medicinal plants: structure, activity and biological fate," *Asian Journal of Pharmaceutical Sciences*, vol. 13, no. 1, pp. 12–23, 2018.
- [7] M. Abotaleb, S. M. Samuel, E. Varghese et al., "Flavonoids in cancer and apoptosis," *Cancers (Basel)*, vol. 11, no. 1, p. 28, 2019.
- [8] P. Skehan, R. Storeng, D. Scudiero et al., "New colorimetric cytotoxicity assay for anticancer-drug screening," *JNCI Journal of the National Cancer Institute*, vol. 82, no. 13, pp. 1107–1112, 1990.
- [9] A. Itharat, P. J. Houghton, E. Eno-Amooquaye, P. J. Burke, J. H. Sampson, and A. Raman, "In vitro cytotoxic activity of Thai medicinal plants used traditionally to treat cancer," *Journal of Ethnopharmacology*, vol. 90, no. 1, pp. 33–38, 2004.
- [10] Z. H. Jia, M. C. Tang, and J. M. Wu, "The determination of flavonoid contents in mulberry and their scavenging effects on superoxide radicals," *Food Chemistry*, vol. 64, pp. 555–559, 1999.
- [11] W. Deng, Y. Wang, Z. Liu, H. Cheng, and Y. Xue, "HemI: a toolkit for illustrating heatmaps," *PLoS One*, vol. 9, no. 11, Article ID e111988, 2014.
- [12] Wardihan, M. Rusdi, G. Alam, Lukman, and M. A. Manggau, "Selective cytotoxicity evaluation in anticancer drug screening of *Boehmeria virgata* (Forst) Guill leaves to several human cell lines: HeLa, WiDr, T47D and Vero," *Dhaka University Journal of Pharmaceutical Sciences*, vol. 12, no. 2, pp. 87–90, 2013.
- [13] V. K. Bhatia, S. R. Gupta, and T. R. Seshadri, "C-glycosides of tamarind leaves," *Phytochemistry*, vol. 5, no. 1, pp. 177–181, 1966.

- [14] R. S. Mohammed, A. H. Abou Zeid, S. S. El Hawary, A. A. Sleem, and W. E. Ashour, "Flavonoid constituents, cytotoxic and antioxidant activities of *Gleditsia triacanthos* L. leaves," *Saudi Journal of Biological Sciences*, vol. 21, no. 6, pp. 547–553, 2014.
- [15] N. A. Yusuf, M. Suffian, M. Annuar et al., "Existence of bioactive flavonoids in rhizomes and plant cell cultures of *Boesenbergia rotunda* (L.) Mansf. Kulturpfl.," *Australian Journal of Crop Science*, vol. 7, no. 6, pp. 730–734, 2013.
- [16] C. Kirana, G. P. Jones, I. R. Record, and G. H. McIntosh, "Anticancer properties of panduratin A isolated from *Boesenbergia pandurata* (Zingiberaceae)," *Journal of Natural Medicines*, vol. 61, no. 2, pp. 131–137, 2007.
- [17] J. Kang, L. Zhou, J. Sun et al., "Chromatographic fingerprint analysis and characterization of furocoumarins in the roots of *Angelica dahurica* by HPLC/DAD/ESI-MSⁿ technique," *Journal of Pharmaceutical and Biomedical Analysis*, vol. 47, no. 4–5, pp. 778–785, 2008.
- [18] P. N. Thanh, W. Jin, G. Song, K. Bae, and S. S. Kang, "Cytotoxic coumarins from the root of *Angelica dahurica*," *Archives of Pharmacal Research*, vol. 27, no. 12, pp. 1211–1215, 2004.
- [19] C. Noysang, N. Kretschmer, O. Kunert et al., "Cytotoxic activity of mammea type coumarins from *Mammea siamensis* flowers," *Planta Medica*, vol. 75, no. 9, p. 981, 2009.
- [20] J. R. Patel, P. Tripathi, V. Sharma, N. S. Chauhan, and V. K. Dixit, "*Phyllanthus amarus*: ethnomedicinal uses, phytochemistry and pharmacology: a review," *Journal of Ethnopharmacology*, vol. 138, no. 2, pp. 286–313, 2011.
- [21] A. Pintatum, W. Maneerat, E. Logie et al., "*In vitro* anti-inflammatory, anti-oxidant, and cytotoxic activities of four curcuma species and the isolation of compounds from *curcuma aromatica* Rhizome," *Biomolecules*, vol. 10, no. 5, p. E799, 2020.
- [22] A. Gursale, V. Dighe, and G. Parekh, "Simultaneous quantitative determination of cinnamaldehyde and methyl eugenol from stem bark of *Cinnamomum zeylanicum* Blume using RP-HPLC," *Journal of Chromatographic Science*, vol. 48, no. 1, pp. 59–62, 2010.

Research Article

Carvacrol: An *In Silico* Approach of a Candidate Drug on HER2, PI3K α , mTOR, hER- α , PR, and EGFR Receptors in the Breast Cancer

Oscar Herrera-Calderon ¹, Andres F. Yepes-Pérez ², Jorge Quintero-Saumeth ³,
Juan Pedro Rojas-Armas ⁴, Miriam Palomino-Pacheco ⁵,
José Manuel Ortiz-Sánchez ⁶, Edwin César Cieza-Macedo ⁴,
Jorge Luis Arroyo-Acevedo ⁴, Linder Figueroa-Salvador ⁷, Gilmar Peña-Rojas ⁸,
and Vidalina Andía-Ayme ⁹

¹Academic Department of Pharmacology, Bromatology and Toxicology, Faculty of Pharmacy and Biochemistry, Universidad Nacional Mayor de San Marcos, Jr Puno 1002, Lima 15001, Peru

²Chemistry of Colombian Plants, Institute of Chemistry, Faculty of Exact and Natural Sciences, University of Antioquia-UdeA, Calle 70 No. 52-21 A.A, Medellín 1226, Colombia

³University of Pamplona, Faculty of Basic Sciences, Colombia, Km 1 Vía Bucaramanga Ciudad Universitaria, Pamplona, Colombia

⁴Laboratory of Pharmacology, Faculty of Medicine, Universidad Nacional Mayor de San Marcos, Av. Miguel Grau 755, Lima 15001, Peru

⁵Laboratory of Biochemistry, Faculty of Medicine, Universidad Nacional Mayor de San Marcos, Av. Miguel Grau 755, Lima 15001, Peru

⁶Laboratory of Physiology, Faculty of Medicine, Universidad Nacional Mayor de San Marcos, Av. Miguel Grau 755, Lima 15001, Peru

⁷School of Medicine, Faculty of Health Sciences, Universidad Peruana de Ciencias Aplicadas, Prolongación Primavera 2390, Lima 15023, Peru

⁸Laboratory of Cellular and Molecular Biology, Biological Sciences Faculty, Universidad Nacional de San Cristóbal de Huamanga, Portal Independencia 57, Ayacucho 05003, Peru

⁹Laboratory of Food Microbiology, Biological Sciences Faculty, Universidad Nacional de San Cristóbal de Huamanga, Portal Independencia 57, Ayacucho 05003, Peru

Correspondence should be addressed to Oscar Herrera-Calderon; oherreraca@unmsm.edu.pe

Received 23 August 2020; Revised 30 September 2020; Accepted 5 October 2020; Published 26 October 2020

Academic Editor: Azis Saifudin

Copyright © 2020 Oscar Herrera-Calderon et al. This is an open access article distributed under the Creative Commons Attribution License, which permits unrestricted use, distribution, and reproduction in any medium, provided the original work is properly cited.

Carvacrol is a phenol monoterpene found in aromatic plants specially in Lamiaceae family, which has been evaluated in an experimental model of breast cancer. However, any proposed mechanism based on its antitumor effect has not been reported. In our previous study, carvacrol showed a protective effect on 7,12-dimethylbenz[α]anthracene- (DMBA-) induced breast cancer in female rats. The main objective in this research was to evaluate by using *in silico* study the carvacrol on HER2, PI3K α , mTOR, hER- α , PR, and EGFR receptors involved in breast cancer progression by docking analysis, molecular dynamic, and drug-likeness evaluation. A multilevel computational study to evaluate the antitumor potential of carvacrol focusing on the main targets involved in the breast cancer was carried out. The *in silico* study starts with protein-ligand docking of carvacrol followed by ligand pathway calculations, molecular dynamic simulations, and molecular mechanics energies combined with the Poisson-Boltzmann (MM/PBSA) calculation of the free energy of binding for carvacrol. As result, the *in silico* study led to the identification of carvacrol with strong binding affinity on mTOR receptor. Additionally, *in silico* drug-likeness index for carvacrol showed a good predicted therapeutic profile of druggability. Our findings suggest that mTOR signaling pathway could be responsible for its preventive effect in the breast cancer.

1. Introduction

Carvacrol (2-methyl-5-(1-methylethyl)-phenol) is a phenol monoterpene and represents the major phytochemical in the essential oil of aromatic vegetable species belonging to the family Lamiaceae [1]. Some species with high content of carvacrol are *Origanum vulgare* (16.2%–81.92%), *Origanum acutidens* (76.21%) [2], *Thymus vulgaris* (43.8%), *Thymus kotschyanus* (24.4%), *Thymus kotschyanus* (24.4%), *Thymus capitatus* (>80%) *Thymus caramanicus*, *Thymus fallax* (from 50% to 70%), and *Thymus algeriensis* (7.8%) [3]. In regard to *Thymus vulgaris*, which is a species very cosmopolite in the world, the content of carvacrol can vary; this is due to the different chemotypes based on its volatile chemical composition. In Europe, *Thymus vulgaris* revealed at least 20 different chemotypes types, which carvacrol may range between 2% and 8% [4]. Otherwise, the essential oil of *Origanum vulgare* known as oregano also presents high variability of carvacrol linked to stage of harvest, ecological and climatic parameters ranging in countries such as Saudi Arabia (70.2%), Brazil (4.7%) [5], Italy (21.89%) [6], and Kashmir in the Himalaya region (52.3%–84.54%) [7].

Investigations related to its pharmacological activity have been tested by using *in vitro* assays overall in cell cultures such as anti-inflammatory, anticancer, antimicrobial, antifungal, antioxidant, antiapoptotic, antiproliferative, anti-invasion, and cytotoxic activities in order to establish any involved molecular mechanisms of carvacrol [8, 9]. Many molecules from nature sources are studied to determine if there could be a novel candidate as an antitumor potential drug yearly. When a molecule is isolated and characterized chemically, the *in silico* studies are the first step in the basic research that leads to the following stage of evaluation as the *in vitro* and *in vivo* studies. The *in silico* tests could exert the main mechanism on a biological target as well as its pharmacokinetic profile.

Nowadays, some citable works corresponding with the antitumor activity of carvacrol *in vitro* and *in vivo* have been reported. Although carvacrol is an old chemical component isolated from the essential oils of aromatic plants, recently, in the last decade, mechanisms involved in the tumorigenesis of certain types of cancer as prostate, lung, breast, gastric and colon have been evaluated only *in vitro* and recently employing experimental animals in breast and colon cancer. Even though the toxicity of carvacrol was evaluated in animals, this data is limited. It has been reported that the median lethal dose of carvacrol in rats is 810 mg/kg of body weight by oral gavage. Additionally, in an animal model of cancer induction, the maximum doses tested were 200 mg/kg of body weight and side effects linked to body weight loss and death were not evidenced [10].

The autophagy and adipogenic differentiation of about 30%–40% produced by carvacrol could be the cause to stop the cancer progression. It has been demonstrated that inhibition of mTOR by MEK signaling and LC3B-II expression promotes autophagy induction in an *in vitro* model of human cervical cancer. Additionally, carvacrol

nanoemulsion suppresses autophagy through enhancing the decreased conversion of autophagy-related genes LC-3 I to II, downregulating ATG5 (autophagy related 5) and ATG7 (autophagy related 7), and upregulating the protein P62. On the other hand, carvacrol downregulated the PI3K/AKT signaling on MCF-7 cells (human breast adenocarcinoma cells) [11]. Even though carvacrol has shown antiproliferative effects on a human metastatic breast cancer cell line (MDA-MB 231) and human non-small-cell lung cancer cell line (A-549), its mechanism is associated with biochemical changes in the mitochondria such as depolarization of the membrane potential, release of cytochrome c, and activation of caspase producing apoptosis [12, 13].

Additionally, carvacrol has demonstrated cytotoxicity against human cervical cancer cells HeLa [14], as well as antiproliferative and apoptotic on human liver cancer cells HepG-2 [15], cytotoxicity in AGS human gastric adenocarcinoma cells [15], liver cancer in rats [16], apoptosis in human oral squamous cell carcinoma (OSCC), and antiproliferative in N2a neuroblastoma cells; in PC-3 prostate cancer cells reduced the IL-6 protein levels, pSTAT3, pERK1/2, and pAKT signaling proteins. Furthermore, it exerted an antiproliferative effect on DU-145 prostate cancer cells by inhibiting TRPM7 channels and suppression of PI3K/Akt and MAPK signaling pathways [17, 18].

We proposed an *in silico* analysis and molecular docking studies on the main targets involved in the progression of the mammary tumors such as phosphatidylinositol-3-kinase- α wild type (PI3K α), human estrogen receptor- α (hER- α), progesterone receptor (PR), human epidermal growth factor receptor-2 (HER2), the mammalian target of rapamycin (mTOR), and epidermal growth factor receptor (EGFR), as well as molecular dynamic simulation and molecular mechanics energies combined with the Poisson-Boltzmann (MM/PBSA) studies, as well as evaluating its drug-likeness properties *in silico* in order to demonstrate druggability.

2. Results and Discussion

2.1. Multitarget Molecular Docking Investigation. Cancer in mammals involved multiple biological targets responsible for tumor cell proliferation and survival. Indeed, these receptors are included within key cellular signaling pathways which commonly appear to be genetically amplified in different tumors like breast cancer, including PI3K/Akt/mTOR signaling, HER2/EGFR-AKT system, and the classical hormone receptor-positive (ER+) pathway, which are implicated in the tumor self-renew, survival, and proliferation in breast cancer [19–22]. Targeting a single or multiple signaling pathways is considered nowadays a promising strategy for anticancer chemotherapy. Despite drugs available to treat breast cancer (i.e., lapatinib, alpelisib, rapamycin, tamoxifen, gefitinib, and the repurposing drug ulipristal acetate) have beneficial profiles, the severe and life-threatening side effects many of them have are notable. It has led to accelerated development of novel chemotherapy

alternatives, which computational approaches have been strongly employed for understanding drug-protein interactions, as well as mechanistic study when the potential drugs are placed within target-active site and binding affinity is calculated.

In this context, marked biological effects both *in vitro* and *in vivo* for carvacrol against breast cancer cells described here inspired further studies. For the current investigation, we hypothesized that carvacrol at least might target one of the signaling pathways, providing a plausible explanation from the observed experimental results. Thus, in order to afford an insight at a possible molecular-level mechanism for this compound, we performed docking investigations against the most valuable therapeutic targets for breast cancer therapy, such as phosphatidylinositol-3-kinase- α wild type (PI3K α), human estrogen receptor- α (hER- α), progesterone receptor (PR), human epidermal growth factor receptor-2 (HER2), the mammalian target of rapamycin (mTOR), and epidermal growth factor receptor (EGFR), which as previously mentioned play a fundamental role in breast cancer growth, invasiveness, and metastasis. Rigid receptor docking was performed in order to provide structural insights into the binding mode of carvacrol into every refined cancer signaling proteins.

To accomplish this goal, we calculated the binding energy scoring function of carvacrol docked against the X-ray crystallographic structures of these key proteins associated with breast cancer as follows: HER2 (PDB ID: 3PP0), PI3K α wild type (PDB ID: 4JPS), mTOR (PDB ID: 4DRI), hER- α (PDB ID: 3ERT), PR (PDB ID: 4OAR), and EGFR (PDB ID: 3POZ). In addition, we have screened six FDA-approved drugs for breast cancer, as well as strong inhibitors and its binding affinities were also determined to ensure certain amount of confidence regarding the Autodock scoring function of this project. The binding free energies produced by docking action of carvacrol and the known inhibitors on each catalytic site of the selected key protein targets are tabulated in Table 1.

As shown in Table 1, docking results showed that the best binding interaction was founded when carvacrol was docked with mTOR. In fact, a critical exploration of the selected active sites revealed that the binding pockets for the majority of these targets are too large to accommodate well carvacrol and achieve protein docking interactions, but not for the mTOR protein complex. Carvacrol had a docking score value of -7.5 kcal-mol against mTOR, which notably appears to be close to those founded for the rapamycin in this work (-8.6 kcal-mol) and previous works (-8.4 kcal-mol).

2.1.1. Docking Profile inside mTor Active Domain for Carvacrol: A Single-Target Approach. Due to interestingly binding energy founded for carvacrol against X-ray crystallographic structure of mTOR, an effective multilevel computational study based on single-objective involved docking followed by MD simulation and MM/PBSA free energy calculations was performed aiming to explore the potential of carvacrol to inhibit the mTOR function. The mammalian or mechanistic target of rapamycin (mTOR) is a

complex metabolic pathway responsible for activating cellular sensor to nutrients, cell growth, and proliferation in breast cancer; its inhibition is a promising therapeutic opportunity for breast cancer therapy [23, 24]. The architecture of mTOR complexes has been solved in detail by März et al. and cocrystallized with the cyclic macrolide rapamycin. The structure explains how rapamycin is capable of inhibiting mTOR function by binding to small protein termed as FKBP12, and how resulting complex then interacts with the FRB-mTor domain. This interaction disrupts the association of mTOR with the catalytic domain of mTORC1 and may block nutrient signaling and cell growth in breast cancer [25]. Thus, the most important active pocket into the mTOR pathway comprise the interface between FKBP12 and the FRB-mTor domain (namely, as rapamycin-binding pocket) and enclosing key binding interactions which play a crucial role in the catalytic activity of the kinase, including twelve contacts into FRB-mTor domain with His2028, Glu2033, Tyr2104, Leu2097, Gln2099, Trp2101, Tyr2038, Arg2036, Phe2108, Leu2031, Tyr2105, and Phe2039 and twenty residues from FKBP12, such as Arg73, Tyr113, Ile87, Asp68, Gln85, Gly84, Val78, Phe79, Leu128, Gly59, Lys121, Phe130, Lys88, Ser118, Ile122, Phe67, Tyr57, Trp90, Val86, and Phe77. Thus, docking investigations were carried out using final dimensions of the grid box of $32 \text{ \AA} \times 32 \text{ \AA} \times 32 \text{ \AA}$ and set on $X = 34.343$, $Y = 48.363$, and $Z = 38.034$, centering around key residues.

In order to accomplish high throughput, AutoDock Vina protocol inside mTOR binding pocket was firstly validated through self-docking. We performed a comparison of the crystallographic binding mode of the rapamycin deposited in PDB by März et al. and the lowest energy docking pose. To carry out this validation, root-mean-square deviation (RMSD) value was calculated to correlate the differences between the atomic distances. As shown in Figure 1, the docked conformation predicted for rapamycin (in violet) is spatially close to the crystallographic structure pose (in yellow) with an optimal RMSD value of 1.44 \AA . In addition, as shown in Table 1, the best binding energy calculated for rapamycin (-8.6 kcal-mol) was in good agreement with the literature data (-8.4 kcal-mol) [26]. These findings indicate a high-level of the feasibility in our protein-ligand docking procedure, which was able to reproduce the binding pose of the cocrystallized ligand deposited in the PDB ID: 4DRI.

After the docking protocol is validated, an exhaustive search in the binding pocket was carried out in order to establish key binding site points when carvacrol was docked into rapamycin binding Site of the mTOR catalytic domain. To this purpose, the best binding conformation for carvacrol and rapamycin was analyzed to make a valid comparison. A simple visual inspection to the superimposition of the docked inhibitors and carvacrol revealed that the carvacrol had a docked structure that fit well within the rapamycin-binding site with a low binding energy of -7.5 kcal-mol (Figure 2).

As rapamycin, carvacrol was also able to bind to mTOR with at least eleven essential amino acids for the catalytic activity of mTOR as follows: His2028, Glu2033, Tyr2104, Phe2108, Leu2031, Tyr2105, and Trp2101 at the mTOR-FRB

TABLE 1: Calculated binding affinity for carvacrol and current inhibitors into the active site of the most important targets involved in breast cancer.

	Target	Carvacrol	Lapatinib/ TAK-285 ^a	Alpelisib ^d /PIK-93 ^e	(-)-Rapamycin (sirolimus) ^c	4- OHT ^f	Ulipristal acetate (UPA)	Gefitinib/ TAK-285 ^a
Target protein docking score (kcal/mol)	HER2	-6.6	-10.4/-12	—	—	—	—	—
	PI3K α	-6.0	—	-8.1/-7.5	—	—	—	—
	mTOR ^b	-7.5	—	—	-8.6	—	—	—
	hER- α	-6.3	—	—	—	-9.7	—	—
	PR	-5.4	—	—	—	—	-10.6	—
	EGFR	-6.2	—	—	—	—	—	-8.2/-10.7

^aPotent, selective, ATP-competitive, and orally active HER2 and EGFR inhibitor; ^bmammalian active site of rapamycin was used; ^cspecific mTOR inhibitor with IC₅₀ of ~0.1 nM; ^dpotent and selective PI3K α inhibitor with IC₅₀ of 5 nM into the ATP pocket in PI3K α ; ^epotent PI3K α inhibitor (IC₅₀ at 19 nM) into the ATP pocket in PI3K α ; ^f4-hydroxytamoxifen, the active metabolite of tamoxifen.



FIGURE 1: Self-docking validation. Alignment of the best-docked pose of rapamycin (in violet) and the crystallographic binding mode (in yellow).

domain, as well as Val78, Phe79 Val86, and Phe77 with the FKBP12 protein (Table 2). This particular result supports our proposal: carvacrol might block mTOR function with similar binding affinity to rapamycin preventing the cell growth and proliferation.

Furthermore, this preliminary finding was also supported by an inspection of the 2D protein-ligand interaction plot after the docking protocol for carvacrol, which revealed similar key interactions in comparison with rapamycin (Figure 3(a)). Thus, carvacrol displays the occurrence of seven σ/π - π interactions into the mTOR-FRB domain with key Phe2108, Leu2031, Tyr2105, Trp2101 residues, as well as hydrophobic interactions with three residues postulated to bring about the catalytic function of mTOR (His2028, Glu2033, and Tyr2104). Furthermore, van der Waals contacts were formed between carvacrol with four residues of FKBP12 protein, such as Val78, Phe79 Val86, and Phe77. Finally, we also observed further interactions of carvacrol with mTOR, including five contacts with mTOR-FRB domain that have not been reported yet for current mTOR inhibitors as follows: one π -H-bond interaction with Ser2035 and four hydrophobic interactions surrounded by side chains of Arg2106, Glu2032, and His2106 (Figure 3(b)). Both crucial interactions and those additional binding

interactions might contribute to increasing mTOR affinity; hence carvacrol can tightly bind to the mTOR and potentially could inhibit its activity, suggesting that this small molecule may become a better drug prototype against breast cancer by targeting mTOR pathway.

2.1.2. Docking-Based Molecular Dynamics Simulation.

Molecular docking followed by MD simulation and MM/PBSA studies is a multilevel computational strategy to facilitate the process of drug designing against cancer. In fact, combining these computational protocols may conduce to develop safe and effective therapeutic options in response to the breast cancer [27]. Thus, in order to verify the docking computational solution obtained for carvacrol against the potential target mTOR protein, the best-docked pose of carvacrol into rapamycin-binding site was subjected to MD dynamic studies at 50 ns to explore the stability for ligand-protein complex, followed by MM/PBSA studies aiming to calculate the binding free energy of mTOR-carvacrol complex. Atom positional RMSD values in general equilibrate quickly during MD simulation, whereas an average RMSD value of 2.52 ± 0.02 Å was obtained and fall within the optimal range around 2 Å [28, 29]. This interesting finding suggest that the mTor-carvacrol complex predicted by molecular docking tends to reach dynamic stability at least in the time of 50 ns.

As illustrated in Figures 4(a) and 4(b), after 50 ns MD simulation the starting carvacrol docking pose exhibited two strong fluctuations in RMSD at around 10 and 18 ns, but notably achieved equilibrium beyond 20 ns within cavity-ligand binding. RMSD fluctuations primarily can be attributed as binding pocket large and elongated promoting large accommodations of the aromatic ring into the active site. Within the limitations of this study, this preliminary conclusion is based on the observations provided by Figures S1 and S2 in the supplementary material.

On the other side, the radius of gyration (Rg) represents the compactness of the protein structure and conformational stability of the whole systems (i.e., protein-ligand complexes). We performed Rg analysis to observe the conformational alterations and dynamic stability of the carvacrol into the mTOR-FRB domain. The predicted values of Rg for carvacrol (2.05 ± 0.64 Å) are listed in Figure 4(c). Rg value confirms the stabilization and suggests there was no

TABLE 2: Detailed interactions profile between carvacrol and rapamycin at the interface cavity of FKBP12 and mTOR–FRB domain.

Ligand	Interactions with FKBP12 protein			Interactions with mTOR–FRB domain		
	H-bond interactions <3 Å (n)	Van der Waals contacts (n)	σ/π - π /alkyl interactions (n)	H-bond interactions <3 Å (n)	Van der Waals contacts (n)	σ/π - π interactions (n)
Carvacrol	0	4Val78, Phe79 Val86, Phe77	0	0	6His2028, Glu2033, Tyr2104, Arg2106, Glu2032, His2106	7Phe2108, Leu2031, Tyr2105, Trp2101, Ser2035
Rapamycin	6Arg73, Tyr113, Ile87, Asp68, Gln85, Gly84	8Val78, Phe79, Leu128, Gly59, Lys121, Phe130, Lys88, Ser118	10Ile122, Phe67, Tyr57, Trp90, Val86, Phe77	0	8His2028, Glu2033, Tyr2104, Leu2097, Gln2099, Trp2101, Tyr2038, Arg2036	4Phe2108, Leu2031, Tyr2105, Phe2039

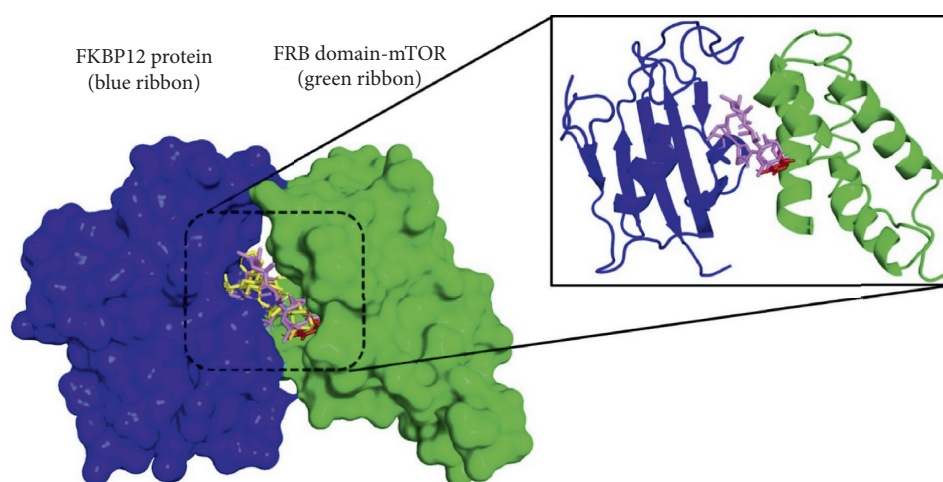


FIGURE 2: Superposition of the best pose-docked of carvacrol and rapamycin at the interface cavity of FKBP12 and mTOR–FRB domain. Carvacrol (in red), cocrystallized pose for rapamycin (in yellow), and best-docked pose for rapamycin (in violet).

significant change in the residual backbone and folding of the mTor protein after the binding process with carvacrol. This finding suggests not only that ligand-protein interactions remain intact during the simulation period, but also the protein-ligand structure is not disturbed over the entire trajectory (50 ns). The above-mentioned statement was also supported by 2D-binding interactions maps and 3D representation of carvacrol in the mTOR catalytic pocket (see supporting information in Figures S1–S3). Notably, trajectory snapshots extracted along MD simulation every 10 ns revealed that four of those key interactions established by the docking studies, which are essential to the mTOR function, were maintained stable during the simulation period, such as Leu2031, Trp2101, Ser2035, and Tyr2105. In addition, further interaction was evidenced with residue Phe2039 (FRB domain), which has been demonstrated to play an important role in the mTOR function [19, 30, 31] and also as part of those interactions with the rapamycin inhibitor (Table 2). These crucial interactions of mTOR with carvacrol are the probable reason for its marked antiproliferative activity.

Furthermore, 3D representation of carvacrol into mTOR binding pocket was used to make a comparison between the top-scoring binding pose and the equilibrated conformation after 50 ns MD simulations; hence we plotted the superposition of the docked complex 3D-structures before and

after MD simulation into the catalytic domain (see supporting information in Figures S2 and S3). In general, there are no dramatic differences between the structures extracted after 50 ns MD simulation and the best docking pose of carvacrol. Figure S3 showed that the aromatic ring in the small molecule is slightly shifted; indeed this slight rotational motion favored its contact with the key residue Phe2039, which as above-mentioned apparently plays a critical role in mTOR activation.

The obtained MD simulation results suggest (1) the initial docking conformation of the binding pocket and carvacrol were stable during the 50 ns MD simulations, (2) carvacrol does not leave the binding pocket while running MD simulation, and (3) crucial binding interactions initially shown by the docking results were maintained throughout the MD simulation; indeed we could find strong evidence that carvacrol may be able to interact with the key Phe2039 residue located within receptor binding domain of FRB, which becomes clearly visible when MD simulations were carried out. These findings not only suggested the rationality and validity of the active conformations obtained using AutoDock, but also proposed that carvacrol could act as rapamycin-like inhibitor of mTOR complex, which is highly implicated in the protein synthesis, cell growth, and cell proliferation in human breast cancer tissues.

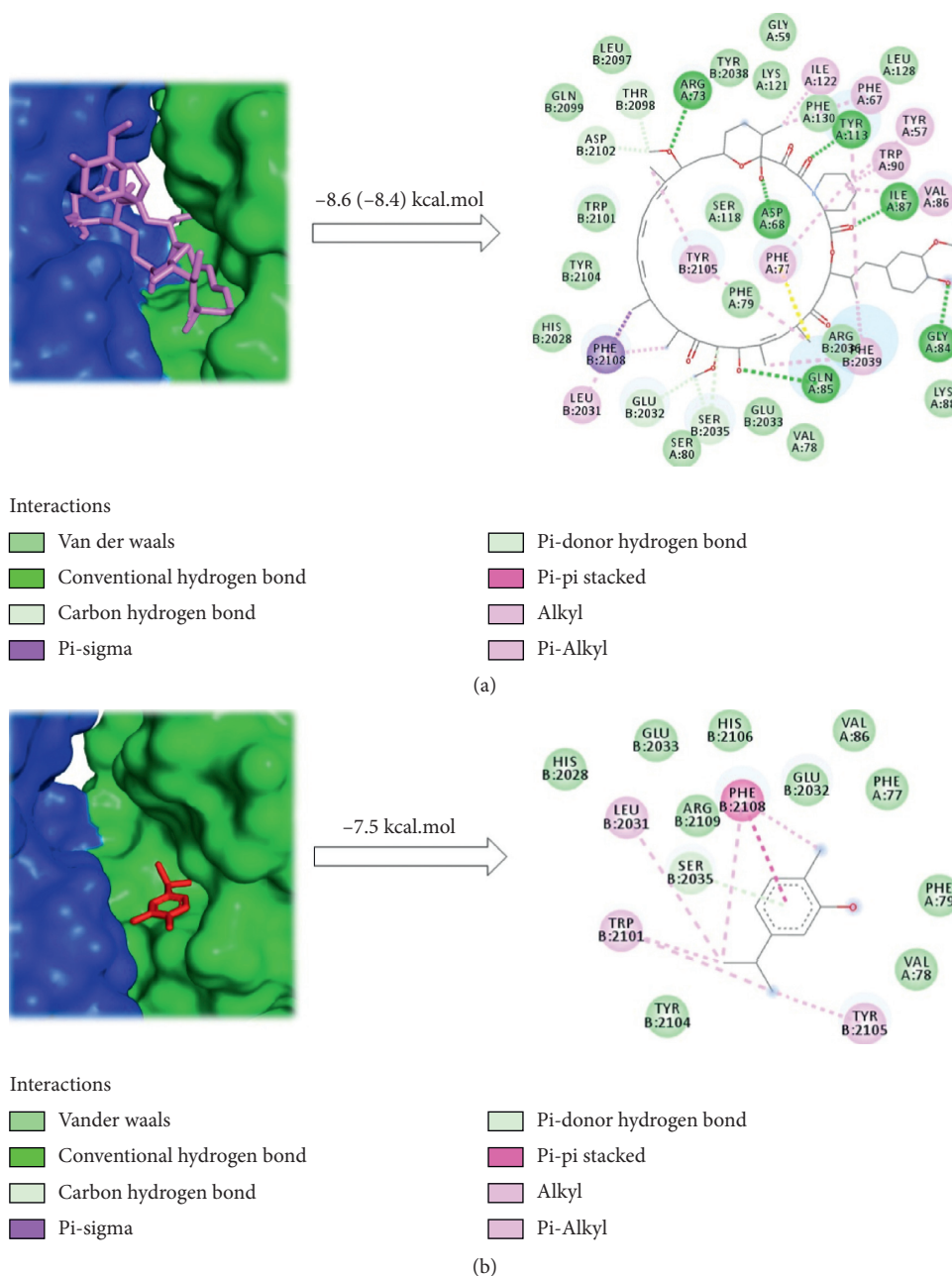


FIGURE 3: 2D ligand-protein interaction plots with the 3D-crystal structure of mTOR: (a) rapamycin and (b) carvacrol.

2.1.3. MM/PBSA Binding Free Energy Calculations. Finally, molecular mechanics combined with Poisson–Boltzmann and surface area (MM/PBSA) calculations were carried out in order to estimate the different contributions to the binding free energy during mTOR-carvacrol complex formation, which were obtained from a standard single-trajectory MMPBSA protocol. Use of a postdocking procedure based on MMPBSA approach plays an increasingly important role in understanding many subjects in molecular modeling studies focus on clinical applications, leading to development of anticancer compounds [32, 33]. To address this, MM/PBSA calculations were performed using the *g_mmpbsa* package [34] (from the last 40 ns of

trajectories from the production stage) to obtain free-energy contributions to the mTOR-carvacrol complex stabilization, which are summarized in Table 3.

From the results of MM/PBSA studies (Table 3), a molecular understanding of the binding interaction between carvacrol to the potential target (mTOR) by estimating different components of interaction energy that contributes to this binding was performed. Carvacrol possesses high nonbonded interaction energy with mTOR indicating its strong binding affinity (ΔG_{bind} value of $-18.03 \pm 1.57 \text{ kcal}\cdot\text{mol}^{-1}$). Moreover, van der Waals contacts have a greater energy contribution ($\Delta G_{\text{vdw}} = -19.28 \pm 1.46 \text{ kcal}\cdot\text{mol}^{-1}$) favoring the carvacrol bind to

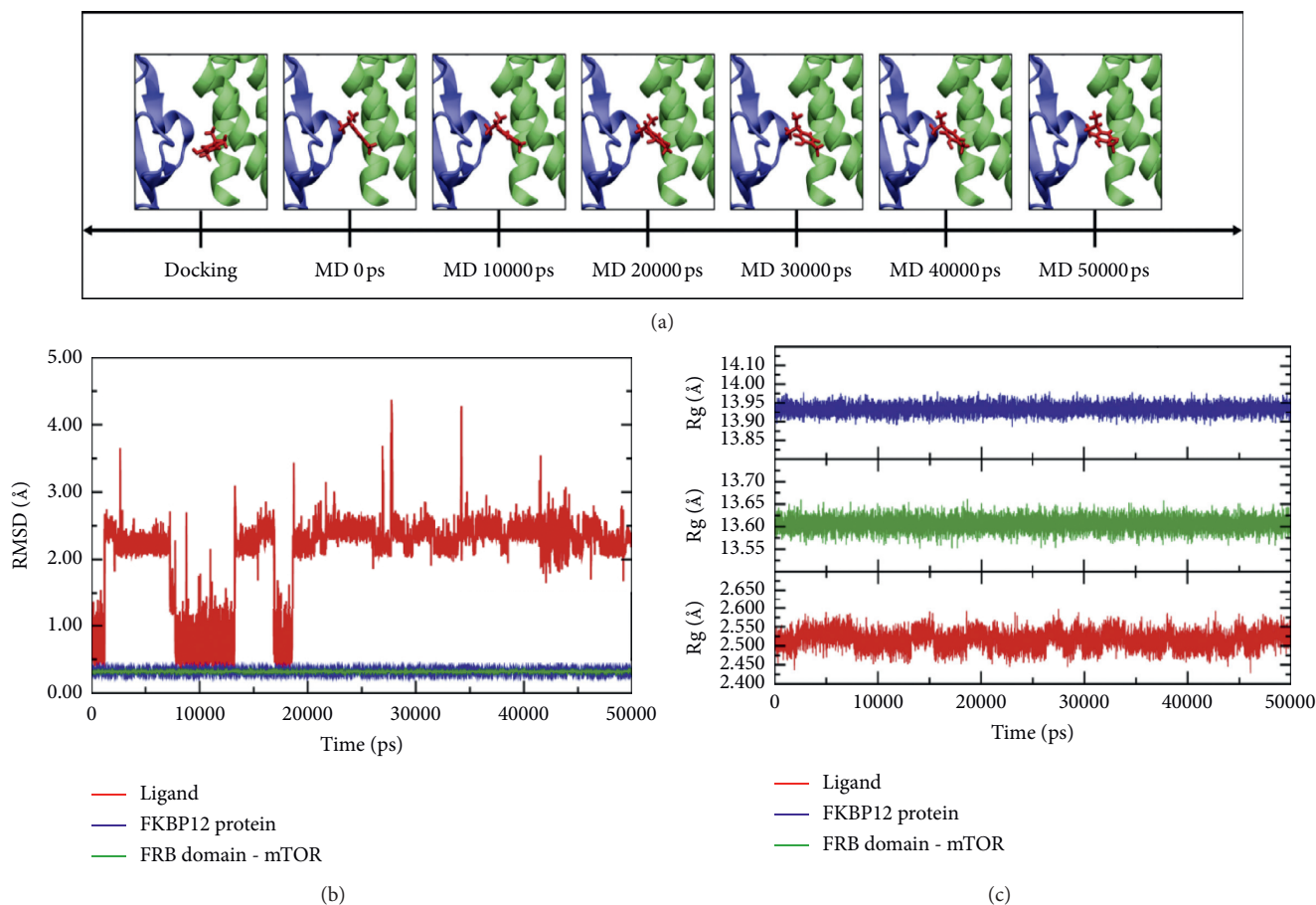


FIGURE 4: (a) Graphical snapshots at different periods during the MD simulation. (b) RMSD of the backbone of the carvacrol into the mTOR binding domain (in red). (c) Radius of gyration (Rg) plot for carvacrol into the binding pocket (in red) and every protein without ligand (green and blue).

TABLE 3: Calculated MM/PBSA binding free energy in $\text{kcal}\cdot\text{mol}^{-1}$ for complex mTOR carvacrol.

Energy contribution	Value ($\text{kcal}\cdot\text{mol}^{-1}$)
ΔG_{vdw}^a	-9.28 ± 1.46
$\Delta G_{\text{Electr}}^b$	-0.38 ± 0.70
$\Delta G_{\text{Polar}}^c$	3.85 ± 1.46
ΔG_{SASA}^d	-2.21 ± 0.14
ΔG_{bind}^e	-18.03 ± 1.57

^aVan der Waals energy terms. ^bElectrostatic energy contribution. ^cPolar contributions between the solute and solvent to the solvation energy. ^dNonpolar solvation energy using the solvent accessible surface area. ^e ΔG_{bind} is the total free binding energy.

mTOR, while solvent accessibility ($\Delta G_{\text{SASA}} = -2.21 \pm 0.14 \text{ kcal}\cdot\text{mol}^{-1}$) and electrostatic interactions ($\Delta G_{\text{Electr}} = -0.38 \pm 0.70 \text{ kcal}\cdot\text{mol}^{-1}$) only slightly contributed to total free binding energy. These findings revealed that those favorable ligand binding contributions could play a crucial role in the inhibition of mTOR with carvacrol inside the rapamycin binding site. Besides, unfavorable polar contributions were seen for carvacrol binding by the positive value obtained after MM/PBSA runs ($3.85 \pm 1.46 \text{ kcal}\cdot\text{mol}^{-1}$).

In addition, a per residue binding free energy decomposition using MM/PBSA was carried out in order to estimate individual energy contributions of each residue to the total binding free energy. As listed in Figure S4 in the Supplementary Information, per residue binding energy decompositions by using Amber MMPBSA showed that the key surrounding residues on complex carvacrol-mTOR resulted in being consistent with those found to be important to mTOR function and were in good agreement with close contacts resulting from MD simulations; among them, we can highlight Asp68, Glu75, Phe77, Gln85, and Asp91 (from the FKBP12 protein) and Leu2031, Ser2035, Phe2039, Trp2101, Asp2102, Tyr2104, Tyr2105, and Phe2108, from the FRB domain. From the calculations, we also observed that Lys52, Arg73, Lys83, and Lys121 (from the FKBP12 protein) and Arg2042, Arg2109, and Arg2110 (from the FRB domain) represent energetically unfavorable contacts during the ligand-binding event.

From the data collected by MM/PBSA calculations, it is suggested that van der Waals forces together with electrostatic interactions and the solvation free energy contributes to the mTOR-carvacrol complex stability. Importantly, not only carvacrol may bind to mTOR primarily through hydrophobic interactions mostly from the mTOR-FRB

domain, but also may equally bind favorably and strongly to the rapamycin-binding site compared to rapamycin.

2.1.4. Carvacrol Drug-Likeness Evaluation. Currently, early prediction of drug-likeness filters provides a useful guideline for further optimization of small molecules for cancer therapy, surviving clinical trials and becoming a drug. In general, these filters are based on empirical rules targeting several pharmacokinetic indices that confer crucial information for the speed and success in drug discovery. Herein, we predicted for carvacrol thirteen of the most crucial drug-likeness filters recommended during the design of cancer drug candidates [35, 36], which are shown in Table 4.

Calculated data sets for carvacrol fit well within recommended parameters for an optimal therapeutic option, suggesting the druggability of the carvacrol and demonstrating their potential as likely orally active oncology medicine. According to Lipinski’s rule of five (no more than one violation is acceptable) [37], the tested compound could be used as orally dosed drugs in humans. In addition, carvacrol exhibited a great %HIA, which would suggest that the molecule could be absorbed throughout the intestinal segments upon oral administration. This latter statement has been also confirmed by using Caco-2 cell monolayers or MDCK cells as predicting model, in which both models are recommended as a simplified *in vitro* model of intestinal absorption in drug development [38, 39]. In this case, carvacrol displayed recommended values ranges for an ideal drug of 3712 and 2042 nm/s, respectively. Compared to reference values taken from 95% of currently known drugs, carvacrol has an optimal lipophilicity index ($\text{LogP}_{o/w}$) of 3.280, may be implying the ability of the molecule to penetrating the lipid bilayers of the malignant cells. This fact was also verified using the calculated polar surface area (PSA) value, which is the most important physicochemical property to correlate passive molecular transport through membranes and drug-membrane interactions [40]. Predicted PSA for carvacrol showed an acceptable therapeutic value of 21.271 Å², indicating again that this compound should have good cellular membrane permeability. Finally, binding to serum albumin (calculated as LogK_{HSA}) is the most important indices for distribution and transport of drugs in the systemic circulation. Early prediction of this parameter reduces the amount of wasted time and resources for drug development candidates for anticancer therapy. Notably, carvacrol has a LogK_{HSA} value of 0.023 that fits well within the permitted range for 95% of marketed drugs (from -5 to 2.0). With respect to future pharmaceutical applications, the optimal pharmacokinetic properties make carvacrol a potential therapeutic alternative for specific treatment of breast cancer.

3. Materials and Methods

3.1. Molecular Modelling Studies

3.1.1. Protein Structure and Setup. To explore the potential mechanism of action of carvacrol, the most representative

TABLE 4: Drug-likeness evaluation of carvacrol.

Properties	Carvacrol
MW ^a	150.220
PSA ^b (7–200 Å ²)	21.271
<i>n</i> -Rot bond (<10)	2
<i>n</i> -ON ^c (<10)	1
<i>n</i> -OHNH ^d (<5)	1
Log <i>p</i> _{o/w} ^e (-2.0–6.5)	3.280
LogK _{HSA} ^g (-1.5–2.0)	0.023
Caco-2 ^h (nm/s) <25 poor; >500 great	3712
App. MDCK (nm/s) ⁱ <25 poor; >500 great	2042
% HIA ^j	100
Lipinski’s rule of five (≤1)	0
% HOA ^k >80% is high <25% is low	>80

^aMolecular weight of the molecule; ^bpolar surface area; ^c*n*-ON number of hydrogen bond acceptors; ^d*n*-OHNH number of hydrogen bonds donors; ^epredicted octanol-water partition coefficient; ^faqueous solubility; ^g*in vitro* binding constant to human serum albumin; ^hpredicted human intestinal permeability model (nonactive gut-blood barrier transport; ⁱapparent permeability across cellular membranes of Madin–Darby Canine Kidney (MDCK) cells; ^jhuman intestinal absorption (% HIA); ^kpercent of human oral absorption (HOA %).

proteins involved in intracellular signaling pathways driving breast cancer progression, including phosphatidylinositol-3-kinase- α wild type (PI3K α), human estrogen receptor- α (hER- α), progesterone receptor (PR), human epidermal growth factor receptor-2 (HER2), the mammalian target of rapamycin (mTOR), and epidermal growth factor receptor (EGFR), were used, respectively. Thus, the crystal structures were obtained from the Protein Data Bank as follows: HER2 (PDB ID: 3PP0) [41], PI3K α -wild type (PDB ID: 4JPS) [42], mTOR (PDB ID: 4DRI) [43], hER- α (PDB ID: 3ERT) [44], PR (PDB ID: 4OAR) [45], and EGFR (PDB ID: 3POZ) [41]. Discovery Studio (DS) Visualizer 2.5 was used to edit the protein structures and to remove water molecules together with bound ligands. The structures of the selected proteins were parameterized using AutoDockTools [46]. In general, hydrogens were added to polar side chains to facilitate the formation of hydrogen bonds, and the Gasteiger partial charges were calculated.

3.1.2. Ligand Dataset Preparation and Optimization.

Ligands used in this study are carvacrol and nine well-known anticancer inhibitors, including six FDA-approved cancer drugs (lapatinib, alpelisib, (-)-rapamycin, 4-OHT, ulipristal acetate, and gefitinib) and two emerging inhibitors for breast cancer therapy: TAK-285 and PIK-93. The selected 2D structures of the ligands were retrieved as CSV files from the PubChem database (<https://pubchem.ncbi.nlm.nih.gov/>); then DS visualizer was used to rewrite the data files into pdb format. The structures of the ligands were parameterized using AutodockTools to add full hydrogens to the ligands, to assign rotatable bonds, to compute Gasteiger partial atomic charges and save the resulting structure in the required format for use with AutoDock. All possible flexible torsions of the ligand molecules were defined using AUTOTUTORS in

AutoDockTools [47] to facilitate the simulated binding with the receptor structure.

3.1.3. Docking and Subsequent Analysis. Docking simulations were performed with AutoDock 5.6 using the Lamarckian genetic algorithm and default procedures for docking a flexible ligand to a rigid protein. Docking calculations were carried out into the binding catalytic site of each protein target. Once potential binding sites were identified, docking of carvacrol to these sites was carried out to determine the most probable and most energetically favorable binding conformations. To accomplish that, rigorous docking simulations involving a grid box to the identified binding site, Autodock Vina 1.1.2 [48], was used. The exhaustiveness was 20 for each protein-compound pair. The active site was surrounded by a docking grid of 32 Å³ with a grid spacing of 0.375 Å. Affinity scores (in kcal/mol) given by AutoDock Vina for carvacrol were obtained and ranked based on the free energy binding theory (more negative value means greater binding affinity). The resulting structures and the binding docking poses were graphically inspected to check the interactions using the DS Visualizer 2.5 (<http://3dsbiovia.com/products/>) or The PyMOL Molecular Graphics system 2.0 programs.

3.1.4. Molecular Dynamics (MD) Simulation and Free Energy Calculations. In order to verify the molecular interaction stability of mTOR-carvacrol complex, molecular dynamics (MD) simulations were carried out by using the Gromacs program [49] considering the most potential protein target for carvacrol extracted from docking results and the best docking pose. Force field parameters for protein and ligand were derived independently. For the selected protein, the amber03 force field was selected and assigned by using the pdb2gmx tool of the Gromacs program packages; meanwhile, ligand force field parameters were prepared with the generalized AMBER force field (GAFF) using the molecular geometries previously optimized in gas phase using the HF/6-31* level of theory, [50] with the Gamess-US program [51]. In addition, ligand was verified as a minimum through a harmonic vibrational normal mode analysis. Atomic charges were obtained with the Merz-Kollman scheme [52] by fitting a restricted electrostatic potential (RESP) model [53] by the Gamess-US program, and the output file was used into the resp. subprogram of the AmberTools program package [54]. Assignment of GAFF force field parameters was carried out by the Antechamber program [55] and the required input files for molecular dynamics simulations were prepared using the ACPYPE python interface [56]. Protein and protein-ligand complex were solvated in a rectangular box of TIP3P waters and chloride (Cl⁻) or sodium (Na⁺) ions were added to the system by random replacement of water molecules until neutralization of total charge. In order to remove spurious contact, molecular geometries were optimized with the steepest descent algorithm with 100000 steps and protein backbones atoms were constrained with a force constant of 1000 kJ mol⁻¹. Then, the MD simulations were allowed to run for 1000 ps in the NpT ensemble.

Additionally, 50 ns in the NpT ensemble were calculated for the production stage. All simulations were carried out under periodic boundary conditions. A 12 Å cutoff distance was used to calculate nonbonded interactions. Electrostatic interactions were treated with the Ewald particle mesh (PME) method [57], while van der Waals interactions were introduced by using the cutoff scheme [58]. Finally, the V-rescale thermostat at 300 K with a coupling constant of 1.0 ps was used and the pressure was kept constant at 1 atm using the Parrinello-Rahman barostat [59] with a coupling constant of 2.0 ps and a compressibility factor of 4.5×10^{-5} bar⁻¹. All covalent bonds were constrained using the LINCS algorithm and the contact list was updated every 40 fs. The binding free energy was analyzed using the molecular mechanics Poisson-Boltzmann surface area (MM/PBSA) method [60] implemented in Gromacs program. For MMPBSA calculations, the g_mmpbsa software [34] was used for electrostatic interactions, van der Waals interactions, polar solvation energy, and nonpolar solvation energy calculations. The binding free energy was calculated using the last 40 ns of trajectories from the production stage MD simulations, for example, 500 snapshots. The SASA model was used for nonpolar contributions with a surface tension of 0.0226778 (kJ/mol²) and a probe radius of 1.4 Å. An ionic strength of 0.150 M-NaCl with radii of 0.95 and 1.81 Å for sodium and chloride ions, respectively, was used for all polar calculations. In addition, dielectric constants of 6, 80 and 1 were used for the protein, water, and vacuum, respectively. To calculate the average binding free energy over the previously selected snapshots, a bootstrap analysis was performed.

3.1.5. Carvacrol Drug Likeness Evaluation. *In silico* drug-likeness indices were evaluated for carvacrol in order to explore its druggability for further clinical studies. To find out the drug-like properties, carvacrol was screened for its pharmacokinetic properties using open-source cheminformatics toolkits such as Molinspiration software (for: MW, rotatable bonds and topographical polar surface area (PSA) descriptors, ALOGPS 2.1 algorithm from the Virtual Computational Chemistry Laboratory (for: Log Po/w descriptor), and Pre-ADMET 2.0 program to predicted various pharmacokinetic parameters and pharmaceutical relevant properties such as apparent predicted intestinal permeability (App. Caco-2), binding to human serum albumin (LogK_{HSA}), MDCK cell permeation coefficients, and intestinal or oral absorption (%HIA). These key parameters define absorption, permeability, motion, and action of drug molecule. The interpretation of two predicted ADMET properties using the Pre-ADMET program was shown in the following.

Value of Caco-2 permeability is classified into three classes:

(1) If permeability < 4, low permeability; (2) if permeability < 70, moderate permeability; and (3) if permeability > 70, higher permeability.

Value of MDCK cell permeability can be classified into three classes:

(1) If permeability < 25, low permeability; (2) if 25 < permeability < 500, moderate permeability; and (3) if permeability > 500, higher permeability.

4. Conclusions

Multilevel computational studies suggested that the candidacy of carvacrol for future drugs investigations in the breast cancer treatment should be strongly considered. Virtual screening revealed that mTOR is the main target of carvacrol which has shown a good interaction with this regulating protein with respect to other evaluated proteins responsible of the mammary tumorigenesis. ADME prediction of carvacrol shows that it is a good candidate to oral drug formulation and could be useful as alternative therapy in breast cancer. However, in spite of showing a good prediction on mTOR receptor with values near to rapamycin in docking modeling, our findings in the histological evaluation of our previous research suggest that carvacrol could be protective or preventive against an exposure with any carcinogenic agent. Further studies with other target proteins should be analyzed in order to elucidate how carvacrol is acting in breast cancer.

Data Availability

The data that support the findings of this study are available from the corresponding author upon reasonable request.

Conflicts of Interest

The authors declare no conflicts of interest.

Authors' Contributions

O.H.-C., A.F.Y.-P., and J.Q.-S. were responsible for conceptualization; A.F.Y.-P., J.Q.-S., and J.P.R.-A. were responsible for methodology; A.F.Y.-P. and J.Q.-S. were responsible for software; L.F.-S. and G.P.-R. were responsible for validation; V.A.-A. was responsible for formal analysis; O.H.-C., J.L.A.-A., and J.M.O.-S. was responsible for investigation; O.H.-C., A.F.Y.-P., and J.Q.-S. were responsible for writing and editing and original draft preparation; O.H.-C., M.P.-P., and J.Q.-S. were responsible for writing, reviewing, and editing; E.C.C.-M. was responsible for visualization; A.F.Y.-P. was responsible for supervision. All authors have read and agreed to the published version of the manuscript.

Acknowledgments

The authors thank Universidad Nacional Mayor de San Marcos for supporting this work.

Supplementary Materials

S1: 2D-binding interactions maps from MD simulations for carvacrol-mTOR complex. S2: 3D plots for comparison pose docking, snapshot of carvacrol backbone atoms at 10 and 20 ns, and after 50 ns MD simulations for carvacrol-mTOR

complex. Best docking pose (red) snapshot at 10 ns (grey), snapshot at 20 ns (orange), and pose post-50 ns MD simulation (yellow). S3: 3D plots for comparison pose docking and pose after MD simulations for carvacrol-mTOR complex (best docking pose in red and pose post-50 ns MD simulation in yellow). S4: the individual energy contributions of each residue from MM/PBSA calculations in carvacrol-mTOR complex. FKBP12 protein is colored blue and FRB domain green. (*Supplementary Materials*)

References

- [1] E. R. Silva, F. O. De Carvalho, L. G. B. Teixeira et al., "Pharmacological effects of carvacrol in in Vitro studies: a review," *Current Pharmaceutical Design*, vol. 24, no. 29, pp. 3454–3465, 2018.
- [2] N. Leyva-López, E. P. Gutiérrez-Grijalva, G. Vazquez-Olivo, and J. B. Heredia, "Essential oils of oregano: biological activity beyond their antimicrobial properties," *Molecules*, vol. 22, no. 6, 989 pages, 2017.
- [3] S. M. Nabavi, A. Marchese, M. Izadi, V. Curti, M. Daglia, and S. F. Nabavi, "Plants belonging to the genus thymus as antibacterial agents: from farm to pharmacy," *Food Chemistry*, vol. 173, pp. 339–347, 2015.
- [4] P. Satyal, B. Murray, R. McFeeters, and W. Setzer, "Essential oil characterization of thymus vulgaris from various geographical locations," *Foods*, vol. 5, no. 4, p. 70, 2016.
- [5] S. Fikry, N. Khalil, and O. Salama, "Chemical profiling, biostatic and biocidal dynamics of *Origanum vulgare* L. essential oil," *AMB Express*, vol. 9, no. 1, p. 41, 2019.
- [6] L. De Martino, V. De Feo, C. Formisano, E. Mignola, and F. Senatore, "Chemical composition and antimicrobial activity of the essential oils from three chemotypes of *origanum vulgare* l. ssp. *hirtum* (link) *ietswaart* growing wild in campania (southern Italy)," *Molecules*, vol. 14, no. 8, pp. 2735–2746, 2009.
- [7] S. Jan, M. Rashid, E. F. Abd-Allah, and P. Ahmad, "Biological efficacy of essential oils and plant extracts of cultivated and wild ecotypes of *Origanum vulgare* L.," *BioMedical Research International*, vol. 2020, Article ID 8751718, 2020.
- [8] Z. Mbese and B. A. Aderibigbe, "Biological efficacy of carvacrol analogues," *Recent Patents on Anti-Infective Drug Discovery*, vol. 13, no. 3, pp. 207–216, 2018.
- [9] Z. E. Suntres, J. Coccimiglio, and M. Alipour, "The bioactivity and toxicological actions of carvacrol," *Critical Reviews in Food Science and Nutrition*, vol. 55, no. 3, pp. 304–318, 2015.
- [10] J. P. Rojas-Armas, J. L. Arroyo-Acevedo, M. Palomino-Pacheco et al., "The essential oil of *cymbopogon citratus* stapt and carvacrol: an approach of the antitumor effect on 7,12-dimethylbenz- $[\alpha]$ -anthracene (DMBA)-Induced breast cancer in female rats," *Molecules*, vol. 25, no. 14, p. 3284, 2020.
- [11] A. Mari, G. Mani, S. N. Nagabhishek et al., "Carvacrol promotes cell cycle arrest and apoptosis through PI3K/AKT signaling pathway in MCF-7 breast cancer cells," *Chinese Journal of Integrative Medicine*, 2020.
- [12] A. T. Koparal and M. Zeytinoglu, "Effects of carvacrol on a human non-small cell lung cancer (NSCLC) cell line, A549," *Cytotechnology*, vol. 43, no. 1, pp. 149–154, 2003.
- [13] K. M. Arunasree, "Anti-proliferative effects of carvacrol on a human metastatic breast cancer cell line, MDA-MB 231," *Phytomedicine*, vol. 17, no. 8-9, pp. 581–588, 2010.
- [14] I. Potočnjak, I. Gobin, and R. Domitrović, "Carvacrol induces cytotoxicity in human cervical cancer cells but causes cisplatin

- resistance: involvement of MEK-ERK activation,” *Phytotherapy Research: PTR*, vol. 32, no. 6, pp. 1090–1097, 2018.
- [15] Q.-H. Yin, F.-X. Yan, X.-Y. Zu et al., “Anti-proliferative and pro-apoptotic effect of carvacrol on human hepatocellular carcinoma cell line HepG-2,” *Cytotechnology*, vol. 64, no. 1, pp. 43–51, 2012.
- [16] S. Jayakumar, A. Madankumar, S. Asokkumar et al., “Potential preventive effect of carvacrol against diethylnitrosamine-induced hepatocellular carcinoma in rats,” *Molecular and Cellular Biochemistry*, vol. 360, no. 1–2, pp. 51–60, 2012.
- [17] Y. Luo, J.-Y. Wu, M.-H. Lu, Z. Shi, N. Na, and J.-M. Di, “Carvacrol alleviates prostate cancer cell proliferation, migration, and invasion through regulation of PI3K/akt and MAPK signaling pathways,” *Oxidative Medicine and Cellular Longevity*, vol. 2016, Article ID 1469693, 11 pages, 2016.
- [18] F. Khan, V. K. Singh, M. Saeed, M. A. Kausar, and I. A. Ansari, “Carvacrol induced program cell death and cell cycle arrest in androgen-independent human prostate cancer cells via inhibition of notch signaling,” *Anti-Cancer Agents in Medicinal Chemistry*, vol. 19, no. 13, pp. 1588–1608, 2019.
- [19] L. Yang, P. Shi, G. Zhao et al., “Targeting cancer stem cell pathways for cancer therapy,” *Signal Transduction and Targeted Therapy*, vol. 5, no. 1, p. 8, 2020.
- [20] M. A. Ortega, O. Fraile-Martínez, Á Asúnsolo, J. Buján, N. García-Honduvilla, and S. Coca, “Signal transduction pathways in breast cancer: the important role of PI3K/Akt/mTOR,” *Journal of Oncology*, vol. 2020, Article ID 9258396, 11 pages, 2020.
- [21] F. J. Velloso, A. F. Bianco, J. O. Farias et al., “The crossroads of breast cancer progression: insights into the modulation of major signaling pathways,” *OncoTargets and Therapy*, vol. 10, pp. 5491–5524, 2017.
- [22] B. R. B. Pires, Í. S. S. De Amorim, L. D. E. Souza, J. A. Rodrigues, and A. L. Mencialha, “Targeting cellular signaling pathways in breast cancer stem cells and its implication for cancer treatment,” *Anticancer Research*, vol. 36, no. 11, pp. 5681–5692, 2016.
- [23] S. H. Hare and A. J. Harvey, “mTOR function and therapeutic targeting in breast cancer,” *American Journal of Cancer Research*, vol. 7, no. 3, pp. 383–404, 2017.
- [24] I. Mayer, “Role of mTOR inhibition in preventing resistance and restoring sensitivity to hormone-targeted and HER2-targeted therapies in breast cancer,” *Clinical Advances in Hematology & Oncology*, vol. 11, no. 4, pp. 217–224, 2013.
- [25] J. Kim and K.-L. Guan, “mTOR as a central hub of nutrient signalling and cell growth,” *Nature Cell Biology*, vol. 21, no. 1, pp. 63–71, 2019.
- [26] R. Kist and R. A. Caceres, “New potential inhibitors of mTOR: a computational investigation integrating molecular docking, virtual screening and molecular dynamics simulation,” *Journal of Biomolecular Structure and Dynamics*, vol. 35, no. 16, pp. 3555–3568, 2017.
- [27] M. Rosales-Hernandez, J. Bermudez-Lugo, J. Garcia, J. Trujillo-Ferrara, and J. Correa-Basurto, “Molecular modeling applied to anti-cancer drug development,” *Anti-Cancer Agents in Medicinal Chemistry*, vol. 9, no. 2, pp. 230–238, 2012.
- [28] H. Gohlke, M. Hendlich, and G. Klebe, “Knowledge-based scoring function to predict protein-ligand interactions,” *Journal of Molecular Biology*, vol. 295, no. 2, pp. 337–356, 2000.
- [29] B. Kramer, M. Rarey, and T. Lengauer, “Evaluation of the flexx incremental construction algorithm for protein-ligand docking,” *Proteins Structure. Function.Bioinformatics*, vol. 37, no. 2, pp. 228–241, 1999.
- [30] V. Thiagarajan, K. W. Lee, M. K. Leong, and C. F. Weng, “Potential natural mTOR inhibitors screened by in silico approach and suppress hepatic stellate cells activation,” *Journal of Biomolecular Structure and Dynamics*, vol. 36, no. 16, pp. 4220–4234, 2018.
- [31] J. C. Chamcheu, V. M. Adhami, S. Esnault et al., “Dual inhibition of PI3K/akt and mTOR by the dietary antioxidant, delphinidin, ameliorates psoriatic features in vitro and in an imiquimod-induced psoriasis-like disease in mice,” *Antioxidants & Redox Signaling*, vol. 26, no. 2, pp. 49–69, 2017.
- [32] B. R. Miller, T. D. McGee, J. M. Swails et al., “MMPBSA.py: an efficient program for end-state free energy calculations,” *Journal of Chemical Theory and Computation*, vol. 14, no. 11, pp. 6035–6049, 2012.
- [33] B. Kuhn, P. Gerber, T. Schulz-Gasch, and M. Stahl, “Validation and use of the MM-PBSA approach for drug discovery,” *Journal of Medicinal Chemistry*, vol. 48, no. 12, pp. 4040–4048, Jun. 2005.
- [34] R. Kumari, R. Kumar, O. S. D. D. Consortium, and A. Lynn, “g _ mmpbsa—a GROMACS tool for MM-PBSA and its optimization for high-throughput binding energy calculations,” *Journal of Chemical Information and Modeling*, 2014.
- [35] C. Y. Jia, J. Y. Li, G. F. Hao, and G. F. Yang, “A drug-likeness toolbox facilitates ADMET study in drug discovery,” *Drug Discovery Today*, vol. 25, no. 1, pp. 248–258, 2020.
- [36] T. Maziasz, V. J. Kadambi, L. Silverman, E. Fedyk, and C. L. Alden, “Predictive toxicology approaches for small molecule oncology drugs,” *Toxicologic Pathology*, vol. 38, no. 1, pp. 148–164, Jan. 2010.
- [37] C. A. Lipinski, F. Lombardo, B. W. Dominy, and P. J. Feeney, “Experimental and computational approaches to estimate solubility and permeability in drug discovery and development settings,” *Advanced Drug Delivery Reviews*, vol. 23, no. 1, pp. 3–25, 2012.
- [38] F. Broccatelli, L. Salphati, E. Plise et al., “Predicting passive permeability of drug-like molecules from chemical structure: where are we?” *Molecular Pharmaceutics*, vol. 13, no. 12, pp. 4199–4208, 2016.
- [39] B. Press and D. Di Grandi, “Permeability for intestinal absorption: caco-2 assay and related issues,” *Current Drug Metabolism*, vol. 9, pp. 893–900, 2008.
- [40] P. Ertl, B. Rohde, and P. Selzer, “Fast calculation of molecular polar surface area as a sum of fragment-based contributions and its application to the prediction of drug transport properties,” *Journal of Medicinal Chemistry*, vol. 43, no. 20, pp. 3714–3717, 2000.
- [41] K. Aertgeerts, R. Skene, J. Yano et al., “Structural analysis of the mechanism of inhibition and allosteric activation of the kinase domain of HER2 protein,” *Journal of Biological Chemistry*, vol. 286, no. 21, pp. 18756–18765, 2011.
- [42] P. Furet, V. Guagnano, R. A. Fairhurst et al., “Discovery of NVP-BYL719 a potent and selective phosphatidylinositol-3 kinase alpha inhibitor selected for clinical evaluation,” *Bioorganic & Medicinal Chemistry Letters*, vol. 23, no. 13, pp. 3741–3748, 2013.
- [43] A. M. Marz, A.-K. Fabian, C. Kozany, A. Bracher, and F. Hausch, “Large FK506-binding proteins shape the pharmacology of rapamycin,” *Molecular and Cellular Biology*, vol. 33, no. 7, pp. 1357–1367, 2013.
- [44] A. K. Shiau, D. Barstad, P. M. Loria et al., “The structural basis of estrogen receptor/coactivator recognition and the

- antagonism of this interaction by tamoxifen,” *Cell*, vol. 95, no. 7, pp. 927–937, 1998.
- [45] I. Petit-Topin, M. Fay, M. Resche-Rigon et al., “Molecular determinants of the recognition of ulipristal acetate by oxosteroid receptors,” *The Journal of Steroid Biochemistry and Molecular Biology*, vol. 144, pp. 427–435, 2014.
- [46] G. M. Morris, W. Huey R Fau - Lindstrom, M. F. Lindstrom W Fau - Sanner et al., “Autodock4 and autodocktools4: automated docking with selective receptor flexibility,” *Journal of Computational Chemistry*, vol. 30, no. 16, pp. 2785–2791, 2009.
- [47] G. M. Morris, D. S. Goodsell, R. S. Halliday et al., “Automated docking using a lamarckian genetic algorithm and an empirical binding free energy function,” *Journal of Computational Chemistry*, vol. 16, no. 14, pp. 1639–1662, 1998.
- [48] O. Trott and A. J. Olson, “Autodock vina: improving the speed and accuracy of docking with a new scoring function, efficient optimization, and multithreading,” *Journal of Computational Chemistry*, vol. 31, no. 2, pp. 455–461, 2009.
- [49] M. J. Abraham, T. Murtola, R. Schulz et al., “Gromacs: high performance molecular simulations through multi-level parallelism from laptops to supercomputers,” *SoftwareX*, vol. 1, pp. 19–25, 2015.
- [50] D. A. Case, I. Y. Ben-Shalom, S. R. Brozell et al., “Amber,” vol. 54, no. 7, pp. 1951–1962, University of California, San Francisco, CA, USA, 2018.
- [51] M. W. Schmidt, K. K. Baldridge, J. A. Boatz et al., “General atomic and molecular electronic structure system,” *Journal of Computational Chemistry*, vol. 14, no. 11, pp. 1347–1363, 2016.
- [52] J. Koca, Z. Jirouskova, R. Svobodova Varekova, and J. Vanek, “Electronegativity equalization method: parameterization and validation for organic molecules using the merz-kollman-singh charge distribution scheme,” *Journal of Computational Chemistry*, vol. 30, no. 7, pp. 1174–1178, 2009.
- [53] C. I. Bayly, P. Cieplak, W. D. Cornell, and P. A. Kollman, “A well-behaved electrostatic potential based method using charge restraints for deriving atomic charges: the RESP model,” *The Journal of Physical Chemistry*, vol. 97, no. 40, pp. 10269–10280, 1993.
- [54] L. F. Song, T. S. Lee, C. Zhu, D. M. York, and K. M. Merz, “Using AMBER18 for relative free energy calculations,” *Journal of Chemical Information and Modeling*, vol. 59, no. 7, pp. 3128–3135, 2019.
- [55] J. Wang, W. Wang, P. A. Kollman, and D. A. Case, “Automatic atom type and bond type perception in molecular mechanical calculations,” *Journal of Molecular Graphics and Modelling*, vol. 25, no. 2, pp. 247–260, 2006.
- [56] A. W. Sousa Da Silva and W. F. Vranken, “Acpype—antechamber python parser interface,” *BMC Research. Notes*, vol. 5, p. 367, 2012.
- [57] U. Essmann, L. Perera, M. L. Berkowitz et al., “A smooth particle mesh ewald method,” *The Journal of Chemical Physics*, vol. 103, no. 19, 1995.
- [58] P. L. Silvestrelli, “Van der waals interactions in density functional theory using wannier functions,” *The Journal of Physical Chemistry*, vol. 113, no. 17, pp. 5224–5234, 2009.
- [59] G. J. Ackland, K. D’Mellow, S. L. Daraszewicz et al., “The moldy short-range molecular dynamics package,” *Computer Physics Communications*, vol. 182, pp. 55–56, 2011.
- [60] N. Homeyer and H. Gohlke, “Free energy calculations by the molecular mechanics poisson-boltzmann surface area method,” *Molecular Informatics*, vol. 31, no. 2, pp. 114–122, 2012.

Research Article

Potential Molecular Mechanisms of Chaihu-Shugan-San in Treatment of Breast Cancer Based on Network Pharmacology

Kunmin Xiao,^{1,2} Kexin Li,¹ Sidan Long,¹ Chenfan Kong,¹ and Shijie Zhu ^{1,2}

¹Graduate School, Beijing University of Chinese Medicine, Beijing 100029, China

²Department of Oncology, Wangjing Hospital, China Academy of Chinese Medical Sciences, Beijing 100102, China

Correspondence should be addressed to Shijie Zhu; 20180941234@bucm.edu.cn

Received 16 May 2020; Accepted 5 August 2020; Published 25 September 2020

Guest Editor: Azis Saifudin

Copyright © 2020 Kunmin Xiao et al. This is an open access article distributed under the Creative Commons Attribution License, which permits unrestricted use, distribution, and reproduction in any medium, provided the original work is properly cited.

Breast cancer is one of the most common cancers endangering women's health all over the world. Traditional Chinese medicine is increasingly recognized as a possible complementary and alternative therapy for breast cancer. Chaihu-Shugan-San is a traditional Chinese medicine prescription, which is extensively used in clinical practice. Its therapeutic effect on breast cancer has attracted extensive attention, but its mechanism of action is still unclear. In this study, we explored the molecular mechanism of Chaihu-Shugan-San in the treatment of breast cancer by network pharmacology. The results showed that 157 active ingredients and 8074 potential drug targets were obtained in the TCMSP database according to the screening conditions. 2384 disease targets were collected in the TTD, OMIM, DrugBank, GeneCards disease database. We applied the Bisogenet plug-in in Cytoscape 3.7.1 to obtain 451 core targets. The biological process of gene ontology (GO) involves the mRNA catabolic process, RNA catabolic process, telomere organization, nucleobase-containing compound catabolic process, heterocycle catabolic process, and so on. In cellular component, cytosolic part, focal adhesion, cell-substrate adherens junction, and cell-substrate junction are highly correlated with breast cancer. In the molecular function category, most proteins were addressed to ubiquitin-like protein ligase binding, protein domain specific binding, and Nop56p-associated pre-rRNA complex. Besides, the results of the KEGG pathway analysis showed that the pathways mainly involved in apoptosis, cell cycle, transcriptional dysregulation, endocrine resistance, and viral infection. In conclusion, the treatment of breast cancer by Chaihu-Shugan-San is the result of multicomponent, multitarget, and multipathway interaction. This study provides a certain theoretical basis for the treatment of breast cancer by Chaihu-Shugan-San and has certain reference value for the development and application of new drugs.

1. Introduction

Breast cancer is one of the most common cancers endangering women's health all over the world. The GLOBOCAN 2018 statistics show alarming results that there are 8.6 million new cases of female cancer and 4.2 million female cancer deaths worldwide. The proportion of breast cancer is 24.2% and 15.0%, respectively, ranking first in female cancer incidence and death [1]. It is predicted that, by the 2050s, the global incidence of breast cancer will reach nearly 3,200,000 new cases of breast cancer each year. These datasets reflect the high incidence of breast cancer and the urgent global need for breast cancer prevention and treatment measures [2].

Traditional Chinese medicine (TCM) has a long history in the etiology, pathogenesis, prevention, and treatment of breast cancer. According to the principle of TCM syndrome differentiation and treatment, the clinical syndrome of breast cancer is mainly "Liver-Qi" stagnation. Chaihu-Shugan-San is one of the classical prescriptions for the treatment of "Liver-Qi" stagnation. It has the effect of soothing "Liver-Qi." It has a history of 485 years and is widely used in clinical practice [3–5]. Chaihu-Shugan-San includes seven kinds of traditional Chinese medicine such as *Bupleurum chinense* DC (Chinese name: Chaihu), *Radix Paeoniae Alba* (Chinese name: Baishao), *Citrus reticulata* Blanco (Chinese name: Chenpi), *Cyperus rotundus* L (Chinese name: Xiangfu), *Glycyrrhiza uralensis* Fisch

(Chinese name: Gancao), *Citrus aurantium* L (Chinese name: Zhiqiao), and *Ligusticum chuanxiong* Hort (Chinese name: Chuanxiong) [6]. Traditional Chinese medicine meridian tropism is one of the core components of the theory of TCM. According to the theory of TCM, the characteristics of the selective distribution of the effective components of traditional Chinese medicine in the body are basically consistent with the relationship between the viscera and viscera of the corresponding meridian tropism. Chaihu, Chenpi, Xiangfu, Chuanxiong, and Baishao in Chaihu-Shugan-San belong to the liver meridian, which can soothe the liver and regulate Qi well. In traditional Chinese medicine theory, the main location of breast cancer is in the liver and often related to the spleen and kidney in the process of disease. Chaihu-Shugan-San meridian attribution is consistent with breast cancer meridian attribution and can better play the therapeutic effect.

As a classical prescription, Chaihu-Shugan-San has been widely studied in pharmacology. Chaihu-Shugan-San has the pharmacological effects of antidepressant [7], regulation of neuro-endocrine-immune network [8, 9], anti-inflammation, antioxidative stress [10], lipid-lowering and glucose-lowering, and antifibrosis [11]. In terms of antitumor, in a study of 86 patients with stage III breast cancer, the control group was given a standardized CAF regimen (cyclophosphamide + doxorubicin + 5-fluorouracil), and the experimental group was treated with Chaihu-Shugan-San on the basis of CAF. The short-term effective rate of the observation group was significantly higher than that of the control group (81.4% vs. 58.14%); the Karnofsky improvement rate of the observation group was significantly higher than that of the control group (48.84% vs. 34.88%) [12]. As a safe complementary alternative therapy, Chaihu-Shugan-San combined with other chemotherapy regimens can improve the therapeutic effect, alleviate the myelosuppression caused by chemotherapeutic drugs, and improve the prognosis of breast cancer patients [13, 14]. However, the mechanism of Chaihu-Shugan-San in the treatment of breast cancer remains to be further explored.

Classical prescriptions are currently the preferred way to treat diseases in TCM clinic, but they lack a scientific basis to reasonably explain the mechanism of TCM prescriptions from the whole to the local level or from the cellular to the molecular level [15]. Network pharmacology is an emerging discipline based on the integration of systems biology, molecular biology, pharmacology, and a variety of network computing platforms in the context of the era of big data, which can more directly explain the association between TCM prescriptions and diseases [16]. Therefore, this study constructed a multidimensional network of “ingredient-target-pathway” through network pharmacology to explore the potential molecular mechanism of Chaihu-Shugan-San in the treatment of breast cancer and to provide a certain theoretical basis for Chaihu-Shugan-San in the treatment of breast cancer.

2. Materials and Methods

2.1. Screening of Active Components and Target Prediction in Chaihu-Shugan-San. In this study, the chemical components of the seven herbs were searched on Traditional

Chinese Medicine Systems Pharmacology Database and Analysis Platform (TCMSP, <http://tcmssp.com/tcmssp.php>, updated on May 31, 2014) [17]. Search keywords are Chaihu, Baishao, Chenpi, Xiangfu, Gancao, Zhiqiao, and Chuanxiong, and only oral bioavailability (OB) $\geq 30\%$ and drug-likeness (DL) ≥ 0.18 were considered in this study. The Canonical SMILES sequence of the compound was searched in the PubChem database (<https://pubchem.ncbi.nlm.nih.gov/>) [18], and this sequence was used to predict the target of the compound in the Swiss Target Prediction online database (<http://www.swisstargetprediction.ch/>) [19] and collect target protein gene names and UniProt ID in the prediction results.

2.2. Network Construction of Components and Targets.

The chemical composition and potential targets of the above Chaihu-Shugan-San were uploaded to Cytoscape 3.7.1 [20] software to build up the component-target network. In the network, the degree centrality (DC) represents the number of nodes in the network that directly interacts with the node. The greater the degree, the more the biological functions it participates in; the betweenness centrality (BC) refers to the proportion of the number of nodes passing through the shortest path in the network, and the larger the BC is, the more influential the node is. Closeness centrality (CC) reflects the degree of proximity between nodes, and the reciprocal of the shortest path distance from one node to other nodes is CC. The closer the nodes are, the larger the CC is; the average shortest path length (ASPL) is the average of the shortest path length between all points in the network. The smaller the average path of a node, the more crucial this node is in the network.

2.3. Prediction of Breast Cancer Targets. With “breast cancer” or “malignant breast tumors” as keywords, we searched in Online Mendelian Inheritance in Man (OMIM, <http://www.omim.org/>, updated on May 4, 2018) [21], DrugBank (<https://www.drugbank.ca/>, version 5.1.6, updated on Apr 22, 2020) [22], Therapeutic Target Database (TTD, <http://db.idrblab.net/ttd/>, updated on Nov 11, 2019) [23], and GeneCards (<https://www.genecards.org/>, version 4.14.0) [24] to collect breast cancer-related targets. In the GeneCards database, the higher the score value is, the closer the relationship between the target and disease is, and the score value greater than the median is used as the screening condition to extract the key target. The above retrieval results were combined to remove duplicates and serve as the prediction target library of breast cancer.

2.4. Protein-Protein Interaction (PPI) Network Construction and Selection of Core Targets.

The BisoGenet plug-in in Cytoscape 3.7.1 draws the PPI network and maps the Chaihu-Shugan decoction component targets and breast cancer-related disease targets into the protein interaction relationship network, using Cytoscape 3.7.1 merge two protein interaction networks, to extract the intersection of the network. Based on the intersection network, the

CytoNCA plug-in [25] is used to screen out the nodes whose degree centrality (DC) is greater than 2 times the median of all nodes. After multiple screening, the core PPI network is finally obtained.

2.5. GO Functional Enrichment Analysis and KEGG Pathway Enrichment Analysis. The core target of PPI network selected above was imported into Metascape (<https://metascape.org/gp/index.html>, updated on March 20, 2020) [26] database for KEGG (Kyoto Encyclopedia of Genes and Genomes) pathway analysis and GO (Gene Ontology) biological process enrichment analysis. Parameter is set to min overlap >3, p value cutoff <0.01, and min enrichment >1.5. Taking p value as parameter and sorting from small to large as screening condition, KEGG pathway and GO biological process of the top 20 eligible were selected and uploaded to OmicShare (<http://www.omicshare.com/tools>) platform for data visualization.

2.6. Constructing PPI Network of Ingredient-Disease-KEGG Pathway. The top 20 KEGG pathways, Chaihu-Shugan-San active ingredients, and disease common targets were uploaded to Cytoscape 3.7.1 software to obtain the multi-dimensional network diagram of component-disease-KEGG pathway.

3. Results

3.1. Active Ingredient and Target of Chaihu-Shugan-San. OB $\geq 30\%$, DL ≥ 0.18 as the screening conditions, after searching TCMSp database, Chaihu-Shugan-San obtained a total of 157 chemical components, 13 compounds from Baishao, 17 compounds from Chaihu, 5 compounds from Chenpi, 7 compounds from Chuanxiong, 5 compounds from Zhiqiao, 92 qualified compounds from Gancao, and 18 compounds from Xiangfu (as shown in Table S1 in Supplementary Materials). 8074 targets were obtained by inputting 158 chemical components into Swiss Target Prediction online database.

3.2. Compound-Target Network Construction. The compound-target network consists of 945 nodes and 8200 edges. 29 of 157 compounds were not found in the database and not involved in the network construction (Figure 1). In this network, the average degree value is 15.647, and most of the proteins share common ligands with other proteins, which reflects the mechanism of the joint action between multi-components and multitargets of Chaihu-Shugan-San, and conform to the characteristics of the traditional Chinese formula. Table 1 shows the detailed topological parameters of the top 10 compounds with high DC.

3.3. Screening of Breast Cancer Targets. Breast cancer or malignant breast tumors were used as keywords to search in TTD, OMIM, DrugBank, and GeneCards databases. 37 disease targets were obtained from TTD database, 1163 disease targets were screened from OMIM database, 202

disease targets were screened from Drugbank database, and 1286 disease targets with score >13.96 were obtained from GeneCards database. The duplicates were deleted after merging, and 2,384 breast cancer-related targets were finally obtained.

3.4. Construction of PPI Network of Chaihu-Shugan-San and Disease Targets. To further explore the pharmacological mechanism of Chaihu-Shugan-San on breast cancer, Chaihu-Shugan-San and breast cancer protein were input into the BisoGenet plug-in of Cytoscape 7.2.1 software for merging. CytoNCA plug-in performs topological analysis and takes 2 times of the average degree value as the screening condition. In the first screening, a network composed of 2,728 nodes and 109,005 edges was obtained by the median DC >46. Finally, a PPI network with 451 nodes and 17,140 edges was constructed by further screening with the median DC >156. The process is shown in Figure 2. Topological parameters of the top 10 targets with high DC are shown in Table 2, and other detailed results are shown in Table S2.

3.5. GO Biological Process and Enrichment Analysis of KEGG Pathway. GO biological process consists of molecular function (MF), biological process (BP), and cellular component (CC) to interpret antitumor biological processes at key targets. Kyoto Encyclopedia of Genes and Genomes (KEGG) enrichment analysis studies the key target of antitumor signaling pathways. The results of GO enrichment analysis showed that there were 2000 biological processes, 274 cell components, and 564 molecular functions. KEGG enrichment has 154 signaling pathways. According to the ranking of p values, the top 20 were selected to plot the bubble chart (Figure 3). The left side of each chart is the top enriched name. The color of bubbles from blue to red represents the p value from large to small. The larger the bubbles, the larger the gene count of the pathway. The horizontal axis represents the ratio of the pathway genes to the total input genes. The top 20 signal pathways of KEGG enrichment are shown in Table S3.

3.6. The Multidimensional Network of “Component-Target Disease-KEGG Signaling Pathway” Was Constructed. Combining the component-target network and the first 20 KEGG signaling pathway targets, a multidimensional network of “component-disease target-KEGG signaling pathway” was obtained by Cytoscape 7.2.1 software (as shown in Figure 4). The results showed that the effective components of Chaihu-Shugan-San could treat breast cancer by multi-target and multisignal pathways.

4. Discussion

Traditional Chinese medicine compound acts on diseases through multimolecule, multitarget, and multipathway and plays a certain therapeutic effect. Network pharmacology is a science based on the macroconnection under the background of the big data era. It systematically analyzes the

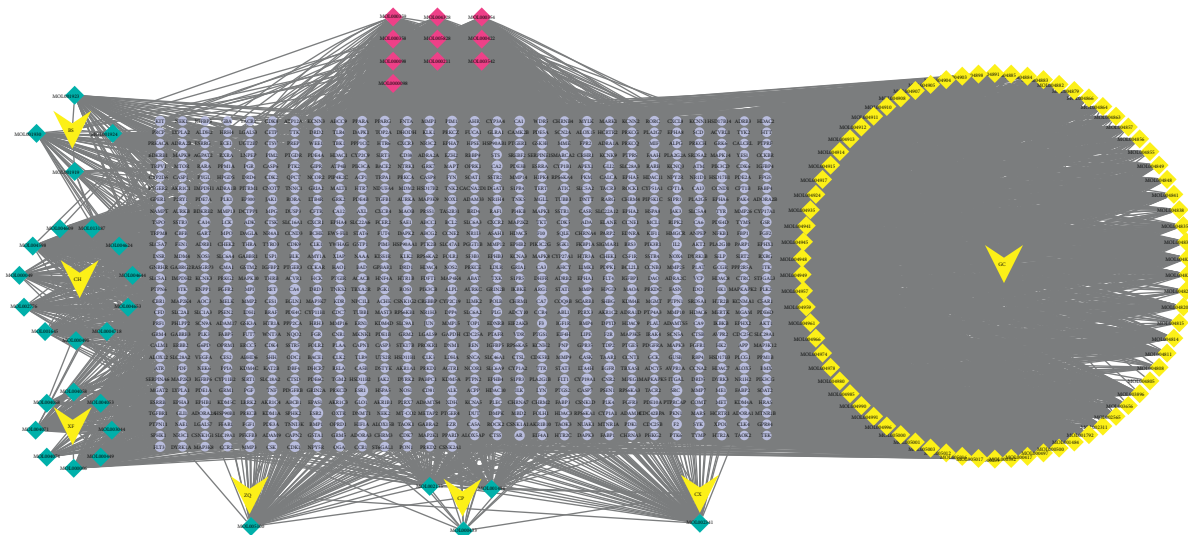


FIGURE 1: Compound-target network: green diamond nodes represent compounds, red diamond nodes represent common compounds, yellow v nodes represent herb names, and purple circular nodes represent corresponding potential targets of compounds.

molecular mechanism of action from all levels, which is consistent with the holistic view of TCM and the thought of syndrome differentiation and treatment. Chaihu-Shugan-San prescription, in which Chaihu is the monarch drug, is good at soothing the “Liver-Qi.” Xiangfu and Chuanxiong are the minister drugs, which can relieve “Liver-Qi.” Chenpi and Zhiqiao, regulating “Qi” stagnation and Baishao, nourishing “Blood” and softening the “Liver,” are adjuvants. Gancao is used as a guide medicine to reconcile various drugs. The combination of various drugs can regulate “Liver-Qi” and smooth “Qi.” Chaihu-Shugan-San has a history of more than 480 years. The basic compatibility of clinical medication is Chenpi 6g, Chaihu 6g, Chuanxiong 4.5g, Xiangfu 4.5g, Zhiqiao 4.5g, Shaoyao 4.5g, and Gancao 1.5g, which is added or subtracted according to the actual situation of patients. The official preparation method is to add 250 ml of water to the herbs and boil them for 30 min. Su [27] and his team identified 33 chemical constituents in Chaihu-Shugan-San. Among them, gallic acid (source: Shaoyao), oxidized paeoniflorin (source: Shaoyao), paeoniflorin (source: Shaoyao), paeoniflorin (source: Shaoyao), glycyrrhizin (source: Gancao), naringin (source: Chenpi, Zhiqiao), hesperidin (source: Chenpi, Zhiqiao), and ferulic acid (source: Chuanxiong) had higher contents, all above 1000 mg/g [28]. Although some studies have comprehensively elucidated the treatment of depression [6, 29], non-alcoholic fatty liver disease [30, 31] and functional dyspepsia [5] by Chaihu-Shugan-San, no studies have comprehensively elucidated the mechanism of Chaihu-Shugan-San in the treatment of breast cancer. Therefore, with the aid of network pharmacology, this study analyzed the specific molecular mechanism of Chaihu-Shugan-San in the treatment of breast cancer from a microscopic perspective.

The results of network analysis showed that the active ingredients in Chaihu-Shugan-San mainly included beta-sitosterol, kaempferol, quercetin, naringenin, isorhamnetin, and nobiletin. Beta-sitosterol can promote the apoptosis of

TABLE 1: Topological parameter of top 10 compounds.

ID	Molecule name	DC	BC	CC	ASPL
MOL000422	Kaempferol	317	0.011	0.377	2.651
MOL000354	Isorhamnetin	303	0.008	0.373	2.681
MOL000359	Sitosterol	233	0.005	0.360	2.774
MOL004328	Naringenin	199	0.058	0.397	2.520
MOL000358	Beta-sitosterol	139	0.004	0.357	2.802
MOL000098	Quercetin	116	0.009	0.377	2.654
MOL004609	Areapillin	101	0.008	0.372	2.690
MOL003044	Chrysoeriol	101	0.008	0.371	2.690
MOL000006	Luteolin	101	0.008	0.371	2.690
MOL004071	Hyndarin	101	0.063	0.374	2.677

breast cancer cells by activating the Fas signaling pathway and caspase-8 activity [32] and is expected to be an orphan nutrition drug against cancer [33]. Kaempferol has shown a good affinity for PAK4 in molecular docking and is considered to be a potential inhibitor in triple-negative breast cancer [34], and kaempferol can prevent G2/M phase of the cell cycle by downregulating CDK1 in human breast cancer MDA-MB-453 cells [35], and blocking RhoA and Rac1 signaling pathways to inhibit breast cancer cell migration and invasion [36] is a powerful antioxidant inducer and can inhibit oncogene transformation and induce cancer cell apoptosis and DNA damage. Quercetin, naringenin, and isorhamnetin, such as flavonoids, can prevent breast cancer cell migration through inflammatory and apoptotic cell signaling [37, 38], and quercetin can induce autophagy by inhibiting the Akt-mTOR pathway [39].

The PPI network showed that the active components in Chaihu-Shugan-San may function through the core targets such as histone deacetylase 1 (HDAC1), huntingtin (HTT), RAC-alpha serine/threonine-protein kinase (AKT1), hepatoma-derived growth factor (HDGF), roquin-1 (RC3H1), chromobox protein homolog 8 (CBX8), histone deacetylase

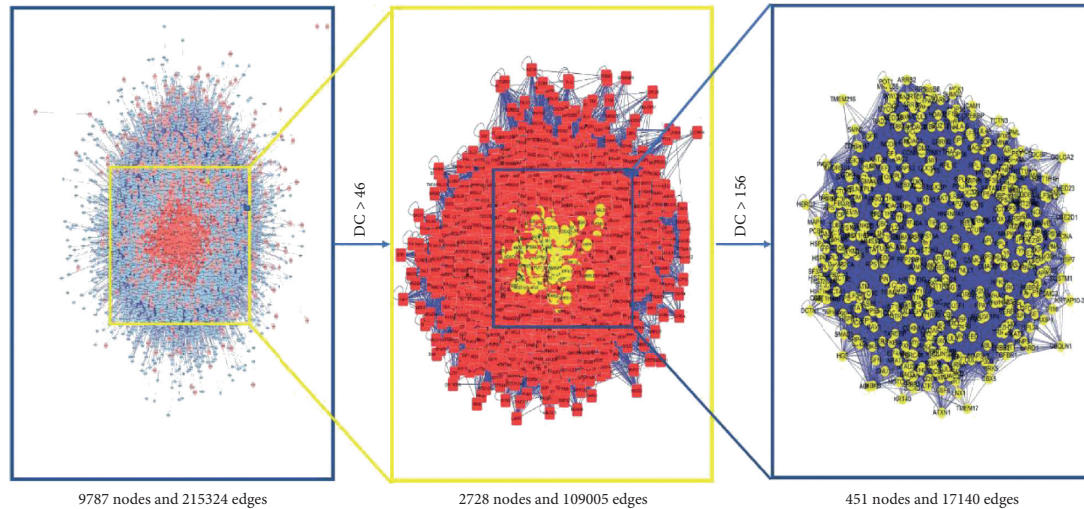


FIGURE 2: Network topology analysis of PPI.

TABLE 2: Topological parameter of top 10 core targets.

Target	DC	BC	CC	ASPL
HDAC1	1976	0.075	0.534	1.874
HTT	1695	0.094	0.526	1.900
AKT1	1136	0.031	0.495	2.019
HDGF	1095	0.021	0.499	2.002
RC3H1	930	0.026	0.501	1.996
CBX8	836	0.013	0.488	2.050
HDAC2	813	0.015	0.493	2.029
SUMO1	810	0.021	0.500	1.999
RPSA	761	0.013	0.489	2.047
RPLP0	736	0.011	0.481	2.081

2 (HDAC2), small ubiquitin-related modifier 1 (SUMO1), 40 S ribosomal protein SA (RPSA), and 60 S acidic ribosomal protein P0(RPLP0). HDAC1 plays an important role in transcriptional regulation and cell cycle progression [40]. HDAC1 can promote the proliferation and migration of breast cancer cells by activating the Snail/IL-8 signaling pathway [41]. Downregulation of HTT transcription and protein levels is a key factor in poor prognosis and metastasis development of breast cancer [42]. AKT1 is involved in the regulation of many tumor processes, including tumor proliferation, cell survival, metabolism, growth, and angiogenesis. The mutation frequency of AKT1 in Chinese breast cancer patients is 3.2%, and it is considered to be a sensitive target for the treatment of breast cancer. A study involving 313 Chinese breast cancer patients found that the mutation frequency of AKT1 in Chinese breast cancer patients was 3.2%, and it is considered a sensitive target for the treatment of breast cancer [43]. HDAC2 is a poor prognostic factor in patients receiving anthracycline therapy and is positively correlated with breast cancer metastasis, progression, increased Ki-67, multidrug resistance protein, and negatively correlated with overall survival of patients [44]. The occurrence and development of breast cancer are closely related to the core proteins, which fully prove that the

treatment of breast cancer by Chaihu-Shugan-San is the result of multimolecular, multitarget, and multipathway interaction.

The biological process of Gene Ontology (GO) involves the mRNA catabolic process, RNA catabolic process, telomere organization, nucleobase-containing compound catabolic process, heterocycle catabolic process, and so on. In cellular component, cytosolic part, focal adhesion, cell-substrate adherens junction, and cell-substrate junction are highly correlated with breast cancer. In the molecular function category, most proteins were addressed to ubiquitin-like protein ligase binding, protein domain specific binding, and Nop56p-associated pre-rRNA complex. In addition, the results of KEGG pathway analysis showed that the pathways mainly involved in apoptosis, cell cycle, transcriptional dysregulation, endocrine resistance, and viral infection. Estrogen receptor (ER) signal transduction pathway plays a central role in the development of breast cancer. ER can not only regulate the expression of certain genes through its mediated signal transduction pathway but also has extensive connections with many other signal transduction pathways, forming a signal transduction regulatory network [45]. ER binds to receptor proteins in the nucleus, and the receptor is activated. Activated ER- α and ER- β form homodimers or heterodimers. Some coregulators form complexes with dimers. The complexes bind to ER response elements to initiate transcription, thereby regulating the function of target genes, leading to abnormal cell proliferation and differentiation, and ultimately leading to tumorigenesis [46]. The increased mutation rate of ER- α in precancerous lesions of breast cancer affects the junction between ER- α zinc finger region and ligand binding domain, resulting in high sensitivity of the body to estrogen. Under the action of low levels of hormones, ER- α is highly bound to TNF-2 co-activator, which leads to the occurrence of tumors. For ER receptor-positive breast cancer patients, quantitative expression of ER receptor is an independent imaging factor to evaluate their prognosis, recurrence, and metastasis [47]. Abnormal activation of MAPK signal

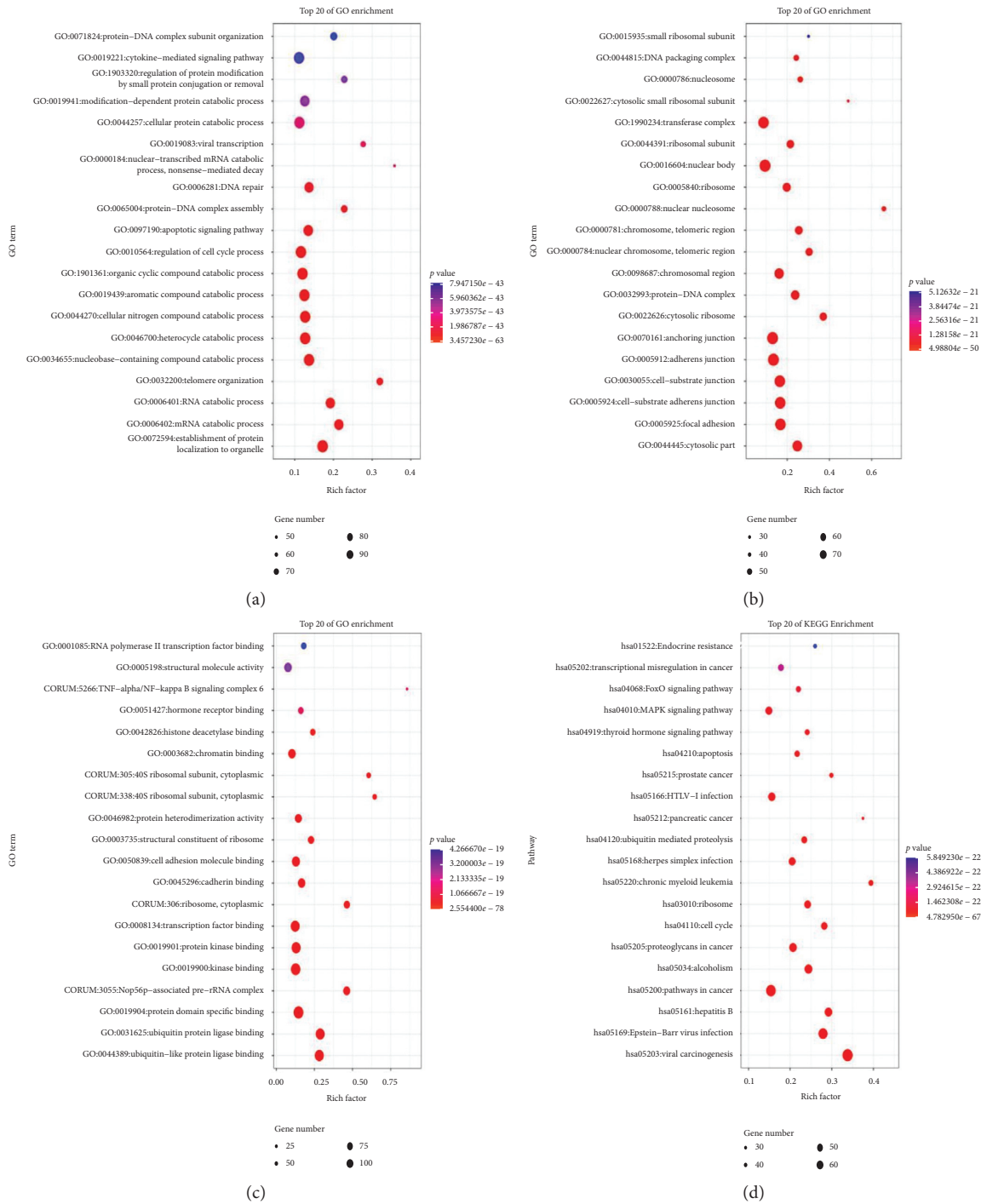


FIGURE 3: GO function enrichment analysis and enrichment analysis of KEGG signaling pathway (top 20). (a) BP. (b) CC. (c) MF. (d) KEGG.

transduction pathway can lead to cell loss of apoptosis and differentiation ability, promote malignant transformation, abnormal proliferation, produce tumors, and further promote the proliferation of tumor cells. Therefore, inhibitors of some key kinases in the MAPK signaling pathway have become a hotspot in the treatment of breast cancer in recent years. Studies have found that Kruppel-like factor 4 [48] and pre-mRNA processing factor 4 [49] affect the growth,

migration, and apoptosis of breast cancer cells through MAPK and are expected to become new targets for the treatment of breast cancer. Studies found that the activation or loss of FOXO function can inhibit the growth and metastasis of breast tumors [50], and the dysregulation of FOXO transcription factors has also become a key molecule in the endocrine resistance mechanism [51]. More and more attention has been paid to the relationship between

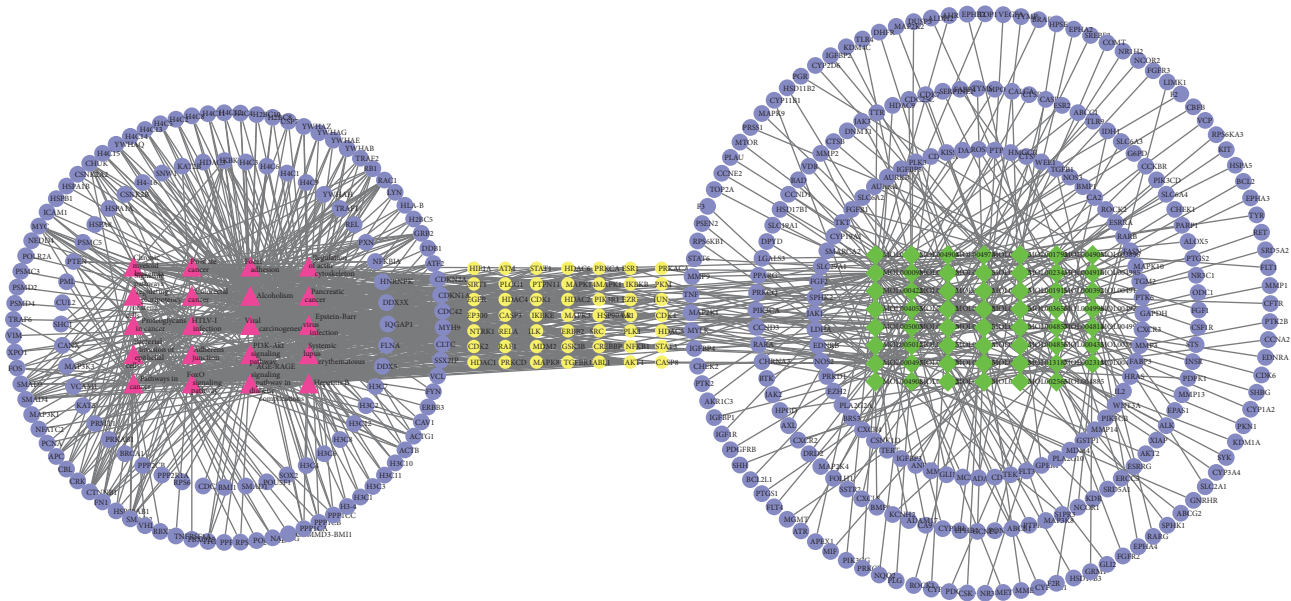


FIGURE 4: Component-disease target-KEGG signaling pathway. Green represents active ingredients of drugs; purple represents targets; yellow represents common targets; and red represents signaling pathways.

viral infection and breast cancer. In particular, human papilloma virus (HPV) has a strong cause-and-effect relationship with breast cancer. Many studies have found that different HPV genotypes are associated with the prevalence of breast cancer and the nuclear prognosis. The relationship between viral infection and breast cancer has been paid more and more attention [52–54]. The relationship between Epstein–Barr Virus (EBV) and breast cancer has also been extensively studied, but the current evidence is less and more controversial [55]. It is proved again that Chaihu-Shugan-San treatment of breast cancer is through a combination of multiple biological pathways and multiple signaling pathways, but this multifeature is not only found in a single disease. Chaihu-Shugan-San is mainly involved in the regulation of neurotransmitters, regulation of inflammatory mediators of TRP channels, calcium signaling pathways, cyclic adenosine monophosphate signaling pathways, and neuroactive ligand-receptor interactions to play an antidepressant role [56]. Chaihu-Shugan-San can improve cognitive impairment in Alzheimer’s disease through multitarget action, and its effect is verified by biological experiments [57]. These all embody the principle of “treating different diseases with the same treatment” in TCM.

Data Availability

All data generated or analyzed during this study are included in this paper.

Disclosure

Kunmin Xiao and Kexin Li are the first authors.

Conflicts of Interest

All authors state that they have no conflicts of interest regarding the publication of this paper.

Authors’ Contributions

Shijie Zhu conceived and designed the experiments. Kunmin Xiao and Kexin Li performed the experiments and wrote the manuscript. Sidan Long and Chenfan Kong contributed to analysis tools.

Acknowledgments

This work was supported by grants from the China National Natural Science Foundation (Grant no. 81973640).

Supplementary Materials

Table S1: active ingredients of Chaihu-Shugan-San. Table S2: topological parameters of Chaihu-Shugan-San targets. Table S3: the top 20 signal pathways of KEGG enrichment. (*Supplementary Materials*)

References

- [1] F. Bray, J. Ferlay, I. Soerjomataram et al., “Global cancer statistics 2018: GLOBOCAN estimates of incidence and mortality worldwide for 36 cancers in 185 countries,” *CA: A Cancer Journal for Clinicians*, vol. 68, no. 6, pp. 394–424, 2018.
- [2] J. R. Benson and I. Jatoi, “The global breast cancer burden,” *Future Oncology*, vol. 8, no. 6, pp. 697–702, 2012.
- [3] N. Yang, X. Jiang, X. Qiu, Z. Hu, L. Wang, and M. Song, “Modified Chaihu shugan powder for functional dyspepsia: meta-analysis for randomized controlled trial,” *Evidence-*

- Based Complementary and Alternative Medicine*, vol. 201310 pages, Article ID 791724, 2013.
- [4] Y. Wang, R. Fan, and X. Huang, "Meta-analysis of the clinical effectiveness of traditional Chinese medicine formula Chaihu-Shugan-San in depression," *Journal of Ethnopharmacology*, vol. 141, no. 2, pp. 571–577, 2012.
 - [5] F. Qin, J. Y. Liu, and J. H. Yuan, "Chaihu-Shugan-San, an oriental herbal preparation, for the treatment of chronic gastritis: a meta-analysis of randomized controlled trials," *Journal of Ethnopharmacology*, vol. 146, no. 2, pp. 433–439, 2013.
 - [6] Z. He, R. Fan, C. Zhang et al., "Chaihu-Shugan-San reinforces CYP3A4 expression via pregnane X receptor in depressive treatment of liver-Qi stagnation syndrome," *Evidence-Based Complementary and Alternative Medicine*, vol. 201911 pages, Article ID 9781675, 2019.
 - [7] K. K. Jia, S. M. Pan, H. Ding et al., "Chaihu-shugan san inhibits inflammatory response to improve insulin signaling in liver and prefrontal cortex of CUMS rats with glucose intolerance," *Biomedicine & Pharmacotherapy*, vol. 103, pp. 1415–1428, 2018.
 - [8] X. Huang, Y. Guo, W. H. Huang et al., "Searching the cytochrome P450 enzymes for the metabolism of meranzin hydrate: a prospective antidepressant originating from Chaihu-Shugan-San," *PLoS One*, vol. 9, no. 11, Article ID e113819, 2014.
 - [9] Z. H. Su, H. M. Jia, H. W. Zhang, Y. F. Feng, L. An, and Z. M. Zou, "Hippocampus and serum metabolomic studies to explore the regulation of Chaihu-Shu-Gan-San on metabolic network disturbances of rats exposed to chronic variable stress," *Molecular BioSystems*, vol. 10, no. 3, pp. 549–561, 2014.
 - [10] Y. Liang, Y. Zhang, Y. Deng et al., "Chaihu-Shugan-San decoction modulates intestinal microbe dysbiosis and alleviates chronic metabolic inflammation in NAFLD rats via the NLRP3 inflammasome pathway," *Evidence-Based Complementary and Alternative Medicine*, vol. 201811 pages, Article ID 9390786, 2018.
 - [11] Q. H. Yang, Y. J. Xu, G. H. Feng et al., "p38 MAPK signal pathway involved in anti-inflammatory effect of Chaihu-Shugan-San and Shen-ling-Bai-zhu-San on hepatocyte in non-alcoholic steatohepatitis rats," *African Journal of Traditional, Complementary and Alternative Medicines*, vol. 11, no. 1, pp. 213–221, 2013.
 - [12] L. Liu, Y. Ni, and F. Yin, "Effect of Chaihu Shugan powder combined with CAF in the treatment of stage III breast cancer and its effect on serum MMPs, estrogen level and tumor markers," *Journal of Chinese Medicinal Materials*, vol. 43, no. 1, pp. 220–221, 2020.
 - [13] F. Quan, B. Shi, and M. Yu, "Clinical effects of Chaihu Shugan powder combined with Paclitaxel and cyclophosphamide in treatment of breast cancer," *Grassroots Medical Forum*, vol. 23, no. 26, pp. 3703–3704, 2019.
 - [14] W. He, "Advanced breast cancer treated with Bupleurum powder for soothing the liver combined with chemotherapy randomized parallel group study," *Journal of Practical Traditional Chinese Internal Medicine*, vol. 28, no. 8, pp. 83–86, 2014.
 - [15] S. Li and B. Zhang, "Traditional Chinese medicine network pharmacology: theory, methodology and application," *Chinese Journal of Natural Medicines*, vol. 11, no. 2, pp. 110–120, 2014.
 - [16] A. L. Hopkins, "Network pharmacology: the next paradigm in drug discovery," *Nature Chemical Biology*, vol. 4, no. 11, pp. 682–690, 2008.
 - [17] J. Ru, P. Li, J. Wang et al., "TCMSP: a database of systems pharmacology for drug discovery from herbal medicines," *Journal of Cheminformatics*, vol. 6, no. 1, 2014.
 - [18] W.-D. Ihlenfeldt, "A virtual file system for the PubChem chemical structure and bioassay database," *Chemistry Central Journal*, vol. 2, no. 1, 2008.
 - [19] D. Gfeller, O. Michielin, and V. Zoete, "Shaping the interaction landscape of bioactive molecules," *Bioinformatics*, vol. 29, no. 23, pp. 3073–3079, 2013.
 - [20] P. Shannon, A. Markiel, O. Ozier et al., "Cytoscape: a software environment for integrated models of biomolecular interaction networks," *Genome Research*, vol. 13, no. 11, pp. 2498–2504, 2003.
 - [21] A. Hamosh, A. F. Scott, J. S. Amberger, C. A. Bocchini, and V. A. McKusick, "Online Mendelian Inheritance in Man (OMIM), a knowledgebase of human genes and genetic disorders," *Nucleic Acids Research*, vol. 33, pp. D514–D517, 2004.
 - [22] D. S. Wishart, Y. D. Feunang, A. C. Guo et al., "DrugBank 5.0: a major update to the DrugBank database for 2018," *Nucleic Acids Research*, vol. 46, no. 1, pp. D1074–D1082, 2018.
 - [23] Y. Wang, S. Zhang, F. Li et al., "Therapeutic target database 2020: enriched resource for facilitating research and early development of targeted therapeutics," *Nucleic Acids Research*, vol. 48, no. 1, pp. D1031–D1041, 2020.
 - [24] G. Stelzer, N. Rosen, I. Plaschkes et al., "The GeneCards suite: from gene data mining to disease genome sequence analyses," *Current Protocols in Bioinformatics*, vol. 54, no. 1, 2016.
 - [25] Y. Tang, M. Li, J. Wang, Y. Pan, and F. X. Wu, "CytoNCA: a cytoscape plugin for centrality analysis and evaluation of protein interaction networks," *Biosystems*, vol. 127, pp. 67–72, 2015.
 - [26] Y. Zhou, B. Zhou, L. Pache et al., "Metascape provides a biologist-oriented resource for the analysis of systems-level datasets," *Nature Communications*, vol. 10, no. 1, p. 1523, 2019.
 - [27] Z. H. Su, G. A. Zou, A. Preiss, H. W. Zhang, and Z. M. Zou, "Online identification of the antioxidant constituents of traditional Chinese medicine formula Chaihu-Shu-Gan-San by LC-LTQ-Orbitrap mass spectrometry and microplate spectrophotometer," *Journal of Pharmaceutical and Biomedical Analysis*, vol. 53, no. 3, pp. 454–461, 2010.
 - [28] X. Ni, M. Cao, Z. Wu, and L. Li, "Research progress on chemical components and pharmacological effects of Chaihu Shugan powder," *Shanghai Journal of Traditional Chinese Medicine*, vol. 51, no. 9, pp. 109–113, 2017.
 - [29] Q. Liu, N. N. Sun, Z. Z. Wu, D. H. Fan, and M. Q. Cao, "Chaihu-Shugan-San exerts an antidepressive effect by downregulating miR-124 and releasing inhibition of the MAPK14 and Gria3 signaling pathways," *Neural Regeneration Research*, vol. 13, no. 5, pp. 837–845, 2018.
 - [30] H. Nie, Y. Deng, C. Zheng et al., "A network pharmacology-based approach to explore the effects of Chaihu Shugan powder on a non-alcoholic fatty liver rat model through nuclear receptors," *Journal of Cellular and Molecular Medicine*, vol. 24, no. 9, pp. 5168–5184, 2020.
 - [31] W. N. Jiang, D. Li, T. Jiang et al., "Protective effects of chaihu shugan san () on nonalcoholic fatty liver disease in rats with insulin resistance," *Chinese Journal of Integrative Medicine*, vol. 24, no. 2, pp. 125–132, 2018.
 - [32] A. B. Awad, M. Chinnam, C. S. Fink, and P. G. Bradford, "Beta-Sitosterol activates Fas signaling in human breast cancer cells," *Phytomedicine*, vol. 14, no. 11, pp. 747–754, 2007.

- [33] M. S. B. Sayeed and S. S. Ameen, "Beta-sitosterol: a promising but orphan nutraceutical to fight against cancer," *Nutrition and Cancer*, vol. 67, no. 8, pp. 1216–1222, 2015.
- [34] M. A. Arowosegbe, O. T. Amusan, S. A. Adeola et al., "Kaempferol as a potential PAK4 inhibitor in triple negative breast cancer: extra precision glide docking and free energy calculation," *Current Drug Discovery Technologies*, vol. 16, 2019.
- [35] L. Zhu and L. Xue, "Kaempferol suppresses proliferation and induces cell cycle arrest, apoptosis, and DNA damage in breast cancer cells," *Oncology Research Featuring Preclinical and Clinical Cancer Therapeutics*, vol. 27, no. 6, pp. 629–634, 2019.
- [36] S. Li, T. Yan, R. Deng et al., "Low dose of kaempferol suppresses the migration and invasion of triple-negative breast cancer cells by downregulating the activities of RhoA and Rac1," *Onco Targets and Therapy*, vol. 10, pp. 4809–4819, 2017.
- [37] Z. Zhao, G. Jin, Y. Ge, and Z. Guo, "Naringenin inhibits migration of breast cancer cells via inflammatory and apoptosis cell signaling pathways," *Inflammopharmacology*, vol. 27, no. 5, pp. 1021–1036, 2019.
- [38] J. Hu, Y. Zhang, X. Jiang et al., "ROS-mediated activation and mitochondrial translocation of CaMKII contributes to Drp1-dependent mitochondrial fission and apoptosis in triple-negative breast cancer cells by isorhamnetin and chloroquine," *Journal of Experimental & Clinical Cancer Research*, vol. 38, no. 1, p. 225, 2019.
- [39] L. Jia, S. Huang, X. Yin, Y. Zan, Y. Guo, and L. Han, "Quercetin suppresses the mobility of breast cancer by suppressing glycolysis through Akt-mTOR pathway mediated autophagy induction," *Life Sciences*, vol. 208, pp. 123–130, 2018.
- [40] N. Zhang, H. Zhang, Y. Liu et al., "SREBP1, targeted by miR-18a-5p, modulates epithelial-mesenchymal transition in breast cancer via forming a co-repressor complex with Snail and HDAC1/2," *Cell Death & Differentiation*, vol. 26, no. 5, pp. 843–859, 2019.
- [41] Z. Tang, S. Ding, H. Huang et al., "HDAC1 triggers the proliferation and migration of breast cancer cells via upregulation of interleukin-8," *Biological Chemistry*, vol. 398, no. 12, pp. 1347–1356, 2017.
- [42] M. S. Thion, J. R. McGuire, C. M. Sousa et al., "Unraveling the role of Huntingtin in breast cancer metastasis," *Journal of the National Cancer Institute*, vol. 107, no. 10, d1v208 pages, 2015.
- [43] G. Li, X. Guo, M. Chen et al., "Prevalence and spectrum of AKT1, PIK3CA, PTEN and TP53 somatic mutations in Chinese breast cancer patients," *PLoS One*, vol. 13, no. 9, Article ID e0203495, 2018.
- [44] H. Zhao, Z. Yu, L. Zhao et al., "HDAC2 overexpression is a poor prognostic factor of breast cancer patients with increased multidrug resistance-associated protein expression who received anthracyclines therapy," *Japanese Journal of Clinical Oncology*, vol. 46, no. 10, pp. 893–902, 2016.
- [45] S. I. Hayashi and Y. Yamaguchi, "Estrogen signaling and prediction of endocrine therapy," *Cancer Chemotherapy & Pharmacology*, vol. 56, no. 1, pp. 27–31, 2005.
- [46] A. J. Knox, M. J. Meegan, and D. G. Lloyd, "Estrogen receptors: molecular interactions, virtual screening and future prospects," *Current Topics in Medicinal Chemistry*, vol. 6, no. 3, pp. 217–243, 2006.
- [47] M. V. Dieci, F. Piacentini, M. Dominici et al., "Quantitative expression of estrogen receptor on relapse biopsy for ER-positive breast cancer: prognostic impact," *Anticancer research*, vol. 34, no. 7, pp. 3657–3662, 2014.
- [48] Y. Jia, J. Zhou, X. Luo et al., "KLF4 overcomes tamoxifen resistance by suppressing MAPK signaling pathway and predicts good prognosis in breast cancer," *Cellular Signalling*, vol. 42, pp. 165–175, 2018.
- [49] S. Park, S. H. Han, H. G. Kim et al., "PRPF4 is a novel therapeutic target for the treatment of breast cancer by influencing growth, migration, invasion, and apoptosis of breast cancer cells via p38 MAPK signaling pathway," *Molecular and Cellular Probes*, vol. 47, Article ID 101440, 2019.
- [50] M. Hornsveld, L. M. Smits, M. Meerlo et al., "FOXO transcription factors both suppress and support breast cancer progression," *Progression. Cancer Research*, vol. 78, no. 9, pp. 2356–2369, 2018.
- [51] M. Bullock, "FOXO factors and breast cancer: outfoxing endocrine resistance," *Endocrine-Related Cancer*, vol. 23, no. 2, pp. R113–R130, 2016.
- [52] K. U. Petry, "HPV and cervical cancer," *Scandinavian Journal of Clinical and Laboratory Investigation*, vol. 74, pp. 59–62, 2014.
- [53] C. Y. Kan, B. J. Iacopetta, J. S. Lawson, and N. J. Whitaker, "Identification of human papillomavirus DNA gene sequences in human breast cancer," *British Journal of Cancer*, vol. 93, no. 8, pp. 946–948, 2005.
- [54] N. Khodabandehlou, S. Mostafaei, A. Etemadi et al., "Human papilloma virus and breast cancer: the role of inflammation and viral expressed proteins," *BMC Cancer*, vol. 19, no. 1, 61 pages, 2019.
- [55] S. L. Glaser, J. L. Hsu, and M. L. Gulley, "Epstein-barr virus and breast cancer: state of the evidence for viral carcinogenesis," *Cancer Epidemiology, Biomarkers & Prevention*, vol. 13, no. 5, pp. 688–697, 2004.
- [56] Y. Y. Liu, D. Hu, Q. Q. Fan et al., "Study on mechanism of chaihu shugan powder () for treating depression based on network pharmacology," *Chinese Journal of Integrative Medicine*, 2019.
- [57] Q. Zeng, L. Li, W. Siu et al., "A combined molecular biology and network pharmacology approach to investigate the multi-target mechanisms of Chaihu Shugan San on Alzheimer's disease," *Biomedicine & Pharmacotherapy*, vol. 120, Article ID 109370, 2019.

Research Article

Efficacy and Safety of Cinobufacin Combined with Chemotherapy for Advanced Breast Cancer: A Systematic Review and Meta-Analysis

Jing Xu,^{1,2} Dongyun Li ¹, Kexin Du,^{1,2} and Jing Wang ¹

¹Department of Hematology and Oncology, Dongzhimen Hospital Affiliated with Beijing University of Chinese Medicine, Beijing 100700, China

²Beijing University of Chinese Medicine, Beijing 100029, China

Correspondence should be addressed to Dongyun Li; lidy0039@sina.com and Jing Wang; jwang2936@126.com

Received 22 July 2020; Revised 24 August 2020; Accepted 2 September 2020; Published 19 September 2020

Academic Editor: Mohd Fadzelly Abu Bakar

Copyright © 2020 Jing Xu et al. This is an open access article distributed under the Creative Commons Attribution License, which permits unrestricted use, distribution, and reproduction in any medium, provided the original work is properly cited.

Background. Cinobufacin is a Chinese patent medicine widely used for breast cancer in China. However, no systematic review and meta-analysis have been published to validate its effects in breast cancer treatment. We, therefore, summarize the efficacy and safety of Cinobufacin combined with chemotherapy in order to provide rigid evidence for its clinical application. **Methods.** By searching multiple databases incepted to December 2019, the RCTs of breast cancer patients treated with Cinobufacin were screened according to the inclusion criteria, and the meta-analysis and sensitivity analysis were conducted using RevMan5.3. **Results.** A total of 1163 articles were retrieved, and 16 studies were included. The total sample size was 1331 cases, including 666 cases in the treatment group receiving Cinobufacin combined with chemotherapy and 665 cases in the control group receiving chemotherapy alone. Our study found that the ORR (overall response rate) (RR = 1.35, 95% CI: [1.23, 1.49], $P < 0.00001$), CBR (clinical benefit rate) (RR = 1.14, 95% CI: [1.08, 1.21], $P < 0.00001$), KPS scores (RR = 1.98, 95% CI: [1.45, 2.68], $P < 0.0001$), and pain relief rate (RR = 1.34, 95% CI: [1.01, 1.78] $P = 0.04$) of the Cinobufacin combined with chemotherapy group were better than those of the chemotherapy group, and the difference was statistically significant. Our study also discovered that the tumor markers (CA125, CA153, and CEA) in the Cinobufacin combined with chemotherapy group were lower than those in the chemotherapy group, which heterogeneity was derived from the low-quality literature included in the study, but the results were robust. In addition, in terms of safety, we found that the incidences of gastrointestinal reactions (RR = 0.58, 95% CI: [0.48, 0.70], $P < 0.00001$), liver and kidney damage (RR = 0.57, 95% CI: [0.38, 0.84], $P = 0.004$), and hair loss (RR = 0.61, 95% CI: [0.40, 0.92], $P = 0.02$) in the Cinobufacin combined chemotherapy group were lower than those in the chemotherapy group, and the difference was statistically significant, but the incidences of peripheral neurotoxicity (RR = 0.69, 95% CI: [0.26, 1.85], $P = 0.46$) and myelosuppression (RR = 0.78, 95% CI: [0.46, 1.34], $P = 0.37$) in the combined group were similar to those of the chemotherapy group, and the difference was not statistically significant. **Conclusions.** Cinobufacin combined with chemotherapy can improve the clinical efficacy of breast cancer patients, enhance the quality of life of the patients, reduce the value of tumor markers such as CA125, CA153, and CEA, and lower the occurrence of adverse reactions such as gastrointestinal reactions, liver and kidney damage, and hair loss.

1. Introduction

Breast cancer is the malignant tumor with the highest female morbidity and the second highest mortality after lung cancer in the world. According to global cancer data statistics, there were more than 2 million new cases of breast cancer in 2018,

accounting for 11.6% of the total number of new cancers. Among them, the incidence of breast cancer in China is as high as 36.1/100,000. More than 600,000 women die from breast cancer, accounting for 6.6% of total cancer-related deaths each year [1, 2]. Chemotherapy is one of the commonly used treatment methods for advanced breast cancer,

but its application is limited because of its severe side effects, including gastrointestinal symptoms, myelosuppression, liver and kidney damage, etc [3].

Cinobufacin is a traditional Chinese patent medicine extracted from the skin of *Bufo bufo gargarizans*. Its components are toadotoxin, dehydroxytoluotoxin, serotonin, amino acids, reducing sugar, arginine complex, etc. It has the functions of clearing away heat and detoxification, promoting blood circulation, and removing and resolving blood stasis [4]. In recent years, many studies have shown that Cinobufacin has antitumor effects, which may be related to its inhibition of tumor cell growth, induction of tumor cell apoptosis, and enhancement of immune function in the body [5]. Multiple meta-analyses have proved that Cinobufacin combined with chemotherapy can improve the efficacy and reduce adverse reactions in gastric cancer, liver cancer, non-small-cell lung cancer, rectal cancer, and other malignant tumors [6–9]. However, there are currently no evidence-based medicine data to demonstrate the efficacy and safety of Cinobufacin for breast cancer. Therefore, we carried out a meta-analysis of Cinobufacin based on the RCT literature of breast cancer to evaluate the efficacy and safety of its treatment and to provide guidance for the clinical application of Cinobufacin.

2. Methods

2.1. Protocol and Registration. First, the study was according to the statements of the Preferred Reporting Items for Systematic Reviews and Meta-Analyses (PRISMA) [10]. The protocol for this review has been registered on PROSPERO, and the registration number is CRD42020154411.

2.2. Literature Search. Our research retrieved the three major English databases of PubMed, Web of Science, Cochrane Library, and the four major Chinese databases of CNKI, WanFang, VIP, and SinoMed, with “Huachansu”, “cinobufotalin”, “cinobufacin”, “cinobufagin”, “cinobufatini”, “toad skin” and “breast cancer”, “breast carcinoma”, and “breast tumor” as main inscriptions or keywords as well as subject words or free words. For example, the PubMed retrieval strategy was as follows: (Huachansu OR cinobufotalin OR cinobufacini OR cinobufagin OR cinobufatini OR toad skin) AND (breast cancer OR breast carcinoma OR breast tumor). The retrieval deadline is until December 2019. In addition, the references that were reviewed and included in the study were searched twice.

2.3. Inclusion and Exclusion Criteria. Our inclusion criteria include, first, randomized controlled trials published in China and abroad, regardless of language; second, all patients are confirmed as advanced breast cancer by pathology and imaging examination; third, the treatment group was treated with Cinobufacin combined with conventional chemotherapy, while the control group was treated with conventional chemotherapy; and fourth, inclusion of research outcome indicators is required (contains one of the following outcome indicators).

Our exclusion criteria include, first, no relevant outcome indicators; second, repeated publications, incomplete data, and second, repetitive, and incomplete data. It should be noted that incomplete data refer to per-protocol analysis instead of intention-to-treat analysis; and third, the intervention measures are Cinobufacin vs chemotherapy, or the control group is not chemotherapy alone.

The outcome indicators included in our study mainly involve clinical efficacy, KPS score, pain relief rate, tumor markers (CA125, CA153, and CEA), and adverse reactions (gastrointestinal reaction, myelosuppression, alopecia, liver and kidney damage, and peripheral neurotoxicity). The clinical efficacy includes overall response rate (ORR) and clinical benefit rate (CBR)— $ORR = CR + PR / \text{total cases} \times 100\%$ and $CBR = CR + PR + SD / \text{total cases} \times 100\%$ [11].

2.4. Data Extraction. We first use EndNote to search and remove duplicate documents and read the remaining documents in depth. Two researchers (JX and KXD) independently screened the literature, extracted data, and cross-checked according to the inclusion and exclusion criteria. For those in doubt, they will be discussed or decided by a third researcher (DYL). The data extracted by this research include first author, year of publication, age, number of cases in each group, intervention measures, course of treatment, outcome indicators, etc.

2.5. Quality Evaluation. Two researchers (KXD and JW) used the risk bias assessment tool in the Cochrane evaluation manual [12] to evaluate the quality of the included literature and then cross-checked it. The evaluation criteria include random sequence generation, allocation concealment, blinding participants and personnel, blinding of outcome assessment, incomplete outcome data, selective reporting, and other bias. Disagreements are resolved through discussion or consultation with a third evaluator (DYL).

2.6. Statistical Analysis. We used RevMan5.3 software to conduct meta-analysis, heterogeneity test, sensitivity analysis and publication bias test on the included studies. The significance level is set to $\alpha = 0.05$, and the heterogeneity is quantitatively analyzed by I^2 . If $P < 0.05$, $I^2 \geq 50\%$, there is obvious heterogeneity between the results of each study, and the random effect model is used for analysis. Mean difference (MD) is used for those with the same measurement unit, and relative risk (RR) and 95% confidence interval (95% CI) are used for binary classification variables. If the clinical heterogeneity is obvious, then the subgroup analysis or sensitivity analysis should be used for treatment.

3. Results

3.1. Search Results. We initially retrieved 163 related literature studies, and through reading the title, abstract, and full text of the literature studies, excluding animal experiments, repeated studies, and reviews, we finally met the inclusion criteria of 16 RCTs (Figure 1).

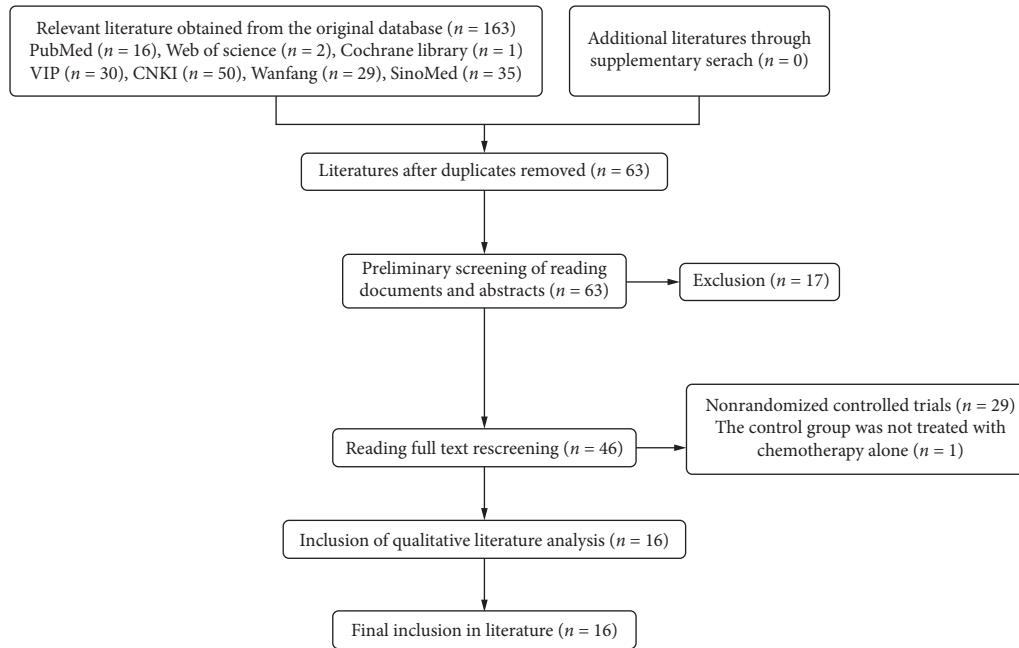


FIGURE 1: Flowchart of literature screening.

3.2. Basic Characteristics of Included Studies. The 16 literature studies [13–28] included in our study included 1331 patients, of which 666 patients in the Cinobufacin combined with chemotherapy group and 665 patients in the chemotherapy-alone group. All the subjects were adult women, and the baseline of each study was comparable. The time span included in the study was 18 years. It should be pointed out that there are no randomized controlled trials of Cinobufacin in breast cancer treatment in foreign literature. The related studies Cinobufacin and breast cancer are reviews or related mechanism studies (Table 1).

3.3. Quality Evaluation of Included Studies. Nine of the 16 studies in our study reported specific random sequence generation methods, among which three studies [17, 18, 21] were grouped according to the order of admission or time and were rated as high-risk bias, while six studies [13, 16, 20, 26–28] were rated as low-risk bias, and the remaining seven studies only mentioned random and did not report the implementation of a specific random scheme. One study [20] was randomly grouped using the sealed envelope method, and no studies reported the implementation of the blind method. None of the studies reported the concealment of random allocation. Sixteen studies did not fully report the predetermined indicators, and there were cases where the results were selectively reported (Figure 2).

3.4. Meta-Analysis Results

3.4.1. Clinical Efficacy. The clinical efficacy of our research includes ORR (overall response rate) and CBR (clinical benefit rate). The 16 studies [13–28] (1331 cases) we included all reported ORR. The meta-analysis results found that the ORR of Cinobufacin combined with chemotherapy was

superior to simple chemotherapy (RR = 1.35, 95% CI: [1.23, 1.49], $P < 0.00001$). We included 15 studies [14–28] (1239 cases) reported CBR. The results of meta-analysis showed that the CBR of Cinobufacin combined with chemotherapy was better than that of chemotherapy alone (RR = 1.14, 95% CI: [1.08, 1.21], $P < 0.00001$) (Figure 3).

3.4.2. KPS Score and Pain Relief Rate. Five studies [13, 19, 21, 22, 25] (368 cases) reported KPS scores, and three studies [17, 19, 22] (153 cases) reported pain relief rate. The results of meta-analysis showed that the KPS score and pain relief rate of the Cinobufacin combined with chemotherapy group were better than those of chemotherapy-alone group, the RR of KPS scores was 1.98, 95% CI was 1.45 to 2.68, P -value was less than 0.0001, and the RR of pain relief rate was 1.34, 95% CI was 1.01 to 1.78, $P = 0.04$ (Figures 4 and 5).

3.4.3. Tumor Markers. The six studies [13, 14, 18, 20, 26, 28] were reported the changes of CA153 and CEA, of which 4 studies [14, 18, 20, 26] reported changes in CA125. Through a comparative analysis of tumor markers before and after treatment in 1372 patients, we found that the heterogeneity between CA125, CA153, and CEA groups before treatment was relatively small and the fixed effects model was selected for meta-analysis. The results showed that there was no statistical difference in tumor markers before treatment ($P > 0.05$) (Figure 6). After treatment, the heterogeneity among CA125, CA153, and CEA groups was large and the random effects model was selected for meta-analysis. The results showed that the tumor markers of Cinobufacin combined with chemotherapy after treatment were lower than those of chemotherapy alone, and the difference was statistically significant; the MD of CA125 was -7.36 , 95% CI was -10.92 to -3.80 , P -value was less than 0.0001, the MD of

TABLE 1: Basic characteristics of 16 included studies.

Author and Year	Treatment Course (weeks)	Age (T/C)	Number (T/C)	Interventions (T/C)	Outcome Indicators
Chen 2019 [13]	6w	46.34 ± 7.88/ 45.67 ± 7.91	46/46	Cinobufacin + NX/NX	A1C2C3
Guo 2019 [14]	8w	45.37 ± 7.68/ 45.54 ± 7.82	60/60	Cinobufacin + pirarubicin/Pirarubicin	A1A2C1C2C3D1D4
Lei 2019 [15]	6w	50.42 ± 3.62/ 50.46 ± 3.68	29/29	Cinobufacin + DC/DC	A1A2D1D2D5
He 2018 [16]	8w	43.7 ± 1.9/ 44.33 ± 2.1	68/68	Cinobufacin + TEC/TEC	A1A2D1
Wang 2018 [17]	6w	Median age 54	35/35	Cinobufacin + DC/DC	A1A2B2D1D2D5
Tian 2017 [18]	9-18w	50.27 ± 6.23/ 49.57 ± 5.86	31/31	Cinobufacin + basic scheme containing capecitabine/ Basic scheme containing capecitabine	A1A2C1C2C3
Ke 2017 [19]	12w	38.3 ± 8.9/39.5 ± 8.8	20/21	Cinobufacin + CAF/CAF	A1A2B1B2D1D3D4
Deng 2017 [20]	6w	50.27 ± 6.23/ 49.57 ± 5.86	31/31	Cinobufacin + basic scheme containing capecitabine/ Basic scheme containing capecitabine	A1A2C1C2C3
Yang 2016 [21]	8w	34.58 ± 14.44	40/41	Cinobufacin + TAC/TAC	A1A2B1D1D2D3
Dong 2011 [22]	6w	Average age 53	20/22	Cinobufacin + DC/DC	A1A2B1B2D1D2D5
Pan 2011 [23]	6w	Average age 56	80/80	Cinobufacin + CAF/CAF	A1A2D1D2D4
Song 2002 [24]	4w	Median age 54	26/21	Cinobufacin + CAF/CAF	A1A2D1D2D3
Sun 2019 [25]	6w	41.85 ± 2.25/ 43.56 ± 3.02	56/56	Cinobufacin + TEC/TEC	A1A2B1D1D2D3
Li 2019 [26]	9w	49.34 ± 7.34/ 48.36 ± 8.52	30/30	Cinobufacin + Basic scheme containing capecitabine/ Basic scheme containing capecitabine	A1A2C1C2C3D1
Mai 2019 [27]	6w	44.10 ± 2.92/ 43.50 ± 3.71	25/25	Cinobufacin + docetaxel sequential CEF/Docetaxel sequential CEF	A1A2D1D3
Li 2018 [28]	—	47.5 ± 11.2/ 48.5 ± 10.8	69/69	Cinobufacin + pemetrexed combined with DDP/ Pemetrexed combined with DDP	A1A2C2C3D1D3D4

Notes: T/C: treatment group/control group. A1(ORR); A2(CBR); B1(KPS score); B2(pain relief rate); C1(CA125); C2(CA153); C3(CEA); D1(gastrointestinal reaction); D2(myelosuppression); D3(liver and kidney damage); D4(alopecia); D5(peripheral neurotoxicity). TAC: docetaxel + pirarubicin + cyclophosphamide; TEC: docetaxel + epirubicin + cyclophosphamide; NX: capecitabine + vinorelbine; CAF: cyclophosphamide + pirarubicin + 5-FU; DC: docetaxel + capecitabine; CEF: cyclophosphamide + epirubicin + 5-FU.

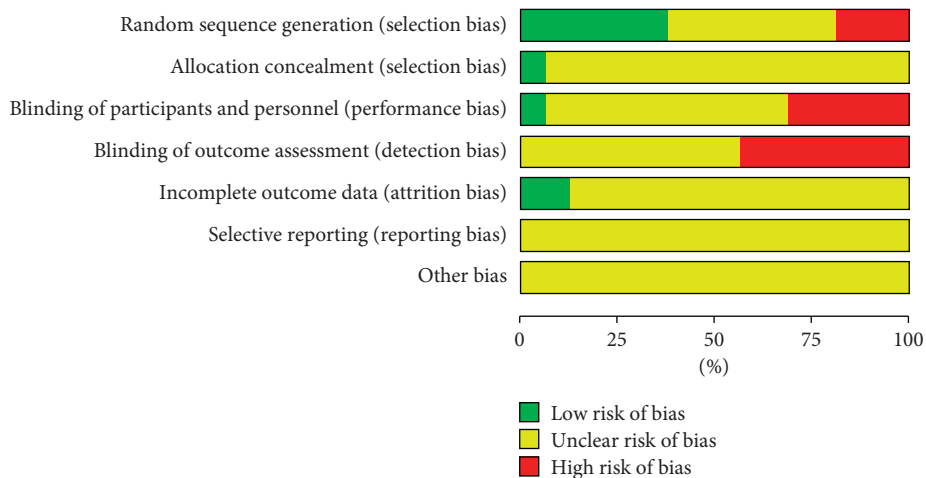


FIGURE 2: The diagram of risk of bias in included studies.

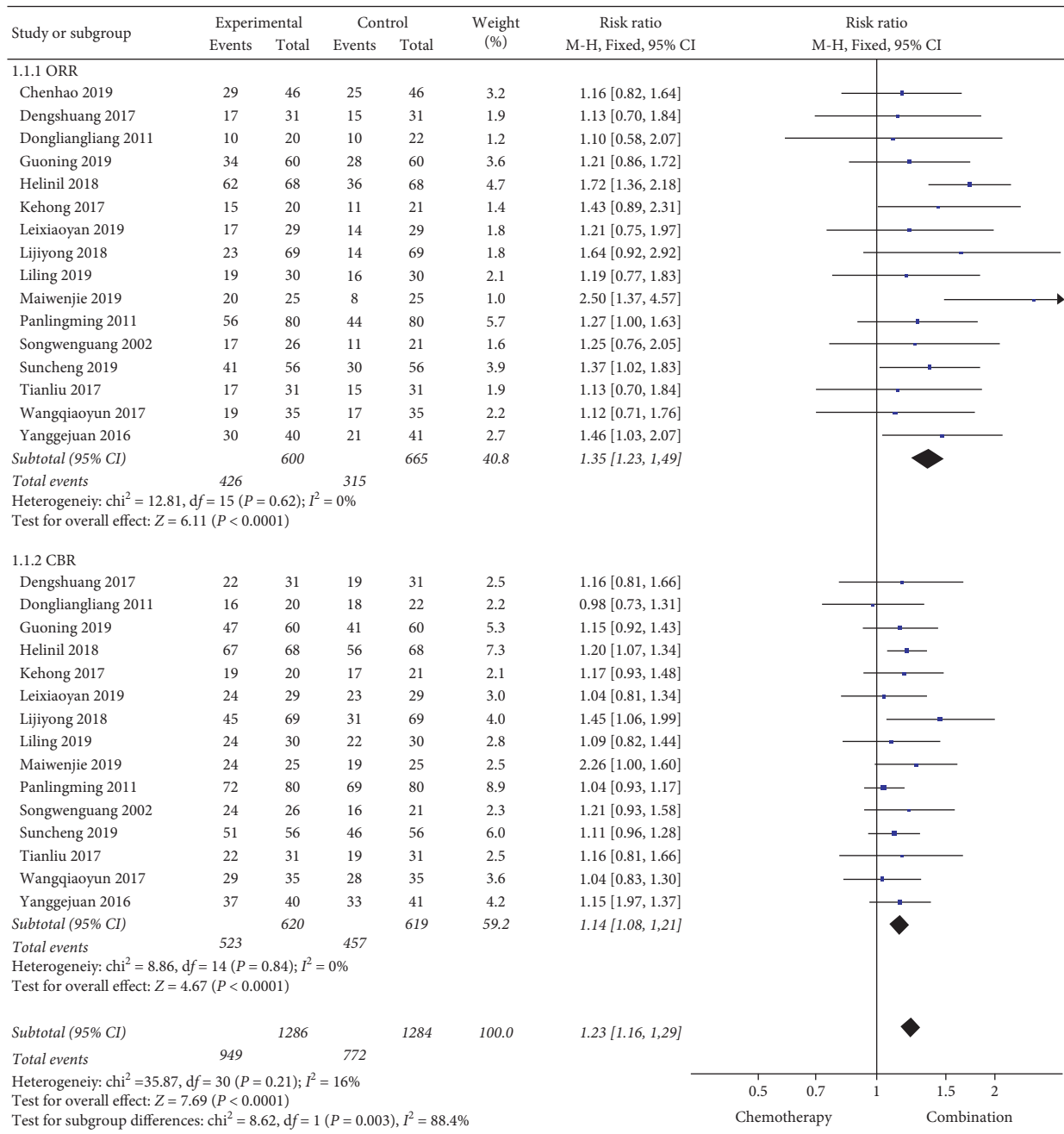


FIGURE 3: A meta-analysis of chemotherapy combined with Cinobufacin and chemotherapy alone for clinical efficacy.

CA153 was -5.20 , 95% CI was -7.36 to -3.03 , P -value was less than 0.00001 , and the MD of CEA was -2.47 , 95% CI was -3.31 to -1.62 , P -value was less than 0.00001 (Figure 7).

3.4.4. Adverse Reactions. 14 studies reported adverse reactions, including gastrointestinal reactions, liver and kidney damage, hair loss, peripheral neurotoxicity, bone marrow suppression, and so on. According to the heterogeneity test, the heterogeneity of gastrointestinal reaction, liver and kidney damage, hair loss, and peripheral neurotoxicity was small, and hence the fixed effects model was used for meta-

analysis, while the heterogeneity of bone marrow suppression study was large, and hence the random effects model was used for meta-analysis. The results of meta-analysis showed that the incidences of gastrointestinal reaction, liver and kidney damage, and hair loss in the Cinobufacin combined with chemotherapy group were lower than those in the chemotherapy-alone group, and the RR of gastrointestinal reaction was 0.58 , 95% CI was 0.48 to 0.70 , P -value was less than 0.00001 , the RR of liver and kidney damage was 0.57 , 95% CI was 0.38 to 0.84 , $P = 0.004$, and the RR of hair loss was 0.61 , 95% CI was 0.40 to 0.92 , $P = 0.02$. The incidences of peripheral neurotoxicity and myelosuppression

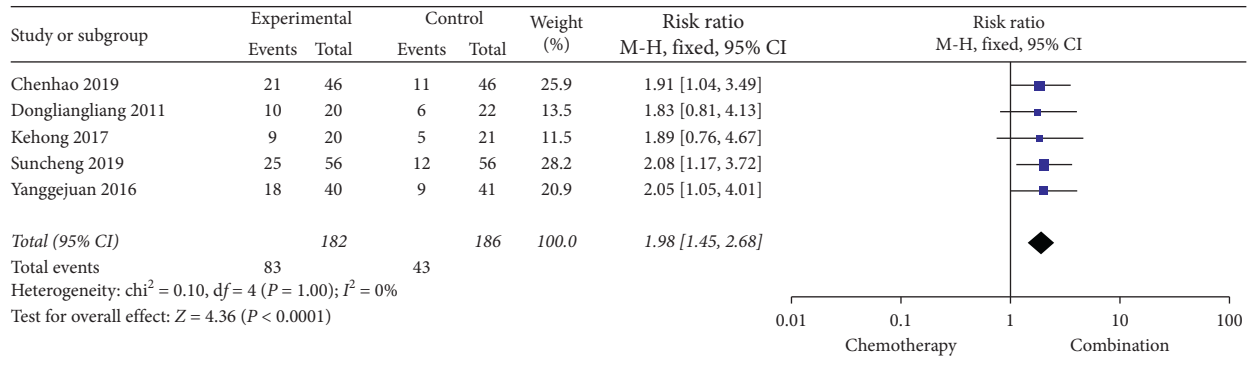


FIGURE 4: A meta-analysis of chemotherapy combined with Cinobufacin and chemotherapy alone for KPS scores after treatment.

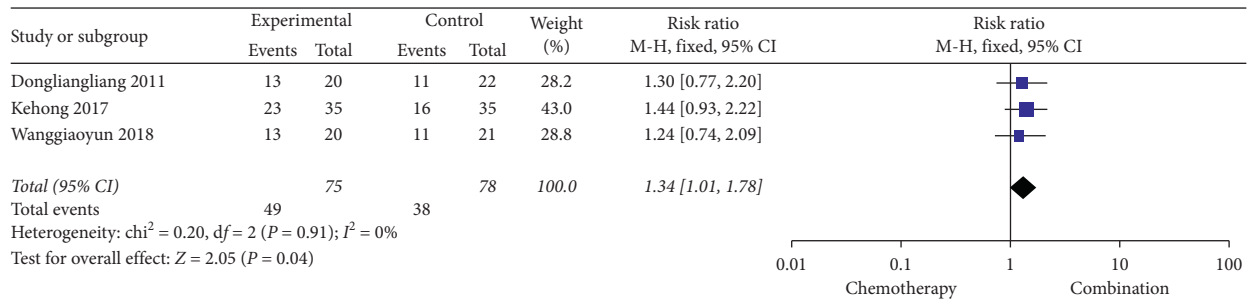


FIGURE 5: A meta-analysis of chemotherapy combined with Cinobufacin and chemotherapy alone for pain relief rate.

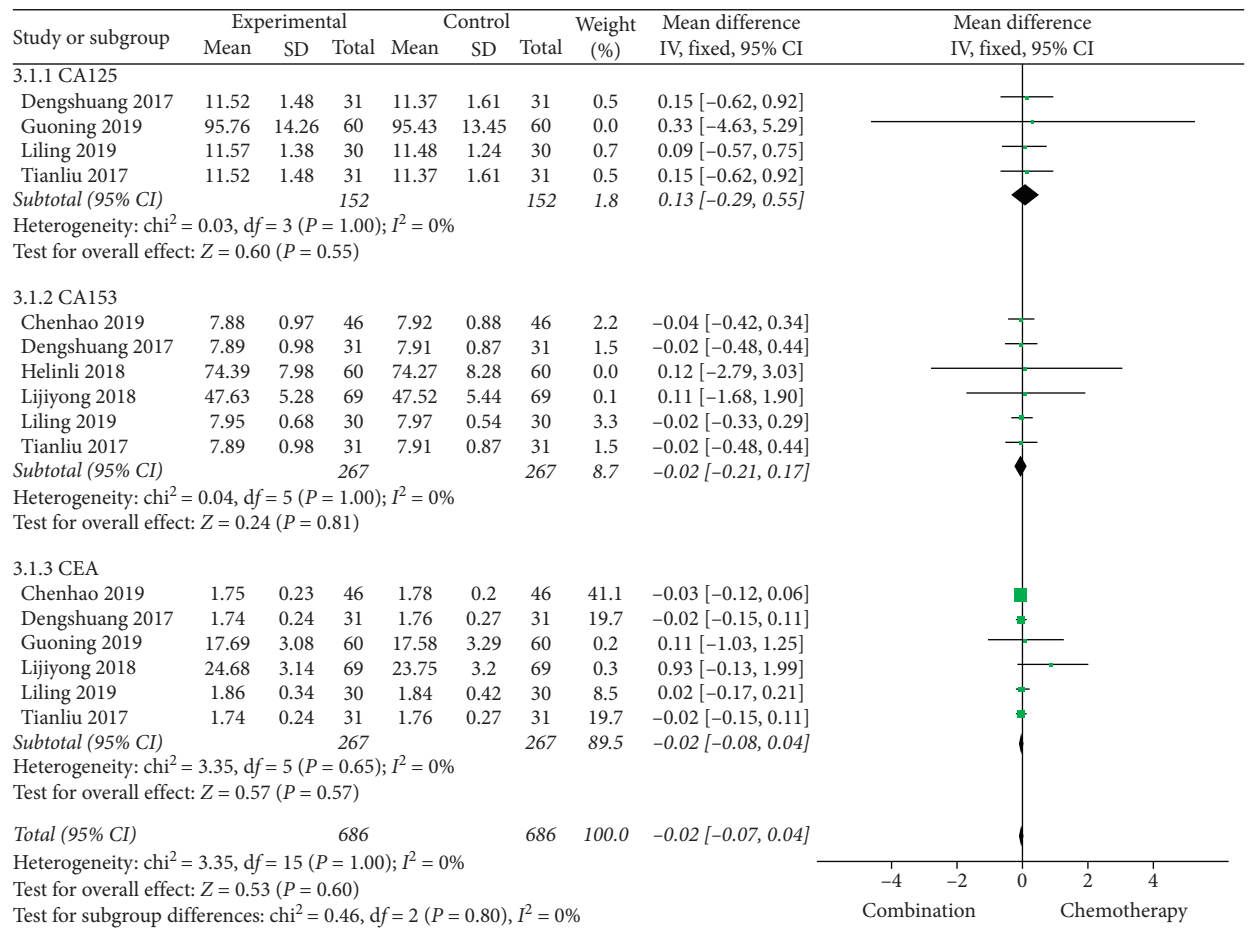


FIGURE 6: A meta-analysis of chemotherapy combined with Cinobufacin capsules and chemotherapy alone in tumor markers (CA125, CA153, and CEA) before treatment.

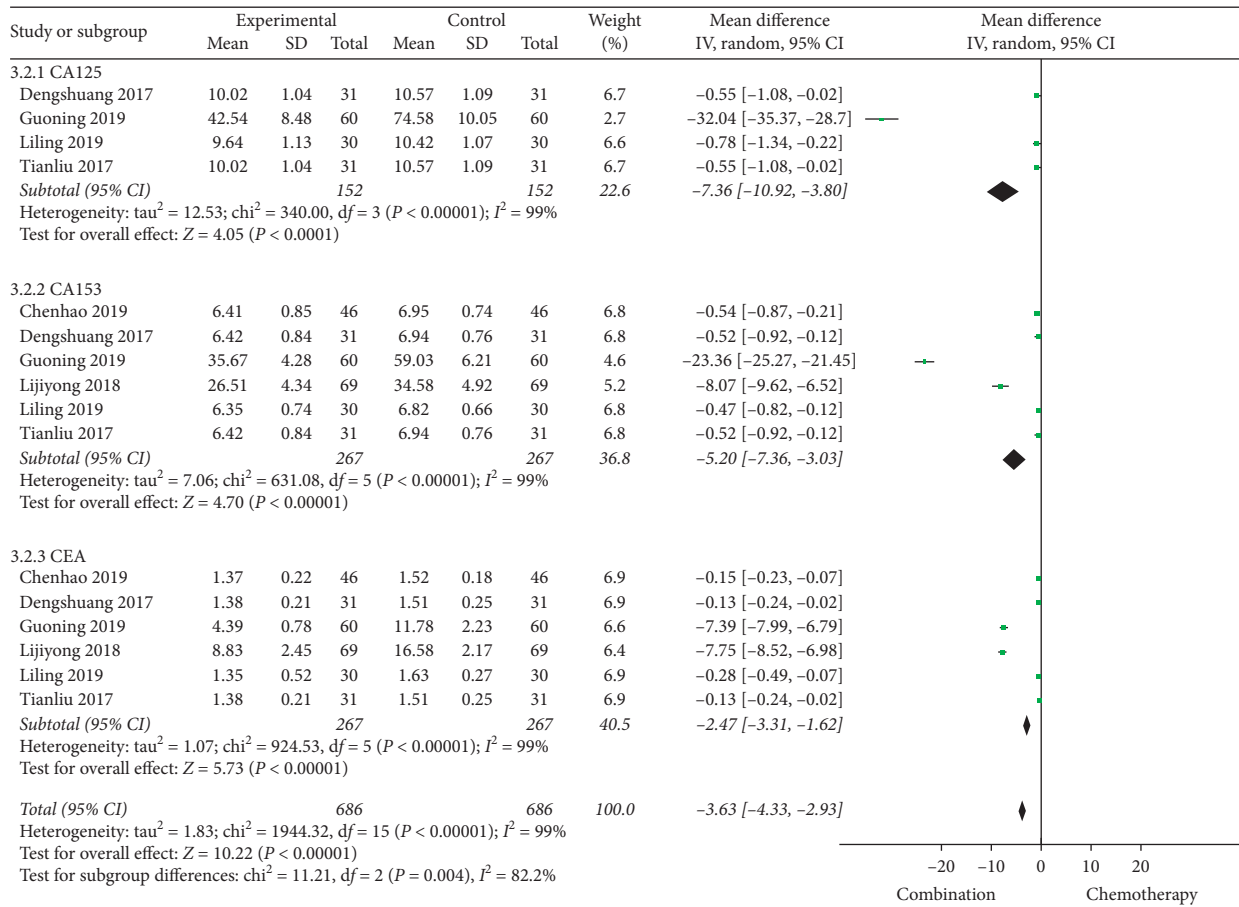


FIGURE 7: A meta-analysis of chemotherapy combined with Cinobufacin capsules and chemotherapy alone in tumor markers (CA125, CA153, and CEA) after treatment.

in the combination group were similar to those in the chemotherapy group, and the difference was not statistically significant, the RR of peripheral neurotoxicity was 0.69, 95% CI was 0.26 to 1.85, *P*-value was 0.46, and the RR of myelosuppression was 0.78, 95% CI was 0.46 to 1.34, *P* = 0.37 (Figures 8 and 9).

3.5. Sensitivity Analysis. Our results showed that the heterogeneity of tumor markers (CA125, CA153, and CEA) after treatment was relatively large (*I*² = 99%). After the comparative analysis was included in the literature, the heterogeneity of tumor markers after treatment was significantly reduced (*I*² = 0) after the removal of the studies by Guo et al. [14] and Li [28], so we considered that the heterogeneity of tumor markers after treatment was mainly related to the quality of the included study (Figure 10).

3.6. Publication Bias Analysis. The funnel chart analysis of clinical efficacy showed that the results were not completely symmetrical, which was related to the low quality of the study and the small sample size (Figure 11).

4. Discussion

In this study, the meta-analysis method was used to merge and analyze 16 randomized controlled literature studies on the efficacy and safety of Cinobufacin combined with chemotherapy for breast cancer. The results of meta-analysis showed that the ORR, CBR, KPS scores, and pain relief rate of the Cinobufacin combined with chemotherapy group were better than those of the chemotherapy-alone group, which suggested that Cinobufacin combined with chemotherapy could improve the clinical efficacy and quality of life of the patients with breast cancer. Our study also found that the tumor markers (CA125, CA153, and CEA) of the Cinobufacin combined with chemotherapy group were lower than those of the chemotherapy-alone group. The heterogeneity was related to the low-quality literature of the included studies, but the results were stable. In terms of safety, the incidences of gastrointestinal reactions, liver and kidney damage, and hair loss in the Cinobufacin combined chemotherapy group were lower than those in the simple chemotherapy group, and the difference was statistically significant, but the incidences of peripheral neurotoxicity and myelosuppression in the combined group were similar

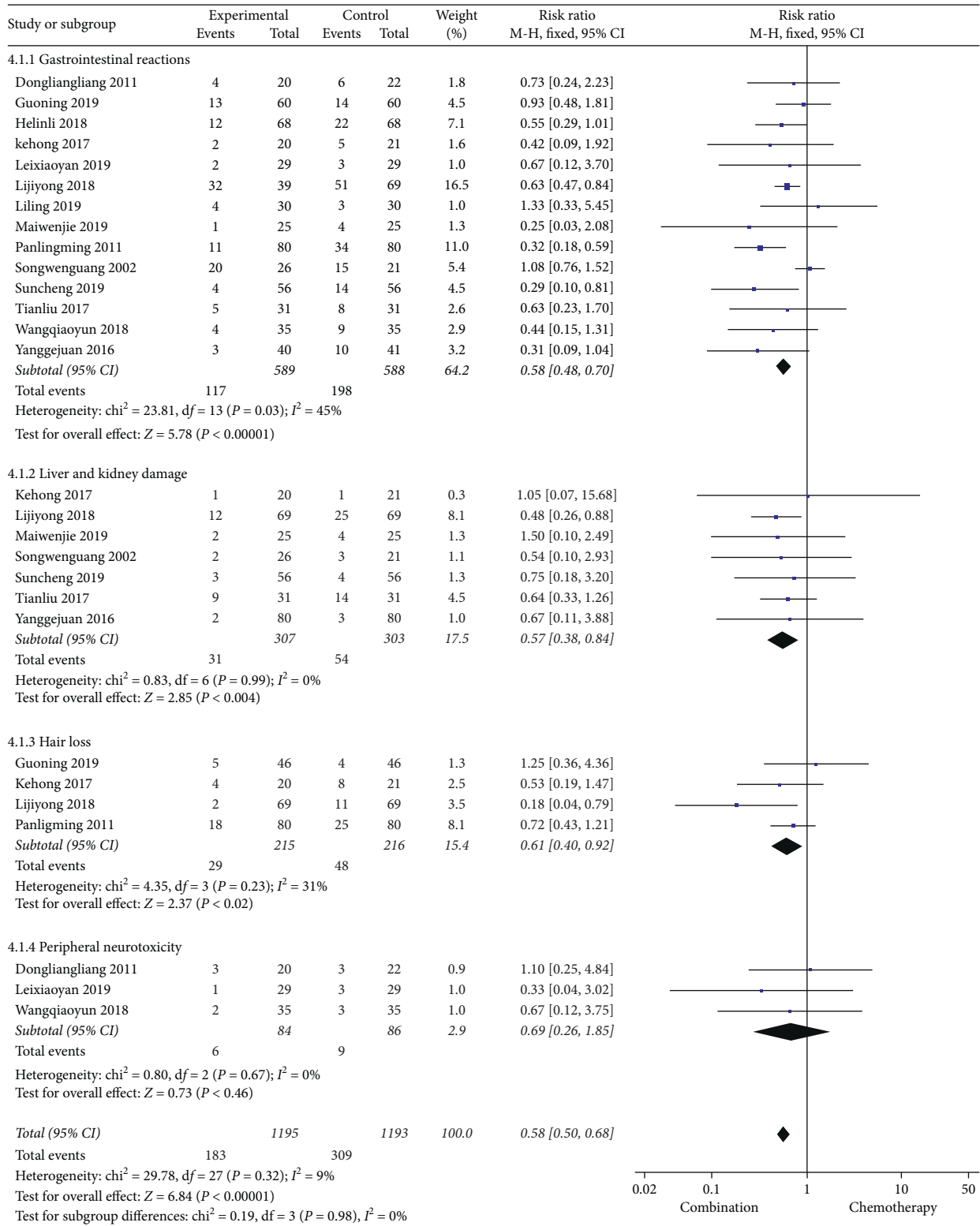


FIGURE 8: A meta-analysis of chemotherapy combined with Cinobufacin and chemotherapy alone for adverse reactions.

to those in the chemotherapy group, and the difference was not statistically significant.

Chemotherapy is the most common and direct clinical treatment for advanced breast cancer, but it usually requires large doses of two or more chemotherapeutic agents, which

will bring corresponding side effects when reaching the treatment dose. The minor side effects will have a certain impact on the daily life of the patients, and the severe toxicities will threaten the physical and mental health of the patients, which will lead to the failure of chemotherapy and

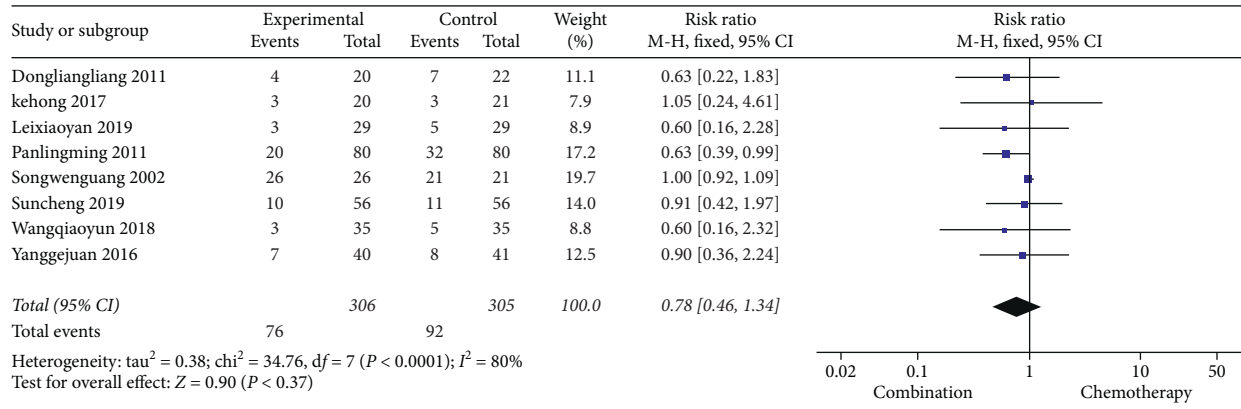


FIGURE 9: A meta-analysis of chemotherapy combined with Cinobufacin and chemotherapy alone in myelosuppression.

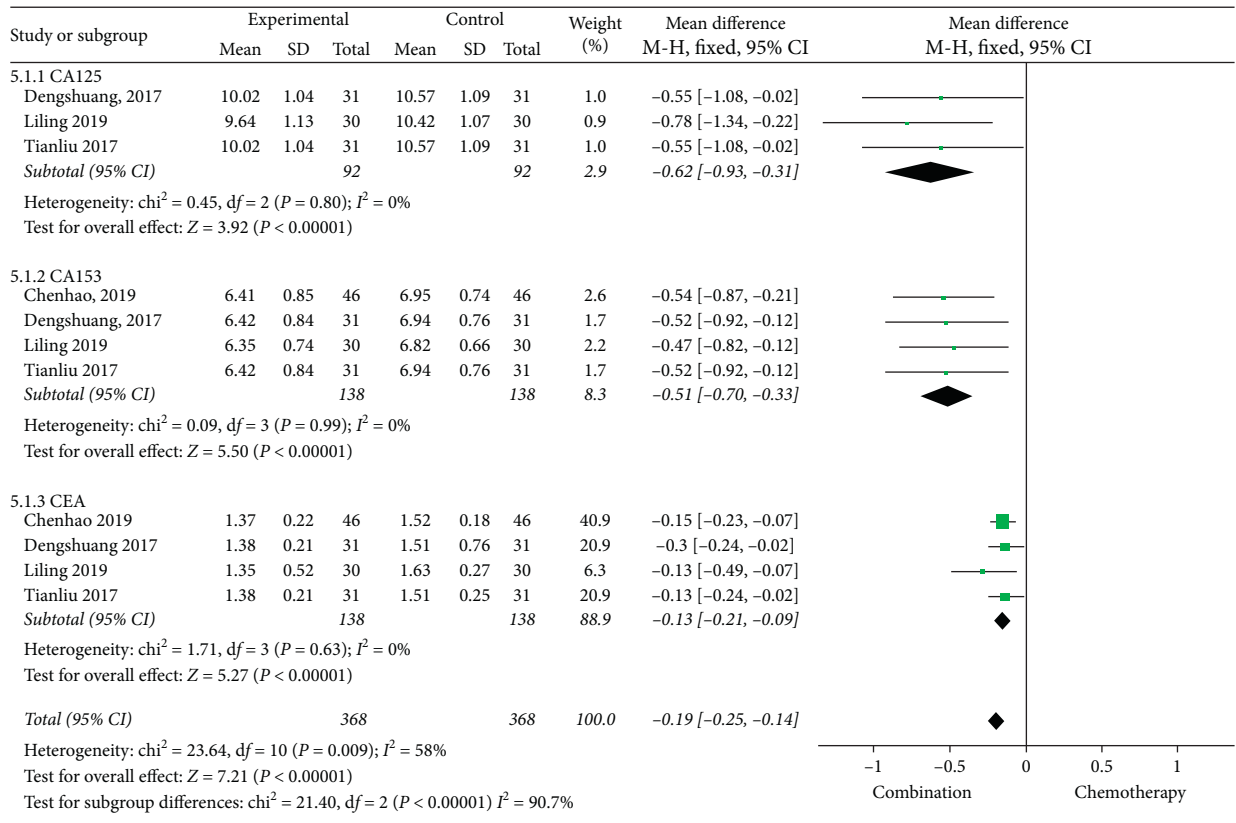


FIGURE 10: A meta-analysis of sensitivity analysis of chemotherapy combined with Cinobufacin and chemotherapy alone in tumor markers (CA125, CA153, and CEA) after treatment.

affect the prognosis [29–31]. Therefore, the combination of traditional Chinese and Western medicine has become a common clinical treatment for malignant tumors [32]. As the incidence of breast cancer increases year by year, an antitumor traditional Chinese medicine preparation independently developed by China, Cinobufacin, can be used in the field of breast cancer in combination with the chemotherapeutics to reduce the adverse reactions of patients and improve the quality of life of patients [33]. The mechanism may be as follows: First, apoptosis of human breast cancer

cell line T-47D can be induced by increasing the expression level of caspase-3 [34]; second, apoptosis of MDA-MB-231 can be induced by destroying the cytoskeleton, resulting in abnormal changes of the cell surface ultrastructure and morphology [35]; Third, it can inhibit the growth and proliferation of human breast cancer cell lines MDA-MB-468 and BT549 by inhibiting their proliferation and migration and the activity of PI3K/Akt signaling pathway [36, 37]; Fourth, many studies have shown that due to a large number of fibrin accumulation and platelet aggregation

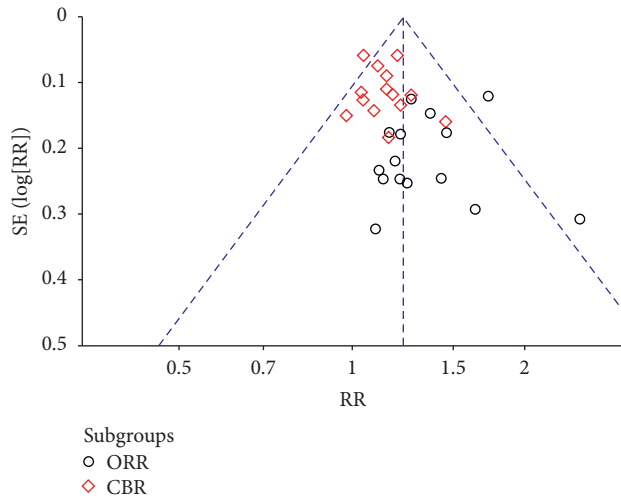


FIGURE 11: Funnel chart of clinical efficacy.

around cancer cells, patients with malignant tumors are prone to coagulation dysfunction, which makes the blood present a hypercoagulable state, while traditional Chinese medicine for promoting blood circulation and removing blood stasis can expose cancer cells, so they are more vulnerable to the attack of chemotherapy drugs [38, 39]. Therefore, the efficacy of Cinobufacin in clearing away heat and detoxification, promoting blood circulation, and removing stasis can play a role of “increasing efficiency and reducing toxicity” when combined with chemotherapy.

At present, a large number of experimental studies have found that Cinobufacin has antitumor effects on breast cancer, lung cancer, esophageal cancer, gastric cancer, liver cancer, bladder cancer, etc. [40]. Ni et al. [41] treated MGC-803 and BGC-823 GC cells with different concentrations of Cinobufacin and found that Cinobufacin has significant antitumor cell proliferation and apoptosis effects both in vivo and in vitro and can inhibit the growth of gastric cancer cells by inhibiting the Akt/mTOR pathway and induce cell apoptosis through the internal pathway. Yin et al. [42] established a nude mouse xenograft model and found that Cinobufacin can inhibit the growth of liver metastases by reducing the expression of MMP-2, MMP-9 and VEGF. Yang et al. [43] also found that Cinobufacin can inhibit the growth of human bladder cancer cells in vivo and in vitro through Fas/FasL and TNF- α /TNFR1 pathways. Not only experimental studies have confirmed the scientific antitumor effect of Cinobufacin but also a large number of clinical studies have confirmed the rationality of its clinical application. Sha et al. [44] through the RCT test on the effect of Cinobufacin capsule combined with raltitrexed and oxaliplatin on advanced colorectal cancer found that Cinobufacin capsule combined with raltitrexed and oxaliplatin can enhance the immune function of patients with advanced colorectal cancer, reduce tumor markers, and inhibit the growth and metastasis of tumor cells and neo-vascularization. Wang et al. [45] found that patients with advanced liver cancer who were treated with Cinobufacin

as a single agent had a lower rate of disease deterioration (11.4%) and a higher total effective rate after treatment (82.86%). Serum total bilirubin and alanine aminotransferase decreased significantly.

Our study also found that Cinobufacin combined with chemotherapy can reduce the incidences of gastrointestinal reactions, liver and kidney damage, and alopecia in breast cancer patients, and there are also relevant clinical reports. Dong [46] found that the incidences of nausea, vomiting, and leukopenia were lower in the combined group than in the control group after randomly dividing 68 patients with advanced colon cancer into the chemotherapy group and chemotherapy combined with Cinobufacin group. Cao, et al. [47] found that the combined group could reduce the incidence of myelosuppression and improve the disease control rate through the RCT trial of Cinobufacin injection combined with first-line chemotherapy in the treatment of advanced non-small-cell lung cancer. In addition, studies on adverse reactions related to Cinobufacin itself have mainly focused on reports of Cinobufacin injection. Cheng [48] retrospectively analyzed 272 cases of adverse reactions/events of Cinobufacin injection and found that the adverse reactions produced by Cinobufacin injection were mainly rapid-onset type, which mainly manifested as rapid-onset skin reactions in addition to venous injury and other adverse reactions. Zhang [49] analyzed 60 cases of adverse reactions caused by Cinobufacin injection and found that the main reactions were allergic and febrile reactions, and no deaths were observed.

Our study is a comprehensive analysis of the RCT literature of Cinobufacin for breast cancer, but there are still some deficiencies. First, the chemotherapy methods used in the studies included in this study are not the same. Although they are all patients with advanced breast cancer, the pathological stage is not exactly the same, which increases the clinical heterogeneity of the study.

Second, blind methods and random allocation concealment were not implemented in some of the included studies, which made the quality of the included studies low. Third, although the Chinese and English databases were searched extensively, the included cases were still from China. Finally, this article has not yet carried out stratified analysis of different dosage forms of Cinobufacin, which may increase the heterogeneity of the study. By consulting the relevant literature, we found that the main components of the three formulations were dried toad skin extract, which could play an antitumor role by inhibiting the growth and reproduction of tumor cells, inducing cell apoptosis and antimetastasis, targeting Na⁺/K⁺-ATPase activity, inhibiting tumor angiogenesis, and inhibiting the steroid receptor coactivator family [50].

5. Conclusion

In summary, the results of this study indicate that Cinobufacin combined with chemotherapy can improve the clinical efficacy of breast cancer patients, enhance the quality of life of the patients, reduce the value of tumor markers such as CA125, CA153, and CEA, and lower the occurrence

of adverse reactions such as gastrointestinal reactions, liver and kidney damage, and hair loss. However, the conclusion of safety should be used carefully especially, the corresponding adverse reactions caused by different dosage forms of Cinobufacini itself should be considered. In future, we will carry out more clinical studies on different dosage forms of Cinobufacini and further compare the efficacy of different dosage forms and the same chemotherapy regimen in the treatment of breast cancer.

Abbreviations

CNKI: Chinese National Knowledge Infrastructure
 RCT: randomized controlled trials
 ORR: overall response rate
 CBR: clinical benefit rate
 KPS: Karnofsky Performance Status
 CR: complete response
 PR: partial response
 SD: stable disease
 RR: relative risk
 CI: confidence interval
 MD: mean difference.

Data Availability

All the data were taken from the published studies.

Conflicts of Interest

The authors declare that there are no conflicts of interest between them.

Authors' Contributions

JX was mainly responsible for research design, literature retrieval, data extraction, data analysis, and writing of papers; DYL was involved in research design, research design, data verification, and quality evaluation; KXD was involved in data extraction and quality evaluation; and JW was involved in research design, quality evaluation, and thesis implication and modification. The author read and approved the final manuscript.

Acknowledgments

The authors wish to thank Ms. Elizabeth Gullen from Yale University for the critical reading of the manuscript. This work was supported by the Key Program (81630080) and Young Scientist Fund (81503575) of National Natural Science Foundation of China, and Young Scientist Development Program 2016 of Dongzhimen Hospital Affiliated to Beijing University of Chinese Medicine (DZMYS-201610).

References



- [1] M. Ghoncheh, Z. Pournamdar, and H. Salehiniya, "Incidence and mortality and epidemiology of breast cancer in the world," *Asian Pacific Journal of Cancer Prevention*, vol. 17, no. sup3, pp. 43–46, 2016.
- [2] F. Bray, J. Ferlay, I. Soerjomataram, R. L. Siegel, L. A. Torre, and A. Jemal, "Global cancer statistics 2018: GLOBOCAN estimates of incidence and mortality worldwide for 36 cancers in 185 countries," *CA: A Cancer Journal for Clinicians*, vol. 68, no. 6, pp. 394–424, 2018.
- [3] G. Miolo, E. Muraro, D. Martorelli et al., "Anthracycline-free neoadjuvant therapy induces pathological complete responses by exploiting immune proficiency in HER2+ breast cancer patients," *BMC Cancer*, vol. 15, no. 14, p. 954, 2014.
- [4] Z. P. Gong, T. Chen, L. R. Deng et al., "Clinical application progress of cinobufagin to cancer pain relief," *Drugs & Clinical*, vol. 25, no. 4, pp. 268–271, 2010.
- [5] S. Kai, J.-H. Lu, P.-P. Hui, and H. Zhao, "Pre-clinical evaluation of cinobufotalin as a potential anti-lung cancer agent," *Biochemical and Biophysical Research Communications*, vol. 452, no. 3, pp. 768–774, 2014.
- [6] Y. Xu, D. Han, F. C. Feng et al., "Meta-analysis of cinobufacini injection combined with platinum-contained first-line chemotherapy in meta-analysis of cinobufacini Injection combined with platinum-contained first-line chemotherapy in treatment of non-small cell lung cancer," *China Journal of Chinese Materia Medica*, vol. 44, no. 21, pp. 4728–4737, 2019.
- [7] Z. Y. Dong, X. T. Qiu, S. A. Kujawa et al., "Cinobufacini injection for moderate and advanced primary liver cancer: a systematic review and meta-analysis," *Journal of Chinese Pharmaceutical Sciences*, vol. 28, no. 4, pp. 264–275, 2019.
- [8] H. Sun, W. Wang, M. Bai, and D. Liu, "Cinobufotalin as an effective adjuvant therapy for advanced gastric cancer: a meta-analysis of randomized controlled trials," *OncoTargets and Therapy*, vol. 12, no. 26, pp. 3139–3160, 2019.
- [9] Y. Y. Peng, Z. Chen, F. Y. Wang et al., "Meta analysis of cinobufacin capsule combined with oxaliplatin chemotherapy in the treatment of colorectal cancer," *Acta Chinese Medicine*, vol. 35, no. 3, pp. 673–678, 2020.
- [10] D. Moher, A. Liberati, J. Tetzlaff, D. G. Altman, and PRISMA Group, "Preferred reporting items for systematic reviews and meta-analyses: the PRISMA statement," *International Journal of Surgery*, vol. 8, no. 5, pp. 336–341, 2010.
- [11] E. A. Eisenhauer, P. Therasse, J. Bogaerts et al., "New response evaluation criteria in solid tumours: revised RECIST guideline (version 1.1)," *European Journal of Cancer*, vol. 45, no. 2, pp. 228–247, 2009.
- [12] H. Steglich-Arnholm, M. Holtmannspötter, C. Gluud et al., "Carotid artery stenting versus no stenting assisting thrombectomy for acute ischaemic stroke: protocol for a systematic review of randomised clinical trials with meta-analyses and trial sequential analyses," *Systematic Reviews*, vol. 5, no. 1, p. 208, 2016.
- [13] H. Chen, "Effect of huachansu capsule combined with NX chemotherapy on serum related tumor markers and median survival in patients with advanced breast cancer," *Hebei Medicine*, vol. 25, no. 3, pp. 533–537, 2019.
- [14] N. Guo, C. X. Li, D. M. Zhu et al., "Clinical study of Huachansu Capsules combined with pirarubicin in treatment of advanced breast cancer," *Drugs & Clinical*, vol. 34, no. 1, pp. 200–204, 2019.
- [15] X. Y. Lei, "To explore the clinical effect of Cinobufacini injection combined with chemotherapy in the treatment of advanced breast cancer," *World Latest Medicine Information*, vol. 19, no. 5, p. 132, 2019.
- [16] L. L. He and B. Zhou, "Efficacy and safety of cinobufacini capsules combined with systemic chemotherapy in treatment of patients with middle-advanced breast cancer," *Evaluation*

- and Analysis of Drug-Use in Hospitals of China, vol. 18, no. 3, pp. 334–336, 2018.
- [17] Q. Y. Wang and Z. Lu, “The clinical efficacy of cinobufacini injection combined chemotherapy in the treatment of advanced breast cancer,” *China & Foreign Medical Treatment*, vol. 37, no. 6, pp. 125–127, 2018.
- [18] L. Tian, “Effects and tolerance of Huachansu Capsule in aided treatment of advanced breast cancer,” *Medical Journal of National Defending Forces in Southwest China*, vol. 27, no. 11, pp. 1173–1175, 2017.
- [19] H. Ke, J. Cui, J. L. Jin et al., “Clinical analysis of cinobufotalin capsule combined CAF scheme in treating moderate and advanced breast cancer,” *World Chinese Medicine*, vol. 12, no. 10, pp. 2358–2361, 2017.
- [20] S. Deng, G. B. Feng, and J. D. Xu, “Curative effects and patients’ tolerance of cinobufotalin capsules combined with capecitabine based regimens in the treatment of advanced breast cancer,” *Pharmaceutical and Clinical Research*, vol. 25, no. 5, pp. 439–443, 2017.
- [21] G. J. Yang, X. H. Wang, R. Pang et al., “Analysis of the efficacy of cinobufotalin injection combined with systemic chemotherapy in the treatment of middle-advanced breast cancer,” *Progress in Modern Biomedicine*, vol. 16, no. 23, pp. 4478–4480, 2016.
- [22] L. L. Dong and L. M. Zhang, “Clinical observation of cinobufotalin injection combined with chemotherapy used to treat advanced breast cancer,” *China Medicine and Pharmacy*, vol. 1, no. 14, pp. 93–94, 2011.
- [23] L. M. Pan, “Analysis of 160 cases of advanced breast cancer combining cinobufacini and chemotherapy,” *China & Foreign Medical Treatment*, vol. 30, no. 1, pp. 59–61, 2011.
- [24] W. G. Song, R. L. Wang, and Z. Z. Fu, “Clinical observation of Cinobufacini combined with chemotherapy in the treatment of advanced breast cancer,” *Chinese Journal of Integrative Medicine*, vol. 13, pp. 158–160, 2002.
- [25] C. Sun, Y. C. Liu, and W. Zhao, “Clinical effect of cinobufotalin Injection combined with systemic chemotherapy in the treatment of advanced breast cancer,” *China Modern Medicine*, vol. 26, no. 20, pp. 43–45, 2019.
- [26] L. Li, “Therapeutic effect of cinobufotalin capsule combined with capecitabine-containing basic regimen in the treatment of advanced breast cancer and its influence on related serum indicators,” *Contemporary Medicine*, vol. 26, no. 1, pp. 91–93, 2020.
- [27] W. J. Mai, Y. X. Fu, K. Ji et al., “Clinical observation on cinobufotalin capsule combined with Docetaxel in treatment of breast cancer,” *Chinese Archives of Traditional Chinese Medicine*, vol. 37, no. 8, pp. 1959–1962, 2019.
- [28] J. Y. Li, “Efficacy and safety of pemetrexed combined with cinobufacini in the first-line treatment of advanced or metastatic breast cancer,” *Chinese Archives of General Surgery (Electronic Edition)*, vol. 12, no. 1, pp. 32–35, 2018.
- [29] R. Kaaks, T. Johnson, K. Tikik et al., “Insulin-like growth factor I and risk of breast cancer by age and hormone receptor status-A prospective study within the EPIC cohort,” *International Journal of Cancer*, vol. 134, no. 11, pp. 2683–2690, 2014.
- [30] K. Tikik, D. Sookthai, T. Johnson et al., “Circulating prolactin and breast cancer risk among pre- and postmenopausal women in the EPIC cohort,” *Annals of Oncology*, vol. 25, no. 7, pp. 1422–1428, 2014.
- [31] M. Brackstone, D. Palma, A. B. Tuck et al., “Concurrent neoadjuvant chemotherapy and radiation therapy in locally advanced breast cancer,” *International Journal of Radiation Oncology*Biophysics*Physics*, vol. 99, no. 4, pp. 769–776, 2017.
- [32] L. K. Xing, J. Wang, Y. Zhang et al., “Cinobufotalin combined with chemotherapy for the advanced gastrointestinal cancer: a Meta-analysis,” *Chinese Journal of Gastroenterology and Hepatology*, vol. 25, no. 7, pp. 779–786, 2016.
- [33] M. McCulloch, C. See, X.-J. Shu et al., “Astragalus-based Chinese herbs and platinum-based chemotherapy for advanced non-small-cell lung cancer: meta-analysis of randomized trials,” *Journal of Clinical Oncology*, vol. 24, no. 3, pp. 419–430, 2006.
- [34] W. Wang, A. Shi, and Z. Fan, “Apoptosis of T-47D cells induced by cinobufacini via a caspase-3-dependent manner,” *Chemical Research in Chinese Universities*, vol. 30, no. 1, pp. 108–113, 2014.
- [35] L. Ma, B. Song, H. Jin et al., “Cinobufacini induced MDA-MB-231 cell apoptosis-associated cell cycle arrest and cytoskeleton function,” *Bioorganic & Medicinal Chemistry Letters*, vol. 22, no. 3, pp. 1459–1463, 2012.
- [36] X. A. He, J. J. Lv, and M. L. Zou, “Clinical research of neoadjuvant chemotherapy with Docetaxel plus epirubicin in patients with advanced breast cancer,” *The Journal of Medical Theory and Practice*, vol. 27, no. 15, pp. 1973–1977, 2014.
- [37] J. J. Mou, *Study on the Effect and Mechanism of Cinobufacini on Breast Cancer*, Dalian Medical University, Dalian, China, 2015.
- [38] J. J. Lv, “To analyze the effect of huachansu tablets on coagulation status, treatment effect and quality of life of patients with advanced lung cancer,” *Guide of China Medicine*, vol. 17, no. 12, p. 194, 2019.
- [39] X. S. Xiao, “Clinical observation of 50 cases of intermediate and advanced liver cancer treated with huachansu intervention chemotherapy,” *China & Foreign Medical Treatment*, vol. 30, no. 25, p. 80, 2011.
- [40] X. Y. Wu, F. Tian, X. J. Zhu et al., “Progress of Cinobufacini Antitumor Research,” *Research and Practice on Chinese Medicines*, vol. 32, no. 5, pp. 82–86, 2018.
- [41] T. Ni, H. Wang, D. Li et al., “Huachansu Capsule inhibits the proliferation of human gastric cancer cells via Akt/mTOR pathway,” *Biomedicine & Pharmacotherapy*, vol. 118, Article ID 109241, 2019.
- [42] J. H. Yin, X. Y. Zhu, W. D. Shi et al., “Huachansu injection inhibits metastasis of pancreatic cancer in mice model of human tumor xenograft,” *BMC Complementary and Alternative Medicine*, vol. 14, p. 483, 2014.
- [43] T. Yang, R. Shi, L. Chang et al., “Huachansu suppresses human bladder cancer cell growth through the fas/fasL and TNF- α /TNFR1 pathway in vitro and in vivo,” *Journal of Experimental & Clinical Cancer Research*, vol. 34, no. 1, p. 21, 2015.
- [44] X. F. Sha, Z. F. Song, J. Ding et al., “Effects of Huachansu capsules combined with raltitrexed and olisaplatin on advanced colorectal cancer immunity, tumor markers, matrix metalloproteinases and angiogenesis,” *Journal of Hainan Medical University*, vol. 24, no. 23, pp. 2066–2069, 2018.
- [45] Z. C. Wang, Z. P. Feng, and H. Wang, “Short-term efficacy of cinobufacini in the treatment of advanced liver cancer,” *Modern Hospitals*, vol. 8, no. 6, pp. 56–57, 2008.
- [46] M. Dong, “Observation on the clinical efficacy of cinobufotalin combined with chemotherapy in the treatment of advanced colon cancer,” *Chinese Community Doctors*, vol. 34, no. 13, pp. 27–28, 2018.
- [47] J. Cao, J. Zhou, D. Yang et al., “Clinical curative effect on non-small cell lung cancer patients by cinobufacini injection

- combined first-line chemotherapy,” *Journal of International Oncology*, vol. 43, no. 10, pp. 741-743, 2016.
- [48] M. Chen, “Analysis on 272 cases of adverse reactions/incidents induced by cinobufacini injection,” *China Pharmaceuticals*, vol. 22, no. 16, pp. 71-72, 2013.
- [49] D. Q. Zhang, “Causes of adverse reactions caused by cinobufacin injection and analysis of rational drug use,” *Anti-Infection Pharmacy*, vol. 14, no. 4, pp. 807-809, 2017.
- [50] C. S. Cheng, J. Wang, J. Chen et al., “New therapeutic aspects of steroidal cardiac glycosides: the anticancer properties of HuaChanSu and its main active constituent bufalin,” *Cancer Cell International*, vol. 19, p. 92, 2019.

Review Article

Efficacy and Safety of Aidi Injection as an Adjuvant Therapy on Advanced Breast Cancer: A Systematic Review and Meta-Analysis of Randomized Controlled Trials

Yihui Chai,¹ Yunzhi Chen,^{1,2} Wen Li ,^{1,3} Zhong Qin,¹ Jie Gao,¹ Zhibin Jiang,⁴ Yuhong Ge,¹ Liancheng Guan,⁵ Mengzhi Zhang,¹ Huaiquan Liu,¹ Haiyang Yu,¹ Qingxue Wang,¹ and Changfu Yang ¹

¹Department of Preclinical Medicine, Guizhou University of Traditional Chinese Medicine, Guiyang, Guizhou, China

²Center for Traditional Chinese Ethnic Minority Medicine, Guizhou University of Traditional Chinese Medicine, Guiyang, Guizhou, China

³Center for Translational Medicine, Guizhou University of Traditional Chinese Medicine, Guiyang, Guizhou, China

⁴Department of Pharmacy, Guizhou University of Traditional Chinese Medicine, Guiyang, Guizhou, China

⁵Second Affiliated Hospital, Guizhou University of Traditional Chinese Medicine, Guiyang, Guizhou, China

Correspondence should be addressed to Changfu Yang; 435140961@qq.com

Received 25 April 2020; Accepted 21 July 2020; Published 21 August 2020

Academic Editor: Norhaizan Mohd Esa

Copyright © 2020 Yihui Chai et al. This is an open access article distributed under the Creative Commons Attribution License, which permits unrestricted use, distribution, and reproduction in any medium, provided the original work is properly cited.

Background. Aidi injection (ADI) is being used widely for breast cancer in China. However, the efficacy and safety of it need to be summarized. We conducted a systematic review and meta-analysis to compare ADI and non-ADI treatment for advanced breast cancer. **Methods.** We searched PubMed, EMBASE, CNKI, SinoMed, and CENTRAL from inception to Jan 2020 for randomized controlled trials (RCTs) with diagnosis of advanced breast cancer that compared the efficacy of ADI with non-ADI treatment. Two researchers screened the literature, extracted data, and evaluated risk of bias separately. The primary outcomes were overall response rate (ORR) and disease control rate (DCR). The secondary outcomes included the QOL, immune cells, and adverse events. Review Manager software was used for estimating risks of bias of included studies, data analysis, and plotting. The sensitivity analysis and the publication bias test were performed using the R language. I^2 and chi-square tests were used to estimate heterogeneity. If $P > 0.1$ or $I^2 < 40\%$, the fixed-effect model meta-analysis was performed. A random or fixed-effect analysis was used depending on the heterogeneity testing. Weighted mean difference (WMD) or standard mean difference (SMD) was used for analysis of continuous data, and the rate ratio (RR) was calculated for the dichotomous variable, respectively. **Results.** We included 14 studies with 1006 patients diagnosed as advanced breast cancer in total. The pooled effect showed that ADI increased ORR in advanced BC patients as an add-on therapy with little heterogeneity ($RR = 1.14$, 95% CI 1.03–1.27). DCR in BC patients could not be improved by ADI. ADI improved the KPS score in BC patients compared with chemotherapy alone (MD = 3.26, 95% CI 1.74–4.78). There were no improvements on immune markers except CD4/CD8 and NK%. Serum tumor markers CEA and CA153 were decreased while treated with ADI, but only one trial was involved. ADI decreased the numbers of myelosuppression in advanced BC patients, and AST, ALT, γ -GT, and CK-MB were all decreased. The sensitivity evaluation indicated that the result of the pooled effect size had good stability. **Conclusion.** This meta-analysis suggested that based on the existing evidence, treatment with ADI significantly changed the ORR of patients with advanced BC and improved their quality of life with few side effects. However, more randomized trials involving larger samples should be considered, and detailed mechanisms are needed to be uncovered.

1. Introduction

Breast cancer (BC) is one of the most usual malignant tumors among women worldwide which results in high rates

of morbidity and mortality [1, 2]. Over the past two decades, the incidence rate of BC has been increasing constantly [3, 4]. Accumulating evidence showed that genes, proteins, and several pathways are involved in the occurrence and

progression of BC, and the precise molecular mechanisms are still unclear. To date, surgery is the first choice for early-stage BC patients, but most clinically diagnosed advanced BC patients are forced to accept chemotherapy [5], radiotherapy [6], endocrine therapy [7], or biotherapy [8]. The management of the disease is primarily to improve quality of life (QOL) and prevent disease from recurring.

Although targeted add-on therapy with monoclonal antibodies such as trastuzumab or pertuzumab has been proved to be efficacious in specific types of BC, the high costs still slowed down the widespread use in developing countries of the world. Therefore, effective and affordable adjunct therapies are needed. Aidi injection (ADI) is a compound preparation injection of Chinese herbs (Z52020236, CFDA), which is composed of the extracts from *Panax ginseng* C. A. Mey, *Astragalus propinquus* Schischkin, *Acanthopanax senticosus* (Rupr. Maxim.) Harms, and *Mylabris phalerata* Pallas [9]. According to a study on chemical constituents in the Aidi injection, 22 chemical components were detected and isolated [10]. These compounds are astragaloside, ginsenoside, eleutheroside, coniferin, etc. Previous studies showed that ADI could significantly improve the clinical response and QOL in patients with non-small cell lung cancer (NSCLC) [11] and gastric cancer. Several clinical trials also revealed that ADI could reduce the toxicity of chemotherapy in breast cancer [12, 13]. However, the efficacy on BC has been inconclusive due to a lack of summary. Therefore, we performed a systematic review and meta-analysis. Findings from such a study may help determine whether to use ADI as an add-on therapy on BC.

2. Methods

2.1. Protocol and Registration. The protocol of the present review was registered in the International Platform of Registered Systematic Review and Meta-Analysis Protocols (Inplasy, <https://inplasy.com/>) and was reported in accordance with PRISMA [14] (Preferred Reporting Items for Systematic Reviews and Meta-Analyses). The registration number is INPLASY202040170, and the DOI number is 10.37766/inplasy2020.4.0170.

2.2. Search Strategy. We conducted an online search for trials from inception up to Jan 2020, in PubMed (<https://www.ncbi.nlm.nih.gov/pubmed>), EMBASE (<http://www.embase.com>), CNKI (<http://www.cnki.net/>), SinoMed (<http://www.sinomed.ac.cn/>), and the Cochrane Central Register of Controlled Trials (CENTRAL) (<http://onlinelibrary.wiley.com/cochranelibrary/>) with the search terms “(Breast Neoplasms [MH] OR breast neoplasm* [TIAB] OR breast carcinoma* [TIAB] OR breast tumor* [TIAB] OR breast tumor* [TIAB] OR breast cancer* [TIAB]) AND (Aidi injection [TIAB]),” following the demonstration of Cochrane handbook (ZM and LH). In addition, we performed handsearches of the references of all identified articles and relevant reviews (GJ).

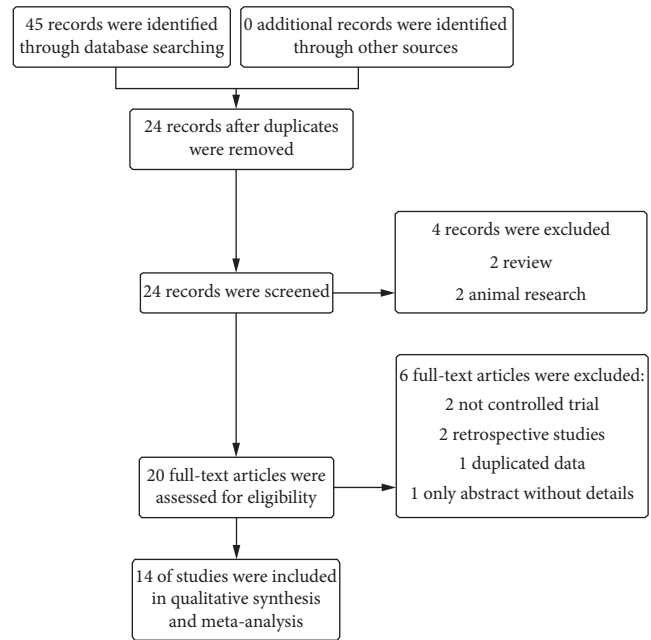


FIGURE 1: Search and selection of clinical trials assessing the efficacy and safety of ADI on advanced BC.

2.3. Study Selection. Eligible clinical trials were defined based on the following criteria: (1) randomized controlled trials of advanced breast cancer (parallel groups or cross-over design); (2) age >18 years; (3) intervention with Aidi injection as an add-on therapy compared with conventional chemotherapy; (4) reported ORR and adverse events or at least one additional outcome.

Exclusion criteria: (1) animal or cell research; (2) observational studies; (3) reviews, letter to the editor, or case reports; (4) duplicates.

Two authors, respectively, reviewed the titles and abstracts (LW and CY). If there were discrepancies between the present reviewers, another author (QZ) was consulted to reach a consensus as the third investigator.

2.4. Data Collection Process. We extracted data from each selected study, including the name of the first author, publication year, geographical location, study design, cases, participants, doses, outcomes, and statistical methods. We followed the recommendations for reporting by the Preferred Reporting Items for Systematic Reviews and Meta-Analyses guidelines [14] (PRISMA). The quality of individual records was assessed according to the Cochrane handbook.

2.5. Outcomes. The primary endpoint was the overall response rate [15] (complete remission + partial remission, ORR) and the disease control rate (complete remission + partial remission + stable disease, DCR). Secondary outcomes included the QOL, immune cells, and adverse events.

TABLE 1: Characteristics of included trials.

Trials	Design	No. of cases T/C	Age T/C	KPS T/C	TNM	Treatment	Control	Outcomes
Yumeng [16]	RCT	24/26	55.08 ± 10.32/ 54.12 ± 10.75	86.25 ± 5.76/ 87.50 ± 5.52	I-IV	Aidi 100 ml/d/1-7 q 21d + CEF or CAF	CEF or CAF	SAS, SDS, QLQC30, ORR, AEs
Weiming [13]	RCT	39/40	46.73 ± 14.2/ 45.98 ± 15.78	>50#	III-IV	Aidi 100 ml/d/1-8 q 21d + CEF	CEF	ICs, QoL, BMs, AEs
Yonghong [12]	RCT	64/64	46.7 ± 20.3	#	I-IV	Aidi 100 ml/d/1-8 q 21d + CEF	CEF	ICs, AEs
Liwang et al. [17]	RCT	78/62	52.5 (24~76)/51.2 (20~70)*	#	I-IV	Aidi 100 ml/d/ 1-14 + CEF or CAF	CEF or CAF	ICs
Mei and Li [18]	RCT	23/23	52 (36~64)*	#	I-III	Aidi 100 ml/d/1-7 q 21d + CEF	CEF	VEGF
Sandi et al. [19]	RCT	26/22	42.27 ± 6.32/ 42.23 ± 6.7	84.23 ± 5.78/ 84.55 ± 5.96	IIA-IIIIC	Aidi 60 ml/d/1-4 q 14d + TC-P	TC-P	ORR, QoL, AEs
Chuanhui et al. [20]	RCT	24/28	57.21 ± 3.52/ 55.66 ± 3.43	#	IIB-IIIIB	Aidi 80 ml/d/1-15 q 21d + TAC	TAC	ORR, ICs
Zhuorong et al. [21]	RCT	30/26	42.47 ± 7.85/ 42.54 ± 8.10	83.67 ± 6.15/ 84.62 ± 5.82	II-III	Aidi 60 ml/d/1-4 q 14d + AC-T	AC-T	ORR, QoL, AEs
Xiangguo and Lin [22]	RCT	28/20	36.2 ± 3.6/ 37.5 ± 4.2	72.87 ± 4.69/ 71.89 ± 5.03	I-III A	Aidi 100 ml/d/ 1-10 q 21d + CTF	CTF	ORR, QoL, AEs
Ling and Xiaoge [23]	RCT	44/44	42 (32~63)/48 (31~65)	#	I-IV	Aidi 100 ml/d/ 1-15 q 28d + NP	NP	ORR, DCR, TTP, AEs
Xiangqiand Shaobo [24]	RCT	32/20	46.2 ± 2.6/ 44.5 ± 3.2	70.78 ± 4.40/ 71.19 ± 4.53	I-III A	Aidi 100 ml/d/ 1-10 q 21d + CEF	CEF	ORR, QoL, AEs
Wenjuan [25]	RCT	30/30	48.4/47.6	#	III-IV	Aidi 100 ml/d/ 1-10 q 21d + CAF	CAF	ORR, ICs, QoL
Zhenzhen [26]	RCT	50/50	45*	#	II-III	Aidi 100 ml/d/ 1-14 q 21d + CAF	CAF	ORR, ICs, QoL, AEs
Ling [27]	RCT	31/28	54.2 (32~69)/53.5 (31~70)	#	II-IV	Aidi 50 ml/d/1-15 q 21d + NT	NT	ORR, ICs, QoL, AEs

BC: breast cancer; T: treatment; C: control; ORR: overall response rate; DCR: disease control rate; TTP: time to progression; AE: adverse events; QoL: quality of life; BM: blood marker; IC: immune cell; SAS: Self-Rating Anxiety Scale; SDS: Self-Rating Depression Scale; QLQC30: Quality Of Life Questionnaire Core 30; CF: cardiac function; ECG: electrocardiogram; CK: creatinine kinase; CEF: cytoxan, epirubicin, and 5-fluorouracil; CAF: cytoxan, adriamycin, and 5-fluorouracil; TC-P: theprubicin, cytoxan, and paclitaxel; TAC: theprubicin, adriamycin, and cytoxan; AC-T: adriamycin, cytoxan, and theprubicin; CTF: cytoxan, theprubicin, and 5-fluorouracil; NT: navelbine and theprubicin. *Data were expressed as medium and interquartile range (IQR). #Details not reported.

2.6. Statistical Analysis. Review Manager software (version 5.3; Cochrane Collaboration, Oxford, UK) was used for estimating risks of bias of included studies, data analysis, and plotting. The sensitivity analysis and the publication bias test were performed using the R language. I^2 and chi-square tests were used to estimate heterogeneity. If $P > 0.1$ or $I^2 < 40\%$, the fixed-effect model meta-analysis was performed. When there was a high degree of heterogeneity, a random-effect analysis was used. For each group, the Aidi injection group was compared to placebo or other active chemotherapy. Weighted mean difference (WMD) or standard mean difference (SMD) was used for analysis of continuous data, and the rate ratio (RR) was calculated for the dichotomous variable, respectively.

3. Results

3.1. Study Description and Risk of Bias. By using the search strategy mentioned above, a total of 24 trials were identified after duplicated records were removed. After screening the title and the abstracts, we retrieved the full texts of 20 records, of which 14 were ultimately included in our analysis

involving 1006 participants totally. The details of the exclusions are shown in Figure 1. In total, 14 trials were included in the present study, and the characteristics of the trials are shown in Table 1. Most of the included trials showed relatively low to medium quality. The Cochrane handbook [28] was used to evaluate the risk of bias for RCTs (Figure 2). The treatments of the 14 included articles were ADI plus chemotherapy.

3.2. Primary Outcomes. Ten trials reported ORR and DCR as the main outcome. The pooled effect showed that ADI increased ORR in BC patients as an add-on therapy with little heterogeneity ($RR = 1.14$, 95% CI 1.03–1.27; $\chi^2 = 5.71$, $P = 0.77$; $I^2 = 0\%$; Figure 3). DCR in BC patients could not be improved by ADI as an add-on therapy ($RR = 1.02$, 95% CI 0.97–1.07; $\chi^2 = 6.55$, $P = 0.6$; $I^2 = 0\%$; Figure 4).

3.3. Secondary Outcomes. ADI plus chemotherapy improved the KPS score in BC patients compared with chemotherapy alone (MD = 3.26, 95% CI 1.74–4.78; $\chi^2 = 0.4$, $P = 0.94$; $I^2 = 0\%$; Figure 5). There were no improvements on CD3%,

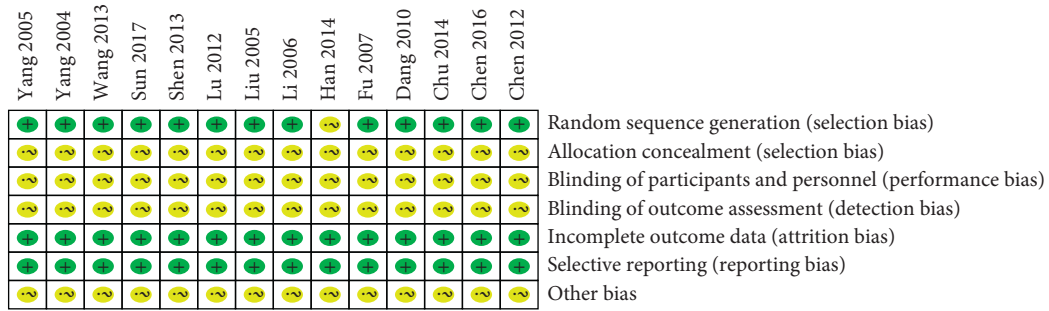


FIGURE 2: Risk of bias of included studies.

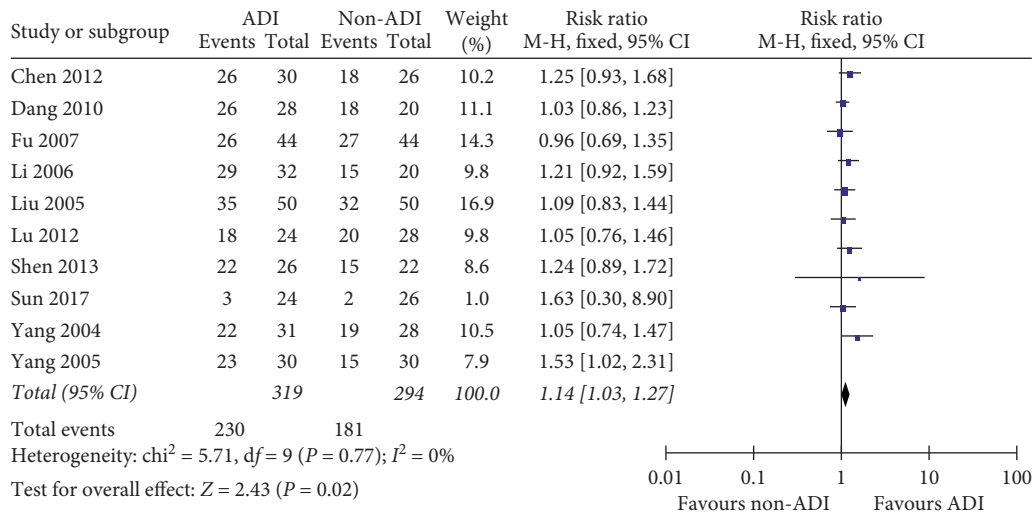


FIGURE 3: ADI increased ORR in advanced BC patients as an add-on therapy ($RR = 1.14, 95\% CI 1.03-1.27; \chi^2 = 5.71, P = 0.77; I^2 = 0\%$).

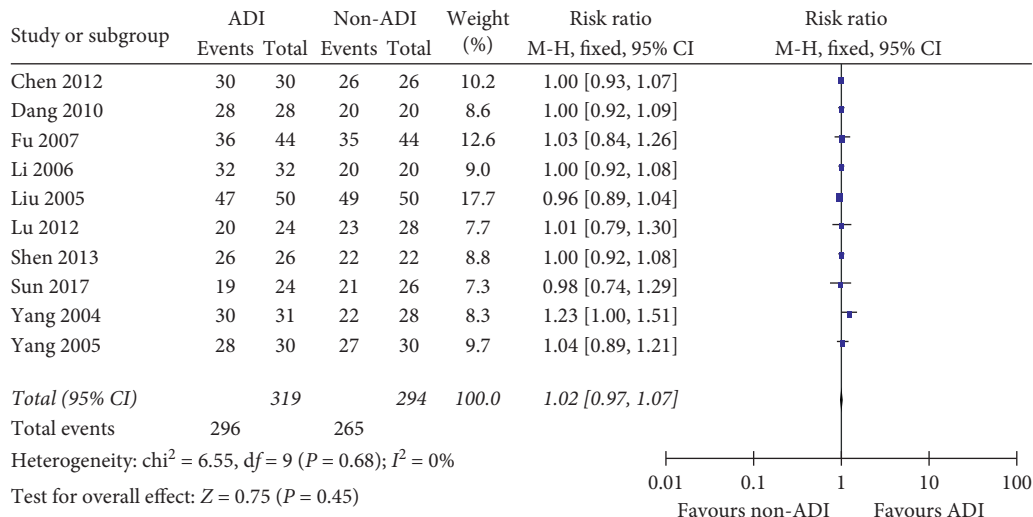


FIGURE 4: ADI did not improve DCR in advanced BC patients as an add-on therapy ($RR = 1.02, 95\% CI 0.97-1.07; \chi^2 = 6.55, P = 0.68; I^2 = 0\%$).

CD4%, and CD8%. The CD4/CD8 ratio was higher while treated with ADI with a high heterogeneity (MD = 0.32, 95% CI 0.07–0.58; $\chi^2 = 48.88, P \leq 0.01; I^2 = 88\%$). NK% data showed the same trend with CD4/CD8. Serum tumor markers CEA and CA153 were decreased while treated with ADI, but only one trial was involved (Table 2).

3.4. Adverse Events. ADI decreased the numbers of myelosuppression in advanced BC patients as an add-on therapy ($RR = 0.69, 95\% CI 0.52-0.92; \chi^2 = 17.95, P = 0.003; I^2 = 72\%$; Figure 6). AST, ALT, γ -GT, and CK-MB were all decreased by ADI treatment. No other side effects were recorded during the studies. Details are shown in Table 3.

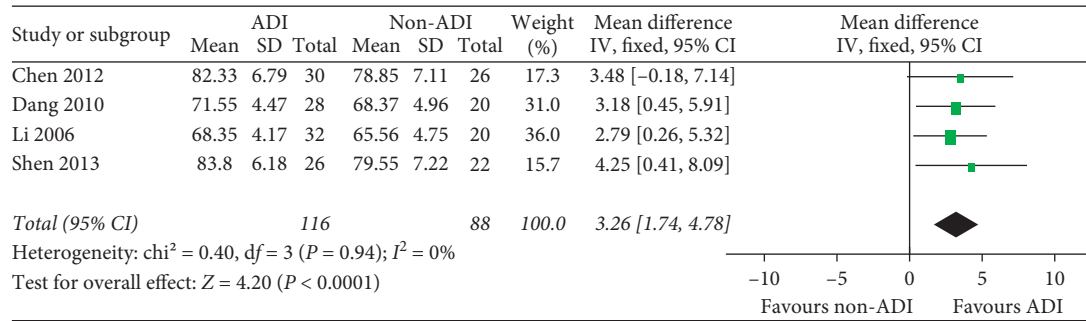


FIGURE 5: ADI improved the KPS score in advanced BC patients as an add-on therapy (MD = 3.26, 95% CI 1.74–4.78; $\chi^2 = 0.4$, $P = 0.94$; $I^2 = 0\%$).

TABLE 2: Secondary outcomes.

Outcomes	No. of trials	Heterogeneity		Effect size with 95% CI	Z with P value
		Chi-squared	I-squared (%)		
Immune cells					
CD3%	7 ^{12,13,18,21,26-28}	514.87 ($P < 0.00001$)	99	3.71 (-3.85~11.27)	0.96 ($P = 0.34$)
CD4%	7 ^{12,13,18,21,26-28}	1302.78 ($P < 0.0001$)	100	6.67 (-2.71~16.06)	1.39 ($P = 0.16$)
CD8%	7 ^{12,13,18,21,26-28}	747.57 ($P < 0.00001$)	99	-0.97 (-7.54~5.6)	0.29 ($P = 0.77$)
CD4/CD8	7 ^{12,13,18,21,26-28}	48.88 ($P < 0.00001$)	88	0.32 (0.07~0.58)	2.5 ($P = 0.01$)
NK%	4 ^{12,13,18,26}	29.39 ($P < 0.00001$)	90	5.54 (4.60~6.47)	11.64 ($P < 0.001$)
Tumor markers					
CEA	1 ¹³	—	—	-2.39 (-3.99~-0.79)	2.93 ($P = 0.003$)
CA153	1 ¹³	—	—	-3.06 (-5.17~-0.95)	2.85 ($P = 0.004$)

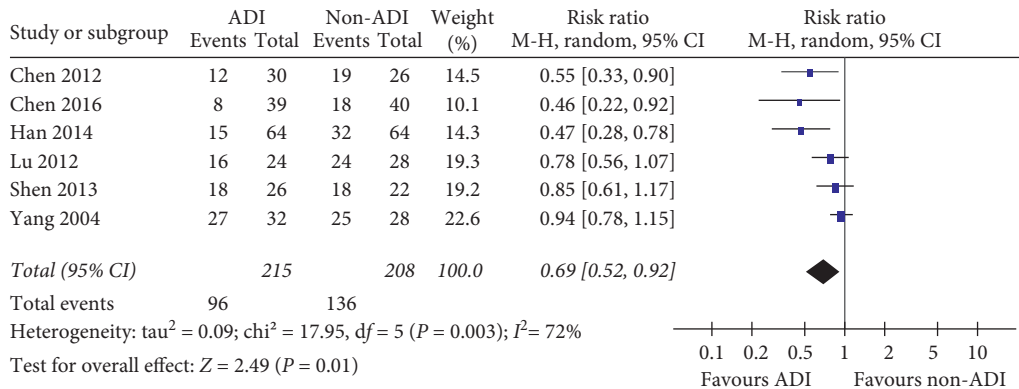


FIGURE 6: ADI decreased the numbers of myelosuppression in BC patients as an add-on therapy (RR = 0.69; 95% CI 0.52–0.92; $I^2 = 72\%$; $P = 0.003$).

TABLE 3: Safety of ADI.

Outcomes	No. of trials	Heterogeneity		Effect size with 95% CI	Z with P value
		Chi-squared	I-squared (%)		
Hepatic function					
AST	3 ^{22,23,25}	112.69 ($P < 0.00001$)	98	-31.21 (-47.06~-15.36)	3.86 ($P = 0.001$)
ALT	3 ^{22,23,25}	4.86 ($P = 0.09$)	59	-4.04 (-5.57~-2.51)	5.16 ($P < 0.0001$)
γ -GT	2 ^{23,25}	0.08 ($P = 0.78$)	0.0	-24.59 (-27.78~-21.40)	15.1 ($P < 0.0001$)
Cardiac function					
CK-MB	2 ^{22,23}	0.64 ($P = 0.42$)	0.0	-4.04 (-5.91~-2.17)	4.23 ($P < 0.0001$)

3.5. Publication Bias. No obvious publication bias was found through the funnel plot (ORR) (Figure 7). Egger's test showed the result of the linear regression test of the funnel plot asymmetry: $t = 1.4319$, $df = 8$, and P value = 0.1901. The result indicated that there was no publication bias.

3.6. Sensitivity Analysis. The sensitivity was evaluated through excluding the poor and overestimated studies about the main outcome ORR. The analysis indicated that the result of the pooled effect size had good stability (Figure 8).

4. Discussion

BC is commonly discovered among women worldwide of which the incidence rate has been increasing constantly. Advanced breast cancer patients do not have many choices but to accept chemotherapy. During a long-term clinical practice, traditional Chinese medicines have played important roles in treating some types of tumors. However, the molecular mechanisms are poorly discovered. ADI is a compound injection of Chinese herbs which is widely used in treating malignant tumors including breast cancer.

The present meta-analysis suggested that based on the existed evidence, treatment with ADI significantly changed the ORR of patients with advanced BC but did not obviously increase the DCR. There were also improvements on quality of life, and an increase in the KPS score was observed. To some extent, the immune system was improved because the CD4/CD8 ratio and NK cells were higher while treated with ADI. However, CD3, CD4, and CD8 did not change because of one study [26] which induced high heterogeneity and showed totally reversed effect to other studies. The participant's age, intervention, and duration were not significantly different from others'. ADI seemed to be safe for patients. ADI decreased the numbers of myelosuppression, AST, ALT, γ -GT, and CK-MB in BC patients as an add-on therapy. No obvious publication bias was found through the funnel plot (ORR).

The mechanism of ADI on BC was suggested that ADI significantly inhibited the proliferation of MCF-7 cells in a dose-dependent manner [29] and the miRNA might serve as potentially therapeutic targets. The modulation of miRNA expression is an important mechanism of ADI inhibiting breast cancer cell growth. Another experiment reported that ADI could inhibit proliferation, promote apoptosis and necrosis of tumor cells, and significantly reduce the cell diameter [30]. But, the research is limited, so more studies should better be involved in and discover the underlying mechanisms.

Several limitations of this meta-analysis should be mentioned. First, the quality of included trials was relatively low, some of which did not report the details of blinding and allocation concealment. This might induce bias of the results. Little research studies provided survival data. Previous studies showed good effect of ADI on patients with BC which may be a potential drug as an adjunct therapy. However, additional high-quality RCTs and larger sample sizes may lead to more reliable results. Second, the records of

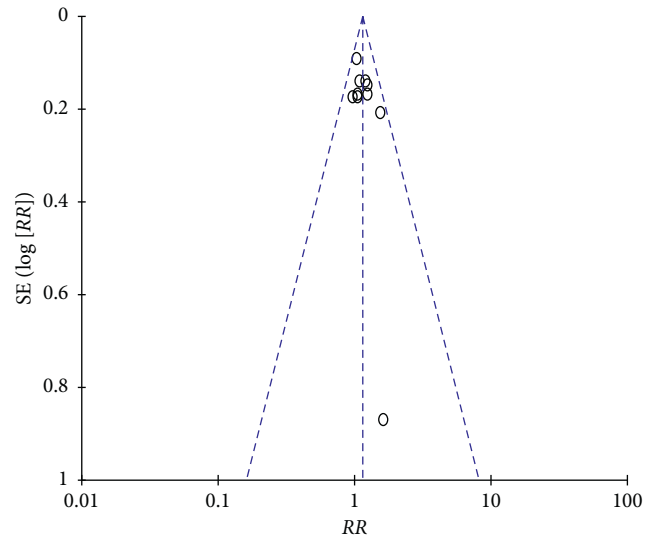


FIGURE 7: Publication bias. There was no publication bias in the included studies.

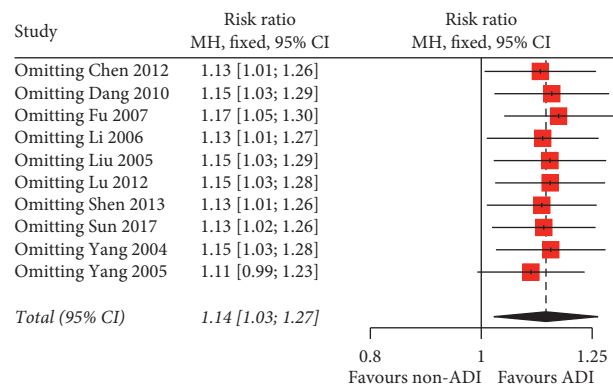


FIGURE 8: Sensitivity analysis showing that the result had good stability.

survival terms were seldomly reported, and we were not able to calculate the overall survival of specific year. Furthermore, the therapeutic duration and designs were not identical, which may lead to heterogeneity. Subgroup analysis was not performed because included articles were limited and difficult to be grouped.

5. Conclusion

In summary, this meta-analysis suggested that based on the existing evidence, treatment with ADI significantly changed the ORR of patients with advanced BC and improved their quality of life with few side effects. More randomized trials involving larger samples should be considered, and detailed mechanisms are needed to be uncovered.

Conflicts of Interest

The authors declare that there are no conflicts of interest regarding the publication of this paper.

Authors' Contributions

Yihui Chai, Yunzhi Chen, and Wen Li contributed equally to this work.

Acknowledgments

This work was supported by the National Natural Science Foundation of China (nos. 81760841, 81874376, and 81660762), the Research Projects on Science and Technology of Science and Technology Program in Guizhou Province (Qiankehe Platform Talents [2017]5735-12), and the Project of Education Department of Guizhou Province (K[2017]041 and KY[2017]172).

References

- [1] A. Kolak, M. Kamińska, K. Sygit et al., "Primary and secondary prevention of breast cancer," *Annals of Agricultural and Environmental Medicine*, vol. 24, no. 4, pp. 549–553, 2017.
- [2] C. G. Yedjou, P. B. Tchounwou, M. Payton et al., "Assessing the racial and ethnic disparities in breast cancer mortality in the United States," *International Journal of Environmental Research and Public Health*, vol. 14, no. 5, 2017.
- [3] M. Wang, C. Zhang, Y. Song et al., "Mechanism of immune evasion in breast cancer," *Oncotargets and Therapy*, vol. 10, pp. 1561–1573, 2017.
- [4] L. Xing, Q. He, Y.-Y. Wang, H.-Y. Li, and G.-S. Ren, "Advances in the surgical treatment of breast cancer," *Chinese Clinical Oncology*, vol. 5, no. 3, p. 34, 2016.
- [5] D. J. Butters, D. Ghersi, N. Wilcken, S. J. Kirk, and P. T. Mallon, "Addition of drug/s to a chemotherapy regimen for metastatic breast cancer," *Cochrane Database of Systematic Reviews*, vol. 11, 2010.
- [6] P. J. Hoskin, K. Hopkins, V. Misra et al., "Effect of single-fraction vs multifraction radiotherapy on ambulatory status among patients with spinal canal compression from metastatic cancer," *Journal of the American Medical Association*, vol. 322, no. 21, pp. 2084–2094, 2019.
- [7] O. Najim, S. Seghers, L. Sergoyne et al., "The association between type of endocrine therapy and development of estrogen receptor-1 mutation(s) in patients with hormone-sensitive advanced breast cancer: a systematic review and meta-analysis of randomized and non-randomized trials," *Biochimica et Biophysica Acta (BBA)-Reviews on Cancer*, vol. 1872, no. 2, Article ID 188315, 2019.
- [8] K. Ishii, N. Morii, and H. Yamashiro, "Pertuzumab in the treatment of HER2-positive breast cancer: an evidence-based review of its safety, efficacy, and place in therapy," *Core Evidence*, vol. 14, pp. 51–70, 2019.
- [9] Z. Xiao, C. Wang, M. Zhou et al., "Clinical efficacy and safety of Aidi injection plus paclitaxel-based chemotherapy for advanced non-small cell lung cancer: a meta-analysis of 31 randomized controlled trials following the PRISMA guidelines," *Journal of Ethnopharmacology*, vol. 228, pp. 110–122, 2019.
- [10] Z. Miaomiao, L. Yanli, C. Zhong, L. Xiaoran, X. Qiongmeng, and Y. Shilin, "Studies on chemical constituents from Aidi injection," *Chinese Traditional and Herbal Drugs*, vol. 43, no. 8, pp. 1462–1470, 2012.
- [11] Z. Xiao, C. Wang, R. Zhou et al., "Can Aidi injection improve overall survival in patients with non-small cell lung cancer? A systematic review and meta-analysis of 25 randomized controlled trials," *Complementary Therapies in Medicine*, vol. 37, pp. 50–60, 2018.
- [12] H. Yonghong, J. Xueqing, Y. Ye, W. Zhiyong, and J. Ming, "Clinical observation of Aidi injection combined with CEF regimen chemotherapy in treatment of postoperative breast cancer," *Hubei Journal of Traditional Chinese Medicine*, vol. 36, no. 05, pp. 7–8, 2014.
- [13] C. Weiming, "Clinical observation of Aidi injection combined with CEF chemotherapy in the treatment of breast cancer after operation," *Chinese Journal of Modern Drug Application*, vol. 10, no. 15, pp. 185–187, 2016.
- [14] D. Moher, A. Liberati, J. Tetzlaff, and D. G. Altman, "Preferred reporting items for systematic reviews and meta-analyses: the PRISMA statement," *British Medical Journal*, vol. 339, 2009.
- [15] V. R. Preedy and R. R. Watson, "Overall response rate," in *Handbook of Disease Burdens and Quality of Life Measures*, Springer, New York, NY, USA, 2010.
- [16] S. Yumeng, *Clinical Observation on Improving Mood and Quality of Life of Breast Cancer Patients with Aidi Injection* [硕士], Liaoning University of Chinese Medicine, Shenyang, China, 2017.
- [17] C. Liwang, W. Zongyan, Z. Liangang, P. Yuzhu, and G. Weiliang, "Effect of Aidi injection on cellular immunity in breast cancer patients," *China Medical Engineering*, vol. 21, no. 12, pp. 36–37, 2013.
- [18] W. Mei and W. Li, "Effect of Aidi injection on serum VEGF level in breast cancer patients," *Chinese Journal of Clinical Research*, vol. 26, no. 11, pp. 1151–1158, 2013.
- [19] S. Sandi, C. Zhuorong, X. Gaofang, L. Zhihui, and H. Zhan, "Clinical observation of dose-intensive TC-P combined with Aidi injection in the treatment of triple negative breast cancer," *Guide of China Medicine*, vol. 11, no. 8, pp. 84–85, 2013.
- [20] L. Chuanhui, H. Ming, Y. Jun, and X. Lin, "Clinical observation of Aidi injection combined with TAC regimen in preoperative neoadjuvant chemotherapy for breast cancer," *Traditional Chinese Medicine Journal*, vol. 11, no. 3, pp. 50–52, 2012.
- [21] C. Zhuorong, S. Sandi, H. Zhan, L. Ruiwen, and L. Yanming, "Clinical observation of dose-intensive AC-T regimen combined with Aidi injection in the treatment of triple negative breast cancer," *Chin Journal of Surgery Oncology*, vol. 4, no. 2, pp. 85–87, 2012.
- [22] D. Xiangguo and W. Lin, "Evaluation of efficacy on breast cancer treated by Aidi injection plus CTF Program of neoadjuvant chemotherapy and the impacts on serum sFas," *World Journal of Integrated Traditional and Western Medicine*, no. 1, pp. 54–56, 2010.
- [23] F. Ling and K. Xiaoge, "Aidi injection combined with chemotherapy for 44 cases of advanced breast cancer," *Jouranal of Practical Traditional Chinese Medicine*, vol. 23, no. 8, p. 517, 2007.
- [24] L. Xiangqi and G. Shaobo, "Efficacy analysis of Aidi injection combined with CEF chemotherapy for breast cancer," *Pharmacology and Clinics of Chinese Materia Medica*, vol. 22, no. C1, pp. 176–177, 2006.
- [25] Y. Wenjuan, "Aidi injection combined with CAF chemotherapy for 30 cases of advanced breast cancer," *Jiangxi Journal of Traditional Chinese Medicine*, vol. 36, no. 7, pp. 46–47, 2005.
- [26] L. Zhenzhen, L. Hui, L. Lianfang, and C. Shude, "Clinical observation of Aidi injection combined with chemotherapy in the treatment of locally advanced breast cancer," *Shandong Medical Journal*, vol. 45, no. 19, p. 62, 2005.

- [27] Y. Ling, "Clinical observation of Aidi injection combined with chemotherapy in the treatment of advanced breast cancer," *Chinese Journal of Integrated Traditional and Western Medicine*, vol. 24, no. 8, pp. 755-756, 2004.
- [28] J. P. Higgins and S. Green, *Cochrane Handbook for Systematic Reviews of Interventions*, Cochrane Book Series, London, UK, 2008.
- [29] H. Zhang, Q.-M. Zhou, Y.-Y. Lu, J. Du, and S.-B. Su, "Aidi injection () alters the expression profiles of MicroRNAs in human breast cancer cells," *Journal of Traditional Chinese Medicine*, vol. 31, no. 1, pp. 10-16, 2011.
- [30] T. Jing and W. Guojun, "Antitumor effect of Aidi injection on ErbB2 positive breast cancer cells cultured in vitro," *Pharmaceutical Journal of Chinese People's Liberation Army*, vol. 34, no. 4, pp. 333-340, 2018.

Research Article

A Bioinformatics Research on Novel Mechanism of Compound Kushen Injection for Treating Breast Cancer by Network Pharmacology and Molecular Docking Verification

Shuyu Liu, Xiaohong Hu, Xiaotian Fan, Ruiqi Jin, Wenqian Yang, Yifei Geng, and Jiarui Wu 

Department of Clinical Chinese Pharmacy, School of Chinese Materia Medica, Beijing University of Chinese Medicine, No. 11 North Three-Ring East Road, Chaoyang District, Beijing, China

Correspondence should be addressed to Jiarui Wu; exogamy@163.com

Received 18 April 2020; Revised 22 June 2020; Accepted 17 July 2020; Published 11 August 2020

Guest Editor: Mohd Fadzelly Abu Bakar

Copyright © 2020 Shuyu Liu et al. This is an open access article distributed under the Creative Commons Attribution License, which permits unrestricted use, distribution, and reproduction in any medium, provided the original work is properly cited.

Compound Kushen injection (CKI) has been extensively used in treating breast cancer (BC). However, the molecular mechanism remains unclear. In this study, 16 active compounds of CKI were obtained from 3 articles for target prediction. Then, a compound-predicted target network and a compound-BC target network were conducted by Cytoscape 3.6.1. The gene ontology (GO) enrichment analysis and Kyoto Encyclopedia of Genes and Genomes (KEGG) pathway enrichment analysis were performed on the DAVID database. The binding energy between the key targets of CKI and the active compounds was studied by molecular docking. As a result, 16 active compounds of CKI were identified, corresponding to 285 putative targets. The key targets of CKI for BC are HSD11B1, DPP4, MMP9, CDK1, MMP2, PTGS2, and CA14. The function enrichment analysis obtained 13 GO entries and 6 KEGG pathways, including bladder cancer, cancer pathways, chemical carcinogenesis, estrogen signaling pathway, TNF signaling pathway, and leukocyte transendothelial migration. The result of molecular docking indicated that DPP4 had strong binding activity with matrine, alicyclic protein, and sophoridine, and MMP9 had strong binding activity with adenine and sophoridine. In conclusion, the therapeutic effect of CKI on BC is based on the overall pharmacological effect formed by the combined effects of multiple components, multiple targets, and multiple pathways. This study provides a theoretical basis for further experimental research in the future.

1. Introduction

Although modern medicine has made great progress in cancer research, breast cancer (BC) remains an important health issue. BC is the most common cancer affecting women's health around the world, and its morbidity and mortality are expected to increase dramatically in the next few years [1]. Current clinical treatments for BC include surgical resection, chemoradiotherapy, and endocrine therapy, but these treatments will bring obvious side effects. Studies have shown that radiotherapy and chemotherapy can increase the risk of myelodysplastic disorder and acute myeloid leukemia in BC patients, which means more pain for patients with poor body function and poor tolerability

[2]. Traditional Chinese medicine (TCM), as a traditional medicine for adjuvant treatment of tumors, has the effect of improving the immune function and tumor microenvironment of the patients and reducing the toxicity of radiotherapy and chemotherapy, so as to improve the survival rate [3–7]. It is shown that compound Kushen injection (CKI), as a TCM compound preparation, has a good synergistic antitumor effect by inhibiting tumor cell proliferation and inducing differentiation. It has been widely used in clinical practice in China [8]. CKI is prepared from a series of refined processes including percolation, boiling, and alcohol absorption of *Sophora flavescens* and *Smilax glabra*, which is able to clear heat and promote diuresis, cool blood and detoxify, resolve stagnation, as well as relieve pain [9].

The chemical composition of CKI is mainly composed of matrine alkaloids such as matrine and oxymatrine, which have significant antitumor activities [10]. *Sophora flavescens* alkaloids can play a role in regulating tumor cell proliferation, inducing tumor cell differentiation and apoptosis, and inhibiting tumor cell invasion and metastasis. It can also reduce tumor neovascularization and regulate body immunity [11]. At present, there are more and more clinical adjuvant treatment methods of CKI combined with radiotherapy and chemotherapy, which can improve the efficacy of radiotherapy or chemotherapy while reducing the resistance of chemotherapeutic drugs [12–18]. However, the mechanisms of CKI in treating BC remain unclear. With the rapid development of human society, the spectrum of human diseases has also undergone tremendous changes. The occurrence and development of complex diseases are closely related to multiple genes and signal pathways in the regulatory network of the body. It is difficult to achieve great therapeutic effects based on a single target. Network pharmacology is combined with high-throughput omics data analysis, computer virtual computing, and network database retrieval foundations. It not only embodies the new concept and mode of modern biomedical research but also changes the traditional mode of “one drug, one target, and one disease” in new drug development. Moreover, it has a profound impact on the concept, strategy, and method of certifying and discovering drugs [19]. Therefore, this study developed network pharmacology method, combined with molecular docking, to explore the anti-BC action mechanism of CKI primarily.

2. Materials and Methods

2.1. Active Ingredients and Potential Targets of CKI. There is a systematic and comprehensive search of published literature on the active compounds of CKI in CNKI, Wanfang, VIP database, and PubMed. The SMILES (Simplified Molecular Linear Input Specification) structures of the screened compounds were obtained using the PubChem database (<https://pubchem.ncbi.nlm.nih.gov>), and putative targets were collected from the Search Tool for Interacting Chemicals (STITCH, <http://stitch.embl.de/>), SuperPred (<http://prediction.charite.de/>), and Swiss Target Prediction (<http://www.swisstargetprediction.ch/>) databases and TCM Pharmacology Database and Analysis Platform (TCMSP, <http://tcmospw.com/tcmosp.php>) [20–23].

2.2. Collection of Target Proteins Related to BC. “Breast cancer” was identified as a keyword to collect proteins related to BC in the TTD databases (Therapeutic Target Database, <http://db.idrblab.net/ttd/>) [24]. At the same time, the Gene Expression Omnibus (GEO, <https://www.ncbi.nlm.nih.gov/geo/>) and The Cancer Genome Atlas (TCGA, <http://cancergenome.nih.gov/>) were applied to search differentially expressed genes of BC and then combined the obtained genes and removed duplicate data. The final results are the targets related to BC [25, 26].

2.3. Network Construction. The active compounds of CKI and the predicted targets were introduced into Cytoscape 3.6.1 to construct a compound-predicted target network. A compound-BC target network was set up by intersecting the predicted targets of the compounds with the targets related to BC. The network analyzer plug-in was used to analyze the key targets on the three key topological parameters of the network: degree, betweenness, and closeness. “Degree” refers to the number of connections between a node and other nodes in the network. “Betweenness” means the ratio of the shortest path through a node to the total number of paths through all nodes. “Closeness” shows the inverse of the sum of the distances of a node from other nodes [27]. The value of the above three topological parameters of a node is directly proportional to the importance of the node in the network.

2.4. Biological Functional and Pathway Enrichment Analysis. In this study, the DAVID (<https://david.ncifcrf.gov/>) platform was applied to perform GO functional enrichment analysis and KEGG pathway enrichment analysis on the potential key genes for anti-BC of the CKI obtained after topology analysis [28]. GO is a database that annotates genes and protein functions into three main items: cellular components (CCs), molecular functions (MFs), and biological processes (BPs). Pathway enrichment analysis revealed possible biological processes for key genes [29, 30]. The results of the enrichment analysis are visualized by the GO plot package in R software.

2.5. Molecular Docking. The SDF format files of compounds were downloaded from the PubChem database and converted into mol2 format files. Protein conformation screening on key targets in the RCSB PDB database (<https://www.rcsb.org/>) was performed, and the PDB format files were downloaded [31]. The following are the screening conditions: (1) the protein structure is obtained by X-crystal diffraction; (2) the resolution of the protein crystal is less than 3 Å; (3) the protein structure reported by molecular docking is preferred; and (4) the biological source of the protein structure is human beings. Water molecules and original small-molecule ligands were deleted from the protein structure. The position of the active pocket was determined after performing hydrogenation, giving charge, and combining nonpolar hydrogen using the AutoDockTools 1.5.6 software. At the same time, grid box coordinates and box size were established. Finally, AutoDock Vina 1.1.2 was used to perform docking operations [32]. The receptor-ligand pairs were sorted and screened according to the affinity (kcal/mol). Ultimately, PyMOL 2.3.2 software was used for visual processing to check the binding status of ligands and receptor binding sites [33].

3. Results

3.1. Compound-Predicted Target Network. As shown in Table 1, a total of 16 active compounds in CKI and 285 predicted targets were obtained [34–36]. The compound-predicted target network (Figure 1) includes 301 nodes

TABLE 1: Active compounds of CKI.

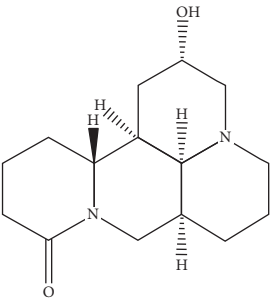
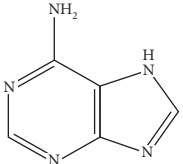
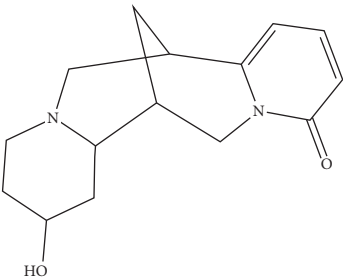
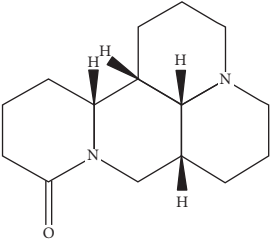
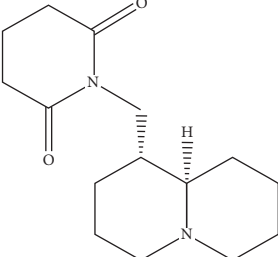
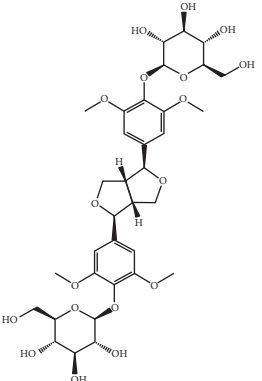
Compounds	PubChem CID	MW (g/mol)	Structure
9 α -Hydroxymatrine	15385684	264.369	
Adenine	190	135.13	
Baptifoline	621307	260.337	
Isomatrine	5271984	248.37	
Lamprolobine	87752	264.369	
Liriodendrin	21603207	742.724	

TABLE 1: Continued.

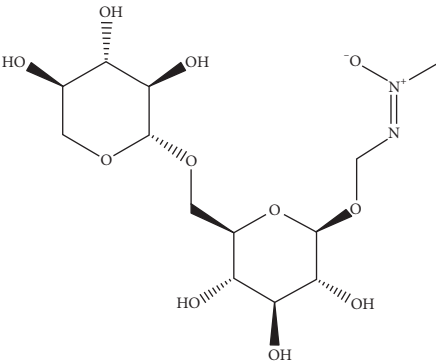
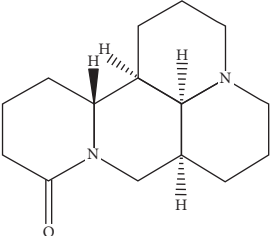
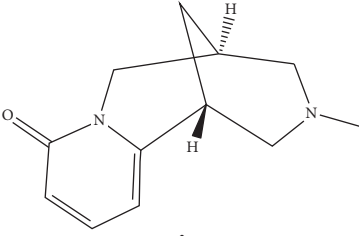
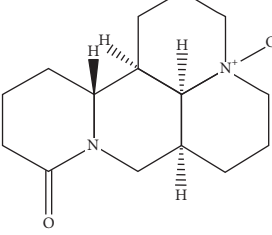
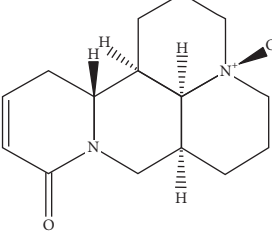
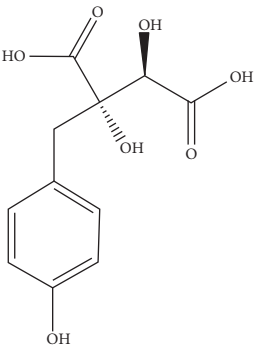
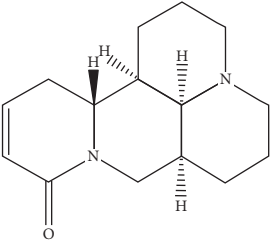
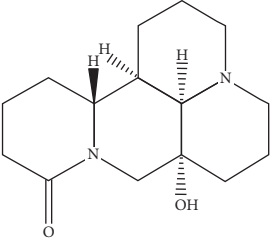
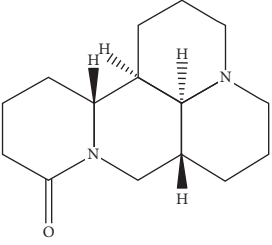
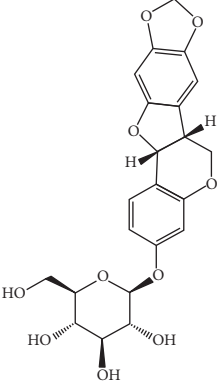
Compounds	PubChem CID	MW (g/mol)	Structure
Macrozamin	9576780	384.338	
Matrine	91466	248.37	
N-Methylcytisine	670971	204.273	
Oxymatrine	114850	264.369	
Oxysophocarpine	24721085	262.353	

TABLE 1: Continued.

Compounds	PubChem CID	MW (g/mol)	Structure
Piscidic acid	6710641	256.21	
Sophocarpine	115269	246.354	
Sophoranol	12442899	264.369	
Sophoridine	165549	248.37	
Trifolirhizin	442827	446.408	

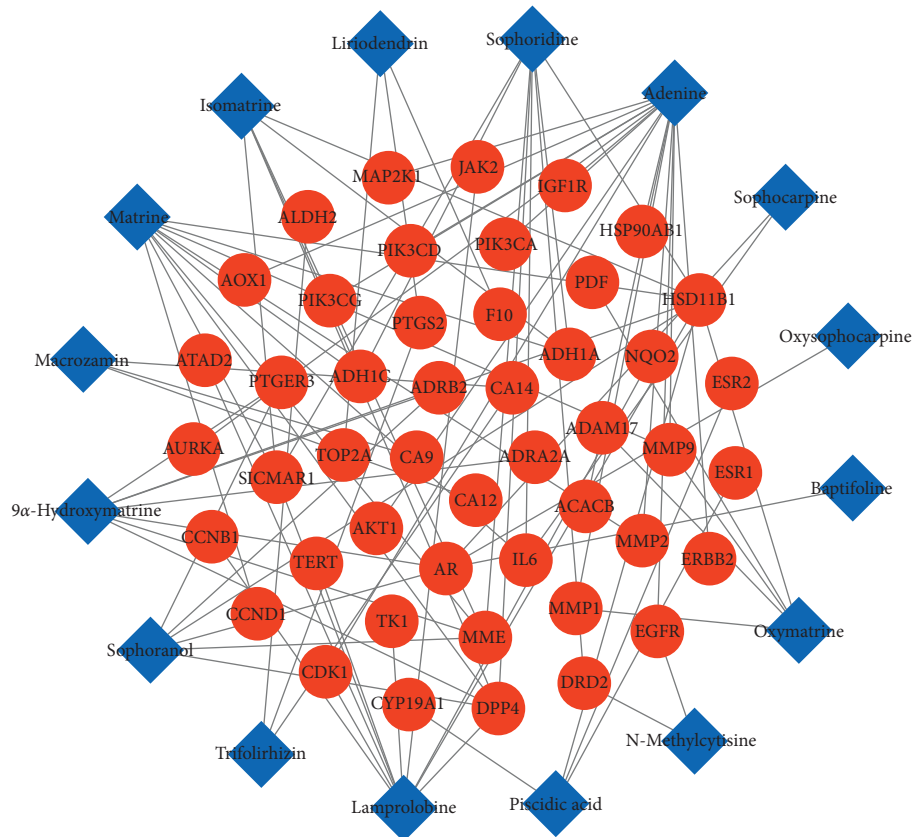


FIGURE 2: Compound-BC target network. Notes: the blue diamonds represent active compounds of CKI, and the red circles represent the common targets.

(GO: 0035987), proteolysis (GO: 0006508), collagen catabolic progress (GO: 0030574), extracellular matrix disassembly (GO: 0022617), ephrin receptor signaling pathway (GO: 0048013), response to hypoxia (GO: 0001666), and angiogenesis (GO: 0001525); items related to molecular function (MF) include serine-type endopeptidase activity (GO: 0004252), metallopeptidase activity (GO: 0008237), and metalloendopeptidase activity (GO: 0004222) related to MF; and the GO entry related to cell composition (CC) is proteinaceous extracellular matrix (GO: 0005578) (Figure 3). It suggests that the active compounds of CKI may exert anti-BC effects by participating in various biological regulation processes.

KEGG enrichment analysis totally obtained 6 pathways, namely, bladder cancer (hsa05219), pathways in cancer (hsa05200), chemical carcinogenesis (hsa05204), estrogen signaling pathway (hsa04915), TNF signaling pathway (hsa04668), and leukocyte transendothelial migration (hsa04670) (Figure 4). These pathways involve cancer, endocrine system, signaling system, and immune system. Figure 5 shows the main biological effects of the key targets of CKI, in addition to the major enriched pathways mentioned above; the whole biological process also involves ErbB signaling pathway, MAPK signaling pathway, and NF-kappa B signaling pathway. Figure 6 illustrates the interaction among compounds, targets, and pathways of CKI in treating BC.

3.4. Molecular Docking. The structure of key targets and compound with highest value were introduced into Auto-DockTools 1.5.6 for molecular docking (Tables 2 and 3). In general, the lower the binding free energy, the more stable the binding between the ligand and protein receptor. According to the results of molecular docking, the macromolecular protein receptor DPP4 has strong binding activity with matrine, lamprolobine, and sophoridine, and MMP9 has strong binding activity with adenine and sophoridine. The hydrogen-bonding relationship between the active small-molecule ligands and the protein receptor is shown in Figure 7.

4. Discussion

BC is a common malignant tumor that threatens women's health and lives. In clinical practice, patients are often treated with integration of TCM and western medicine. Although the effect of traditional Chinese medicine on tumor shrinkage is not as obvious as that of radiotherapy and chemotherapy, it has less toxic and side effects and high safety, which helps slow down the clinical condition and improve the quality of life of patients [37]. A large number of studies have shown that CKI has a good intervention effect against the toxicity of chemotherapeutic drugs, which can enhance the immune function and protect the hematopoietic system.

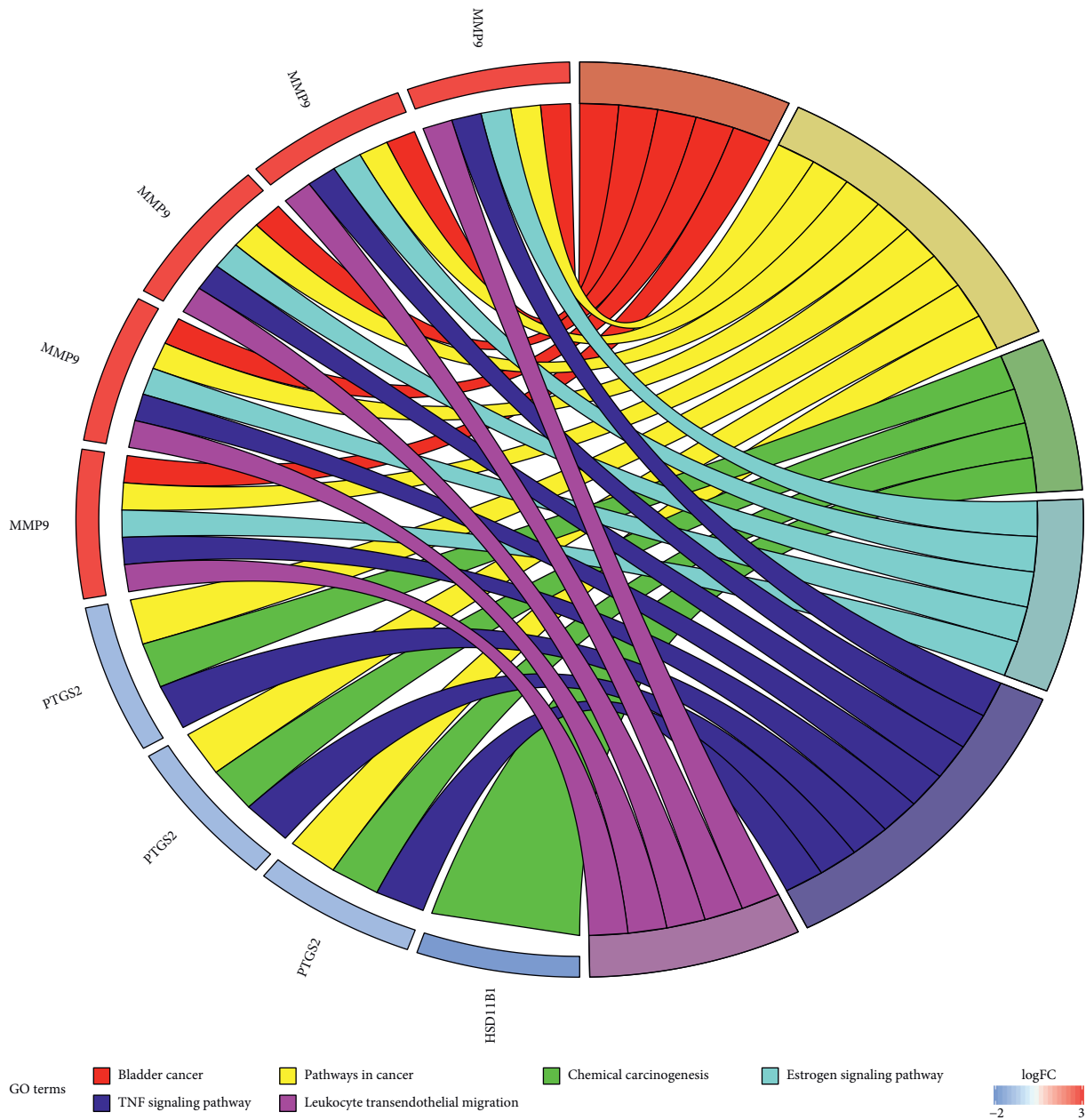


FIGURE 4: KEGG pathway enrichment analysis of key targets.

in the invasion and metastasis of BC, and their levels were significantly increased in the serum and plasma of BC patients [44]. Studies have shown that the expression of MMP2 and MMP9 in BC may be related to the expression of AP-2 and HER2. The positive expression of MMP9 indicates the low survival rate of small hormone reactive tumors, and its expression in cancer cells is beneficial to the survival of tumors [45]. CDK1 is a protein-encoding gene of the cell-cycle-dependent kinase family and also plays an important regulatory role controlling cell cycle. CDK disorder leads to the increase of cell proliferation, which has been found in many cancers including breast cancer. Studies have shown that many genes can negatively regulate the expression of CDK1 mRNA by selectively blocking CDK1 or in combination with other therapies, thus inhibiting the proliferation

of human BC cells and blocking G2/M cells [46–48]. The application is related to anticancer effects, which suggests that CDK1 may be considered to be the best CDK target for BC treatment [49]. PTGS2, also known as cyclooxygenase (COX)-2, is an inflammation-inducing enzyme. Studies have shown that PTGS2 is upregulated in approximately 40% of BC patients (including ductal carcinoma in situ and invasive cancer) and associated with metastasis diseases, which reduced patients' survival rate [50].

According to the GO functional enrichment analysis and KEGG pathway enrichment analysis results, the key targets of the active compound regulation of CKI are significantly enriched in a variety of biological processes, molecular functions, and cellular components, such as embryo implantation, positive regulation of vascular smooth muscle

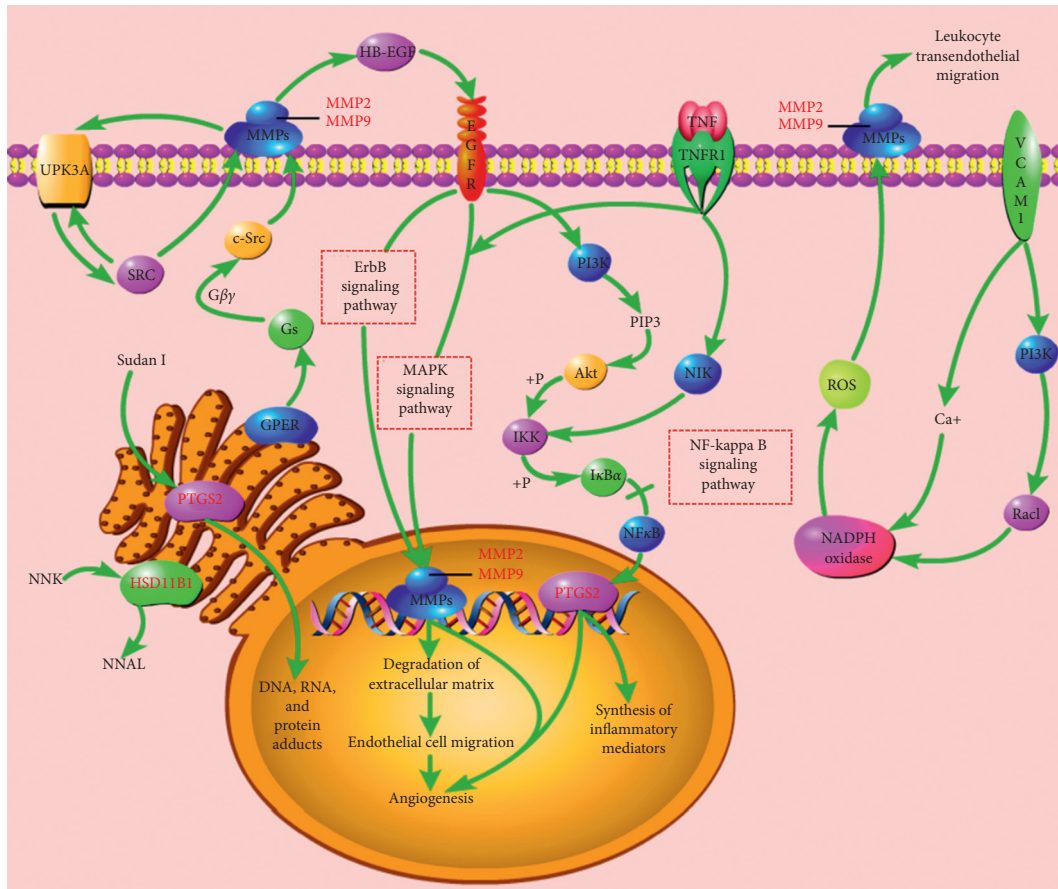


FIGURE 5: Illustration of crucial biological progress caused by key targets and known therapeutic targets for CKI.

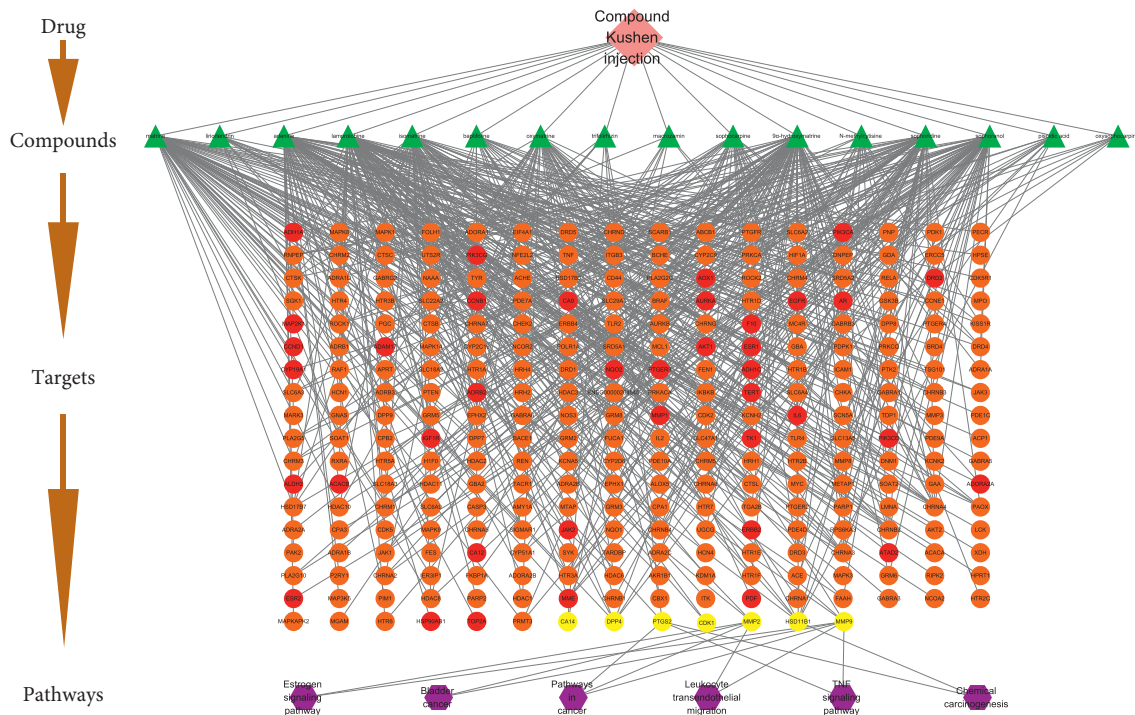


FIGURE 6: Compound-target-pathway network. Notes: The pink diamond refers to CKI. The green triangles represent active compounds in CKI. The orange, red, and yellow circles represent putative targets of CKI. Among them, the red circles represent the common targets of CKI and BC, and the yellow circles represent key targets of CKI for the treatment of BC. The purple hexagons represent the main pathways of key targets.

TABLE 2: The information of key targets.

Protein name	Target	PDB ID
Corticosteroid 11-beta-dehydrogenase isozyme 1	HSD11B1	2ILT
Dipeptidyl peptidase 4	DPP4	4A5S
Matrix metalloproteinase-9	MMP9	5TH6
Cyclin-dependent kinase 1	CDK1	4YC3
72 kDa type-IV collagenase	MMP2	4WKE
Prostaglandin G/H synthase 2	PTGS2	5KIR
Carbonic anhydrase 14	CA14	4LU3

TABLE 3: The docking information.

Compound	Affinity (kal·mol ⁻¹)		
	HSD11B1	DPP4	MMP9
Lamprolobine	-5.4	-7.3	-6.1
Sophoridine	-6.2	-7.9	-7.2
Matrine	-6	-7.4	-6.1
Adenine	-6.1	-5.8	-7

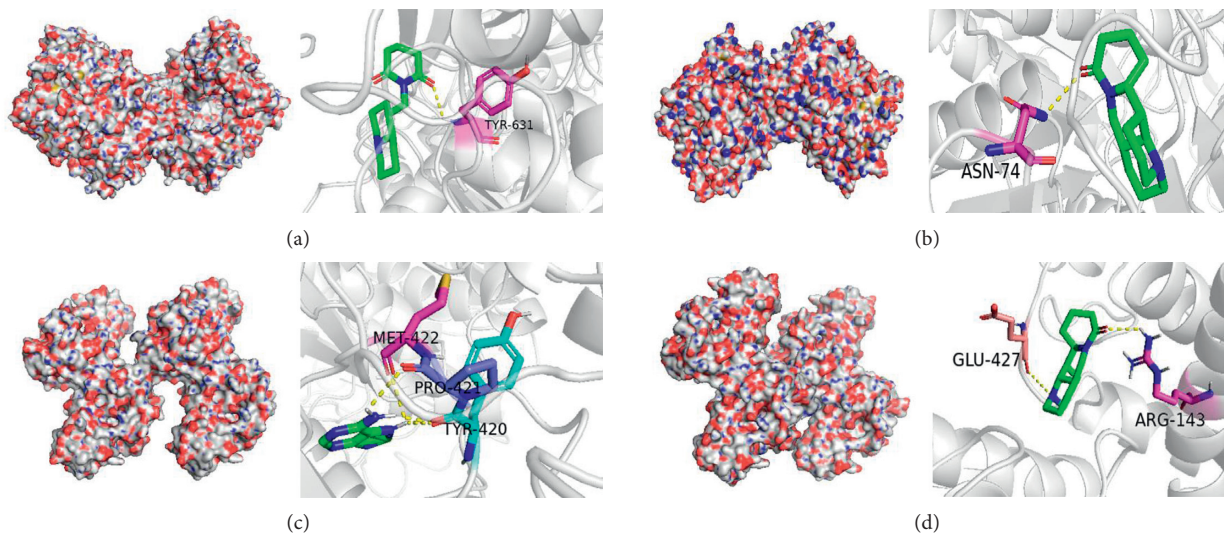


FIGURE 7: Result of molecular docking. Notes: (a) lamprolobine acts on DPP4; (b) sophoridine acts on DPP4; (c) adenine acts on MMP9; (d) sophoridine acts on MMP9.

cell proliferation, endoderm cell differentiation, proteolysis, collagen catabolism, extracellular matrix breakdown, adrenergic receptor signaling pathway, hypoxia, angiogenesis, serine-type endopeptidase activity, metalloproteinase activity, metalloendopeptidase activity, and protein extracellular matrix. The main enriched pathways are cancer pathway, chemical carcinogenesis, estrogen signaling pathway, TNF signaling pathway, and leukocyte transendothelial migration. Chemical carcinogenesis refers to the characteristics of some cancer cells, such as nongenotoxic carcinogens exposed to the environment, which changes the signal transduction pathway and eventually leads to high variability, genomic instability, uncontrolled proliferation, and resistance to apoptosis [51]. The estrogen signaling pathway enables estrogen to bind to the estrogen receptors ER α and ER β . It plays an

opposite role in cell proliferation, apoptosis, and migration and has different effects on the occurrence and development of tumor by inducing different transcription reactions [52]. Tumor necrosis factor (TNF), as an important cytokine, plays an important role in many physiological and pathological processes such as cell proliferation, differentiation, apoptosis, immune regulation, and inflammation induction [53]. Studies have suggested that TNF- α sign plays a key role in BC cell migration and its level has great potential to be prognostic cancer biomarkers [54]. The migration of white blood cells from the blood into tissues is essential for immune surveillance and inflammation. During inflammation or immune surveillance, leukocytes in the blood pass through endothelial cells in the vascular lumen and migrate to the next layer of tissue. This process is called

leukocyte transendothelial cell migration (TEM). The mechanism of CKI against BC may be closely related to the regulation of BC cell proliferation, apoptosis and migration, immune regulation, and inflammation induction.

5. Conclusion

In summary, this study revealed the potential pharmacological mechanism of CKI in the treatment of BC at a system level, which may involve synergistic regulation of cell proliferation, apoptosis, cell migration, immune regulation, and inflammation induction. Besides, the present study provides clues to understand and evaluate the synergistic effect of TCM in the treatment of complex diseases. Considering that this research is mainly based on data analysis, further biological experiments are essential for verifying the result.

Abbreviations

CKI:	Compound Kushen injection
BC:	Breast cancer
TCM:	Traditional Chinese medicine
GO:	Genome ontology
KEGG:	Kyoto Encyclopedia of Genes and Genomes
DAVID:	Database for Annotation, Visualization, and Integrated Discovery
SMILES:	Simplified Molecular Linear Input Specification
STITCH:	Search Tool for Interacting Chemicals
TCMSP:	Traditional Chinese Medicine Systems Pharmacology Analysis Platform
TTD:	Therapeutic Target Database
GEO:	Gene Expression Omnibus
TCGA:	The Cancer Genome Atlas
CCs:	Cellular components
MFs:	Molecular functions
BPs:	Biological processes
TNF:	Tumor necrosis factor
TEM:	Transendothelial cell migration
NA:	Neuronal acetylcholine
SRD5A1:	3-Oxo-5-alpha-steroid 4-dehydrogenase 1
HSD11B1:	Corticosteroid 11-beta-dehydrogenase isozyme 1
DPP4:	Dipeptidyl peptidase 4
MMP9:	Matrix metalloproteinase-9
CDK1:	Cyclin-dependent kinase 1
MMP2:	72 kDa type-IV collagenase
PTGS2:	Prostaglandin G/H synthase 2
CA14:	Carbonic anhydrase 14
MMPs:	Matrix metalloproteinases.

Data Availability

The data used to support the findings of this study are available from the corresponding author upon request.

Conflicts of Interest

All the authors declare that there are no conflicts of interest.

Acknowledgments

This work was supported by the Young Scientists Training Program of Beijing University of Chinese Medicine and the National Nature Science Foundation of China (Grant nos. 81473547 and 81673829).

Supplementary Materials

Supplementary Table 1: Degree of compounds in compound-compound target network. Supplementary Table 2: the topological analysis of key targets. Supplementary Table 3: the result of GO enrichment analysis. Supplementary Table 4: the result of KEGG pathway enrichment. (*Supplementary Materials*)

References

- [1] Z. Anastasiadi, G. D. Lianos, E. Ignatiadou, H. V. Harissis, and M. Mitsis, "Breast cancer in young women: an overview," *Updates in Surgery*, vol. 69, no. 3, pp. 313–317, 2017.
- [2] H. G. Kaplan, G. S. Calip, and J. A. Malmgren, "Maximizing breast cancer therapy with awareness of potential treatment-related blood disorders," *The Oncologist*, vol. 25, no. 5, pp. 391–397, 2020.
- [3] K. R. Wu, Z. H. Zhu, Y. X. He, L. Huang, X. Yan, and D. Wan, "Efficacy and safety of Xiao Ai Ping Injection combined with chemotherapy in advanced gastric cancer: a systematic review and meta-analysis," *Evidence-Based Complementary and Alternative Medicine*, vol. 2019, Article ID 3821053, 12 pages, 2019.
- [4] L. Wang, X. Liu, J. Wang, Y. Sun, G. Zhang, and L. Liang, "Comparison of the efficacy and safety between dezocine injection and morphine injection for persistence of pain in Chinese cancer patients: a meta-analysis," *Bioscience Reports*, vol. 37, no. 3, 2017.
- [5] X. Zhang, Y. Yuan, Y. P. Xi et al., "Cinobufacini injection improves the efficacy of chemotherapy on advanced stage gastric cancer: a systemic review and meta-analysis," *Evidence-Based Complementary and Alternative Medicine*, vol. 2018, Article ID 7362340, 12 pages, 2018.
- [6] S. Q. Huang, W. J. Peng, D. Mao et al., "Kangai injection, a traditional Chinese medicine, improves efficacy and reduces toxicity of chemotherapy in advanced colorectal cancer patients: a systematic review and meta-analysis," *Evidence-Based Complementary and Alternative Medicine*, vol. 2019, Article ID 8423037, 15 pages, 2019.
- [7] J. L. Liu, L. B. Yu, and W. Ding, "Efficacy and safety of kanglaite injection combined with radiochemotherapy in the treatment of advanced pancreatic cancer: a prisma-compliant meta-analysis," *Medicine (Baltimore)*, vol. 98, no. 32, Article ID e16656, 2019.
- [8] J. Wang and Y. Ren, "Clinical study on Compound Kushen Injection combined with ET regimen in treatment of breast cancer," *Drugs Clinic*, vol. 34, no. 7, pp. 2137–2141, 2019.
- [9] W. L. Li, S. J. Wu, W. J. Qin et al., "Research progress on the quality control of compound kushen injection," *Chinese Journal of Ethnomedicine and Ethnopharmacology*, vol. 28, no. 11, pp. 48–51, 2019.
- [10] L. Y. Yang and H. Z. Fan, "Progress in research on action mechanisms and clinical application of matrine and oxymatrine in treatment of gastrointestinal tumors," *Practical Clinical Medicine*, vol. 17, no. 5, pp. 97–100, 2016.

- [11] J. Dong, F. Yan, J. Deng, Y. L. Ma et al., "Antitumor mechanism of compound Kushen injection and its clinical application progress," *Tianjin Pharmacy*, vol. 31, no. 1, pp. 71–74, 2019.
- [12] H. W. Chen, X. J. Yao, T. Li et al., "Compound kushen injection plus platinum-based chemotherapy for stage iiib/iv non-small cell lung cancer: a protocol for meta-analysis of randomized clinical trials following the PRISMA Guidelines," *Medicine (Baltimore)*, vol. 98, no. 52, Article ID e18552, 2019.
- [13] Y. Shi, P. W. Yu, D. Z. Zeng et al., "Effects of compound kushen injection on the immunologic function of patients after gastric cancer resection," *Pharmaceutical Care Res*, vol. 6, no. 3, pp. 183–185, 2006.
- [14] Y. N. Dai, Y. Tian, X. J. Chen et al., "Observation on the therapeutic effect of Compound Kushen injection combined with neoadjuvant chemotherapy on breast cancer," *Shanxi Journal of Traditional Chinese Medicine*, vol. 36, no. 4, pp. 23–24, 2020.
- [15] M. Chen, M. W. Ni, W. Zhou et al., "Meta analysis based systematic evaluation of the treatment of non-small cell lung cancer with Compound Kushen injection combined with chemotherapy," *Evaluation and Analysis of Drug-Use in Hospitals of China*, vol. 19, no. 9, pp. 1051–1064, 2019.
- [16] W. S. Lu, S. Chen, and J. Fang, "Effect of Compound Kushen injection combined with radiotherapy and chemotherapy on serum CEA, CA199 and CA125 levels and cellular immune function in elderly patients with esophageal cancer," *Chinese Journal of Gerontology*, vol. 40, no. 6, pp. 1186–1189, 2020.
- [17] G. Li, "Clinical effect of Compound Kushen injection combined with TACE in the treatment of primary liver cancer," *Practical Clinical Journal of Integrated Traditional Chinese and Western Medicine*, vol. 20, no. 3, pp. 45–85, 2020.
- [18] Z. W. Shi, "Effect of Compound Kushen injection combined with DF chemotherapy on advanced esophageal cancer," *Henan Medical Research*, vol. 29, no. 3, pp. 491–492, 2020.
- [19] J. J. Zhang, Y. T. Bai, K. Y. Shao et al., "Application research and development of network pharmacology," *Journal of Comparative Chemistry*, vol. 3, no. 2, pp. 11–15, 2019.
- [20] S. Kim, P. A. Thiessen, E. E. Bolton et al., "PubChem substance and compound databases," *Nucleic Acids Research*, vol. 44, no. 1, pp. D1202–D1213, 2016.
- [21] M. Kuhn, C. von Mering, M. Campillos et al., "STITCH: Interaction networks of chemicals and proteins," *Nucleic Acids Research*, vol. 36, pp. D684–D688, 2008.
- [22] J. Nickel, B. O. Gohlke, J. Erehman et al., "SuperPred: update on drug classification and target prediction," *Nucleic Acids Research*, vol. 42, no. 1, pp. W26–W31, 2014.
- [23] D. Gfeller, A. Grosdidier, M. Wirth, A. Daina, O. Michielin, and V. Zoete, "Swiss target prediction: a web server for target prediction of bioactive small molecules," *Nucleic Acids Research*, vol. 42, pp. W32–W38, 2014.
- [24] X. Chen, Z. L. Ji, and Y. Z. Chen, "TTD: therapeutic target database," *Nucleic Acids Research*, vol. 30, no. 1, pp. 412–415, 2002.
- [25] T. Barrett, S. E. Wilhite, P. Ledoux et al., "NCBI GEO: archive for functional genomics data sets--update," *Nucleic Acids Research*, vol. 41, 2013.
- [26] K. Tomczak, P. Czerwińska, and M. Wizniewicz, "Review the cancer genome Atlas (TCGA): an immeasurable source of knowledge," *Contemporary Oncology/Współczesna Onkologia*, vol. 19, no. 1, pp. A68–A77, 2015.
- [27] X. K. Liu, J. R. Wu, M. J. Lin et al., "Mechanism of Si Junzitang based on network pharmacology," *Chinese Journal of Experimental Traditional Medical Formulae*, vol. 23, no. 16, pp. 194–202, 2017.
- [28] G. J. Dennis, B. T. Sherman, D. A. Hosack et al., "DAVID: Database for annotation, visualization, and integrated discovery," *Genome Biology*, vol. 4, no. 5, 2003.
- [29] M. Ashburner, C. A. Ball, J. A. Blake et al., "Gene ontology: Tool for the unification of biology," *Nature Genetics*, vol. 25, no. 1, pp. 25–29, 2000.
- [30] J. Wixon and D. Kell, "The Kyoto encyclopedia of genes and genomes—KEGG," *Yeast*, vol. 17, no. 1, pp. 48–55, 2000.
- [31] A. Kouranov, "The RCSB PDB information portal for structural genomics," *Nucleic Acids Research*, vol. 34, no. 90001, pp. D302–D305, 2006.
- [32] M. Garrett, Morris, H. Ruth et al., "Using AutoDock for ligand-receptor docking," *Current Protocols in Bioinformatics*, vol. 24, no. 1, 2008.
- [33] M. A. Lill and M. L. Danielson, "Computer-aided drug design platform using PyMOL," *Journal of Computer-Aided Molecular Design*, vol. 25, no. 1, pp. 13–19, 2011.
- [34] Y. Ma, *Study on Chemical Composition and Quality Control of Compound Kushen Injection*, China Academy of Chinese Medical Sciences, Beijing, China, 2012.
- [35] Y. Ma, H. Gao, J. Liu, L. Chen, Q. Zhang, and Z. Wang, "Identification and determination of the chemical constituents in a herbal preparation, compound kushen injection, by hplc and lc-dad-ms/ms," *Journal of Liquid Chromatography & Related Technologies*, vol. 37, no. 2, pp. 207–220, 2014.
- [36] W. Wang, R.-L. You, W.-J. Qin et al., "Anti-tumor activities of active ingredients in compound kushen injection," *Acta Pharmacologica Sinica*, vol. 36, no. 6, pp. 676–679, 2015.
- [37] H. Yang, "Value of compound Kushen injection in patients with breast cancer after chemotherapy," *Shenzhen Journal of Integrated Traditional Chinese and Western Medicine*, vol. 29, no. 1, pp. 2932–2934, 2019.
- [38] C. G. Zhao and Z. B. Li, "Pharmacological study of matrine alkaloids," *Veterinary Orientation*, no. 10, pp. 50–52, 2009.
- [39] M. F. Zhang, J. X. Wang, and Y. Q. Shen, "Research progress of matrine in the treatment of breast cancer and ovarian cancer," *Drug Evaluation and Research*, vol. 42, no. 10, pp. 2111–2118, 2019.
- [40] R. K. Zhang and C. Wang, "Effect of matrine on tumor growth and inflammatory factors and immune function in Wistar rat with breast cancer," *Chinese Journal of Applied Physiology*, vol. 34, no. 4, pp. 375–378, 2018.
- [41] L. L. Ren, W. J. Mo, L. L. Wang et al., "Matrine suppresses breast cancer metastasis by targeting ITGB1 and inhibiting epithelial-to-mesenchymal transition," *Experimental Therapeutic Medicine*, vol. 19, no. 1, pp. 367–374, 2020.
- [42] J. Q. Yu and Y. X. Jiang, "Advances in pharmacological research of sophoridine and oxysophoridine," *Journal of Ningxia Medical College*, vol. 1, pp. 78–80, 2005.
- [43] H. S. Feigelson, L. R. Teras, W. R. Diver et al., "Genetic variation in candidate obesity genes ADRB2, ADRB3, GHRL, HSD11B1, IRS1, IRS2, and SHC1 and risk for breast cancer in the cancer prevention study II," *Breast Cancer Research*, vol. 10, no. 4, p. R57, 2008.
- [44] S. B. Somiari, R. I. Somiari, C. M. Heckman et al., "Circulating MMP2 and MMP9 in breast cancer-Potential role in classification of patients into low risk, high risk, benign disease and breast cancer categories," *International Journal of Cancer*, vol. 119, no. 6, pp. 1403–1411, 2006.
- [45] J. M. Pellikainen, K. M. Ropponen, V. V. Kataja et al., "Expression of matrix metalloproteinase (MMP)-2 and MMP-9 in breast cancer with a special reference to activator protein-2, HER2, and prognosis," *Clinical Cancer Research*, vol. 10, no. 22, pp. 7621–7628, 2004.

- [46] D. Xie, H. M. Song, T. Q. Wu et al., "MicroRNA-424 serves an anti-oncogenic role by targeting cyclin-dependent kinase 1 in breast cancer cells," *Oncology Reports*, vol. 40, no. 6, pp. 3416–3426, 2018.
- [47] X. Zhang, Y. Pan, H. Fu, and J. Zhang, "Nucleolar and spindle associated protein 1 (NUSAP1) inhibits cell proliferation and enhances susceptibility to epirubicin in invasive breast cancer cells by regulating cyclin D kinase (CDK1) and DLGAP5 expression," *Medical Science Monitor*, vol. 24, no. 24, pp. 8553–8564, 2018.
- [48] J.-Y. Qian, J. Gao, X. Sun et al., "KIAA1429 acts as an oncogenic factor in breast cancer by regulating CDK1 in an N6-methyladenosine-independent manner," *Oncogene*, vol. 38, no. 33, pp. 6123–6141, 2019.
- [49] S. Izadi, A. Nikkhoo, M. Hojjat-Farsangi et al., "CDK1 in breast cancer: implications for theranostic potential," *Anti-Cancer Agents in Medicinal Chemistry*, vol. 20, no. 7, pp. 758–767, 2020.
- [50] M. Majumder, L. Dunn, L. Liu et al., "COX-2 induces oncogenic micro RNA miR655 in human breast cancer," *Scientific Reports*, vol. 8, no. 1, p. 327, 2018.
- [51] https://www.kegg.jp/dbget-bin/www_bget?hsa05204, 2020.
- [52] https://www.genome.jp/dbget-bin/www_bget?pathway+hsa04915, 2020.
- [53] J. Bradley, "TNF-mediated inflammatory disease," *The Journal of Pathology*, vol. 214, no. 2, pp. 149–160, 2008.
- [54] Y. Ma, Y. Ren, Z.-J. Dai, C.-J. Wu, Y.-H. Ji, and J. Xu, "IL-6, IL-8 and TNF- α levels correlate with disease stage in breast cancer patients," *Advances in Clinical and Experimental Medicine*, vol. 26, no. 3, pp. 421–426, 2017.